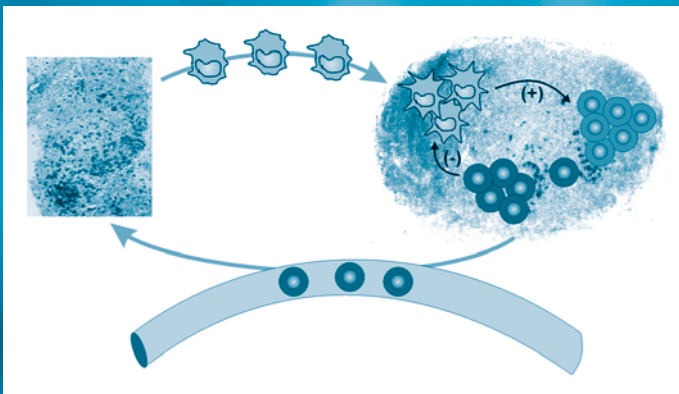# Adoptive Immunotherapy

Methods and Protocols

Edited by

Burkhard Ludewig
Matthias W. Hoffmann

Adoptive Immunotherapy

METHODS IN MOLECULAR MEDICINE™

Adoptive Immunotherapy

Methods and Protocols

Edited by

Burkhard Ludewig

Research Department, Kantonsspital St. Gallen, Switzerland

and

Matthias W. Hoffmann

*Department of Abdominal and Transplant Surgery,
Hannover Medical School, Hannover, Germany*

This publication is printed on acid-free paper. ∞
ANSI Z39.48-1984 (American Standards Institute) Permanence of Paper for Printed Library Materials.

Printed in the United States of America. 10 9 8 7 6 5 4 3 2 1

Preface

Over the last decade, the advances in cellular and molecular immunology have been tremendous. Our continuously improving understanding of the immune system and the appreciation of the mechanisms by which tumors and viral or bacterial infections are controlled have led to promising new treatment strategies. Adoptive transfer of tailored antigen-specific immune cells and/or optimally designed immunological effector molecules is an elegant and promising approach to the establishment or restoration of protective immune responses. At this point, it appears timely to publish the present volume on *Adoptive Immunotherapy* for the *Methods in Molecular Medicine*™ series.

Experts from various fields contributed to this comprehensive collection of state-of-the-art methods for adoptive immunotherapy. Recent technical advances and specific methods from the areas of dendritic cell therapy, generation of antigen-specific cytotoxic T cells, and antitumor treatment with specific antibodies have been compiled. Particular emphasis is placed on preclinical and clinical applications. These chapters are complemented by articles describing the progress of selected approaches in clinical trials. Leading experts in the field provide theoretical overviews and point out future directions for the improvement of adoptive immunotherapy. Additional chapters on the molecular definition of target antigens, mathematical modeling approaches to immunotherapy, and the utilization of regulatory T cells complete the volume. We were fortunate to receive support from leading scientists from all over the world who contributed their most recent experimental protocols and shared their practical advice. Special emphasis was placed on the "Notes" section to include helpful troubleshooting advice for daily work at the lab bench, which is a unique feature of the *Methods in Molecular Medicine*™ series. It is our hope that we have achieved our main objective to provide helpful information for scientists just entering the field of adoptive immunotherapy. Furthermore, this volume attempts to encourage more experienced researchers to try novel experimental approaches.

We are indebted to all our authors for generously making their time available in contributing to this volume and for the excellent quality of their work. Marcel Kremer's help in the final editing process is greatly appreciated. Finally, we want to thank the Series Editor, John Walker, and the staff of Humana Press for their support and continuous encouragement.

Burkhard Ludewig
Matthias Hoffmann

Contents

Contributors

GOSSE J. ADEMA • *Department of Tumor Immunology, Nijmegen Center for Molecular Life Sciences, University Medical Center Nijmegen, Nijmegen, the Netherlands*

SONJA BAILEY • *Protagen AG, Dortmund, Germany*

NINA BHARDWAJ • *NYU Cancer Institute Tumor Vaccine Center, New York University School of Medicine, New York, NY*

GEORG BARTSCH • *Department of Urology, University of Innsbruck, Innsbruck, Austria*

CHRISTIAN BECKER • *Department of Dermatology, Universitätsklinik Mainz, Mainz, Germany*

HELGA BERNHARD • *Department of Hematology/Oncology, Klinikum rechts der Isar, Technical University of Munich, Munich, Germany*

MARTIN BLUEGGEL • *Protagen AG, Dortmund, Germany*

GENNADY BOCHAROV • *Institute of Numerical Mathematics, Russian Academy of Sciences, Moscow, Russia, and Department of Mathematics, University College Chester, Chester, UK*

ATTILIO BONDANZA • *Experimental Hematology Laboratory, Cancer Immunotherapy and Gene Therapy Program, San Raffaele Scientific Institute, Milan, Italy*

CHIARA BONINI • *Experimental Hematology Laboratory, Cancer Immunotherapy and Gene Therapy Program, San Raffaele Scientific Institute, Milan, Italy*

PETER BROSSART • *Department of Hematology, Oncology, Immunology, and Rheumatology, University of Tübingen, Tübingen, Germany*

DIRK H. BUSCH • *Department of Microbiology/Immunology, Klinikum rechts der Isar, Technical University of Munich, Munich, Germany*

JOHN D. M. CAMPBELL • *Miltenyi Biotec GmbH, Bisley, Surrey, UK*

LUCIENNE CHATENOUD • *Immunologie biologie-IRNEM-INSERM U580, Hôpital Necker Enfants Malades, Paris, France*

FABIO CICERI • *Experimental Hematology Laboratory, Cancer Immunotherapy and Gene Therapy Program, San Raffaele Scientific Institute, Milan, Italy*

DIPANKAR DAS • *Faculty of Pharmacy and Pharmaceutical Sciences, University of Alberta, Edmonton, Alberta, Canada*

I. JOLANDA M. DE VRIES • *Department of Tumor Immunology, Nijmegen Center for Molecular Life Sciences, University Medical Center Nijmegen, Nijmegen, The Netherlands*

HANS JOACHIM DEEG • *Clinical Research Division, Fred Hutchinson Cancer Research Center, Seattle, WA*

ANNE-MARIE DOWNS • *Tumour Immunology Section, Department of Immunology, Division of Medicine, Imperial College London, London, UK*

NIKOS EMMANOUILIDIS • *Department of Abdominal and Transplant Surgery, Hannover Medical School, Hannover, Germany*

CARL G. FIGDOR • *Department of Tumor Immunology, Nijmegen Center for Molecular Life Sciences, University Medical Center Nijmegen, Nijmegen, The Netherlands*

NEVILLE J. FORD • *Department of Mathematics, University College Chester, Chester, UK*

BRUNO GANDER • *Institute of Pharmaceutical Sciences, Swiss Federal Institute of Technology (ETH) Zürich, Zürich, Switzerland*

HUBERT GANDER • *Department of Urology, University of Innsbruck, Innsbruck, Austria*

LIQUAN GAO • *Tumour Immunology Section, Department of Immunology, Division of Medicine, Imperial College London, London, UK*

MARCUS GROETTRUP • *Research Department, Cantonal Hospital St. Gallen, St. Gallen, Switzerland, and Division of Immunology, Department of Biology, University of Constance, Konstanz, Germany*

FRANK GRÜNEBACH • *Department of Hematology, Oncology, Immunology, and Rheumatology, University of Tübingen, Tübingen, Germany*

GUSTAVO HELGUERA • *Department of Microbiology, Immunology, and Molecular Genetics, and the Molecular Biology Institute, University of California, Los Angeles, CA*

SONJA HENNEMANN • *Miltenyi Biotec GmbH, Bergisch Gladbach, Germany*

ROB HOEBEN • *Department of Molecular Cell Biology, Leiden University Medical Center, Leiden, The Netherlands*

MATTHIAS W. HOFFMANN • *Department of Abdominal and Transplant Surgery, Hannover Medical School, Hannover, Germany*

WILLIAM J. HOGAN • *Clinical Research Division, Fred Hutchinson Cancer Research Center, Seattle, WA, and Division of Hematology, Mayo Clinic, Rochester, MN*

LORENZ HÖLTL • *Department of Urology, University of Innsbruck, Innsbruck, Austria*

CHRISTOPH HUELS • *Protagen AG, Dortmund, Germany*

HELMUT JONULEIT • *Department of Dermatology, Universitätsklinik Mainz, Mainz, Germany*

HELMUT W. H. G. KESSELS • *Department of Immunology, The Netherlands Cancer Institute, Amsterdam, The Netherlands*

JOACHIM KLOSE • *Institute for Human Genetics, Charité, Berlin, Germany*

ILAN KRAUSE • *Center for Autoimmune Diseases, Sheba Medical Center, Tel-Hashomer, and Sackler Faculty of Medicine, Tel-Aviv University, Tel-Aviv, Israel*

JÜRGEN KUBALL • *Department of Hematology and Oncology, Johannes Gutenberg-University Mainz, Mainz, Germany*

KITTY KWAPPENBERG • *Department of Immunohematology and Blood Transfusion, Leiden University Medical Center, Leiden, The Netherlands*

XIAN CHANG LI • *Division of Immunology, Department of Medicine, Harvard Medical School, Boston, MA*

CHRISTIAN P. LARSEN • *Emory Transplant Center and Department of Surgery, Emory University School of Medicine, Atlanta, GA*

BURKHARD LUDEWIG • *Research Department, Kantonsspital St. Gallen, Switzerland*

PETRA LUTTER • *Protagen AG, Dortmund, Germany*

ANDREAS MACKENSEN • *Department of Hematology/Oncology, University of Regensburg, Regensburg, Germany*

MARKUS Y. MAPARA • *Division of Hematology/Oncology, University of Pittsburgh Cancer Institute, Pittsburgh, PA*

CORNELIA MARTY • *Molecular Cell Biology, Paul Scherrer Institute, Villigen, Switzerland*

NORBERT MEIDENBAUER • *Department of Hematology/Oncology, University of Regensburg, Regensburg, Germany*

KEES MELIEF • *Leiden University Medical Center and University of Leiden, Leiden, The Netherlands*

HELMUT E. MEYER • *Medical Proteom-Center, Ruhr-University Bochum, Bochum, Germany*

DANIELA MICHELI • *Miltenyi Biotec GmbH, Bergisch Gladbach, Germany*

MARTIN R. MÜLLER • *Department of Hematology, Oncology, Immunology, and Rheumatology, University of Tübingen, Tübingen, Germany*

WALTER NUSSBAUMER • *Central Institute of Blood Transfusion, University of Innsbruck, Innsbruck, Austria*

DAVID O'NEILL • *NYU Cancer Institute Tumor Vaccine Center, New York University School of Medicine, New York, NY*

RIENK OFFRINGA • *Department of Immunohematology and Blood Transfusion, Leiden University Medical Center, Leiden, The Netherlands*

MANUEL L. PENICHET • *Department of Microbiology, Immunology, and Molecular Genetics, and the Molecular Biology Institute, University of California, Los Angeles, CA*

CHRISTIAN PESCHEL • *Department of Hematology/Oncology, Klinikum rechts des Isar, Technical University of Munich, Munich, Germany*

CHRISTOPH PIECHACZEK • *Miltenyi Biotec GmbH, Bergisch Gladbach, Germany*

CORNELIS J. A. PUNT • *Departments of Tumor Immunology and Medical Oncology, University Medical Center Nijmegen, Nijmegen, The Netherlands*

THOMAS PUTZ • *Department of Urology, University of Innsbruck, Innsbruck, Austria*

MARTIJN RABELINK • *Department of Molecular Cell Biology, Leiden University Medical Center, Leiden, The Netherlands*

ANDREA RAHM • *Department of Urology, University of Innsbruck, Innsbruck, Austria*

KEVIN P. RAISCH • *Division of Radiation Biology, Department of Radiation Oncology, and Comprehensive Cancer Center, University of Alabama at Birmingham, Birmingham, AL*

REINHOLD RAMONER • *Department of Urology, University of Innsbruck, Innsbruck, Austria*

DELPHINE REA • *Department of Immunohematology and Blood Transfusion, Leiden University Medical Center, Leiden, The Netherlands*

PATRICK REICHENBACH • *Swiss Institute for Experimental Cancer Research (ISREC), Epalinges, Switzerland*

VOLKER L. REICHARDT • *Department of Hematology, Oncology, Immunology, and Rheumatology, University of Tübingen, Tübingen, Germany*

PEDRO ROMERO • *Division of Clinical Onco-Immunology, Ludwig Institute for Cancer Research, Lausanne Branch, University Hospital, Lausanne, Switzerland*

NATHALIE RUFER • *NCCR Molecular Oncology, Swiss Institute for Experimental Cancer Research (ISREC), Epalinges, Switzerland*

AHMAD SAFAVY • *Division of Radiation Biology, Department of Radiation Oncology, and Comprehensive Cancer Center, University of Alabama at Birmingham, Birmingham, AL*

UGUR SAHIN • *Department of Internal Medicine, Johannes Gutenberg-University, Mainz, Germany*

BURKHARD SCHMIDT • *Department of Hematology/Oncology, Klinikum rechts der Isar, Technical University of Munich, Munich, Germany*

EDGAR SCHMITT • *Institute of Immunology, University of Mainz, Germany*

JÜRGEN SCHMITZ • *Miltenyi Biotec GmbH, Bergisch Gladbach, Germany*

SANDRA SCHNEIDER • *Research and Development, Ganymed Pharmaceuticals, Mainz, Germany*

TON N. M. SCHUMACHER • *Department of Immunology, The Netherlands Cancer Institute, Amsterdam, The Netherlands*

EDITH SCHWAMBORN • *Miltenyi Biotec GmbH, Bergisch Gladbach, Germany*

SEBASTIAN SCHWARTE • *Department of Radiooncology, Hannover Medical School, Hannover, Germany*

RETO A. SCHWENDENER • *Paul Scherrer Institute, Molecular Cell Biology, Villigen, Switzerland*

YEHUDA SHOENFELD • *Sackler Faculty of Medicine, Tel-Aviv University, Israel*

HANS J. STAUSS • *Tumour Immunology Section, Department of Immunology, Division of Medicine, Imperial College London, London, UK*

MAVANUR R. SURESH • *Faculty of Pharmacy and Pharmaceutical Sciences, University of Alberta, Edmonton, Alberta, Canada*

MEGAN SYKES • *Bone Marrow Transplantation Section, Transplantation Biology Research Center, Massachusetts General Hospital, Harvard Medical School, Boston, MA*

MATTHIAS THEOBALD • *Department of Hematology and Oncology, Johannes Gutenberg-University, Mainz, Germany*

MARTIN THURNHER • *Department of Urology, University of Innsbruck, Innsbruck, Austria*

ÖZLEM TÜRECI • *Department of Internal Medicine, Johannes Gutenberg-University, Mainz, Germany*

DIRK USENER • *Research and Development, Ganymed Pharmaceuticals, Mainz, Germany*

RALF-HOLGER VOSS • *Department of Hematology and Oncology, Johannes Gutenberg-University, Mainz, Germany*

MINH DIEM VU • *Division of Immunology, Department of Medicine, Harvard Medical School, Boston, MA*

YING WAECKERLE-MEN • *Research Department, Cantonal Hospital St. Gallen, St. Gallen, Switzerland*

ANDREAS WATTENBERG • *Protagen AG, Dortmund, Germany*

PETRA WEINGARTEN • *Protagen AG, Dortmund, Germany*

GREGOR WINKELS • *Miltenyi Biotec GmbH, Bergisch Gladbach, Germany*

MONIKA C. WOLKERS • *Department of Immunology, The Netherlands Cancer Institute, Amsterdam, The Netherlands*

CLAUDIA ZELLE-RIESER • *Department of Urology, University of Innsbruck, Innsbruck, Austria*

1

Exploiting Dendritic Cells for Active Immunotherapy of Cancer and Chronic Infection

David O'Neill and Nina Bhardwaj

Summary

Dendritic cells (DC) are important antigen-presenting cells (APC) that can prime naive T-cells and control lymphocyte-mediated adaptive immune responses with respect to magnitude, memory, and self-tolerance. Understanding the biology of these cells is central to the development of new generation immunotherapies for cancer and chronic infection. This chapter presents a brief overview of DC biology and the preparation and use of DC-based vaccines.

Key Words: Dendritic cells; antigen presentation; cancer vaccine; apoptotic cells; cytotoxic T-lymphocytes.

1. DC Biology

Protective immunity results from the concerted action of innate and adaptive immune systems *(1)*. The innate immune system includes phagocytic cells, natural killer (NK) cells, and complement, and has evolved to respond rapidly to pathogens to protect the host early in infection. The adaptive immune system, which consists of B- and T-lymphocytes, is required for the eventual clearance of many infections and for the generation of immunologic memory. Both innate and adaptive immunity apparently function to protect against the development of malignant tumors *(2–4)*. APC form an important link between innate and adaptive immunity. APC process intracellular and extracellular proteins into antigenic peptides, which are then presented on cell-surface major histocompatibility complex (MHC) molecules to cells of the adaptive immune system *(5)*. Because of their ability to express co-stimulatory molecules and cytokines, APC can stimulate the expansion of lymphocytes that recognize the displayed peptides, initiating an adaptive immune response. Although monocytes, macrophages, B-cells, and DC can all function as APC, DC are thought to be the principle initiators of immune responses *(6)*. In culture with lymphocytes, relatively few DC and very little antigen are needed to stimulate T-cell responses, and primary responses to antigens may be achieved using DC in long-term culture *(7,8)*. In both in vitro and in vivo assays, DC are by far the most potent APCs *(9)*.

1.1. DC Subtypes

DC are bone marrow-derived cells that are present in trace amounts in the blood (<0.1% of blood mononuclear cells) and virtually every tissue. Cell-surface pheno-typing has shown that in mice and apparently in humans there are as many as five distinct subpopulations of DC *(10,11)*. It is not completely clear, however, whether all of these represent distinct cell lineages or are a reflection of functional plasticity. In humans, the three best-characterized DC subsets may be derived by culturing precur-sor cells obtained from the blood *(10)*. Cells closely resembling epidermal Langerhans cells may be obtained from CD34+ hematopoietic progenitor cells (HPC) cultured with granulocyte/macrophage colony-stimulating factor (GM-CSF), tumor necrosis factor (TNF)-α, and transforming growth factor (TGF)-β. Cells resembling so-called dermal or interstitial DC (also known as DC1) may be obtained by culturing monocytes in GM-CSF and interleukin (IL)-4 followed by stimulation with proinflammatory cytokines such as TNF-α or with microbial products such as lipopolysaccharide (LPS). Circulating CD11c− BDCA2+ so-called plasmacytoid DC precursors in the blood may be differentiated into a third type of DC (plasmacytoid DC, or DC2) following expo-sure to viruses or bacterial (unmethylated CpG motif) DNA. Plasmacytoid DC are unique in that they travel to the lymph nodes directly from the blood (instead of through the lymphatics), and that upon stimulation they produce very high levels of type I interferon (interferon [IFN]-α and -β) *(10)*. Although it has been thought that most DC are of myeloid origin, with the exception of plasmacytoid DC, the precise origin of the different DC subtypes is not completely clear. In mice, which have been studied in more detail than humans, there is evidence that all DC types can be derived from both common myeloid and common lymphoid progenitors *(12,13)*, as well as from a third progenitor cell type that does not have myeloid or lymphoid potential *(14)*.

1.2. Antigen Uptake and Maturation

DC exist in a resting state in virtually every tissue and are recruited to sites of inflammation by chemokines such as MIP1-α (CCL3), MIP1-β (CCL4), and RANTES (CCL5). In tissues, DC and DC precursors capture antigens from a wide range of sources including bacteria, viruses, dead or dying cells, and extracellular proteins, peptides, and immune complexes. DC have a host of different antigen uptake recep-tors for this purpose, including toll-like receptors (TLR) *(15,16)*, Fc receptors *(17,18)*, and C-type lectins *(19)*. Some of these receptors induce simultaneous uptake and stimu-latory signals, whereas others are inhibitory receptors that induce suppressive signals upon antigen uptake.

DC continuously sample their environment for antigens, but they must be stimu-lated or "matured" before they can become strong stimulators of the immune system *(9)*. In fact, there is accumulating evidence that in the absence of maturation stimulus, DC function to maintain immunologic tolerance to captured antigens *(20–22)*.

DC maturation is induced by two classes of stimuli, or "danger" signals, termed *exogenous* and *endogenous (15,23,24)*. Exogenous stimuli are associated with micro-bial infections and are mediated by signaling through DC pattern-recognition recep-tors such as TLR *(9,15,25)*. There are at least 10 different TLR, each recognizing

different sets of pathogen-associated molecules. For example, TLR3 recognizes double-stranded RNA, TLR4 recognizes LPS, and TLR9 recognizes bacterial CpG motif DNA. Myeloid (as opposed to plasmacytoid) DC express TLRs 2 through 8, whereas plasmacytoid DC express TLRs 7 and 9, so these different DC subtypes respond differentially to different TLR ligands. DC may secrete a number of important inflammatory cytokines following TLR stimulation, including high levels of IL-12, IFN-α, and TNF-α, but the specific cytokine profile induced depends upon the subtype of DC stimulated as well as the nature of the stimulus. For example, plasmacytoid DC secrete abundant IFN-α when stimulated, whereas myeloid dermal DC do not.

Endogenous maturation stimuli originate from inflammatory molecules produced by cells of the host immune system or by damaged tissues *(9,24)*, and stimulate signaling through specific receptors on the DC. Examples of endogenous stimuli include TNF-α and related molecules expressed on activated lymphocytes such as CD40L and TRANCE, proinflammatory cytokines such as IL-1, heat shock proteins, growth factors such as TSLP, adhesion molecules, costimulatory molecules, ligation of Fc receptors, and contact with activated T-cells, $\gamma\delta$T-cells, and NKT-cells.

DC maturation is characterized by decreased phagocytic capacity, enhanced processing and presentation of antigens, induced ability to migrate to T-cell areas of lymph nodes, and increased ability to stimulate T-cell proliferation and cytokine production *(26)*. In culture, it is at this stage that DC acquire their characteristic dendritic appearance, with numerous cytoplasmic processes, or "veils." Maturation is accompanied by phenotypic changes that include increased cell-surface expression of MHC and co-stimulatory molecules, including members of the TNF receptor (CD40), TNF (OX40L, CD27L), and B7 (CD80 and CD86, B7-H3) families. There is downregulation of chemokine receptors such as CCR2 and CCR5 that direct DC to sites of inflammation (via MCP1, MIP1-α, MIP1-β, and RANTES) and upregulation of CCR7, which targets the DC to lymphatic vessels and lymph nodes via interaction with CCL19 (MIP-3-β, ELC), and CCL21 (SLC).

Antigen processing is highly regulated and controlled by maturation. For example, following receipt of a maturation signal, DC reduce the pH of endosomes (this facilitates processing of exogenously acquired antigens through activation of endosomal proteases), remove invariant chains from the antigen binding pockets of MHC class II molecules (so that processed peptides can access the empty pockets), and exocytose peptide-bound MHC class II molecules to the cell surface together with co-stimulatory molecules. Maturation also upregulates the activity of certain proteasome members to create "immunoproteasomes" that may enhance the processing of antigens that access the MHC class I pathway.

The process of maturation is also accompanied by upregulation of adhesion molecules such as CD54 (ICAM1), cytokines (e.g., TNF-α, IL-12, IL-18), and chemokines (RANTES, MIP1, IP-10). The latter enable the recruitment of T-cells, monocytes, and other DC into the local environment. In their mature state, DC express other markers such as CD83 (a molecule involved in thymic T-cell selection and DC–DC interactions) and DC-LAMP, a lysosomal protein that can distinguish mature from immature DC. In the T-cell areas of lymphoid organs, mature DC live for only 1–2 d *(27)*, but

their life span can be prolonged if they encounter T-cells that are activated and expressing membrane-bound activators such as CD40L and TRANCE *(9)*.

1.3. Antigen Presentation

Through their T-cell antigen receptor (TCR), T-lymphocytes specifically recognize peptide antigens bound to the highly polymorphic MHC molecules on the APC surface. MHC class I molecules present peptide antigens to CD8^{+} T-cells, whereas MHC class II molecules present peptide antigens to CD4^{+} T-cells. In addition, other, less polymorphic antigen-presenting molecules structurally similar to MHC class I are also found on DC. This would include CD1 molecules, which function to present microbial lipids to antigen-specific T-cells *(28,29)*. As with TLR and endocytic receptors, different DC subtypes have different sets of CD1 molecules. For example, CD1a is found on epidermal Langerhans cells, whereas CD1b and CD1c are found on dermal dendritic cells. CD1d presents specific glycolipids (galactosyl ceramides) to NKT-cells, cytokine-secreting cells that are important mediators of T-cell immunity *(30,31)*. CD1 molecules have not been found on plasmacytoid DC.

Infection of host cells with viruses results in the processing of viral peptides onto MHC class I via the so-called classical or endogenous pathway *(26,32)*. DC and most other cell types can process peptides this way from endogenously synthesized cytoplasmic proteins. In this pathway, viral proteins are ubiquitinated and degraded by the proteasome, and the resulting peptides are transported via transporters for antigen presentation (TAP) molecules into the endoplasmic reticulum (ER), where they are loaded onto MHC class I. The MHC class I/peptide complexes exit the ER via the trans-Golgi network and are transported to the cell surface, where the bound peptide is presented to the TCR on CD8^{+} T-cells.

In contrast, processing of antigens onto MHC class II occurs only in APC *(26,32)*. MHC class II/peptide complexes are formed through endocytosis of extracellular sources of protein. Endosomes containing the ingested protein mature and fuse with lysosomes, where acid proteases degrade the proteins into peptide fragments that are then loaded onto MHC class II molecules. The MHC class II/peptide complexes are transported to the cell surface within specialized vesicles, where the bound peptide is presented to the TCR on CD4^{+} T-cells.

DC are also uniquely capable of so-called exogenous presentation onto MHC class I, also known as cross-presentation, when processing extracellular antigens *(26,32–35)*. Through this pathway biosynthesis does not need to take place within the DC for presentation onto MHC class I to occur, permitting DC to elicit CD8^{+} T-cell responses to exogenous as well as endogenous antigens. Because of cross-presentation, DC can display exogenous antigens on both MHC class I and class II, because these antigens are also processed by the endosomal/lysosomal pathway simultaneously. Cross-presentation by DC has been shown to be necessary for inducing T-cell immunity to viruses or other intracellular pathogens that do not infect DC directly *(35)*. In addition, dead cells and immune complexes can specifically target the cross-presentation pathway through dedicated receptors on the DC surface (e.g., the Fcγ receptor for immune complexes and LOX1 for necrotic cell debris) *(17,18,36,37)*.

1.4. Lymphocyte Activation

DC can migrate very rapidly to lymph nodes, where they can dynamically interact with many T-cells at a time *(38,39)*. In the lymph node, triggering of a T-cell response is dependent upon the intensity and length of the DC–T-cell interaction *(40)*. Activation requires two types of signal at the immunological synapse between a DC and a T-cell, the first between the MHC/peptide complex on the DC and the T-cell antigen receptor, and the second through assorted co-stimulatory molecules and cytokines. Through these signals, mature DC can induce T-cells to expand clonally and to differentiate into memory and effector cells. There is a plasticity of this response that is dependent on many factors, including the antigen dose, the nature of the DC maturation stimulus (in the form of pathogen-derived products and the DC microenvironment), and the state of maturation of the DC. All of these influence the secreted cytokine profile of the DC and the polarization of responding T-helper (Th) cells in the form of a Th1 or Th2 response *(27,41,42)*. DC maturation is critical for this induction of immunity. Immature DCs that circulate through lymph nodes in the steady state can induce T regulatory responses and are important at maintaining immune tolerance toward self antigens *(21,22,43)*.

The generation of effector CD8^{+} T-cells (cytotoxic T-lymphocytes, or CTL) is particularly important in establishing immunity to tumors and intracellular infections, but the type of T-helper response is important as well, especially for maintaining immunologic memory *(44)*. Th1 cells, which produce IFN-γ and TNF-α, support CTL responses, whereas Th2 cells (which produce IL-4, IL-5, and IL-13) support humoral immunity and down-regulate Th1 responses. Th1 polarization is potently induced by DC secretion of IL-12, although IL-12 is not an absolute requirement for this, perhaps because of other DC-generated cytokines such as IL-23 or IL-27 *(27,45)*. In addition to activating T-cells, it is now known that DCs can also directly interact with and activate B-cells *(46,47)*, NK cells *(48)*, and NKT-cells *(49)*. All these cells may play a critical role in the induction of antitumor immunity.

2. Ex Vivo Manipulation of DCs for Active Immunotherapy

Vaccines against microbial pathogens are traditionally prepared by isolating an attenuated or killed version of the pathogen and mixing it with an adjuvant that serves to boost the immune response. The success of this type of vaccine often depends on its ability to stimulate the production of neutralizing antibodies *(50)*. For a number of chronic intracellular infections such as HIV, hepatitis C, tuberculosis, or malaria, however, this approach has not proved sufficient to generate protective immunity. To control these disorders, the generation of Th1 and CTL responses appears to be very important *(50)*.

The induction and maintenance of CTL-mediated immunity also appears to be of great importance for immunotherapies for patients with cancer. *(2,3,51)*. By studying cellular immune responses in cancer patients, a variety of tumor-associated antigens have been identified that are recognized by T-cells. These antigens can be used to "vaccinate" individuals against their own tumors *(52–54)*. Attempts to vaccinate cancer patients with killed tumor cells, cell lysates, or tumor antigen proteins or peptides

have produced immunologic and clinical responses, some of them complete and long-lasting *(55–60)*. However, it remains to be demonstrated in large, prospective, randomized trials that these antigen/adjuvant preparations can provide a clinically significant benefit in the form of improved survival *(58,61,62)*.

Cancer vaccine adjuvants such as QS-21, GM-CSF, or Incomplete Freund's Adjuvant (IFA, or Montanide) have all been shown to boost CTL responses to tumor-associated antigens, but these responses are often weak and often require in vitro restimulation of T-cells to be detected *(57,63)*. Because of their potent immunostimulatory capacity and their ability to prime naïve T-cells, the manipulation of DC as a "natural" vaccine adjuvant has generated great interest *(9,50,63–67)*. To date, the most common approach has been to isolate large numbers of DC by culturing bone marrow-derived progenitors ex vivo in the presence of cytokines, loading the DC with antigens and re-injecting them back into the subject. In mice, bone marrow-derived DC loaded ex vivo with tumor antigens by a variety of methods have been shown to induce potent antigen-specific CTL responses. These vaccines can protect mice from challenge with tumors bearing the antigenic peptide in association with cell-surface MHC, and can cure animals bearing established tumors *(68–71)*.

In human subjects, vaccination of healthy volunteers with peptide-pulsed DC is well tolerated and clearly induces antigen-specific T-cell immunity in the form of CTL and Th1 responses *(72,73)*. In addition, CTL responses and tumor regressions have been noted in small clinical trials in cancer patients vaccinated with tumor-associated antigens loaded by a variety of methods onto ex vivo generated DC. Clinical and immune responses have been reported in patients with metastatic melanoma *(74–77)*, metastatic renal cell carcinoma *(78)*, B-cell lymphoma *(79,80)*, prostate cancer *(81–86)*, breast and ovarian cancer *(87)*, and colon and lung cancer *(88)*. Because early results have been encouraging, larger trials are now underway to determine whether DC vaccines can improve survival in cancer patients *(89)*.

Three general methods have been described for the preparation of DC from human subjects for use in clinical trials. The methods differ in the starting population of blood cells used and in the different mixtures of cells obtained in the finished product. The methods involve, respectively: (1) differentiating DC from nonproliferating monocyte precursors; (2) differentiating DC from proliferating CD34$^+$ hematopoietic progenitor cells; or (3) directly isolating DC from peripheral blood. The optimal route of administration for the cells has not yet been determined. They are typically injected intradermally, subcutaneously, or intravenously. Other routes such as direct injection into lymph nodes or tumors have also been described.

2.1. Monocyte-Derived DC

By far the most popular method is to prepare DCs from blood monocytes. Monocyte-derived DCs (MoDC) can be generated from peripheral blood mononuclear cells (PBMC) obtained from whole blood, although to obtain yields sufficient for the production of multiple vaccines, PBMC are usually obtained by leukapheresis *(90)*. To prepare MoDC, CD14$^+$ monocytes are first selected from PBMC, using either a simple plastic adherence step (monocytes adhere to plastic, whereas lymphocytes do not), or by large-scale cell sorting using immunomagnetic beads. The monocytes are induced

to differentiate into immature CD14⁻ CD83⁻ DC by culturing for several days in the presence of IL-4 and GM-CSF. The DC are then typically stimulated to mature by culturing for an additional period of time (1–2 d) in the presence of proinflammatory cytokines or soluble CD40L. Mature MoDC are large, CD14⁻ CD83⁺ cells that express high levels of MHC class I and II molecules and high levels of co-stimulatory molecules such as CD40, CD80, and CD86. Peptide antigens may be loaded or "pulsed" onto the DC either before or after maturation. Cell lysates or purified or recombinant proteins are typically loaded just before the maturation stimulus. Viruses or RNA may be added either before or after maturation.

2.2. DC Derived From CD34⁺ Hematopoietic Progenitor Cells

This method begins with the collection of CD34⁺ proliferating progenitors from the peripheral blood *(91,92)*. This requires mobilizing CD34⁺ progenitor cells from the bone marrow by treating patients with granulocyte colony-stimulating factor (G-CSF) prior to leukapheresis *(63,76)*. The cells are expanded in culture for a week or more in the presence of GM-CSF and TNF-α. The final product is a more complex mixture of cells than MoDC. It includes a population similar to MoDC and another population phenotypically identical to epidermal Langerhans cells. Differentiation may be skewed toward Langerhans cells by adding TGF-β to the culture. A fairly large percentage of the final product consists of myeloid cells at varying stages of differentiation, including some CD14⁺ cells. These do not function as antigen-presenting cells but do not appear to interfere with the potency of the vaccine, although this has not been well studied. CD34⁺ progenitor cell-derived DC may be matured and loaded with antigens similarly to Mo-DC.

2.3. DC Enriched From Peripheral Blood

In the first clinical trial to use DC-based immunotherapy for cancer, DC were purified directly from PBMC by a series of density gradient centrifugation steps *(80)*. In this procedure, the PBMC were first depleted of monocytes by centrifugation through discontinuous Percoll gradients. The monocyte-depleted PBMC were then cultured for 24 h in the presence of antigen, and then the DC were separated from lymphocytes by sequential centrifugation through 15% and then 14% metrizamide gradients. The low-density fraction containing the DC was then cultured overnight again in the presence of antigen, washed, and injected back into the patient *(80)*. The final product contained 50–90% DC, and in subsequent studies it was found that although the DC obtained at the time of leukapheresis had an immature phenotype, by the end of the 2-d procedure they express maturation markers such as CD80, CD86, CD83, and CCR7 *(88)*. DC preparations based on this method are currently being used in phase III trials for the immunotherapy of prostate cancer *(89)*.

The yield of DC obtained by this procedure can be significantly enhanced by stimulating the patient with FMS-like tyrosine kinase-3 ligand (Flt3 ligand, or FL) prior to leukapheresis *(88)*. FL mobilizes and expands peripheral blood DC, and increases the final DC yield approx 20-fold. Taking advantage of the increased numbers of DC obtained in the leukapheresis product following administration of FL, a modification of the DC isolation procedure has been described that omits the initial Percoll gradient and the 14% metrizamide gradient (only the 15% metrizamide gradient is used) *(88)*.

Unfortunately, pharmaceutical-grade FL is no longer commercially available. Still, the development of commercial closed systems that take advantage of cell-separation technology based on immunomagnetic beads, and the short preparation time involved, may make the enrichment of DC directly from blood an attractive option in the future.

2.4. Choice of Cell Type

All three types of DC preparation have been shown to stimulate proliferation and cytokine production of antigen-specific T-cells, and have been associated with clinical responses in trials involving human subjects with cancer. However, no direct comparisons of these cells have been performed in human subjects. In vitro data from one group has indicated an advantage of CD34+ cell-derived DC over MoDC in the presentation of peptides *(93)*, but MoDC have many advantages for clinical use. They are considerably simpler to prepare and are a well characterized, homogenous population of cells. In addition, patients do not need to be prestimulated with cytokines prior to leukapheresis to prepare MoDC.

2.5. Ex Vivo Maturation of DC

Whatever the method used to prepare the DC, it is clearly important that the DCs be matured prior to clinical use *(43)*. Clinical studies with DC-based vaccines indicate that DCs that have been matured ex vivo more effectively stimulate T-cell responses *(94)*, and there is accumulating evidence that the use of antigen-loaded immature DC in vaccines actually leads to immune tolerance, perhaps due to anergy or T-regulatory cell mechanisms *(20,21,95)*.

In early work on DC-based vaccines, DC were matured using supernatants from cultured monocytes (monocyte-conditioned medium, or MCM) as a source of pro-inflammatory cytokines *(90,96,97)*. Currently, the most popular method is to use a cocktail of three cytokines (IL-1-β, IL-6, and TNF-α) plus prostaglandin E2 (PGE2), originally described by Jonuleit et al., which mimics the effect of MCM on DC maturation *(98)*. One concern with this method is that DC matured in the presence of PGE2 do not secrete IL-12 *(99)*. However, the addition of PGE2 is important for inducing DC migratory ability *(100)*, and DC matured with this cocktail still strongly stimulate CTL responses both in vitro and in vivo. This may be due to the action of other IL-12-related cytokines, such as IL-23 and IL-27 *(45)*.

2.6. Loading DCs With Antigens Ex Vivo: Peptide Antigens

There are many ways to load DC with antigens. One of the more commonly used methods is to co-culture them directly with peptides *(72,74–77)*. This has been made possible because of progress in identifying immunodominant peptide epitopes for tumor-associated and microbial antigens that are recognized by T-cells *(52,54)*. Use of peptides requires knowledge of a patient's HLA type and the existence of relevant MHC-restricted peptide epitopes. HLA-A2-restricted peptides are commonly used, often in combinations, although other MHC class I-restricted epitopes and even MHC class II-restricted T-helper epitopes may be used as well. Altered or enhanced peptide antigens have also been used to boost immunity to less immunogenic self antigens *(50,88)*. Peptides from microbial antigens such as influenza matrix protein are

frequently included to test for recall immune responses. Peptides may be loaded onto DC either before or after DC maturation, since short peptides can apparently bind directly to MHC molecules on the DC surface without having to be processed within the cell *(9)*. In our hands, pulsing peptides onto mature DC has resulted in somewhat better specific T-cell stimulation in vitro.

The optimal peptide dose with which to load DC is not entirely clear. Intuitively it might be thought that increasing the concentration of peptide would result in better antigen loading and more potent stimulation of T-cells. The opposite, however, appears to be true. Alexander-Miller et al. showed that APC loaded with very low concentrations of peptide (as little as 0.1 n*M*) stimulate high-avidity T-cell clones that much more effectively recognize and lyse antigen-expressing target cells *(50, 101)*. For clinical use it will be very important to load DC with a peptide dose that stimulates expansion of high-avidity T-cell clones. Most protocols currently pulse DC with peptide concentrations of 1 to 10 µ*M*, although the optimal dose will most likely need to be determined through dose escalation studies in human subjects.

2.7. Proteins and Cell Lysates

One disadvantage of using peptide-pulsed DC is that the dominant epitopes of the antigen of interest must be known for the HLA type of the patient. This often restricts peptide vaccination studies to individuals with common HLA types. Alternatively, DC can be loaded prior to maturation with purified or recombinant proteins *(79)*, or even with whole tumor cell lysates *(74,102,103)*. This method allows host HLA molecules to select epitopes from an antigen's entire sequence, and in the case of loading with tumor lysates permits vaccination with the complete antigenic content of the tumor.

The immunogenicity of protein-loaded DC can be enhanced by using proteins coupled to cytokine or carrier-protein sequences *(79,104)*, or using proteins of xenogeneic origin *(83)*. Keyhole limpet hemocyanin (KLH), a powerful immunogen derived from a marine mollusk, is one such protein that is commonly used to nonspecifically boost the immunogenicity of a vaccine. It is also added as a control to test for the ability of a vaccine to prime T-helper responses to a neoantigen *(6,32)*.

One disadvantage of loading DC with purified protein antigens is that the MHC class I pathway is not specifically targeted. In practice, however, pulsing DC with crude protein mixtures such as tumor cell lysates seems to produce vaccines that generate clinical responses *(74,102,103)*. This may be because of the ability of DC to cross-present exogenous antigens onto MHC class I.

2.8. DNA, RNA, and Viruses

Loading DC with antigens by DNA transfection has been successfully performed *(105,106)*; however, it is often associated with a significant amount of cell death. DC tolerate RNA transfection well, however, and this has been used to successfully load DC with RNA encoding specific antigens or even whole tumor RNA *(68,81,107–109)*. Typically, DC are transfected with RNA by co-culture with naked RNA or by RNA electroporation prior to maturation. DC can also be loaded with antigens by infecting with nonreplicating viral vectors such as recombinant adenovirus or pox viruses *(110–114)*.

As with loading DC with proteins or RNA, this method allows vaccines to be generated for patients of any HLA type, since the encoded proteins are cleaved and processed onto MHC molecules within the host cell.

2.9. Apoptotic Cells, Immune Complexes, and Other Methods

Apoptotic tumor cells can be used as an antigen source to take advantage of cross-presentation of extracellular antigens onto MHC class I *(34,115,116)*. Cross-presentation of specific protein antigens may also be targeted by loading DC with IgG immune complexes of those antigens, which are taken up via Fc receptors on the DC *(17,18,36)*. A number of other methods have also been employed to manipulate DCs ex vivo to create cellular or cell-derived vaccines. Cell fusions between DC and tumor cells create heterokaryons that can stimulate anti-tumor T-cell responses in vitro, in laboratory animals, and in humans with cancer *(78,117,118)*. DC can also be used as a source of exosomes, antigen-presenting vesicles which can be loaded with antigens and used to stimulate T-cell immunity *(119–121)*.

3. Treatment Strategies for the Use of Dendritic Cell Vaccines

It is clearly established that antigen-loaded DC generated by a number of different methods can induce antigen-specific immunity in the form of CTL and Th1 responses in human subjects. Numerous technical variables need testing before this approach is optimized, however, and large controlled studies are needed to prove efficacy in the treatment of cancer or serious chronic infections.

Most of the reports on the therapeutic use of DC vaccines published to date have been on patients with advanced cancer. Although occasional dramatic clinical responses have been noted, it is likely that DC immunizations may be most effective in the adjuvant setting when the patient is in remission or the tumor burden is low but risk of disease progression and death is high. This needs to be investigated in controlled clinical trials. In addition, the possibility of using DC vaccines in combination with novel therapies such as anti-angiogenesis agents *(122)*, antibodies that target tumor antigens, or immunostimulatory agents such as anti-CTLA-4 *(123–125)* has not been addressed. Such synergistic approaches could significantly enhance the vaccine's anti-tumor effect and should be tested in clinical trials.

One significant drawback of DC vaccines is that the ex vivo production of individually tailored cellular therapies is both laborious and expensive. For this reason the use of novel *in situ* approaches that take advantage of the biological properties of DC in vivo has generated great interest. Approaches that can mobilize DC to an accessible site where they can be matured and pulsed with antigens in vivo are being developed that may hopefully lead to potent therapies that do not require expensive facilities or labor-intensive cell processing *(9)*. Such approaches include the systemic mobilization of DC using Flt3 ligand, the local injection of chemokines such as MIP-3β, the use of DNA vaccines containing bacterial CpG motifs (which can target DC and B cells via TLR9), or the use of topical compounds such as Imiquimod (a TLR7 ligand) in conjunction with peptide vaccines *(16,50,126,127)*. As more is discovered about the biological properties of DC, we should be better able to manipulate these important cells to take advantage of their potent immunoregulatory function for the treatment of human disease.

References

1 Palucka, K. and Banchereau, J. (1999) Linking innate and adaptive immunity. *Nat. Med.* **5,** 868–870.

2 Dunn, G. P., Bruce, A. T., Ikeda, H., Old, L. J., and Schreiber, R. D. (2002) Cancer immunoediting: from immunosurveillance to tumor escape. *Nat. Immunol.* **3,** 991–998.

3 Smyth, M. J., Godfrey, D. I., and Trapani, J.A. (2001) A fresh look at tumor immunosurveillance and immunotherapy. *Nat. Immunol.* **2,** 293–299.

4 Pardoll, D. (2003) Does the immune system see tumors as foreign or self? *Annu. Rev. Immunol.* **21,** 807–839.

5 Sant, A. and Yewdell, J. (2003) Antigen processing and recognition. *Curr. Opin. Immunol.* **15,** 66–68.

6 Banchereau, J., Briere, F., Caux, C., et al. (2000) Immunobiology of dendritic cells. *Annu. Rev. Immunol.* **18,** 767–811.

7 Bhardwaj, N., Friedman, S. M., Cole, B. C., and Nisanian, A. J. (1992) Dendritic cells are potent antigen-presenting cells for microbial superantigens. *J. Exp. Med.* **175,** 267–273.

8 Fonteneau, J. F., Larsson, M., Somersan, S., et al. (2001) Generation of high quantities of viral and tumor-specific human CD4$^+$ and CD8$^+$ T-cell clones using peptide pulsed mature dendritic cells. *J. Immunol. Methods.* **258,** 111–126.

9 Steinman, R. M. and Pope, M. (2002) Exploiting dendritic cells to improve vaccine efficacy. *J. Clin. Invest.* **109,** 1519–1526.

10 Shortman, K. and Liu, Y. J. (2002) Mouse and human dendritic cell subtypes. *Nat. Rev. Immunol.* **2,** 151–161.

11. MacDonald, K.P., Munster, D.J., Clark, G.J., Dzionek, A., Schmitz, J., and Hart, D.N. (2002) Characterization of human blood dendritic cell subsets. *Blood* **15,** 15.

12 Manz, M. G., Traver, D., Miyamoto, T., Weissman, I. L., and Akashi, K. (2001) Dendritic cell potentials of early lymphoid and myeloid progenitors. *Blood* **97,** 3333–3341.

13 Wu, L., D'Amico, A., Hochrein, H., O'Keeffe, M., Shortman, K., and Lucas, K. (2001) Development of thymic and splenic dendritic cell populations from different hemopoietic precursors. *Blood* **98,** 3376–3382.

14 del Hoyo, G. M., Martin, P., Vargas, H. H., Ruiz, S., Arias, C. F., and Ardavin, C. (2002) Characterization of a common precursor population for dendritic cells. *Nature* **415,** 1043–1047.

15 Medzhitov, R. (2001) Toll-like receptors and innate immunity. *Nat. Rev. Immunol.* **1,** 135–145.

16 Takeda, K., Kaisho, T., and Akira, A. (2003) Toll-like receptors. *Annu. Rev. Immunol.* **21,** 335–376.

17 Rafiq, K., Bergtold, A., and Clynes, R. (2002) Immune complex-mediated antigen presentation induces tumor immunity. *J. Clin. Invest.* **110,** 71–79.

18 Schuurhuis, D. H., Ioan-Facsinay, A., Nagelkerken, B., et al. (2002) Antigen-antibody immune complexes empower dendritic cells to efficiently prime specific CD8$^+$ CTL responses in vivo. *J. Immunol.* **168,** 2240–2246.

19 Figdor, C. G., van Kooyk, Y., and Adema, G. J. (2002) C-type lectin receptors on dendritic cells and Langerhans cells. *Nat. Rev. Immunol.* **2,** 77–84.

20 Steinman, R. M., and Nussenzweig, M. C. (2002) Avoiding horror autotoxicus: the importance of dendritic cells in peripheral T cell tolerance. *Proc. Natl. Acad. Sci. USA* **99,** 351–358.

21 Steinman, R. M., Hawiger, D., and Nussenzweig, M. C. (2003) Tolerogenic dendritic cells. *Annu. Rev. Immunol.* **21,** 685–711.

22 Hawiger, D., Inaba, K., Dorsett, Y., et al. (2001) Dendritic cells induce peripheral T cell unresponsiveness under steady state conditions in vivo. *J. Exp. Med.* **194,** 769–779.

23 Aderem, A. and Ulevitch, R. J. (2000) Toll-like receptors in the induction of the innate immune response. *Nature* **406,** 782–787.

24 Gallucci, S. and Matzinger, P. (2001) Danger signals: SOS to the immune system. *Curr. Opin. Immunol.* **13,** 114–119.

25 Pulendran, B., Palucka, K., and Banchereau, J. (2001) Sensing pathogens and tuning immune responses. *Science* **293,** 253–256.

26 Mellman, I. and Steinman, R. M. (2001) Dendritic cells: specialized and regulated antigen processing machines. *Cell* **106,** 255–258.

27 Lanzavecchia, A. and Sallusto, F. (2001) The instructive role of dendritic cells on T cell responses: lineages, plasticity and kinetics. *Curr. Opin. Immunol.* **13,** 291–289.

28 Moody, D. B. and Porcelli, S. A. (2002) Intracellular pathways of CD1 antigen presentation. *Nature Rev. Immunol.* **3,** 11–22.

29 Porcelli, S. A. and Modlin, R. L. (1999) The CD1 system: antigen presenting molecules for T cell recognition of lipids and glycolipids. *Annu. Rev. Immunol.* **17,** 297–329.

30 Fujii, S., Shimizu, K., Kronenberg, M., and Steinman, R. M. (2002) Prolonged IFN-gamma-producing NKT response induced with alpha-galactosylceramide-loaded DCs. *Nat. Immunol.* **3,** 867–874.

31 Kronenberg, M. and Gapin, L. (2002) The unconventional lifestyle of NKT cells. *Nature Rev. Immunol.* **2,** 557–568.

32 Bhardwaj, N. (2001) Processing and presentation of antigens by dendritic cells: implications for vaccines. *Trends Mol. Med.* **7,** 388–394.

33 Heath, W. R. and Carbone, F. R. (1999) Cytotoxic T lymphocyte activation by cross-priming. *Curr. Opin. Immunol.* **11,** 314–318.

34 Albert, M. L., Sauter, B., and Bhardwaj, N. (1998) Dendritic cells acquire antigen from apoptotic cells and induce class I- restricted CTLs. *Nature* **392,** 86–89.

35 Heath, W. R. and Carbone, F. R. (2001) Cross-presentation in viral immunity and self-tolerance. *Nat. Rev. Immunol.* **1,** 126–134.

36 Kalergis, A. M. and Ravetch, J. V. (2002) Inducing tumor immunity through the selective engagement of activating Fcgamma receptors on dendritic cells. *J. Exp. Med.* **195,** 1653–1659.

37 Savill, J., Dransfield, I., Gregory, C., and Haslett, C. (2002) A blast from the past: clearance of apoptotic cells regulates immune responses. *Nat. Rev. Immunol.* **2,** 965–975.

38 Stoll, S., Delon, J., Brotz, T. M., and Germain, R. N. (2002) Dynamic imaging of T cell–dendritic cell interactions in lymph nodes. *Science* **296,** 1873–1876.

39 Norbury, C. C., Malide, D., Gibbs, J. S., Bennink, J. R., and Yewdell, J. W. (2002) Visualizing priming of virus-specific CD8+ T cells by infected dendritic cells in vivo. *Nat. Immunol.* **3,** 265–271.

40 Langenkamp, A., Casorati, G., Garavaglia, C., Dellabona, P., Lanzavecchia, A., and Sallusto, F. (2002) T cell priming by dendritic cells: thresholds for proliferation, differentiation and death and intraclonal functional diversification. *Eur. J. Immunol.* **32,** 2046–2054.

41 Palucka, K. and Banchereau, J. (2002) How dendritic cells and microbes interact to elicit or subvert protective immune responses. *Curr. Opin. Immunol.* **14,** 420–431.

42 Boonstra, A., Asselin-Paturel, C., Gilliet, M., 'et al. (2003) Flexibility of mouse classical and plasmacytoid-derived dendritic cells in directing T helper type 1 and 2 cell development: dependency on antigen dose and differential toll-like receptor ligation. *J. Exp. Med.* **197,** 101–109.

43 Lutz, M. and Schuler, G. (2002) Immature, semi-mature and fully mature dendritic cells: which signals induce tolerance or immunity? *Trends Immunol.* **23,** 445.

44 Kaech, S. M. and Ahmed, R. (2003) CD8 T cells remember with a little help. *Science* **300,** 263–265.

45 Trinchieri, G. (2003) Interleukin-12 and the regulation of innate resistance and adaptive immunity. *Nat. Rev. Immunol.* **3,** 133–146.

46 Balazs, M., Martin, F., Zhou, T., and Kearney, J. (2002) Blood dendritic cells interact with splenic marginal zone B cells to initiate T-independent immune responses. *Immunity* **17,** 341–352.

47 Jego, G., Palucka, A. K., Blanck, J. P., Chalouni, C., Pascual, V., and Banchereau, J. (2003) Plasmacytoid dendritic cells induce plasma cell differentiation through type I interferon and interleukin 6. *Immunity* **19,** 225–234.

48 Ferlazzo, G., Tsang, M. L., Moretta, L., Melioli, G., Steinman, R. M., and Munz, C. (2002) Human dendritic cells activate resting natural killer (NK) cells and are recognized via the NKp30 receptor by activated nk cells. *J. Exp. Med.* **195,** 343–351.

49 Fujii, S., Shimizu, K., Kronenberg, M., and Steinman, R. M. (2002) Prolonged IFN-gamma-producing NKT response induced with alpha-galactosylceramide-loaded DCs. *Nat. Immunol.* **3,** 867–874.

50 Berzofsky, J. A., Ahlers, J. D., and Belyakov, I. M. (2001) Strategies for designing and optimizing new generation vaccines. *Nat. Rev. Immunol.* **1,** 209–219.

51 Shankaran, V., Ikeda, H., Bruce, A. T., et al. (2001) IFNgamma and lymphocytes prevent primary tumour development and shape tumour immunogenicity. *Nature* **410,** 1107–1111.

52 Boon, T. and Old, L.J. (1997) Cancer tumor antigens. *Curr. Opin. Immunol.* **9,** 681–683.

53 Houghton, A. N., Gold, J. S., and Blachere, N. E. (2001) Immunity against cancer: lessons learned from melanoma. *Curr. Opin. Immunol.* **13,** 134–140.

54 Stevanovic, S. (2002) Identification of tumour-associated T-cell epitopes for vaccine development. *Nat. Rev. Cancer* **2,** 514–520.

55 Bendandi, M., Gocke, C. D., Kobrin, C. B., et al. (1999) Complete molecular remissions induced by patient-specific vaccination plus granulocyte-monocyte colony-stimulating factor against lymphoma. *Nat. Med.* **5,** 1171–1177.

56 Livingston, P. (2001) The unfulfilled promise of melanoma vaccines. *Clin. Cancer Res.* **7,** 1837–1838.

57 Nestle, F. O. (2002) Vaccines and melanoma. *Clin. Exp. Dermatol.* **27,** 597–601.

58 Machiels, J. P., van Baren, N., and Marchand, M. (2002) Peptide-based cancer vaccines. *Semin. Oncol.* **29,** 494–502.

59 Marchand, M., van Baren, N., Weynants, P., et al. (1999) Tumor regressions observed in patients with metastatic melanoma treated with an antigenic peptide encoded by gene MAGE-3 and presented by HLA⁻ A1. *Int J. Cancer* **80,** 219–230.

60 Rosenberg, S. A., Yang, J. C., Schwartzentruber, D. J., et al. (1998) Immunologic and therapeutic evaluation of a synthetic peptide vaccine for the treatment of patients with metastatic melanoma. *Nat. Med.* **4,** 321–327.

61 Sabel, M. S., and Sondak, V. K. (2002) Tumor vaccines: a role in preventing recurrence in melanoma? *Am. J. Clin. Dermatol.* **3,** 609–616.

62 McClay, E. F. (2002) Adjuvant therapy for patients with high-risk malignant melanoma. *Semin. Oncol.* **29,** 389–399.

63 Banchereau, J., Schuler-Thurner, B., Palucka, A. K., and Schuler, G. (2001) Dendritic cells as vectors for therapy. *Cell* **106,** 271–274.

64 Brossart, P., Wirths, S., Brugger, W., and Kanz, L. (2001) Dendritic cells in cancer vaccines. *Exp. Hematol.* **29,** 1247–1255.

65 Fong, L. and Engleman, E. G. (2000) Dendritic cells in cancer immunotherapy. *Annu. Rev. Immunol.* **18,** 245–273.

66 Jefford, M., Maraskovsky, E., Cebon, J., and Davis, I. D. (2001) The use of dendritic cells in cancer therapy. *Lancet Oncol.* **2,** 343–353.

67 Nestle, F. O., Banchereau, J., and Hart, D. (2001) Dendritic cells: on the move from bench to bedside. *Nat. Med.* **7,** 761–765.

68 Ashley, D. M., Faiola, B., Nair, S., Hale, L. P., Bigner, D. D., and Gilboa, E. (1997) Bone marrow-generated dendritic cells pulsed with tumor extracts or tumor RNA induce antitumor immunity against central nervous system tumors. *J. Exp. Med.* **186,** 1177–1182.

69 Celluzzi, C. M. and Falo, L. D., Jr. (1998) Physical interaction between dendritic cells and tumor cells results in an immunogen that induces protective and therapeutic tumor rejection. *J. Immunol.* **160,** 3081–3085.

70 Gilboa, E., Nair, S. K., and Lyerly, H. K. (1998) Immunotherapy of cancer with dendritic-cell-based vaccines. *Cancer Immunol. Immunother.* **46,** 82–87.

71 Porgador, A., Snyder, D., and Gilboa, E. (1996) Induction of antitumor immunity using bone marrow-generated dendritic cells. *J. Immunol.* **156,** 2918–2926.

72 Dhodapkar, M. V., Steinman, R. M., Sapp, M., et al. (1999) Rapid generation of broad T-cell immunity in humans after a single injection of mature dendritic cells. *J. Clin. Invest.* **104,** 173–180.

73 Dhodapkar, M. V., Krasovsky, J., Steinman, R. M., and Bhardwaj, N. (2000) Mature dendritic cells boost functionally superior CD8(+) T-cell in humans without foreign helper epitopes. *J. Clin. Invest.* **105,** R9–R14.

74 Nestle, F. O., Alijagic, S., Gilliet, M., et al. (1998) Vaccination of melanoma patients with peptide- or tumor lysate-pulsed dendritic cells. *Nat. Med.* **4,** 328–332.

75 Thurner, B., Haendle, I., Roder, C., et al. (1999) Vaccination with mage-3A1 peptide-pulsed mature, monocyte-derived dendritic cells expands specific cytotoxic T cells and induces regression of some metastases in advanced stage iv melanoma. *J. Exp. Med.* **190,** 1669–1678.

76 Banchereau, J., Palucka, A. K., Dhodapkar, M., et al. (2001) Immune and clinical responses in patients with metastatic melanoma to CD34(+) progenitor-derived dendritic cell vaccine. *Cancer Res.* **61,** 6451–6458.

77 Schuler-Thurner, B., Schultz, E. S., Berger, T. G., et al. (2002) Rapid induction of tumor-specific type 1 T helper cells in metastatic melanoma patients by vaccination with mature, cryopreserved, peptide-loaded monocyte-derived dendritic cells. *J. Exp. Med.* **195,** 1279–1288.

78 Kugler, A., Stuhler, G., Walden, P., et al. (2000) Regression of human metastatic renal cell carcinoma after vaccination with tumor cell–dendritic cell hybrids. *Nat. Med.* **6,** 332–336.

79 Timmerman, J. M., Czerwinski, D. K., Davis, T. A., et al. (2002) Idiotype-pulsed dendritic cell vaccination for B-cell lymphoma: clinical and immune responses in 35 patients. *Blood* **99,** 1517–1526.

80 Hsu, F. J., Benike, C., Fagnoni, F., et al. (1996) Vaccination of patients with B-cell lymphoma using autologous antigen-pulsed dendritic cells. *Nat. Med.* **2,** 52–58.

81 Heiser, A., Coleman, D., Dannull, J., et al. (2002) Autologous dendritic cells transfected with prostate-specific antigen RNA stimulate CTL responses against metastatic prostate tumors. *J. Clin. Invest.* **109,** 409–417.

82 Fong, L., Brockstedt, D., Benike, C., Wu, L., and Engleman, E. G. (2001) Dendritic cells injected via different routes induce immunity in cancer patients. *J. Immunol.* **166,** 4254–4259.

83 Fong, L., Brockstedt, D., Benike, C., et al. (2001) Dendritic cell-based xenoantigen vaccination for prostate cancer immunotherapy. *J. Immunol.* **167,** 7150–7156.

84 Small, E. J., Fratesi, P., Reese, D. M., et al. (2000) Immunotherapy of hormone-refractory prostate cancer with antigen-loaded dendritic cells. *J. Clin. Oncol.* **18,** 3894–3903.

85 Burch, P. A., Breen, J. K., Buckner, J. C., et al. (2000) Priming tissue-specific cellular immunity in a phase I trial of autologous dendritic cells for prostate cancer. *Clin. Cancer Res.* **6,** 2175–2182.

86 Tjoa, B. A., Simmons, S. J., Bowes, V. A., et al. (1998) Evaluation of phase I/II clinical trials in prostate cancer with dendritic cells and PSMA peptides. *Prostate* **36,** 39–44.

87 Brossart, P., Wirths, S., Stuhler, G., Reichardt, V. L., Kanz, L., and Brugger, W. (2000) Induction of cytotoxic T-lymphocyte responses in vivo after vaccinations with peptide-pulsed dendritic cells. *Blood* **96,** 3102–3108.

88 Fong, L., Hou, Y., Rivas, A., et al. (2001) Altered peptide ligand vaccination with Flt3 ligand expanded dendritic cells for tumor immunotherapy. *Proc. Natl. Acad. Sci. USA* **98,** 8809–8814.

89 Valone, F. H., Small, E., MacKenzie, M., et al. (2001) Dendritic cell-based treatment of cancer: closing in on a cellular therapy. *Cancer J.* **7(Suppl. 2),** S53–S61.

90 Thurner, B., Roder, C., Dieckmann, D., et al. (1999) Generation of large numbers of fully mature and stable dendritic cells from leukapheresis products for clinical application. *J. Immunol. Meth.* **223,** 1–15.

91 Caux, C., Massacrier, C., Dezutter-Dambuyant, C., et al. (1995) Human dendritic Langerhans cells generated in vitro from CD34+ progenitors can prime naive CD4+ T cells and process soluble antigen. *J. Immunol.* **155,** 5427–5435.

92 Caux, C., Dezutter-Dambuyant, C., Schmitt, D., and Bancherea u, J. (1992) GM-CSF and TNF-alpha cooperate in the generation of dendritic Langerhans cells. *Nature* **360,** 258–261.

93 Mortarini, R., Anichini, A., Di Nicola, M., et al. (1997) Autologous dendritic cells derived from CD34+ progenitors and from monocytes are not functionally equivalent antigen-presenting cells in the induction of melan-A/Mart-1(27–35)-specific CTLs from peripheral blood lymphocytes of melanoma patients with low frequency of CTL precursors. *Cancer Res.* **57,** 5534–5541.

94 Jonuleit, H., Giesecke-Tuettenberg, A., Tuting, T., et al. (2001) A comparison of two types of dendritic cell as adjuvants for the induction of melanoma-specific T-cell responses in humans following intranodal injection. *Int. J. Cancer* **93,** 243–251.

95 Dhodapkar, M. V., Steinman, R. M., Krasovsky, J., Munz, C., and Bhardwaj, N. (2001) Antigen-specific inhibition of effector T cell function in humans after injection of immature dendritic cells. *J. Exp. Med.* **193,** 233–238.

96 Bender, A., Sapp, M., Schuler, G., Steinman, R. M., and Bhardwaj, N. (1996) Improved methods for the generation of dendritic cells from nonproliferating progenitors in human blood. *J. Immunol. Meth.* **196,** 121–135.

97 Romani, N., Reider, D., Heuer, M., et al. (1996) Generation of mature dendritic cells from human blood. An improved method with special regard to clinical applicability. *J. Immunol. Meth.* **196,** 137–151.

98 Jonuleit, H., Kuhn, U., Muller, G., et al. (1997) Pro-inflammatory cytokines and prostaglandins induce maturation of potent immunostimulatory dendritic cells under fetal calf serum-free conditions. *Eur. J. Immunol.* **27,** 3135–3142.

99 Lee, A.W., Truong, T., Bickham, K., et al. (2002) A clinical grade cocktail of cytokines and PGE(2) results in uniform maturation of human monocyte-derived dendritic cells: implications for immunotherapy. *Vaccine* **20(Suppl. 4),** A8–A22.

100 Scandella, E., Men, Y., Gillessen, S., Forster, R., and Groettrup, M. (2002) Prostaglandin E2 is a key factor for CCR7 surface expression and migration of monocyte-derived dendritic cells. *Blood* **100,** 1354–1361.

101 Alexander-Miller, M. A., Leggatt, G. R., and Berzofsky, J. A. (1996) Selective expansion of high- or low-avidity cytotoxic T lymphocytes and efficacy for adoptive immunotherapy. *Proc. Natl. Acad. Sci. USA* **93,** 4102–4107.

102 Geiger, J., Hutchinson, R., Hohenkirk, L., McKenna, E., Chang, A., and Mule, J. (2000) Treatment of solid tumours in children with tumour-lysate-pulsed dendritic cells. *Lancet* **356,** 1163–1165.

103 Chang, A. E., Redman, B. G., Whitfield, J. R., et al. (2002) A phase I trial of tumor lysate-pulsed dendritic cells in the treatment of advanced cancer. *Clin. Cancer Res.* **8,** 1021–1032.

104 Kim, D. T., Mitchell, D. J., Brockstedt, D. G., et al. (1997) Introduction of soluble proteins into the MHC class I pathway by conjugation to an HIV tat peptide. *J. Immunol.* **159,** 1666–1668.

105 Tuting, T., Wilson, C. C., Martin, D. M., et al. (1998) Autologous human monocyte-derived dendritic cells genetically modified to express melanoma antigens elicit primary cytotoxic T cell responses in vitro: enhancement by cotransfection of genes encoding the Th1⁻ biasing cytokines IL-12 and IFN-alpha. *J. Immunol.* **160,** 1139–1147.

106 Yang, S., Vervaert, C. E., Burch, J., Jr., Grichnik, J., Seigler, H. F., and Darrow, T. L. (1999) Murine dendritic cells transfected with human gp100 elicit both antigen-specific CD8(+) and CD4(+) T-cell responses and are more effective than DNA vaccines at generating anti-tumor immunity. *Int. J. Cancer* **83,** 532–540.

107 Boczkowski, D., Nair, S. K., Snyder, D., and Gilboa, E. (1996) Dendritic cells pulsed with RNA are potent antigen-presenting cells in vitro and in vivo. *J. Exp. Med.* **184,** 465–472.

108 Nair, S. K., Heiser, A., Boczkowski, D., et al. (2000) Induction of cytotoxic T cell responses and tumor immunity against unrelated tumors using telomerase reverse transcriptase RNA transfected dendritic cells. *Nat. Med.* **6,** 1011–1017.

109 Sullenger, B. A. and Gilboa, E. (2002) Emerging clinical applications of RNA. *Nature* **418,** 252–258.

110 Jenne, L., Schuler, G., and Steinkasserer, A. (2001) Viral vectors for dendritic cell-based immunotherapy. *Trends Immunol.* **22,** 102–107.

111 Dietz, A. B., and Vuk-Pavlovic, S. (1998) High efficiency adenovirus-mediated gene transfer to human dendritic cells. *Blood* **91,** 392–398.

112 Chaux, P., Luiten, R., Demotte, N., et al. (1999) Identification of five MAGE-A1 epitopes recognized by cytolytic T lymphocytes obtained by in vitro stimulation with dendritic cells transduced with MAGE-A1. *J. Immunol.* **163,** 2928–2936.

113 Larsson, M., Fonteneau, J.F., Somersan, S., et al. (2001) Efficiency of cross presentation of vaccinia virus-derived antigens by human dendritic cells. *Eur. J. Immunol.* **31,** 3432–3442.

114 Engelmayer, J., Larsson, M., Lee, A., et al. (2001) Mature dendritic cells infected with canarypox virus elicit strong anti-human immunodeficiency virus CD8⁺ and CD4⁺ T-cell responses from chronically infected individuals. *J. Virol.* **75,** 2142–2153.

115 Kotera, Y., Shimizu, K., and Mule, J. J. (2001) Comparative analysis of necrotic and apoptotic tumor cells as a source of antigen(s) in dendritic cell-based immunization. *Cancer Res.* **61,** 8105–8109.

116 Berard, F., Blanco, P., Davoust, J., et al. (2000) Cross-priming of naive CD8 T cells against melanoma antigens using dendritic cells loaded with killed allogeneic melanoma cells. *J. Exp. Med.* **192,** 1535–1544.

117 Gong, J., Avigan, D., Chen, D., et al. (2000) Activation of antitumor cytotoxic T lymphocytes by fusions of human dendritic cells and breast carcinoma cells. *Proc. Natl. Acad. Sci. USA* **97,** 2715–2718.

118 Gong, J., Koido, S., Chen, D., et al. (2002) Immunization against murine multiple myeloma with fusions of dendritic and plasmacytoma cells is potentiated by interleukin 12. *Blood* **99,** 2512–2517.

119 Zitvogel, L., Regnault, A., Lozier, A., et al. (1998) Eradication of established murine tumors using a novel cell-free vaccine: dendritic cell-derived exosomes. *Nat. Med.* **4,** 594–600.

120 Wolfers, J., Lozier, A., Raposo, G., et al. (2001) Tumor-derived exosomes are a source of shared tumor rejection antigens for CTL cross-priming. *Nat. Med.* **7,** 297–303.

121 Schartz, N. E., Chaput, N., Andre, F., and Zitvogel, L. (2002) From the antigen-presenting cell to the antigen-presenting vesicle: the exosomes. *Curr. Opin. Molec. Ther.* **4,** 372–381.

122 Kerbel, R., and Folkman, J. (2002) Clinical translation of angiogenesis inhibitors. *Nat. Rev. Cancer* **2,** 727–739.

123 Egen, J. G., Kuhns, M. S., and Allison, J. P. (2002) CTLA-4: new insights into its biological function and use in tumor immunotherapy. *Nat. Immunol.* **3,** 611–618.

124 Hodi, F. S., Mihm, M. C., Soiffer, R. J., et al. (2003) Biologic activity of cytotoxic T lymphocyte-associated antigen 4 antibody blockade in previously vaccinated metastatic melanoma and ovarian carcinoma patients. *Proc. Natl. Acad. Sci. USA* **100,** 4712–4717.

125 Phan, G. Q., Yang, J. C., Sherry, R. M., et al. (2003) Cancer regression and autoimmunity induced by cytotoxic T lymphocyte-associated antigen 4 blockade in patients with metastatic melanoma. *Proc. Natl. Acad. Sci. USA* **100,** 8372–8377.

126. Homey, B., Muller, A., and Zlotnik, A. (2002) Chemokines: agents for the immunotherapy of cancer? *Nat. Rev. Immunol.* **2,** 175–184.

127. Schwarz, K., Storni, T., Manolova, V., et al. (2003) Role of toll-like receptors in costimulating cytotoxic T cell responses. *Eur. J. Immunol.* **33,** 1465–1470.

2

A Mathematical Approach for Optimizing Dendritic Cell-Based Immunotherapy

Gennady Bocharov, Neville J. Ford, and Burkhard Ludewig

Summary

Adoptive dendritic cell (DC)-based immunotherapy represents a promising approach to overcome peripheral tolerance against autologous tumor antigens and to maintain protective antitumor immunity. The translation of successful preclinical studies, however, appears to be hampered by new complexities associated with the clinical situation. Mathematical modeling provides the means for qualitative and quantitative analysis, predictions for complex dynamic systems in immunology, and for the design and improvement of therapeutic approaches. We present here a workable computational methodology for developing meaningful data- and hypothesis-driven mathematical models for DC-based immunotherapy with a particular focus on numerical parameter estimation and sensitivity analysis.

Key Words: Mathematical model; immune response; computer simulation; data fitting; parameter estimation; sensitivity analysis; predator–prey dynamics; dendritic cell; cytotoxic T-lymphocyte; numerical software.

1. Introduction

Immunotherapeutic approaches based on adoptive transfer of dendritic cells (DC) expressing relevant antigens may be used for active mobilization of cellular immune responses (cytotoxic T-lymphocytes [CTL], T-helper cells, and natural killer [NK] cells) against tumors *(1,2)*. The efficacy of this active immunization depends on the complex biology of the DC life cycle and their interaction with T-cells. The kinetics of this interaction and its sensitivity to relevant parameters are still incompletely understood. These parameters include antigen loading, DC maturation stage, frequency and route of DC injection, frequency and activation status of T-cells, and the homing rate of DC to and their persistence within lymphoid tissues. Mathematics provides the means for an integrative description of simplified models of various immunological phenomena, including those arising in the context of adoptive immunotherapy. Its primary role is to assist in parameter estimation (e.g., the cellular interaction kinetic rates, life spans, delays, activation thresholds) and analysis (the "numbers game"), and to make testable predictions in advance of experiments and clinical applications.

Table 1
Decision Making Before and During the Modeling Process *[a]*

Modeling objectives
Determine the focus of the investigation.   • General understanding of the rules underlying the observed behavior (e.g., causality inferences and/or critical parameters of system dynamics)   • Reliable calculations of system dynamics   • Specific predictions about new observations—experimental design   • Characterize and analyze the data

Modeling approaches
Decide on the approach to develop the model.   • Building block (models are formulated by applying the governing physical laws/constraints and constitute relations to the subsystems)   • Black box (models are formulated on the basis of the input-output characteristics of the system, no consideration of its internal functioning)

Model types
Decide on the types of equations that provide the appropriate compromise between simplicity and tractability on the one hand, and accuracy on the other.   • Continuous in time   • Discrete in time   • Deterministic   • Stochastic

Types of building block models
• Microscopic (spatially distributed)   • Macroscopic (lumped)

[a] Summarized from **refs. *3–5***

Mathematical modeling involves a number of distinct steps. In order to establish a mathematical model, many simplifying assumptions have to be specified and decisions must be made, either explicitly or implicitly *(3–5)* (**Table 1**). The translation process, starting from a particular (immunological) phenomenon and ending in a mathematical formalism (i.e., a set of equations), is the hardest part of applying mathematics, because it involves the conversion of imprecise assumptions into formulas. We describe here one possible approach to modeling the interaction of DC with CTL. In the presented model, the DC–CTL interaction is described by adapting different theoretical frameworks, such as predator–prey models from population biology *(6)* and Monod-type kinetics with saturation which are applied in biochemistry *(7)*. We are considering these deterministic models at the macroscopic level of the whole immune system, and neglect details such as spatial structures of lymphoid organs or cytokine networks. The overall aim of this approach is to produce a scientifically meaningful mathematical model that is both descriptive and predictive.

In the "Methods" section we explain the use of the computational techniques for *in silico* simulations, using the models, parameter estimation, information-theoretical assessment of the mathematical model given the data, and sensitivity analysis. These represent the major aspects of the general problem of valid inference *(8)*. Although our main interest has been the mathematical modeling of the population dynamics of DC–CTL interaction in mice, the computational methodology has widespread applicability. To describe the kinetics of the population densities of immune cells, we utilize either ordinary or delay differential (in the case of memory effects) equations, which describe the rate of change of cell population densities as a function of time *t*.

2. Materials

2.1. Experimental Data

Reliable input from experimental or clinical research in terms of precise and comprehensive datasets is a core part of an interdisciplinary modeling approach. The data set presented in **Table 2** was generated using established protocols *(9,10)*. Briefly, major histocompatibility complex (MHC) class I tetramers complexed with the immunodominant CTL epitope (gp33) derived from the glycoprotein of the lymphocytic choriomeningitis virus (LCMV-GP) *(11)* were used to follow activation of gp33-specific CTL after immunization with DC. DC derived from transgenic mice ubiquitously expressing the first 60 aa of LCMV-GP including gp33 (H8-DC) *(12)* were injected intravenously (i.v.) into naïve C57BL/6 recipient mice. At the indicated time points following immunization, the densities of the following cell populations as a function of time *t* were determined:

- "Activated" $CD8^+62L^-$ T-cells staining with the gp33-tetramer (tet^+) in spleen that have downregulated the CD62L molecule, $E_a(t)$
- "Quiescent" $CD8^+CD62L^+tet^+$ cells in spleen $E_m(t)$.

Furthermore, to assess the availability of adoptively transferred DC for productive interaction with T-cells within secondary lymphoid organs, ^{51}Cr-labeled H8-DC were injected i.v. into naïve recipient mice, and the accumulated radioactivity was determined in spleen at different time points using established protocols *(13)*. The data set for homing of adoptively transferred DC from blood to spleen has been published elsewhere *(14)*.

2.2. Simulation Software

The practical way to study mathematical models is based on using numerical techniques to approximate the solutions. To understand the DC–CTL interaction dynamics, model equations were evaluated under different parameter settings—a "direct" approach. Differential equations of the model were programmed using the universal computer language FORTRAN. Efficient and reliable software packages such as MATLAB (Website: http://www.mathworks.com) or Berkeley Madonna (Website: http://www.berkeleymadonna.com) represent more convenient alternatives to the "classical" programming approach, because they automate a number of steps (e.g., programming of equations, selection of the numerical method) of the process of solving initial value problems for ordinary or delay differential equations.

Table 2
Example of the Original Data Set (Mean ± Standard Deviation) for the Kinetics of tet⁺ CD8 T-Cells Expansion Induced after Intravenous (i.v.) Injection of 2×10^5 H8-DC[a]

Days after i.v. injection	Splenocytes (cells)	CD8⁺ T-cells	tet⁺ CD8 T-cells	% CD62L⁻	E_a (activated gp33-specific CTL)	$E_a + E_m$ (total gp33-specific CTL)
					Derived data used for fitting of the model variable	
d4	$(7.0 \pm 0.66) \times 10^7$	$(1.0 \pm 0.02) \times 10^7$	$(1.4 \pm 0.19) \times 10^5$	$43 \pm 6.7\%$	1.4×10^5	—
d7	$(4.0 \pm 1.5) \times 10^7$	$(7.0 \pm 2.7) \times 10^6$	$(3.6 \pm 1.8) \times 10^5$	$82 \pm 5.6\%$	3.6×10^5	—
d12	$(6.1 \pm 0.67) \times 10^7$	$(6.1 \pm 0.71) \times 10^6$	$(1.7 \pm 0.55) \times 10^5$	$71 \pm 8.2\%$	—	1.7×10^5
d18	$(5.5 \pm 0.73) \times 10^7$	$(5.1 \pm 1.2) \times 10^6$	$(6.6 \pm 1.3) \times 10^4$	$49 \pm 5.2\%$	—	6.6×10^4

[a] The data set used for fitting the model predictions for activated cytotoxic T-lymphocytes (CTL) (E_a) and the total CTL ($E_a + E_m$) variables of the mathematical model.
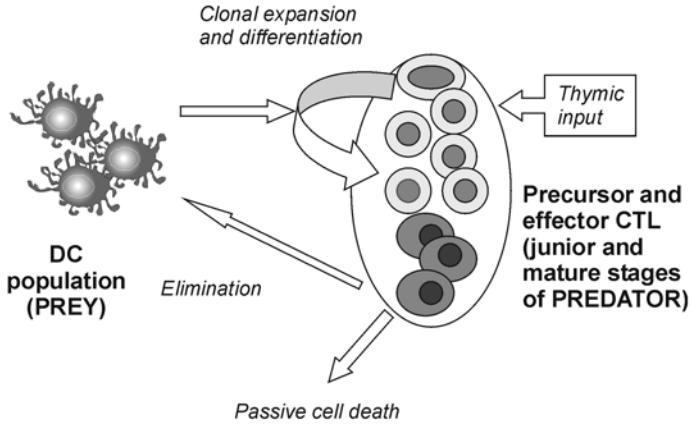
Fig. 1. Conceptual model for the predator–prey type induction/regulation of CD8^{+} T-cell responses by dendritic cells (DC). Antigen-expressing DC migrate from blood to spleen, where they induce clonal expansion of naïve antigen-specific cytotoxic T-lymphocytes (CTL), whereas activated CTL eliminate DC. Arrows indicate the modeled processes.

3. Methods

3.1. Generation of a Conceptual Scheme (Model) of the System

The first task in a data- and hypothesis-driven modeling approach is to choose/specify the functional form of the model to represent the data of the system under analysis *(3)*. Although many variables and parameters might seem necessary to describe the effect of DC on CTL, one must *a priori* restrict the model to the most important interactions. We quote from Burnham and Anderson *(8)*: "Development of the a priori set of candidate models often should include a global model: a model that has many parameters, includes all potentially relevant effects, and reflects causal mechanisms thought likely, based on the science of situation." This type of a global model for a systemic dynamics of DC–CTL interaction has recently been developed by Ludewig et al. *(14)*. Our conceptual model is based on the spatio-temporal view of the organization and predator–prey type regulation of CD8^{+} T-cell responses by DC *in vivo*. Antigen-expressing DC migrate irreversibly from blood to the spleen, where they induce clonal expansion of naïve antigen-specific CTL. Activated CTL eliminate the DC and recirculate among spleen, blood, and peripheral tissues. The key element of the model is the predator–prey-type interaction of DC with antigen-specific CTL (**Fig. 1**). We present here our modeling methodology for the splenic compartment of the immune system.

3.2. Specifying Assumptions and Selecting Quantities

To formulate equations for DC–CTL interaction following i.v. injection, we make the following simplifying biological assumptions. Such a list is also helpful for the evaluation of the modeling results from the viewpoint of the underlying biology.

1. DC do not re-circulate from lymphoid organs into the blood after intravenous injection *(15)*.
2. Adoptively transferred DC are in mature state *(10)*.
3. DC-mediated induction of antigen-specific CTL is due to their interaction in the spleen *(14)*.
4. DC do not divide in secondary lymphoid organs *(16)*.
5. DC decay due to a short life span *(17)* and their killing by activated CTL *(9,18)*.
6. The population of antigen-specific CTL in spleen is split into quiescent (naïve or central memory-like) and activated CTL (effector or effector memory-like) *(19)*.
7. CTL re-circulate among spleen, blood, and peripheral organs (e.g., liver).

The required quantities for the specific model depend on the conceptual scheme and the assumptions. The quantities include here time as an independent variable, time-dependent variables (population densities of cells), and the parameters that characterize the kinetics of the specified processes. The biological meaning and units of the parameters considered in the presented model of DC–CTL interaction are listed in **Table 3**.

3.3. Derivation of Model Equations

The cell population dynamics can be represented by the following prototype mass balance equation (*see* **Note 1**):

Change rate of number of cells of *j*-th type at time *t* =

± *transfer* between compartments + cell *division* – cell *death* ± *transition* between states   (1)

We model the localized population dynamics of DC–CTL interaction, i.e., in the spleen, and ignore the DC re-circulation between spleen and blood.

The rate of change in the density of DC in the spleen is modeled as:

$$\frac{d}{dt}D(t) = \mu_{BS} \cdot \frac{Q_{Blood}}{Q_{Spleen}} \cdot D_{Blood}(t) - \alpha_D \cdot D(t) - b_{DE} \cdot E_a(t) \cdot D(t) \tag{2}$$

The first term represents the trafficking of DC from blood to spleen (Q_{Blood} and Q_{Spleen} being the volumes of the blood and spleen compartments, respectively), and the other two take into account the natural death of the cells and their elimination by activated CTL. We substitute the formulae identified in *(14)* for the kinetics of DC in the blood $D_{Blood}(t)$.

The dynamics of activated CTL is modeled by the following equation:

$$\frac{d}{dt}E_a(t) = \alpha_{E_a} \cdot \left[E^{naive} - E_a(t) \right] + b_p \cdot \frac{D(t-\tau_d) \cdot E_a(t-\tau_d)}{\theta_D + D(t-\tau_d)} - r_{am} \cdot E_a(t) + b_a \cdot D(t) \cdot E_m(t) \tag{3}$$

The first term considers the homeostasis of naïve CTL in the spleen, the second term represents the DC-induced division of CTL proceeding at the rate that saturates at a high number of DC. The time lag between the cognate interaction of CTL with DC represents the duration of "preprogramming" of CTL for division and differentiation *(20)*. The last two terms take into account the silencing of activated CTL into quiescent "memory" cells (third term) and the activation of the memory cells by DC.

Table 3
Parameters of the DC–CTL Model in Spleen

Notation	Biological Definition	Estimate (units) [99% Confidence Interval]
μ_{BS}	Transfer rate of H8-DCs from blood to spleen	2.832 d^{-1}
$t_{1/2} = \ln2/\alpha_D$	Half-life of gp-33-expressing DC	3 d (ad hoc fixed value)
b_{DE}	Per capita elimination rate of H8-DCs by activated CTL	0.487×10^{-5} $mL/cell/d$ [0.13×10^{-6}, 0.6×10^{-5}]
E^{naive}	The number of naïve gp-33-specific CTL contributing to primary clonal expansion	370 $cells$ (ad hoc fixed value)
τ_d	Duration of antigen preprogrammed CTL divisions	1 d (ad hoc fixed value)
$t_{1/2}^{E_a} = \ln 2 / \alpha_{E_a}$	Half-life of activated CTL	5.78 d [0.12, $+\infty$)
$t_{1/2}^{E_m} = \ln 2 / \alpha_{E_m}$	Half-life of resting "memory" CTL	69 d (ad hoc fixed value)
b_p	Maximal expansion factor of activated CTL per d	12 d^{-1} [10, 85]
θ_D	DC density in the spleen for half-maximal proliferation rate of CTL	2.12×10^3 $cell/mL$ [7.5×10^2, 1.2×10^4]
r_{am}	Fraction of activated CTL reverting into resting "memory" cells per day	0.01 d^{-1} [0.4×10^{-3}, 1.2]
b_a	Activation rate of quiescent CTL by DCs	10^{-3} $mL/cell/d$

The equation for the dynamics of quiescent "memory" CTL is:

$$\frac{d}{dt}E_m(t) = r_{am} \cdot E_a(t) - \left[\alpha_{E_m} + b_a \cdot D(t)\right] \cdot E_m(t) \tag{4}$$

which considers the transition of the activated CTL into the quiescent "memory" state, the death of *memory* CTL at some slow rate, and the activation of memory CTL depending on the availability of DC.

3.4. Computer Simulation of the System Dynamics

A typical computer simulation includes the following steps:

1. Program the set of differential equations of the model, either following protocols specified in specialized simulation packages (*see* **Methods**) or using universal computer languages such as FORTRAN or C++.
2. Set initial values for the time-dependent population densities of DC and CTL.
3. Set the values for the model parameters (*see* **Note 2** for an example of how to derive the initial guess for CTL proliferation parameters b_p, θ_D).
4. Set run-time parameters—the start and finish times as well as the report times for the solution and the error-per-step tolerance in the solver.

There are several difficulties in obtaining efficiently a numerical approximation to the solution of the model equations (*see* **Note 3**). It follows that the computer simulations require specification of values for the model parameters. The parameter values can be obtained from experimental data sets either directly, or using special numerical procedures for the "inverse" modeling approach.

3.5. Estimation of Parameters and Confidence Intervals Via Data-Fitting

Estimation of adjustable parameters of a mathematical model with specified architecture is another central task of data-driven modeling *(3)*. The purpose of data-fitting is to calculate values of the model parameters that optimize some objective function which is a measure of the fit (agreement) between the simulated values (predictions of the model) and the data (*see* **Note 4**). **Figure 2** shows the experimental data and the corresponding best-fit solution of the mathematical model.

3.5.1. Least-Squares Fitting Functions

Let the set of observation times $\{t_j\}_{j=1}^N$ and observations $\{y_j^i\}_{j=1}^N$ for M ($1 \leq i \leq M$) of the model variables be specified. An example of the experimental data set representing the kinetics of tet$^+$ CD8 T-cells expansion after i.v. injection of 2×10^5 H8-DC used in parameter estimation is given in **Table 2**. Simulation of the system with the model suggests prediction (a regression function) for the observed variable $y^i(t_j, \mathbf{p})$, which depends on the adjustable parameters $\mathbf{p}$, i.e., the model parameter vector with L components. The common ordinary least-squares (LSQ) error measure of the match between the model and data is given by the objective function determined by the square of the absolute deviation between the model and data:

$$\Phi(\mathbf{p}) = \sum_{j=1}^{N}\sum_{i=1}^{M}\left[y_j^i - y^i(t_j, \mathbf{p})\right]^2 \tag{5}$$
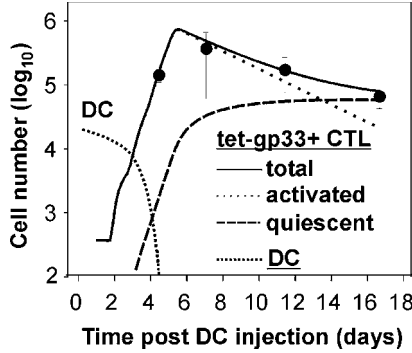
Fig. 2. Data vs model description for the population dynamics of dendritic cells (DC) and cytotoxic T-lymphocytes (CTL) in spleen induced by intravenous injection of 2×10^5 gp33-presenting H8-DC. The symbols represent averages of 3 mice ± standard deviation. The smooth lines predict the population dynamics of the total tet+, activated tet+, and quiescent memory tet+ CTLs and H8-DCs for the best-fit estimates of the model parameters. DC elimination follows a biphasic kinetics; the first, slower phase reflects their life span and the accelerated decay phase results from the killing effect by activated CTLs.

The weighted LSQ objective function

$$\Phi(\mathbf{p}) = \sum_{j=1}^{N} \sum_{i=1}^{M} w_j^i \left[y_j^i - y^i (t_j, \mathbf{p}) \right]^2 \tag{6}$$

can be used when different weights have to be given to particular observations. A natural choice for the weights could be the inverse variances $w_j^i = \left(\sigma_j^i \right)^{-2}$ of the observations. The LSQ approach proves to be efficient when the variation in scale of the data set over the observation time interval is within one order of magnitude. This is exactly the case with the data for the initial biodistribution kinetics of DC after intravenous injection (*see* **ref. *14*** and **Note 5**).

3.5.2. Minimization of the Least-Squares Function

The numerical technique for finding the best-fit parameter estimates for a given data set, mathematical model, and objective function requires (1) providing an initial guess for the model parameters; (2) solving the model equations to compute $\Phi(\mathbf{p})$; and (3) adjusting the parameter values by some minimization routine available, for example, in the MATLAB library (– fmins). Because the parameters of the model are constrained to be nonnegative, we used a $\log_{10}$-transformation for the parameters, so that the resulting sequence of reduced order data-fitting problems were treated as an unconstrained minimization (*see* **Note 6**).

There are software packages such as Berkeley Madonna that can automatically find the values of a number of parameters in a model that minimize the deviation between the model's output and a data set. In principle, these facilities greatly enhance the capability of treating the parameter estimation problem. However, data-fitting with non-linear differential equations-based models is a type of expertise that can be learned only in actual practice (*see* **refs. *21–23*** for extensive discussion of various aspects of statistical techniques and computational methods).

3.5.3. Computation of Confidence Intervals

To characterize the precision or reliability of best-fit parameter estimates (**p***) a number of approaches exist, of which we consider (1) the variance-covariance matrix for estimated parameters *(23)*; and (2) the profile-likelihood-based method *(24)* (*see* **Note 7**). Alternatively, a bootstrap approach may be used *(21,25)*. The confidence interval analysis is a computation-intensive procedure. The simplest approach is to approximate the 95% confidence intervals using estimates of the standard errors $p_*^l \pm 1.96\sigma_l$, where $\sigma_l = \sqrt{v_{ll}}$, $1 \le l \le L$ stand for the diagonal elements of the variance-covariance matrix. In turn, the matrix elements are determined via the residual sum of LSQ function, the number of degrees of freedom, and the Hessian matrix *(22,23)*, according to the formula

$$
\begin{bmatrix}
v_{11} & c_{12} & c_{13} & \cdots & c_{1L} \\
c_{21} & v_{22} & c_{23} & \cdots & c_{2L} \\
c_{31} & c_{32} & v_{33} & \cdots & c_{3L} \\
\cdots & \cdots & \cdots & \cdots & \cdots \\
c_{L1} & c_{L2} & c_{L3} & \cdots & v_{LL}
\end{bmatrix}
= 2\frac{\Phi(\mathbf{p}_*)}{N_{obs}-L}
\begin{bmatrix}
\frac{\partial^2}{\partial p_1^2}\Phi(\mathbf{p}_*) & \frac{\partial^2}{\partial p_1 \partial p_2}\Phi(\mathbf{p}_*) & \frac{\partial^2}{\partial p_1 \partial p_3}\Phi(\mathbf{p}_*) & \cdots & \frac{\partial^2}{\partial p_1 \partial p_L}\Phi(\mathbf{p}_*) \\
\frac{\partial^2}{\partial p_2 \partial p_1}\Phi(\mathbf{p}_*) & \frac{\partial^2}{\partial p_2^2}\Phi(\mathbf{p}_*) & \frac{\partial^2}{\partial p_2 \partial p_3}\Phi(\mathbf{p}_*) & \cdots & \frac{\partial^2}{\partial p_2 \partial p_L}\Phi(\mathbf{p}_*) \\
\frac{\partial^2}{\partial p_3 \partial p_1}\Phi(\mathbf{p}_*) & \frac{\partial^2}{\partial p_3 \partial p_2}\Phi(\mathbf{p}_*) & \frac{\partial^2}{\partial p_3^2}\Phi(\mathbf{p}_*) & \cdots & \frac{\partial^2}{\partial p_3 \partial p_L}\Phi(\mathbf{p}_*) \\
\cdots & \cdots & \cdots & \cdots & \cdots \\
\frac{\partial^2}{\partial p_L \partial p_1}\Phi(\mathbf{p}_*) & \frac{\partial^2}{\partial p_L \partial p_2}\Phi(\mathbf{p}_*) & \frac{\partial^2}{\partial p_L \partial p_3}\Phi(\mathbf{p}_*) & \cdots & \frac{\partial^2}{\partial p_L^2}\Phi(\mathbf{p}_*)
\end{bmatrix}^{-1}
\tag{7}
$$

where N_{obs} and L stand for the total number of scalar observations and the number of model parameters, respectively. The Hessian matrix can be approximated using the complete information matrix or via numerical differentiation provided in MATLAB.

The estimates of the parameters for DC–CTL interaction in spleen and their confidence intervals are shown in **Table 3** (*see* **Note 7**).

3.5.4. Evaluation of the Model Parsimony and Accuracy

In general, the biological model architectures are not comprehensively justified on the basis of proven mechanisms, but reflect a parsimonious characterization of the system under study *(26)*. The mathematical model presented here is not the only plausible model for studying the dynamics of DC–CTL interaction in vivo. Other formulations may be preferable given a different context (e.g., data) or a different set of goals. It is important, therefore, not only to rank plausible models with respect to their consistency with the data (as measured by the best-fit objective function), but also to consider their distance to an unknown "true model" underlying the data set.

The information-theoretic framework provides a basis for such assessment of information complexity of the model (the model parsimony) and the selection of the best ones with respect to the information in the data *(8)*. Using the maximized-likelihood function, one can compute the value of the corrected Akaike's information criterion (AIC) (appropriate for data sets smaller than 40 units):

$$\mu_{cAIC} = -2\ln\left[\mathscr{L}(\mathbf{p}_*,\sigma)\right] + 2(L+1)\left[1 + \frac{L+2}{N_{obs} - (L+2)}\right] \tag{8}$$

with $\mathscr{L}(\mathbf{p}_*,\sigma)$ being the maximized likelihood function, or the revised relative indicator

$$\Delta\mu_{cAIC} = N_{obs}\ln\Phi(\mathbf{p}_*) + 2(L+1)\left[1 + \frac{L+2}{N_{obs} - (L+2)}\right] \tag{9}$$

in which extraneous terms are discarded and the relationship between the maximum-likelihood estimation and the LSQ estimation (either ordinary- or Log-LSQ) is used. The best model is considered to be that which yields the lowest value of the indicators. The indicators can be regarded as taking parsimony into account.

3.6. Sensitivity Analysis

The major advantage of a mathematical model is that the model parameters can be easily altered and the effect on system dynamics can be examined via sensitivity analysis (*see* **Note 8**). We present an example in which the initial numbers of injected DC and naïve CTL were changed to predict the effect on the peak expansion of CTL. In this process, the model equations were run using various combinations of the numerical values of the initial numbers of DC and CTL; other parameter values are shown in **Table 3**. The computer experiments summarized in **Fig. 3** suggest that the peak CTL expansion is a conserved feature of the DC–CTL interaction dynamics once the initial numbers of DC and CTL have reached a saturation level. Furthermore, this simulation indicates that increasing the initial number of CTL above a certain threshold does not lead to further expansion because of the accelerated elimination of the antigen-presenting DC.

4. Notes

1. Various functional forms can be suggested for process terms in the above equation, as illustrated for the DC-induced proliferation rate of T-cells in **Table 4**. To model dose-response curves, there is a broad set of phenomenological equations available that allow one to get the desired shape, including one-site saturation, sigmoidal with variable slope, four-parameter logistic equation, and so on. It has to be determined which of these forms is most consistent with the system under consideration, and this can be judged either by using *a priori* biological arguments, or by confronting against experimental data as presented, for example in *(27)*, or using the information-theoretic model selection criteria (*see* **Subheading 3.5.4.**).

2. Experimental data on CTL priming with DC *(10)* indicate that 100–1000 DC have to reach the spleen to achieve protective levels of CTL activation. These numbers directly suggest the range for the initial estimates of the threshold parameter of half-maximal CTL activation, i.e., $100 \leq \theta_D \leq 1000$ (cells). The doubling time of CTL during the
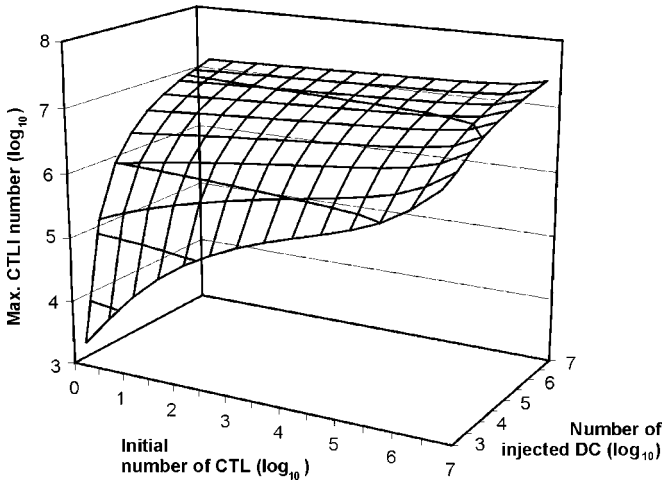
Fig. 3. Sensitivity analysis of CTL expansion to parameters variation. The maximal expansion of gp33-specific CTL as a function of the initial number of intravenously injected H8-DC and the initial number of the specific CTL.

Table 4
Some Functional Forms for DC-Induced CTL Growth
and the Associated Qualitative Implications

Process					
DC-induced per capita T cell division rate					
Form1	Dose/Effect	Form2	Dose/Effect	Form3	Dose/Effect
~DC		$\sim \dfrac{DC}{\theta + DC}$		$\sim \dfrac{DC}{\theta + (DC)^2}$	

expansion phase ranges from 6 to 24 h. This suggests a plausible range for the CTL amplification per day parameter $1 \leq b_p \leq 2^4 = 16$ (d^{-1}). Data-fitting procedures are required to further refine these initial estimates (*see* **Subheading 3.5.**).

3. Voit *(7)* presents a useful practical guide to doing simulations with mathematical models formulated using systems of ordinary differential equations. They offer a basic, easy to install and start software for Power Law Analysis and Simulation (PLAS). Some differential equations model processes with widely separated decay times (called *stiff*) require special stiff solvers (based upon either implicit Runge-Kutta or Gear's methods) to produce simulations. These are available, for example, in the software package Berkeley Madonna. In the case of models formulated with delay (rather than ordinary) differential equations, software development is still an active area of research. Some interesting guidelines and recipes on how to conduct *in silico* experiments on the model system are discussed in *(7)* for biochemical models.

4. We have available observations as input data, which typically arise from a multiple series of observations, in which case the individual data have to be summarized in some way (e.g., as means and standard errors). Since the basis of the data-fitting usually includes assumptions about distributions (e.g., normal or Log-normal) of the errors in observations, it is important to ensure that those assumptions are realistic. A general statistical framework is the Bayesian approach, which under some natural assumptions reduces to Maximum A Posteriori Estimation and, further down, to Maximum Likelihood (ML) Estimation *(3,23)*. The choice depends on the knowledge of the statistical features of the data, expectations in advance about the model parameter values, and the selected set of models. If one uses a single model and assumes a uniform prior on the parameter values, then the ML approach would be the natural choice *(3,23)*. The LSQ parameter estimation is equivalent to the ML estimation under the set of assumptions (often made implicitly) that (1) the observational errors are normally distributed, (2) equivalent positive and negative deviations from expected values differ by equal amounts; and (3) the errors between samples are independent and identically distributed. Other powers of the deviation between the model and the data can be used depending on the error distribution—for example, the first power would correspond to an exponential distribution of the errors *(3)*.

5. Immunological characteristics may vary over several orders of magnitude. In such cases logarithmic scaling should be applied in order to make the data-fitting problem equally sensitive to differences between the model and data in the lower end of the observed values. Statistically, this implies an assumption of geometric normality of observational errors, in which equivalent deviations differ by equal proportions. Minimizing the Log-LSQ function is equivalent to maximizing the likelihood function under the assumption that the observational errors are independent and Log-normally distributed. The parameter estimation problem corresponds to a choice of Log-LSQ (relative deviation) objective function

$$\Phi_{LogLS}(\mathbf{p}) = \sum_{j=1}^{N}\sum_{i=1}^{M}\left\{\ln\left(y_j^i\right) - \ln\left[y^i\left(t_j, \mathbf{p}\right)\right]\right\}^2 \tag{10}$$

The DC-induced population dynamics of tet$^+$ CD8$^+$ T-cells is exactly such a case. To estimate the model parameters characterizing the DC–CTL interaction, we minimized the Log-LSQ function in an iterative way over sequentially expanding time intervals dominated by different sets of parameters.

6. In terms of efficiency, it may be advantageous to try a number (or a combination) of minimization methods. Whereas the initial estimates of model parameters can first be improved by a computationally simple, slowly converging method (e.g., derivative-free Simplex method), the resulting better guess can further be improved using a computationally extensive but rapidly converging procedure (e.g., quasi-Newton method). Good starting values for parameter estimates can sometimes be obtained by a sequential process of refining the estimates via fitting the subsets of the data, which are obtained by subdividing the observation interval. As the size of the subinterval increases, the best-fit parameter values can be improved in a step-by-step manner. The limited accuracy of the numerical solution of the mathematical model and, therefore, the correct number of digits in the value of the LSQ function must be accounted for in the minimization process, especially if it uses finite-difference approximations to the derivatives of the objective functions.

7. For complex mathematical models the variance-covariance matrix approach to assess the precision of parameter estimates is more difficult to implement because of the complexity

(this is the case for the mathematical model of systemic DC–CTL interaction). We used a different approach: approximate (e.g., 99%) confidence regions for every best-fit parameter estimate (α_*) of the whole parameter vector $\mathbf{p}_* \equiv \left[\mathbf{p}_*^{(L-1)}, \alpha_* \right]$ were obtained using the profile-likelihood-based method *(24)*, by searching for those values of α that satisfied the following inequality

$$\frac{\Phi_{LogLS}\left(\mathbf{p}_*^{[L-1]}, \alpha\right)}{\Phi_{LogLS}\left(\mathbf{p}_*^{[L-1]}, \alpha_*\right)} \leq e^{\frac{\chi_{1,1-0.01}^2}{N_{obs}}} \tag{11}$$

The value of $\chi_{1,0.99}^2$, which stands for the 0.99th quantile of the χ^2-distribution on one degree of freedom is 6.635 (*see* standard statistical textbooks), N_{obs} stands for the number of observations. Therefore, numerically one needs to find the two extreme values of α (the endpoints of the confidence range) that enable

$$\Phi_{LogLS}\left(\mathbf{p}_*^{[L-1]}, \alpha\right) = e^{\frac{6.635}{N_{obs}}} \cdot \Phi_{LogLS}\left(\mathbf{p}_*^{[L-1]}, \alpha_*\right) \tag{12}$$

8. Sensitivity analysis in modeling of biochemical and bioengineering systems has been discussed elsewhere *(7,28)*. To summarize, the sensitivity analysis has multiple functions: it can indicate the controllability of the system dynamics, the parameter redundancy in the model, the effect of errors in the data on parameter estimates, and the predictability of the system, as well as assisting in ranking the importance of the modeled processes. In addition to the simplest form of sensitivity analysis—i.e., how a permanent perturbation in parameter(s) around the best-fit value affects the solution (transient or steady-state)—one may study the effect of time-varying perturbation(s), or the sensitivity of more complex system features, like the clonal burst size, the transition time to a particular state, and so on. The practical details of sensitivity analysis with PLAS software created by Ferreira are discussed in detail by Voit *(7)*. The simplest sensitivity computations require that the parameter of interest be independent of the remaining parameters in the model; otherwise one has to take into account all functional dependences upon other parameters.

Acknowledgments

References

1. Schuler, G., Schuler-Thurner, B., and Steinman, R. M. (2003) The use of dendritic cells in cancer immunotherapy. *Curr. Opin. Immunol.* **15,** 138–147.
2. Steinman, R. M. and Pope, M. (2002) Exploiting dendritic cells to improve vaccine efficacy. *J. Clin. Invest.* **109,** 1519–1526.
3. Gershenfeld, N. (2002) *The Nature of Mathematical Modelling*. Cambridge University Press, Cambridge, UK.
4. Kutz, M. (2002) *Standard Handbook of Biomedical Engineering and Design*. McGraw-Hill Professional Publishing, New York, NY.

5. Blanchard, P., Devaney, R. L., and Hall, G. R. (1998) *Differential Equations*. Brooks/Cole Publishing Company, Pacific Grove, CA.

6. Volterra, V. (1926) Variations and fluctuations in the numbers of co-existing animal species. In: *The Golden Age of Theoretical Biology 1923–1940*. Scudo, F. M., and Ziegler, J. R., eds. Springer, Berlin, Heidelberg, Germany, pp. 65–236.

7. Voit, E. O. (2000) *Computational Analysis in Biochemical Systems. A Practical Guide for Biochemists and Molecular Biologists*. Cambridge University Press, Cambridge, UK.

8. Burnham, K. P. and Anderson, D. R. (2002) *Model Selection and Multimodel Inference— a Practical Information-Theoretic Approach, 2nd Ed*. Springer, New York, NY.

9. Ludewig, B., Bonilla, W. V., Dumrese, T., Odermatt, B., Zinkernagel, R. M., and Hengartner, H. (2001) Perforin-independent regulation of dendritic cell homeostasis by CD8(+) T cells in vivo: implications for adaptive immunotherapy. *Eur. J. Immunol.* **31,** 1772–1779.

10. Ludewig, B., Ehl, S., Karrer, U., Odermatt, B., Hengartner, H., and Zinkernagel, R. M. (1998) Dendritic cells efficiently induce protective antiviral immunity. *J. Virol.* **72,** 3812–3818.

11. Gallimore, A., Glithero, A., Godkin, A., et al. (1998) Induction and exhaustion of lymphocytic choriomeningitis virus-specific cytotoxic T lymphocytes visualized using soluble tetrameric major histocompatibility complex class I–peptide complexes. *J. Exp. Med.* **187,** 1383–1393.

12. Ehl, S., Hombach, J., Aichele, P., et al. (1998) Viral and bacterial infections interfere with peripheral tolerance induction and activate CD8+ T cells to cause immunopathology. *J. Exp. Med.* **187,** 763–774.

13. Eggert, A. A., Schreurs, M. W., Boerman, O. C., et al. (1999) Biodistribution and vaccine efficiency of murine dendritic cells are dependent on the route of administration. *Cancer Res.* **59,** 3340–3345.

14. Ludewig, B., Krebs, P., Junt, T., et al. (2004) Determining control parameters for dendritic cell–cytotoxic T lymphocyte interaction. *Eur. J. Immunol.* **34,** 2407–2418.

15. Fossum, S. (1988) Lymph-borne dendritic leukocytes do not recirculate, but enter the lymph node paracortex to become interdigitating cells. *Scand. J. Immunol.* **27,** 97–105.

16. Ardavin, C., Martinez, del Hoyo, G., Martin, P., et al. (2001) Origin and differentiation of dendritic cells. *Trends Immunol.* **22,** 691–700.

17. Ruedl, C., Koebel, P., Bachmann, M., Hess, M., and Karjalainen, K. (2000) Anatomical origin of dendritic cells determines their life span in peripheral lymph nodes. *J. Immunol.* **165,** 4910–4916.

18. Hermans, I. F., Ritchie, D. S., Yang, J., Roberts, J. M., and Ronchese, F. (2000) CD8+ T cell-dependent elimination of dendritic cells in vivo limits the induction of antitumor immunity. *J. Immunol.* **164,** 3095–3101.

19. Wherry, E. J., Teichgraber, V., Becker, T. C., et al. (2003) Lineage relationship and protective immunity of memory CD8 T cell subsets. *Nat. Immunol.* **4,** 225–234.

20. van Stipdonk, M. J., Lemmens, E. E., and Schoenberger, S. P. (2001) Naive CTLs require a single brief period of antigenic stimulation for clonal expansion and differentiation. *Nat. Immunol.* **2,** 423–429.

21. Armitage, P., Berry, G., and Matthews, J. N. S. (2002) *Statistical Methods in Medical Research*. Blackwell Science, Oxford, UK.

22. Baker, C. T. H., Bocharov, G., Paul, C. A. H., and Rihan, F. A. (2004) Computational modeling with functional differential equations: identification, selection and sensitivity, *Appl. Num. Math.*, in press.

23. Bard, Y. 1974. *Nonlinear Parameter Estimation*. Academic, New York, NY.

24. Venzon, D. J. and Mooogavkor, S. H. (1988) A method for computing profile-likelihood-based confidence intervals. *Appl. Statistician* **37,** 87–94.

25 De Boer, R. J., Oprea, M., Antia, R., Murali-Krishna, K., Ahmed, R., and Perelson, A. S. (2001) Recruitment times, proliferation, and apoptosis rates during the CD8(+) T-cell response to lymphocytic choriomeningitis virus. *J. Virol.* **75,** 10,663–10,669.

26 Wood, S. N. and Thomas, M. B. (1999) Super-sensitivity to structure in biological models. *Proc. R. Soc. Lond. B Biol. Sci.* **266,** 565–570.

27. Borghans, J. A., Taams, L. S., Wauben, M. H., and De Boer, R. J. (1999) Competition for antigenic sites during T cell proliferation: a mathematical interpretation of in vitro data. *Proc. Natl. Acad. Sci. USA* **96,** 10,782–10,787.

28. Rabitz, H. (1981) Chemical sensitivity analysis theory with applications to molecular dynamics and kinetics. *Comput. Chem.* **5,** 167–180.

3

Delivery of Tumor Antigens to Dendritic Cells Using Biodegradable Microspheres

Ying Waeckerle-Men, Bruno Gander, and Marcus Groettrup

Summary

Poly(D,L-lactide-co-glycolide) (PLGA) polymers have been used for the production of biodegradable medical sutures and for controlled drug release for decades. Useful characteristics such as in vivo biodegradability, an adjustable release profile, and the very high encapsulation capacity have stimulated immunologists to explore PLGA microspheres (MS) as antigen delivery systems for vaccination for more than 15 yr. In previous studies aiming at the development of "single-dose" vaccines, direct immunization with PLGA MS containing various antigens induced strong and sustained immune responses. We have observed that human immature monocyte-derived dendritic cells (MoDC) prepared for clinical application are able to internalize high numbers of MS without negative effects on their pivotal properties. Furthermore, PLGA-MS-incorporated antigens are effectively processed for presentation on major histocompatibility complex (MHC) class I and MHC class II molecules by dendritic cells (DCs) in vitro and induced strong cytotoxic T-lymphocyte (CTL) responses in vivo. Taken together, PLGA MS is a promising delivery vehicle for the improvement of current DC-based tumor vaccine protocols.

Key Words: Antigen processing; dendritic cells; immunotherapy; microspheres; poly(lactide-co-glycolide); vaccine delivery.

1. Introduction

DC-based immunotherapy for various cancers is increasingly being tested in clinical trials. In some cases, vaccination with tumor antigen-pulsed autologous DC correlated well with tumor regression, although the average response rates (10–20 %) were quite low *(1,2)*. The high rate of clinical failures is most likely due to the inability to induce strong and sustained cellular immune responses. Although it has emerged that mature rather than immature DC should be applied, most parameters of DC-based tumor vaccine development still need to be optimized in order to improve the clinical efficacy. Among these parameters are the vaccination schedule, the route of injection, the cell number used for inoculation, tumor antigen selection, and, especially, the mode of antigen loading into DC. In many current DC-based cancer vaccine trials, short
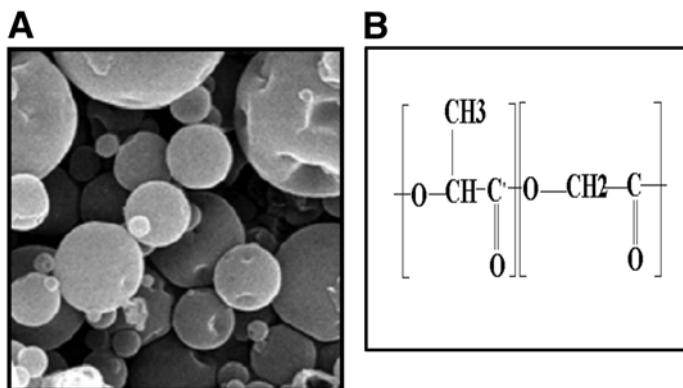
Fig. 1. Microscopic image of poly(D,L-lactide-co-glycolide) microspheres (PLGA MS) and chemical formula of PLGA. **(A)** Scanning electron micrograph of PLGA MS, and **(B)** formula of PLGA, composed of lactic acid (left bracket) and glycolic acid (right bracket).

tumor antigen-derived peptide ligands of certain MHC alleles, e.g., HLA-A*0201, are used for antigen loading. This strategy excludes many cancer patients from the therapy because they lack the specific MHC allele. Another problem resides in the short half-life of peptide/MHC class I molecule complexes on the cell surface of externally loaded DC *(3)*. The use of tumor-derived lysate or mRNA as a source of antigens may overcome the problem of MHC restriction and represent a useful alternative when tumor-specific antigens are difficult to define. However, sufficient amounts of autologous tumor material are not easily obtained, and the in vitro cultivation of tumors for long-term vaccine supply often fails. In addition, cross-presentation of soluble proteins by antigen-presenting cells (APC) is extremely inefficient.

1.1. PLGA Microspheres for Antigen Delivery

An interesting alternative to the exogenous supply of soluble peptides is to administer antigens in particulate form. One prominent example is the incorporation of antigens into biodegradable PLGA MS (**Fig. 1**). PLGA polymers have been widely used for the manufacturing of surgical sutures and controlled drug-delivery systems for human use. They are aliphatic polyesters composed of varying proportions (50:50 up to 100:0) of lactate and glycolate (**Fig. 1B**). In contact with aqueous media, PLGA is partly hydrated and slowly hydrolyzed to lactic and glycolic acids, which are further metabolized via the citric acid cycle. Medical-grade PLGA polymers differ in molecular mass and co-polymer composition, two properties that determine mainly the extent of swelling, degradation kinetics, and the release of entrapped drugs or antigens. We mostly use a relatively low molecular weight (14–17 kDa) PLGA 50:50 or PLGA 75:25, either with free carboxylic end groups (uncapped) or esterified (capped) end groups (*see* **Note 1**). These fairly hydrophilic PLGA polymers were found suitable for the release of antigens from MS over a period of 30–60 d, a period of time after which the polymer is largely hydrolyzed *(4)*.

Microencapsulation of antigens into PLGA can be achieved by several methods. Most of them involve the dissolution of PLGA in an organic solvent, formation of PLGA solution droplets, and extraction of the organic solvent into an aqueous phase or warm air. Most commonly employed methods encompass solvent extraction from a water-in-oil-in-water (w/o/w) dispersion, polymer coacervation, spray-drying, or spray freeze-drying *(5)*. In this chapter, we describe the spray-drying technique at laboratory scale, which yields small MS with diameters of less than 10 µm, a size range ideally suited for the uptake by macrophages and DC *(6,7)*. Further, we also describe methods to determine the content of microencapsulated tetanus toxoid (TT) in PLGA MS and a test to assess the in vitro release of antigens from PLGA MS.

1.2. Evaluation of PLGA-MS Uptake by MoDC

The presence of PLGA MS inside phagocytic cells can be observed through conventional light microscopy *(6)* or by fluorescence microscopy when the MS contain a fluorescent dye such as coumarin 6 *(8)*. In addition, the proportion of cells that have ingested coumarin 6-labeled MS (MS-C6) can be determined by flow cytometry (FL1-H channel for green fluorescence). Here, we outline the determination of PLGA MS uptake by human MoDC. Since PLGA MS tend to adhere to the cell surface, a method to remove externally adhering MS is also described. Detailed protocols for MoDC preparation can be found in Chapters 6 and 8 of this book.

1.3. Quality Control of Monocyte-Derived DC After PLGA-MS Uptake

As the hydrolysis of PLGA MS produces lactic and glycolic acids, one might expect that the resulting acidification during PLGA degradation alters the cellular functions of MoDC such as their maturation capability, recovery and survival rate, the capability to stimulate naïve T-cells, and the pattern of proinflammatory cytokine secretion. Therefore, the quality control of PLGA-MS-loaded MoDC is necessary, because a sensitive and long-lasting presentation of CTL and T helper epitopes can occur only when the essential functional properties of MoDC are not adversely affected after MS loading. In addition, for use as cellular tumor vaccines, MS-loaded DC should still be able to migrate from the site of injection to the secondary lymphoid organs, where they may encounter and stimulate antigen-specific T-cells. We have recently found that immature DC loaded with PLGA MS can be fully matured with different DC maturation stimuli, and that the functional and phenotypical hallmarks of MoDC maturation were not changed through PLGA MS uptake. We also observed that the migration capacity of matured, PLGA-MS-loaded MoDC did not decline. Interestingly, the survival of these cells was even consistently improved by approx 50% after treatment with Fas mAb, when the cells were matured with lipopolysaccharide (LPS). In addition, MS-carrying MoDC maintained the capacity to stimulate naïve allogeneic T helper cells and secrete amounts of the cytokines interleukin (IL)-12, IL-10, and tumor necrosis factor (TNF)-α comparable to those of untreated control cells *(8)*. The phenotypic and functional characterization of clinical-grade DC is covered in Chapter 9. Therefore, only special parameters related to PLGA MS loading are illustrated in this chapter.

1.4. Presentation of Antigens Contained in PLGA MS by Dendritic Cells

Previous studies in our laboratories demonstrated that immunization with various antigens, including natural proteins and synthetic antigenic peptides, gave rise to high antibody titers as well as strong and sustained T helper and CTL responses in vivo *(9–12)*. Protein antigens were presented both on MHC class I and class II molecules when administered to macrophages or DC in association with PLGA MS *(6)*. Based on these findings and the evidence that DC are essential for T-cell priming, we have evaluated PLGA MS as antigen-delivery and -targeting devices, specifically regarding their potential to prolong antigen presentation by DC and, hence, to improve DC-based tumor vaccines.

Although presentation of MHC class II-restricted antigens by DC is, in general, rather efficient with soluble exogenous proteins such as TT, we could still observe that a 10-fold lower concentration of antigen was sufficient to obtain the same level of T-cell proliferation when TT was offered to DC by PLGA MS loading. In addition, when we determined the kinetics of antigen presentation with MoDC by using a low concentration of TT (e.g., 0.01 µg/mL), MoDC pulsed with soluble TT ceased to stimulate TT-specific T-cells after 6 d, whereas MS-TT-charged DC were still able to activate T-cells 10 d after MS-TT loading (Y. Waeckerle-Men, manuscript in preparation). Thus, antigen delivery via PLGA MS can lead to a prolongation of MHC class II-restricted antigen presentation.

Cross-presentation of soluble proteins by DC can occur, but is extremely inefficient, while strong cross-presentation of exogenous protein antigens in particulate forms such as iron oxide beads *(13)*, latex beads *(14)*, and polysaccharides *(15)* or in PLGA MS *(6)* has been observed in phagocytic APC. We have shown that MoDC loaded with microencapsulated $FluM_{58-66}$ peptide prolonged the antigen presentation time for up to 9 d, as compared with the soluble peptide (for up to 3 d) (*16*, **Fig. 2**)*.* This prolongation of antigen presentation might be due to the slow hydrolysis of PLGA MS within DC, which provide a continuous supply of peptide ligands for newly synthesized MHC class I molecules (**Fig. 3**). In this chapter, we describe two examples of studying the presentation of MS-encapsulated antigens to specific $CD4^+$ or $CD8^+$ T-cells by MoDC, using MS charged with the TT protein and $FluM_{58-66}$ peptide (designated MS-TT and MS-Flu).

2. Instruments and Materials

2.1. Microencapsulation by Spray-Drying

1. Spray-dryer, e.g., Mini Spray-Dryer 191 (Büchi, Flawil, Switzerland).
2. Ultrasonicator, e.g., Vibra-cell® (Sonics & Materials, Danbury, CT).
3. Resomer® RG502H (Boehringer-Ingelheim, Ingelheim, Germany, *see* **Note 1**).
4. Ethyl formate (analytical grade, Fluka, Buchs, Swizerland).
5. Fluorescent dye, e.g., Coumarin 6 (Fluka).
6. Tetanus toxoid (Pasteur Mérieux, Paris, France).
7. Membrane filters (0.2 µm) of regenerated cellulose (RC 58, Schleicher and Schuell, Dassel, Germany).

2.2. Uptake of Microspheres by Dendritic Cells

1. Immature monocyte-derived dendritic cells and DC culture medium (for details *see* Chapters 6 and 8).
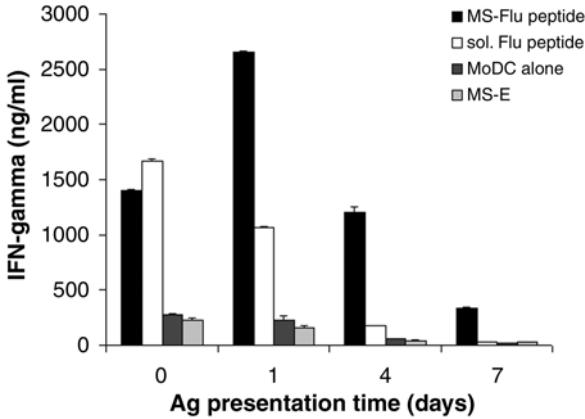
Fig. 2. Prolonged presentation of a cytotoxic T-lymphocyte (CTL) epitope by monocyte-derived dendritic cells (MoDC) after antigen delivery via PLGA MS. Immature MoDC generated from HLA-A*0201 positive donors were loaded with 1 µg/mL of Flu peptide in poly-(D,L-lactide-co-glycolide) microspheres (PLGA MS) (MS-Flu peptide), in soluble form (sol. Flu peptide), with empty MS (MS-E) or left untreated. The cells were then matured with lipopolysaccharide (5 µg/mL) for 48 h. After washing and being irradiated (20 Gy), MoDC were seeded into 96-well flat bottom plates (2×10^4/well). Subsequently, Flu peptide-specific cytotoxic T-lymphocytes (CTL) (1×10^5 per well) were added to MoDC either immediately (d 0), or on d 1, 4, or 7 after peptide/MS loading. After 20 h of co-incubation of MoDC and CTL, supernatants were collected for determining interferon-γ production by ELISA. The data represent the mean of duplicate cultures ± standard error of the mean.

2. 24-well Cell-culture plates (Cellstar, Greiner Bio-One, Frickenhausen, Germany).
3. Sterilized 15-mL centrifugation tubes.
4. Dimethylsulfoxide (DMSO) (Sigma D-2650, Switzerland).
5. Phosphate-buffered saline (PBS), pH 7.4.
6. FACS buffer (2% FCS in PBS containing 0.05% sodium azide).
7. Optical microscope.
8. Fluorescent microscope, e.g., Leica DMR fluorescence microscope with digital camera.
9. Flow cytometer, e.g., FACScan™ flow cytometer (Becton Dickinson).

2.3. Quality Control of PLGA MS-Loaded MoDC

1. FITC-labeled anti-human CD80, CD83, CD86, HLA-DR, CD95, and the respective isotype controls FITC-labeled mouse IgG1, IgG2a, IgG2b (BD Pharmingen, Basel, Switzerland).
2. Rat antihuman-CCR7 mAb (**Note 3**) and FITC-conjugated goat-antirat IgG (Jackson Immunoresearch, La Roche, Switzerland) was used as secondary antibody for anti-CCR7 staining.
3. Human chemokines CCL19 and CCL21 (R&D Systems, Wiesbaden-Nordenstadt, Germany).
4. Annexin V-FITC (BD Pharmingen).
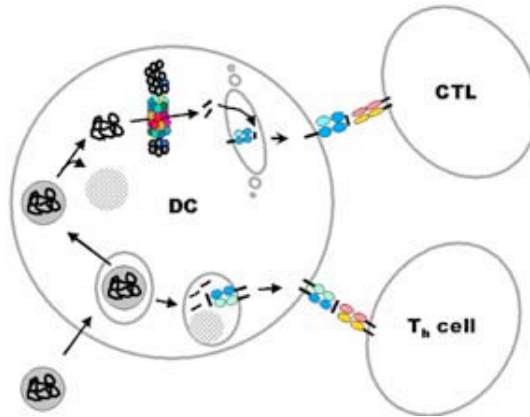
Fig. 3. Schematic illustration of antigen processing of poly(D,L-lactide-co-glycolide) microspheres (PLGA MS)-encapsulated proteins. Proteins encapsulated in PLGA MS are phago-cytosed by dendritic cells (DC). PLGA MS can escape the endosome and are hydrolyzed in the cytoplasm, thereby slowly releasing the protein for degradation by the proteasome. Resulting peptides are transported via TAP transporter into the endoplasmic reticulum, where they bind major histocompatibility complex (MHC) class I heavy chain/β_2-microglobulin complexes and migrate via the Golgi apparatus to the cell surface for recognition by cytotoxic T-lymphocytes (CTL). Alternatively, PLGA MS are hydrolzyed in endo-lysosomes; incorporated proteins are processed by cathepsins for presentation on MHC class II molecules on the cell surface, where they are recognized by T helper cells.

5. Propidium iodide (BD Pharmingen).
6. Transwell® plates with polycarbonate filters of 5 µm pore size (e.g., Corning Costar, Cambridge, MA).
7. CD4+/CD45RO- Multi Sort Kit (Miltenyi, Bergisch Gladbach, Germany).
8. ELISA kits for TNF-α, IL-10, and IL-12p70 (BD Pharmingen).

2.4. Presentation of Microencapsulated Antigens to T-Cells

1. Immature monocyte-derived dendritic cells and the relevant DC medium (e.g., AIM V medium with GM-CSF and IL-4) (*see* Chapters 6 and 8).
2. Lipopolysaccharide (LPS, from *Salmonella abortus equi,* Fluka).
3. Soluble TT (1 mg/mL).
4. MS-TT (e.g., 10 µg TT per mg of MS).
5. Soluble HPLC-purified FluM$_{58-66}$ (amino acid sequence: GILGFVFTL).
6. TT-specific CD4+ cell lines generated by repeated in vitro re-stimulation with TT in the presence of human IL-2 by using a standard protocol.
7. T-cell culture medium: Iscove's Modified Dulbecco's Medium (IMDM) with GlutaMAX-1 supplemented with 10% human AB serum, 10 m*M* HEPES and 1% peni-cillin/streptomycin (Gibco-BRL Life Technologies, Paisley, UK).
8. ELISA kit for human interferon (IFN)-γ (BD Pharmingen).

3. Methods

3.1. Microsphere Preparation by Laboratory Spray-Drying

Spray-drying is a continuous process suitable for small- and large-scale PLGA MS production. Here, we specially outline the preparation of three types of MS: MS without content ("empty" or placebo MS, MS-E); MS containing coumarin 6 (MS-C6), a green fluorescent dye used for evaluation of MS uptake by DC; and MS containing tetanus toxoid (MS-TT), which have been used for antigen presentation studies. For spray-drying, 1 g of Resomer® RG502H is first dissolved in 20 mL ethyl formate to obtain a 5% (m/v) polymer solution. This polymer solution is then spray-dried at a flow rate of 2 mL/min, and at inlet and outlet temperatures of 48°C and 40°C, respectively, to yield MS-E. Further technical details on the process are described elsewhere *(4)*. MS-C6 is prepared by directly dissolving 5 µg/mL coumarin 6 in a solution of 5% PLGA in ethyl formate. Spray-drying is performed as described above for MS-E. For preparing MS-TT, 1 mL of TT in phosphate-buffered saline (PBS) (10 mg/mL) is added to 20 mL of 5% PLGA in ethyl formate; the aqueous TT-PBS is dispersed in the organic PLGA solution under ultrasonication for 2×30 s on ice. Then, the water in oil emission dispersion is spray-dried under the conditions outlined above. The spray-dried MS are collected, washed with water to remove non-encapsulated protein, and dried under vacuum for 24 h. Numerous methods have been proposed for the quantification of the actual antigen content of PLGA MS *(17)*. The choice of method depends on the properties of particular antigen and the desired or required assay (*see* **Note 2**).

The in vitro release of antigen from PLGA MS can be monitored by incubating 30–40 mg of MS in 4 mL PBS containing 0.02% sodium azide at 37°C under mild rotational movement. At regular intervals, 1 mL of release test medium is withdrawn for analysis and replaced by fresh buffer. The sampled test medium is assayed photometrically, fluorometrically, or by ELISA for protein concentration. During release testing, the pH of the release medium should be monitored and adjusted if necessary. All determinations should be performed in triplicate. In addition, the amount of unreleased antigen remaining inside the PLGA MS can also be monitored at different time points by antigen extraction and assay (*see* **Note 2**).

3.2. Evaluation of PLGA-MS Uptake by MoDC

Fluorescent PLGA MS (e.g., MS-C6) are dispersed in DC culture medium and subsequently added to MoDC at a concentration of 0.2 mg of particles per 1×10^6 cells/well in 24-well cell-culture plates. Incubation is performed at 37°C for 4–18 h, or at 4°C as control. After incubation, MoDC are collected and washed three times with PBS. The MS-C6 uptake can be examined directly by fluorescence microscopy. Phase-contrast and fluorescence micrographs are acquired for a semi-quantitative estimation of MS uptake.

The uptake of fluorescent MS can also be evaluated with flow cytometry. After co-incubation of MS-C6 and MoDC, as described previously, 1×10^5 MoDC are collected, washed, and resuspended in 500 µL of FACS buffer. The MS uptake efficiency is analyzed by flow cytometry. MoDC that have not been co-incubated with PLGA MS

are used as negative control. The whole DC population is first gated in the forward scatter/side scatter dot plot. Then, the number of FL1-H-positive cells observed within the forward scatter/FL1-H dot plot is scored as DC loaded with PLGA MS.

Flow-cytometric analysis is a very convenient method to quantify the uptake of fluorescent MS. However, this technique *per se* cannot distinguish between externally adhering and intracellularly localized PLGA MS. To remove PLGA MS adhering to MoDC surface after MoDC/MS co-incubation, pure DMSO is added to the cells and left for exactly 3 s, after which the mixture is immediately diluted with growth medium. This treatment with DMSO dissolves quantitatively externally adhering PLGA MS without affecting the viability or integrity of the MoDC. After overnight incubation, DC are collected for uptake analysis by FACS as described.

3.3. Quality Control of PLGA-MS-Loaded MoDC

3.3.1. Phenotype and Maturation of DC Loaded With PLGA MS

Immature MoDC loaded with PLGA MS can be fully matured with different DC maturation stimuli such as LPS, CD40 ligand, poly I:C, or a cocktail of the proinflammatory cytokines IL-1β, IL-6, TNF-α· *(8)*. The phenotype of MoDC after MS loading is characterized, in our studies, by the expression of the maturation markers CD80, CD83, CD86, and HLA-DR. Another important DC maturation marker is the chemokine receptor CCR7, which is up-regulated after DC stimulation in order to enable and promote DC migration towards the lymph-node-derived chemokines CCL19 and CCL21.

3.3.2. Survival of DC Loaded With PLGA MS

One important issue in DC vaccination is the duration of DC survival after MS-loading. After vaccination with DC, the cells should remain alive for a sufficiently long period to fully activate T-cells. DC viability can be determined by staining with annexin V-FITC and propidium iodide (PI), as live cells resist annexin V and PI staining. We have observed that PLGA-MS loading does not trigger the apoptosis of immature or matured MoDC. Interestingly, the survival of matured, PLGA-MS-loaded MoDC were even consistently improved by approx 50% after treatment with Fas mAb, when the cells were matured with LPS *(8)*.

3.3.3. Migration Capacity of DC Loaded With PLGA MS

The migration capacity of DC can be tested with an in vitro chemotaxis Transwell migration assay described previously *(18)*. Briefly, 600 μL of DC medium alone or DC medium containing either 250 ng/mL CCL19 or 250 ng/mL CCL21 are added to the bottom chamber of 24-well Transwell plates with polycarbonate filters of 5 μm pore size. In each well, 1×10^5 MoDC are added to the upper chamber in a total volume of 100 μL of DC medium. The plates are then incubated for 3 h at 37°C. After careful removal of the upper chamber, 500 μL of cells (migrated cells) in the bottom chamber are collected to count for 60 s by flow cytometry. The percentage of migrated cells can be calculated as: % Migrated DC = (number of migrated DC/total DC number) × 100%.

3.3.4. T-Cell Stimulatory Functions of MoDC Loaded With PLGA MS

T-cell stimulation by MoDC can be measured by the mixed lymphocyte response (MLR). Briefly, naïve CD4^{+}CD45RA^{+} T-cells are purified by negative selection using the CD4^{+}/CD45RO^{-} Multi Sort Kit. Then, allogeneic MoDC are γ-irradiated (30 Gy) before or after PLGA MS ingestion and cultured with CD4^{+}CD45RA^{+} T-cells in 96-well flat-bottom plates at different T-cell/DC ratios in duplicate. On d 4, ^{3}H-thymidine (1 μCi/well) is added and its incorporation determined after 16–18 h. Culture medium from immature MoDC and from MoDC stimulated under indicated experimental conditions in the presence or absence of PLGA MS is collected for evaluating the cytokine production pattern by TNF-α, IL-10, and IL-12p70 ELISA.

3.4. MHC Class II-Restricted Antigen
Presentation by MoDC Charged With PLGA MS

One million immature MoDC are loaded with 2 μg/mL of TT in solution or entrapped in PLGA MS, and the loaded MoDC are cultured at 37°C in 24-well cell-culture plates. After overnight co-culture, the uptake of PLGA MS is checked by microscopic inspection. Then, the cells are collected and extensively washed. The DC loaded with PLGA MS are counted and resuspended at 2×10^5/mL in IMDM medium. Next, 2×10^4 DC (100 μL/well) are seeded into 96-well flat-bottom plates in the presence of 2 μg/mL LPS. TT-specific CD4^{+} T-cells are added to the DC culture immediately, or 1, 3, 5, or 7 d later, for co-incubation in duplicate. After 3 d of co-culture, ^{3}H-thymidine (1 μCi/well) is added, and the incorporation determined after 16–18 h.

3.5. MHC Class I-Restricted Antigen
Presentation by MoDC Charged With PLGA MS

One million immature MoDC are loaded with 2 μg/mL of Flu M1 peptide in solution or entrapped in PLGA MS, and MoDC are cultured at 37°C in 24-well cell-culture plates. After overnight co-culture, the uptake of PLGA MS is checked by visual inspection under a microscope. The cells are collected and extensively washed to remove free antigen. DC loaded with PLGA MS are counted and resuspended at 2×10^5/mL in IMDM medium. Aliquots of 100 μL (2×10^4 DC) per well are seeded in 96-well round-bottom plates in the presence of 2 μg/mL LPS. Flu-specific CTL (10^5/well) are added to DC culture immediately, or 1, 3, 5, or 7 d later, for co-incubation in duplicate. After 24 h co-culture, the supernatants are collected and determined for IFN-γ production by ELISA.

4. Future Perspectives

In our earlier studies on immunization in animals *(9–12)*, we observed that micro-encapsulated antigens elicited strong and concomitant antibody, T helper, and CTL responses, which emphasized the potential of PLGA MS as adjuvant. It is now evident that immature DC can engulf a large number of PLGA MS, and that this phagocytic process does not adversely affect DC maturation in terms of DC phenotype and capacity to stimulate T-lymphocytes. Considering that PLGA particles can escape from endo-lysosomes into the cytosol *(19)*, we may expect that the direct targeting of

MS-formulated antigens into DC not only prolongs antigen presentation, but may also mediate strong cross-priming of CTL in vivo. We have indeed observed that immunization of mice with bone-marrow-derived dendritic cells (BMDC) that had been loaded with microencapsulated β-galactosidase (β-gal) protein induced strong CTL responses, whereas injection of BMDC externally charged with soluble β-gal failed to do so (Y. Waeckerle-Men, manuscript in preparation). Our data, combined with a recent report that vaccination with BMDC loaded with a fragment from HER-2 in polysaccharide microparticles has achieved complete tumor eradication *(15)*, indicate that the delivery of tumor antigens via MS is clearly more potent than exogenous supply of proteins or peptides to DC. In vivo studies have to be performed now in mice with BMDC loaded with PLGA MS in order to evaluate the potential of this approach in a therapeutic setup of tumor immunotherapy; the efficacy of this system will have to be compared to that of other approaches. Given that PLGA is approved for clinical use, a successful outcome will set the stage for testing PLGA MS in a phase I clinical trial of tumor immunotherapy. Some efforts are still needed to produce sterile PLGA MS. Terminal sterilization may be performed by gamma irradiation of the antigen-containing PLGA MS. However, we will have to ascertain that this treatment does not hamper the properties of the antigen-containing PLGA MS. If gamma irradiation fails, the aseptic production of PLGA MS in a sterile environment will be a feasible but costly alternative.

Concerns have been raised that vaccination with autologous MoDC in general will turn out to be too labor intensive and costly to be established as a standard therapy. It has been argued that antigen loading of DC would be more practical in vivo. Along this avenue, PLGA MS may turn out to be a valuable tool, as it should be possible to co-microencapsulate chemo-attractants of DC along with the antigen. The slow release of chemo-attractants may lead to the recruitment of immature DC, which could ingest intradermally deposited PLGA MS. Since PLGA MS loading *per se* does not lead to DC maturation, the co-encapsulation of a maturation stimulus like poyI:C or CpG oligos should be necessary. A continuous flow of matured and antigen-loaded DC to the draining lymph nodes could ensue, which would be an ideal stimulus for the T-cell response. The development of PLGA MS as an in vivo antigen delivery device for DC would be even more attractive for treating malignant diseases.

5. Notes

1. PLGA 50:50 or PLGA 75:25 polyesters are available from, e.g., Boehringer Ingelheim, Germany, under the trade name of Resomer® RG502(H) or Resomer® RG752.
2. For water-soluble antigens like TT, total antigen content in MS can be determined by dissolving 10–30 mg of PLGA MS in dichloromethane, collecting the undissolved TT on a 0.2 µm cellulose membrane filter, eluting the TT from the filter with PBS, and quantifying the total ultraviolet-spectrophotometrically, fluorimetrically, or by a colorimetric protein assay. To estimate the amount of antibody-reactive TT, we recommend the use of antigen-specific ELISA. The encapsulation efficiency is calculated as the determined amount of encapsulated antigen relative to nominal antigen content. All determinations should be performed in triplicate.
3. Rat antihuman-CCR7 mAb clone 3D12 commercially available from BD Biosciences.

Acknowledgments

References

1. Nestle, F. O., Alijagic, S., Gilliet, M., et al. (1998) Vaccination of melanoma patients with peptide- or tumor lysate-pulsed dendritic cells. *Nat. Med.* **4,** 328–332.

2. Thurner, B., Haendle, I., Roder, C., et al. (1999) Vaccination with mage-3A1 peptide-pulsed mature, monocyte-derived dendritic cells expands specific cytotoxic T cells and induces regression of some metastases in advanced stage IV melanoma. *J. Exp. Med.* **190,** 1669–1678.

3. Ludewig, B., McCoy, K., Pericin, M., et al. (2001) Rapid peptide turnover and inefficient presentation of exogenous antigen critically limit the activation of self-reactive CTL by dendritic cells. *J. Immunol.* **166,** 3678–3687.

4. Thomasin, C., Corradin, G., Men, Y., Merkle, H. P., and Gander, B. (1996) Tetanus toxoid and synthetic malaria antigen containing poly(lactide)/poly(lactide-co-glycolide) microspheres, importance of polymer degradation and antigen release for immune response. *J. Control. Release* **41,** 131–145.

5. Johansen, P., Men, Y., Merkle, H. P., and Gander, B. (2000) Revisiting PLA/PLGA microspheres: an analysis of their potential in parenteral vaccination. *Eur. J. Pharm. Biopharm.* **50,** 129–146.

6. Men, Y., Audran, R., Thomasin, C., et al. (1999) MHC class I- and class II-restricted processing and presentation of microencapsulated antigens. *Vaccine* **17,** 1047–1056.

7. Walter, E., Dreher, D., Kok, M., et al. (2001) Hydrophilic poly(DL-lactide-co-glycolide) microspheres for the delivery of DNA to human-derived macrophages and dendritic cells. *J. Control. Release* **76,** 149–168.

8. Waeckerle-Men, Y., Scandella, E., Uetz-von Allmen, E., et al. (2004) Phenotype and functional analysis of human monocyte-derived dendritic cells loaded with biodegradable poly(lactide-co-glycolide) microspheres for immunotherapy. *J. Immunol. Meth.* **287(1–2),** 109–124.

9. Men, Y., Thomasin, C., Merkle, H., Gander, B., and Corradin, G. (1995) A single administration of tetanus toxoid in biodegradable microspheres elicits T cell and antibody responses similar or superior to those obtained with aluminum hydroxide. *Vaccine* **13,** 683–689.

10. Men, Y., Gander, B., Merkle, H. P., and Corradin, G. (1996) Induction of sustained and elevated immune responses to weakly immunogenic synthetic malarial peptides by encapsulation in biodegradable polymer microspheres. *Vaccine* **14,** 1442–1450.

11. Men, Y., Tamber, H., Audran, R., Gander, B., and Corradin, G. (1997) Induction of a cytotoxic T lymphocyte response by immunization with a malaria specific CTL peptide entrapped in biodegradable polymer microspheres. *Vaccine* **15,** 1405–1412.

12. Peter K., Men, Y., Pantaleo, G., Gander, B, and Corradin, G. (2001) Induction of a cytotoxic T-cell response to HIV-1 proteins with short synthetic peptides and human compatible adjuvants. *Vaccine* **19,** 4121–4129.

13. Kovacsovics-Bankowski, M., Clark, K., Benacerraf, B., and Rock, K. L. (1993) Efficient major histocompatibility complex class I presentation of exogenous antigen upon phagocytosis by macrophages. *Proc. Natl. Acad. Sci. USA* **90,** 4942–4946.

14 Shen, Z., Reznikoff, G., Dranoff, G., and Rock, K. L. (1997) Cloned dendritic cells can present exogenous antigens on both MHC class I and class II molecules. *J. Immunol.* **158,** 2723–2730.

15 Ikuta, Y., Katayama, N., Wang, L. J., et al. (2002) Presentation of a major histocompatibility complex class 1-binding peptide by monocyte-derived dendritic cells incorporating hydrophobized polysaccharide-truncated HER2 protein complex: implications for a polyvalent immuno-cell therapy. *Blood* **99,** 3717–3724.

16 Audran, R., Peter, K., Dannull, J., et al. (2003) Micro-encapsulation of peptides prolongs their presentation to cytotoxic T cells by antigen presenting cells in vitro. *Vaccine* **21,** 1250–1255.

17 Sah, H. 1997. A new strategy to determine the actual protein content of poly(lactide-co-glycolide) microspheres. *J. Pharm. Sci.* **86,** 1315–1318.

18. Scandella, E., Men, Y., Gillessen, S., Förster, R., and Groettrup, M. (2002) Prostaglandin E2 is a key factor for CCR7 surface expression and migration of monocyte-derived dendritic cells. *Blood* **100,** 1354–1361.

19. Panyam, J., Zhou, W. Z., Prabha, S., Sahoo, S. K., and Labhasetwar, V. (2002) Rapid endo-lysosomal escape of poly(D,L-lactide-co-glycolide) nanoparticles: implications for drug and gene delivery. *FASEB J.* **16,** 1217–1226.

4

RNA Transfection of Dendritic Cells

Frank Grünebach, Martin R. Müller, and Peter Brossart

Summary

Dendritic cells (DC) are the most powerful antigen-presenting cells that induce and maintain primary immune responses in vitro and in vivo. The development of protocols for the ex vivo generation of DC provided a rationale to design and develop DC-based vaccination studies for the treatment of infectious and malignant diseases. The efficacy of antigen loading and delivery into DC is pivotal for the optimal induction of T-cell-mediated immune responses. Recently it was shown that DC transfected with RNA coding for a tumor-associated antigen (TAA) or whole-tumor RNA are able to induce potent antigen- and tumor-specific T-cell responses directed against multiple epitopes. The latter technique does not require the definition of the TAA or HLA haplotype of the patients and has the potential of broad clinical application. Such a polyvalent vaccine might be able to reduce the probability of clonal tumor escape and to elicit CTL responses directed against naturally processed and presented immunodominant tumor antigens. Additional targeting of HLA class II restricted epitopes may further amplify and prolong the induced T-cell responses.

Key Words: Dendritic cells; RNA transfection; electroporation; CTL induction; immunotherapy.

1. Introduction

DC are the most powerful antigen-presenting cells, with the unique ability to initiate and maintain primary immune responses in vitro and in vivo *(1,2)*. The development of protocols for the ex vivo generation of DC provided a rationale to design and develop DC-based vaccination strategies for the treatment of infectious and malignant diseases *(3–6)*. The efficacy of antigen delivery into DC is pivotal for the optimal induction of T-cell-mediated immune responses.

Various viral and nonviral transfection methods are available for introducing DNA into mammalian cells, depending on the purpose of the experiment. Retroviruses are particularly useful in this respect, since their life cycle involves the stable integration of viral DNA into the genome of infected cells, making them an important vehicle for a broad range of applications including gene therapy. Nonviral transfection methods include direct microinjection of DNA into the cell nucleus, incorporation of DNA into

lipid vesicles (liposomes) that fuse with the plasma membrane, and exposure of cells to a brief electric pulse that transiently opens pores in the plasma membrane (electroporation). However, plasmid DNA transfer into DC is not very efficient and the use of viral vectors for transduction of DC implies a more complex and laborious manipulation associated with safety issues. Moreover, DC transfected by viral vectors have been reported to have impaired capacity in stimulating T-lymphocytes *(7–9)*.

In contrast, it was recently shown that DC transfected with RNA coding for a TAA or whole-tumor RNA are able to induce potent antigen- and tumor-specific T-cell responses directed against multiple epitopes *(10–12)*. We analyzed the efficiency of RNA transfection into DC using different sources of RNA as well as applying different delivery strategies, including electroporation, lipofection, and CD71 receptor-based endocytosis, and found that electroporation was most effective *(13)*.

Electroporation is a technique used to permeabilize cell membranes by means of an electric discharge applied directly to living cells. This permeabilization is probably due to the creation of pores in the cell membrane. Whenever a cell is exposed to the action of an electrical field the components of its membrane polarize until the establishment of a transmembranous difference of potential. If the potential difference produced in this way reaches a certain threshold (variable according to the cell type), the membrane will be disorganized or degraded at various spots, and the cell will become permeable to different exogenous molecules *(14)*. Nevertheless, the actual mechanism is still not fully understood.

To evaluate the sensitivity of these different approaches, we utilized in vitro RNA transcripts from a vector coding for the enhanced green fluorescence protein (EGFP) and RNA isolated from a cell line that was transfected with an EGFP plasmid. EGFP is a GFP variant that contains chromophore mutations that make the protein 35 times brighter than the wild-type and that is codon optimized for higher expression in mammalian cells. It is readily detectable using techniques of fluorescence microscopy, flow cytometry, or macroscopic imaging *(15,16)*.

2. Materials

1. Ficoll Paque Plus™, density 1.077 g/mL (Amersham Biosciences, Freiburg, Germany).
2. BD Falcon™ 6-well Multiwell™ plate. Tissue-culture treated polystyrene, flat bottom, with low-evaporation lid (BD Biosciences, Heidelberg, Germany).
3. PBS: phospate-buffered saline (Invitrogen, Karlsruhe, Germany).
4. PBS/FCS: PBS containing 0.5% heat-inactivated fetal calf serum (FCS).
5. RPMI Medium 1640.
6. RP10 medium: RPMI 1640 supplemented with 10% heat-inactivated FCS, 2 m*M* L-glutamine, 50 µ*M* 2-mercaptoethanol, and antibiotics streptomycin (100 µg/mL) and penicillin (100 U/mL).
7. X-VIVO 20™ medium (Cambrex Bio Science, Apen, Germany) .
8. Granulocyte/macrophage colony-stimulating factor (GM-CSF; Leukomax; Novartis, Nürnberg, Germany).
9. Interleukin (IL)-4 (Genzyme, Cambridge, MA).
10. Tumor necrosis factor (TNF)-α (Genzyme).
11. Propidium iodide (PI) staining solution: 50 µg PI/mL in PBS (pH 7.4) (BD Biosciences).
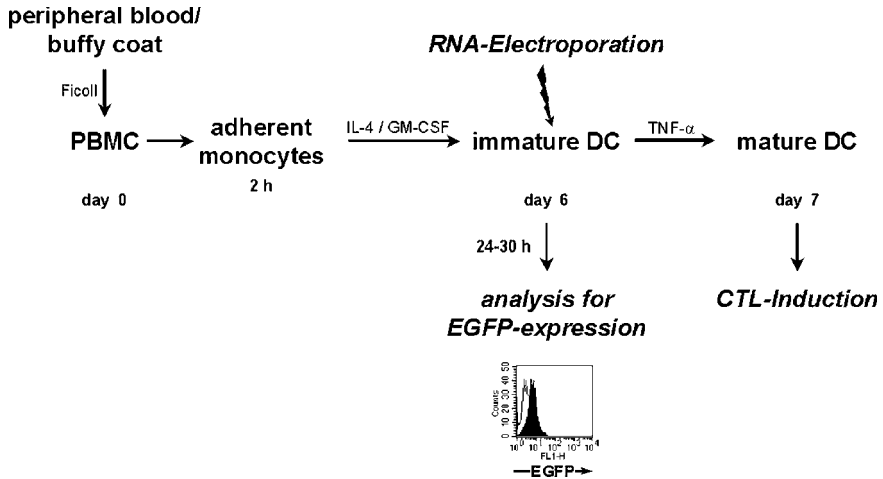
Fig. 1. Process flow of in vitro generation of dendritic cells (DC) from adherent peripheral blood mononuclear cells (PBMC) and RNA electroporation. IL-4, interleukin 4; GM-CSF, granulocyte macrophage-colony stimulating factor; TNF-α, tumor necrosis factor-α; CTL, cytotoxic T-lymphocytes; EGFP, enhanced green fluorescence protein.

12. FACSCalibur™ flow cytometer (BD Biosciences).
13. RNeasy™ anion-exchange spin columns (Qiagen, Hilden, Germany).
14. 10X MOPS-EDTA-sodium acetate buffer (MESA buffer): 3-[*N*-morpholino]propanesulfonic acid (MOPS), 0.4 *M*, pH 7.0, 0.1 *M* sodium acetate, 10 m*M* EDTA.
15. Agarose-LE™, RNase-free (Ambion, Huntingdon, UK).
16. 1% Ethidium bromide stock solution (10 mg/mL).
17. RNA sample loading buffer: 62.5% deionized formamide, 1.14 *M* formaldehyde, 1.25 X MOPS-EDTA-sodium acetate buffer, 200 µg/mL bromphenol blue, 200 µg/mL xylene cyanole, 50 µg/mL ethidium bromide.
18. Plasmid pSP64-EGFP-2 (V. F. I. Van Tendeloo).
19. Restriction enzyme *Nde*I .
20. QIAEX II Gel Extraction Kit™ (Qiagen).
21. 10 m*M* Tris-Cl, pH 8.5.
22. SP6 Cap Scribe Kit™ (Roche Applied Science, Mannheim, Germany).
23. RNA Millenium Markers™ (Ambion).
24. Easyject Plus™ electroporator (EquiBio; Peqlab, Erlangen, Germany).
25. 4-mm electroporation cuvets.

3. Methods

The methods described below outline (1) cell isolation and generation of DC from adherent peripheral blood mononuclear cells (PBMC), (2) the RNA isolation from animal cells and formaldehyde agarose gel electrophoresis, (3) the generation of EGFP mRNA by in vitro transcription, (4) the electroporation of DC, and (5) the detection of EGFP fluorescence by flow cytometry (**Fig. 1**).

3.1. Cell Isolation and Generation of Human DC From Adherent Peripheral Blood Mononuclear Cells (PBMC)

1. Dilute fresh human heparinized blood by addition of an equal volume of PBS. Alternatively, leukocyte-rich buffy coat not older than 8 h is diluted 1:4 with PBS.
2. Pipet 12 mL Ficoll-Paque Plus in a 50-mL sterile conical centrifuge tube.
3. Carefully layer the diluted blood sample on Ficoll-Paque Plus.
4. Centrifuge at 650g for 20 min at 18–20°C in a swing-out rotor without brake.
5. After centrifugation the PBMC (lymphocytes and monocytes) form a distinct band at the sample/medium interface. Carefully transfer the interphase cells to a new 50-mL conical tube. The cells are best removed from the interface using a sterile plastic Pasteur pipet without removing the upper layer.
6. Wash the cells twice or thrice: add PBS/FCS (*see* **Note 1**) to 50 mL, mix and centrifuge 120g for 10 min at 18–20°C (*see* **Note 2**).
7. Resuspend the cell pellet in RP10 medium (*see* **Note 3**).
8. Seed the cells at a concentration of 1×10^7 cells/3 mL/well into 6-well plates.
9. Incubate for 2 h in a humidified 37°C/5% CO_2 incubator for adherence of monocytes.
10. Gently shake and remove medium containing non-adherent lymphocytes.
11. Wash the adherent monocytes three times with 3 mL PBS (*see* **Note 4**).
12. Add RP10 medium supplemented with human recombinant GM-CSF (100 ng/mL) and IL-4 (20 ng/mL) for the generation of immature DC (*see* **Note 3**). Every other d add cytokines.
13. Culture cells in a humidified 37°C/5% CO_2 incubator for 6 d. After 6 d the loosely adherent or nonadherent cells should display immature DC morphology and phenotype (CD14$^{+/-}$, CD1a^{++}, CD40$^+$, CD83$^-$, CD86$^+$, HLA-DR^{++}).
14. Harvest the immature monocyte-derived DC and electroporate with RNA.
15. For maturation, culture DC with TNF-α (10 ng/mL) for an additional 24 h (after d 6).
16. Analyze the phenotype of DC by flow cytometry after 7 d of culture: CD14$^-$, CD1a$^+$, CD80$^+$, CD83$^+$, CD86^{++}, HLA-DR^{+++}.

3.2. Total RNA Isolation From Human Cells and Formaldehyde Agarose Gel Electrophoresis

Total RNA is isolated from cell lysates using RNeasy™ Midi or Maxi anion-exchange spin columns according to the protocol for isolation of total RNA from animal cells provided by the manufacturer (*see* **Note 5**). To avoid exogenous sources of RNase contamination, always apply RNase-free techniques when working with RNA (*see* **Note 6**).

Quantity and purity of RNA is determined by measuring the absorbance at 260 nm in a spectrophotometer. The ratio of the readings at 260 nm and 280 nm provides an estimate of the purity of RNA with respect to contaminants that absorb in the ultraviolet (UV), such as protein. Pure RNA has an A260/A280 ratio of 1.9–2.1. Furthermore, RNA samples are routinely checked by formaldehyde/agarose gel electrophoresis for size and integrity and stored at –80°C in small aliquots.

Preparation of 1.2% formaldehyde/agarose gel of size $10 \times 14 \times 0.7$ cm:

1. Add 1.2 g RNase-free agarose, 10 mL 10X MESA buffer, and RNase-free water to 100 mL.
2. Heat the mixture to melt agarose and cool to 65°C.
3. Add 1.8 mL of 37% (12.3 M) formaldehyde and 1 µL of a 10 mg/mL ethidium bromide stock solution.
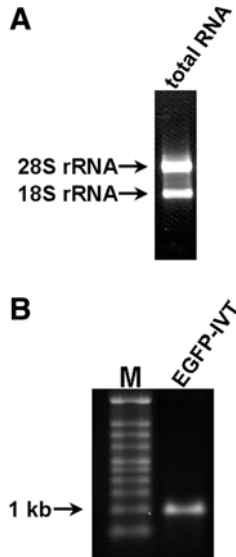
Fig. 2. **(A)** 1.2% formaldehyde agarose gel of total human RNA showing the 18S and 28S ribosomal RNA (rRNA). **(B)** 1.2% formaldehyde agarose gel of enhanced green fluorescence protein in vitro transcript (EGFP-IVT). M, RNA Millenium Markers™ (Ambion).

4. Pour the mixture into the gel tray.
5. Equilibrate the gel prior to running in 1X MESA buffer for at least 30 min.
6. Add RNA sample loading buffer to the RNA sample in ratio 1:2 to 1:5. The RNA marker is treated equally.
7. Heat the RNA samples just before loading onto the gel to 65°C for 10 min and chill on ice.
8. Run the gel at <5 V/cm in 1X MESA buffer. When resolved, the 18S and 28S ribosomal RNA (rRNA) bands should appear as sharp bands on the stained gel. 28S rRNA bands should be present with an intensity approximately twice that of the 18S rRNA band, indicating that no degradation of RNA has occurred (**Fig. 2A**).

3.3. Generation of EGFP mRNA by In Vitro Transcription

For generation of EGFP mRNA, the plasmid pSP64-EGFP-2 (*see* **Note 7**), which allows in vitro transcription under the control of the phage SP6 promoter, is used (**Fig. 3**) *(16)*. The plasmid is linearized with the restriction enzyme *Nde*I (*see* **Notes 8 and 9**) and then purified with the QIAEX II Gel Extraction Kit using the protocol for desalting and concentrating DNA solutions (*see* **Note 10**). In vitro transcription is done with the SP6 Cap Scribe kit according to the protocol provided by the manufacturer, except that 2.0 µg linearized plasmid DNA is used per transcription reaction and the synthesis time is extended to 3 h. Purification of in vitro transcripts is performed with RNeasy Mini anion-exchange spin columns according to the RNA
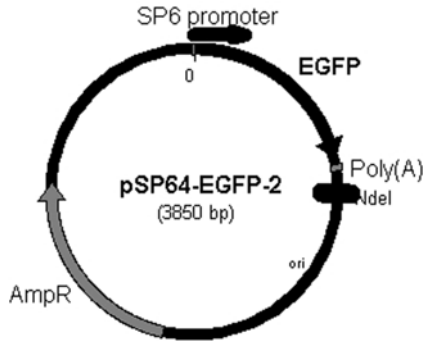
Fig. 3. Schematic drawing of plasmid pSP64-EGFP-2 for in vitro transcription of EGFP. EGFP, enhanced green fluorescence protein; ori, origin of replication; AmpR, β-lactamase coding region.

cleanup protocol provided by the manufacturer. RNA in vitro transcripts (IVT) are routinely checked by formaldehyde/agarose gel electrophoresis for correct size and integrity, and stored at –80° in small aliquots (**Fig. 2B**).

3.4. Electroporation of DC

Electroporation is done on d 6 of DC generation (**Fig. 1**).

1. Prepare 6-well plates with 3 mL RP10 medium supplemented with cytokines and pre-warm in the incubator (*see* **Note 3**).
2. Wash immature DC twice with serum-free X-VIVO 20 medium and resuspend to a final concentration of 2×10^7 cells/mL.
3. Mix 200 µL of the cell suspension with 10 µg RNA (2.5 µg RNA/10^6 DC, *see* **Note 11**) and transfer into a 4-mm electroporation cuvet (*see* **Note 12**). EGFP in vitro transcribed RNA is recommended as a positive control.
4. Adjust the parameters of the electroporator apparatus as follows: voltage of 300 V, capacitance of 150 µF, and resistance of 1540 Ω.
5. Insert the cuvet into the electroporation chamber and trigger the pulse.
6. Transfer the cells immediately into the 6-well plate with prewarmed RP10 medium and return it to the incubator (*see* **Note 13**).
7. Treat the control cells equally but use PBS instead of RNA.

3.5. EGFP Analysis by Flow Cytometry

EGFP-RNA-transfected DC are checked for EGFP expression 24–30 h post electroporation by flow cytometric analysis. Briefly, 2×10^5 cells are washed once with 5 mL PBS and are then resuspended in 200 µL of PBS/FCS buffer. Gating is performed on cells exhibiting a large forward scatter (FSC) and side scatter (SSC) profile in order to allow exclusion of contaminating autologous lymphocytes. Gated DC are then evaluated for EGFP expression (excitation maximum = 488 nm; emission maximum = 507 nm). As a control, nontransfected DC (PBS control) are used.

The vitality of the cells after electroporation can be assessed by propidium iodide (PI) staining (*see* **Note 14**). 10 μL of PI staining solution are added to the cell sample in ratio 1:10. PI is detected in the orange range of the spectrum using a 562–588 nm band-pass filter.

4. Notes

1. For clinical use, FCS can be omitted.
2. The washings remove thrombocytes, which are not spun down at this centrifugal force.
3. For clinical use the RP10 medium can be replaced with serum-free X-VIVO 20 medium.
4. In our experience the purity of the adherent monocytes after the wash steps varies considerably from donor to donor.
5. RNeasy kits provide a fast and simple method for preparation of total RNA from animal cells and tissues, but other methods producing high-quality RNA can be applied.
6. See manuals of the RNA isolation kits.
7. An in vitro transcription vector can be constructed by subcloning the coding sequence of any gene into the vector pSP64 Poly(A) (Promega) by standard cloning procedures *(17)*. For linearization of the vector, a singular restriction site should be present approx 50–200 bp downstream of the termination codon of the respective gene. If this is not the case, an adequate restriction site must be created by site-directed mutagenesis.
8. Plasmid DNA must be linearized with a restriction enzyme downstream of the insert to be transcribed, since linearized templates give transcripts of defined length and usually higher yields of transcripts. Circular plasmid templates will generate extremely long, heterogeneous RNA transcripts.
9. Remove an aliquot for an analytical gel in order to confirm that cleavage is complete.
10. Plasmid DNA from some isolation procedures may be contaminated with residual RNase A. The plasmid template used for transcription should be sufficiently purified and not contain high amounts of bacterial RNA or RNases. The QIAEX II Gel Extraction Kit avoids phenol/chloroform extraction and ethanol precipitation. The DNA is eluted with an appropriate volume of 10 mM Tris-Cl, pH 8.5, to achieve a concentration of 0.5–1.0 μg/μL.11. The preparation can be downscaled, but keep the ratio between RNA and cells of 2.5 μg /10^6.
12. The RNA must be added to the cell suspension shortly before the pulse to prevent degradation due to RNases.
13. During the electroporation pulse, electrolysis of the medium and electrodes is a major event. This electrolysis strongly and unfavorably affects the characteristics of the medium, notably the pH. Therefore it is absolutely advisable to transfer the electroporated cells to fresh medium as soon as possible after the pulse (within seconds); failure to do so will considerably increase the mortality rate.
14. PI intercalates into double-stranded nucleic acids. It is excluded by viable cells but can penetrate cell membranes of dying or dead cells.

Acknowledgments

References

1. Banchereau, J. and Steinman, R. M. (1998) Dendritic cells and the control of immunity. *Nature* **392,** 245–252.
2. Cella, M., Sallusto, F., and Lanzavecchia, A. (1997) Origin, maturation and antigen presenting function of dendritic cells. *Curr. Opin. Immunol.* **9,** 10–16.
3. Sallusto, F. and Lanzavecchia, A. (1994) Efficient presentation of soluble antigen by cultured human dendritic cells is maintained by granulocyte/macrophage colony stimulating factor plus interleukin 4 and down regulated by tumour necrosis factor. *J. Exp. Med.* **179,** 1109–1118.
4. Zhou, L. and Tedder, T. F. (1996) CD14 blood monocytes can differentiate into functionally mature CD83+ dendritic cells. *Proc. Natl. Acad. Sci. USA* **93,** 2588–2592.
5. Brossart, P., Grünebach, F., Stuhler, G., et al. (1998) Generation of functional human dendritic cells from adherent peripheral blood monocytes by CD40 ligation in the absence of granulocyte-macrophage colony-stimulating factor. *Blood* **92,** 4238–4247.
6. Brossart, P., Wirths, S., Brugger, W., and Kanz, L. (2001) Dendritic cells in cancer vaccines. *Exp. Hematol.* **29,** 1247–1255.
7. Brossart P., Goldrath, A. W., Butz, E. A., Martin, S., and Bevan, M. J. (1997) Virus-mediated delivery of antigenic epitopes into dendritic cells as a means to induce CTL. *J. Immunol.* **158,** 3270–3276.
8. Reeves, M. E., Royal, R. E., Lam, J. S., Rosenberg, S. A., and Hwu, P. (1996) Retroviral transduction of human dendritic cells with a tumor-associated antigen gene. *Cancer Res.* **56,** 5672–5677.
9. Van Tendeloo, V. F., Snoeck, H. W., Lardon, F., et al. (1998) Nonviral transfection of distinct types of human dendritic cells: high-efficiency gene transfer by electroporation into hematopoietic progenitor—but not monocyte-derived dendritic cells. *Gene Ther.* **5,** 700–707.
10. Boczkowski, D., Nair, S. K., Snyder, D., and Gilboa, E. (1996) Dendritic cells pulsed with RNA are potent antigen-presenting cells in vitro and in vivo. *J. Exp. Med.* **184,** 465–472.
11. Nair, S. K., Boczkowski, D., Morse, M., Cumming, R. I., Lyerly, H. K., and Gilboa, E. (1998) Induction of primary carcinoembryonic antigen (CEA)-specific cytotoxic T lymphocytes in vitro using human dendritic cells transfected with RNA. *Nat. Biotechnol.* **16,** 364–369.
12. Müller, M. R., Grünebach, F., Nencioni, A., and Brossart, P. (2003) Transfection of dendritic cells with RNA induces CD4- and CD8-mediated T cell immunity against breast carcinomas and reveals the immunodominance of presented T cell epitopes. *J. Immunol.* **170,** 5892–5896.
13. Grünebach, F., Müller, M. R., Nencioni, A., and Brossart, P. (2003) Delivery of tumor-derived RNA for the induction of cytotoxic T-lymphocytes. *Gene Ther.* **10,** 367–374.
14. Andreason, G. L. and Evans, G. A. (1989) Optimization of electroporation for transfection of mammalian cell lines. *Anal. Biochem.* **180,** 269–275.
15. Zhang, G., Gurtu, V., and Kain, S. R. (1996) An enhanced green fluorescent protein allows sensitive detection of gene transfer in mammalian cells. *Biochem. Biophys. Res. Commun.* **227,** 707–711.
16. Van Tendeloo, V. F., Ponsaerts, P., Lardon, F., et al. (2001) Highly efficient gene delivery by mRNA electroporation in human hematopoietic cells: superiority to lipofection and passive pulsing of mRNA and to electroporation of plasmid cDNA for tumor antigen loading of dendritic cells. *Blood* **98,** 49–56.
17. Sambrook, J., Fritsch, E. F., and Maniatis, T. (1989) *Molecular Cloning: A Laboratory Manual*, 2nd Ed. Cold Spring Harbor Laboratory, Cold Spring Harbor, NY.

5

Isolation and Generation of Clinical-Grade Dendritic Cells Using the CliniMACS System

John D. M. Campbell, Christoph Piechaczek, Gregor Winkels, Edith Schwamborn, Daniela Micheli, Sonja Hennemann, and Jürgen Schmitz

Summary

Dendritic cells (DC) can either be generated from progenitors such as stem cells or CD14+ monocytes, or isolated directly from the blood. Blood-derived DC are present as at least two distinct populations—myeloid and plasmacytoid DC. Here we describe methods for the clinical-grade isolation of blood DC and DC precursors using the CliniMACS™. We describe the isolation of ultra-pure monocytes in order to generate large numbers of monocyte-derived DC, and also new methods for the direct isolation of blood DC. Isolation of blood DC in large numbers means that natural DC with different properties can be investigated for their clinical function for the first time.

Key Words: Dendritic cells; myeloid DC; plasmacytoid DC; magnetic separation; CliniMACS.

1. Introduction

DC are the most efficient antigen-presenting cells (APC) of the immune system. DC are present at low levels in most tissues, acting as sentinels that patrol the boundaries against foreign enemies, such as infectious agents, toxins, and allergens *(1)*. The potent antigen (Ag)-presenting ability of the DC is currently of great interest in the clinical manipulation of immune responses. Vaccination with DC, particularly in cancer and viral-induced disease, may lead to the establishment of Ag-specific immune responses in the patient, which ultimately may eliminate the pathogen or tumor.

In humans, DC have been identified that develop from at least two different progenitor cell types—DC of myeloid origin (mDC, or DC1), and DC of plasmacytoid origin (pDC, or DC2) *(2,3)*. There is also heterogeneity within each DC group *(2,3)*. The mDC and pDC subsets react to differing maturation signals, and produce different cytokines in response to stimulus. DC are present in relatively small numbers in the bloodstream (less than 1% of mononuclear cells) *(4)*, and until recently, no suitable

specific markers were available to isolate these cells. DC for therapy were therefore generated in large numbers from precursor cells, such as CD34⁺ cells or CD14⁺ monocytes *(5,6)*. Using CD14 selection on the CliniMACS device, it is possible to isolate very large numbers of precursors for the generation of monocyte-derived DC (MoDC) for therapy. MoDC are analogous to mDC, and have already been successfully used in early clinical trials.

We have also now generated novel reagents to isolate blood DC for therapy, using the antibodies BDCA-1 (CD1c) and BDCA-4 to isolate mDC and pDC respectively. This means that for the first time, the potent Ag-presenting abilities of natural DC can be exploited for clinical use, and the specific functions of mDC and pDC *(7–10)* can be investigated in clinical trials.

In this chapter we detail the three methods for isolation of DC for therapy—direct isolation of blood mDC and pDC, and the purification of CD14⁺ cells for generation of MoDC. The application of CD14-derived DC for vaccination of tumor patients is described elsewhere in Chapter 6 of this volume. Here we will describe:

1. The isolation of ultra-pure CD14⁺ cells for MoDC generation.
2. The optimal culture conditions for the generation of large numbers of MoDC.
3. The isolation of mDC and pDC.

Each method is described separately, as the specific materials required differ for each isolation.

2. Materials

2.1. Clinical-Scale Separation of CD14⁺ Monocytes

1. Leukapheresis product from unmobilized donor containing $10–20 \times 10^9$ leukocytes (white blood cells [WBC]).
2. CliniMACS CD14 Reagent (Miltenyi Biotec, cat. no. 281-01).
3. CliniMACS ᵖˡᵘˢ Instrument (Miltenyi Biotec, cat. no.155-01); software version 2.3.1.
4. CliniMACS Tubing Set (Miltenyi Biotec, cat. no.161-01).
5. PreSystem-Filter (Miltenyi Biotec, cat. no.181-01).
6. Luer/Spike Interconnector, (Miltenyi Biotec, cat. no.187-01).
7. CliniMACS PBS/EDTA Buffer (Miltenyi Biotec, cat. no. 700-25).
8. Human serum albumin (HSA) (e.g., Aventis Behring).
9. Transfer Packs 600 mL (Miltenyi Biotec, cat. no. 190-01).
10. Transfer Set Coupler/Coupler (Miltenyi Biotec, cat. no.186-01).
11. Centrifuge, suitable for bag processing.
12. Balance for weighing bags.
13. Plasma extractor.
14. Orbital shaker.
15. Sampling Site Coupler (Miltenyi Biotec, cat. no.189-01).
16. Tubing slide clamps/scissor clamps.
17. Sample tubes, size 2 mL.
18. CD14-FITC (e.g., Miltenyi Biotec GmbH, cat. no. 130-080-701).
19. CD15-PE (e.g., BD-Pharmingen).
20. Propidium iodide solution (1 mg/mL).
21. Ammonium chloride red blood cell lysing solution (final concentration: 155mM NH₄Cl; 10 mM KHCO₃; 0.1 mM EDTA, pH 7.3). Make fresh before use from a 10X stock solution.

2.2. Generation of Immature Dendritic Cells From Monocytes

1. Cell culture bags (e.g., CellGenix) or flasks (e.g., NUNC™).
2. 50- or 250-mL conical centrifuge tubes (e.g., Falcon).
3. Syringes.
4. Medium, e.g., X-VIVO 15 (BioWhittaker).
5. Human AB serum (e.g., Sigma).
6. Granulocyte/macrophage colony-stimulating factor (GM-CSF; e.g., Leucomax®, Sandoz).
7. Interleukin (IL)-4 (e.g., R&D Systems).
8. DC generation medium—X-VIVO 15 medium supplemented with 1% AB serum; 1000 IU/mL GMCSF; 1000 IU/mL IL-4.
9. Trypan blue solution for viability testing.
10. Biological safety cabinet.
11. CO_2 incubator with 5 % CO_2.
12. Variable volume pipettors.
13. Microscope.
14. Anti-CD14-FITC (e.g., Miltenyi Biotec GmbH).
15. Anti-CD80-FITC (e.g., BD-Pharmingen).
16. Anti-CD83-PE (e.g., BD-Pharmingen).
17. Anti -CD86-PE (e.g., BD-Pharmingen).
18. Anti -HLA-DR-FITC (e.g., BD-Pharmingen).
19. Isotype controls.
20. Propidium iodide (1 mg/mL).

2.3 Blood DC

2.3.1 Plasmacytoid Dentritic Cells (pDC)

1. Leukapheresis product from unmobilized donor containing $10–40 \times 10^9$ WBC.
2. CliniMACS Anti-BDCA-4 MicroBeads (Miltenyi Biotec GmbH, cat. no. 291-01).
3. CliniMACS [plus] instrument (Miltenyi Biotec GmbH , cat. no. 155-01 or 155-02), software version 2.3.1+.
4. CliniMACS Tubing Set (Miltenyi Biotec GmbH, e.g., cat. no. 165-01 or 161-01).
5. CliniMACS PBS/EDTA buffer (P/E; $3 \times 1L$; Miltenyi Biotec, ref. no. 700-25).
6. Pre-System Filter (Miltenyi Biotec GmbH, cat. no. 181-01).
7. Luer/Spike Interconnector (Miltenyi Biotec GmbH, cat. no. 187-01).
8. Transfer packs, 150 mL and 600 mL.
9. Centrifuge, suitable for bag processing, bags to balance centrifuge.
10. Plasma extractor.
11. Sterile tubing welder.
12. Orbital shaker.
13. Sampling site coupler.
14. Tubing slide clamps/scissor clamps.
15. Flow cytometer (properly equipped and compensated to allow simultaneous analysis of FITC, PE, and PI. If equipped with a 633-nm laser, additionally APC).
16. Automated hematology analyzer or Neubauer hemocytometer.
17. Human serum albumin (HSA) or bovine serum albumin (BSA) as supplement to P/E (final concentration 0.5%, P/E/H or P/E/B) (*see* **Note 7**).
18. Ammonium chloride lysing solution (155 m*M* NH_4Cl, 10 m*M* $KHCO_3$, 0.1 m*M* EDTA).
19. FcR-Blocking Reagent (Miltenyi Biotec, ref. no. 130-059-901). Titer 1:5.

20. CD45.FITC (Miltenyi Biotec, ref. no. 130-080-202). Titer 1:11.
21. Anti-BDCA-2.PE (Miltenyi Biotec, ref. no. 130-090-511). Titer 1:11.
22. CD123.APC (Miltenyi Biotec ref. no. 130-090-901). Titer 1:11.
23. Propidium iodide, stock: 1mg/mL (Sigma, ref. no. P4170). Titer 1:1000.
24. 12×75 mm (4 mL) tubes (Falcon-2052 or equivalent).

2.3.2 Myeloid Dentritic Cells (mDC)

1. Leukapheresis product from unmobilized donor containing $10–40 \times 10^9$ WBC.
2. CliniMACS CD1c (Anti-BDCA-1)-Biotin (Miltenyi Biotec GmbH, CliniMACS Anti-Biotin MicroBeads, ref. no. 192-01).
3. CliniMACS CD19 (MicroBeads, ref. no. 193-01).
4. CliniMACS ^plus instrument (Miltenyi Biotec GmbH , cat. no. 155-01 or 155-02), software version 2.3.1+.
5. 2X CliniMACS Tubing Set (Miltenyi Biotec, e.g., ref. no. 165-01 or 161-01 or 162-01).
6. 2X CliniMACS PBS/EDTA buffer (3×1L; Miltenyi Biotec, e.g., ref. no. 700-25 or 705-25).
7. 2X Pre-System Filter (Miltenyi Biotec, ref. no. 181-01).
8. 2X Luer/Spike Interconnector (Miltenyi Biotec, ref. no. 187-01).
9. Transfer packs, 150 mL and 600 mL.
10. Centrifuge suitable for bag processing, bags to balance centrifuge.
11. Plasma extractor.
12. Sterile-tubing welder.
13. Orbital shaker.
14. Sampling site coupler.
15. Tubing slide clamps/scissor clamps.
16. Flow cytometer (properly equipped and compensated to allow simultaneous analysis of FITC, PE, and PI. If equipped with a 633-nm laser, additionally APC).
17. Automated hematology analyzer or Neubauer hemocytometer.
18. Human serum albumin (HSA) or bovine serum albumin (BSA) as supplement to P/E (final concentration 0.5%, P/E/H or P/E/B) (*see* **Note 7**).
19. Ammonium chloride lysing solution (155 m*M* NH$_4$Cl, 10 m*M* KHCO$_3$, 0.1 m*M* EDTA).
20. FcR-Blocking Reagent (Miltenyi Biotec, ref. no. 130-059-901). Titer 1:5.
21. CD1c.PE (Clone AD5-8E7; Miltenyi Biotec GmbH 130-090-508). Titer 1:11.
22. CD20.APC (Clone LT20; Miltenyi Biotec GmbH). Titer 1:11.
23. CD45.FITC (Miltenyi Biotec, ref. no. 130-080-202). Titer 1:11.
24. Propidium iodide, stock: 1 mg/mL (Sigma, ref. no. P4170). Titer 1:1000.
25. 12×75 mm FCM tubes (Falcon-2052 or equivalent).

3. Methods

3.1. Isolation of CD14+ Cells for the Generation of Immature MoDC

In this section we describe the separation of CD14+ monocytes; the cultivation procedure for generation of immature DC (iDC) from monocytes; flow cytometry analysis of the CD14 separation and iDC.

3.1.1. Isolation of CD14+ Cells Using the CliniMACS

Isolation of CD14+ monocytes is performed by immunomagnetic labeling of target cells followed by an automated separation process using the CliniMACS^plus.

3.1.1. Immunomagnetic Labeling

Determine the total number of leukocytes in your sample. This protocol is designed for leukapheresis products containing $10-20 \times 10^9$ WBC (*see* **Notes 1–3**). Before starting, it is useful to determine the number of monocytes in the sample (either by automated hematology analyzer or flow cytometry), as this number of target cells must be entered into the CliniMACS cell-separation software before separation. Supplement CliniMACS PBS/EDTA buffer with HSA (final concentration 0.5%) before starting. The HSA is required to inactivate and to coat the surfaces of tubing and bags.

1. Determine the weight of an empty 600-mL transfer pack to be used as a cell-preparation bag. Transfer the leukapheresis product into the cell-preparation bag and record the weight.
2. Fill the bag with HSA-supplemented CliniMACS PBS/EDTA buffer to a total volume of 600 mL and centrifuge the cell suspension for 15 min at $300g$ (room temperature, 19–25°C), no brake.
3. Remove supernatant carefully using the plasma expressor to a final sample volume of 50 mL, taking care not to resuspend the cell pellet.
4. Resuspend cell pellet and add the entire content of one vial CliniMACS CD14 Reagent (7.5 mL), and mix carefully (*see* **Note 4**).
5. Incubate the cell-preparation bag for 15 min at room temperature (19–25°C) on an orbital shaker at 25 rpm maximum.
6. Add HSA-supplemented CliniMACS PBS/EDTA buffer to a final volume of 600 mL for cell washing and centrifuge for 15 min at $300g$ (room temperature), no brake.
7. Remove as much supernatant as possible from the cell pellet, resuspend the cells, and add CliniMACS PBS/EDTA/HSA buffer to a final volume of 100 mL.
8. Retain a 0.5-mL sample from the cell suspension and place into a sample tube for analysis. It is recommended to determine at least total cell number, viability, and frequency/number of CD14$^+$ cells.

3.1.2. Automated Separation

1. Determine the weight of an empty 600-mL transfer pack with a Luer/Spike Interconnector inserted and attach this bag to the cell collection port of the CliniMACS Tubing Set. Ensure that all slide clamps are open. Switch on the instrument and choose selection program "ENRICHMENT 1.1."
2. Confirm your choice and enter the parameters requested on the screen. Check the calculated number of labeled total and target cells and confirm by pressing "ENT." Check buffer and bag requirements and confirm displayed data after preparation of tubing set and buffer bags as mentioned above.
3. Follow the tubing-set installation instructions on the screen and start the automated separation program.
4. Determine the weight of the cell collection bag after the separation and take a 0.5-mL sample for cell-count determination and flow-cytometry analysis. The weight can be used to determine the volume of the positive fraction.
5. Take a 0.5-mL sample from the negative fraction collection bag for cell-count determination and flow-cytometry analysis.

3.1.3. Analysis of CD14 Separation (**Fig. 1**)

Analysis of all four fractions obtained—original, positive, negative and buffer waste bags—allows the most accurate determination of yield (*see* **Notes 5** and **6**).

Unseparated Fraction   **Positive Fraction**
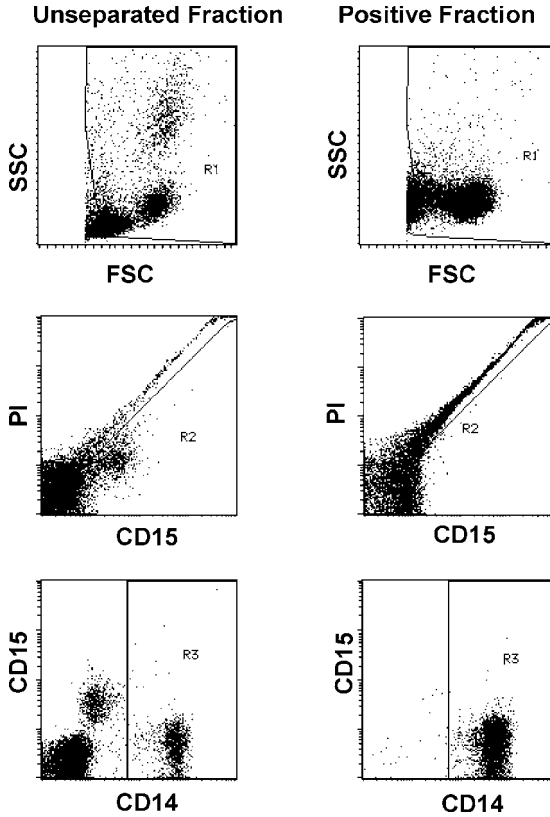
Fig. 1. Determination of CD14+ cell purity and yield. Representative flow cytometry analysis of a leukapheresis sample before and after CliniMACS CD14 separation. Samples are first gated on Forward vs Side Scatter (FSC vs SSC) to exclude any debris (R1). Results from R1 are then plotted CD15-PE vs PI to exclude dead cells (R2). A combined gate is then made (e.g., G3 = R1*R2 in "Cell Quest" software, BD biosciences). G3 therefore contains all viable cells. CD14 is plotted against CD15 to evaluate the numbers of live CD14+CD15– cells (viable monocytes) in the samples (R3). In this example, the start population has 13.2% CD14+CD15– cells, which is enriched to >99% after CliniMACS sorting.

To calculate yield:

$$\text{Total, viable monocytes} = \frac{\text{total WBC} * \% \text{ viable monocytes (purity)}}{100\%}$$

Example:

Total cell number positive fraction: 1.9×10^9

Viability of positive fraction = 99.9% (G3)

Purity of positive fraction = 99.3% (R3)

Percentage viable monocytes = 99.9% * 99.3% = 99.2%

$$\text{Total, viable monocytes} = \frac{1.9 \times 10^9 * 99.2\%}{100\%} = 1.885 \times 10^9 \text{ viable CD14+ monocytes}$$

1. Determine the cell count from the samples and ensure that the total amount of WBC is no greater than $1 \times 10^6/100\,\mu L$. If necessary, dilute the samples with PBS/EDTA/0.5% HSA.
2. Determine the viability of each fraction either using trypan blue exclusion or propidium iodide exclusion during the flow-cytometry analysis (recommended).
3. Label four tubes as follows: (1) original fraction; (2) positive fraction; (3) negative fraction; and (4) wash fraction. Place 100 μL of cell suspension in each tube.
4. Add 20 μL of CD14-PE and 10 μL of CD15-FITC to each tube.
5. Incubate the tubes for 10 min in the dark at 2–8°C.
6. Add 1 mL of ammonium chloride red blood cell lysing solution and incubate for 10 min at room temperature.
7. Spin down the cells for 5 min at $300g$ ($\pm 10g$) at room temperature.
8. Wash cells with 1 mL of PBS/EDTA/0.5% HSA. Spin down the cells for 5 min at $300g$ ($\pm 10g$) at room temperature. Remove supernatant completely.
9. Resuspend cells in an adequate volume of buffer for flow-cytometric analysis according to routine laboratory practice. To assess cell viability and to exclude the effects of non-specific binding of antibodies by dead cells, add propidium iodide (PI) in a concentration of 1μg/mL to each tube immediately prior to acquisition.
10. Acquire at least 10,000 events per sample—*see* **Fig. 1** for detailed gating strategy.

3.2. Immature Monocyte-Derived Dentritic Cells (MoDCs)

3.2.1. Generation of Immature DC From CD14⁺ Cells

1. Calculate the required volume of medium to achieve a final concentration of 2×10^6 CD14⁺ cells per mL.
2. Transfer the CD14⁺ cells of the positive fraction to centrifuge tubes or a 150-mL collection bag and centrifuge for 10 min at $300g$ without brake.
3. Freshly prepare DC generation medium.
4. Resuspend cells in DC generation medium, prewarmed to 37°C, at a density of $2 \times 10^6/$ mL and transfer them into culture bags or flasks. Incubate cells in a CO_2 incubator with 5% CO_2 and 37°C.

After 72 h:

5. Prepare fresh DC generation medium.
    Add a volume of DC generation medium, prewarmed to 37°C, to each flask equal to one third of the original culture volume. Replace cells in incubator.

After 120 h (5 d):

6. Repeat step 5.

After 7 d:

7. Gently mix cultures and pool their contents into centrifuge tubes or centrifugable bags. If cells remain in culture vessel, add 10 mL PBS/EDTA buffer, prewarmed to 37°C, into each flask or bag and incubate for 5 min at 37°C. Add all supernatants into centrifuge tubes.
8. Centrifuge for 10 min at $300g$ without brake at room temperature; remove supernatant.
    Pool cells into a single tube and suspend with PBS/EDTA solution. Remove a small sample for cell count, viability testing, and flow-cytometry analysis.

3.2.2. Flow-Cytometry Analysis of Immature Dendritic Cells (*Fig. 2*)

A minimum suggested panel of Ab to evaluate the generation of DC from CD14⁺ cells is anti-CD14, anti-HLA-DR, anti-CD86, anti-CD80, and anti-CD83. Immature
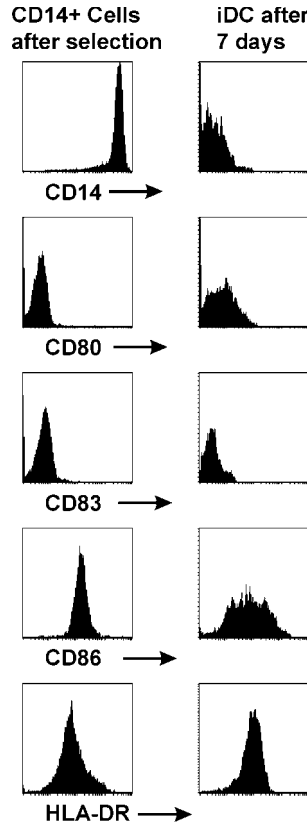
Fig. 2. Generation of iDC from CD14+ cells. Representative flow cytometry analysis of freshly isolated CD14+ monocytes, and the same cells after 7-d culture with granulocyte-macrophage colony-stimulating factor and interleukin-4. The cells rapidly lose expression of CD14 (in this case from a mean fluorescence of 2850 for the monocytes reduced to only 5 for the dendritic cells [DC]). The DC also do not express CD80 or CD83, and only low levels of CD86 and HLA-DR, indicating that these are homogeneous, immature DC.

DC should have a CD14 low/negative, CD83⁻, CD80⁻, CD86⁺, HLA⁻DR⁺ phenotype— *see* **Fig. 2**.

Cells should be stained for flow cytometry as detailed under **Subheading 3.1.3.**, without the RBC lysis step. Acquire at least 10,000 events; *see* **Fig. 2** for detailed gating strategy.

3.3. Blood DC

This section details the isolation of mDC and pDC. Each method is detailed separately, but the notes are combined in a single section at the end.

3.3.1. Plasmacytoid Dendritic Cells (pDC)

pDC were previously identified as CD11c$^-$/ CD123$^+$ DC. We have developed a panel of new antibodies against blood DC. pDC are specifically recognized by the antibodies BDCA-2 and BDCA-4. These reagents are used in tandem to carry out, and determine the success of, pDC selection—BDCA-4 is used to isolate the cells, and BDCA-2 to validate the purity of the isolated pDC.

This method describes the separation of BDCA-4$^+$ cells from a leukapheresis product containing up to 40×10^9 cells. The expected yield from this starting population is up to 0.2×10^9 BDCA-4$^+$ pDC. The range of pDC in peripheral blood is 0.17–0.22% of leukocytes (median $0.21\% \cong 1.1 \times 10^4$ cells/mL blood).

3.3.1.1. IMMUNOMAGNETIC LABELING

Determine the total number of leukocytes. The following protocol is designed for leukapheresis products containing 10–40×10^9 WBC. Use only CliniMACS PBS/EDTA buffer (referred to as PBS/EDTA buffer) supplemented with HSA or BSA (final concentration 0.5%), which is required to inactivate and to coat the surfaces of tubing and bags.

1. Determine the weight of an empty 600-mL transfer pack to be used as a cell preparation bag. Transfer the leukapheresis product into the cell preparation bag and record the weight.
2. Dilute the leukapheresis product with HSA- or BSA-supplemented PBS/EDTA buffer to maximal filling volume and centrifuge the cell suspension for 15 min at 200g (room temperature, 19–25°C), no brake.
3. Discard supernatant carefully and repeat washing step.
4. Resuspend the cell pellet and adjust to a final sample volume of 95 mL.
5. Add the entire contents of one vial CliniMACS Anti-BDCA-4 MicroBeads (7.5 mL) and mix carefully.
6. Incubate the cell preparation bag for 30 min at room temperature (19–25°C) on an orbital shaker at 25 rpm maximum (*see* **Note 8**).
7. Add HSA- or BSA-supplemented CliniMACS PBS/EDTA buffer to a final volume of 600 mL for cell washing and centrifuge for 15 min at 300g (19–25°C), no brake. Remove as much supernatant as possible from the cell pellet and carefully resuspend cells. Repeat washing procedure (*see* **Note 9**).
8. Remove supernatant and then adjust volume to 100 mL.
9. Retain a 0.5-mL sample from this original cell suspension (*see* **Note 10**) and place into a sample tube for analysis (*see* **Subheading 3.3.1.3.**). Store at room temperature until analyzed.

3.3.1.2. AUTOMATED SEPARATION

1. Determine the weight of an empty 150-mL transfer pack with a Luer/Spike Interconnector inserted and attach this bag (cell collection bag) to the cell collection port. Ensure that all slide clamps are open.
2. Switch on CliniMACS^{plus} instrument and select separation program "ENRICHMENT 3.1."
3. Confirm your choice by pressing "ENT" and enter the parameters requested on the screen.
4. Follow the tubing set installation instructions on the screen and start the automated separation program.

5. Determine the weight of the filled cell collection bag after separation and take a well-mixed sample for flow cytometric analysis and determination of the total cell number.
6. The enriched pDC can be washed further in the cell collection bag and then transferred into cell-culture bags or flasks for culturing. They also can be frozen in HSA containing 10% DMSO.

3.3.1.3. FLOW CYTOMETRIC ANALYSIS OF ISOLATED CELLS (**FIG. 3**)

The yield of pDC is determined from cell counts and phenotype analysis of the original and positive fractions. Determine the cell count from the samples and ensure that the total amount of WBC is no greater than $1 \times 10^6/100$ µL. If necessary, dilute the samples with PBS/EDTA/0.5% HSA. For accurate determination of pDC numbers in peripheral blood, samples are stained with anti-CD45 to positively identify leukocytes, and BDCA-2 to identify pDC. Additionally, anti-CD123 staining as a second pDC marker may be used if sufficient channels are available on the flow cytometer.

1. Centrifuge 5 min at 300*g*, remove supernatant, and resuspend pellet in 20 µL P/E/B.
2. Staining volume is 110 µL. Add 22 µL FcR-blocking reagent, 58 µL P/E/B, 10 µL CD45.FITC, 10 µL anti-BDCA-2.PE, and 10 µL CD123.APC or P/E/B to each sample. Incubate for 10 min at 4°C.
3. Add 900 µL of ammonium chloride lysing solution to all fractions and incubate for another 10 min in the dark at room temperature.
4. Centrifuge 5 min at 300*g*, remove supernatant, and add 1 mL P/E/B. Mix and centrifuge again 5 min at 300*g*.
5. Remove supernatant and resuspend cells in an adequate volume of buffer (e.g., 0.5 mL) for flow-cytometric analysis. To assess cell viability and to exclude the events of nonspecific binding of antibodies by dead cells, add PI in a concentration of 1µg/mL to each tube immediately prior to acquisition.
6. For optimal analysis of the original fraction, a minimum of 100 BDCA-2^{+} events should be counted (i.e., at a frequency of 0.2% BDCA-2^{+} among unseparated cells, 50,000 viable cells have to be acquired). For the highly pure positive fraction, it is sufficient to acquire 10,000 events. For detailed gating strategy *see* **Fig. 3**.
7. For a sample calculation of pDC purity and yield *see* **Fig. 3**.

3.3.2. Myeloid DC

Isolation of CD1c^{+} myeloid dendritic cells is performed by two magnetic separation steps. In the first step, CD1c-expressing cells are indirectly labeled with CliniMACS CD1c(anti-BDCA-1)-biotin. In the same step, CD19-expressing B-cells are directly labeled with CliniMACS CD19 MicroBeads. There is a small population of CD1c-expressing B-cells, and this subpopulation of B-cells and all other CD19^{+} cells are depleted using the CliniMACS device in the first step. In the second step, the CD19-depleted fraction is magnetically labeled by CliniMACS Anti-Biotin MicroBeads to enrich CD1c^{+} dendritic cells.

This method describes the separation of CD1c^{+} cells from a leukapheresis product containing up to 40×10^9 cells. The expected yield from this starting population is up to 0.2×10^9 CD1c^{+} mDC. The range of mDC in peripheral blood is 0.17–0.24% of leukocytes (median 0.21% $\cong 1.1 \times 10^4$ cells/mL blood).

Unseparated Fraction   **Positive Fraction**

Fig. 3. Determination of PDC purity and yield. Representative flow cytometry analysis of a leukapheresis sample before and after CliniMACS Anti-BDCA-4 separation. Samples are first gated on CD45.FITC vs Side Scatter to exclude debris and focus on white blood cells (WBC). Results from R1 are plotted Anti-BDCA-2.PE vs PI to exclude dead cells (R2). A combined gate is then made (e.g., G3 = R1*R2 in "Cell Quest" software, BD biosciences). G3 therefore contains all viable WBC. Anti-BDCA-2.PE is plotted against CD123.APC to evaluate the numbers of live BDCA-2+CD123+ cells (viable PDC) in the samples (R3). In this example, the start population has 0.31% PDC cells, which is enriched to 92.5% after CliniMACS sorting.

To calculate yield:

$$\text{Total, viable PDC} = \frac{\text{total WBC} * \% \text{ viable PDC (purity)}}{100\%}$$

Example:

      Total cell number positive fraction: 2.84×10^7

      Viability of positive fraction = 97.6% (G3)

      Purity of positive fraction = 92.5% (R3)

      Percentage viable PDC = 97.6% * 92.5% = 90.28%

$$\text{Total, viable PDC} = \frac{2.84 \times 10^7 * 90.28\%}{100\%} = 2.56 \times 10^7 \text{ viable PDC}$$

3.3.2.1. Immunomagnetic Labeling—1

Determine the total number of leukocytes. The following protocol is designed for leukapheresis products containing $10–40 \times 10^9$ WBC. Use only PBS/EDTA buffer supplemented with HSA or BSA (final concentration 0.5%), which is required to inactivate and to coat the surfaces of tubing and bags. During the depletion phase, it is necessary to know the percentage of CD19$^+$ cells in the sample—this must be determined by flow-cytometry analysis beforehand.

1. Determine the weight of an empty 600-mL transfer pack to be used as a cell preparation bag. Transfer the leukapheresis product into the cell preparation bag and record the weight.
2. Dilute the leukapheresis product (1:3) with CliniMACS PBS/EDTA buffer (supplemented with 0.5% HSA) and centrifuge the cells at 200*g* for 15 min without brake.
3. Remove supernatant, taking care not to resuspend the pellet, and adjust sample to a final volume of 90 mL.
4. Resuspend cell pellet, add entire contents of one vial of CliniMACS CD1c (anti-BDCA-1)-biotin (5 mL) and one vial CliniMACS CD19 MicroBeads (7.5 mL) and mix carefully.
5. Incubate the cell preparation bag for 30 min at room temperature (19–25°C) on an orbital shaker at 25 rpm maximum.
6. Add HSA- or BSA-supplemented CliniMACS PBS/EDTA buffer to a final volume of 600 mL for cell washing and centrifuge for 15 min at 300*g* (19–25°C), no brake.
7. After centrifugation, remove supernatant, taking care not to resuspend the cell pellet, and adjust sample to a volume of 100 mL.
8. Remove a sample of 0.5 mL with a 10-mL syringe, taking care to get a well mixed aliquot (*see* **Note 10**), and place into a sample tube for analysis (*see* **Subheading 3.3.2.5.**). Store at room temperature (19–25°C) until analyzed.

3.3.2.2. Automated Separation—1

1. Connect a 600-mL transfer pack with a Luer/Spike Interconnector to the cell-collection port of the CliniMACS tubing set. Ensure that all Luer/Spike slide clamps are open.
2. Switch on CliniMACS^{plus} instrument and select the separation program called "DEPLETION 2.1."
3. Confirm your choice by pressing "ENT" and enter the Ref-number of the CliniMACS LS tubing set (ref. no. 162-01). Follow instructions given on the instrument screen for installation of the tubing set (*see* **Note 11**).
4. Enter WBC concentration of the sample after CD19 labeling, ready to be loaded to the instrument. Then enter frequency of labeled (CD19$^+$) cells and sample loading volume.
5. Start the separation process.

3.3.2.3 Immunomagnetic Labeling—2

1. After finishing the depletion process, centrifuge the cell preparation bag (CD19-depleted fraction) at 300*g* for 15 min without brake.
2. Remove supernatant, taking care not to resuspend the pellet, and adjust sample to a final volume of 95 mL.
3. Add the entire contents of one vial CliniMACS Anti-Biotin MicroBeads (7.5 mL) and mix carefully.
4. Incubate the cell preparation bag for 30 min at room temperature (19–25°C) on an orbital shaker at 25 rpm maximum.

5. Add HSA-supplemented PBS/EDTA buffer to a final volume of 600 mL for cell washing, and centrifuge for 15 min at 300g, 19–25°C, no brake.
6. After centrifugation, adjust the volume of the leukapheresis product for loading on the CliniMACS^{plus} instrument to 100 mL.
7. Resuspend cells, and remove a 0.5-mL sample using a 10-mL syringe, taking care to get a well mixed aliquot for analysis. Determine at least the cell concentration, viability, and BDCA-1 cell frequency/cell number.

3.3.2.4. AUTOMATED SEPARATION—2

1. Connect a 150-mL or 600-mL transfer pack with a Luer/Spike Interconnector to the cell collection port of the CliniMACS tubing set. Ensure that all Luer/Spike slide clamps are open.
2. Switch on CliniMACS^{plus} instrument and select separation program "ENRICHMENT 3.1."
3. Confirm your choice by pressing "ENT" and enter the parameters requested on the screen.
4. Follow the tubing set installation instructions on the screen and start the automated separation program.
5. When the separation has finished, determine the weight of the filled cell collection bag, and take a well mixed sample for flow-cytometric analysis and determination of total cell number.
6. The enriched mDC can be washed further in the cell collection bag and then transferred into cell-culture bags or flasks for culturing. They also can be frozen in HSA containing 10% DMSO.

3.3.2.5. FLOW-CYTOMETRIC ANALYSIS OF ISOLATED CELLS (**FIG. 4**)

Analysis of the following fractions—original, CD19-depleted, and BDCA-1$^+$—allows the most accurate determination of yield. Determine the cell count from the samples and ensure that the total amount of WBC is no greater than $1 \times 10^6/100$ µL. If necessary, dilute the samples with PBS/EDTA/0.5% HSA. For accurate determination of mDC numbers, cells are stained for analysis with a combination of CD1c (PE), CD20 (APC), and CD45 (FITC) monoclonal antibody reagents. Samples are stained with anti-CD45 to positively identify leukocytes; CD1c (BDCA-1) is a marker specific for mDC and a subpopulation of B-cells in blood. CD20 is used to stain B-cells to control the depletion efficiency, since the antigen is specifically expressed upon B-cells and labeling with a CD19 fluorochrome is not optimal after CD19 Micro-Beads incubation.

1. Place each sample in a suitable tube for flow cytometry. Centrifuge 5 min at 300g, remove supernatant, and resuspend pellet in 20 µL P/E/B.
2. Staining volume is 110 µL. Add 58 µL P/E/B, 22 µL FcR-blocking reagent, 10 µL CD45.FITC, 10 µL CD1c.PE, and 10 µL CD20.APC. Incubate for 10 min at 4°C.
3. Add 900 µL of ammonium chloride lysing solution to the fractions and incubate for another 10 min in the dark at room temperature.
4. Centrifuge 5 min at 300g, remove supernatant, and add 1 mL P/E/B. Mix and centrifuge again 5 min at 300g.
5. Remove the supernatant, resuspend the cell pellet, add 1000 µL P/E/B and 1 µL PI immediately before FCM analysis.
6. For optimal analysis of the original fraction, a minimum of 100 BDCA-1$^+$ events should be counted (i.e., at a frequency of 0.2% BDCA-1$^+$ among unseparated cells, 50,000 viable

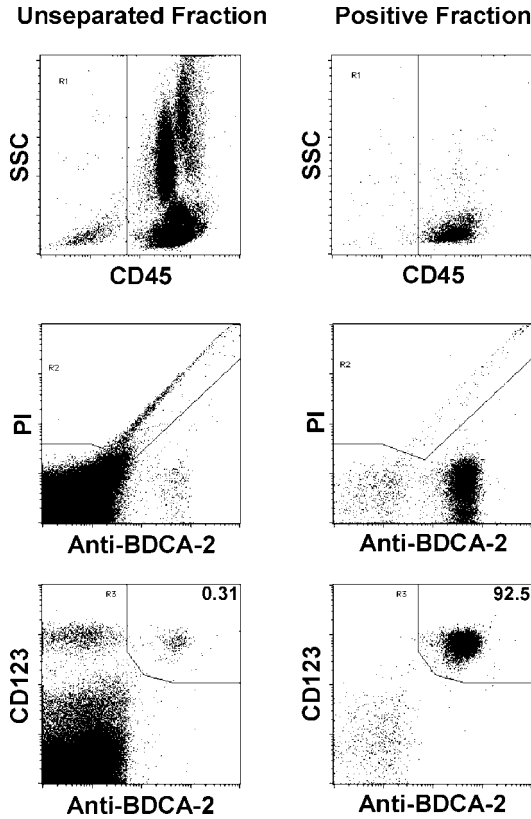**Unseparated Fraction**   **CD19 depleted Fraction**   **Positive Fraction**
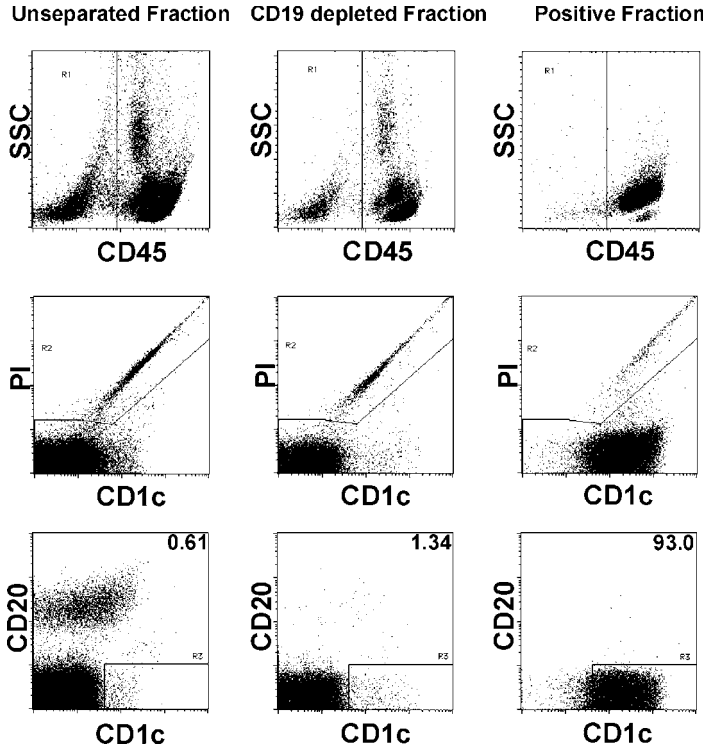
Fig. 4. Determination of MDC purity and yield. Representative flow cytometry analysis of a leukapheresis sample before separation, after CliniMACS CD19 depletion and following CliniMACS CD1c (Anti-BDCA-1) separation. Samples are first gated on CD45.FITC vs Side Scatter to exclude debris and focus on white blood cells (WBC). Results from R1 are plotted CD1c.PE vs PI to exclude dead cells (R2). A combined gate is then made (e.g., G3 = R1*R2 in "Cell Quest" software, BD biosciences). G3 therefore contains all viable WBC. CD1c.PE is plotted against CD20.APC to evaluate the numbers of live CD1c+CD20– cells (viable MDC) in the samples (R3). In this example, the start population has 0.61% MDC cells, which is pre-enriched to 1.34% after CD19 depletion and finally enriched using CD1c (Anti-BDCA-1)-Biotin and Anti-Biotin MicroBeads up to 93.0%.

To calculate yield:

$$\text{Total, viable MDC} = \frac{\text{total WBC} \ * \ \% \ \text{viable MDC} \ (\text{purity})}{100\%}$$

Example:

Total cell number positive fraction: 7.41×10^7

Viability of positive fraction = 97.5% (G3)

Purity of positive fraction = 93.0% (R3)

Percentage viable MDC = 97.5% * 93.0% = 90.68%

$$\text{Total, viable MDC} = \frac{7.41 \times 10^7 \ * 90.68\%}{100\%} = 6.72 \times 10^7 \ \text{viable MDC}$$

cells have to be acquired). For the highly pure positive fraction, it is sufficient to acquire 10,000 events. For detailed gating strategy, *see* **Fig. 4**.

7. For a sample calculation of mDC purity and yield, *see* **Fig. 4**.

4. Notes

1. Leukapheresis procedures can lead to the activation of monocytes, which ultimately decreases the yield of DC obtained from the isolated cells. Reducing the inlet flow rate of leukapheresis (ideally to 50 mL/min) substantially reduces monocyte activation.

2. Storage of leukapheresis samples decreases the quality of the CD14 separation and the yield of DC. Preparation and separation of the leukapheresis product should be performed immediately after leukapheresis. If the leukapheresis product must be stored, it should be kept at controlled room temperature (19–25°C) and should not be stored for more than 24 h before separation. Storage of isolated monocytes is also not recommended.

3. One vial of CliniMACS CD14 Reagent is capable of labeling up to 4×10^9 CD14$^+$ monocytes out of a total leukocyte number of up to 20×10^9 cells.

4. The CliniMACS CD14 Reagent is for single use only. Storage at +2°C to +8°C is recommended. Do not freeze. Do not use after expiration date.

5. If samples are also kept from the negative and waste fractions, in the unlikely event of lower yield, it is easier to trace the CD14$^+$ cells.

6. The target cells for the separation are the CD14^{high} monocytes. For accurate analysis, any CD14^{dim} cells have to be excluded by using CD15 as an exclusion marker for granulocytes.

7. During preclinical work-up, BSA may be substituted for HSA on the grounds of cost.

8. As an alternative, cell bags can be gently shaken every 5 min by hand during magnetic labeling.

9. To get highest purities of PDC, it is essential to get rid of platelets, which otherwise block the anti-BDCA-4 reagent. Never omit one of the initial two washing steps to abbreviate the protocol.

10. To get a representative aliquot from a cell fraction out of a bag, use at least a 10-mL syringe and refill it repeatedly before taking the sample.

11. Make sure that the tubing set is correctly inserted. If one valve is blocked, the whole separation can fail. All bags (cell collection bag, negative fraction bag, buffer waste bag) must be unsealed when procedure is started.

References

1 Banchereau, J. (1997) Dendritic cells: therapeutic potentials. *Transfus. Sci.* **18,** 313–326.

2 Dzionek, A., Fuchs, A., Schmidt, P., et al. (2000) BDCA-2, BDCA-3, and BDCA-4: three markers for distinct subsets of dendritic cells in human peripheral blood. *J. Immunol.* **165,** 6037–6046.

3 Dzionek, A., Inagaki, Y., Okawa, K., et al. (2002) Plasmacytoid dendritic cells: from specific surface markers to specific cellular functions. *Hum. Immunol.* **63,** 1133–1148.

4 Fay, J. (1998) Dendritic cells in the treatment of cancer. *Baylor Univ. Med. Cent. Proc.* **11(4),** 217–219.

5 Pickl, W. F., Majdic, O., Kohl, P., et al. (1996) Molecular and functional characteristics of dendritic cells generated from highly purified CD14+ peripheral blood monocytes. *J. Immunol.* **157,** 3850–3859.

6 Thurner, B., Röder, C., Dieckmann, D., et al. (1999) Generation of large numbers of fully mature and stable dendritic cells from leukapheresis products for clinical application. *J. Immunol. Meth.* **223,** 1–15.

7 Cella, M., Facchetti, F., Lanzavecchia, A., and Colonna, M. (2000) Plasmacytoid dendritic cells activated by influenza virus and CD40L drive a potent TH1 polarization. *Nat. Immunol.* **1,** 305–310.

8 Cella, M., Jarrossay, D., Facchetti, F., et al. (1999) Plasmacytoid monocytes migrate to inflamed lymph nodes and produce large amounts of type I interferon. *Nat. Med.* **5,** 919–923.

9. Fong, L., Hou, Y., Rivas, A., et al. (2001) Altered peptide ligand vaccination with Flt3 ligand expanded dendritic cells for tumor immunotherapy. *PNAS* **98,** 8809–8814.

10. Ito, T., Inaba, M., Inaba, K., et al. (1999) A CD1a+/CD11c+ subset of human blood dendritic cells is a direct precursor of Langerhans cells. *J. Immunol.* **163,** 1409–1419.

6

Generation of Clinical-Grade Monocyte-Derived Dendritic Cells Using the CliniMACS System

Thomas Putz, Hubert Gander, Reinhold Ramoner, Claudia Zelle-Rieser, Andrea Rahm, Walter Nussbaumer, Georg Bartsch, Lorenz Höltl, and Martin Thurnher

Summary

We describe the generation of monocyte-derived dendritic cells (MoDC) from leukapheresis products using the CliniMACS system from Miltenyi Biotec. In a clinical setting, the method turned out to be feasible for the generation of clinical-grade MoDC from patients with metastatic renal-cell carcinoma. MoDC generated with this system exhibited a fully mature phenotype as well as high migratory and T-cell stimulatory capacity.

Key Words: Monocyte-derived dendritic cells; immunomagnetic isolation; leukapheresis; purity; CD14; CD83; CCR7; migration; proliferation.

1. Introduction

Dendritic cells (DC) are antigen-presenting cells (APC) that can induce vigorous T-lymphocyte responses *(1)*. DC pick up and process antigens to present antigenic peptides in a major histocompatibility complex (MHC)-restricted fashion to the T-cell receptor of T-cells. DC also provide co-stimulatory signals required for T-cell activation *(1)* and bias T helper cell differentiation *(2)*. In addition, DC can enhance B-lymphocyte and natural killer (NK)-cell responses *(1,3)*. The in vivo immunogenicity of DC has meanwhile been tested and confirmed in numerous clinical trials *(4)*.

One way to generate DC in vitro is to differentiate them from CD14$^+$ monocytes in a two-step culture system *(5,6)* (**Fig. 1**). In a first step, granulocyte/macrophage colony-stimulating factor (GM-CSF) and interleukin (IL)-4 promote the development of immature DC with high antigen-capturing capacity. In the second step, proinflammatory factors induce the terminal maturation of CD83$^+$ DC *(7,8)*, which stably express MHC-peptide complexes *(9)*, abundant T-cell adhesion, and co-stimulatory molecules (CD80 and CD86) *(10)* , as well as chemokine receptors such as CCR7, which direct DC migration to lymph nodes *(11)*.
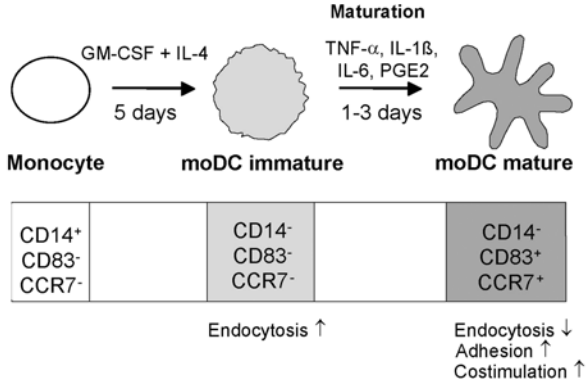
Fig. 1. Monocyte-derived dendritic cell generation in the two-step granulocyte/macrophage colony-stimulating factor (GM-CSF)/interleukin (IL)-4 culture system.

Various methods such as adherence to plastic or centrifugal elutriation have been used to isolate monocytic precursors for subsequent DC differentiation *(12,13)*. Yet another approach to isolate monocytes is based on the immunomagnetic isolation of CD14+ cells. In the present work we have used the immunomagnetic isolation system from Miltenyi Biotec to generate monocyte-derived DC (MoDC). We analyzed MoDC with regard to phenotype as well as migratory and T-cell stimulatory capacity. In a clinical setting, we also used the CliniMACS system to generate MoDC from leukapheresis products.

2. Materials

2.1. Leukapheresis

1. Cobe Spectra Apheresis System (Gambro BCT, Lakewood, CO).
2. Anticoagulant Citrate Dextrose Solution (ACD-A) (Baxter, Austria).
3. Cell-culture flasks, 162-cm^2 (Costar, Germany).
4. Luer/Spike Interconnector (Miltenyi Biotec, Bergisch Gladbach, Germany).
5. CliniMACS PBS/EDTA buffer (Miltenyi Biotec).
6. Heat-inactivated human AB plasma: human AB plasma (local Institute of Blood Transfusion) from individuals tested negative for various viruses 6 mo after donation. In addition, after heat-inactivation (30 min at 56°C) plasma was subjected to sterility testing at the local Institute of Hygiene (bacteria, fungi).
7. Neubauer chamber.
8. Plaxan (Gatt, Austria).

2.2. Enrichment of Monocytes

1. CliniMACS CD14 Reagent (Miltenyi Biotec).
2. CliniMACS Tubing Set 600 (Miltenyi Biotec).
3. CliniMACS instrument (Miltenyi Biotec).
4. Luer/Spike Interconnector (Miltenyi Biotec).
5. Cell-culture flasks, 162-cm^2 (Costar).

6. AIM-V (Invitrogen, Carlsbad, CA).
7. Heat-inactivated human AB plasma.
8. HEPES (Bio Whittaker, Europe).
9. 2-Mercaptoethanol (Merck, Germany).
10. Recombinant human GM-CSF (Leucomax, Novartis).
11. Recombinant human IL-4 (Strathmann Biotech, Hannover, Germany).
12. Dimethylsulphoxide (DMSO) (Sigma, Germany).
13. Six-well plates (Costar).
14. Renal-cell carcinoma lysate *(12)*.
15. Keyhole limpet hemocyanin (KLH), endotoxin-free/pyrogen-free (Calbiochem-Nova-biochem, San Diego, CA).
16. Tumor necrosis factor (TNF)-α* (R&D Systems, Minneapolis, MN).
17. IL-1β* (R&D Systems).
18. IL-6* (R&D Systems).
    These cytokines can now be purchased in GMP quality.
19. Prostaglandin E2 (Prostin E2) (Pharmacia & Upjohn, Vienna, Austria).
20. Lactated Ringer's solution (Mayerhofer Pharmazeutika, Linz, Austria).
21. Luer/Spike Interconnector (Miltenyi Biotec).

2.3. Flow-Cytometric Analysis

1. PE conjugated antihuman CD83 (cat. no. 556855, BD, Mountain View, CA).
2. PE conjugated mouse IgG1-κ monoclonal immunglobulin isotype control (BD, cat. no. 555749).
3. Rat IgG2a anti-human CCR7 (Dr. Reinhold Förster, Hannover, Germany, or BD).
4. FITC conjugated mouse anti-rat IgG2a monoclonal antibody (BD, cat. no. 553896).
5. Rat IgG2a-κ monoclonal immunoglobulin isotype control (BD, cat. no. 555841).
6. FACSCalibur and CellQuest software (BD).

2.4. Migration Assay

1. Twenty-four-well Transwell chambers (Corning Costar, Cambridge, MA) with polycarbonate filters of 6.5 mm in diameter and 5 µm pore size.
2. AIM-V (Invitrogen).
3. Heat-inactivated human AB plasma.
4. Macrophage inflammatory protein (MIP)-3β (CCL19) (R&D Systems).
5. Lipopolysaccharide (LPS) from *Salmonella abortus equi* (Sigma, Austria).
6. FACSCalibur and CellQuest software (BD).

2.5. Mixed Leukocyte Reaction

1. Peripheral blood mononuclear cells (PBMC) from healthy donors for T-cell isolation.
2. CD4 MicroBeads (Miltenyi Biotec).
3. Irradiated MoDC (3000 rad).
4. Ninety-six-well flat-bottomed tissue-culture plates (BD Falcon).
5. AIM-V (Invitrogen).
6. Heat-inactivated human AB plasma.
7. [^{3}H]thymidine (1 µCi/well = 37 kBq/well, ICN Biomedicals).
8. Skatron cell harvester, glass fiber filters and scintillation vials (Skatron, Lier, Norway).
9. OptiPhase "Hi-Safe2" Scintillator (cat. no. 0197435241 Wallac, Fisher).
10. Liquid-scintillation counter (Wallac 1410, Pharmacia).
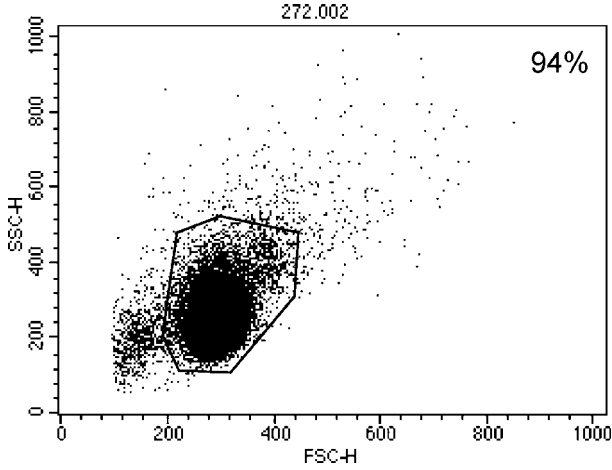
Fig. 2. Purity of monocytes isolated with the CliniMACS system. A representative sample with 94% CD14+ cells is shown.

3. Methods

3.1. Leukapheresis

At the local Institute for Blood Transfusion, renal-cell carcinoma (RCC) patients underwent a standard leukapheresis procedure performed with the Cobe Spectra cell separator. Using the MNC program at a continuous whole-blood inlet flow rate ranging from 50 to 70 mL/min (*see* **Note 1**), 3–5 L of whole blood were processed. ACD-A at a 1:12 ratio was used for anticoagulation.

Transfer the apheresis product (50–100 mL) to a cell-culture flask using a Luer/ Spike Interconnector and adjust to 200 mL using CliniMACS PBS/EDTA buffer supplemented with 2% heat-inactivated human AB plasma. Determine the total cell number with a Neubauer chamber in the presence of Plaxan (to lyse red blood cells). **Table 1** lists the numbers of cells obtained from 16 RCC patients.

3.2. Generation of MoDC From Leukapheresis Products Using the CliniMACS System

3.2.1. Enrichment of Monocytes

1. CD14+ monocytes were separated from apheresed cells by positive selection using the CD14 reagent, the CliniMACS Tubing Set 600 (for up to 20×10^9 cells), and the Clini-MACS instrument. All steps were carried out according to the manufacturer's instructions. (For a detailed protocol *see* Chapter 5 in this volume.)
2. Remove an aliquot of your final isolated positive fraction using the Luer/Spike Interconnector for flow-cytometric determination of monocyte purity (**Fig. 2**). Yields of CD14+ cells from RCC patients are listed in **Table 1**.

Table 1
Monocyte Enrichment and MoDC Generation From PBMC of RCC Patients Using the CliniMACS System

Patients	PBMC ($\times10^8$)	CD14$^+$ cells ($\times10^8$)	MoDC ($\times10^8$)	CD14$^+$ (% of PBMC)	MoDC (% of PBMC)	MoDC yield (% of CD14$^+$)	lymphocyte contamination of MoDC (%) [a]
Patient 1	15.00	2.25	1.80	15	12	80	1.7
Patient 2	19.00	3.50	1.60	18	8	46	1.1
Patient 3	20.00	5.80	1.00	29	5	17	2.7
Patient 4	79.00	6.00	2.65	8	3	44	4.6
Patient 5	50.00	8.20	1.40	16	3	17	6.7
Patient 6	100.00	7.48	2.97	7	3	40	3.2
Patient 7	23.00	7.00	2.30	30	10	33	1.7
Patient 8	60.00	7.30	2.00	12	3	27	1.8
Patient 9	39.00	4.00	0.60	10	2	15	2.8
Patient 10	90.00	8.00	6.50	9	7	81	1.9
Patient 11	50.00	5.00	1.70	10	3	34	6.5
Patient 12	90.00	20.00	8.00	22	9	40	1.8
Patient 13	90.00	13.00	3.36	14	4	26	5.1
Patient 14	48.00	6.50	2.00	14	4	31	1.5
Patient 15	118.00	6.70	0.88	6	1	13	1.6
Patient 16	74.00	7.00	5.90	9	8	84	ND
mean	**60.31**	**7.36**	**2.79**	**14**	**5**	**39**	**3**
SD	31.30	4.00	2.09	7	3	23	2

[a] Lymphocyte contamination was determined by selective forward/sideward scatter gating (*see also* **Fig. 3B**).

ND, Not determined; MoDC, monocyte-derived dendritic cells; PBMC, peripheral blood mononuclear cells; RCC, renal-cell carcinoma; SD, standard deviation.

3. CD14$^+$ cells (50×10^6 in 50 mL) were cultured in 162-cm^2 cell-culture flasks in AIM-V containing 1% heat-inactivated human AB plasma, 10 mM HEPES, and 50 µM 2-mercaptoethanol as well as a combination of recombinant human GM-CSF (1000 U/mL) and recombinant human IL-4 (1000 U/mL).

4. After 2 d of culture, 50 mL of fresh medium containing supplements were added.

5. On d 5, MoDC were harvested and frozen in liquid nitrogen using a standard protocol (50% AIM-V, 40% human AB plasma, 10% DMSO).

6. Two days before vaccination, d-5 MoDC were thawed, counted, and replated in 6-well plates at 1.8×10^6 cells per well in 6 mL of fresh medium containing GM-CSF (1000 U/mL) and IL-4 (250 U/mL) as well as 1% heat-inactivated human AB plasma (*see* **Notes 2–4**). All cells were pulsed with autologous RCC lysate (10 µg/mL) and half of the cells also with KLH (10 µg/mL). Maturation of thawed d-5 MoDC was induced simultaneously with the RCC lysate/KLH pulses by stimulation with a "cocktail" consisting of 1000 U/mL of recombinant human TNF-α, IL-1β (5 ng/mL), IL-6 (10 ng/mL), and 1 µM prostaglandin E2 *(14,15)*.

7. After 48 h, MoDC were harvested, washed, counted, and resuspended in lactated Ringer's solution containing 1% heat-inactivated human AB serum.

8. Remove an aliquot of your final MoDC suspension using the Luer/Spike Interconnector for flow-cytometric determination of CD83 expression.

Only samples with CD83 expression >85% were released (**Fig. 3A**). Purity of MoDC ranged from 93 to 99% (mean: 97%). Sterility testing was performed at the local Institute of Hygiene; all tests were negative (100% sterility).

3.3. Flow-Cytometric Analysis

To determine surface expression of CD83 or CCR7, cell suspensions were labeled for 30 min on ice with mouse anti-CD83-PE or rat anti-CCR7 followed by anti-rat IgG2a-FITC. The samples were analyzed using the FACSCalibur and CellQuest software from BD.

3.4. Migration Assay

Chemotactic capacity of MoDC was measured by assessing migration through a polycarbonate filter (6.5 mm in diameter and 5 µm pore size) in 24-well Transwell chambers *(16)*.

1. 600 µL AIM-V supplemented with 1% heat-inactivated human AB plasma with or without 300 ng/mL MIP-3β (CCL19) was added to the lower chamber. Immature MoDC or MoDC matured with either LPS or "cocktail" for 48 h were added to the upper chamber (1×10^5 cells in a total volume of 100 µL) and incubated for 3 h at 37°C.

Fig. 3. *(opposite page)* Purity and homogeneity of monocyte-derived dendritic cells (MoDC) generated with the CliniMACS system. Monocytes were propagated for 5 d in the granulocyte/macrophage colony-stimulating factor (GM-CSF)/interleukin (IL)-4 cell-culture system, pulsed with autologous tumor lysate, and stimulated for 2 d with the maturation cocktail. A representative example is shown. **(A)** Ninety percent of all MoDC generated expressed the maturation marker CD83. **(B)** The MoDC portion represented 97% of all cells (gate 1); contaminating lymphocytes were approx 3% (gate 2). **(C)** MoDC displayed a homogenous morphology with typical veils.
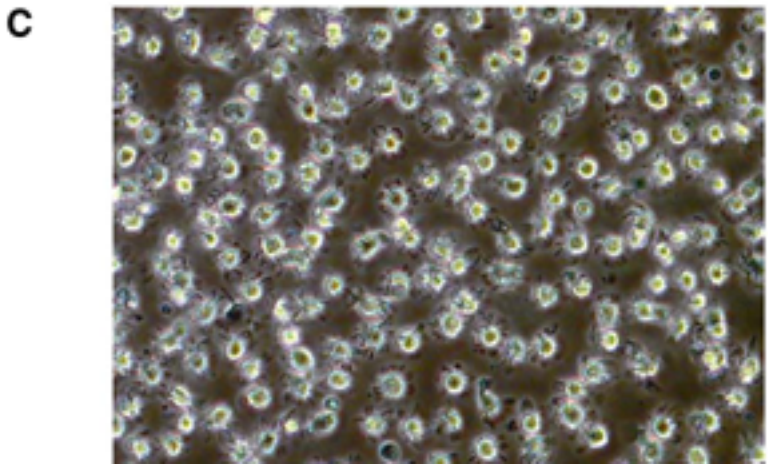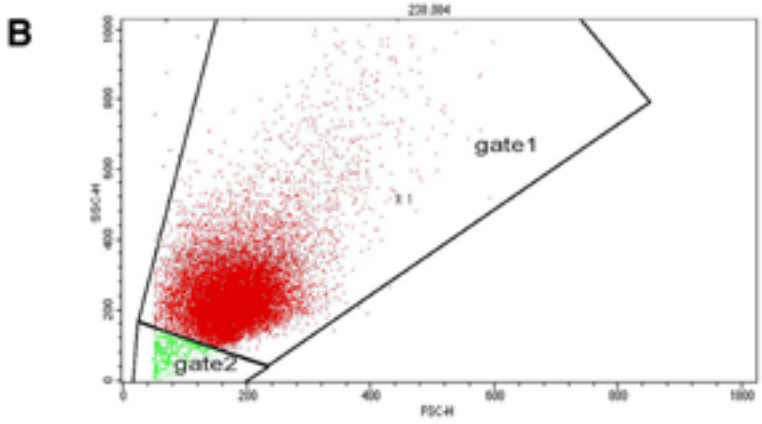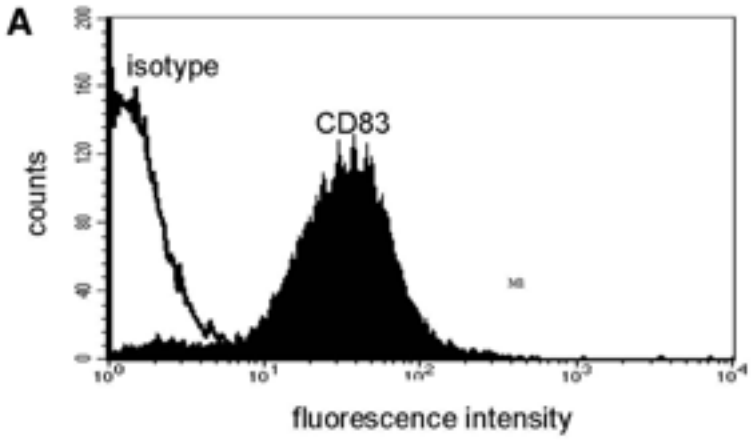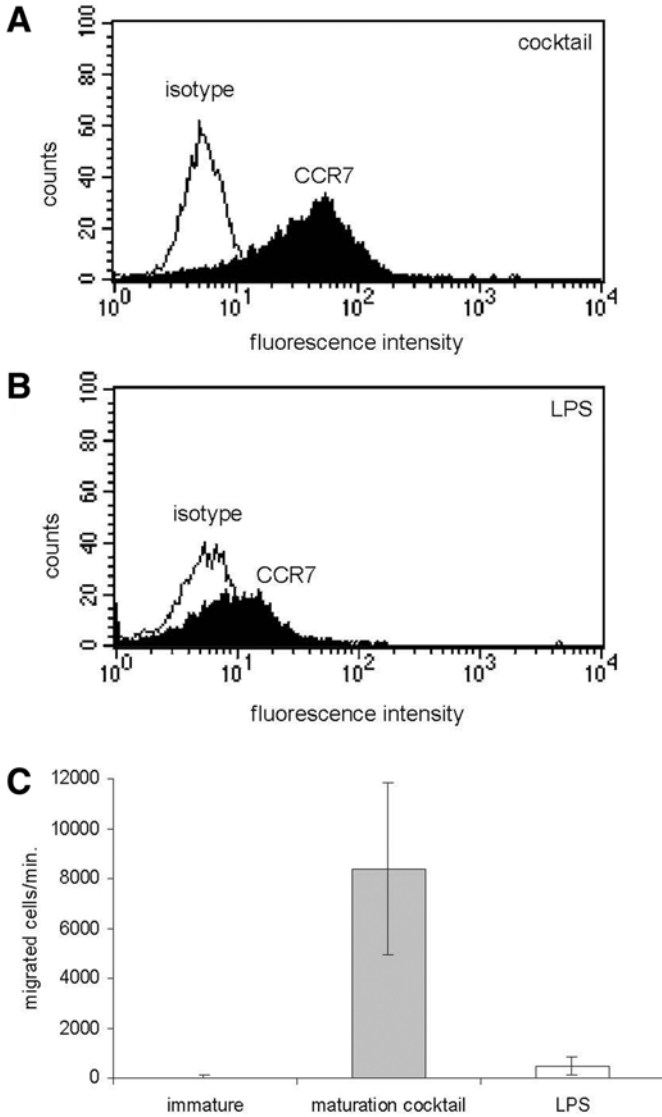
Fig. 4. Monocyte-derived dendritic cells (MoDC) generated with the CliniMACS system express CCR7 and migrate in response to macrophage inflammatory protein (MIP)-3β. Monocytes were maintained for 5 d in the granulocyte/macrophage colony-stimulating factor (GM-CSF)/interleukin (IL)-4 cell-culture system and matured for 2 d with either the maturation cocktail or lipopolysaccharide (LPS), or left unstimulated (immature). **(A)** MoDC treated with the maturation cocktail exhibited high levels of CCR7. **(B)** LPS treatment of MoDC resulted in low CCR7 expression. **(C)** Migration of MoDC was determined in a Transwell chamber assay. Accumulation of migrating MoDC in the lower chamber containing MIP-3β/CCL19 was determined by counting cells for 1 min in a flow cytometer.
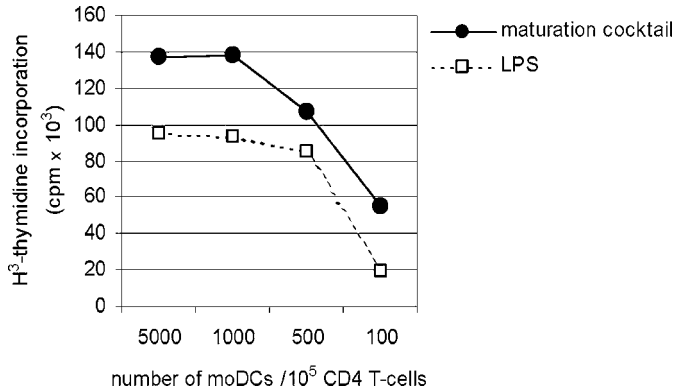
Fig. 5. Monocyte-derived dendritic cells (MoDC) generated with the CliniMACS system exhibit high CD4+ T-cell stimulatory capacity. Monocytes were propagated for 5 d in the granulocyte/macrophage colony-stimulating factor (GM-CSF)/interleukin (IL)-4 cell-culture system and stimulated for 2 d with the maturation cocktail or lipopolysaccharide. Subsequently, MoDC were irradiated and co-cultured with CD4+ T-cells. Proliferation of CD4+ T-cells was determined by ^{3}H-thymidine incorporation. Background proliferation of CD4+ T-cells was negligible (data not shown).

2. A 500-μL aliquot of the cells that migrated to the bottom chamber was counted by flow cytometry as the number of events acquired during 1 min. Each experiment was performed in duplicates.

The mean number of spontaneously migrated MoDC (in the absence of MIP-3β) was subtracted from the total number of MoDC that migrated in response to MIP-3β (*see* **Note 4**).

Fig. 4A,B shows CCR7 expression of MoDC and **Fig. 4C** shows MoDC migration in response to MIP-3β.

3.5. Mixed Leukocyte Reaction

1. CD4+ T-cells were positively selected using CD4 MicroBeads according to the manufacturer's instructions.
2. CD4+ T-cells (2×10^5/well) were stimulated with various numbers of allogeneic, irradiated (3000 rad) MoDC. Cells were cultured in triplicates in 96-well flat-bottomed tissue-culture plates in a final volume of 200 μL/well in medium containing 1% heat-inactivated human AB plasma.
3. T-cell proliferation was measured as [^{3}H]-thymidine incorporation (1 μCi/well = 37 kBq/well). Cells were pulsed during the last 16 h of a 5-d culture period, harvested on glass fiber filters using a Skatron cell harvester, and analyzed in a liquid-scintillation counter. Results are expressed as the mean counts per minute (cpm) of six independent experiments.

Fig. 5 confirms that MoDC generated with this system have high T-cell stimulatory capacity.

4. Notes

1. Although rare, early apoptosis may cause considerable cell loss during the first step of MoDC culture (immature MoDC, **Fig. 1**). The reason for this phenomenon is unclear, but flow rates during leukapheresis may be critical and should therefore not exceed 80 mL/min (50 mL/min is recommended by Miltenyi Biotec).

2. Immature MoDC, 18×10^6, are thawed to prepare one vaccine. This usually results in 11–14×10^6 mature, antigen-loaded MoDC, corresponding to a recovery of 61–77%. The stress induced by the pro-inflammatory "cocktail," as well as the addition of tumor lysate, which signals massive necrosis, is likely to be responsible for apoptotic cell loss.

3. Thawing of MoDC is also critical. Cryo-vials should be transferred directly from liquid nitrogen to 37°C. As soon as the cell suspension is thawed, it is diluted with plasma-supplemented buffer. However, dilution has to be performed dropwise with gentle shaking of the cryo-tube, to allow the DMSO to diffuse from the MoDC. Otherwise, the DMSO in the MoDC would cause a rapid influx of water and osmotic lysis of the MoDC.

4. The maturation step is carried out at a cell density of 3×10^5 MoDC/mL (i.e., 1.8×10^6 cells per 6 mL). We have previously shown that efficient MoDC maturation requires cell densities below 5×10^5 cells/mL *(8)*. Both LPS, a component of the outer cell wall of Gram-negative bacteria, as well as a "cocktail" consisting of TNF-α, IL-1β, IL-6, and prostaglanding E2 induce MoDC maturation. However, it has to be noted that the use of different maturation stimuli can cause phenotypic and functional differences. As shown in **Fig. 4A**, the cocktail is more potent at inducing the expression of CCR7, the chemokine receptor that directs migration of DC to MIP-3β-producing lymph nodes *(17)*. Consequently, MoDC matured with the cocktail migrated much more efficiently towards MIP-3β in a Transwell chamber migration assay (**Fig. 4C**). Furthermore, the T-cell stimulatory capacity of MoDC treated with the maturation cocktail was higher compared to MoDC treated with LPS (**Fig. 5**).

5. MoDC prepared with the CliniMACS system have been administered to 16 patients with metastatic RCC (Höltl et al., manuscript in preparation). No adverse effects were observed. Mean follow up time was 9 mo (range: 2–16 mo). Taken together, our data indicate that the CliniMACS system is feasible for the generation of functional, clinical-grade MoDC. Preliminary clinical data also suggest that MoDC prepared with the CliniMACS system are well tolerated.

Acknowledgments

References

1   Banchereau, J. and Steinman, R. M. (1998) Dendritic cells and the control of immunity. *Nature* **392,** 245–252.

2   Rissoan, M. C., Soumelis, V., Kadowaki, N., et al. (1999) Reciprocal control of T helper cell and dendritic cell differentiation. *Science* **283,** 1183–1186.

3   Fernandez, N. C., Lozier, A., Flament, C., et al. (1999) Dendritic cells directly trigger NK cell functions: cross-talk relevant in innate anti-tumor immune responses in vivo. *Nat. Med.* **5,** 405–411.

4   Schuler, G., Schuler-Thurner, B., and Steinman, R. M. (2003) The use of dendritic cells in cancer immunotherapy. *Curr. Opin. Immunol.* **15,** 138–147.

5 Sallusto, F. and Lanzavecchia, A. (1994) Efficient presentation of soluble antigen by cultured human dendritic cells is maintained by granulocyte/macrophage colony-stimulating factor plus interleukin 4 and downregulated by tumor necrosis factor alpha. *J. Exp. Med.* **179,** 1109–1118.

6 Romani, N., Reider, D., Heuer, M., et al. (1996) Generation of mature dendritic cells from human blood. An improved method with special regard to clinical applicability. *J. Immunol. Meth.* **196,** 137–151.

7 Lechmann, M., Zinser, E., Golka, A., and Steinkasserer, A. (2002) Role of CD83 in the immunomodulation of dendritic cells. *Intl. Arch. Allergy Immunol.* **129,** 113–118.

8 Thurnher, M., Papesh, C., Ramoner, R., et al. (1997) In vitro generation of CD83+ human blood dendritic cells for active tumor immunotherapy. *Exp. Hematol.* **25,** 232–237.

9 Cella, M., Engering, A., Pinet, V., Pieters, J., and Lanzavecchia, A. (1997) Inflammatory stimuli induce accumulation of MHC class II complexes on dendritic cells. *Nature* **388,** 782–787.

10 Carreno, B. M. and Collins, M. (2002) The B7 family of ligands and its receptors: new pathways for costimulation and inhibition of immune responses. *Ann. Rev. Immunol.* **20,** 29–53.

11 Moser, B. and Loetscher, P. (2001) Lymphocyte traffic control by chemokines. *Nat. Immunol.* **2,** 123–128.

12 Holtl, L., Zelle_Rieser, C., Gander, H., et al. (2002) Immunotherapy of metastatic renal cell carcinoma with tumor lysate-pulsed autologous dendritic cells. *Clin. Cancer Res.* **8,** 3369–3376.

13 Rieser, C., Papesh, C., Herold, M., et al. (1998) Differential deactivation of human dendritic cells by endotoxin desensitization: role of tumor necrosis factor-alpha and prostaglandin E2. *Blood* **91,** 3112–3117.

14 Jonuleit, H., Kuhn, U., Muller, G., et al. (1997) Pro-inflammatory cytokines and prostaglandins induce maturation of potent immunostimulatory dendritic cells under fetal calf serum-free conditions. *Eur. J. Immunol.* **27,** 3135–3142.

15 Rieser, C., Bock, G., Klocker, H., Bartsch, G., and Thurnher, M. (1997) Prostaglandin E2 and tumor necrosis factor alpha cooperate to activate human dendritic cells: synergistic activation of interleukin 12 production. *J. Exp. Med.* **186,** 1603–1608.

16. Scandella, E., Men, Y., Gillessen, S., Forster, R., and Groettrup, M. (2002) Prostaglandin E2 is a key factor for CCR7 surface expression and migration of monocyte-derived dendritic cells. *Blood* **100,** 1354–1361.

17. Robbiani, D. F., Finch, R. A., Jager, D., Muller, W. A., Sartorelli, A. C., and Randolph, G. J. (2000) The leukotriene C(4) transporter MRP1 regulates CCL19 (MIP-3beta, ELC)-dependent mobilization of dendritic cells to lymph nodes. *Cell* **103,** 757–768.

7

Adenoviral Transduction of Dendritic Cells

**Rienk Offringa, Kitty Kwappenberg, Martijn Rabelink,
Delphine Rea, and Rob Hoeben**

Summary

Recombinant adenoviral (rAd) vectors are highly suitable for efficient genetic modification of dendritic cells (DC). In certain cases, the high immunogenicity of rAd may be a disadvantage. This chapter describes the essential aspects of optimal rAd-mediated gene transfer into DC, discusses the consequences of the immunogenicity of rAd vectors, and provides suggestions to minimize these complications.

Key Words: Dendritic cells; recombinant adenovirus; genetic transduction; monocytes.

1. Introduction

DC are generally considered the crucial antigen-presenting cells (APC) for the induction and regulation of T-cell-dependent immune responses *(1)*. This notion has prompted extensive research aiming at genetic modification of human DC—for instance, to program these APC for presentation of large amounts of peptide antigens of interest into their surface HLA molecules, or to secrete immuno-regulatory cytokines. rAd vectors are widely used for genetic modification of a variety of cell types, including DC (*see* **Note 1**). Adenoviral vectors can harbor one, or even multiple transgenes, as well as strong promoter/enhancer sequences to direct high expression of the transgene(s) of interest. They are considered attractive and relatively safe viral vectors for clinical applications, because rAd batches free of replication-competent adenovirus (RCA) can reliably be obtained, high titers of up to 1×10^{11} infectious particles/mL can be reached with relative ease, and rAd batches can be stored for prolonged periods without significant loss of infectivity *(2,3)*. A prominent advantage of rAd as vehicles for gene transfer into DC is that, unlike for retroviral vectors, this process does not depend on mitotic activity of the targeted cells. This is crucial, because (until proven otherwise) human DC, even in their immature stage, constitute terminally differentiated cells that have lost the capacity for cell division. Furthermore, unlike the case with poxvirus vectors, high transduc-

tion efficiencies ranging between 50 and 90% can readily be achieved without compromising the vitality and the key immunological functions of DC.

In spite of these advantages, certain drawbacks of rAd-mediated gene transfer into DC should not be ignored. Even though high transduction rates can be obtained, this generally requires a high multiplicity of infection (MOI), in the range of 200–1000 infectious particles per DC *(4)*. Notably, rAd-infection will therefore not only introduce the rAd genome harboring the transgene into the DC, but also a considerable amount of adenoviral antigens. Peptides derived from these highly immunogenic proteins, for which the majority of the human population exhibits potent memory T-cell immunity, are processed into class I and II MHC molecules at the DC surface. As a result, rAd-infected DC readily trigger Ad5-specific responses by human T-cells both in vitro and in vivo, which may very well dominate over immunity against transgene-encoded antigens of interest. The HLA-restricted presentation of adenoviral antigens by rAd-modified DC is not restricted to the capsid antigens derived from the rAd particles that have infected the DC, but can also include various other adenoviral antigens encoded by the viral backbone. Even though replication-deficient rAd generally lack the E1 region required for efficient expression of the adenoviral gene program, the other viral genes that were retained in the vector can nevertheless be expressed in cells that are infected at high MOI *(5,6)*, as is the case for rAd-modified DC. Importantly, the contribution of rAd vector components to the antigenic load of rAd-modified DC can be limited by employing rAd vectors that use other cell-surface molecules as receptor and that, as a result, infect DC with higher efficiency, permitting the use of a lower MOI. Alternatively, rAd vectors can be used in which additional genes have been deleted from the viral backbone (*see* **Note 2**).

In conclusion, rAd are highly efficient and versatile vectors for genetic modification of DC, but like most other viral vectors they are also highly immunogenic. Consequently, it is recommended to weigh the pros and cons of rAd vectors against those of alternative vector systems before embarking on genetic modification of DC.

2. Materials

2.1. Preparation of rAd Stocks

1. Infection medium: DMEM (Gibco-BRL, Gaithersburg, MD) supplemented with 0.3 g/L glucose, 0.6 g/L glutamine, 0.1 g/L biotin, 10 mM MgCl$_2$ (for PER.C6 helper cells only), and 2% heat-inactivated horse serum (HS).
2. Postinfection medium: DMEM (Gibco-BRL) supplemented with 0.3 g/L glucose, 0.6 g/L glutamine, 0.1 g/L biotin, and 8% heat-inactivated fetal bovine serum (FBS).
3. PBS/HS: phosphate-buffered saline supplemented with 2% heat-inactivated horse serum (HS).
4. 2X F15 medium: For preparation of 5 L, dissolve into 4 L of milli-Q water: 1 jar of MEM powder (MEM, minimal essential medium for 10 L, with Earle's salts, with L-glutamine, without NaHCO$_3$; Gibco-BRL cat. no. 61100-087). Subsequently add and dissolve 22 g NaHCO$_3$ and 6 g glutamine. Finally add 200 mL of a 0.1 g/L biotin solution, 120 mL of a 15% glucose solution, 200 mL MEM amino acids solution (50X) (Gibco-BRL), 100 mL MEM nonessential amino acids solution (100X) (Gibco-BRL), 100 mL Basal Medium Eagle (BME) vitamins solution (100X) (Gibco-BRL). Adjust volume to 5 L, set pH to 7.15 with 3N NaOH, sterilize through a 0.22 µm filter, and aliquot.

5. One *M* HEPES pH 7.4, sterilized through a 0.22 µm filter.
6. Agar solution, 1.7%: 8.5 g agar noble (Difco) in 475 mL milli-Q water; sterilized through autoclave.
7. Agar 1.7%, pH 7.4: cool freshly autoclaved agar to <60°C, add 25.0 mL 1 *M* HEPES (pH 7.4), prewarmed at 37°C, per 475 mL agar.
8. Cesium chloride (CsCl) stock solutions: prepare 500 mL of a 1.45 g/cm^3 (3.6 *M*) CsCl solution by dissolving 305 g CsCl (MW 168.37) in 500 mL $T_{10}E_1$ (10 m*M* Tris, 1 m*M* EDTA , pH 8.1). Use part of this solution to prepare the other CsCl solutions: 300 mL + 106.7 mL $T_{10}E_1$ = 1.33 g/cm^3 CsCl; 100 mL + 120.2 mL $T_{10}E_1$ = 1.20 g/cm^3 CsCl.
9. TD dialysis buffer (pH 7.8): prepare a 10X TD stock solution by dissolving into 1000 mL milli-Q water 80 g NaCl (1.37 *M*), 3.8 g KCl (51 m*M*), 1.0 g $Na_2HPO_4·2H_2O$ (5.6 m*M*) and 30 g Tris-HCl (248 m*M*). Also prepare a 200X Ca/Mg stock solution by dissolving into 200 mL milli-Q water 5.3 g $CaCl_2$ (180 m*M*) and 4.0 g $MgCl_2·6H_2O$ (98 m*M*). Now prepare 1000 mL of 1X TD dialysis buffer by adding to 900 mL milli-Q water 100 mL 10X TD and 5mL Ca/Mg stock solution.
10. Sucrose dialysis buffer (pH 7.8): add to 4000 mL of milli-Q water 40.9 g NaCl (140 m*M*), 4.4 g $Na_2HPO_4.2H_2O$ (5,0 m*M*), 1.0 g KH_2PO_4 (1.5 m*M*), 250 g sucrose (730 m*M*, 5 %) and adjust the final volume to 5000 mL.

2.2. Isolation, rAd-Infection, and Phenotypical Analysis of Immature Monocyte-Derived DC

1. MACS buffer: PBS supplemented with 2 m*M* EDTA and 0.5% BSA.
2. Antibodies for analysis of the DC surface phenotype by flow cytometry: phycoerythrin (PE)-anti-CD1a (Caltag Laboratories, Burlingame, CA), PE-anti-CD80 (BB1), PE-anti-CD86 (FUN-1), FITC-anti-CD40 (5C3) (all from Pharmingen, San Diego, CA), PE-anti-CD14 (L243), PE-anti-HLA-DR (mfP9), and PE- and fluorescein isothio-cyanate (FITC)-conjugated isotype controls (all from Becton Dickinson), PE-anti-CD83 (Immunotech), and FITC-anti-HLA class I (Serotec Inc., Raleigh, NC). Of course, this selection should merely be regarded as a suggestion, and in many cases several alternative antibodies that also work very well will be available.
3. The origin and/or composition of other materials used is described under **Subheading 3**.

3. Methods

The methods described below outline (1) the production of high-titer batches of rAd; (2) the isolation of immature DC from peripheral blood mononuclear cells (PBMC); (3) the infection of DC with rAd; and (4) the phenotypical and functional analysis of uninfected and rAd-infected DC.

3.1. Production of High-Titer rAd

Efficient gene transfer into human DC with rAd derived from human adenovirus type 5 can require an MOI of up to 1000 *(4)*. It is therefore essential to use rAd stocks of high titer (>1 × 10^{10} plaque-gorming units (pfu) per mL) and purity that have been isolated by two-step cesium chloride (CsCl) density centrifugation. Although the introduction into the DC of highly immunogenic vector-derived antigens is inherent to the procedure of rAd-mediated gene-transfer, the balance between the transgenic and vector components can be optimized by making use of rAd batches that have a minimal content of defective rAd particles. To check the quality of CsCl-purified rAd batches, the concentration of viral particles (VP/mL) can be assessed next to the con-

centration of pfu/mL. High-quality rAd batches typically display a VP:pfu ratio of smaller than 30. Please note that a VP:pfu ratio of 30 does not mean that 29 out of 30 viral particles are defective. Instead, this value indicates that during standard infection conditions, using highly permissive target cells, 1 out of 30 viral particles will be able to elicit a productive infection *(7)*. It should be noted that the ratio obtainable may depend on the rAd construct used, and can be negatively affected if the transgene encodes a gene product that interferes with efficient rAd production. Furthermore, care should be taken to refrain from repeated freeze-thawing of the purified rAd stocks, as this may lead to irreversible vector inactivation and aggregation.

Virus stocks are routinely tested for the presence of RCA by polymerase chain reaction (PCR). The absence of RCA is especially important if the rAd used harbor transgenes encoding potentially hazardous proteins, such as (proto-) oncogenes or growth factors, and/or if the rAd-mediated gene transduction is part of a procedure that is aimed at clinical applications.

All handling of rAd and rAd-infected cells must be performed in functional biosafety cabinets in an appropriate biological containment laboratory.

3.1.1. Large-Scale rAd Multiplication

PER.C6 cells are the host of choice for generating batches of rAd that are free of RCA *(8)*. As alternatives cell lines 911 *(9)* or 293 *(10)* helper cells can be used, provided that suitable RCA checks are performed on all stocks. PER.C6 cells are routinely split in a ratio of 1:5 twice a week. When setting up cultures for infection, a ratio of 1:4 is recommended. As an example, use six 15-cm dishes (133 cm^2) of PER.C6 cells to seed 20 T-180 flasks (180 cm^2). This quantity of cells will usually produce 1–20×10^{10} pfu of virus, depending on the vector and insert.

Approximately 3 d after seeding, at the time when each flask contains 3×10^7 cells, PER.C6 is infected with an MOI of 3 to 5.

1. Add 2×10^9 pfu virus to 120 mL infection medium (*see* **Subheading 2.1.**), and mix well.
2. Replace the medium in the flasks with 6 mL of inoculum and gently rock the flasks to spread the medium over the cells.
3. Incubate for 2 h at 37°C in a well leveled 5% CO$_2$ incubator. To enhance viral uptake it is recommended to gently rock the flasks several times during these 2 h.
4. Add 12 mL/flask of postinfection medium (*see* **Subheading 2.1.**) and put flasks back into incubator.

Usually 40–48 h postinfection a cytopathic effect (CPE) is achieved. All cells are rounded up, the medium has changed from red to orange/yellow, and about half of the cells can be detached by gentle agitation of the flasks. It is important to check the cells regularly, because some rAd require a longer incubation time to induce CPE. Harvesting of virus-infected cells is performed as follows:

1. Gently rock flasks until all cells are detached. Avoid heavy shaking and formation of foam and aerosols.
2. Transfer medium with cells to 50-mL conical tubes. Centrifuge at 250*g* for 5 min.
3. Remove supernatant. This medium usually contains approx 1–5×10^8 pfu/mL of rAd. It can be stored for future use, for instance as viral stock for starting up new, large-scale amplifications.

4. Use 40 mL of this supernatant to collect all cell pellets into one 50-mL tube, and centrifuge this tube again.

5. Remove supernatant, resuspend cells in 3 mL PBS supplemented with 2% HS, and transfer to smaller conical tubes.

6. Release the virus from the cells by processing the cell suspension through three rapid freeze/thaw cycles, centrifuge at 1100g for 10 min, and collect supernatant.

This rAd preparation can be stored at –20°C and can be used for CsCl purification, infecting a new batch of cells, or for RCA screening by PCR. Occasionally, a large fraction of the rAd produced is not associated with the cell pellet, but rather resides in the supernatant. This virus can be concentrated from the supernatant with ammonium sulphate precipitation *(11)*.

3.1.2. CsCl Purification of rAd

The rAd preparation is first purified over a discontinuous CsCl gradient. For this purpose use open (no cap) 10-mL Ultra Clear tubes (Beckmann, cat. no. 344059).

1. First pour 2.0 mL of the high-density CsCl (1.45 g/cm^3) solution in each tube. Carefully overlay with 4.5 mL of the second CsCl (1.20 g/cm^3) solution on top of the first one. The final virus purity depends on the quality of the gradient.

2. Finally, load your viral stock on top of the gradient. This volume should be less than 4 mL, and less than 1×10^9 cells, otherwise the gradient will be overloaded.

3. Centrifuge at 30,000 rmp (110,000g) in a Beckman Sw41 rotor for 2 h at 16°C (brake switched off).

4. Carefully place the rotor into a biosafety cabinet, take out the tubes, and fix these in a clamp attached to a stand.

5. After centrifugation, the gradient should reveal a pellet of high-density cell components at the bottom, a turbid layer of low-density cell components at the top, and two bands in the middle. The upper band is yellow-white and consists of defective viral particles. The lower one, bluish-white, contains the infectious virus.

6. Puncture the tubes just below the lowest band containing the virions using a 2.5-mL syringe with a 19G needle. Gently aspirate the virus. Avoid collecting other bands and impurities, and keep the volume as small as possible (usually less than 2 mL).

The virus is further purified on a continuous CsCl gradient:

7. Transfer the virus isolated from first gradient to a 14-mL Quick Seal tube (Beckman, cat. no. 342413).

8. Fill up the tube with additional 1.33 g/cm^3 CsCl solution.

9. Spin sealed tubes for approx 18 h at 48,000 rpm (160,000g) in a Beckman 70.1Ti rotor (brake switched off).

10. After centrifugation, only one clear band should be visible. Isolate this band as described in **step 6**, but before extracting the virus, puncture a hole in the top of the tube to allow the inflow of air into the sealed tubes.

For dialysis of the virus isolate, a dialysis cassette (Pierce; Slide-A-Lyzer Cassette; 10,000 MWCO) is used, which can hold 0.5–3.0 mL of solution. For smaller volumes (approx 0.1 up to 0.5 mL), dialysis tubes (Pierce; Slide-A-Lyzer Mini Dialysis Unit; 10,000 MWCO) are used.

11. Fill the dialysis cassette using a 5-mL syringe with a 23G needle. Dialyze against 500 mL TD dialysis buffer at 4°C. Refresh the buffer at the end of the day, and continue dialysis overnight.

Table 1
Dilution Scheme for Virus Titration

Dilution 10^E–x	Volume of infection medium in tube (mL)	Volume of virus (μL) [from tube 10^{-X}]
2	1.98	20 [stock]
3	1.80	200 [10^{-2}]
4	1.80	200 [10^{-3}]
5	1.80	200 [10^{-4}]
6	1.80	200 [10^{-5}]
7	1.80	200 [10^{-6}]
8	1.80	200 [10^{-7}]
9	1.80	200 [10^{-8}]
10	1.80	200 [10^{-9}]
11	1.80	200 [10^{-10}]

12. The next morning, replace buffer with a 5% sucrose buffer. Dialyze for 2–3 h (not longer).
13. Take the virus from the cassette with a 5-mL syringe with a 23G needle.
14. Aliquot in small portions of 100 μL or less. In addition, make two or three portions of 15 μL, which can be used to determine virus titer in plaque assays.
15. Store aliquots at –80°C as soon as possible.

3.1.3. Analysis of rAd Titer

Analyses of rAd titers are best performed with 911 cells, as these cells, in contrast to Per.C6 and 293, grow well under agar overlays *(9)*. From a subconfluent culture of 911 cells, seed six wells of a six-well plate for each plaque assay and allow the cells to adhere overnight. Next day, make sure that the cultures are approx 80–90% confluent. Infect cells with six different dilutions of the viral stock, starting with one of the 15-μL aliquots. When testing CsCl-purified preparations, it is recommended to test dilutions in the range of 10^{-6} to 10^{-11}. For nonconcentrated rAd preparations, test dilutions in the range of 10^{-4} to 10^{-10} (*see* **Table 1** for dilution scheme).

Infect host cells with viral dilutions as follows:

1. Remove all medium from the wells and replace by 1.0 mL of the selected viral dilutions; six serial dilutions are tested on one six-well plate. Spread medium over surfaces of the wells.
2. Incubate for 2 h at 37°C in 5% CO_2 incubator. To enhance viral uptake it is recommended to gently rock the plate several times during these 2 h.
3. Subsequently, the inoculum of each well is replaced by 2 mL of a 1:1 agar/F15 overlay. The solutions for this overlay need to be prepared in advance as follows: Prepare a 1.7% agar, pH 7.4 (*see* **Subheading 2.1.**). Before use, while incubating the cells with viral dilutions, melt the agar in a microwave oven. Keep the molten agar at 42°C in a water bath. Also prepare 2X F15 complete medium (2xF15c). This should be prepared fresh (on d of use) (*see* **Table 2**). Keep at 37°C in a water bath. To prepare the overlay, mix melted agar and prepared 2xF15c in 1:1 ratio (2.0 mL needed for each well).

Table 2
Scheme for Preparation of 2X F15 Complete
(2XF15c) Medium and 1:1 Agar/F15 Overlay [a]

Volumes per number of plaque assays	1	2	3	4	5	6	7	8
2xF15 (mL; *see* **Subheading 2.**)	7	15	20	25	30	40	45	50
Glutamine 30g/L (µL)	140	300	400	500	600	800	900	1000
MgCl$_2$ 1 *M* (µL)	175	375	500	625	750	1000	1125	1250
Horse serum (HS) (µL)	280	600	800	1000	1200	1600	1800	2000
Pen./strep. (µL)	50	50	100	100	150	150	200	200
Fungizone 250 µg/mL (µL)	50	50	100	100	150	150	200	200
2xF15c (mL)	7.6	16.3	21.8	27.2	32.7	43.6	49.0	54.5
Agar pH 7.4 (mL)	7.6	16.3	21.8	27.2	32.7	43.6	49.0	54.5
Agar/2xF15c (mL)	15.2	32.6	43.6	65.5	65.4	87.2	98.0	109.0

[a] The upper part of this table lists the volumes of the various stock solutions (in µL, unless indicated otherwise) that need to be added to make up the amount of 2xF15c sufficient for 1–8 plaque assays (each plaque assay consists of 6 wells on a 6-well plate). After mixing, the 2xF15c should be warmed to 37°C in a waterbath. The lower part of the table lists the volume 2F15c obtained. Just before overlaying the wells, add 1 volume of agar pH 7.4, prewarmed at 42°C, mix and apply to the wells (2 mL/well).

Plaques will start to appear from d 5. At d 7–12, depending on the virus used, the number of plaques will reach its maximum. Calculate the titer as follows: number of plaques/dilution = plaque forming units per mL (pfu/mL). For CsCl-purified rAd batches, expect titers to range between 1×10^8 and 10^{11}; for nonconcentrated batches, expect titers between 1×10^5 and 10^9.

3.1.4. Determination of the Concentration of VP/mL

The viral particle concentration of CsCl-purified adenovirus (after dialysis, in 5% sucrose buffer) can be determined by an $OD_{260\,nm}$ measurement. Before measurement, the virus needs to be inactivated with NaOH/SDS.

Measurement of virus sample (for cuvets with a capacity of 100 µL):

1. Add 20 µL of a virus sample to an Eppendorf tube filled with 60 µL 5% sucrose buffer and 20 µL of an 0.1 *M* NaOH/1% SDS solution.
2. Transfer to a quartz cuvet.
3. Measure optical density (OD) at a wavelength of 260 nm.
4. Use a solution of 80 µL sucrose + 20 µL of NaOH/SDS as a blank.
5. If the OD reading exceeds the linear range, repeat measurement with an appropriate dilution of the virus stock sucrose buffer.

   Calculation:

$$1.0\ OD_{260\,nm} = \text{dilution factor} \times 1.1 \times 10^{12}\ \text{particles/mL}$$

Table 3
PCR Reactions

For the polymerase chain reactions (PCR), add per tube:

Volume (µL)	Solution	Stock concentration
4.5	PCR buffer, Perkin Elmer	10X
3.5	MgCl$_2$	25 mM
2.0	dNTP	10 mM total (2.5 mM each)
2.0	F1 forward primer	10 pmol/µL
2.0	R2 reverse primer	10 pmol/µL
1.0	tRNA	5 mg/mL
0.3	Taq-polymerase, Perkin Elmer	5 U/µL
33.7	Milli Q	

3.1.5. RCA Screening

   Screening of rAd stocks for RCA is routinely performed by PCR on nonconcentrated preparations isolated from freeze-thawed rAd-infected cells that result from the procedure described under **Subheading 3.1.1.** PCR reactions on purified or medium samples are less sensitive. Before performing PCR reactions, the virus samples need to be inactivated. This will be done by a proteinase K (prot. K) treatment, followed by heat inactivation.

   1. Heat inactivation: in 1.5-mL Eppendorf tube, mix 45.0 µL virus sample with 5.0 µL 10X PCR buffer (Perkin Elmer) and 0.5 µL prot. K (40 mg/mL) (ICN).
   2. Incubate at 44°C overnight.
   3. Tighten caps of tubes very well by plastic multicap locks or tape, and incubate the tubes in boiling water for 5 min.
   4. Centrifuge for 5 min at maximum speed in Eppendorf centrifuge.
   5. The supernatant can be directly used in the PCR assay or stored at –20°C until further use.
   6. The PCR reactions are performed with primers that are specific for the Ad5E1 region, which should be absent for rAd, but which is present in RCA as well as in the host cells used for virus multiplication:

   Forward primer: 5'-GGG.TGG.AGT.TTG.TGA.CGT.G (19-mer)

   Reverse primer: 5'-TCG.TGA.AGG.GTA.GGT.GGT.TC (20-mer)

   These primers correspond to nt 52–70 and 674–693 of the adenovirus type 5 sequence (GenBank gi:33694637), respectively. PCR reactions are set up according to the scheme in **Table 3**. Add 1.0 µL of virus sample into one of these tubes. Add 1.0 µL of water to one of the tubes as negative control. DNA isolated from a wild-type Ad5 stock can be used as a positive control. A series of 1, 10, 100, and 1000 pfu/µL (or similar range) of control DNA is to be used. Perform 30-cycle PCR reactions as follows:

   Step 1: block temp 94.0°C, time 30 s.

   Step 2: block temp 63.0°C, time 45 s.

   Step 3: block temp 72.0°C, time 1 min (8 min for final cycle).

7. Analyze PCR products by electrophoresis on a standard 2% agarose gel. Before loading onto the gel, remove tRNA from samples by adding 1 μL RNAse (10 mg/mL stock) and incubating at 37°C for 10 min. If a sample is contaminated with RCA, a band of 640 bp will appear. The sensitivity of the assay can be checked on the basis of the wild-type Ad5 control samples. The 10-pfu sample should result in a visible band, while the samples containing 100 pfu and more should give rise to heavy bands. Note: this PCR reaction is not suitable for 293-derived rAd stocks, because 293 cells contain the entire amplified region.

3.2. Isolation of Immature, Monocyte-Derived DC

PBMC from healthy blood donors constitutes the most readily accessible source of DC precursors: the monocytes. For the proper interpretation of most immunologically oriented experiments, it is advisable to make use of PBMC from fully HLA-typed blood donors.

3.2.1. Isolation of Human PBMC From Buffy Coat

We routinely isolate PBMC from a 50–60 mL buffy coat, derived from 500 mL of peripheral blood, as follows:

1. Add 15 mL Ficoll-Hypaque solution (1.077 g/L) to each of six Leucosep tubes (Greiner, cat. no. 227290) and spin tubes for 2 min at 650g to force the ficoll under the filter.
2. Apply 10–15 mL (maximally; do not overload gradient) onto the filter and fill up tubes with 25–30 mL of PBS. Mix buffy coat and PBS by pipetting the solution up and down.
3. Centrifuge at room temperature for 10 min at 650g, brake set to "low."
4. Collect the cells from the ficoll/PBS interphase in a 50-mL tube, fill up this tube with PBS, mix and spin down cells for 5 min at 350g.
5. Wash the cells with PBS two more times.
6. For healthy donor buffy coats, this isolation typically results in the isolation of 5–10×10^8 PBMC that are free of erythrocytes. We routinely freeze these PBMC in aliquots of 0.5–1×10^8 cells.

3.2.2. Isolation of CD14$^+$ Monocytes

Before proceeding, it is important to consider how many DC will be needed. On average, the preparation of 10×10^6 immature DC requires the isolation of 20×10^6 monocytes, which requires approx 200×10^6 PBMC. Please note that recovery rates may vary and are certainly expected to be lower if one intends to isolate DC from diseased subjects such as cancer patients.

Although monocytes can be isolated from both fresh and frozen PBMC samples, best results are usually obtained when starting from freshly isolated cells, in particular because thawed cells tend to form clumps that will negatively affect the efficiency of the isolation procedure. Therefore, we generally use part of the PBMC to immediately proceed with the monocyte isolation, while the remainder of the PBMC is frozen in aliquots to be used as autologous responder cells in subsequent immunological assays.

In order to obtain a highly homogenous DC population, we highly recommend isolating monocytes through MACS with anti-CD14-coated beads, as follows:

1. Spin down the required amount of PBMC in a 50-mL conical tube (5 min at 350g). It is recommended to start with at least 20×10^6 PBMC, because with lower amounts the isolation procedure tends to become less efficient.

2. To the cell pellet add MACS buffer (*see* **Subheading 3.2.2.**) and CD14 beads (Milteny Biotech, cat. no. 130-050-201). Per 1×10^7 PBMC add respectively 90 µL and 10 µL of these compounds.

3. Resuspend cells and incubate at 4°C (not on ice) for 30 min.

4. Fill up the tube with MACS buffer (0–4°C), spin down cells in a cooled centrifuge, and resuspend cell pellet in MACS buffer: 1 mL of buffer per 2×10^8 cells.

5. Place an LS MACS column (Milteny Biotech, cat. no. 130-042-401) into the magnetic device, and equilibrate it with 3 mL of MACS buffer. Elute column and apply cell suspension to column.

6. Wash column with three loads of 3 mL MACS buffer.

7. Remove column from magnetic device and elute the beads with the CD14-positive cells with 3 mL of MACS buffer (*see* **Subheading 3.2.2.** for expected recovery rates). At this stage, the monocytes can either be differentiated into DC, or aliquotted and frozen for future use. We have not found that the presence of the magnetic beads has any negative influence on monocyte growth, function, survival, or their capacity to differentiate into DC.

3.2.3. Preparation of Monocyte-Derived DC

In order to allow the CD14$^+$ monocytes to differentiate into DC, set up cultures in a six-well plate (2 mL culture per well) of 1×10^6 cells/mL in RPMI medium supplemented with 10% FBS, 500 U/mL interleukin (IL)-4 (Sanvertech), and 800 U/mL granulocyte/macrophage colony-stimulating factor (GM-CSF; Leucomax, Novartis). After 2 d, add 2 mL of fresh medium to each well containing 1000 U/mL IL-4 and 1600 U/mL GM-CSF. After another 2 d of culture, take 2 mL of medium out off each well and replace it by 2 mL of fresh medium containing 1000 U/mL IL-4 and 1600 U/mL GM-CSF. Repeat this procedure after another 2 d.

Fully differentiated, immature DC are obtained after 6–7 d of culture. The quality of this cell preparation can be analyzed through FACS analysis for a limited set of critical surface markers—in particular, CD1a, CD14, CD83, CD86, and HLA class II (*see* **Subheading 2.2.** for suitable antibodies). The desired DC population should exclusively consist of cells that are positive for CD1a and negative for CD14 and CD83, while expressing low levels of CD86 and moderate levels of CD80, CD40, HLA-class II, and HLA-class I *(4)*. The presence of a subpopulation of CD14$^+$ cells usually indicates that the differentiation process was incomplete, while increased levels of CD86 and CD83 usually indicate that a fraction of the DC has (partially) matured.

3.2.4. rAd Infection of DC

For most applications, it is preferable to infect DC in their immature stage (*see* **Note 3**). After 6–7 d of differentiation, the immature DC cultures can be infected with rAd as follows:

1. Harvest cells, transfer to conical 10–15 mL tube and spin down for 5 min at 650*g*.

2. Resuspend cell pellet in 10 mL of serum-free RPMI, count vital cells, and spin cells again.

3. Resuspend cells in serum-free RPMI at a concentration of 2.5×10^6 cells/mL.

4. Plate cell suspension in 24-well plate at 200 µL/well and add the desired amount of rAd suspension to each well. In our hands, optimal results (maximal gene transduction efficiency in combination with minimal cytotoxicity) for rAd5- and rAd2-based vectors is

usually obtained at an MOI of 500–1000. To reach this MOI, add 2.5×10^8 pfu rAd per well. Infection is performed in a minimal volume to optimize infection efficiency. In view of this, we recommend using rAd stocks with high titer. Efficient rAd-mediated gene transduction can also be obtained at lower MOI if one makes use of certain modified rAd vectors (*see* **Note 2**).

5. Incubate for 6 h at 37°C in tissue-culture incubator.
6. After 6 h, add to each well 1 mL of RPMI medium supplemented with 10% FBS, 500 U/ mL IL-4, and 800 U/mL GM-CSF. If full maturation of rAd-transduced DC is desired, certain DC-maturation agents can be added to the cultures at this stage (*see* **Note 4**).

We generally perform phenotypical and functional analysis of our rAd-infected DC on the following d, after overnight culturing. Assessment of the results of rAd infection involves two primary analyses:

7. The efficiency of rAd-mediated gene transduction is preferably analyzed through FACS analysis, and may require extracellular or intracellular staining of the DC, depending on the transgen-encoded antigen. In order to validate the rAd-mediated gene-transfer procedure, rAd vectors encoding either EGFP or β-galactosidase are ideal, because gene-transfer efficiency can be readily assessed at the level of individual cells without the need for antibody-mediated detection. At MOI of 500–1000, gene transduction efficiencies are expected to range between 50 and 80%. However, due to the character of the transgene-encoded protein concerned, certain rAd constructs may result in lower transduction efficiencies, a lower recovery of vital rAd-infected DC, and/or a decreased lifespan of these DC.
8. Analysis of a limited set of surface markers, in particular CD83, CD86, and HLA-class II. Our previous work has shown that rAd infection of DC induces partial maturation of these cells, as compared to the full maturation induced by LPS or CD40 ligand, in that the expression levels of CD86 and HLA-class II are strongly increased, whereas only very modest levels of CD83 expression are reached *(4)* (*see* **Notes 3** and **4** for additional information on DC maturation and polarization).

We use our rAd-infected DC for functional analyses and immunological experiments anywhere between 18 and 48 h after rAd infection. Although for most applications we expect this timing not to be critical, certain applications may require the use of rAd-infected DC at an earlier time point, 6–18 h after infection (*see* **Note 3**).

4. Notes

1. An overview of the cumulative published work on rAd-transduced DC lies beyond the scope of this chapter, but information on this subject can readily be obtained through a MedLine/PubMed search with the Boolean term *adenovirus* AND *dendritic*. This search, which at present results in more than 350 hits, can be narrowed down, for instance by providing in addition the name of the transgene of interest.
2. The initial attachment of rAd to the majority of human cell types is mediated by its fiber capsid protein, which binds to the high-affinity coxsacky-adenovirus receptor (CAR). The absence of CAR on human DC is in accordance with the fact that rAd infection of these cells requires high MOI *(4)*. In view of this notion, several labs have constructed rAd vectors with modified fiber proteins that target other cell-surface proteins that are expressed on DC, and thereby allow efficient rAd infection of DC at 100-fold lower MOI *(12–17)* and references therein). Alternatively, bispecific antibodies directed against fiber and DC-surface markers, in particular CD40, have be successfully used to reduce the effective dose of rAd (*see* **ref. 18** and references therein).

A major advantage of the use of lower MOI is that a lower dose of adenoviral antigens is applied to the DC and, therefore, that the balance between the immunogenicity of transgene-encoded and rAd-derived antigens is shifted towards the transgene-encoded antigens of interest (*see also* **Subheading 3.2.4.**). Furthermore, these modifications can be used to improve rAd-mediated gene targeting of DC in vivo.

3. It is generally preferable to infect DC at the immature stage in view of the following considerations. Although both immature and mature DC can be infected to high efficiencies with rAd, efficiencies reached with immature DC are usually higher *(4)*. If rAd infection is intended to introduce presentation of transgene-encoded antigenic peptide epitopes into surface HLA molecules, access to especially the HLA class II processing route is best before DC maturation *(1)*. If DC infected with rAd-encoding antigens of interest are to be injected in vivo with the aim of inducing (or modulating) T-cell immune responses against these antigens, most injection routes (except intranodal injection) will require the DC to home to lymphoid organs where encounter with antigen-specific T-cells can take place. DC migration is guided by the programmed expression of chemokine and adhesion receptors, which evolves during DC maturation *(19)*. It is conceivable that fully matured DC have already lost some of the chemotactic homing qualities that they displayed at an earlier stage after receiving their maturation triggers *(20)*. Moreover, if the rAd-infected DC are to be used for induction of T-helper (Th)1-type CD4+ T-cell responses and/or Th1-dependent cellular immunity (i.e., by CD8+ cytotoxic T-lymphocytes), maximal secretion of the Th1-polarizing cytokine IL-12 is desired. DC that have been triggered for maturation secrete large quantities of this cytokine during the first 24–36 h, but lose this capacity afterwards *(21)*.

4. As originally described by us *(4)* and confirmed in studies by many others, rAd infection of DC induces partial maturation of DC in the absence of polarization. The latter essentially means that DC triggering by rAd infection, unlike through ligation of its CD40 receptor, does not cause the DC to secrete IL-12. When DC are to be used for inducing potent T-cell immunity against rAd-transgene-encoded antigens, the latter is usually desired. Therefore, it is usually recommendable to induce full maturation of rAd-infected DC by stimulating their CD40 receptors or their Toll-like receptors *(22)*. The combination of these triggers with rAd infection will result in an exacerbation of the matured DC phenotype and secretion of very high levels of IL-12 *(4,12)*. When inducing DC maturation, either by rAd infection and/or other stimuli, one should always keep in mind that certain important features of DC maturation such as expression of homing receptors and cytokine genes are only transiently induced, and are lost at later time points after initiation of the maturation process (*see* **Note 3**).

References

1 Banchereau, J., Briere, F., Caux, C., et al. (2000) Immunobiology of dendritic cells. *Annu. Rev. Immunol.* **18,** 767–811.

2 Russell, W. C. (2000) Update on adenovirus and its vectors. *J. Gen. Virol.* **81,** 2573–604.

3. St. George, J. A. (2003) Gene therapy progress and prospects: adenoviral vectors. *Gene Ther.* **10,** 1135–1141.

4 Rea, D., Schagen, F. H., Hoeben, R. C., et al. (1999) Adenoviruses activate human dendritic cells without polarization toward a T-helper type 1-inducing subset. *J. Virol.* **73,** 10,245–10,253.

5 Nevins, J. R., Imperiale, M. J., Kao, H. T., Strickland, S., and Feldman, L. T. (1984) Detection of an adenovirus E1A-like activity in mammalian cells. *Curr. Top. Microbiol. Immunol.* **113,** 15–19.

6 Amalfitano, A., Hauser, M. A., Hu, H., Serra, D., Begy, C. R., and Chamberlain, J. S. (1998) Production and characterization of improved adenovirus vectors with the *E1*, *E2b*, and *E3* genes deleted. *J. Virol.* **72,** 926–933.

7 Nyberg-Hoffman, C., Shabram, P., Li, W., Giroux, D., and Aguilar-Cordova, E. (1997) Sensitivity and reproducibility in adenoviral infectious titer determination. *Nat. Med.* **3,** 808–811.

8 Fallaux, F. J., Bout, A., van der Velde, I., et al. (1998) New helper cells and matched early region 1–deleted adenovirus vectors prevent generation of replication-competent adeno-viruses. *Hum. Gene Ther.* **9,** 1909–1917.

9 Fallaux, F. J., Kranenburg, O., Cramer, S. J., et al. (1996) Characterization of 911: a new helper cell line for the titration and propagation of early region 1–deleted adenoviral vec-tors. *Hum. Gene Ther.* **7,** 215–222.

10 Graham, F. L., Smiley, J., Russell, W. C., and Nairn, R. (1977) Characteristics of a human cell line transformed by DNA from human adenovirus type 5. *J. Gen. Virol.* **36,** 59–74.

11 Schagen, F. H., Rademaker, H. J., Rabelink, M. J., et al. (2000) Ammonium sulphate precipitation of recombinant adenovirus from culture medium: an easy method to increase the total virus yield. *Gene Ther.* **7,** 1570–1574.

12 Rea, D., Havenga, M. J., van Den Assem, M., et al. (2001) Highly efficient transduction of human monocyte-derived dendritic cells with subgroup B fiber-modified adenovirus vec-tors enhances transgene-encoded antigen presentation to cytotoxic T cells. *J. Immunol.* **166,** 5236–5244.

13 Belousova, N., Korokhov, N., Krendelshchikova, V., et al. (2003) Genetically targeted adenovirus vector directed to CD40-expressing cells. *J. Virol.* **77,** 11,367–11,377.

14 Fontana, L., Nuzzo, M., Urbanelli, L., and Monaci, P. (2003) General strategy for broad-ening adenovirus tropism. *J. Virol.* **77,** 11,094–11,104.

15 Gaggar, A., Shayakhmetov, D. M., and Lieber, A. (2003) CD46 is a cellular receptor for group B adenoviruses. *Nat. Med.* **9,** 1408–1412.

16 Okada, N., Masunaga, Y., Okada, Y., et al. (2003) Dendritic cells transduced with gp100 gene by RGD fiber-mutant adenovirus vectors are highly efficacious in generating anti-B16BL6 melanoma immunity in mice. *Gene Ther.* **10,** 1891–1902.

17 Vogels, R., Zuijdgeest, D., van Rijnsoever, R., et al. (2003) Replication-deficient human adenovirus type 35 vectors for gene transfer and vaccination: efficient human cell infec-tion and bypass of preexisting adenovirus immunity. *J Virol.* **77,** 8263–8271.

18 de Gruijl, T. D., Luykx-de Bakker, S. A., Tillman, B. W., et al. (2002) Prolonged matura-tion and enhanced transduction of dendritic cells migrated from human skin explants after in situ delivery of CD40-targeted adenoviral vectors. *J. Immunol.* **169,** 5322–5331.

19 Sallusto, F. and Lanzavecchia, A. (2000) Understanding dendritic cell and T-lymphocyte traffic through the analysis of chemokine receptor expression. *Immunol. Rev.* **177,** 134–140.

20 Watanabe, S., Kagamu, H., Yoshizawa, H., et al. (2003) The duration of signaling through CD40 directs biological ability of dendritic cells to induce antitumor immunity. *J. Immunol.* **171,** 5828–5836.

21. Langenkamp, A., Messi, M., Lanzavecchia, A., and Sallusto, F. (2000) Kinetics of den-dritic cell activation: impact on priming of TH1, TH2 and nonpolarized T cells. *Nat. Immunol.* **1,** 311–316.

22. Kaisho, T. and Akira, S. (2002) Toll-like receptors as adjuvant receptors. *Biochim. Biophys. Acta* **1589,** 1–13.

8

Generation of Autologous Peptide- and Protein-Pulsed Dendritic Cells for Patient-Specific Immunotherapy

David O'Neill and Nina Bhardwaj

Summary

This chapter presents a detailed protocol for the generation of mature, monocyte-derived dendritic cells (DC) that are loaded or "pulsed" with tumor-associated peptide antigens for use as patient-specific immunotherapy. The protocol can easily be adapted for the treatment of patients with a variety of tumors or chronic viral infections by simply changing the peptide antigens used. The vaccine may use major histocompatibility complex (MHC) class I- or class II-restricted peptides to elicit stimulation of CD8$^+$ cytotoxic T-lymphocytes (CTL) or CD4$^+$ T-helper cells, respectively. It also provides an example of loading DC with a purified protein antigen—in this instance, keyhole limpet hemocyanin (KLH). KLH may be used to boost the immunogenicity of the vaccine and as a control to test for the induction of CD4$^+$ T-helper-cell responses. Other antigenic proteins may be added or substituted. Once prepared, the DC are frozen in aliquots and samples are tested for identity, purity, viability, and sterility. After these "release" criteria are met, vaccine aliquots can be thawed, drawn up into syringes, and injected back into the patient.

Key Words: Cancer; dendritic cells; immunotherapy; melanoma; monocytes; vaccine.

1. Introduction

This protocol is adapted from the method of Thurner et al. for the large-scale generation of monocyte-derived DC (Mo-DC) from leukapheresis products *(1)*. Mo-DC are the most commonly used DC preparation for clinical use, although DC derived from CD34$^+$ hematopoietic progenitor cells or enriched directly from peripheral blood have also been used successfully *(2,3)*. Our modifications to the Thurner method include omitting an initial overnight incubation of the monocytes in the absence of interleukin (IL)-4 and granulocyte/macrophage colony-stimulating factor (GM-CSF), and the use of a cocktail of three proinflammatory cytokines (IL-1β, IL-6, tumor necrosis factor [TNF]-α) and prostaglandin E$_2$ (PGE$_2$) to mature the DC in the place of monocyte-conditioned medium (MCM). The cocktail, first described by Jonuleit et al. *(4)* and referred to here as "MCM mimic," allows potent, reproducible DC maturation in less than 24 h *(5)*.

The protocol begins with the preparation of frozen aliquots of peripheral blood mononuclear cells (PBMC) and heat-inactivated plasma from apheresis products obtained from the patient *(1)*. To prepare the DC, frozen PBMC are thawed and plated in medium containing 1% autologous plasma into 10-cm tissue-culture dishes. Monocytes adhere to the plastic dishes during a 1-h incubation, after which the dishes are washed to remove lymphocytes, which do not adhere to plastic. The monocytes (CD14+ cells) are then induced to differentiate into immature DC by culturing for 5 d in the presence of IL-4 and GM-CSF. During this time they become non-adherent and differentiate into immature DC (CD14− CD83− cells). The DC are harvested then and transferred to six-well plates, where they are cultured for an additional d. They are then pulsed with protein antigens and stimulated to mature by culturing for another 18 to 24 h in the presence of MCM mimic. On the final d of culture the DC, which have matured into CD14− CD83+ cells with characteristic cytoplasmic projections, or "veils," are loaded with peptide antigens for 1 h, washed, and frozen in aliquots in a controlled-rate freezing device. After testing control aliquots for specified release criteria, the cells may be thawed and injected directly into the patient from whom they were prepared. Following this protocol we routinely obtain cell yields of 5 to 10% relative to the number of PBMC plated, with 80 to 90% of the cells having morphologic and phenotypic characteristics of mature DC.

Earlier methods for the generation of Mo-DC for clinical use relied on the use of whole human blood as starting material *(6,7)*. The advantage of using leukapheresis products as opposed to whole blood is that over 3 billion PBMC can routinely be obtained from one product. Whole blood yields approx 1 million PBMC per mL of blood drawn, so a 100-mL blood sample typically yields only 5 to 10 million mature DC, enough for just one injection. Our protocol uses an "open" system of tissue-culture dishes and plates, although it is potentially adaptable to closed or semi-closed culture systems using bags *(8)* or cell "factories" *(9)*. There is no general consensus as to the best culture medium to use. Various laboratories use plasma, serum, or even serum-free medium. We currently use RPMI 1640 medium with 1% autologous heat-inactivated plasma, and have not observed significant improvements in yield using serum or serum-free medium.

DC-based vaccines are currently used primarily for the immunotherapy of cancer. One very common method to generate a DC-based cancer vaccine is to load MHC-restricted peptides carrying dominant epitopes of tumor-associated antigens directly onto DC *(2,3,10,11)*. HLA-A2-restricted peptides are commonly used, often in combinations. Other MHC class I-restricted epitopes and even MHC class II-restricted T-helper epitopes are also available. Control peptides carrying dominant epitopes from antigens the patient has been previously exposed to may also be included to test for recall immune responses. Influenza virus peptides are commonly used for this purpose *(12)*. Peptides may be loaded onto DC before or after DC maturation, although in our hands pulsing mature DC with peptides has resulted in somewhat better specific T-cell stimulation in vitro.

DC are also commonly loaded with protein antigens to produce vaccines, and we have included an example of this in the protocol. We use KLH, a purified protein that

is a powerful immunogen derived from a marine mollusk. It may be used to boost the immunogenicity of the vaccine by inducing a T-helper response (proteins taken up from the extracellular fluid are largely processed by the endosomal , or MHC class II, pathway) *(13,14)*. Because it is a xenoantigen, KLH may also be used as a control antigen to test the vaccine's ability to prime naïve T-cells *(2,10,12)*. The DC are pulsed with KLH just prior to maturation, since immature DC are most adept at acquiring complex antigens exogenously.

DC prepared following this protocol may also be loaded with antigens by RNA transfection *(15,16)* or by co-culturing with whole-cell lysates *(10,17,18)*, immune complexes *(19–21)*, or apoptotic cells *(22–24)*. Regardless of the antigen source, it is important to mature the DC prior to injection into patients, since there is increasing evidence that injection of antigen-loaded immature DC results in ineffective immunization or even immune tolerance *(25,26)*.

For clinical use, many groups prepare DC fresh from PBMC prior to each vaccine injection. One problem with this approach is that freshly prepared cells cannot be fully tested for sterility prior to injection into the patient. For improved safety, reliability, and efficiency of large-scale production, several laboratories have begun preparing DC-based vaccines in large batches that can be aliquotted and tested for sterility prior to use *(27)*. In our hands, cryopreserved DC work just as well as fresh DC in in vitro assays measuring antigen-specific T-cell stimulatory capacity and migration in response to chemokines (unpublished observations). We have outlined our method for DC cryopreservation in this protocol.

2. Materials (*see* Note 1)

2.1. Special Equipment (see **Note 2**)

1. Controlled-Rate Freezer (Planer Kryo 10 Series III, Planer Products, Sunbury-on-Thames, UK).
2. Portable 50-L liquid nitrogen dewar with roller base and transfer hose (Cryo-Cyl 50 LP; Minnesota Valley Engineering, Burnsville, MN).

2.2. Supplies

1. Ten-cm tissue-culture dishes (Falcon 353003; Becton Dickinson, Franklin Lakes, NJ).
2. Six-well tissue-culture plates (Falcon 353046, Becton Dickinson).
3. Fifteen-mL conical tubes (Falcon 352097, Becton Dickinson).
4. Fifty-mL conical tubes (Falcon 352098, Becton Dickinson).
5. Conical tubes, 250 mL (430776, Corning, Corning, NY).
6. Tube support cushions, 250 mL (430236, Corning,).
7. Thirteen-mL sterile screw cap tubes (60.540, Sarstedt, Newton, NC).
8. Nunc CryoTube vials, 1.8 mL (375418, Nalge Nunc, Rochester, NY).
9. One-mL Nunc CryoTube vials (377224, Nalge Nunc).
10. Millex-LG 25-mm syringe-driven filter unit (SLLG025SS, Millipore, Bedford, MA).

2.3. Blood Products (see **Note 3**)

1. Leukapheresis product (200 mL peripheral blood mononuclear cells, obtained from patient).
2. Plasmapheresis product (100 to 200 mL, obtained from patient).

2.4. Cell Culture Reagents (see Note 4)

1. RPMI 1640 medium with L-glutamine (12-702F, Cambrex, Walkersville, MD).
2. X-VIVO 15 serum-free medium with gentamicin and phenol red (04-418Q, Cambrex).
3. One *M* HEPES-buffered saline (17-737E, Cambrex).
4. Phosphate-buffered saline (PBS) without Ca^{++} and Mg^{++} (17-516F, Cambrex).
5. Trypan blue vital stain, 0.4% (17-942E, Cambrex).
6. Albumin (human) 25%, USP (Plasbumin-25, Bayer, Elkhart, IN).
7. Ficoll-Paque Plus (Amersham Biosciences, Piscataway, NJ).
8. DMSO, USP (Cryoserv, CRY-VB00, Edwards Life Sciences, Irvine, CA).
9. Sterile 0.9% sodium chloride for injection, USP (Abbott Laboratories, North Chicago, IL).
10. Gentamicin, 10 mg/mL (American Pharmaceutical Partners, Los Angeles, CA).

2.5. Cytokines

1. Leukine (recombinant human GM-CSF), 500 µg/mL, 5600 IU/µg (Berlex, Seattle, WA).
2. Recombinant human IL-4, lyophilized, 50 µg vial, 6700 IU/µg (CellGenix, Gaithersburg, MD).
3. Recombinant human TNF-α, lyophilized, 25 µg vial (CellGenix).
4. Recombinant human IL-1β, lyophilized, 50 µg vial (CellGenix).
5. Recombinant human IL-6, lyophilized, 150 µg vial (CellGenixD).
6. One mg/mL PGE_2 (Prostin E2, Pharmacia & Upjohn, Puurs, Belgium).

2.6. Protein Antigen

1. VACMUNE (keyhole limpet hemocyanin subunits, 20 mg/mL, Biosyn, Carlsbad, CA).

2.7. MHC-Restricted Peptide Antigens

1. Pharmaceutical-grade peptides carrying MHC class I- or MHC class II-restricted immunodominant epitopes for a variety of viral or tumor-associated antigens may be obtained aliquotted in lyophilized form from Clinalfa, Laufelfingen, Switzerland. Other companies also provide this service.

2.8. Solutions

1. Freezing solution 1 (X-VIVO 15 medium with 10% human albumin and 10% DMSO): Mix 25 mL of X-VIVO 15 medium with 20 mL of 25% human albumin and 5 mL of DMSO. Sterile filter using a Millex-LG filter unit attached to a 60-mL syringe. Chill the filtered solution on ice if using right away or store refrigerated (*see* **Note 5**). Expires in 1 mo.
2. RPMI/1% autologous plasma (RPMI 1640 medium with 1% autologous heat-inactivated plasma, 10 m*M* HEPES-buffered saline, and 20 µg/mL gentamicin): Mix 489 mL of RPMI-1640 medium with 5 mL of thawed autologous heat-inactivated plasma, 5 mL of 1 *M* HEPES-buffered saline, and 1 mL of 10 mg/mL gentamicin. Sterile filter and store refrigerated (2–8°C). Expires in 8 d. We use autologous plasma in place of fetal calf serum so that the cells may be injected back into human subjects (FDA does not permit biologic products from ruminants to be used in the preparation of therapeutic cells).
3. PBS/5% albumin. Mix 40 mL of phosphate-buffered saline with 10 mL of 25% human albumin. Sterile filter and store refrigerated. Expires in 1 mo.
4. 400 IU/µL IL-4. Dissolve the contents of a frozen 50-µg vial of lyophilized IL-4 in 840 µL PBS/5% albumin. Mix thoroughly but gently. Do not vortex excessively. Store refrigerated (2–8°C). Keep this solution on ice when using. The solution expires in 8 d.

5. 100 IU/μL GM-CSF. Combine 36 μL of leukine with 964 μL of PBS/5% human albumin in a sterile 1-mL Nunc tube. Mix thoroughly but gently. Do not vortex excessively. Store refrigerated (2–8°C). Keep this solution on ice when using. It expires in 8 d.

6. RPMI/1% autologous plasma with cytokines. For every 10 mL of medium with cytokines needed, combine 10 mL RPMI/1% autologous plasma with 5 μL of 400 IU/μL IL-4 and 10 μL of 100 IU/μL GM-CSF. Mix thoroughly but gently. The final concentration of cytokines in this solution is 200 IU/mL of IL-4 and 100 IU/mL of GM-CSF. Use this solution immediately (do not prepare and store in advance).

7. RPMI/1% autologous plasma with 10X cytokines. For every 1 mL of medium with 10X cytokines needed, combine 1 mL RPMI/1% autologous plasma with 5 μL of 400 IUμL IL-4 and 10 μL of 100 IU/μL GM-CSF. Mix thoroughly but gently. This is a 10X working solution with a concentration of 2000 IU/mL IL-4 and 1000 IU/μL GM-CSF. It is used to refresh the cytokines in dendritic cell cultures on d 3. Use this solution immediately (do not prepare and store in advance).

8. Frozen stock solutions of TNF-α, IL-1β, and IL-6. Working aseptically, reconstitute lyophilized TNF-α in 0.5 mL of PBS/5% albumin (concentration of 50 μg/mL). Store frozen (–20 to –80°C) in 20-μL aliquots. Reconstitute lyophilized IL-1β in 1 mL of PBS/5% albumin (concentration of 50 μg/mL). Store frozen (–20 to –80°C) in 20-μL aliquots. Reconstitute lyophilized IL-6 in 1 mL of PBS/5% albumin (concentration of 150 μg/mL). Store frozen (–20 to –80°C) in 200-μL aliquots.

9. 100X monocyte conditioned medium mimic (100X MCM mimic): Combine 200 μL of PGE$_2$ (Prostin E2) with 1560 μL of PBS/5% albumin in a 1.8-mL Nunc tube. Mix thoroughly (the alcohol in Prostin E2 will cause some of the albumin to precipitate, but this goes back into solution after thorough mixing). Use this solution to rinse out one vial each of frozen TNF-α, IL-1β, and IL-6 stock solutions, pooling back into the 1.8-mL Nunc tube. The final volume should be 2 mL. 100X MCM mimic contains 0.5 μg/mL TNF-α, 0.5 μg/mL IL-1β, 15 μg/mL IL-6, and 100 μg/mL PGE$_2$.

10. Freezing solution 2 (90% autologous plasma, 10% DMSO): Mix 9 mL of autologous plasma with 1 mL of DMSO. Sterile filter using a Millex-LG filter unit attached to a 10-mL syringe. Chill the filtered solution on ice if using right away or store refrigerated (*see* **Note 5**). Expires in 8 d.

3. Methods (*see* **Note 6**)

3.1. Preparation of Frozen Stocks of Autologous Peripheral Blood Mononuclear Cells (PBMC) and Heat-Inactivated Plasma

3.1.1. PBMC (allow 4 to 5 h)

1. Fill the portable 50-L dewar with liquid nitrogen to between 1/2 and 3/4 full. Prepare freezing solution 1 as outlined under **Subheading 2.8.** and pre-heat a water bath to 56°C.

2. Record the volume stated on the leukapheresis product bag. Store the plasmapheresis product bag at 4°C until ready to process.

3. After gentle mixing, sterilely transfer the entire contents of the leukapheresis bag into a labeled 250-mL conical tube. Record the volume collected.

4. Distribute the leukapheresis product in 15-mL aliquots into labeled 50-mL conical tubes. Then add 25 mL of RPMI 1640 medium to each tube, cap, and gently mix.

5. For each tube, remove the cap and gently layer 12 mL of Ficoll-Paque Plus beneath the cell suspension, starting by placing the tip of your pipet at the bottom of the tube. Be careful not to disturb the interface as it develops and not to blow bubbles into the Ficoll layer. Re-cap the tubes.

6. Centrifuge the tubes at 900*g* for 30 min at room temperature (20°C) with no brake.
7. For each tube, gently aspirate the cloudy PBMC layer with a new pipet. Transfer to new labeled 250-mL tubes, pooling the aspirated PBMC (add up to 60 mL of pooled PBMC per tube). When finished, discard the 50-mL tubes containing the residual Ficoll, granulocytes, red blood cells, plasma, and platelets.
8. Dilute the contents of each tube of pooled PBMC with approx 3 vol of RPMI 1640 medium. Cap and mix gently by inversion.
9. Centrifuge at 400*g* for 10 min at room temperature (20°C) with full brake.
10. Remove the supernatant and resuspend each pellet in approx 100 mL RPMI 1640 medium. Centrifuge again at 400*g* for 10 min at room temperature (20°C) with full brake (*see* **Note 7**).
11. Resuspend each pellet in a small volume of RPMI 1640 medium and pool all of the cells into one 50-mL tube. Bring up to a final volume of 50 mL with more medium.
12. Thoroughly mix to ensure a uniform cell suspension by capping the tube tightly and inverting the tube several times. Transfer 10 µL of cell suspension to a small tube containing 990 µL of medium. Mix thoroughly. Mix 10 µL of this diluted suspension with 10 µL of 0.4% Trypan blue solution and count the number of viable cells using a hemacytometer. Be sure not to count residual red cells and platelets.
13. Calculate the percent viable PBMC, the number of viable PBMC/mL, and the total number of viable PBMC. Then calculate the number of 1-mL aliquots to be frozen assuming a concentration of 200 million viable PBMC/mL (*see* **Note 8**). Prepare labels for this many aliquots and apply the labels to sterile 1.8-mL Nunc cryovials.
14. Prepare the controlled-rate freezing device so that it is ready to perform a run, following the manufacturer's instructions. This usually involves attaching the liquid nitrogen dewar using a hose connection and initializing the machine's freezing program. It should take 2 to 3 min for the machine to stabilize at its start temperature (4°C).
15. Centrifuge the PBMC at 400*g* for 10 min at 4°C.
16. Aspirate the supernatant and loosen the pelleted cells by flicking or slapping the tube. Resuspend the cells at a final concentration of 200 million cells/mL in cold freezing solution 1.
17. Aliquot 1 mL of cell suspension per tube into the labeled Nunc tubes.
18. Load the filled cryovials into the freezer chamber of the mechanical freezing device and start the freezing run.
19. At the end of the run, remove the frozen samples and place in a transfer container with crushed dry ice. Transfer the cryovials immediately into a liquid-nitrogen freezer for long-term storage (cells for clinical use should be stored in the vapor phase of the freezer, not submerged in liquid nitrogen).

3.1.2. Heat-Inactivated Plasma (allow at least 1 h)

1. Record the volume stated on the plasmapheresis product bag.
2. After gentle mixing, sterilely transfer the entire contents of the bag into labeled 50-mL conical tubes.
3. Centrifuge the 50-mL tubes at 2000*g* for 20 min at 4°C to pellet platelets.
4. Remove the supernatant plasma, transferring 40-mL volumes into labeled 50-mL conical tubes.
5. Heat-inactivate the plasma by incubating in a water bath at 56°C for 35 min.
6. Centrifuge the heat-inactivated plasma at 2000*g* for 20 min at 4°C to remove any precipitated material.

7. Transfer 10-mL volumes of the supernatant to labeled 13-mL sterile Sarstedt tubes. Place the tubes in a –80°C freezer for long-term storage.

3.1.3. Quality-Control Testing of Frozen Intermediates

1. Aliquots of PBMC and plasma should be tested for sterility and for the presence of bacterial endotoxin. It is best to outsource sterility testing to a qualified microbiology laboratory. A commercially available kit (Limulus amoebocyte lysate assay, Cambrex) may be used to test for the presence of endotoxin. Since high concentrations of plasma interfere with the endotoxin assay, samples should be diluted at least 1:10 before testing, and a sensitive kinetic chromogenic assay should be used.

3.2. Dendritic Cell Processing: Day 0 (allow 3 to 4 h)

1. Thaw one 10-mL aliquot of autologous heat-inactivated plasma in a 37°C water bath with constant agitation. Make sure the cap of the tube is fully tightened while thawing. Periodically remove the tube from the water bath during this process and invert the tube several times to mix the contents thoroughly. When completely thawed, put the tube on ice.
2. Prepare two 500-mL batches of RPMI/1% autologous plasma as directed in **Subheading 2.8.**
3. Prepare PBS/5% albumin as outlined in **Subheading 2.8.**
4. Prepare a 400 IU/µL (60 ng/µL) working solution of interleukin-4 (IL-4) by dissolving the contents of a frozen vial of lyophilized IL-4 in PBS/5% albumin as outlined in **Subheading 2.8.**
5. Prepare a 100 IU/µL (18 ng/µL) working solution of GM-CSF by diluting a refrigerated aliquot of Leukine in PBS/5% albumin as described in **Subheading 2.8.**
6. Thaw six vials (1.2 billion cells) of frozen autologous PBMC in a 37°C water bath with constant agitation. Make sure the caps of the tubes are fully tightened while thawing. When completely thawed, sterilely transfer and pool the thawed cells into a labeled sterile 50-mL tube containing 30 mL of RPMI/1% autologous plasma. Mix well.
7. Centrifuge the cells for 5 min at 500*g*. Pipet off the supernatant and loosen the pellet by slapping the bottom of the tube with your fingers until the pellet is loosely coating the lower portion of the tube. Resuspend the cells in 30 mL RPMI/1% autologous plasma, tighten the cap of the tube, and mix thoroughly by swirling the tube and by inversion (do not vortex cells excessively).
8. Centrifuge the cells again for 5 min at 500*g*. Pipet off the supernatant, loosen the pellet as described above, and resuspend in 50 mL RPMI/1% autologous plasma. Tighten the cap of the tube and mix well by inversion.
9. Dilute 10 µL of cell suspension with 190 µL RPMI/1% autologous plasma in a 1-mL Nunc tube. Mix well. Remove 10 µL of this diluted cell suspension and mix with 10 µL 0.4% Trypan blue solution for cell counting. Count the cells and calculate the percent viability, the number of viable cells/mL, and the total number of viable cells.
10. Plate 35 million viable PBMC/dish on Falcon 353003 10-cm tissue-culture dishes (*see* **Note 9**). Adjust the volume in each dish to 10 mL by adding RPMI/1% autologous plasma. Mix the contents of each dish thoroughly by gently swirling and rocking.
11. Incubate the cells for 1 to 2 h at 37°C in the tissue-culture incubator. Don't stack the tissue-culture dishes for this step so that they can rapidly equilibrate to 37°C.
12. During the incubation, pre-warm an unopened bottle of RPMI 1640 medium in a 37°C water bath. This will be used for washing off nonadherent cells.

13. Prepare RPMI/1% autologous plasma with cytokines as directed in **Subheading 2.8.** You will need 10 mL for each tissue-culture dish (*see* **Note 10**). This will be used to culture the adherent monocytes following the wash step.

14. When the incubation is complete, remove a tissue-culture dish from the incubator and wash twice—first with the medium already present in the plate, then with the prewarmed RPMI 1640 medium. When washing, pipet up and down several times, gently rocking the dish. When pipetting up, tilt the plate toward you while aspirating up the medium. When pipetting down, direct the stream of medium over the entire surface of the dish by moving your pipet. Don't scrape the surface of the dish with the pipet. Pipet out all of the medium after each wash, but work quickly so that you don't let the cells dry out between washes.

15. After the second wash, add 10 mL of RPMI/1% autologous plasma with cytokines. Check the dish under the inverted microscope after adding the medium with cytokines. There should be very few freely floating cells (these can be identified by tapping the plate and looking for moving cells). You may need to wash again if many cells are still free-floating. When finished, return the dish to the tissue-culture incubator on a new shelf.

16. Repeat the previous two steps (washing twice, adding medium with cytokines, and returning to the incubator) with all of the tissue-culture dishes.

17. Incubate the plates for 3 d at 37°C in the tissue-culture incubator.

3.3. Dendritic Cell Processing: Day 3 (allow at least 30 min)

1. Prepare RPMI/1% autologous plasma with 10X cytokines as directed in **Subheading 2.8.** You will need 1 mL for each tissue-culture dish.

2. View the cells under an inverted microscope and assess on a scale of 0 (worst) to 5 (best) for cell density, cell viability/relative lack of debris, relative number of non-adherent cells, relative number of large cells, and for dendritic or veiled appearance (*see* **Note 11**).

3. Add 1 mL of medium with 10X cytokines to each plate. Mix each plate well by swirling and gentle rocking.

4. Incubate the plates for two more days at 37°C.

3.4. Dendritic Cell Processing: Day 5 (allow 1 to 2 h)

1. View the cells under an inverted microscope and assess on a scale of 0 (worst) to 5 (best) as described in **Subheading 3.3., Note 2** (*see* **Note 11**).

2. Harvest the cultures by pipetting up and down with a 10-mL pipet to resuspend all non-adherent cells (*see* **Note 11**). Transfer and pool the harvested non-adherent cells into a labeled 250-mL tube. Discard the empty tissue-culture dishes.

3. Cap the tube and record the total volume of harvested cells. Mix the tube thoroughly. Remove 10 μL of cell suspension and mix with 10 μL of 0.4% Trypan blue solution for cell counting.

4. Count the cells using a hemacytometer and calculate the percent cell viability, the number of viable cells per mL, and the total number of viable cells. Calculate the d 5 yield of viable cells by dividing the total number of viable cells harvested by the number of cells plated on d 0 (read **Note 12** before proceeding).

5. The harvested cells are to be washed, resuspended at approx 500,000 cells/mL in medium with cytokines, and then plated at 3 mL/well in six-well tissue-culture plates (*see* **Note 13**). Calculate the volume (in mL) of medium you will need to resuspend the cells in by dividing the total number of viable cells harvested by 500,000 (*see* **Note 13**). Measure out this amount of RPMI/1% autologous plasma and add IL-4 and GM-CSF to make RPMI/1% autologous plasma with cytokines as outlined in **Subheading 2.8.**

6. Centrifuge the cell suspension at 500*g* for 5 min. Discard the supernatant and loosen the pellet(s) as described previously. Resuspend the cells in all of the medium with cytokines prepared and mix thoroughly.

7. Transfer 3 mL of cell suspension per well into labeled six-well plates. Incubate the plates in the 37°C tissue-culture incubator overnight.

3.5. Dendritic Cell Processing: Day 6 (allow at least 1 h)

1. View the cells under an inverted microscope and assess on a scale of 0 (worst) to 5 (best) as described in **Subheading 3.3., Note 2**.

2. Add 1.5 µL of 20 µg/µL KLH to each well (final KLH concentration of 10 µg/mL). Mix the cultures thoroughly by swirling the plates. Return the plates to the tissue-culture incubator.

3. If not already done, prepare frozen stocks of TNF-α, IL-1β, and IL-6 as outlined in **Subheading 2.8.**

4. Prepare 100X monocyte-conditioned medium mimic (100X MCM mimic) as described in **Subheading 2.8.** You will need 30 µL for each well. Keep 100X MCM mimic on ice while working with it (*see* **Note 14**).

5. Add 30 µL of 100X MCM mimic to each well. Mix thoroughly by swirling the plates. Return the plates to the tissue-culture incubator and incubate overnight.

3.6. Dendritic Cell Processing: Day 7 (allow at least 5 h)

1. Fill the portable 50-L dewar with liquid nitrogen to between 1/2 and 3/4 full.

2. Prepare freezing solution 2 (90% autologous plasma, 10% DMSO) as outlined in **Subheading 2.8.** Chill on ice.

3. Prepare labels for Nunc cryovials, with five labels designated "for injection" and two labels designated "QC." Apply the labels to sterile 1.8-mL Nunc cryovials.

4. View the cells under an inverted microscope and assess on a scale of 0 (worst) to 5 (best) as described in **Subheading 3.3., Note 2**.

5. Return the plates to the 37°C incubator.

6. Aseptically transfer 1 mL sterile 0.9% NaCl, USP, to a sterile 1-mL Nunc tube labeled "saline."

7. Aseptically transfer 1 mL DMSO, USP, to a sterile 1-mL Nunc tube labeled "DMSO."

8. Reconstitute lyophilized peptides at a concentration of 1 m*M* (for MHC class I-restricted peptides, this would be a concentration of approx 1 µg/µL, since most class I-restricted peptides have 9 to 10 amino acids and a molecular weight of approx 1000 Da). This results in a 1000X peptide working solution (final concentrations of peptides in culture will be 1 µ*M*). Use saline to reconstitute peptides that are soluble in water and DMSO for peptides that are poorly soluble in water (solubility for each peptide must be determined empirically). For peptides obtained frozen in solution, thaw quickly in a 37°C water bath.

9. Keep all peptide solutions on ice except for those brought up in DMSO (DMSO will freeze when placed on ice).

10. Remove the plates from the incubator. On the lid of each plate, use a marking pen to mark each well with the name of the peptide it will receive. Each well is to receive only a single peptide, 3 µL per well (*see* **Note 13**).

11. Add the peptides to their designated wells, 3 µL per well. Mix the cultures thoroughly by swirling the six-well plates. The final peptide concentration should be 1 µ*M* (*see* **Note 15**).

12. Place the plates back in the 37°C incubator and incubate for at least 1 h.

Table 1
Resuspending Day 7 DC in Freezing Solution 2

Day 7 cell yield (millions)	Vol. freezing solution 2 (mL)	Final DC conc. (millions/mL)
130	8.7	15
120	8.0	15
110	7.3	15
100	6.7	15
90	6.0	15
80	6.2	13
70	6.4	11
60	6.0	10
50	6.2	8
40	6.7	6
30	6.0	5

13. When the incubation is finished, use a 10-mL pipet to harvest the non-adherent cells from each plate (by pipetting up and down as described for d 5). Pool the harvested cell suspension into a labeled sterile tube of appropriate size.

14. Centrifuge the harvested cells at 500g for 5 min. Pipet off the supernatant and loosen the pellet. Resuspend the cells in 50 mL RPMI/1% autologous plasma. Transfer to a new 50-mL tube if desired.

15. Centrifuge again at 500g for 5 min. Pipet off the supernatant, loosen the pellet, and resuspend the cells in 50 mL sterile PBS.

16. Cap the tube and mix thoroughly. Remove 10 µL of cell suspension and mix with 10 µL of 0.4% Trypan blue solution for cell counting.

17. Count the cells using a hemacytometer and calculate the percent cell viability, the number of viable cells per mL, and the total number of viable cells for each batch. Calculate the d 7 yield of viable cells by dividing the total number of viable cells harvested by the number of cells plated on d 0.

18. Prepare the controlled-rate freezing device so that it is ready to perform a run, following the manufacturer's instructions. This usually involves attaching the liquid-nitrogen dewar using a hose connection and initializing the machine's freezing program. It should take 2 to 3 min for the machine to stabilize at its start temperature (4°C).

19. Centrifuge the cells again at 500g for 5 min. Pipet off the supernatant and loosen the pellet. Resuspend the cells in 10 mL sterile 0.9% NaCl, USP. Transfer to a new labeled 15-mL conical tube and centrifuge again at 500g for 5 min. Discard the supernatant and resuspend the cell pellet in freezing solution 2 as outlined in **Table 1**.

20. Mix the cell suspensions thoroughly. Transfer 1 mL of cell suspension to each Nunc tube designated "for injection," and transfer the remaining cell suspension equally to the two remaining tubes designated "QC."

21. Load the filled cryovials into the freezer chamber of the mechanical freezing device and start the freezing run.

22. At the end of the run, remove the frozen samples and place in a transfer container with crushed dry ice. Transfer the cryovials immediately into a liquid-nitrogen freezer for long-term storage (cells for clinical use should be stored in the vapor phase of the freezer, not submerged in liquid nitrogen).

Table 2
Sample Controlled-Rate Freezing Program

Step	Start temp.	End temp.	Rate	Comment
a.	4°C	–6°C	–1°C/min	Chamber temp. lowered to –6°C at –1°C/min
b.	–6°C	–6°C	—	Hold at –6°C for 10 min.
c.	–6°C	–50°C	–25°C/min	Chamber temp. lowered rapidly to absorb heat of fusion.
d.	–50°C	–14°C	+15°C/min	Chamber temp. allowed to approx sample temp.
e.	–14°C	–60°C	–1°C/min	Sample temp. lowered to –60°C at –1°C/min.
f.	–60°C	–90°C	–5°C/min	Sample temp. lowered to –90°C at –5°C/min.
g.	Hold at –90°C and signal end of run.			

3.7. Quality-Control (Release) Testing

1. One QC aliquot for each batch of DC must be thawed and tested to ensure that the DC preparation conforms to specifications for identity, purity, and viability before the cells can be injected into human subjects (*see* **Note 16**). The second QC aliquot for each batch is to be kept frozen in case future testing is needed.

3.8. Injection Preparation

1. Thaw an aliquot of DC designated "for injection" in a 37°C water bath filled with sterile water. Working in the BSC, use a blunt cannula to draw the cell suspension up equally into two labeled 1-mL syringes. Place the syringes on ice and transport to the clinic for injection (*see* **Note 17**).

4. Notes

1. We have not included in the materials list required items that are routinely found in a modern cell-culture laboratory. This list would include a class II biological safety cabinet; a water-jacketed, 37°C, 5% CO_2 tissue-culture incubator; a refrigerated centrifuge (Beckman Coulter Allegra 6KR or equivalent) with a rotor and buckets/carriers suitable for 15-, 50-, and 250-mL conical tubes; a water bath; standard and inverted microscopes; a vortex; a hemacytometer; a refrigerator; and –20°C, –80°C, and liquid-nitrogen freezers. The laboratory should be supplied with assorted sterile filtration units, pipets and pipetting devices, pipet tips, needles, syringes, and cell-culture flasks. Sources of liquid nitrogen, dry ice, and wet ice should be available. We would also like to note that the sources of itemized equipment, reagents, and supplies are only suggested; other manufacturers may offer equivalent products that give excellent results.

2. We have achieved superior results with cryopreservation of PBMC and dendritic cells using a commercially available mechanical controlled-rate freezing device (Planer Kryo-10). In our hands, antigen-loaded DC frozen using such a device have significantly better immunostimulatory capacity than cells frozen using inexpensive isopropanol freezing baths (such as the Nalgene Cryo 1°C chamber). DC prepared using the controlled-rate freezer are identical to freshly prepared DC when assessed for cell-surface phenotype, immunostimulatory capacity, and migratory response to chemokines (unpublished observations). The freezer should be programmed by a qualified service technician authorized by the manufacturer. A sample program is shown in **Table 2**. The program takes approx 75 min to run.

3. Leukapheresis and plasmapheresis products must be obtained by a qualified cell-collection facility or contractor. To obtain PBMC we typically request that the facility process 10 L of blood (approx two blood volumes) with the blood cell separator set to obtain mononuclear cells. The cells and plasma should be processed as soon as possible following collection, although we have obtained good results with products that have been shipped overnight on wet ice.

4. *Cytokines, peptides and protein antigens*. In addition to cytokines from CellGenix, we have obtained excellent results with cytokines from R&D Systems, Minneapolis, MN. It is important that cytokines used to prepare clinical-grade DC have a detailed certificate of analysis and have been tested for sterility. It is also desirable to purchase reagents that did not come into contact with animal products during their production; otherwise, they may need to be tested for the presence of adventitious viral agents before they can be used in clinical trials. Clinalfa (Laufelfingen, Switzerland) is a good source for a variety of pharmaceutical-grade peptides that carry CD8 or T-helper epitopes for viral and tumor-associated antigens. Alternatively, if accompanied by a detailed certificate of analysis and tested for sterility, peptides manufactured by somewhat less exacting standards may be acceptable if they are not to be directly injected into patients. KLH is an animal product and must be tested for the presence of adventitious viral agents before use in human subjects. Biosyn KLH comes tested for adventitious viral agents and in the United States is approved for use by the FDA.

5. For the preparation of freezing media we specify the use of the Millex-LG filter unit because the membrane and filter housing are compatible with DMSO. Do not substitute an incompatible filter when filtering any DMSO-containing solution. As an alternative, since the DMSO stock solution is certified sterile, the solution may be prepared without DMSO, then filtered, and then the DMSO can be added. Freezing solutions must be chilled completely to 0 to 4°C prior to use to achieve best results.

6. In the United States, clinical protocols using antigen-loaded dendritic cells for immunotherapy in human subjects must first be approved by the Food and Drug Administration and your institutional review board. All cell-processing steps should be carried out in an appropriate controlled environment (i.e., a clean room with HEPA-filtered air) following current good manufacturing practices (cGMP). This is especially true when working with an open culture system such as described here. Work with open vessels should be carried out in a class II biological safety cabinet (BSC) using aseptic technique. Workers should be fully gowned and gloved, including shoe covers, a head cover, and a face mask. Be mindful that the finished cell product is for autologous use only: throughout the procedure, all tubes and plates should be labeled with two unique identifiers (such as a patient ID number and a product batch number) to avoid mix-ups and cross-contamination with other products.

7. The three "soft" spins at $400g$ remove most of the platelets, which remain in the supernatant.

8. We typically obtain yields of about 3 billion PBMC, enough for 15 frozen aliquots.

9. We plate 35 million cells per 10-cm tissue-culture plate because in our hands this is the lowest number of cells that can reproducibly saturate the plate (these plates will only yield a maximum of 5 to 6 million immature DC on d 5). There may be donor to donor variability in the optimal number of cells to plate (we have plated up to 50 million PBMC/plate), but the objective is always to use just enough cells to yield at least 5 million cells/plate on d 5.

10. IL-4 and GM-CSF induce the differentiation of monocytes (large CD14$^+$ cells) into immature DC (which are large, nonadherent, CD14$^-$ CD83$^-$ cells). It is a good idea to

carry out titration experiments to determine the optimal amount of these cytokines needed to achieve the desired effect. GM-CSF is required to keep the cells viable in culture, whereas IL-4 prevents monocyte differentiation into macrophages. Macrophages are easily identified as large, adherent cells with a "fried egg" appearance. In our hands, 100 IU/mL GM-CSF and 200 IU/mL IL-4 are sufficient to induce monocyte differentiation into immature DC. Increasing the concentration of these cytokines has no adverse effects, but tends not to improve the yield of immature DC on d 5.

11. It is important to understand the morphological changes to expect in the cell culture. After washing out most of the lymphocytes on d 0, the remaining monocytes can be seen adhering tightly to the plastic surface of the tissue-culture dish, many of them with a flattened appearance. A fair number of adherent platelets will also be seen, which are much smaller than monocytes or lymphocytes. Most of the platelets will not survive the wk-long culture period, and platelets are not noticeably present by d 7. During the first 5 d of culture, the monocytes will detach from the plastic as they differentiate into immature DC. There will be a fair amount of cell death and debris visible, but it is reasonable to expect a viable cell yield of 10 to 15% (relative to the number of PBMC plated) by d 5. Immature DC are large, relatively round cells with few or no cytoplasmic projections. They are two to three times the size of lymphocytes. Over 90% of the cells should be non-adherent by d 5, with the vast majority having the morphological characteristics of immature DC (most of the remaining cells are lymphocytes). Once the cells are washed and re-plated on d 5, much less cell debris should be seen. You should expect about two thirds of the cells to survive from d 5 to d 7. By d 5, some of the DC may begin to show early changes associated with DC maturation—the characteristic cytoplasmic projections (dendrites) or veils. These changes are much more evident on d 7 following the overnight maturation stimulus (culture in MCM mimic). By d 7, approx 80% of the cells in the culture should be large, nonadherent cells with numerous cytoplasmic projections and/or veils. Most of the remaining cells will be lymphocytes (small round cells). There will be some cell debris and evidence of cell death, but this should not be a predominant feature. It is reasonable to expect a 5 to 10% yield of mature DC (relative to the number of PBMC plated) on d 7.

12. Planning for d 6. KLH is a very potent immunogen, so it may not be desirable to inject a patient with KLH for every injection in a series of immunizations. In our current trial of DC for immunotherapy of malignant melanoma, we prepare two parallel batches of DC, one loaded with peptides and KLH to be used in the first injection, and one loaded with peptides alone that is used for the following three injections. This way all of the injections are prepared at the same time but in two parallel batches. If you wish to similarly inject differently pulsed DC at different time points during a clinical trial, we recommend that you also break the preparation up into parallel batches at this point.

13. It is a good idea to plan ahead for the peptide-loading step on d 7 at this point. If you plan to pulse the DC with more than one peptide, it is best to pulse with only one peptide per well—i.e., do not pool peptides before adding to the DC culture. By not pooling the peptides you avoid the possibility that some of the peptides may be preferentially recognized on a given DC due to competition *(28)*. To efficiently pulse DC with more than one peptide, plate the day 5 DC into a number of wells that is a multiple of the number of peptides you will be adding. This allows each peptide to be distributed to the same number of wells. You can adjust the concentration of DC to anywhere from 1.5 to 2 million cells/well to ensure that you plate into the multiple of wells needed.

14. MCM mimic is a potent cocktail of proinflammatory cytokines and PGE$_2$ that reproducibly results in high-level stimulation of dendritic cell maturation following overnight

(18 to 24 h) culture *(4,5,9)*. Most laboratories use this cocktail in place of monocyte-conditioned medium because it is better defined and provides more reproducible DC maturation. Of its four components, we use final concentrations in tissue-culture medium of 5 ng/mL TNF-α, 5 ng/mL IL-1β, 150 ng/mL IL-6, and 1 μg/mL PGE$_2$.

15. The optimal concentration of peptides to use to load DC is not currently known. In our hands, mature d-7 DC pulsed with peptide concentrations of 1 and 10 μM are clearly able to stimulate antigen-specific T-cell clones in vitro. We have obtained better immuno-stimulatory capacity using a 1- to 2-h pulse on d 7 than with an overnight pulse beginning on d 6 (unpublished results). A discussion on the dosing of DC with peptides may be found in Chapter 1.

16. In the United States, the Food and Drug Administration (FDA) requires that therapeutic cells be tested or validated for identity, purity, potency, and stability before they can be used in human subjects. We have validated this method to ensure the identity, potency, and stability of the cells by testing frozen/thawed DC for cell-surface phenotype (high-level expression of HLA-DR, CD86, CCR7, CD83, negative staining for CD14), immuno-stimulatory capacity, and viability under transport conditions. Frozen/thawed DC routinely and specifically stimulate MHC-restricted antigen-specific T-cell clones in lymphocyte proliferation and interferon γ Elispot assays, with activity in these assays indistinguishable from freshly prepared DC. The frozen/thawed DC are stable for at least 2 h in freezing solution 2 when kept on ice. In addition, we test a QC aliquot of each batch of DC for viability (Trypan blue staining), sterility (bacterial, fungal, and mycoplasma cultures, mycoplasma DNA fluorescence), absence of bacterial endotoxin (Limulus amoebocyte lysate assay), and identity (flow cytometry). Plasma and DMSO will interfere with the Limulus amoebocyte lysate (LAL) assay, so samples need to be diluted 10- to 20-fold and tested using a sensitive kinetic chromogenic assay (this can be outsourced or done with a commercially available kit from Cambrex). Our current QC (release) criteria include >70% viable cells, negative results for all sterility and endotoxin tests, and >50% of the cells having the characteristics of mature DC by flow cytometry (large, CD14$^-$ CD83$^+$ cells). We routinely obtain close to 90% mature DC, with cell viability usually >90%. Most of the remaining cells are lymphocytes.

17. The optimal route of administration of dendritic cell vaccines is still a matter of debate. DC vaccines may be administered by subcutaneous, intradermal, or intravenous injection, or may be injected directly into lymph nodes or tumors. We currently administer bilateral subcutaneous injections, 0.5 mL each, into the medial aspect of the upper arm (a region that drains into the axillary lymph nodes). If the axillary lymph nodes have been removed surgically, we inject into a similar location in the thighs. The freezing solution contains 10% DMSO, USP, in autologous plasma, which is compatible with injection into human subjects.

References

1 Thurner, B., Roder, C., Dieckmann, D., et al. (1999) Generation of large numbers of fully mature and stable dendritic cells from leukapheresis products for clinical application. *J. Immunol. Methods* **223,** 1–15.

2 Banchereau, J., Palucka, A. K., Dhodapkar, M., et al. (2001) Immune and clinical responses in patients with metastatic melanoma to CD34(+) progenitor-derived dendritic cell vaccine. *Cancer Res.* **61,** 6451–6458.

3 Fong, L., Hou, Y., Rivas, A., et al. (2001) Altered peptide ligand vaccination with Flt3 ligand expanded dendritic cells for tumor immunotherapy. *Proc. Natl. Acad. Sci. USA* **98,** 8809–8814.

4 Jonuleit, H., Kuhn, U., Muller, G., et al. (1997) Pro-inflammatory cytokines and prostaglandins induce maturation of potent immunostimulatory dendritic cells under fetal calf serum-free conditions. *Eur. J. Immunol.* **27,** 3135–3142.

5 Lee, A. W., Truong, T., Bickham, K., et al. (2002) A clinical grade cocktail of cytokines and PGE(2) results in uniform maturation of human monocyte-derived dendritic cells: implications for immunotherapy. *Vaccine* **20(Suppl 4),** A8–A22.

6 Bender, A., Sapp, M., Schuler, G., Steinman, R. M., and Bhardwaj, N. (1996) Improved methods for the generation of dendritic cells from nonproliferating progenitors in human blood. *J. Immunol. Methods* **196,** 121–135.

7 Romani, N., Reider, D., Heuer, M., et al. (1996) Generation of mature dendritic cells from human blood. An improved method with special regard to clinical applicability. *J. Immunol. Methods* **196,** 137–151.

8 Pullarkat, V., Lau, R., Lee, S. M., Bender, J. G., and Weber, J. S. (2002) Large-scale monocyte enrichment coupled with a closed culture system for the generation of human dendritic cells. *J. Immunol. Methods* **267,** 173–183.

9 Berger, T., Feuerstein, B., Strasser, E., et al. (2002) Large-scale generation of mature monocyte-derived dendritic cells for clinical application in cell factories. *J. Immunol. Methods* **268,** 131.

10 Nestle, F. O., Alijagic, S., Gilliet, M., et al. (1998) Vaccination of melanoma patients with peptide- or tumor lysate-pulsed dendritic cells. *Nat. Med.* **4,** 328–332.

11 Schuler-Thurner, B., Schultz, E. S., Berger, T. G., et al. (2002) Rapid induction of tumor-specific type 1 T helper cells in metastatic melanoma patients by vaccination with mature, cryopreserved, peptide- loaded monocyte-derived dendritic cells. *J. Exp. Med.* **195,** 1279–1288.

12 Dhodapkar, M. V., Steinman, R. M., Sapp, M., et al. (1999) Rapid generation of broad T-cell immunity in humans after a single injection of mature dendritic cells. *J. Clin. Invest.* **104,** 173–180.

13 Banchereau, J., Briere, F., Caux, C., et al. (2000) Immunobiology of dendritic cells. *Annu. Rev. Immunol.* **18,** 767–811.

14 Bhardwaj, N. (2001) Processing and presentation of antigens by dendritic cells: implications for vaccines. *Trends Mol. Med.* **7,** 388–394.

15 Mitchell, D. A. and Nair, S. K. (2000) RNA-transfected dendritic cells in cancer immunotherapy. *J. Clin. Invest.* **106,** 1065–1069.

16 Sullenger, B. A. and Gilboa, E. (2002) Emerging clinical applications of RNA. *Nature* **418,** 252–258.

17 Geiger, J., Hutchinson, R., Hohenkirk, L., McKenna, E., Chang, A., and Mule, J. (2000) Treatment of solid tumours in children with tumour-lysate-pulsed dendritic cells. *Lancet* **356,** 1163–1165.

18 Chang, A. E., Redman, B. G., Whitfield, J. R., et al. (2002) A phase I trial of tumor lysate-pulsed dendritic cells in the treatment of advanced cancer. *Clin. Cancer Res.* **8,** 1021–1032.

19 Rafiq, K., Bergtold, A., and Clynes, R. (2002) Immune complex-mediated antigen presentation induces tumor immunity. *J. Clin. Invest.* **110,** 71–79.

20 Kalergis, A. M. and Ravetch, J. V. (2002) Inducing tumor immunity through the selective engagement of activating Fcgamma receptors on dendritic cells. *J. Exp. Med.* **195,** 1653–1659.

21 Schuurhuis, D. H., Ioan-Facsinay, A., Nagelkerken, B., et al. (2002) Antigen-antibody immune complexes empower dendritic cells to efficiently prime specific CD8+ CTL responses in vivo. *J. Immunol.* **168,** 2240–2246.

22 Larsson, M., Fonteneau, J. F., Somersan, S., et al. (2001) Efficiency of cross presentation of vaccinia virus-derived antigens by human dendritic cells. *Eur. J. Immunol.* **31,** 3432–3442.

23 Albert, M. L., Sauter, B., and Bhardwaj, N. (1998) Dendritic cells acquire antigen from apoptotic cells and induce class I- restricted CTL. *Nature* **392,** 86–89.

24 Kotera, Y., Shimizu, K., and Mule, J. J. (2001) Comparative analysis of necrotic and apoptotic tumor cells as a source of antigen(s) in dendritic cell-based immunization. *Cancer Res.* **61,** 8105–8109.

25 Dhodapkar, M. V., Steinman, R. M., Krasovsky, J., Munz, C., and Bhardwaj, N. (2001) Antigen-specific inhibition of effector T cell function in humans after injection of immature dendritic cells. *J. Exp. Med.* **193,** 233–238.

26 Jonuleit, H., Giesecke-Tuettenberg, A., Tuting, T., et al. (2001) A comparison of two types of dendritic cell as adjuvants for the induction of melanoma-specific T-cell responses in humans following intranodal injection. *Int. J. Cancer* **93,** 243–251.

27. Feuerstein, B., Berger, T. G., Maczek, C., et al. (2000) A method for the production of cryopreserved aliquots of antigen- preloaded, mature dendritic cells ready for clinical use. *J. Immunol. Methods* **245,** 15–29.

28. Palmowski, M. J., Choi, E. M., Hermans, I. F., et al. (2002) Competition between CTL narrows the immune response induced by prime- boost vaccination protocols. *J. Immunol.* **168,** 4391–4398.

9

Phenotypical and Functional Characterization of Clinical-Grade Dendritic Cells

I. Jolanda M. de Vries, Gosse J. Adema, Cornelis J. A. Punt, and Carl G. Figdor

Summary

Dendritic cells (DC) are the most potent antigen-presenting cells and form a promising new treatment modality. Fully activated DC loaded with antigen are very useful in stimulating immune responses, in particular those to combat cancer. Immature DC can either cause immunological tolerance or induce regulatory T-cells, opening up future application in transplantation, autoimmunity, and perhaps chronic inflammation.

For these clinical applications, generation of DC under Good Manufacturing Practice conditions and without the use of animal products is a main prerequisite. To date, there are many different DC culture protocols, which subsequently lead to different types of DC. Protocols differ not only in DC preparation techniques, but also many other variables, like maturation status, dose and timing interval, route of administration, and antigen loading. DC vaccination, although very promising, is far from standardized. In this chapter we discuss the usefulness of standardized clinical and immunological criteria and the need for careful study design to further optimize the use of dendritic cells and to unequivocally prove their efficacy.

Key Words: Quality control; Good Manufacturing Practice; maturation; migration; immunotherapy.

1. Introduction

A role for dendritic cells (DC) has been implicated in several diseases, including cancer. DC loaded with tumor antigens have been shown to be potent inducers of T-cell responses in vitro. The ability to culture large amounts of DC from monocytes in vitro combined with the availability of class I-restricted peptides derived from tumor-associated antigens, such as gp100, tyrosinase, MAGEs, and NY-ESO-1, gives the opportunity to vaccinate cancer patients with peptide-loaded DC *(1–5)*. Recently, DC pulsed with tumor antigens have been successfully used in vivo for the induction of antitumor T-cell reactivity in melanoma patients *(1,2)*. Therefore, DC have the potential to be used as vaccine adjuvants in immunotherapy against cancer. Currently, many

clinical trials using DC-based immunotherapies are ongoing for the treatment of a wide range of malignancies. It is not surprising that in these international trials, huge variations occur in both culturing of DC and in study design *(6)*. DC can be directly isolated from blood and by culturing from peripheral blood monocytes or CD34$^+$ bone-marrow cells in the presence of interleukin (IL)-4 and granulocyte/monocyte colony-stimulating factor (GM-CSF), tumor necrosis factor-α (TNF-α), stem cell factor, and FLT3 ligand, respectively *(7–9)*.

So far, most DC vaccines have been used to stimulate immune responses, in particular those to combat cancer *(10,11)*. Recent findings indicate that immature DC can either cause immunological tolerance or induce regulatory T-cells, opening up future application in transplantation, autoimmunity, and perhaps chronic inflammation. Furthermore, generation of DC under Good Manufacturing Practice (GMP) conditions is a main prerequisite for their use in clinical trials. In this chapter we will discuss current issues relating to monocyte-derived DC (MoDC) culturing under GMP guidelines as well as the function of these cells for specific goals.

2. Generation of Monocyte-Derived DC Under GMP Conditions

Today, all DC vaccines appear to be safe and nontoxic, with only occasional and mild side effects. However, generation of MoDC according to GMP-guidelines, without the use of animal products like fetal calf serum (FCS), is necessary for their use in clinical trials. Especially the use of animal-derived products is reported by Mackensen et al. to be of risk *(12)*. They show the presence of antibodies to FCS and bovine serum albumin (BSA) in patients vaccinated with DC cultured in FCS/BSA. Moreover, in their study one patient had a type I hypersensitivity anaphylactic reaction after repetitive vaccination with autologous peptide-pulsed DC. On the basis of these data, DC cultured either in human serum or plasma or under serum-free conditions are recommended for therapeutic applications in vivo.

To generate DC in the absence of FCS for clinical applications, many laboratories set out to optimize the differentiation of monocytes to DC in the presence of clinical-grade media either serum-free or supplemented with human serum/plasma (pooled or autologous). This has led to the use of many different protocols and subsequently to different types of DC. Protocols differ not only in DC preparation but also many other variables, such as maturation status, dose and timing interval, route of administration, and antigen loading. DC vaccination, although very promising, is far from standardized, preventing the introduction of this type of therapy as standard cancer treatment. To make this possible, there is a strong need for standardization and quality control of ex vivo-generated DC and for the implementation of large two-pronged double-blind clinical studies to unequivocally prove clinical efficacy. This is needed to let this form of immunotherapy move away from bulky disease to patients with low tumor burden. Most studies conducted so far concern late-stage cancer patients with metastatic lesions. The current lack of standardization prevents the inclusion of early-stage patients. In these patients, long-term side effects due to prolonged survival might be foreseen, and therefore DC must be grown in molecularly well-defined culture media, cytokine cocktails, and/or molecularly defined triggers for DC activation (e.g., toll-

like receptor ligands). Additionally, DC have to be cultured in closed culture systems, which will simplify handling, thus limiting the use of expensive and labor-intensive GMP facilities.

3. Culturing and Phenotypical Characterization of Immature and Mature Monocyte-Derived DC

To isolate monocytes after a leukapheresis, several options are available. Counter-flow centrifugation (centrifugal elutriation), adherence of peripheral blood mono-nuclear cells to plastic, or isolation of CD14$^+$ cells by magnetic sorting, using clinical-grade anti-CD14 microbeads. We used counter-flow centrifugation (centrifu-gal elutriation) and compared these DC with those generated from adherent peripheral blood mononuclear cells. Both GMP-approved methods yield highly purified mono-cytes, from which, with the use of IL-4 and GM-CSF, immature DC *(7)* could be generated that express MHC I and II and low levels of costimulatory molecules. Strik-ingly, maturation of the immature DC generated from elutriated monocytes using either monocyte-conditioned medium (MCM) or MCM/prostaglandin (PG)E$_2$/ TNF-α appeared to be difficult and resulted in a significantly lower yield. This lack of matu-ration of elutriated DC might be due to the fact that the elutriated monocytes are first activated by the leukapheresis process, a phenomenon also described by Thurner and colleagues *(2)*, and subsequently by the counter-flow centrifugation procedure, in which they are subjected to shear stress.

The optimal maturation stimulus to obtain mature DC from immature DC is still unclear. Recent clinical trials have tended to use either MCM *(2)* or the cytokine TNF-α, either alone *(13–15)* or in combination with IL-1β, IL-6, and PGE$_2$ *(16–18)*. Cytokines may be preferable to MCM, as they can be standardized and are molecu-larly defined. The combination of TNF-α, IL-1β, IL-6, and PGE$_2$ has become popular as a result of analyses in vitro demonstrating enhanced capacity to stimulate T-cells under FCS-free conditions *(16)*. Despite the previously observed lack of IL-12 pro-duction and subsequent Th1 development of PGE$_2$-matured DC in vitro (FCS-cul-tured) *(19)*, after vaccination with MCM/TNF-α/PGE$_2$-matured DC we observed polarization of T-cells towards interferon (IFN)-γ production in patients *(20)*. Further-more, exposure to PGE$_2$ is required for optimal migration of mature DC towards the chemokine receptor (CCR)7 ligands CC-chemokine ligand (CCL)19 and CCL21, chemokines which attract DC to lymph nodes *(21,22)*.

A significant issue to be taken into account when discussing DC maturation is the possibility of exhaustion. DC that are maximally stimulated have a relatively short window in which to produce Il-12—on the order of 48 h *(19,23)*. Maturation of DC in vitro sets the clock ticking, and therefore it is hoped that, after migration of antigen-expressing DC from the site of injection to the lymph node, these DC are still capable of stimulating Th1-type tumor-specific response. The ideal maturation cocktail there-fore may be one that induces migratory capacity yet leaves them responsive to further stimulation by CD40 ligand through engagement of antigen-specific T-cells in vivo, resulting in release of bioactive IL-12 in the microenvironment where it is most needed. Maturation with IFN-α appears to cause this effect *(24)*, and more recent studies sug-

Table 1

General Quality Criteria for DC to be Used in Clinical Trials

Microbiological controls	Negative for bacteria and fungal contamination
Viability	>50% determined by tryphan blue exclusion
Purity	>70% determined by light scatter or staining with non-DC lineage markers
Morphology	Immature: Adherent, stretched cells with some extensions
	Mature: Loosely attached, veiled and clustered cells
Phenotype	Immature: $CD14^{neg/low}$, $CD83^{neg}$, $CD80^{neg/low}$, $CD86^{low}$, MHC class I^{pos}, MHC class II^{pos}, DC-SIGN^{pos}, CCR5^{pos}
	Mature: $CD83^{pos}$, $CD80^{pos}$, $CD86^{pos}$, MHC class I^{pos}, MHC class II^{pos}, DC-SIGN^{pos}, CCR7^{pos}
Induction of immune response	Mixed lymphocyte reaction: T cell proliferation at DC:PBMC ratio 1:20 in at least one donor.
	Recognition of the loaded antigen by T cells: Cytotoxicity assay or cytokine production

gest that transient exposure to maturation stimuli may also be useful *(25)*. Another approach for the generation of mature DC is based on an alternate DC activation pathway, using calcium-mobilizing agents to drive differentiation of fully mature DC from monocytes in only 2 d *(26)*. The validity of these approaches awaits testing in a controlled clinical setting.

4. Quality Control

DC have to be evaluated for multiple DC markers and meet release criteria. There is an urgent task for the research community to define these criteria. The DC preparations should be tested for sterility/pyrogenicity, viability (after thawing), purity, phenotype (surface antigens), migratory capacity, and function. Here, we would like to introduce general quality criteria that DC should meet before use in a clinical setting (**Table 1**, **Fig. 1**).

4.1. Sterility/Pyrogenicity, Viability, and Purity

Samples of the DC vaccine harvested at day 4 and on the day of the first DC vaccination should be sent for microbiologic analysis for clearance.

For release, viability of the DC vaccine, determined for example by trypan blue exclusion, should be more than 50%. This is a percentage that can easily be reached at the first vaccination day, when DC are harvested, loaded with antigen, and then immediately administrated to the patient. However, subsequent DC vaccines are often frozen and thawed at the required vaccination day. In these samples, the viability is lower,
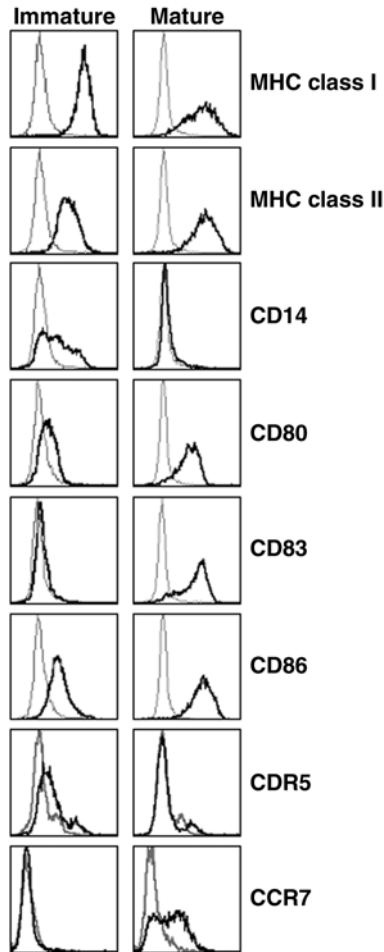
Fig. 1. Flow-cytometric analysis of immature dendritic cells and mature dendritic cells (cultured from adherent monocytes). Gray lines represent isotype-matched controls, whereas the dark overlays are the markers as indicated on the right.

but it is possible to reach the criterion of 50% when optimized freezing and thawing methods are used *(21,27)*. These methods describe viabilities up to 80% of frozen/ thawed DC *(27)*.

The purity of the DC preparation can be evaluated based on light scatter (flow cytometry) as well as staining for specific markers (non-DC lineage markers) for contaminating cells. Berger et al. have reported that DC preparations are often contaminated with T-cells (CD3^{+}), NK cells (CD56^{+}), and especially by B-cells (CD19^{+}), but they still reached purities of >85% DC *(27)*. We propose that DC preparations with purities of >70% can be released for clinical use.

4.2. Morphology, Phenotype, and Function

Before administration of DC, these cells should be evaluated extensively by flow cytometry and microscopy. The morphology of the generated DC can be analyzed under an inverted phase-contrast microscope. The typical morphology (nonadherent veiled cells) of mature DC is easy to distinguish from the adherent and stretched morphology of immature DC and from the very large round adherent macrophages *(20)*. To determine the stability of the DC, the "wash-out" test is proposed. In this test, DC are washed and deprived of cytokines. Under these conditions, only fully mature DC remain nonadherent, veiled, and viable *(28)*.

Phenotypically, the quality of the mature DC vaccine could be monitored by flow cytometry, evaluating surface expression of the maturation marker CD83, as well as the costimulatory molecules CD80 and CD86. These markers should be low or even absent on immature DC preparations. Both DC types should have high levels of DC-SIGN and MHC class I and class II; on mature DC, an increase of the latter two molecules is preferred.

Migration of DC to lymph nodes is a prerequisite in the induction of an immune response. Therefore the expression of CCR molecules, allowing directed migration, is highly important. Immature DC do not express CCR7, but do express CCR5, whereas mature DC are lacking CCR5 but do express (when fully mature) CCR7, allowing them to migrate to the T-cell areas of lymph nodes and carry out their function *(20–22)*.

Next to reaching the T-cells, DC samples should be able to stimulate T-cell proliferation in a mixed lymphocyte reaction in vitro. A drawback of this assay is that it is not only dependent on the quality of DC but also on the responder cells, in particular the extent of the HLA-mismatch, and therefore the data generated in different individuals cannot easily be compared. However, DC should display a potent stimulatory capacity at low DC/peripheral blood mononuclear cell ratios.

Mixed lymphocyte reactions provide information about the competence of DC to stimulate an immune response. However, in immunotherapy we are aiming at inducing immune responses towards well-defined antigens. Therefore, DC should be recognized by cytotoxic T-cells with specificity for the loaded antigens. This should be tested on freshly harvested and antigen-loaded DC as well as on frozen/thawed DC with preloaded antigen. Since this testing requires a lot of the mostly rare cytotoxic T-cells, we propose to load antigenic peptides after thawing of the DC to ensure optimal peptide loading *(21)*.

5. Functional Characterization of Immature and Mature DC

5.1. DC Function In Vivo

In vivo, immature DC originating from the bone marrow and present in nonlymphoid tissues are potent in antigen uptake and processing *(29)*. Upon antigenic stimulation under inflammatory conditions, DC change their chemokine receptor expression pattern and migrate to the secondary lymphoid tissues *(30–32)*. Here, DC become fully mature and secrete an array of chemokines to recruit B-cells, T-cells, and other DC to efficiently induce an immune response *(29,33)*.

5.2. Antigen Uptake and T-Cell Activation

DC can take up a wide array of antigens and present them to T-cells as peptides bound to both MHC class I and II. They mediate diverse functions in the immune system with high efficiency. These functional stages are related to the maturation state of the DC. Immature cells are adept at endocytosis and express relatively low levels of surface MHC class I and II and costimulatory molecules. Therefore, it is useful to maintain cells in an immature state when preparing for antigen loading. Exogenous antigens such as proteins or apoptotic cells are taken up by immature DC and processed and subsequently retained for use as immunogenic peptides days later. After stimulation with microbial products or inflammatory cytokines, immature DC transform into mature DC. These cells have a reduced capacity for antigen uptake but are extremely well equipped for T-cell stimulation: high MHC class I and II and costimulatory molecules on their surface as well as T-cell adhesion molecules *(34)*. Maturation also leads to the extension of long dendrites, which may increase the capacity to capture T-cells. Furthermore, upon maturation DC remodel their chemokine receptor repertoire and thereby gain the ability to migrate to lymph nodes and stimulate T-cells, the ultimate goal in DC-based immunotherapy *(31)*.

5.3. Migration

Upon exposure to pathogens in peripheral tissues, resident immature DC become activated through toll-like receptors *(35)* and take up and process antigen, while migrating to the draining lymph nodes to present their antigenic load *(36)*. To facilitate migration, CCR5 is down-regulated, while CCR7 is upregulated, the latter being required for trafficking and entry into the T-cell areas of the lymph node *(31,37–39,40)*.

DC injected into patients must actively migrate to lymph nodes and subsequently into the T-cell areas of lymph nodes. Mature DC are migratory both in vitro and in vivo, irrespective of whether they are administered into the skin or intranodally *(20)*. By contrast, in vitro-generated immature DC are unable to leave the skin after intradermal injection. The low migratory capacity of immature DC relates directly to their strong adhesive properties in vitro, which is mediated by highly expressed β1 integrins, in particular α5β1 *(20,41)*. Similar findings have been reported by Gunzer et al., who show in a collagen matrix model that the immature state of murine DC is characterized by low migration, whereas mature murine DC exhibit high migratory activity *(42)*.

In vitro-generated monocyte-derived immature DC lack the chemokine receptor CCR7, required for migration into the T-cell areas of lymph nodes *(43,44)*. Hence, immature DC generated in vitro do not co-localize and interact with naïve T-cells in the lymph nodes, a prerequisite for the induction of an effective immune response *(20)*. In contrast to immature DC, monocyte-derived mature DC express CCR7 and, as expected, these cells migrate into the T-cell areas of the lymph nodes *(20)*. The inability of immature DC to migrate into the T-cell areas could explain why vaccination with antigen-loaded immature DC in melanoma patients fails to induce proliferative as well as DTH responses. The failure of immature DC to induce an immune response correlates with the observation that immature DC, when used as a vaccine adjuvant, give rise to T-cells that display the typical properties of regulatory T-cells—non-proliferative, IL-10-pro-

ducing T-cells that can dampen pre-existing antigen-specific effector T-cell function *(45,46)*.

5.4. Chemokine Production

DC are known to secrete a variety of chemokines that allow them to attract and interact with lymphocytes to induce an immune response *(40,61)*.We have showed that the chemokine profiles of clinical-grade mature and immature DC are similar, as previously observed for DC cultured in the presence of FCS *(47,48)*, including high expression of DC-CK1 that preferentially attracts naïve T-cells in mature DC *(21,49)*. DC also express high levels of TARC and MDC, which have recently been reported to attract memory T-cells in addition to NK- and T-helper-2 cells *(50–52)*.

6. Application of Immature and Mature DC

6.1. DC Immunotherapy to Induce Tolerance

An increasing number of preclinical studies focus on the capacity of immature DC to induce antigen-specific unresponsiveness or tolerance following antigen capture. DC in the steady state are immature and can silence immunity in an antigen-specific manner through two recently identified mechanisms *(11)*. In one tolerance mechanism, due to the absence of DC maturation stimuli, interacting T-cells proliferate but are soon deleted. Effector functions and, therefore, memory do not develop, resulting in peripheral tolerance. A second tolerance mechanism involves the induction of IL-10-producing T-cells by immature DC, which in turn can silence other effector T-cells. Immature DC incubated with immunosuppressive agents such as dexamethasone *(53)*, vitamin D *(54)*, and more recently the Rel B inhibitor Bay *(55)* all result in IL-10-producing T-cells and thereby in the induction of peripheral tolerance.

While most clinical DC-vaccination studies so far are aimed at stimulating immune responses, the finding that immature DC are extremely suitable to silence immune responses opens up new clinical applications in transplantation, allergy, autoimmunity, and perhaps chronic inflammation.

6.2. DC Immunotherapy to Induce Immunity

Most DC vaccines have been generated from myeloid precursors or monocytes grown in GM-CSF/IL-4, further matured with cytokine cocktails and loaded with antigen ex vivo. Comparative studies with immature and mature DC clearly demonstrated that only mature DC stimulate protective T-cell responses *(20,45,46)*. Additionally, only mature DC show enhanced migration to draining lymph nodes when compared with immature DC *(20)*. The inability of immature DC to induce an immune response also indicates that monocyte-derived DC do not mature after injection in vivo *(56)*. Thus, for active immunization in cancer patients it appears to be critical that DC are matured in vitro before injection *(6)*.

Most studies conducted so far concern late-stage cancer patients with metastatic lesions. Clinical results are variable, although in several studies remarkable long-lasting objective clinical responses were observed. Therefore, DC vaccination represents a promising approach, which does not meet expectations yet due to the current lack of

knowledge. Evidence is accumulating that the dose and timing interval, route of administration, and antigen loading play a critical role in determining the quality and quantity of the immune response *(38,57)*. Especially the route of injection and the migration of DC from the injection site might highly influence clinical outcome. We recently showed that migration of DC is highly dependent on their maturation status *(20)*. Furthermore, we demonstrated that the majority of injected monocyte-derived DC matured in vitro, reside at the injection depot, despite the fact that they express CCR7 and are highly motile in vitro *(20,58–61)*. Gunzer et al. reasoned that the microenvironment largely influences emigration *(42)*. In addition, the relatively high local density of DC at the site of injection may affect this microenvironment, thereby having a major impact on emigration. Matrix metalloproteinases are good candidates to enhance the emigration of DC *(7)*. Certainly a better understanding of this lack of emigration is of importance for future DC vaccine development.

With regard to optimization of antigen loading of DC, one should keep in mind that monovalent antigen specificity is likely to be insufficient in patients with large tumor burden, also in view of the tumor minus variants that arise. Vaccination against multiple tumor antigens or against tumor antigens plus tumor-associated antigens expressed by stromal or endothelial cells in the tumor is currently being explored in preclinical models. Vaccination with these mixtures of antigens could induce a combined immune response that could have an additive if not synergistic effect.

7. Perspectives

To further optimize clinical efficacy, DC vaccination strategies need to be optimized, standardized, and quality controlled. DC must be grown in molecularly well-defined culture media, cytokine cocktails, and/or molecularly defined triggers of DC activation. Most importantly, DC have to be cultured in closed culture systems, which will simplify handling, thus limiting the use of expensive and labor-intensive GMP facilities. In the future, implementation of DC in large two-pronged double-blind studies are necessary to unequivocally prove clinical efficacy.

References

1. Nestle, F. O., Alijagic, S., Gilliet, M., et al. (1998) Vaccination of melanoma patients with peptide- or tumor lysate-pulsed dendritic cells. *Nat. Med.* **4(3),** 328–332.
2. Thurner, B., Haendle, I., Roder, C., et al. (1999) Vaccination with mage-3A1 peptide-pulsed mature, monocyte-derived dendritic cells expands specific cytotoxic T cells and induces regression of some metastases in advanced stage IV melanoma. *J. Exp. Med.* **190(11),** 1669–1678.
3. Hsu, F. J., Benike, C., Fagnoni, F., et al. (1996) Vaccination of patients with B-cell lymphoma using autologous antigen-pulsed dendritic cells. *Nat. Med.* **2(1),** 52–58.
4. Cochand, L., Isler, P., Songeon, F., and Nicod, L. P. (1999) Human lung dendritic cells have an immature phenotype with efficient mannose receptors. *Am. J. Respir. Cell Mol. Biol.* **21(5),** 547–554.
5. Vissers, J. L. M. De Vries, I. J. M., Oosterwijk, E., Figdor, C. G., and Adema, G. J. (2000) Towards specific immunotherapy employing dendritic cells in melanoma and renal cell carcinoma, in *Peptide-Based Cancer Vaccines.* Eurekah.com, Austin, TX, pp. 200–214.

6. McIlroy, D. and Gregoire, M. (2003) Optimizing dendritic cell-based anticancer immuno-therapy: maturation state does have clinical impact. *Cancer Immunol. Immunother.* **52(10),** 583–591.

7. Steinman, R. M. (1991) The dendritic cell system and its role in immunogenicity. *Annu. Rev. Immunol.* **9,** 271–296.

8. Hart, D. N. (1997) Dendritic cells: unique leukocyte populations which control the primary immune response. *Blood* **90(9),** 3245–3287.

9. Levin, D., Constant, S., Pasqualini, T., Flavell, R., and Bottomly, K. (1993) Role of dendritic cells in the priming of CD4+ T lymphocytes to peptide antigen in vivo. *J. Immunol.* **151(12),** 6742–6750.

10. Bancherau, J., Schuler-Thurner, B., Palucka, A. K., and Schuler, G. (2001) Dendritic cells as vectors for therapy. *Cell* **106(3),** 271–274.

11. Steinman, R. M. and Nussenzweig, M. C. (2002) Avoiding horror autotoxicus: the importance of dendritic cells in peripheral T cell tolerance. *Proc. Natl. Acad. Sci. USA* **99(1),** 351–358.

12. Mackensen, A., Drager, R., Schlesier, M., Mertelsmann, R., and Lindemann, A. (2000) Presence of IgE antibodies to bovine serum albumin in a patient developing anaphylaxis after vaccination with human peptide-pulsed dendritic cells. *Cancer Immunol. Immunother.* **49(3),** 152–156.

13. Marten, A., Flieger, D., Renoth, S., et al. (2002) Therapeutic vaccination against metastatic renal cell carcinoma by autologous dendritic cells: preclinical results and outcome of a first clinical phase I/II trial. *Cancer Immunol. Immunother.* **51(11–12),** 637–644.

14. Lin, C. L., Lo, W. F., Lee, T. H., et al. (2002) Immunization with Epstein-Barr Virus (EBV) peptide-pulsed dendritic cells induces functional CD8+ T-cell immunity and may lead to tumor regression in patients with EBV-positive nasopharyngeal carcinoma. *Cancer Res.* **62(23),** 6952–6958.

15. Stift, A., Friedl, J., Dubsky, P., et al. (2003) Dendritic cell-based vaccination in solid cancer. *J. Clin. Oncol.* **21(1),** 135–142.

16. Jonuleit, H., Kuhn, U., Muller, G., et al. (1997) Pro-inflammatory cytokines and prostaglandins induce maturation of potent immunostimulatory dendritic cells under fetal calf serum-free conditions. *Eur. J. Immunol.* **27(12),** 3135–3142.

17. Schuler-Thurner, B., Schultz, E. S., Berger, T. G., et al. (2002) Rapid induction of tumor-specific type 1 T helper cells in metastatic melanoma patients by vaccination with mature, cryopreserved, peptide-loaded monocyte-derived dendritic cells. *J. Exp. Med.* **195(6),** 1279–1288.

18. Holtl, L., Zelle-Rieser, C., Gander, H., et al. (2002) Immunotherapy of metastatic renal cell carcinoma with tumor lysate-pulsed autologous dendritic cells. *Clin. Cancer Res.* **8(11),** 3369–3376.

19. Kalinski, P., Hilkens, C. M., Wierenga, E. A., and Kapsenberg, M. L. (1999) T-cell priming by type-1 and type-2 polarized dendritic cells: the concept of a third signal. *Immunol. Today* **20(12),** 561–567.

20. De Vries, I. J., Krooshoop, D. J., Scharenborg, N. M., et al. (2003) Effective migration of antigen-pulsed dendritic cells to lymph nodes in melanoma patients is determined by their maturation state. *Cancer Res.* **63(1),** 12–17.

21. Scandella, E., Men, Y., Gillessen, S., Forster, R., and Groettrup, M. (2002) Prostaglandin E2 is a key factor for CCR7 surface expression and migration of monocyte-derived dendritic cells. *Blood* **100(4),** 1354–1361.

22. Luft, T., Jefford, M., Luetjens, P., et al. (2002) Functionally distinct dendritic cell (DC) populations induced by physiologic stimuli: prostaglandin E(2) regulates the migratory capacity of specific DC subsets. *Blood* **100(4),** 1362–1372.

23. Langenkamp, A., Messi, M., Lanzavecchia, A., and Sallusto, F. (2000) Kinetics of dendritic cell activation: impact on priming of TH1, TH2 and nonpolarized T cells. *Nat. Immunol.* **1(4),** 311–316.

24. Vieira, P. L., Heystek, H. C., Wormmeester, J., Wierenga, E. A., and Kapsenberg, M. L. (2003) Development of Th1-inducing capacity in myeloid dendritic cells requires environmental instruction. *J. Immunol.* **164(9),** 4507–4512.

25. Spisek, R., Bougras, G., Ebstein, F., et al. (2003) Transient exposure of dendritic cells to maturation stimuli is sufficient to induce complete phenotypic maturation while preserving their capacity to respond to subsequent restimulation. *Cancer Immunol. Immunother.* **52(7),** 445–454.

26. Czerniecki, B. J., Carter, C., Rivoltini, L., et al. (1997) Calcium ionophore-treated peripheral blood monocytes and dendritic cells rapidly display characteristics of activated dendritic cells. *J. Immunol.* **159(8),** 3823–3837.

27. Berger, T. G., Feuerstein, B., Strasser, E., et al. (2002) Large-scale generation of mature monocyte-derived dendritic cells for clinical application in cell factories. *J. Immunol. Methods* **268(2),** 131–140.

28. Romani, N., Reider, D., Heuer, M., et al. (1996) Generation of mature dendritic cells from human blood. An improved method with special regard to clinical applicability. *J Immunol Methods* **196(2),** 137–151.

29. Banchereau, J. and Steinman, R. M. (1998) Dendritic cells and the control of immunity. *Nature* **392(6673),** 245–252.

30. Caux, C., Dezutter-Dambuyant, C., Schmitt, D., and Banchereau, J. (1992) GM-CSF and TNF-alpha cooperate in the generation of dendritic Langerhans cells. *Nature* **360(6401),** 258–261.

31. Sallusto, F., Schaerli, P., Loetscher, P., et al. (1998) Rapid and coordinated switch in chemokine receptor expression during dendritic cell maturation. *Eur. J. Immunol.* **28(9),** 2760–2769.

32. Zlotnik, A. and Yoshie, O. (2000) Chemokines: a new classification system and their role in immunity. *Immunity* **12(2),** 121–127.

33. Sallusto, F., Mackay, C. R., and Lanzavecchia, A. (2000) The role of chemokine receptors in primary, effector, and memory immune responses. *Annu. Rev. Immunol.* **18,** 593–620.

34. Mellman, I. and Steinman, R. M. (2001) Dendritic cells: specialized and regulated antigen processing machines. *Cell* **106(3),** 255–258.

35. Cumberbatch, M., Dearman, R. J., and Kimber, I. (1997) Langerhans cells require signals from both tumour necrosis factor-alpha and interleukin-1 beta for migration. *Immunology* **92(3),** 388–395.

36. Hirao, M., Onai, N., Hiroishi, K., et al. (2000) CC chemokine receptor-7 on dendritic cells is induced after interaction with apoptotic tumor cells: critical role in migration from the tumor site to draining lymph nodes. *Cancer Res.* **60(8),** 2209–2217.

37. Kukutsch, N. A., Rossner, S., Austyn, J. M., Schuler, G., and Lutz, M. B. (2000) Formation and kinetics of MHC class I-ovalbumin peptide complexes on immature and mature murine dendritic cells. *J. Invest. Dermatol.* **115(3),** 449–453.

38. Nestle, F. O., Banchereau, J., and Hart, D. (2001) Dendritic cells: On the move from bench to bedside. *Nat. Med.* **7(7),** 761–765.

39 Cox, A. L., Skipper, J., Chen, Y., et al. (1994) Identification of a peptide recognized by five melanoma-specific human cytotoxic T cell lines. *Science* **264(5159),** 716–719.

40 Dieu, M. C., Vanbervliet, B., Vicari, A., et al. (1998) Selective recruitment of immature and mature dendritic cells by distinct chemokines expressed in different anatomic sites. *J. Exp. Med.* **188(2),** 373–386.

41. D'Amico, G., Bianchi, G., Bernasconi, S., et al. (1998) Adhesion, transendothelial migration, and reverse transmigration of in vitro cultured dendritic cells. *Blood* **92(1),** 207–214.

42 Gunzer, M., Friedl, P., Niggemann, B., Brocker, E. B., Kampgen, E., and Zanker, K. S. (2000) Migration of dendritic cells within 3-D collagen lattices is dependent on tissue origin, state of maturation, and matrix structure and is maintained by proinflammatory cytokines. *J. Leukoc. Biol.* **67(5),** 622–629.

43 Eggert, A. A., Schreurs, M. W., Boerman, O. C., et al. (1999) Biodistribution and vaccine efficiency of murine dendritic cells are dependent on the route of administration. *Cancer Res.* **59(14),** 3340–3345.

44 Parlato, S., Santini, S. M., Lapenta, C., et al. (2001) Expression of CCR-7, MIP-3beta, and Th-1 chemokines in type I IFN-induced monocyte-derived dendritic cells: importance for the rapid acquisition of potent migratory and functional activities. *Blood* **98(10),** 3022–3029.

45 Grabmaier, K., Vissers, J. L., De Weijert, M. C., et al. (2000) Molecular cloning and immunogenicity of renal cell carcinoma-associated antigen G250. *Int. J. Cancer* **85(6),** 865–870.

46 Dhodapkar, M. V., Steinman, R. M., Krasovsky, J., Munz, C., and Bhardwaj, N. (2001) Antigen-specific inhibition of effector T cell function in humans after injection of immature dendritic cells. *J. Exp. Med.* **193(2),** 233–238.

47 Vissers, J. L., Hartgers, F. C., Lindhout, E., Teunissen, M. B., Figdor, C. G., and Adema, G. J. (2001) Quantitative analysis of chemokine expression by dendritic cell subsets in vitro and in vivo. *J. Leukoc. Biol.* **69(5),** 785–793.

48 Lindhout, E., Vissers, J. L., Hartgers, F. C., et al. (2001) The dendritic cell-specific CC-chemokine DC-CK1 is expressed by germinal center dendritic cells and attracts CD38-negative mantle zone B lymphocytes. *J. Immunol.* **166(5),** 3284–3289.

49 Adema, G. J., Hartgers, F., Verstraten, R., et al. (1997) A dendritic-cell-derived C-C chemokine that preferentially attracts naive T cells. *Nature* **387(6634),** 713–717.

50 Sallusto, F., Lenig, D., Forster, R., Lipp, M., and Lanzavecchia, A. (1999) Two subsets of memory T lymphocytes with distinct homing potentials and effector functions. *Nature* **401(6754),** 708–712.

51 Godiska, R., Chantry, D., Raport, C. J., et al. (1997) Human macrophage-derived chemokine (MDC), a novel chemoattractant for monocytes, monocyte-derived dendritic cells, and natural killer cells. *J. Exp. Med.* **185(9),** 1595–1604.

52 Inngjerdingen, M., Damaj, B., and Maghazachi, A. A. (2000) Human NK cells express CC chemokine receptors 4 and 8 and respond to thymus and activation-regulated chemokine, macrophage-derived chemokine, and I-309. *J. Immunol.* **164(8),** 4048–4054.

53 Rea, D., van Kooten, C., van Meijgaarden, K. E., Ottenhoff, T. H., Melief, C. J., and Offringa, R. (2000) Glucocorticoids transform CD40-triggering of dendritic cells into an alternative activation pathway resulting in antigen-presenting cells that secrete IL-10. *Blood* **95(10),** 3162–3167.

54 Adorini, L., Penna, G., Giarratana, N., and Uskokovic, M. (2003) Tolerogenic dendritic cells induced by vitamin D receptor ligands enhance regulatory T cells inhibiting allograft rejection and autoimmune diseases. *J. Cell Biochem.* **88(2),** 227–233.

55 Martin, E., O'Sullivan, B., Low, P., and Thomas, R. (2003) Antigen-specific suppression of a primed immune response by dendritic cells mediated by regulatory T cells secreting interleukin-10. *Immunity* **18(1),** 155–167.

56 De Vries, I. J., Lesterhuis, W. J., Scharenborg, N. M., et al. (2003) Maturation of dendritic cells is a prerequisite for inducing immune responses in advanced melanoma patients. *Clin. Cancer Res.* **9(14),** 5091–5100.

57 Fong, L., Brockstedt, D., Benike, C., Wu, L., and Engleman, E. G. (2001) Dendritic cells injected via different routes induce immunity in cancer patients. *J. Immunol.* **166(6),** 4254–4259.

58 Barratt-Boyes, S. M., Zimmer, M. I., Harshyne, L. A., et al. (2000) Maturation and trafficking of monocyte-derived dendritic cells in monkeys: implications for dendritic cell-based vaccines. *J. Immunol.* **164(5),** 2487–2495.

59 Eggert, A. A., Schreurs, M. W., Boerman, O. C., et al. (1999) Biodistribution and vaccine efficiency of murine dendritic cells are dependent on the route of administration. *Cancer Res.* **59(14),** 3340–3345.

60 Morse, M. A., Coleman, R. E., Akabani, G., Niehaus, N., Coleman, D., and Lyerly, H. K. (1999) Migration of human dendritic cells after injection in patients with metastatic malignancies. *Cancer Res.* **59(1),** 56–58.

61. Lindhout E., Vissers J. L. M. Figdor C. G. Adema G. J. (1999) Chemokines and lymphocyte migration. *The Immunologist* **7,** 147–152.

10

Dendritic Cells in Clinical Trials for Multiple Myeloma

Volker L. Reichardt and Peter Brossart

Summary

Due to the existence of the truly specific tumor antigen idiotype in multiple myeloma and based on encouraging data from dendritic cell vaccinated B-cell non-Hodgkin's lymphoma (NHL) patients, dendritic cell-based vaccination was first initiated in myeloma patients in 1995. This overview will summarize published and ongoing clinical trials in patients with multiple myeloma who are treated with idiotype-based dendritic cell (Id/DC) vaccination. All groups of investigators have found that Id/DC vaccination of multiple-myeloma patients is feasible and that myeloma-specific immunity can be induced in heavily pretreated individuals. In future trials, new dendritic cell-based immunization strategies will be investigated based on techniques like RNA transfection of DC.

Key Words: Dendritic cells; immunotherapy; multiple myeloma; clinical trial; idiotype; T-cells.

1. Introduction

Multiple myeloma (MM) is a malignant monoclonal B-cell disorder characterized by plasma cell expansion in the bone marrow compartment and production of a unique monoclonal immunoglobulin (Ig). The diagnosis is often delayed due to unspecific clinical findings, resulting in more advanced disease in most of the patients at presentation. Despite conventional chemotherapy and even high-dose chemotherapy protocols with autologous stem-cell transplantation *(1,2)*, which have markedly improved the response rate, the time to progression, and the overall survival, the course of most multiple myeloma patients remains ultimately fatal. New drugs targeting not only the malignant B and plasma cells but also the tumor environment—such as thalidomide and its derivatives, and very recently, the proteasome inhibitors—have gained much attention and have yielded promising results in early clinical trials *(3,4)*. A different approach of targeted therapy is a therapeutic vaccination of MM patients with the goal of inducing immunological control of residual disease. For such an approach, dendritic cell (DC)-based vaccination strategies have been developed and will be discussed.

2. Idiotype and Tumor-Associated Antigens in MM

The immunoglobulin (Ig) produced by each B-cell and its progeny is homogeneous and unique. The differences responsible for the vast Ig molecule variety are based on the variable regions of Ig heavy and light chains. Individual heavy and light chains are composed of different antigenic determinants in the hyper-variable regions, which form so-called idiotopes . The combination of all individual idiotopes of any given Ig molecule is called the idiotype. Therefore, an idiotype (Id) is a specific protein product and marker of an individual B-cell clone. The amount of secreted Id protein is strongly correlated with the amount of myeloma plasma cells and therefore with the tumor mass. The idiotype protein can be isolated from serum or plasma in the majority of patients if a pretreatment serum sample with an appropriate amount of Id protein is available. Idiotypes are clone specific and have successfully been used as targets of immunotherapy in animal models of MM since the 1970s by Eisen et al. *(5)*, and will be discussed in depth in this chapter.

Tumor-associated antigens in MM comprise a large group of either over-expressed proteins such as mucin 1 (MUC1); telomerase, with its catalytic subunit hTERT; the gene product of PRAME or the sperm protein 17; so-called cancer testis antigens like MAGE, BAGE, GAGE, and NY-ESO-1; or some mutated gene products, such as Ras, as recently reviewed and discussed by Pellat-Deceunynck *(6)*. After thorough investigation in MM cell lines, several groups have also found relevant tumor-associated antigen (TAA) expression in fresh MM cells, especially in increasing the stage of MM in the case of cancer testis antigens *(7)*. An important next step before the clinical application of TAA vaccination in MM is that TAA-specific cytolytic T-cell responses can be induced in vitro, as shown for MUC1 by our group *(8)* and for sperm protein 17 by Lim et al. *(9)*. Many more MM-associated antigens are likely to be identified using either RNA array technology, proteomics, or SEREX technology *(10)*. To the best of our knowledge, no clinical phase I studies have been reported on DC-based vaccination using TAA or TAA peptides in MM patients so far.

3. Id Vaccination in MM

For the unique expression of individual Id on MM B-cells and plasma cells, several groups have focused on this truly tumor-specific antigen for vaccination purposes. Based on encouraging immunological and clinical results of Id vaccination in follicular NHL, as reported initially by Stanford et al. *(11,12)* and continued by Bendandi et al. *(13)*, the first Id vaccination in MM was reported by Mellstedt et al. *(14,15)*. Purified Id protein was either precipitated in aluminum phosphate (Id/alum) and vaccinated subcutaneously (s.c.) or co-injected with granulocyte macrophage colony-stimulating factor (GM-CSF). Id/alum and Id/GM-CSF vaccines induced Id-specific T-cell responses as measured by interferon (IFN)-γ enzyme-linked immunospot (ELISPOT) assay in early-stage MM patients (*n* = 5), proving the concept that the MM-specific self-antigen is able to induce immune responses in the tumor-bearing patient. Based on these promising data, Massaia et al. have performed a phase I clinical trial (*n* = 12) of Id/keyhole limpet hemocyanin (Id/KLH) vaccination in MM patients in first remission after high-dose chemotherapy *(16)*. The ratio-

nale for immunizing MM patients in a status of minimal residual disease—i.e., following high-dose chemotherapy and autologous stem-cell transplantation—has been discussed before *(17)*. All vaccines were given s.c. and co-injected with GM-CSF or interleukin (IL)-2. Only transient local reactions at the injection sites were reported, and cytokine-associated systemic toxicity was mild. The authors found in all patients T-cell proliferative responses to the highly immunogenic xeno-antigen KLH, but only in 2 out of 11 patients could Id-specific T-cell proliferation be detected after in vitro re-stimulation. In 8 of 10 patients studied, an Id-specific delayed-type hypersensitivity (DTH) skin reaction was documented after seven injections of Id/KLH. Five of 11 patients who received all planned vaccines remained in remission 9–30 mo following the first immunization; all other patients relapsed within 9–36 mo.

4. DC in MM Patients

Based on strongly encouraging data from Id/DC vaccination in NHL *(18,19)*, which proved feasibility and immunological responses in B-cell NHL, several investigators studied the feasibility of generating DC vaccines from MM patients either from peripheral blood leukapheresis products *(20–23)*, from peripheral blood monocytes *(21,24,25)*, or from CD34^{+} precursors *(26)*. All authors found it feasible to generate DC vaccines from heavily pretreated MM patients and demonstrated a comparable phenotypic profile in peripheral blood DC (PB-DC) as compared to normal donors *(21,22)*. While Raje et al. reported comparable in vitro T-cell stimulatory capacity in MM patients' DC, Brown and Ratta detected functional defects of PB-DC in MM patients. Most authors agree upon the notion that monocyte-derived DC (MoDC) of MM patients either generated by leukapheresis and plastic adherence or by positive selection of CD14^{+} blood monocytes are phenotypically and functionally normal *(23,25,27)*. In vitro studies have found that MoDC from MM patients can internalize and present idiotype proteins, and can be used to induce Id-specific T-cell responses in vitro *(25,28)*. Thorough in vitro investigations by Tarte et al. have been reported on the generation of MoDC without the use of xenogeneic fetal calf serum to avoid the sensitization against bovine immunogens with repetitive immunizations in a clinical setting *(29)*. We have extended these investigations and have developed an optimized protocol for the generation of serum-free MoDC in MM patients *(30)*. Raje et al. reported on comparable yields, similar phenotype and function of CD34^{+}-derived DC vs MoDC *(21)*, but Ratta et al. found lower yields of CD34^{+}-derived DC in MM patients *(25)*.

5. Clinical Application of Id/DC Vaccination in MM

The Stanford group was the first to report on the initiation of DC-based Id vaccination in MM patients who were responsive to high-dose therapy (HDT) followed by autologous peripheral blood stem-cell transplantation (PBSCT) *(31)*. This protocol followed very closely the very successful approach of using Id-pulsed PB-DC for patients with low-grade B-cell NHL, as earlier published by Hsu et al. *(18)* and updated recently by Timmerman *(19)*.

The first scientific report on the clinical application of Id/DC vaccination in a single MM patient used immature MoDC pulsed with autologous Id and KLH *(24)*. The Id-KLH/DC vaccines were comprised of at least 20% pure MoDC and were injected three times intravenously (i.v.). The authors found an Id-specific T-cell proliferative response in this refractory MM patient and were able to induce Id-specific cytotoxic T-cells after seven rounds of in vitro re-stimulation. Despite large amounts of circulating Id, the authors were able to detect Id-specific IgM antibody responses after vaccination. No clinical response, as determined by significant changes of the circulating Id, could be determined.

In another trial, 12 MM patients who were treated with HDT and PBSCT to induce a status of minimal residual disease were enrolled in a clinical study of Id/DC vaccination followed by Id/KLH booster immunizations *(20)*. All Id/DC vaccines were generated using PB-DC harvested by leukapheresis and given i.v. Id/KLH vaccines were given s.c. and co-injected with the chemical adjuvant ISAF. The authors demonstrated the feasibility of isolating PB-DC from MM patients even 3–7 mo after HDT and PBSCT. The purity of the PB-DC vaccines varied between 3% and 63%, which is a PB-DC enrichment of approx 100-fold as compared to peripheral blood. Id-specific T-cell proliferative responses were detected repeatedly in 2 out of 12 patients. Eleven of 12 patients mounted strong KLH-specific T-cell responses, suggesting immunocompetence to a neo-antigen at the time of vaccination. Cytolytic Id-specific T-cell responses could be found in only one of three patients studied when a single round of in vitro re-stimulation was performed. Id-specific antibody responses were not analyzed because all but two patients had large amounts of circulating Id at the time of vaccination. Interestingly, the two patients who mounted Id-specific T-cell proliferative responses were in clinical complete remission (CR) at the time of vaccination and remained in CR 30 and 17 mo after PBSCT. One patient who stabilized her disease only after HDT and PBSCT and failed to mount a measurable Id-specific T-cell response had declining Id levels in the subsequent 2 yr without any further cytoreductive treatment.

In the next cohort of MM patients treated with DC vaccines after HDT and PBSCT, the Stanford group examined the effect of pulsing the PB-DC with a conjugate of Id and KLH, trying to increase the immunogenicity of the weak self-antigen Id *(32)*. The PB-DC were isolated using a new methodology based on sequential density centri-fugation in a device developed and patented by Dendreon Corporation, Seattle, WA. While the authors achieved markedly higher cell numbers than in leukapheresis products, the purity of infused PB-DC fell significantly. Importantly, the rate of Id-specific immune responses remained comparable to the first cohort *(20)*, with 2 out of 14 patients developing T-cell proliferative responses. In line with the previous observations, all DC infusions were well tolerated, regardless of the much higher dose of cells infused. The authors found decreasing amounts of Id protein in the serum of several patients after Id vaccination, and described two cases of conversion from partial remission (PR) to CR following Id/DC vaccination. Still, the number of patients remains too small to establish a correlation between a modest rate of Id-specific immune response and clinical course.

The same Dendreon device for the enrichment of PB-DC as mentioned above has been used by researchers from Sacramento, CA (M. McKenzie et al.) and by a group at the Mayo Clinic in Rochester (M. Lacy et al.), who have both reported on clinical feasibility, immune responses, and early clinical results. As of February 2004, these results have not been published.

A series of six MM patients vaccinated with Id-pulsed MoDC was reported by Lim et al. *(33)*, who chose MoDC generated after steady-state leukapheresis. All MoDC were immature as judged by their FACS phenotype, were pulsed with Id Fab fragments and KLH, and were given either freshly or thawed for vaccination 2 and 3. Id protein-specific T-cell proliferative responses were detected in five of six patients following Id/DC vaccination, and Id-specific cytotoxic T-cell precursor frequency was increased in some patients. In line with their initial report *(24)*, the authors also detected a specific humoral response to Id despite circulating Id in the postvaccination serum. The authors did not evaluate humoral or cellular immune responses to bovine proteins, which might have been induced due to the repetitive use of fetal calf serum in generating the MoDC. All patients developed proliferative T-cell and antibody responses to KLH. One patient experienced a drop of his Id protein level by 25%; all other patients remained stable with a follow-up of 8 mo or progressed.

A report by Cull and collaborators summarizes the results of two MM patients who received four Id Fab fragment and KLH pulsed immature MoDC vaccines, which were given i.v. *(34)*. Both patients, with advanced refractory disease, developed Id-specific proliferative T-cell responses and KLH-specific T-cell responses. No Id-specific cytotoxicity could be measured in vitro, but in one patient an Id-specific antibody response was noted. One patient progressed quickly after completion of the vaccine trial and the other patient remained stable for some time following the vaccination.

The only report on Id/DC vaccination using DC generated from $CD34^+$ precursors is a study in relapsed and refractory MM patients ($n = 11$) who received a single s.c. Id/DC injection followed by Id/GM-CSF s.c. booster vaccinations ($n = 9$) or Id/DC vaccination again ($n = 2$) *(26)*. All patients received immature DC that were loaded with Id $F(ab')_2$ fragments and proteinase K digested Id peptides. The same randomly digested Id peptides were used for s.c. booster injections with GM-CSF as adjuvant. Id-specific T-cell reactivity, as determined by IFN-γ ELISPOT, was detected in 4 out of 10 patients studied. The authors also found increased anti-Id antibody titers following vaccination in 3 of 10 patients investigated. No significant clinical responses were seen following Id/DC vaccination in this cohort of refractory or relapsed MM patients.

In one small ($n = 5$) but very promising study of Id/DC vaccination of MM patients, Yi et al. reported on Id-pulsed MoDC vaccination *(35)*. All patients were in stable PR 4 to 33 mo following single or double HDT and PBSCT, and received three Id/DC vaccines. To enhance the efficacy of vaccination, low-dose interleukin-2 was given s.c. for 5 consecutive days following each s.c. DC vaccination. The phenotype of the MoDC preparations was clearly that of mature DC. Id-specific T-cell responses were evaluated with IFN-γ and IL-4 ELISPOT and T-cell proliferation assays. Two of five patients developed Id-specific T-cell proliferative responses and four of five patients had a positive IFN-γ immune response following Id/DC vaccination. Anti-Id

B-cell reactivity as determined by ELISPOT technology was found in all five patients. One patient experienced a significant drop of his serum Id protein, possibly due to vaccination or due to a delayed effect of HDT and PBSCT, which he received 4 mo prior to vaccination.

We have developed a protocol to generate Mo-DC from MM patients under serum-free tissue-culture conditions to avoid the immunization with bovine antigens by repetitive vaccinations. Using this technology, a series of MM patients ($n = 12$) responding to single or double HDT and autologous PBSCT have been vaccinated at our institution with Id-pulsed MoDC followed by s.c. Id/KLH booster immunizations *(30)*. Mature Id-pulsed MoDC were given i.v. as in our previous protocol *(20)* and Id/KLH was given with GM-CSF as adjuvant. Two of 12 patients mounted detectable Id-specific T-cell proliferative responses, and one of these patients developed Id-specific cytotoxic T-cell reactivity. This cytotoxic T-lymphocyte (CTL)-responsive patient experiences an ongoing very good PR 40 mo following initiation of the Id/DC vaccination. All patients developed cellular and delayed humoral immune responses to KLH.

6. Perspectives and Newer Protocols

A current clinical trial of DC vaccination in MM patients focuses on tumor lysate-pulsed DC based on encouraging in vitro data as published by the Arkansas group *(36)*. This new approach holds the advantage of potentially targeting a host of individual MM-specific targets and circumvents the necessity of isolation of Id protein. A disadvantage is the need for a certain amount of fresh MM cells to generate individual MM cell lysates.

We and others (R. Raymakers, Nijmengen, Netherlands) have begun to offer Id/DC vaccination to MM patients after HDT and PBSCT who have achieved a clinical CR but still have measurable disease on a molecular level. The goal of vaccinating this group of patients is the induction of a molecular CR, which is most likely to be achieved in a situation of minimal residual disease.

DC-based vaccination with idiotype peptide-loaded DC, as proposed by the studies of Fagerberg and Hansson, is still not being clinically evaluated *(37,38)*. Data generated by Trojan et al. provide evidence that Id peptides are rare in MM patients *(39)*.

Very provocative data from the Boston group regarding vaccination with fusion cells of autologous MM cells with DC will be clinically evaluated in the near future *(40)*.

We have succeeded in the induction of MM cell line-specific cytotoxicity in vitro using RNA transfection of DC *(41)*. These techniques will soon be evaluated in a phase I clinical trial in our institution.

References

1 Attal, M., Harousseau, J. L., Stoppa, A. M., et al. (1996) A prospective, randomized trial of autologous bone marrow transplantation and chemotherapy in multiple myeloma. Intergroupe Francais du Myelome. *N. Engl. J. Med.* **335,** 91–97.

2 Child, J. A., Morgan, G. J., Davies, F. E., et al. (2003) High-dose chemotherapy with hematopoietic stem-cell rescue for multiple myeloma. *N. Engl. J. Med.* **348,** 1875–1883.

3 Singhal, S., Mehta, J., Desikan, R., et al. (1999) Antitumor activity of thalidomide in refractory multiple myeloma. *N. Engl. J. Med.* **341,** 1565–1571.

4 Richardson, P. (2003) Clinical update: proteasome inhibitors in hematologic malignancies. *Cancer Treat. Rev.* **29(Suppl. 1)** 33–39.

5 Lynch, R. G., Graff, R. J., Sirisinha, S., Simms, E. S., and Eisen, H. N. (1972) Myeloma proteins as tumor-specific transplantation antigens. *Proc. Natl. Acad. Sci. USA* **69,** 1540–1544.

6 Pellat-Deceunynck, C. (2003) Tumour-associated antigens in multiple myeloma. *Br. J. Haematol.* **120,** 3–9.

7 van Baren, N., Brasseur, F., Godelaine, D., et al. (1999) Genes encoding tumor-specific antigens are expressed in human myeloma cells. *Blood* **94,** 1156–1164.

8 Brossart, P., Schneider, A., Dill, P., et al. (2001) The epithelial tumor antigen MUC1 is expressed in hematological malignancies and is recognized by MUC1-specific cytotoxic T-lymphocytes. *Cancer Res.* **61,** 6846–6850.

9 Chiriva-Internati, M., Wang, Z., Salati, E., Bumm, K., Barlogie, B., and Lim, S. H. (2002) Sperm protein 17 (Sp17) is a suitable target for immunotherapy of multiple myeloma. *Blood* **100,** 961–965.

10 Tureci, O., Sahin, U., and Pfreundschuh, M. (1997) Serological analysis of human tumor antigens: molecular definition and implications. *Mol. Med. Today* **3,** 342–349.

11 Kwak, L. W., Campbell, M. J., Czerwinski, D. K., Hart, S., Miller, R. A., and Levy, R. (1992) Induction of immune responses in patients with B-cell lymphoma against the surface-immunoglobulin idiotype expressed by their tumors. *N. Engl. J. Med.* **327,** 1209–1215.

12 Hsu, F. J., Caspar, C. B., Czerwinski, D., et al. (1997) Tumor-specific idiotype vaccines in the treatment of patients with B-cell lymphoma—long-term results of a clinical trial. *Blood* **89,** 3129–3135.

13 Bendandi, M., Gocke, C. D., Kobrin, C. B., et al. (1999) Complete molecular remissions induced by patient-specific vaccination plus granulocyte-monocyte colony-stimulating factor against lymphoma. *Nat. Med.* **5,** 1171–1177.

14 Bergenbrant, S., Yi, Q., Osterborg, A., et al. (1996) Modulation of anti-idiotypic immune response by immunization with the autologous M-component protein in multiple myeloma patients. *Br. J. Haematol.* **92,** 840–846.

15 Osterborg, A., Yi, Q., Henriksson, L., et al. (1998) Idiotype immunization combined with granulocyte-macrophage colony-stimulating factor in myeloma patients induced type I, major histocompatibility complex-restricted, CD8- and CD4-specific T-cell responses. *Blood* **91,** 2459–2466.

16 Massaia, M., Borrione, P., Battaglio, et al. (1999) Idiotype vaccination in human myeloma: generation of tumor-specific immune responses after high-dose chemotherapy. *Blood* **94,** 673–683.

17 Reichardt, V. L., Okada, C. Y., Stockerl-Goldstein, K. E., Bogen, B., and Levy, R. (1997) Rationale for adjuvant idiotypic vaccination after high-dose therapy for multiple myeloma. *Biol. Blood Marrow Transplant.* **3,** 157–163.

18 Hsu, F. J., Benike, C., Fagnoni, F., et al. (1996) Vaccination of patients with B-cell lymphoma using autologous antigen-pulsed dendritic cells. *Nat. Med.* **2,** 52–58.

19 Timmerman, J. M., Czerwinski, D. K., Davis, T. A., et al. (2002) Idiotype-pulsed dendritic cell vaccination for B-cell lymphoma: clinical and immune responses in 35 patients. *Blood* **99,** 1517–1526.

20 Reichardt, V. L., Okada, C. Y., Liso, A., et al. (1999) Idiotype vaccination using dendritic cells after autologous peripheral blood stem cell transplantation for multiple myeloma—a feasibility study. *Blood* **93,** 2411–2419.

21 Raje, N., Gong, J., Chauhan, D., et al. (1999) Bone marrow and peripheral blood dendritic cells from patients with multiple myeloma are phenotypically and functionally normal despite the detection of Kaposi's sarcoma herpesvirus gene sequences. *Blood* **93,** 1487–1495.

22 Brown, R. D., Pope, B., Murray, A., et al. (2001) Dendritic cells from patients with myeloma are numerically normal but functionally defective as they fail to up-regulate CD80 (B7-1) expression after huCD40LT stimulation because of inhibition by transforming growth factor-beta1 and interleukin-10. *Blood* **98,** 2992–2998.

23 Ratta, M., Fagnoni, F., Curti, A., et al. (2002) Dendritic cells are functionally defective in multiple myeloma: the role of interleukin-6. *Blood* **100,** 230–237.

24 Wen, Y. J., Ling, M., Bailey-Wood, R., and Lim, S. H. (1998) Idiotypic protein-pulsed adherent peripheral blood mononuclear cell-derived dendritic cells prime immune system in multiple myeloma. *Clin. Cancer Res.* **4,** 957–962.

25 Ratta, M., Curti, A., Fogli, M., et al. (2000) Efficient presentation of tumor idiotype to autologous T cells by CD83(+) dendritic cells derived from highly purified circulating CD14(+) monocytes in multiple myeloma patients. *Exp. Hematol.* **28,** 931–940.

26 Titzer, S., Christensen, O., Manzke, O., et al. (2000) Vaccination of multiple myeloma patients with idiotype-pulsed dendritic cells: immunological and clinical aspects. *Br. J. Haematol.* **108,** 805–816.

27 Tarte, K., Lu, Z. Y., Fiol, G., Legouffe, E., Rossi, J. F., and Klein, B. (1997) Generation of virtually pure and potentially proliferating dendritic cells from non-CD34 apheresis cells from patients with multiple myeloma. *Blood* **90,** 3482–3495.

28 Butch, A. W., Kelly, K. A., and Munshi, N. C. (2001) Dendritic cells derived from multiple myeloma patients efficiently internalize different classes of myeloma protein. *Exp. Hematol.* **29,** 85–92.

29 Tarte, K., Fiol, G., Rossi, J. F., and Klein, B. (2000) Extensive characterization of dendritic cells generated in serum-free conditions: regulation of soluble antigen uptake, apoptotic tumor cell phagocytosis, chemotaxis and T cell activation during maturation in vitro. *Leukemia* **14,** 2182–2192.

30 Reichardt, V.L., Milazzo, C., Brugger, W., Einsele, H., Kanz, L, and Brossart, P. (2003) Idiotype vaccination of multiple myeloma patients using monocyte-derived dendritic cells. *Haematologica* **88,**1139–1149.

31. Reichardt, V., Okada, C., Benike, C., et al. (1996) Idiotypic vaccination using dendritic cells for multiple myeloma patients after autologous peripheral blood stem cell transplantation. *Blood* **88(Suppl 1),** 481a.

32 Liso, A., Stockerl-Goldstein, K. E., Auffermann-Gretzinger, S., et al. (2000) . Idiotype vaccination using dendritic cells after autologous peripheral blood progenitor cell transplantation for multiple myeloma. *Biol. Blood Marrow Transplant.* **6,** 621–627.

33 Lim, S. H. and Bailey-Wood, R. (1999) Idiotypic protein-pulsed dendritic cell vaccination in multiple myeloma. *Int. J. Cancer* **83,** 215–222.

34 Cull, G., Durrant, L., Stainer, C., Haynes, A., and Russell, N. (1999) Generation of anti-idiotype immune responses following vaccination with idiotype-protein pulsed dendritic cells in myeloma. *Br. J. Haematol.* **107,** 648–655.

35 Yi, Q., Desikan, R., Barlogie, B., and Munshi, N. (2002) Optimizing dendritic cell-based immunotherapy in multiple myeloma. *Br. J. Haematol.* **117,** 297–305.

36 Wen, Y. J., Min, R., Tricot, G., Barlogie, B., and Yi, Q. (2002) Tumor lysate-specific cytotoxic T lymphocytes in multiple myeloma: promising effector cells for immunotherapy. *Blood* **99,** 3280–3285.

37 Fagerberg, J., Yi, Q., Gigliotti, D., et al. (1999) T-cell-epitope mapping of the idiotypic monoclonal IgG heavy and light chains in multiple myeloma. *Int. J. Cancer* **80,** 671–680.

38 Hansson, L., Rabbani, H., Fagerberg, J., Osterborg, A., and Mellstedt, H. (2003) T-cell epitopes within the complementarity-determining and framework regions of the tumor-derived immunoglobulin heavy chain in multiple myeloma. *Blood* **101,** 4930–4936.

39 Trojan, A., Schultze, J. L., Witzens, M., et al. (2000) Immunoglobulin framework-derived peptides function as cytotoxic T-cell epitopes commonly expressed in B-cell malignancies. *Nat. Med.* **6,** 667–672.

40. Gong, J., Koido, S., Chen, D., et al. (2002) Immunization against murine multiple myeloma with fusions of dendritic and plasmocytoma cells is potentiated by interleukin 12. *Blood* **99,** 2512–2517.

41. Milazzo, C., Reichardt, V. L., Muller, M. R., Grunebach, F., and Brossart, P. (2003) Induction of myeloma specific cytotoxic T cells using dendritic cells transfected with tumor-derived RNA. *Blood* **101,** 977–982.

11

Identification of Tumor-Associated Autoantigens With SEREX

Özlem Türeci, Dirk Usener, Sandra Schneider, and Ugur Sahin

Summary

Serological analysis of tumor antigens by recombinant cDNA expression cloning (SEREX) allows the systematic cloning of tumor antigens recognized by the spontaneous autoantibody repertoire of cancer patients. For SEREX, cDNA expression libraries are constructed from fresh tumor specimens, packaged into λ-phage vectors, and expressed recombinantly in *Escherichia coli*. Recombinant proteins expressed during the lytic infection of bacteria are transferred onto nitrocellulose membranes to be probed with diluted autologous patient serum for identification of clones reactive with high-titered IgG antibodies. This chapter describes the SEREX technology in detail.

Key Words: Tumor antigens; expression screening; λ-phage libraries; autoantibodies.

1. Introduction

One of the cardinal challenges in tumor immunology is the identification of antigenic structures in human tumors that are recognized by the host's immune system. By using tumor-specific cytotoxic T-lymphocyte (CTL) clones as probes for cDNA expression cloning, a growing number of tumor antigens has been identified *(1,2)*. The necessity of established precharacterized CTL clones with tumor-cell restricted reactivity is a critical obstacle of this methodology and was the main reason why the majority of antigens defined hitherto were identified in malignant melanoma.

A large body of evidence points to a coordinated recruitment of CD4^{+}, CD8^{+}, and B-cell responses to the same tumor antigen, and suggests that once immune recognition of a gene product is elicited, it is not restricted to merely one effector system. Furthermore, it is frequently argued that the CTL repertoire of cancer patients is deleted for many relevant CTL precursors. However, it is quite unlikely that a concomitant antibody response towards antigens (in particular intracellular ones) for which respective CTLs have been be deleted, would also be erased *(3)*. Thus, specific antibodies may be the persisting hallmark of a substantial interaction between tumor and immune system, and may help to trace back not only relevant antigens but also deleted CTL specificities. Based on these rationales, we designed SEREX, a proce-

dure allowing the systematic and unbiased cloning of tumor antigens recognized by the IgG autoantibody repertoire of cancer patients *(4)*.

To this aim, cDNA expression libraries are constructed from fresh tumor specimens, expressed recombinantly and probed with autologous patient serum to identify clones reactive with high-titered IgG-antibodies.

The SEREX approach is technically characterized by several features:

1. There is no need for established tumor cell lines and precharacterized CTL clones.
2. The use of fresh tumor specimens restricts the analysis to genes that are expressed by the tumor cells in vivo and circumvents in vitro artifacts associated with short- and long-term tumor cell culture
3. The use of the polyclonal (polyspecific) patient's serum as a probe for immunoscreening allows for the identification of multiple antigens with one screening course.
4. The screening is restricted to clones against which the patient's immune system has raised high-titered IgG responses indicating the presence of concomitant T-helper lymphocyte responses in vivo.
5. As both the expressed antigenic protein and the coding cDNA are present in the same plaque of the phage immunoscreening assay, identified antigens can be subjected immediately to molecular characterization.
6. The release of periplasmatic proteins involved in protein folding during phage-induced bacterial lysis allows at least partial folding of recombinant proteins and provides the basis for the identification of linear as well as nonlinear epitopes. This has been confirmed by showing that enzymes expressed in lytic plaques do exert their catalytic activity (our unpublished results). In contrast, epitopes derived from eucaryotic posttranslational modification (e.g., glycosylation) are not detected by the page immunoscreening assay.

The proliferation of the technology to many other laboratories and the coordinated analysis of different types of human cancers has resulted in a multitude of tumor-associated antigens identified by the SEREX technique *(5–7)*. Most of these antigens are deposited in the SEREX Database, which harbors more than 2000 entries and provides a comprehensive molecular insight into what is called the "cancer immunome" (*see* Websites: www2.licr.org/CancerImmunomeDB and www.eurice.de/EUCIP) *(8)*.

The use of reverse T-cell immunology on SEREX-discovered antigens led to the identification of epitopes recognized by CD8^{+} as well as CD4^{+} T-cells isolated from cancer patients *(9,10)*. This not only confirmed the original rationale but made these antigens attractive candidates in experimental clinical trials for specific vaccination of cancer patients *(11)*. Moreover, SEREX has opened up new possibilities in the field of tumor serology *(12)*, where it has long been hoped to develop antibody-based screening tests for general use in the monitoring, diagnosis, and prognosis of cancer.

However, it soon became apparent that sera of cancer patients also contain IgG antibodies that are unrelated to their disease and contribute whenever SEREX is applied in a not yet quantified extent to the cloning of antigens. These are, for example, natural antibodies as well as antibodies elicited by infections with pathogens. In addition, antibody entities may be elicited consecutive to necrosis or tissue destruction as accompaniments of tumor growth, with no direct relation at all to the molecular alterations specific for the cancer cell.

Extracting the authentically cancer-related antigens has proven to be a major challenge.

This chapter not only provides a detailed protocol for the powerful SEREX technology. It also outlines how conceptually the validation process downstream of the high-output discovery of antigens should be designed to allow for extraction of the relevant ones.

2. Materials

2.1. Disposables

1. Disposable gloves.
2. Small and large Petri dishes (diameter 8 cm, 13.5 cm), (Greiner Bio-One, Kremsmünster, Austria).
3. Fifty-mL Conical Falcon tube (BD Biosciences, Heidelberg, Germany).
4. Fourteen-mL Sterile Falcon round-bottom tube white caps (BD Biosciences).
5. Tubes:
   a. Safe Lock 0.5 mL (Eppendorf, Hamburg, Germany).
   b. Safe Lock 1.5 mL (Eppendorf).
6. Nitrocellulose Blotting Membranes: 45 μm, (Sartorius AG, Göttingen, Germany).
7. 3MM blotting filters (Whatman, Maidstone, UK).
8. Square Petri dish 24.5×24.5 cm (VWR, Darmstadt, Germany) .
9. Self-made plastic spacers, size $23 \times 2 \times 0.1$ cm to fit into a square Petri dish forming 24 sections of 23×1 cm .
10. Self-made incubator of 3-mm thick plexiglas to allow parallel processing of 24 nitrocellulose membrane slips each in a different serum; floor space of 25×56 cm; separated in 2×24 cm incubation segments.

2.2. Chemicals and Reagents

1. IPTG (AppliChem, Darmstadt, Germany) in water, store 1 *M* stock at –20°C .
2. Nitroblue-tetrazoliumchloride (NBT) (AppliChem), 75 mg/mL stock in 70% *N-N* dimethylformamide .
3. 5-Bromo-4-chloro-3-indol-phosphate-toluidine (BCIP) (AppliChem), 50 mg/mL in 100% *N-N* dimethylformamide .
4. Goat anti-human IgG labeled with alkaline phosphatase (Dianova, Hilden Germany).
5. Affinity adsorbent 669580 (Roche Diagnostic, Mannheim, Germany).
6. Na-acid NaN_3 (AppliChem): prepare a 10% (w/v) solution in water, store at 4°C.
7. Thimerosal: prepare a 10% (w/v) solution in water, store at 4°C.
8. MMLV reverse transcriptase (Stratagene, La Jolla, US).
9. $MgSO_4$ ($MgSO_4 \cdot 7H_2O$) (Roth, Karlsruhe, Germany): 1 *M* in water, sterile filtered.
10. $MgCl_2$ ($MgCl_2 \cdot 6H_2O$) (AppliChem): 1 *M* in water, sterile filtered.
11. Maltose (AppliChem): 10% (w/v) in water.
12. X-Gal (AppliChem): 250 mg/mL in DMF.
13. Ethanol, 96% p.a. (Roth).
14. Tetracycline (Sigma, Taufkirchen, Germany): 5 mg/mL stock in 96% ethanol, store at –20°C.
15. Ampicillin (Sigma): 100 μg/mL stock in water, store at –20°C.
16. Kanamycin (Sigma): 50 μ/mL stock in water, store at –20°C.

2.3. Kits

1. Messenger RNA Isolation Kit (Stratagene).
2. ZAP cDNA Synthesis Kit (Stratagene).

3. Uni Zap XR Vector Kit (Stratagene).
4. Sizesep 400 Spun columns (Amersham-Bioscience, Uppsala, Sweden).
5. ZAP-cDNA Gigapack III Gold Cloning Kit (Stratagene).
6. Max-Plax λ packaging extracts (Epicentre, Madison, WI).

2.4. Buffers and Media

1. LB broth: 10 g NaCl, 10 g tryptone, 5 g yeast extract, add deionized H_2O to a final volume of 1 L .
2. LB agar: 10 g NaCl, 10 g tryptone, 5 g yeast extract, 20 g agar, add deionized H_2O to a final volume of 1 L .
3. LB-tetracyline agar: 1 L autoclaved LB agar, cool to 55°C and add tetracycline to a final concentration of 12.5 µg/mL .
4. LB-ampicillin agar: Prepare 1 L LB agar, autoclave, cool to 55°C, and add ampicillin to a final concentration of 150 µg/mL.
5. LB-kanamycin agar: Prepare 1 L LB agar, autoclave, cool to 55°C, and add kanamycin to a final concentration of 50 µg/mL.
6. LB top agar: Prepare 1 L LB broth, add 0.4% (w/v) agarose (Applichem) and 0.4% agar.
7. SM buffer: 5.8 g NaCl, 2.0 g $MgSO_4$, 50 mL of 1 *M* Tris-HCl (pH 7.5), 5 mL of 2% (w/v) gelatin, add deionized H_2O to a final volume of 1 L .
8. 10X TBS: 0.5 *M* Tris base, 1.5 *M* NaCl, adjust pH 7.5 with concentrated hydrochloric acid .
9. 10X TBST: add 0.5% Tween-20 to 10X TBS.
10. Blocking buffer: 1X TBST with 5% low-fat milk powder (Saliter, Obergünzburg, Germany).
11. 20X PBS: 2.8 *M* NaCl, 54 m*M* KCl, 162 m*M* Na_2HPO_4, 30 m*M* KH_2PO_4, adjust to pH 7.4–7.6 with NaOH or HCl if necessary.
12. Tris-HCl, pH 3.0: 0.05 *M* Tris base, adjust to pH 3 with concentrated HCl.
13. 10X MOPS: 200 m*M* MOPS, 50 m*M* NaAc, 10 m*M* EDTA in 1 L, adjust to pH 7.0 with NaOH.
14. 10X CDS (color development solution): 0.1 *M* Tris-HCl (pH 9.5), 5 m*M* $MgCl_2$, 0.1 *M* NaCl (pH 9.5).

3. Methods

Basic methods of molecular biology are described elsewhere *(13)*.

3.1. Construction of a λ Phage Expression Library

For construction of a large, representative cDNA library, high quality mRNA as starting material is of utmost importance. We propose the guanidium isothiocyanate-phenol-chloroform extraction method *(14)*, which produces large amounts of high-quality, non-degradation total RNA. For subsequent purification of poly(A) RNA, a number of comparable commercial kits are available. We generally use the messenger RNA Isolation Kit (Stratagene). All precautions should be taken to avoid contamination with RNAses. Once high-quality mRNA is obtained, it is subjected to the procedure described in **Subheading 3.1.1.** This protocol for construction of a λ phage library follows basically the instructions of the manufacturer (Uni-ZAP XR cDNA library synthesis kit, Stratagene) with minor modifications (*see* **Note 1**).

3.1.1. Synthesis of Doubled-Stranded cDNA for Directional Ligation

The cDNA-library-synthesis kit (e.g., Stratagene, cat. no. 200400) allows the generation of adaptor-ligated double-stranded cDNA for directional cloning. Fragments suitable for directional cloning are generated using an oligo(dT) primer with an internal XhoI site. 5-methyl-dCTP is used instead of dCTP for first-strand synthesis. The use of RNAse⁻ MMLV-reverse transcriptase (e.g., Superscript, Stratascript) improves amount and quality of the first-strand cDNA. The second-strand synthesis is performed with DNA polymerase I in combination with RNaseH, which generates internal priming sites. Unmodified dNTPs are used here, resulting in the generation of hemimethylated double-stranded cDNA with blocked internal XhoI sites and a single unmethylated XhoI site at the initial 3'-priming region. *Pyrococcus furiosus* polymerase lacking terminal nucleotide transferase activity fills up and blunts cDNA termini. A second restriction site is introduced into the cDNA fragments by ligating adaptors with sticky unphosphorylated EcoR1 overhangs and phosphorylated blunted ends. XhoI digestion of adaptor-ligated cDNA results in the generation of fragments containing a 3' XhoI site (introduced during priming) and a 5' EcoR1 site (introduced by adaptor ligation).

1. Preheat a 37°C water bath. Thaw, vortex, and spin down the contents of the nonenzymatic tubes of the Uni-ZAP XR cDNA library synthesis kit and place them on ice. MMLV-RT is temperature sensitive and should be kept at –20°C until needed.
2. The final volume of the first-strand synthesis reaction is 50 µL. The volume of added reagents and enzymes is 12.5 µL, which allows the mRNA and DEPC-treated water to be added in a volume up to 37.5 µL. Add the following reagents in this order: 5 µL of 10X first-strand buffer, 3 µL of first-strand methyl nucleotide mixture, 2 µL of linker-primer (1.4 µg/µL), X µL of DEPC-treated water, 1 µL of RNase Block Ribonuclease Inhibitor (40 U/µL). Mix the reaction and then add X µL of poly (A) RNA (5 µg). Mix gently.
3. After primer annealing for 10 min at room temperature, add 1.5 µL of MMLV-RT (50 U/µL) to the first-strand synthesis reaction. The final volume of the first-strand synthesis reaction should now be 50 µL. Mix the sample gently and spin down the contents in a microcentrifuge.
4. Incubate the first-strand synthesis reaction at 37°C for 1 h. To stop reaction, place tube on ice.
5. For synthesis of second-strand cDNA, thaw, vortex, and spin all nonenzymatic second-strand components and place them on ice. All reagents should be <16°C when DNA polymerase I is added.
6. Add the following components on ice to the first-strand synthesis reaction in this order: 20 µL of 10X second-strand buffer, 6 µL of second-strand dNTP mixture, 114 µL of sterile distilled water, 2 µL of RNase H (1.5 U/µL), 11 µL of DNA polymerase I (9.0 U/µL).
7. After vortexing and spinning, incubate for 2.5 h at 16°C. Temperatures above 16°C can cause the formation of hairpin structures and decrease efficiency of insertion of correctly synthesized cDNA into the prepared vector.
8. For blunting the cDNA termini, place the reaction tube on ice and add the following to the second-strand synthesis reaction: 23 µL of blunting dNTP mix, 2 µL of cloned Pfu DNA polymerase (2.5 U/µL).
9. After vortexing and spinning, incubate the reaction at 72°C for exactly 30 min.
10. Prepare a 1:1 (v/v) emulsion of phenol (equilibrated to pH 7.0–8.0) and chloroform, and add 200 µL of it to the reaction. Vortex and spin the reaction briefly at maximum speed at

room temperature and transfer the upper aqueous layer, containing the cDNA, to a new tube. Do not remove any interface that may be present.

11. Add an equal volume of chloroform and vortex. Spin the reaction briefly at maximum speed at room temperature and again transfer the upper layer.

12. Precipitate the cDNA by adding 20 µL of 3 *M* sodium acetate and 400 µL of 100% ethanol. Flick the bottom of the tube and precipitate overnight at –20°C.

13. Spin in a microcentrifuge at maximum speed for 60 min at 4°C. Remove and discard the supernatant carefully without disturbing the pellet. Sometimes the pellet is not clearly visible. Keep in mind that it may taper off along the side of the tube.

14. Wash the pellet by adding 500 µL of 70% (v/v) ethanol to the side of the tube opposite to the precipitate. Do not mix or vortex. Spin in a microcentrifuge at maximum speed for 2 min at room temperature in the same orientation as before.

15. Aspirate the ethanol and dry the pellet.

16. Resuspend the pellet in 9 µL of EcoR I adapters and incubate at 4°C for at least 30 min. Repeat mixing to ensure that the cDNA is completely in solution.

17. For adapter ligation, add the following components to the tube containing the blunted cDNA and the EcoR I adapters: 1 µL of 10X ligase buffer, 1 µL of 10 m*M* rATP, 1 µL of T4 DNA ligase (4 U/µL). Spin down and incubate overnight at 8°C.

18. Heat-inactivate the ligase at 70°C for 30 min. Thereafter, spin the reaction briefly and cool it to room temperature for 5 min.

19. Phosphorylate the adapter ends by adding the following components: 1 µL of 10X ligase buffer, 2 µL of 10 m*M* rATP, 6 µL of sterile water, 1 µL of T4 polynucleotide kinase (10 U/µL). Incubate the reaction for 30 min at 37°C.

20. Heat-inactivate the kinase for 30 min at 70°C. Spin down briefly and allow the reaction to equilibrate to room temperature for 5 min.

21. For restriction enzyme digest with Xho I, add the following components to the reaction: 28 µL of Xho I buffer supplement and 3 µL of Xho I (40U/µL). Incubate the reaction for 1.5 h at 37°C.

22. Add 50 µL of a 1:1 (v/v) emulsion of phenol (equilibrated to pH 7.0–8.0) and chloroform to the reaction. Vortex and spin the reaction briefly at maximum speed at room temperature and transfer the upper aqueous layer, containing the cDNA to a new tube. Do not remove any interface that may be present.

23. Add an equal volume of chloroform and vortex. Spin as above and again transfer the upper layer.

3.1.2. cDNA Size Fractionation

Complete elimination of residual adaptors, which are present in great molar excess, is crucial for efficient ligation of the cDNA fragments with the phage vector arms. We recommend the use of Sizesep separation columns, which allow the removal of adaptors as well as size selection of long cDNA fragments.

1. Place the SizeSep™ 400 spin column in 14-mL Falcon tubes to collect the flow-through.

2. Overlay the column with 1X STE buffer.

3. Centrifuge (700*g*) for 1–2 min and discard the flow-through. Repeat this washing step.

4. To dry the column, centrifuge for 3 min at 700*g*.

5. Before inserting the spin column, place a 1.5-mL safe lock tube into the 14-mL Falcon tube and load the cDNA reaction (**Subheading 3.1.1., step 23**) on the middle of the column without touching it.

6. Spin 3 min at 700*g* and collect the flow-through (1st fraction).

7. Pipet 50 µL 1X STE buffer onto the column, spin (3min, 700*g*), and collect the flow-through as 2nd fraction.
8. Repeat this twice to obtain the 3rd and 4th fractions.
9. Add 5 µL 3 *M* NaAc and 55 µL 96% ethanol to each fraction and precipitate the reaction overnight at –20°C.
10. After precipitation, spin the reaction at maximum speed for 60 min at 4°C.
11. Wash the pellet by carefully adding 250 µL of 70% (v/v) ethanol without disturbing the pellet. Centrifuge at maximum speed for 5 min at room temperature in the same orientation as before.
12. Air-dry the pellets and resuspend them in 8 µL of sterile H_2O.
13. For quantification, take 1 µL from each tube and add it to 4 µL H_2O (1:5 dilution). Transfer 0.5 µL of these into new tubes with 4.5 µL H_2O (1:50 dilution). Dot 2.5 µL from both dilutions of each fraction onto an agarose/ethidium-bromide gel. Dot in parallel increasing dilutions of a DNA marker of known concentration.

   By comparison on a UV transilluminator, the amount of cDNA in each reaction can be estimated.

3.1.3. Ligation of cDNA into the λ Phage Vector

1. To prepare the sample ligation, add the following components in the described order: X µL resuspended cDNA (approx 100 ng), 0.5 µL of 10X ligase buffer, 0.5 µL of 10 m*M* rATP (pH 7.5), 1 µL of the Uni-ZAP XR vector (1 µg/µL), 0.5 µL of T4 DNA ligase (4 U/µL), and X µL water for a final volume of 5 µL.
2. Incubate the reaction tubes for 2 d at 4°C.

3.1.4. Packaging Procedure

For packaging of methylated DNA, commercial kits are available from different manufacturers (Gigapack Gold, Stratagene; MaxPlax, Invitrogen). These systems are of comparable convenience and efficacy. We usually use Gigapack III Gold λ packaging extracts. We suggest performing test packaging to determine the appropriate amount of packaging extract.

1. For test packaging, which should be done after one day of ligation, remove one tube of packaging extract from the –80°C freezer and place it on dry ice.
2. Quickly thaw the packaging extract between your fingers, add 1 µL of the ligated DNA to the packaging extract immediately. Mix well by stirring with a pipet tip, avoiding air bubbles.
3. Incubate the tube at room temperature for not longer than 2 h. Extended packaging times may decrease efficacy considerably.
4. Add first 500 µL of SM buffer followed by 20 µL of chloroform, and mix the contents of the tube gently.
5. Make serial dilutions of the packaged phage in SM buffer (10^{-2}–10^{-6}) for plating and titering of this test ligation, as described under **Subheading 3.1.6.**
6. Count the plaques and determine the titer (pfu/mL) and packaging efficiency according to the following equation:

$$\frac{\text{Number of plaques} \times \text{dilution factor} \times \text{total reaction volume}}{\text{volume of dilution plated} \times \text{amount of DNA packaged}} \tag{1}$$

7. The remaining ligation reaction has to be packaged at d 2 of ligation, repeating **steps 1–6**. The number of packaging extracts needed has to be calculated according to the efficiency determined by the test ligation described above in **step 6**.

Spin the tubes briefly to sediment the debris. The supernatants containing the phage are ready for titering and can be stored at 4°C.

3.1.5. Preparing the Host Bacteria

1. Streak the host strain XLl-Blue MRF' onto an LB agar plate containing the appropriate antibiotic and incubate the plate overnight at 37°C.
2. Inoculate LB broth supplemented with 10 mM MgSO$_4$ and 0.2% (w/v) maltose, with a single colony and grow at 37°C, shaking for 4–6 h to an OD$_{600}$ of 0.7–0.9.
3. Spin the cells at 500g for 10 min and discard the supernatant.
4. Gently resuspend the cells in sterile 10 mM MgSO$_4$ to obtain an OD$_{600}$ of 0.5.

3.1.6. Plating and Titering of the Library

The color assay allows determination of the percentage of recombinants within a newly constructed library and is part of the quality control.

1. To plate the packaged ligation product, mix the following components: 1 µL of the final packaged reaction as well as 1 µL of its 1:10 dilution each with 200 µL of XL1-Blue MRF' cells (an OD$_{600}$ of 0.5).
2. Allow the phage to attach to the cells by incubating them at 37°C for 15 min. Add the following components: 4 mL of LB top agar (melted and cooled to approx 47°C), 15 µL of 0.5 M IPTG, 50 µL of X-gal.
3. Plate immediately onto the LB-tetracycline agar plates in small Petri dishes (diameter 8 cm) and allow the plates to set for 10 min. Invert the plates and incubate at 37°C overnight.
4. Count the plaques. Calculate the efficiency using the following equation:

$$\frac{\text{Number of plaques} \times \text{dilution factor} \times \text{total reaction volume}}{\text{Total number of micrograms packaged} \times \text{number of microliters plated}} \tag{2}$$

Background plaques are blue, while recombinant plaques will be white and should be 50- to 100-fold above the background.

3.1.7. Amplification of the Library

The titer of a primary λ phage library may drop with time, resulting in the loss of rare cDNA species. Therefore, one round of library amplification is suggested to obtain a large and stable high-titer stock of the library (*see* **Note 2**). Make sure that as long as the library has not gone through amplification, XL1-Blue MRF' cells are used as host strain (*see* **Note 3**).

1. Plate the entire library on large Petri dishes. Follow **Subheading 3.1.6., steps 1–3**. IPTG is not required, since protein expression is not intended. Subconfluency of phage plaques is ensured at 10^5 pfu per plate. Plates should not be lytic to ensure representation also of slow-growing clones.
2. After overnight incubation, overlay the plates with 8 mL of SM buffer and incubate at 4°C for 4 h with gentle rocking. Recover the bacteriophage suspension from each plate and pool it into a sterile polypropylene container. Do not use glassware, to which the phages would stick.
3. Rinse the plates thoroughly with additional 2 mL of SM buffer and add this to the polypropylene container.

4. Add chloroform to 5% (v/v) final concentration. Mix well and incubate for 15 min at room temperature.
5. Remove the cell debris by centrifugation for 10 min at 500*g*. Recover and transfer the supernatant to a new polypropylene container. Add chloroform to a final concentration of 0.3% (v/v) and store at 4°C. Titer before use.
6. The phage library could be stored for long periods at –80°C with 7% DMSO.

Make sure that you assess and document all quality criteria of your library (*see* **Note 4**).

3.2. Immunoscreening of λ Phage Expression Library

3.2.1. Preparation of Patient Serum

Polyclonal human sera contain antibodies that are reactive with *E. coli* and phage proteins. These contaminating antibodies will increase background and affect sensitivity and reliability of the assay. For elimination of such antibody specificities we have developed an affinity purification protocol consisting of three consecutive steps (*see* **Note 5**). For preabsorption we prefer a batch rather than a column procedure; the batch procedure promotes not only efficient binding of serum to the affinity adsorbent but is also faster and more convenient, in particular for processing of a larger number of different sera.

3.2.1.1. Preabsorption Against Mechanically Disrupted Bacteria

1. Inoculate LB broth supplemented with 10 m*M* MgSO$_4$ and 0.2% (w/v) maltose, with a single colony of XL1-Blue MRF' and grow overnight, shaking at 37°C.
2. Harvest the bacteria by centrifugation (3500*g*, 15 min) and resuspend pellet in 5 mL 1X MOPS buffer.
3. Place cells on ice and disrupt by sonication five × for 20 s (Branson Sonic Power Co. A Smithkline).
4. For each individual serum fill a 50-mL Falcon tube with 2 g of affinity adsorbent, add 3 mL 1X PBS/0.01% NaN$_3$, incubate for 10 min. Spin the tube and discard supernatant.
5. Add lysate obtained by mechanical disruption of bacteria to the affinity adsorbent and rotate on an overhead shaker for 4 h at room temperature or overnight at 4°C.
6. Spin down the matrix (100*g*, 1 min) and discard supernatant.
7. Wash column twice for 10 min with 30 mL 1X PBS/0.01% NaN$_3$ on an overhead shaker. Discard washing buffer.
8. Incubate affinity adsorbent for 2 h at 4°C with 1 *M* glycin and wash subsequently twice for 10 min with 1X PBS/0.01% NaN$_3$. You have now obtained a resin saturated with bacterial proteins.
9. Dilute human serum 1:10 in dilution buffer (0.01% NaN$_3$, 0.01% thimerosal and 0.5% low-fat milk powder in 1X TBS). Transfer the diluted serum (not more than 40 mL per tube) to the 50-mL Falcon tubes with the prepared resin. Incubate for 4 h at room temperature or overnight at 4°C on an overhead shaker.
10. Centrifuge to spin down the resin (100*g*, 1 min). Harvest the preabsorbed sera, which are stored at 4°C until introduction into the second purification step as described under **Subheading 3.2.1.2.**
11. This resin as well as the one generated under **Subheading 3.2.1.2.** can be regenerated and re-used. For regeneration, wash the resin first three times for 10 min with 30 mL 50 m*M*

Tris-HCl, pH 3. Subsequently, wash twice for 10 min with 30 mL TBS and 10 min with 30 mL TBS and 0.01% NaN$_3$ and thimerosal. Store the affinity adsorbent in TBS and 0.01% NaN$_3$ and thimerosal at 4°C. Maximal shelf life of regenerated resin is 3 mo. The binding capacity is sufficient for processing of 6 mL undiluted serum in total (equivalent to 60 mL 1:10 prediluted serum).

3.2.1.2. PREABSORPTION AGAINST BACTERIOPHAGE PROTEINS AND LYTICALLY INFECTED BACTERIA

1. Inoculate LB broth supplemented with 10 m*M* MgSO$_4$ and 0.2% (w/v) maltose with a single colony of XL1-Blue MRF', and grow overnight, shaking at 37°C.
2. Harvest the bacteria by centrifugation (3500*g*, 15 min). Discard supernatant and resuspend the pellet in 2 mL 10 m*M* MgSO$_4$. Transfer 200 μL of it to 4 mL fresh LB broth supplemented with 10 m*M* MgSO$_4$ and 0.2% (w/v) maltose. The rest is kept at 4°C until use in **step 4**.
3. Infect freshly inoculated LB broth with 10^4 pfu of a wild-type λ ZAPII phage. For this purpose, you can harvest "blue phages" obtained under **Subheading 3.1.5.** Shake at 37°C for 4 h.
4. Add remaining bacterial suspension from **step 2** and shake 2 h at 37°C. Under these conditions you will obtain amplification of bacteriophages and lytic infection of bacteria in culture.
5. Place cells on ice and disrupt by sonication five times for 20 s (Branson Sonic Power Co. A, Smithkline).
6. Fill a 50-mL Falcon tube with 2 g of affinity adsorbent, add 3 mL 1X PBS/0.01% NaN$_3$, incubate for 10 min. Spin the tube and discard supernatant.
7. Add lysate obtained by phage lysis of bacteria to the affinity adsorbent and rotate on an overhead shaker for 4 h at room temperature or overnight at 4°C.
8. Spin down the matrix (100*g*, 1 min) and discard supernatant.
9. Wash column twice for 10 min with 30 mL 1X PBS/0.01% NaN$_3$ on an overhead shaker. Discard washing buffer.
10. Incubate affinity adsorbent for 2 h at 4°C with 1 *M* glycin and wash subsequently twice for 10 min with 1X PBS/0.01% NaN$_3$. You have now obtained a resin saturated with phage and bacterial proteins.
11. Transfer the sera processed through the first preabsorption step (**Subheading 3.2.1.1.**) to the 50-mL Falcon tubes with the prepared resin. Incubate for 4 h at room temperature or overnight at 4°C on an overhead shaker.
12. Centrifuge to spin down the resin (100*g*, 1 min). Harvest the sera, which are stored at 4°C until introduction into the third purification step as described under **Subheading 3.2.1.3.**

3.2.1.3. PREABSORPTION AGAINST LYTIC FILTERS

1. Prepare *E. coli* XL1-Blue MRF' as described under **Subheading 3.1.5.**
2. For each large Petri dish agar plate (diameter 13.5 cm) infect 600 μL bacteria (OD$_{600}$ = 0.5) with 10^5 pfu of wild-type λ ZAP II phage ("blue phage"—*see* **Subheading 3.2.1.2., step 3**). Incubate at 37°C for 15 min. Add 40 μL 1 *M* IPTG and 8 mL LB top agar (melted and cooled to 42°C).
3. Poor onto prewarmed LB-tetracycline agar plates, allow the top agar to solidify, and incubate upside down overnight at 37°C. Due to the high multiplicity of infection (MOI) used, the plates will be lytic next morning without spared bacterial lawn.

4. Place nitrocellulose filters on top of the bacteria plaques, incubate 4 h at 37°C.
5. Lift filters and replace each by a second one, repeat incubation for 6 h at 37°C.
6. All filters are immersed in a large container with 1X TBST and incubated with gentle agitation. Take care the top agar is removed entirely.
7. Wash three times for 10 min in 1X TBST.
8. Place each filter into an individual Petri dish. Incubate them in blocking buffer for 1 h at room temperature with gentle agitation to block nonspecific protein-binding sites.
9. Wash filters three times for 10 min in a large container with 1X TBS. The filters can be either air dried and stored at room temperature for up to 6 mo or used directly for the third step of preabsorption.
10. Place each filter blotted side facing upward into a Petri dish. Transfer each individual human serum that has been processed as described under **Subheadings 3.2.1.1.** and **3.2.1.2.** to a filter and incubate for 4 h at room temperature on a horizontal shaker.
11. Remove the membrane, recover the serum completely, and incubate it with a fresh lytic membrane.
12. Transfer serum into a 500-mL bottle or Falcon tubes. The serum is now ready to use for immunoscreening.

3.2.2. Primary Immunoscreening of cDNA Expression Library

If the library has been generated from tissue contaminated with a considerable number of B-lymphocytes, the immunoscreening protocol should be modified either on the level of primary or secondary immunoscreening (*see* **Note 6**).

1. Inoculate a single colony from the freshly plated XL1-Blue MRF' cells in 20 mL LB medium containing 0.2% maltose and 10 mM MgSO$_4$ and grow overnight at 30°C to an OD$_{600}$ of 0.7–0.9.
2. Spin the cells gently in Falcon tubes, remove the supernatant, and resuspend cells in 10 mM MgSO$_4$ to an OD$_{600}$ of 0.5.
3. Add 5×10^4 pfu of the library to 0.6 mL cells. Mix well and incubate at 37°C for 15 min without shaking to allow phages to adhere to cells.
4. Add 15 µL of 1 M IPTG and 9–10 mL of melted LB top agar, mix well, and pour the mixture onto a prewarmed, dry LB-tetracycline agar plate (diameter 13.5 cm) (*see* **Note 7**).
5. After the top agar is solidified, invert the plates and incubate at 37°C overnight.
6. Number nitrocellulose filters with a waterproof pencil. Soak them in TBS until they are completely wet. Discard nitrocellulose that does not wet properly. Place filters on blotting paper to drain residual fluid. Take plates out of the incubator and place filters carefully onto the top agar, starting at an edge. Incubate plates at 37°C overnight.
7. Chill plates at 4°C for at least 1 h. Mark the orientation of the filters relative to the agar plates with a needle by piercing in several places.
8. Remove filters carefully from plates, immerse them in a large container with 1X TBST (*see* **Note 8**). Shake them vigorously on a platform shaker for 30–60 min.
9. Remove any remaining top agar by lightly rubbing filters submerged in 1X TBST with gloved fingers.
10. Transfer filters into a large container with fresh 1X TBST buffer and wash them for an additional 15–30 min under vigorous agitation.
11. Place each filter into an individual Petri dish. Immerse them in blocking buffer for 1 h at room temperature with gentle agitation to block nonspecific protein-binding sites.

12. Wash filters three times for 10 min in a large container with 1X TBS. Make sure that precipitates of milk powder are rubbed off with gloved fingers.
13. Transfer each filter again into an individual Petri dish. Add preabsorbed serum prepared as described under **Subheading 3.2.1.** Incubate on the shaker at room temperature overnight.
14. Wash filters three times for 10 min in a large container with 1X TBS.
15. Transfer each filter again into an individual Petri dish. Add goat anti-human IgG labeled with alkaline phosphatase (1:2500 dilution) in 1X TBS with 1% dry milk. Incubate for 1.5 h on the shaker at room temperature.
16. Wash filters three times for 10 min in a large container with 1X TBS.
17. Prepare staining solution by adding nitroblue tetrazolium chloride (NBT) to a final concentration of 0.3 mg/mL and 5-bromo-4-chloro-3-indol-phosphate-toluidine (BCIP) to a final concentration of 0.15 mg/mL to color development solution under continuous stirring. Filter this staining solution to avoid precipitates.
18. Transfer each filter into an individual Petri dish and immerse them in staining solution. Allow reaction to proceed in the dark until positive reactions are clearly visible. Substrate reaction occurs at the circumference of a phage plaque, so that positive clones appear as darker halo.
19. Identify and mark positives on filters. Determine the respective plaque on the agar plate using needle holes for orientation.
20. Pick positive plaques with two to three adjacent negative plaques using a pipet tip and place each agar plug in a separate tube containing 1 mL of SM and 20 µL of chloroform. Vortex vigorously and incubate at 4°C overnight.

3.2.3. Secondary Round of Immunoscreening and Monoclonalization of Phages

This oligoclonal phage suspension is introduced to a secondary round of immunoscreening. Negative plaques have been included deliberately as internal negative controls for the secondary round of immunoscreening. The objective of the secondary round is to confirm positivity and to enrich positive phages to monoclonality.

1. Divide the LB-tetracycline agar plate in a large Petri dish (diameter 13.5 cm) into four quarters by carving out cross-shaped borders with a scalpel.
2. Dilute the primary stock of oligoclonal phages at 1:500 and 1:100 in SM buffer, add 2 µL from these dilutions and IPTG to 2–3 mL top agar. Pour each of these dilutions on one quarter. Thus two different titers of two different oligoclonal phage stocks can be assayed on one 13.5-cm Petri plate.
3. Repeat **Subheading 3.2.2., steps 5–19** for primary immunoscreening.
4. Confirmation of positivity should be done only for clones resulting in subconfluent phage plaques. If the entire lawn is lytic with both dilutions, repeat the test with a higher dilution.
5. Pick two monoclonal phages for each clone confirmed as positive, as described under **Subheading 3.2.2., step 20**. Transfer them into 0.5 mL SM with 20 µL chloroform for in vivo excision.

3.3. Serological Characterization of Clones

Differential serology, which means testing of a clone with sera from tumor patients as well as appropriate control groups, is an important tool to determine the antigens with tumor-associated sero-responses (*see* **Note 9**).

3.3.1. Conventional "Petite Serology"

1. Divide agar-tetracycline plates in 15-cm Petri dishes into four quarters by carving out cross-shaped borders with a scalpel.
2. Mix monoclonal phages representing individual antigens of interest 5:1 with wild-type λ ZAP phage as a control. Infect 0.6 mL *E. coli* XL1-Blue MRF' host strain ($OD_{600} = 0.5$) in the presence of 0.8 m*M* IPTG with a final pfu of 2×10^3.
3. Add 2–3 mL LB top agar and pour onto one quarter of the prewarmed LB agar plates for overnight incubation. Thus four different clones can be processed in parallel on one plate.
4. After plaque formation, recombinant proteins are blotted onto nitrocellulose filters and processed as described under **Subheading 3.2.2., steps 7–20**. Each filter is incubated with serum from a different donor preabsorbed as described under **Subheading 3.2.1.** In total, 15–20 sera from cancer patients suffering from the tumor under investigation and 15–20 sera of healthy controls are used on the respective set of four clones under investigation.

3.3.2. SeroGRID for "Petite Serology"

Compared to conventional "petite serology," SeroGRID is a rapid, high-throughput procedure that allows multiplex analysis of an entire set of antigens with a selection of different sera *(15)*.

1. Instead of round large Petri dishes (diameter 13.5 cm), use $24.5 \times 24.5 \times 2.5$ cm square Petri dishes to prepare an LB-tetracycline plate.
2. Before pouring phage-infected bacteria in the top agar layer onto the plate, insert 22 plastic spacers into the agar, producing slots 1 cm × 24 cm in size to obtain a separate slot for each individual phage clone.
3. Titer each phage clone, mix approximately in a ratio of 5:1 with wild-type phage as internal negative control, adjust to a final pfu of 6×10^2 and infect *E. coli* XL1-Blue MRF'. Add 3 mL of top agar in the presence of IPTG and pour into the prepared slots.
4. One slot is reserved for wild-type phage as a negative control. As a positive control, a phage containing PINCH (GenBank, accession no. U09284), which reacts with most human sera, is used.
5. After overnight incubation, spacers are removed. For plaque lift of recombinantly expressed proteins, a 24×23 cm nitrocellulose membrane is prepared and placed on the plate.
6. Wash and block as described in **Subheading 3.2.2., steps 7–12**
7. After washing and blocking, cut the membranes in 1×23 cm "multiantigen" strips with the cutting edge at right angles to the direction of individual phage slots. Each strip is placed in an individual segment of the self-made incubation chamber and incubated with a different serum overnight.
8. Proceed as described in **Subheading 3.2.2., steps 9–20** to obtain immunostained filters.

3.4. Molecular Characterization of Clones

3.4.1. In Vivo Excision of the Phagemid From the λ Phage Vector

The Uni-ZAP XR vector is designed to allow simple, efficient in vivo excision from the λ vector, and recircularization to form an ampicillin-resistant pBluescript phagemid containing the cloned insert. The cloning site of the λ vector is flanked by fl bacteriophage origins of replication. Simultaneous infection of *E. coli* with both the λ vector and the fl bacteriophage leads to nicking at these sites and synthesis of a

single-stranded DNA molecule. This molecule includes all sequences of the pBluescript SK(–) phagemid and the insert, if one is present and is circularized by specific proteins from the f1 phage. In addition, a functional f1 origin is generated as found in f1 bacteriophage or phagemids. The ExAssist helper phage used for this procedure contains an amber mutation that prevents replication of the phage genome in a nonsuppressing *E. coli* strain such as SOLR cells. This allows only the excised phagemid to replicate in the host, avoiding co-infection by ExAssist helper phage.

1. Streak the host strain *E. coli* XL1-Blue MRF' and *E. coli* XL1-Blue SOLR onto an LB agar plate containing tetracycline/kanamycin, and incubate the plate overnight at 37°C.
2. Grow separate overnight cultures of XL1-Blue MRF' and SOLR cells in LB broth, supplemented with 0.2% (w/v) maltose and 10 mM MgSO$_4$, at 30°C to an OD$_{600}$ of 0.7–0.9.
3. Spin the cells down and resuspend them to obtain an OD$_{600}$ of 1.0 in 10 mM MgSO$_4$.
4. Combine the following components in a Falcon 2059 polypropylene tube: 200 μL of XL1-Blue MRF' cells at an OD$_{600}$ of 1.0, 250 μL of monoclonal secondary positive phage stock (containing >1 × 10^5 phage particles), 1 μL of the ExAssist helper phage (>1 × 10^6 pfu/μL).
5. Incubate the Falcon 2059 polypropylene tube at 37°C for 15 min.
6. Add 3 mL of LB broth and incubate the Falcon 2059 polypropylene tube for 2.5–3 h at 37°C.
7. Heat the Falcon 2059 polypropylene tube at 65–70°C for 20 min to inactivate the ExAssist helper phage and then spin the tube at 1000g for 15 min.
8. Decant the supernatant into a sterile Falcon 2059 polypropylene tube. This stock contains the excised pBluescript phagemid packaged as filamentous phage particles, and may be stored at 4°C for 1–2 mo.
9. To plate the excised phagemids, add 10 μL and 100 μL of the phage supernatant from step 7 each to 200 μL of freshly grown SOLR cells from step 2 (OD$_{600}$ = 1.0) in 1.5-mL microcentrifuge tubes.
10. Incubate the tubes at 37°C for 15 min.
11. Streak 10–20 μL of the cell mixture from microcentrifuge tubes on LB-ampicillin agar plates (50 μg/mL) and incubate the plates overnight at 37°C. Colonies appearing on the plates contain the pBluescript double-stranded phagemid with the cloned DNA insert. Colonies can now be picked, grown, and subjected to plasmid purification. For long-term storage, prepare a bacterial glycerol stock and store at –80°C.

3.4.2. Further Molecular Characterization of In Vivo Excised Clones

In vivo excised phagemids can be conveniently subjected to state-of-the-art technologies for molecular, structural, and functional analysis (*see* **Note 10**).

4. Notes

1. Three different λ phage expression library systems have been reported for SEREX screening: (1) λ Uni ZAP vector, which allows in vivo excision of pBluescript phagemid using the SOLR strain (Stratagene); (2) λ ZAP Express vector, which allows in vivo excision of pBK-CMV phagemid using the XLOLR strain (Stratagene); (3) λ TRIPLX vector (Clontech Laboratories Inc., Palo Alto, CA).

   Protocols described here refer to the λ ZAP II-based system, which we prefer since it results in large and clearly visible lytic plaques with high amounts of recombinant protein.

2. If primary phage count is $>4 \times 10^6$, primary immunoscreening can be conducted without library amplification. Even so, we recommend one round of amplification of a fraction of the library containing at least 2×10^6 phages. We prefer amplification on agar plates rather than amplification in soluble medium, since this procedure reduces the risk of dramatic changes in the representation of individual clones. Amplification of the library allows generation of large amounts of phages for multiple screening rounds as well as for storing. It may be advisable to conduct an initial screening round directly after the library has been packaged but before amplification, which will allow a more representative coverage of the diversity of transcript species.

3. Messenger RNA is primed in the first-strand synthesis with a Xho I site containing linker primer, and is reverse transcribed using RNase H negative MMLV-RT and 5-methyl dCTP. The hemimethylated cDNA is protected from digestion of the cDNA with Xho I, used later to cleave the linker primer.

   Hemimethylated DNA introduced in a bacterial strain would be efficiently digested by the *mcrA* and *mcrB* restriction systems. It is necessary to pass the library through a McrA$^-$ McrB$^-$ host (e.g., XL1-Blue MRF'). After that, the library is no longer hemimethylated and can be grown on McrA$^+$ McrB$^+$ strains (e.g., XL1-Blue).

4. Three surrogate parameters—(1) number of clones; (2) rate of recombinants; and (3) median and maximal insert size of inserts—are used to determine the quality of an expression library. The number of primary plaques is a good indicator for the representation of individual transcripts in the library. cDNA clones in λ-ZAP libraries are expressed as fusion proteins containing N-terminal β-galactosidase fragments. Having in mind that only one third of directionally cloned cDNA are in the appropriate frame and some cDNA fragments are cloned with a leading 5'-UTR possibly introducing premature stop codons, we recommend that a "good library" should contain $>2 \times 10^6$ primary plaques. To estimate the average and maximum fragment size, we perform agarose gel analysis of inserts, either amplified by PCR using oligonucleotides binding to insert flanking regions of the vector backbone and $>10^5$ phages as template, or by analyzing 20 randomly picked, in vivo excised restriction enzyme-digested clones. The median size of human mRNA-derived inserts should be >1 kb, and the presence of inserts with size >4–5 kb indicates sufficient representation of large cDNAs. The rate of recombinants (white plaque number/total plaque number) is generally clearly above 95%. Lower rates point to inefficient ligation of the cDNA fragments (e.g., mismatched amounts of vector and insert, defective cDNA-fragment or vector ends, contamination with adaptors). Even though rates around 85% are tolerable, we recommend performing sequencing of randomly picked clones to ensure the correctness of inserts (correct direction, presence of adaptor sequences at 5' end, presence of poly(A) tail at the 3' end), if rates of recombinants are below 95%.

5. The quality of the preabsorbed serum is critical. Usually the serum can be used several times (5–15 rounds of screening). It should be stored at 4°C and thimerosal or NaN$_3$ should be added each week to prevent bacterial contamination. Reuse often results in reduced background due to absorption of nonspecific components rather than in diminished activity. This increases sensitivity and specificity. As a consequence, weak positive reactivities are detected in later rounds of the immunoscreening.

   Our protocol of preabsorption uses not only mechanically disrupted bacteria, which deplete antibodies against intracellular components and cell-wall elements of bacteria. We also preabsorb against bacteria lysed by phages. The latter reagent contains additionally phage proteins as well as bacterial proteins induced secondary to infection (e.g., shock proteins).

Many human sera can be used after having been subjected to one round of the described tripartite preabsorption process (**Subheadings 3.2.1.1.–3.2.1.3.**). However, if this does not reduce unspecific cross-reactivity sufficiently, parts of the process can be repeated. If mainly the bacterial lawn in between plaques is contributing to the background, **Subheading 3.2.1.1.** should be repeated. If the plaque circumferences are stained unspecifically, repeat **Subheading 3.2.1.2. or 3.2.1.3.**

6. Libraries derived from tissue specimens contaminated with B-lymphocytes will contain inserts expressing segments of genes encoding human immunoglobulins. Immunoscreening of such libraries derived from tissue will result in the identification of false positives by binding of the second antibody to recombinantly expressed human IgG derived from the B-cell transcriptome. Such inserts may represent up to 90% of all positive clones. These clones should be eliminated early from further characterization. One option is to use a modified primary screening as described previously *(16)*. To this aim, the filters are handled according to the protocol including the blocking step (**Subheading 3.2.2., steps 1–12**), but then preincubated first with enzyme-conjugated anti-human IgG and stained to detect the immunoglobulin inserts, which are marked with a pencil. Subsequently, these membranes go through the standard process starting with incubation with the autologous serum, second antibody, and thereafter staining (**Subheading 3.2.2., steps 12–20**). Only clones appearing now de novo and not marked in context of the prior staining step are recovered. If contamination is modest, this pre-testing by direct incubation with the anti-IgG antibody may be done on the level of secondary immunoscreening after individual phages have been picked and oligo-clonalized.

   A substantial *a priori* reduction of such false positives can be achieved by depletion of immunoglobulin sequences during library construction using subtractive cDNA library approaches *(17)*.

7. A reduced moisture content of plates results in higher quality plaque lifts. Agar plates should be prepared at least 24 h prior to use. Preincubate plates at 37°C 1 h before use. If necessary, wipe dry with a paper tissue before pouring the top agar. If despite these endeavors the top agar and plaques stick to the filter and are removed together with it, the phage traces pertinent on the agar plate under the top agar layer, even though not visible, are sufficient to recover phage clones of interest.

8. Nitrocellulose filters should be handled with care. Never touch with bare hands, always use gloves. Do not allow filters to dry after antigen absorption.

   Because inter-lot differences of nitrocellulose may affect the quality of the assay, we prefer to test batches prior to use. Washes have to be thorough and generous. Top agar has to be removed without scratching but diligently. Parts of the filter covered by gelatinized contents of lytic plaques or sticking traces of top agar are not eligible for immunodetection by antibodies. As described, we prefer to separate filters and process them blotted side facing upward in individual Petri dishes for the critical steps of blocking, antibody incubation, and staining, to ensure adequate exposure. These Petri dishes do not need to be sterile and can be re-used.

9. SEREX is a high-output technology. Comprehensive mapping of even a single patient specimen results in cloning of multiple different antigens. However, as pointed out in the introduction, a considerable proportion of clones detected by SEREX are not primarily cancer related. Evaluation of multiple SEREX-defined clones in serological assays using panels of allogeneic sera from cancer patients as well as appropriate control groups is an important step towards focusing on the relevant antigens worth further extended analysis *(18)*.

Usually, a two-step strategy is used. First, a small-scale serological study based on the plaque lift assay is conducted to define those antigens without reactivity with control sera of healthy individuals but exhibiting reactivity with tumor sera ("petite serology"). Subsequently, those antigens that appear to be cancer related are subjected to ELISA based on purified recombinant protein for further confirmation with a large panel of sera ("grande serology") *(19)*. Since this process is labor intensive, several modified protocols have been established *(20–22)*, one of which is revisited in **Subheading 3.3.2.** *(15)*.

10. SEREX aims at the identification of tumor-related antigens of potential diagnostic or therapeutic use. Conceptually, besides state-of-the-art procedures for characterization of new genes, the molecular characterization should tackle in particular which of the gene products are (1) selectively expressed and/or (2) of tumor biological relevance *(18,23)*.

A first step is sequencing of the antigen encoding cDNAs and subsequent BLAST search to determine clones identical to known autoantigens or to proteins with known tumor biological relevance. Expression profiling by quantitative RT-PCR in a panel of normal and tumor tissues determines genes with tumor-associated tissue distribution.

References

1 Boon, T., Cerottini, J. C., van den Eynde, B., van der Bruggen, P., and van Pel, A. (1994) Tumor antigens recognized by T-lymphocytes. *Annu. Rev. Immunol.* **12,** 337–366.

2 van der Bruggen, P., Traversari, C., Chomez, P., et al. (1991) A gene encoding an antigen recognized by cytolytic T lymphocytes on a human melanoma. *Science* **254,** 1643–1647.

3 Hartley, S. B., Booke, M. P., Fulcher, D. A., et al. (1993) Elimination of self reactive B lymphocytes proceeds in two stages: arrested development and cell death. *Cell* **72,** 325–335.

4 Sahin, U., Türeci, O., Schmitt, H., et al. (1995) Human neoplasms elicit multiple specific immune responses in the autologous host. *Proc. Natl. Acad. Sci. USA* **92,** 11,810–11,813.

5 Sahin, U., Türeci, O., and Pfreundschuh, M. (1997) Serological identification of human tumor antigens. *Curr. Opin. Immunol.* **9,** 709–716.

6. Türeci, O., Sahin, U., and Pfreundschuh, M. (1997) Serological analysis of human tumor antigens: Molecular definition and implications. *Mol. Med. Today* **3,** 342–349.

7 Boon, T. and Old, L. J. (1997) Cancer tumor antigens. *Curr. Opin. Immunol.* **9,** 681–683.

8 Jongeneel, V. (2001) Towards a cancer immunome database. *Cancer Immun.* **1,** 3.

9 Zarour, H. M., Maillere, B., Brusic, V., et al. (2002) NY-ESO-1 119-143 is a promiscuous major histocompatibility complex class II T-helper epitope recognized by Th1- and Th2-type tumor-reactive CD4^{+} T cells. *Cancer Res.* **62,** 213–218.

10 Zeng, G., Li, Y., El-Gamil, M., et al. (2002) Generation of NY-ESO-1-specific CD4^{+} and CD8^{+} T cells by a single peptide with dual MHC class I and class II specificities: a new strategy for vaccine design. *Cancer Res.* **62,** 3630–3635.

11 Jager, E., Gnjatic, S., Nagata, Y., et al. (2000) Induction of primary NY-ESO-1 immunity: CD8^{+} T lymphocyte and antibody responses in peptide-vaccinated patients with NY-ESO-1^{+} cancers. *Proc. Natl. Acad. Sci. USA* **97,** 12,198–12,203.

12 Old, L. J. and Chen, Y. T. (1998) New paths in human cancer serology. *J. Exp. Med.* **187,** 1163–1167.

13. Maniatis, T., Sambrook, J., and Fritsch, E. F., eds. (1989) *Molecular Cloning: A Laboratory Manual*. 2nd Ed. Cold Spring Harbor Laboratory, Cold Spring Harbor, NY, pp.7.11–7.12.

14 Chomczynski, P. and Sacchi, N. (1987) Single-step method of RNA isolation by acid guanidinium thiocyanate-phenol-chloroform extraction. *Anal. Biochem.* **162,** 156–159.

15 Krause, P., Türeci, Ö., Micke, P., Buhl, R., Huber, C., and Sahin, U. (2003) SeroGRID: An improved method for the rapid selection of antigens with disease related immunogenicity. *J. Immunol. Methods* **283,** 261–267.

16. Türeci, Ö., Schmitt, H., Fadle, N., Pfreundschuh, M., and Sahin, U. (1997) Molecular definition of a novel human galectin which is immunogenic in patients with Hodgkin's disease. *J. Biol. Chem.* **272,** 6416–6422.

17 Diatchenko, L., Lukyanov, S., Lau, Y. F., and Siebert, P. D. (1999) Suppression subtractive hybridisation: A versatile method for identifying differentially expressed genes. *Methods Enzymol.* **303,** 349–380.

18. Türeci, O., Sahin, U., Zwick, C., Neumann, F., and Pfreundschuh, M. (1999) Exploitation of the antibody repertoire of cancer patients for the identification of human tumor antigens. *Hybridoma* **18,** 23–28.

19 Stockert, E., Jäger, E., Chen, Y. T., et al. (1998) A survey of the humoral immune response of cancer patients to a panel of human tumor antigens. *J. Exp. Med.* **187,** 1349–1354.

20 Lagarkova, M. A., Koroleva, E. P., Kuprash, D. V., et al. (2003) Evaluation of humoral response to tumor antigens using recombinant expression-based serological mini-arrays (SMARTA). *Immunol. Lett.* **85,** 71–74.

21 Scanlan, M. J., Welt, S., Gordon, C. M., et al. (2002) Cancer-related serological recognition of human colon cancer: identification of potential diagnostic and immunotherapeutic targets. *Cancer Res.* **62,** 4041–4047.

22. Türeci, Ö., Luxemburger, U., Heinen, H., et al. (2004) CrELISA: A fast and robust enzyme linked immuno sorbent assay bypassing the need for purification of recombinant protein. *J. Immunol. Methods*, in press.

23. Türeci, Ö., Sahin, U., Zwick, N., Neumann, F., and Pfreundschuh, M., (1999) Identification of human tumor antigens using the antibody repertoire of cancer patients. *Gann Monograph Cancer Res.* **48,** 93–101.

12

Application of Proteomics and Protein Analysis for Biomarker and Target Finding for Immunotherapy

Petra Weingarten, Petra Lutter, Andreas Wattenberg, Martin Blueggel, Sonja Bailey, Joachim Klose, Helmut E. Meyer, and Christoph Huels

Summary

Regulatory T-cells play a central role in the maintenance of the immunological balance and are powerful inhibitors of T-cell activation both in vivo and in vitro. The enhancement of suppressor-cell function might be a target for immunotherapeutic approaches for the treatment of immune-mediated diseases like multiple sclerosis and Crohn's disease.

The method of choice to elucidate the still unclear effector functions of regulatory T-cells is the differential proteome analyses performed with human and murine T-cell populations. To this end, whole-protein extracts of conventional and regulatory T-cells are separated by high-resolution two-dimensional gel electrophoresis according to Klose *(1)*. The proteomes are analyzed by a 2DE gel image analysis software, ProteomWeaver™. The protein spots that are found differentially expressed are picked from the gels and prepared for matrix-assisted laser desorption/ionization (MALDI) mass spectrometrical analysis automatically. The high-resolution 2DE-PAGE and the automated spot handling and protein identification allows one to rapidly find new potential candidate proteins that are of functional relevance for regulatory T-cells, to be used as targets for drug development or as biomarkers for research and diagnostic purposes.

Key Words: Proteome analysis; T-lymphocytes; mass spectrometry; electrophoresis; image analysis; protein identification; in-gel digestion; silver staining; Coomassie staining; protein database; 2DE; spot picking; sample preparation; T-regulatory cells; peptide mass fingerprint; MALDI; peptide fragmentation; drug target; suppressor T-cells; drug development.

1. Introduction

Proteins as targets are dominating pharmaceutical research and development (R&D). Forty-five percent of the drugs on the market modulate receptor–ligand interactions, and 28% are directed to enzymes. Only 2% of the drugs in therapeutic use interfere directly or indirectly with DNA *(2)*. There is no evidence for a dramatic change of this fact in the future, since antisense and DNA-intercalating drug candidates have yet to show their broader applicability.

Additionally, the pharmaceutical industry is under strong pressure to reduce overall R&D costs. One major chance to achieve this goal is to get access to proprietary and validated targets with a proven role in diseased states and new mode of action (MOA). This allows development of a competitive advantage and longer and stronger patent protection for new drugs. Validated targets with new MOA and corresponding lead compounds are the key for future development of the pharmaceutical industry.

Huge efforts have been put into the sequencing of the human genome, setting the basis for the today's activities in functional genomics. Technological progress led to the generation of vast amounts of data in a short time, and to a high number of new potential targets that have to be validated for the pharmaceutical R&D process. The development of all new technologies for target discovery, and in particular the technological revolution in proteomics, led to new approaches in pharmaceutical R&D and made access to validated targets faster and more cost effective.

The classical way of performing proteomics studies via two-dimensional gel electrophoresis (2DE) and mass spectrometry in combination with sophisticated bioinformatics is still dominating the proteomics world. Reproducible and sensitive 2DE systems are mandatory for the process. The 2DE system from one of the inventors of the 2DE, Joachim Klose, is the most reliable and reproducible compared to the other systems used in the community. It uses the ampholine technology for the first dimension in combination with long-distance separation, leading to superior performance *(1,3,4)*.

The protocols presented here are depicted from studies focused on early drug development. Several mechanisms control the discrimination between self and nonself, including the thymic deletion of auto-reactive T-cells and the induction of anergy in the periphery. In addition to these passive mechanisms, evidence has accumulated for the active suppression of auto-reactivity by a population of regulatory T-cells that co-express CD4 and CD25. Regulatory T-cells play a central role in the maintenance of the immunological balance and are powerful inhibitors of T-cell activation both in vivo and in vitro *(5)*. The enhancement of suppressor-cell function might be a target for immunotherapeutic approaches for the treatment of immune-mediated diseases. By contrast, the elimination of regulatory T-cells or the inhibition of their functions might prove to be beneficial for the induction of tumor immunity or the treatment of chronic infectious diseases.

To elucidate the still unclear effector functions of regulatory T-cells, we performed differential proteome analyses with diverse human and murine T-cell populations *(6)*. The whole protein extracts of conventional and regulatory T-cells of four individual human donors and BALB/c mouse pools were separated by high-resolution two-dimensional gel electrophoresis. The proteomes of resting as well as anti-CD3/CD28-stimulated $CD4^+$ and $CD4^+$ $CD25^+$ T-cells were compared. The identification of candidate proteins that are of functional relevance for both human and murine regulatory T-cells contributes to the understanding of the causes for and mechanisms involved in autoimmune diseases, allergy, and cancer, and will lead to the development of new drugs to manipulate the activity of regulatory T-cells *(7)*.

2. Materials

2.1. Equipment

2.1.1. Sample Preparation

1. Sonication bath to perform sonication in a water bath, e.g., Sonorex super RK 52H (Bandelin Electronic, Berlin, Germany).
2. Glass beads with a diameter of 1.0–2.0 mm (Roth, Karlsruhe, Germany).
3. Complete™ protease inhibitor cocktail (Roche Diagnostics, Penzberg, Germany).
4. Phenylmethylsulfonyl fluoride (PMSF) in ethanol.
5. Pepstatin A.
6. Urea.
7. Thiourea.
8. Dithiothreitol (DTT).
9. Ampholine Servalyt 2-4 (Serva, Heidelberg, Germany).
10. Benzonase.
11. Magnetic stirrer with 5×1 mm stirring bars.
12. Fine tweezers.

2.1.2. Isoelectric Focusing (IEF)

1. Glass tubes for IEF gels: length 40 cm or 20 cm; inner diameter: 0.7 mm for analytical gels or 0.9 mm for preparative gels; outer diameter: 7.0 mm (Schott Glaswerke, Mainz, Germany).
2. Nylon strings (fishing line, 0.8 mm thick; one end is made thicker by melting the end of the string and fitting it quickly into the glass tube).
3. IEF chamber: the apparatus consists of an upper and a lower cylindrical buffer chamber and is equipped with intermediate cylinders in various heights to allow gel tubes of various lengths. Up to eight glass tubes can be inserted into the apparatus and fixed with screws (for detailed view *see* **ref. 3**).
4. Power supply: EPS 3500 XL (Amersham Biosciences Europe, Freiburg, Germany).
5. Gel loader tips (Eppendorf, Hamburg, Germany).
6. IEF gel holder (for detailed view *see* **ref. 3**).
7. Plastic boxes to store the IEF gels on the holder at –18°C to –80°C.

2.1.3. SDS-PAGE

1. Desaphor VA 300 system with equipment (Sarstedt, Nuembrecht, Germany).
2. Plastic spacers, 0.75 mm or 1.5 mm, for analytical or preparative gels (Sarstedt).
3. Power Supply: EPS 3500 XL (Amersham Biosciences Europe).
4. HydroTech Gel Drying System (Bio-Rad Laboratories, München, Germany).
5. Cellophane film (Pütz Folien, Taunusstein, Germany, or Bio-Rad Laboratories, München, Germany).

2.1.4. Gel Staining

1. Staining trough (30 cm × 40 cm).
2. Horizontal gel shaker type 3020 (GFL, Burgwedel, Germany).

2.1.5. Image Analysis

1. Flatbed scanner PowerLook 2100 (Umax Data Systems, Taiwan).
2. ProteomWeaver™ Vers. 2.0 (Definiens, München, Germany).

2.1.6. Spot Excision

1. Spot Picking Robot PROTEINEER sp™ (Bruker Daltonik, Bremen, Germany).
2. Pierced microtiter plates (Bruker Daltonik).

2.1.7. Digestion

1. Digesting robot PROTEINEER dp™ (Bruker Daltonik).
2. Digestion Kit: dp 384 Reagent Kit (Bruker Daltonik).
3. Acetonitrile (p.a.), acetone (p.a.) (Merck, Darmstadt, Germany).

2.1.8. MALDI Analysis

1. Ultraflex TOF/TOF Mass Spectrometer (Bruker Daltonik).
2. MALDI 600 µm AnchorChip™ Target (Bruker Daltonik).

2.1.9. Database Analysis

1. Proteinscape™ Database (Bruker Daltonik).
2. ProFound™ (Genomic Solutions, Ann Arbor, MI).
3. Mascot™ (Matrix Science, London, UK).
4. Sequest™ (Thermo Finnigan, San Jose, CA).

2.2. Buffers and Solutions

2.2.1. Sample Preparation

1. Protease inhibitor solution: 0.2 M KCl, 10% (w/v) glycerol, 0.1 M phosphate buffer (NaH_2PO_4/Na_2HPO_4, 1:2) pH 7.1, 1 mM $MgSO_4$·H_2O, 0.13 M CHAPS, 2.6 µM pepstatin A, 1.8 mM PMSF, 1 pill Complete™/5 mL.

2.2.2. IEF

1. Separation gel solution: The composition is given in **Table 1**. The gel solution is filtered (GF/C glass microfiber filter, diameter 7 cm, Whatman Scientific., Maidstone, Kent, UK), aliquoted into 2-mL portions, and stored at –70°C. To remove acrylic acid, 20 mL of the acrylamide solution (containing 3.5% [w/v] acrylamide and 0.3% [w/v] piperazine diacrylamide) is mixed with 1 g prewashed Amberlite MB-1A and agitated for 1 h. Thereafter, the solution is filtered to remove the ion-exchange material.
2. Cap gel solution: The composition is given in **Table 1**. The gel solution is filtered (GF/C glass microfiber filter, diameter 7 cm, Whatman Scientific), aliquoted into 750-µL portions, and stored at –70°C. To remove acrylic acid, 20 mL of the acrylamide solution (containing 3.5% [w/v] acrylamide and 0.3% [w/v] piperazine diacrylamide) is mixed with 1 g prewashed Amberlite MB-1A and agitated for 1 h. Thereafter, the solution is filtered to remove the ion-exchange material.
3. Ammonium persulfate solution: 0.08 g ammonium persulfate is dissolved in bidistilled water to give a final volume of 10 mL. The solution is filtered, aliquoted into 100-µL portions, and stored at –70°C.
4. Sephadex suspension: 20 g Sephadex G-75 superfine (Amersham Biosciences Europe) is swollen in 500 mL bidistilled water for 5 h at 90°C. The supernatant water is decanted and the Sephadex resuspended into 1000 mL 25% (w/v) glycerol and gently stirred for 2 h. The glycerol solution is changed once during the 2-h period. The supernatant water is then sucked off from the suspension by using a filter funnel. The Sephadex is aliquoted into 272-mg portions and stored at –20°C.

Table 1
Solutions for IEF

Separation gel solution pH 2.0–11.0		Cap gel solution pH 2.0–11.0	
3.5% (w/v)	Acrylamide	12.3% (w/v)	Acrylamide
0.3% (w/v)	Piperazine diacrylamide	0.13% (w/v)	Piperazine diacrylamide
4% (v/v)	Carrier ampholyte solution pH 2.0–11.0	4% (v/v)	Carrier ampholyte solution pH 2.0–11.0
9 *M*	Urea	9 *M*	Urea
5% (w/v)	Glycerol	5% (w/v)	Glycerol
0.06% (v/v)	TEMED	0.06% (v/v)	TEMED
Carrier ampholyte solution pH 2.0–11.0		**Sample protection solution**	
8 mL	Ampholine pH 3.5–10.0	30% (w/v)	Urea
8 mL	Servalyt pH 2.0–11.0	5% (w/v)	Glycerol
16 mL	Pharmalyte pH 5.0–8.0	2% (v/v)	Servalyt 2–4
24 mL	Pharmalyte pH 4.0–6.5		
8 mL	Servalyt pH 6.5–9.0		

The chemicals were dissolved in bidistilled water. Servalytes are from Serva (Heidelberg, Germany) and Pharmalytes are from Amersham Biosciences Europe (Freiburg, Germany).

5. Sample protection solution: The composition is given in **Table 1**. The resulting solution is filtered, aliquoted into 100-μL portions, and stored at –70°C.
6. Anode solution: 0.742 *M* phosphoric acid, 3 *M* urea (prepared freshly).
7. Cathode solution: 5% (v/v) ethylenediamine, 5% (v/v) glycerol, 9 *M* urea. The electrode solutions are prepared freshly before each IEF run. The cathodic solution can be heated up to 30°C to better dissolve the urea (prepared freshly).
8. Equilibration solution: 125 m*M* Tris-base, 40% (v/v) glycerol, 3% (w/v) SDS, 65 m*M* DTT, pH 6.8. The final solution is filtered, aliquoted into 10-mL portions, and stored at –70°C.

2.2.3. SDS-PAGE

1. Gel solution: 1.5 L of the ready-made mixture of 30% acrylamide and 0.4% bisacrylamide (Serva) are added to 1.5 L buffer solution containing 1.5 *M* Tris/Tris-HCl, pH 8.8 (138.0 g Tris and 56.8 g Tris-HCl dissolved in 2 L H_2O will give a pH of 8.8), 0.4% SDS (w/v), and 0.12% (v/v) TEMED. The mixture is divided into two portions, filtered, and degassed for 30 min. The two portions are combined carefully, avoiding a new intake of air. The gel solutions are aliquoted into 70-mL portions for analytical gels and 140-mL portions for preparative gels, and stored at –20°C.
2. Ammonium persulfate solution: 40 g ammonium persulfate are dissolved in bidistilled water to give a final volume of 100 mL. The solution is filtered, aliquoted into 1-mL portions, and stored at –20°C.
3. Underlayering solution: 40 g glycerol are dissolved in distilled water to give a final volume of 100 mL and stored at 4°C.
4. Overlayering solution A: 1-Butanol saturated with Electrode buffer. B: 17.25 g Tris, 7.1 g Tris·HCl, and 0.5 g SDS are dissolved in distilled water to give a final volume of 500 mL. The solution is aliquoted into 20-mL portions and stored at –20°C.

Table 2
Solutions for Silver Staining

Solution	Composition	
Fixation solution (A)	50% (v/v)	Ethanol
	10% (v/v)	Acetic acid
Incubation solution (B)	0.5 M	Sodium acetate
	0.2% (w/v)	Sodium thiosulfate
	30% (v/v)	Ethanol
	0.5% (v/v)	Glutardialdehyde
Silver nitrate solution (C)	0.1% (w/v)	Silver nitrate
	0.01% (v/v)	Formaldehyde
Wash solution (D)	2.5% (w/v)	Sodium carbonate
Developer solution (E)	2.5% (w/v)	Sodium carbonate
	0.1% (v/v)	Formaldehyde
Stop solution (F)	0.05 M	EDTA

Table 3
Solutions for Colloidal Coomassie Staining

Solution	Composition	
Fixation solution (A)	50% (v/v)	Methanol
	2% (v/v)	Phosphoric acid
Incubation solution (B)	34% (v/v)	Methanol
	2% (v/v)	Phosphoric acid
	17% (w/v)	Ammonium sulfate

5. Agarose buffer: 0.2 g SDS (final concentration 0.1%) is dissolved in bidistilled water to give a final volume of 174 mL. 25 mL 125 mM Tris buffer (pH 6.8, titrated with phosphoric acid) are added to this solution. The resulting solution is filtered, aliquoted into 10-mL portions, and stored at –20°C.
6. Agarose solution: 1% low-melt agarose and a few crystals bromphenol blue (both electrophoresis grade, Bio-Rad Laboratories) are added to the agarose buffer. The suspension is dissolved by melting at 70°C. The final solution is used at 40°C.
7. Electrode buffer: The buffer is prepared freshly for each 2DE run. 0.025 M Tris, 0.192 M glycine, and 0.1% (w/v) SDS are dissolved in distilled water. A 10X buffer solution can be prepared and stored for at least one week. Dilute the 10X buffer immediately before the 2DE run.

2.2.4. Gel Staining

2.2.4.1. Solutions for Silver Staining of 2DE Gels

Six solutions are needed for the silver staining according to Heukeshoven *(8)*. The composition of the solutions is given in **Table 2**. All solutions are prepared freshly.

2.2.4.2. Solutions for Colloidal Coomassie Staining

Two solutions are needed for the colloidal Coomassie staining according to Neuhoff *(9)*. Both solutions are prepared freshly. The composition is given in **Table 3**.

3. Methods

3.1. Sample Preparation

Cell lysis and protein preparation are important steps with much influence on the quality and reproducibility of 2D gels. The sample preparation is performed by a modified protocol according to Klose and Kobalz *(10)*. The cells can either be prepared immediately after harvesting and PBS washing or from frozen samples (*see* **Note 1**).

1. The cell pellet is mixed rapidly with the protease inhibitor solution. The amount of the applied solution is calculated as follows: mg of the pellet (wet weight) × 1.25 = µL of the protease inhibitor solution (*see* **Notes 2** and **3**).
2. The resulting sample volume is estimated by adding the wet weight of the cell pellet (mg) and the volume of the protease inhibitor solution in µL.
3. The cells are lysed by sonication in the presence of small glass beads (1–2 mm diameter). The number of glass beads should be one per 30 µL sample solution. Sonication is performed 6 times for 10 s, each time leaving intervals of 50 s at 4°C.
4. Ribonucleic acids are digested with benzonase (0.5 units/µL sample volume) for 20 min at room temperature with gentle stirring (*see* **Note 4**).
5. Then 7 m*M* urea, 2 m*M* thiourea, 70 m*M* DTT, and 2% carrier ampholytes Servalyt pH 2.0–4.0 (Serva) are added and the proteins are solubilized at room temperature.
6. The glass beads and the magnetic stirring bars are removed with fine tweezers.
7. The protein concentration is determined by amino acid analysis or other suitable methods (e.g., Bradford *[11]*) (*see* **Note 5**). The cell lysate is frozen and stored at –70°C.

3.2. IEF

3.2.1. Preparation of IEF Gels

1. The nylon strings are inserted into the glass tubes, which are held vertically.
2. Separation gel solution, cap gel solution, and ammonium persulfate solution are thawed. The separation gel solution, as well as the cap gel solution, are degassed for 5 min.
3. Then 51 µL of ammonium persulfate solution are mixed into the separation gel solution, and the glass tubes are filled by dipping the end of the tubes into the gel solution and lifting the nylon string to suck the separation gel solution to a height of 35.5 cm (for 40-cm IEF gels) or 15.5 cm (for 20-cm IEF gels) into the tubes.
4. Thereafter, 19 µL of ammonium persulfate solution are mixed into the cap gel solution, and the cap gel solution is sucked into the glass tubes for an additional 0.8-cm height.
5. Immediately afterwards, the nylon string is lifted for a further 0.5 cm to obtain at the end of the tube a small space free of gel solution.
6. The filled gel tubes are left in vertical position at room temperature for 20 min to allow polymerization. Afterwards, the gels are stored in the dark in a humid atmosphere. To this end the gels are stored in a sealed plastic bag in the presence of a wet filter paper. The gels are used for isoelectric focusing after keeping them at room temperature for 3 d in the dark.

3.2.2. Sample Application and IEF Run

1. The glass tubes are inserted into the IEF apparatus (cap gel on the cathodic side) and fixed with the screws (*see* **Note 6**). The cathodic buffer is poured into the lower chamber.
2. The gel-free ends of the glass tubes are filled with cathodic buffer and placed into the cathodic buffer. Avoid any air bubbles.

Table 4
Electric Current Gradient for Isoelectric Focusing

20 cm IEF gels		40 cm IEF gels	
60 min	100 V	60 min	100 V
60 min	200 V	60 min	300 V
17.5 h	400 V	23 h	1000 V
60 min	650 V	30 min	1500 V
30 min	1000 V	20 min	2000 V
10 min	1500 V		
10 min	2000 V		
	Σ = 9233 Vh		Σ = 24,817 Vh

3. 330 g of a fine mixture of urea/thiourea (5.1:2, w/w), 25 µL DTT solution, and 25 µL of carrier ampholyte solution pH 2.0–11.0 (*see* **Table 1**) are added to the Sephadex suspension.
4. 1–2 mm of the final Sephadex suspension are pipetted onto the upper (anodic) gel surface. This is best done with fine Pasteur pipets.
5. The protein sample is pipetted onto the Sephadex and carefully overlaid with 1 mm sample protection solution. This is best done with the gel loader tips. The sample volume depends on the protein concentration. For gels used for the image analysis (analytical gels), 60–100 µg protein in 10 to 15 µL are applied to a gel. For preparative gels used for protein identification, 150–300 µg protein in 20 to 35 µL are applied.
6. The glass tubes are filled with anodic buffer, and the rest of the buffer is supplied to the upper chamber covering the glass tubes.
7. Isoelectric focusing is performed using the current gradient, as indicated in **Table 4**.
8. After the focusing is finished, the excess solutions from the lower and upper side of the glass tubes are removed by a Pasteur pipet.
9. The nylon string is used to gently push the IFF gels off the tubes onto a gel holder covered with equilibration solution. The gels are incubated for 10 min in the solution. Then the solution is removed with a pipet and filter paper. Touching the gels with the filter paper is to be avoided.
10. For 40-cm gels, mark on the glass tube the half-length of the IEF gel before extruding the gel. The gels are cut into two halves prior to SDS-PAGE.
11. The IEF gels are stored at –70°C.

3.3. SDS-PAGE

3.3.1. Preparation of Gels for SDS-PAGE

1. All glass plates are cleaned prior to use to avoid point streaking during the silver stain. The gel cassettes are prepared by placing the spacer covered with a thin layer of silicone grease between two identical glass plates to seal the cassette. The plates are fixed according to the manufacturer's instructions with two clamps.
2. The cassettes are placed into the polymerization stand.
3. Ammonium persulfate solution (144 µL) is added to 70 mL of the thawed gel solution and gently mixed by shaking.

Table 5
Silver Staining Procedure

Gel treatment	Volume of solution/gel	Duration of treatment	Remarks
Fixation	0.5 L Solution A	2 h or overnight	
Incubation	0.5 L Solution B	2 h	
Wash	2 L Distilled water	2 × 20 min	
Silver reaction	0.5 L Solution C	30 min	
Wash	0.5 L Distilled water	few s	Remove the water immediately.
Wash	0.5 L Solution D	1 min	Distribute arising silver clouds quickly.
Development	0.5 L Solution E	3–10 min	Watch the staining intensity
Stop reaction	0.5 L Solution F	20 min	

4. The gel solution is poured into the cassette, air bubbles are removed, and the cassette is filled up just 0.5 cm below the upper side of the glass plate. The gel cassettes are carefully filled up with the overlayering solution A.
5. The gels are allowed to polymerize for at least 30 min at room temperature.
6. The overlayering solution A is replaced by overlayering solution B and the gels are stored at 4°C overnight.

3.3.2. Protein Separation

1. For the protein separation in the second dimension, the tube gels are thawed slowly and washed once with SDS running buffer. The buffer is removed with a pipet.
2. The gels should be left wet for a better transfer to the SDS gels.
3. The washed tube gels are transferred onto the SDS gel surface without being stretched or compressed. The inclusion of air or solution should be avoided.
4. The IEF gels are overlaid with 40°C agarose solution, and the agarose is gelatinized at room temperature.
5. The gel cassettes are inserted into the electrophoresis apparatus, and the electrophoresis chamber is filled up with electrode buffer.
6. The temperature during SDS-PAGE run should be kept constant at 15°C.
7. The analytical gels are run for 15 min at 65 mA and than at 100 mA until the bromphenol blue reaches the end of the gel. For preparative gels, the gels are run for 15 min at 75 mA and then at 200 mA.
8. After the run, the gels are transferred into the appropriate fixation buffer.

3.4. Gel Staining

3.4.1. Silver Staining

1. The 2DE gels are fixed in the fixation solution for at least 2 h, better overnight. The gels are shaken gently to avoid the gels sticking together during the fixation process.
2. Afterwards, each gel is transferred into a trough. The staining protocol is listed in **Table 5**. During the staining process, the gels stay in the same trough while the solutions are being sucked away.

A silver-stained 2DE gel of human regulatory T-cells is displayed in **Fig. 1**.
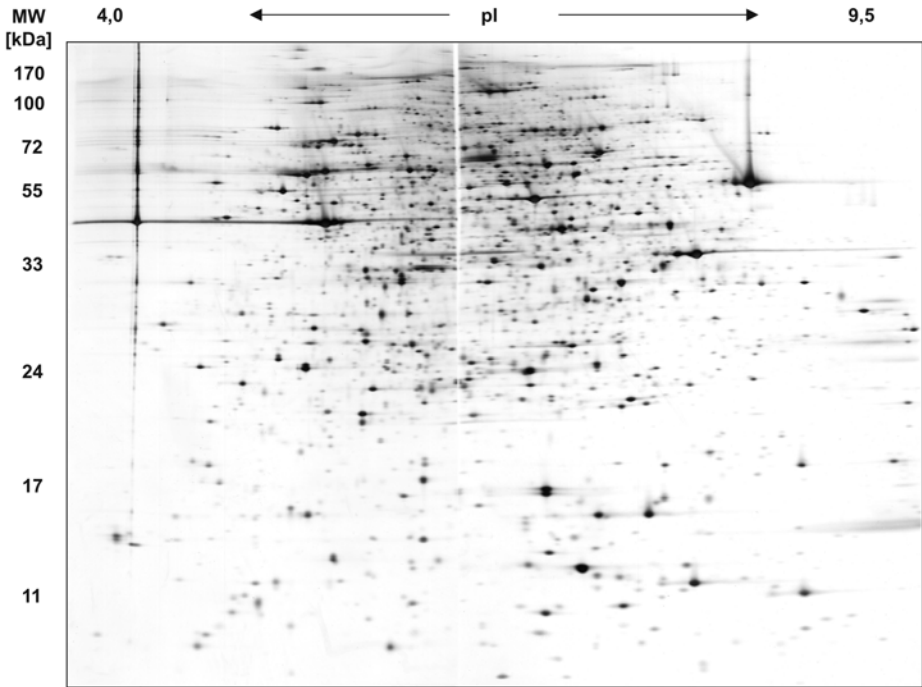
Fig. 1. Large-gel 2DE pattern of human CD4+ CD25+ T-regulatory cells. The sample preparation and production of the 2DE gel was performed as described in the text. The sample load was 60 μg protein /10 μL sample. The gel was stained with silver according to Heukeshoven. Approximately 3500 protein spots were detected using the ProteomWeaver™ image analysis software.

3.4.2. Colloidal Coomassie G-250 Staining

The colloidal Coomassie G-250 staining according to Neuhoff *(9)* is less sensitive than silver staining but compatible with mass spectrometry based protein analysis methods. Depending on the protein properties, the detection limit is approx 10 ng protein per spot.

1. The 2DE gels are fixed in the fixation solution for at least 2 h, better overnight. The gels are shaken gently to avoid the gels sticking together during the fixation process.
2. Afterwards, the gels are transferred into a large trough. The staining protocol is listed in **Table 6**.
3. For the destaining process, the gels are placed into a new trough and the water is changed several times.
4. For highest sensitivity in the mass spectrometrical analysis, the gels should be processed immediately after the destaining, but they can be stored for several days at 4°C in a plastic foil.

Table 6
Staining Process With Colloidal Coomassie G-250

Gel treatment	Volume of solution/gel	Duration of treatment	Remarks
Fixation	0.5 L Solution A	overnight	
Wash	0.5 L Distilled water	3 × 30 min	
Incubation	0.5 L Solution B	1 h	
Staining	0.5 L Solution C (add 660 mg Coomassie G-250 to solution B)	up to 6 d	
Destaining	Distilled water	several h	Change the water several times during the destaining process.

3.5. Image Analysis

Image analysis is perhaps the most crucial element of proteome analysis. There are many systems available for image capture—e.g., CCD cameras and white light or laser scanners. For visible stains like silver, or Coomassie stain, conventional scanners can be used successfully if they have a resolution of 16-bit grayscale or better. A typical work flow of 2DE gel image analysis comprises the following steps: scanning of the gel image (image capture), image capture (data acquisition), spot detection, gel matching, data analysis and interpretation, and database creation or export to a database.

1. The gels are dried between two cellophane films prior to the image-capture process with a gel dryer. To digitize large 2D gels, a 440 × 355 mm flatbed scanner is utilized.
2. In case of gels used for the image analysis and determination of spot intensities, the gel is placed in the scanner and scanned as a transmissive 16-bit grayscale image with 200-dpi image resolution and a γ value of 1.0. Coomassie-stained gels are scanned without drying as transmissive 48-bit-depth color image with 200-dpi resolution (*see* **Note 7**).
3. To ensure high reproducibility, the scanning parameters should always be kept constant.
4. Gels are analyzed semi-automatically with the ProteomWeaver™ software. Gels of the same sample (replicates) are sorted into the same group. Different groups are compared according to the analytical request.
5. Spot detection and pre-matching normalization are performed within the same experiment automatically. To eliminate spots with low signal-to-noise ratios, pre-matching filters are set and saturated spots are eliminated manually. Then the gel images are matched with each other. Obvious mismatches and incorrect spot detection are corrected manually.
6. To achieve more precise results, a pair-match basis normalization is carried out after spot matching.
7. Spots with a standard deviation >50% within the same group are eliminated by the spot filter tool for reliable analysis and interpretation of differential spots.
8. For inter-group comparison, several statistical filters are used to localize spots that increased or decreased or are present uniquely in one group. Spot ratios >2 for increased

and <0.5 for decreased spots are considered as differential if confirmed by the software-implemented statistical tests.

9. The calibration is performed on the basis of a set of protein spots with known isoelectric points (pI) and molecular weights (MW).

In **Fig. 2**, enlargements of gel regions of the different T-cell populations are shown. Using the ProteomWeaver™ software, the marked spots were analyzed as differentially expressed, comparing the T-cell populations.

3.6. Spot Excision

The spots of interest as identified by image analysis are then located on a preparative gel, excised, and digested *(12,13)*. The spot excision, digestion, and MALDI analysis are fully automated in order to minimize keratin contamination (*see* **Note 8**), to maximize reproducibility, and to facilitate consistent sample tracking and data handling. The identification of proteins from a 2DE gel is a multistep process that is outlined in **Fig. 3** and described in detail below.

The spot-picking robot (PROTEINEER sp™) is employed to excise the protein spots from the preparative 2DE gels and to deposit them into specially pierced microtiter plates for further analysis (*see* **Notes 9,10**). The robot has a high-resolution scanner integrated on its platform for acquisition of high-quality images. A spot-detection algorithm integrated into the software localizes the exact position of the spots of interest.

1. The preparative gel is laid into a so-called sandwich assembly (*see* **Fig. 4**), which consists of a glass plate and a metal frame. This assembly simplifies the subsequent handling especially of unbacked gels, and prevents the gel from moving during the picking process.
2. The gel in this sandwich assembly is then fitted onto the scanner surface, and an image of the gel is acquired on the spot-picker platform and stored in a relational database.
3. Four pierced PCR plates in a plate holder (*see* **Note 11**) are put onto the robot deck, and accommodate the picked gel plugs. All samples are given a unique identifier that is written to a transponder attached to the plate holder.
4. Then the spots of interest are selected either by using a simple point-and-click interface or by employing the integrated spot-detection capability.
5. Before initiating the picking process, all processing steps for the samples, including the digestion and the MALDI acquisition method, are defined. For the spot picker, an optimized picking protocol is used that is provided by the manufacturer.
6. The picking is then initiated. Using this setup, usually >99% of the gel plugs from the 2DE gels are successfully ejected into the microtiter plate. Using such an automated setup, keratin contamination can be minimized in this step and the exact *x-y* coordinates of every picked spot can be stored in a database.

3.7. Digestion

After picking has ended, the microtiter plates with the gel plugs are transferred to the digestion robot (PROTEINEER dp™). This robot is capable of washing and digesting 384 gel cores at a time. The microtiter plates from the spot picker are put onto the appropriate positions of the digestion robot (*see* **Note 12**).

1. A reagent kit containing all reagents needed for the process (apart from organic solvents) in sealed vessels is mounted in the reagent rack. This reagent kit is supplied by the vendor
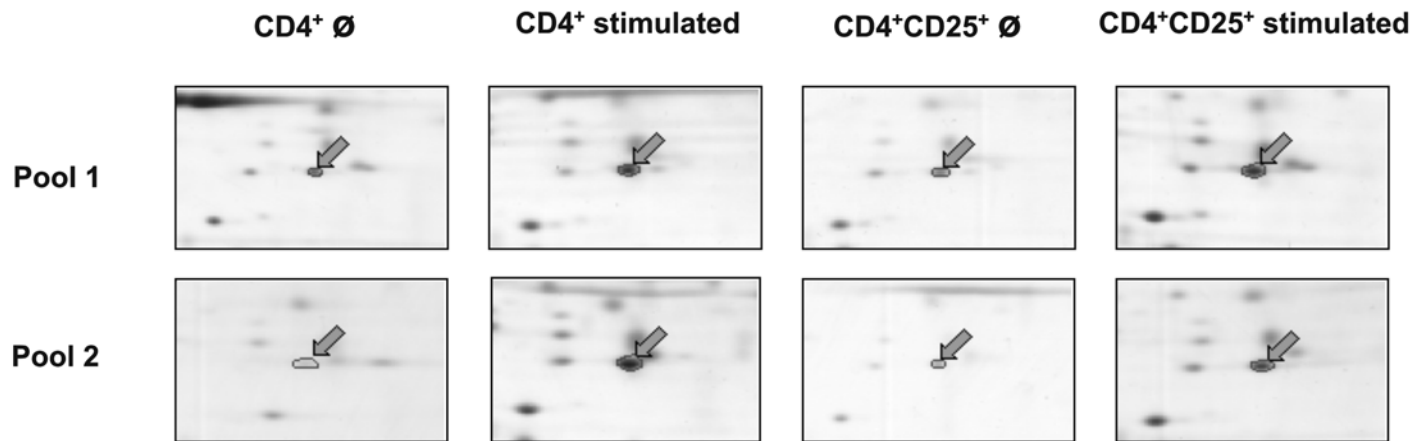
Fig. 2. Selected gel regions showing different proteins expressed in murine resting (⊘) and anti-CD3/CD28 stimulated conventional CD4^{+} and CD4^{+} CD25^{+} T-regulatory cells. The differential proteins were found by image analysis with ProteomWeaver™ image analysis software. The expression profiles of the four cell types of two independent mouse pools were analyzed.
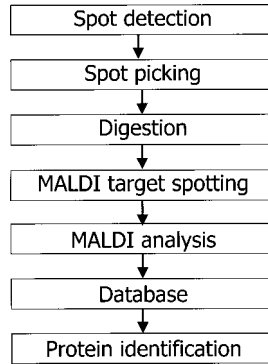
Fig. 3. Schematic representation of the protein identification process from 2DE gels.
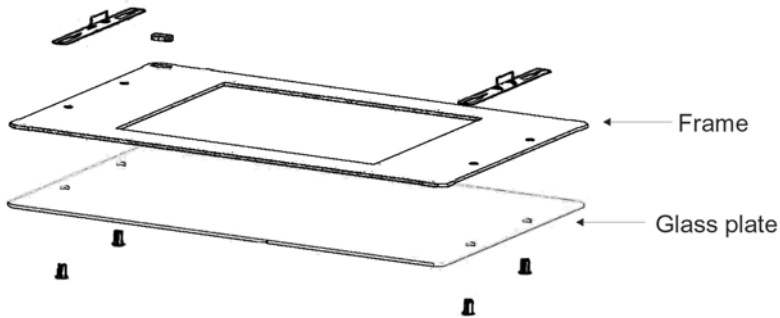
Fig. 4. The sandwich assembly used for the spot picking robot. The 2DE gel is put on the glass plate and held in place by the frame on top. Two handles allow the easy removal of the assembly from the scanner surface.

    of the robot, together with optimized protocols. The organic solvents are poured into troughs (*see* **Note 13**).

2. A clean MALDI target is fitted into the appropriate position of the robot deck.
3. As the protocol used for digestion was already defined when picking the spots, the user only needs to press the "Full-Automode" button.
4. The robot then automatically identifies the samples on the deck and in a sample-tracking database and processes them accordingly. Again, an optimized digestion protocol is supplied by the manufacturer.
   a. The gel plugs are washed briefly to remove the Coomassie stain and dried using acetonitrile.
   b. Trypsin is applied to the gel plugs and the samples are incubated for 4–8 h at 30°C.
   c. The resulting peptides are extracted and spotted onto an AnchorChip® MALDI target that was precoated with α-cyano-4-hydroxy-cinnamic acid and washed.

3.8. MALDI Analysis

1. When the digestion process is finished, the MALDI target is taken from the digestion robot and inserted into the MALDI mass spectrometer. In a first analysis, the masses of the intact peptides generated in the digestion process are measured. As each protein gives rise to a unique set of peptides, these sets are as unique as a fingerprint; thus the spectra are termed peptide mass fingerprint (PMF) spectra.

2. The target spots are analyzed by summing up 200 shots per spot while the laser attenuation is adjusted automatically to an optimal level by utilizing a fuzzy-logic feedback algorithm.

3. The peaks in the spectrum are labeled using the SNAP algorithm provided by the vendor of the mass spectrometer (Bruker Daltonik, Bremen, Germany) in order to identify the monoisotopic peak of each peptide signal. The spectra are then exported to the proteinscape™ database for protein identification (**Fig. 5**).

4. In a second round of analysis, the individual peptides from the digest are fragmented in order to obtain PFF spectra that allow identification of a protein from only one peptide. The acquisition of these PFF spectra is more time-consuming than the acquisition of PMF spectra. Therefore, the acquisition of PFF spectra is triggered by an intelligent algorithm in the database that can choose peptides suitable for fragmentation based on different criteria, such as intensity or protein identification.

3.9. Database Analysis

1. The spectra that are imported into the database are automatically linked to the appropriate spots in the 2DE gel image that were imported from the spot picker. The fully automated flow of information ensures the integrity of the data set, as it eliminates user intervention.

2. In the database, the spectra are recalibrated using known contaminant peaks (from keratin, trypsin, and so on) in order to obtain precise peptide masses. The masses of the contaminant peaks are then removed from the spectra so that only peaks with unknown masses are used for database searching (*see* **Note 14**).

3. Protein identification is achieved by searching the mass spectra against a protein database using several external search algorithms (ProFound™, Mascot™). The results are collated into one table with a unified scoring system (*see* **Note 15**) that allows a comparison of the different algorithms. The significance of the search result is then evaluated based on the unified score.

4. Notes

1. Normally, cell-culture media contain serum (e.g., fetal calf serum). To remove the serum proteins from the sample, the cells are washed well with PBS.

2. The amount of all reagents for the sample preparation is calculated on the basis of the wet weight of the cells. After harvesting and washing the cells, they are centrifuged at max. 300*g* at 4°C and the PBS is removed. Make sure that no excess buffer dilutes the sample.

3. Proteases are included in all cells. To inhibit their activity, suitable protease inhibitors against all types of proteases should be added to the sample. They are best added before or during the thawing process or immediately prior to cell lysis.

4. The sample preparation can be performed without nucleic acid digestion, but 2DE gels will exhibit much better performance (well-defined spots, less streaking) if the nucleic acids are digested either with benzonase or other RNases and DNases.
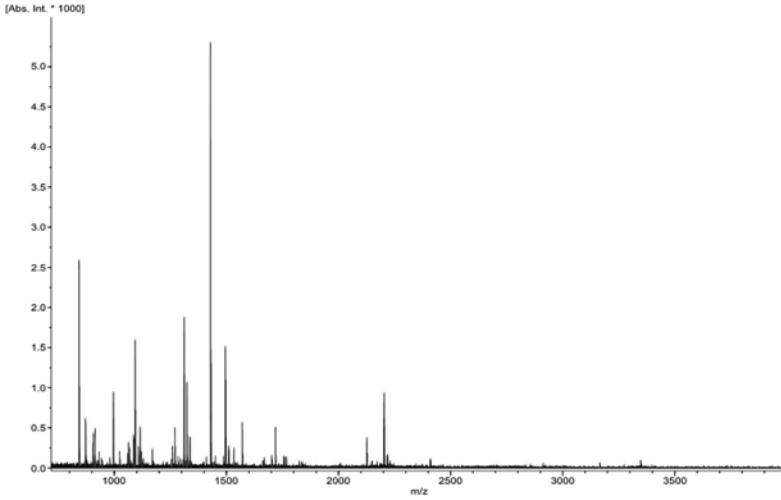
```
gi|2119204 A25074 vimentin - human
           10         20         30         40         50
MSTRSVSSSS YRRMFGGPGT ASRPSSSRSY VTTSTRTYSL GSALRPSTSR
           60         70         80         90        100
SLYASSPGGV YATRSSAVRL RSSVPGVRLL QDSVDFSLAD AINTEFKNTR
          110        120        130        140        150
TNEKVELQEL NDRFANYIDK VRFLEQQNKI LLAELEQLKG QGKSRLGDLY
          160        170        180        190        200
EEEMRELRRQ VDQLTNDKAR VEVERDNLAE DIMRLREKLQ EEMLQREEAE
          210        220        230        240        250
NTLQSFRQDV DNASLARLDL ERKVESLQEE IAFLKKLHEE EIQELQAQIQ
          260        270        280        290        300
EQHVQIDVDV SKPDLTAALR DVRQQYESVA AKNLQEAEEW YKSKFADLSE
          310        320        330        340        350
AANRNNDALR QAKQESTEYR RQVQSLTCEV DALKGTNESL ERQMREMEEN
          360        370        380        390        400
FAVEAANYQD TIGRLQDEIQ NMKEEMARHL REYQDLLNVK MALDIEIATY
          410        420        430        440        450
RKLLEGEESR ISLPLPNFSS LNLRETNLDS LPLVDTHSKR TLLIKTVETR
          460
DGQVINETSQ HHDDLE
```

 5. For the determination of the protein concentration, the methods of Bradford *(11)*, Lowry *(14)*, or Popov *(15)* can be used. The most accurate method for the determination of protein concentration is amino acid analysis.

 6. Within one proteome study, always run the same number of gels in parallel to yield maximum reproducibility during IEF. Different numbers of gels result in different values of resistance and current, and therefore in different migration distances of the proteins during the isoelectric focusing process.

 7. If 40-cm IEF gels are used, the 2DE gels consist of two halves. After the gels are scanned, they are merged together digitally with suitable software (Corel Photo-Paint or Adobe Photoshop). The merged gel images allow easier spot matching than the analysis of individual halves.

 8. When analyzing 2D gel spots, especially of low-abundance proteins, it is of great importance to keep the contamination of the sample at an absolute minimum. When handling the preparative 2D gel and for all subsequent sample handling steps, gloves should be worn, as keratin (from the skin) is one of the most persistent contaminants. Also, the reagents should be stored in a way that minimizes exposure to the environment, and regularly checked for keratin contamination.

 9. Disposables such as tips or plates should not be washed and re-used. In our experience, cross-contamination cannot be ruled out. This is especially true for 2D gel samples, where the concentration of protein in a spot can vary by several orders of magnitude. Thus, when re-using disposables, peptides from an abundant protein can contaminate the subsequent analysis of a low-concentration sample.

10. The quality of plastic used for disposables can vary widely from manufacturer to manufacturer. For example, when considering which brand of pipet tip to use, it is advisable to spot a few microliters of organic solvent onto a MALDI target plate together with matrix and to check the MALDI spectrum for polymer peaks. We recommend using tips obtained from Eppendorf, Hamburg, Germany.

11. The microtiter plates are enclosed in a special storage container, which carries a transponder in order to identify the samples and which utilizes a special lid that minimizes the exposure of the samples to contamination in the lab. The gel pieces are processed in specially designed microtiter plates that function as flow-through reaction vessels, where the liquid is applied from the top and is removed through small orifices in the bottom of the wells by applying nitrogen gas pressure.

12. The order of the four-sample carrier on the robot deck of the digester does not have to be the same as on the spot picker. As the digest robot reads the unique identifier of each carrier prior to starting the protocol, a mismatch of the sample is prevented.

13. When storing organic solvents, special care must be taken not to contaminate these. It is therefore strongly advisable to use the original bottle for long-term storage and to portion the liquids by pouring only. For portioning we recommend the use of teflon-coated plastic bottles (Nunc, Wiesbanden, Germany).

14. The recalibration and peak filtering is an important feature of the proteinscape™ database used. For a typical data set, the identification rate for the MALDI PMF analysis can be raised by 50–100%.

Fig. 5. *(opposite page)* Schematic representation of the protein identification from MALDI PMF data. The spectrum (top) is imported into the proteinscape™ database and processed by different algorithms (such as ProFound™ or Mascot™). The sequence of the identified protein is then reported for further analysis.

15. Algorithms that can identify proteins from mass spectra are available from different vendors. All these algorithms give slightly different results, especially in their ranking. As each algorithm uses a different approach to calculate the quality of the protein identification, the results cannot be compared directly. The database used in our setup can therefore calculate a separate score that is independent of the algorithm used in order to restore the comparability.

Acknowledgments

References

1. Klose, J. (1975). Protein mapping by combined isoelectric focusing and electrophoresis of mouse tissues. A novel approach to testing for induced point mutations in mammals. *Humangenetik.* **26,** 231–243.
2. Drews, J. (2000) Drug discovery: a historical perspective. *Science* **287,** 1960–1964.
3. Klose, J. (1999) Large-gel 2-D electrophoresis. *Methods Mol. Biol.* **112,** 147–172.
4. Lutter, P. (2003) Untersuchung des Einflusses vasoaktiver Substanzen auf das Proteom humaner Endothelzellen, Dissertation. Ruhr-University Bochum, Bochum Germany.
5. Jonuleit, H., Schmitt, E., Kakirman, H., Stassen, M., Knop, J., and Enk, A. H. (2002) Infectious tolerance: human CD25+ regulatory T cells convey suppressor activity to conventional CD4+ T helper cells. *J. Exp. Med.* **196,** 255–260.
6. Jonuleit, H. and Schmitt, E. (2004) Regulatory T Cells in Antitumor Therapy: Isolation and Function of CD4$^+$CD25$^+$ Regulatory T Cells. In: *Methods in Molecular Medicine, vol. 109: Adoptive Immunotherapy: Methods and Protocols.* (Ludewig, B. and Hoffman, M. W., eds.) Humana, Totowa, NJ, pp. 285–296.
7. Lutter, P., Jonuleit, H., Schmitt, E., et al. (2003) Proteome analysis of regulatory t cells—promising targets for innovative immunotherapeutical approaches. *Mol. Cell. Proteomics* **9,** 990.
8. Heukeshoven, J. and Dernick, R. (1988). Improved silver staining procedure for fast staining in PhastSystem Development Unit. I. Staining of sodium dodecyl sulfate gels. *Electrophoresis* **9,** 28–32.
9. Neuhoff, V., Arold, N., Taube, D., and Ehrhardt, W. (1988). Improved staining of proteins in polyacrylamide gels including isoelectric focusing gels with clear background at nanogram sensitivity using Coomassie Brilliant Blue G-250 and R-250. *Electrophoresis* **9,** 255–262.
10. Klose, J. and Kobalz, U. (1995) Two-dimensional electrophoresis of proteins: an updated protocol and implications for a functional analysis of the genome. *Electrophoresis* **16,** 1034–1059.
11. Bradford, M. M. (1976). A rapid and sensitive method for the quantitation of microgram quantities of protein utilizing the principle of protein-dye binding. *Anal. Biochem.* **72,** 248–254.
12. Lutter, P., Meyer, H. E., Langer, M., et al. (2001) Investigation of charge variants of rViscumin by two-dimensional gel electrophoresis and mass spectrometry. *Electrophoresis* **22,** 2888–2897.

13 Shevchenko, A., Wilm, M., Vorm, O., and Mann, M. (1996) Mass spectrometric sequencing of proteins from silver-stained polyacrylamide gels. *Anal. Chem.* **68,** 850–858.

14 Lowry, O. H., Rosebrough, N. J., Farr A. L., and Randall, R. J. (1951) Protein measurement with the folin phenol reagent. *J. Biol. Chem.* **193,** 265–275.

15. Popov, N., Schmitt, M., Schulzeck, S., and Matthies, H. (1975), Eine störungsfreie Mikromethode zur Bestimmung des Proteingehaltes in Gewebehomogenaten. *Acta. Biol. Me. Germ.* **34,** 1441–1461.

13

Isolation and Expansion of Tumor-Reactive Cytotoxic T-Cell Clones for Adoptive Immunotherapy

**Helga Bernhard, Burkhard Schmidt,
Dirk H. Busch, and Christian Peschel**

Summary

Attempts to treat patients with tumor-reactive cytotoxic T-lymphocytes (CTL) have been limited. This is due to the difficulty of isolating and expanding functionally active T-cells, which are present at extremely low frequencies in the peripheral blood. Recently developed multimers of the HLA–peptide complex mimic the natural ligand of the T-cell receptor and, therefore, fluorochrome-labeled multimers allow visualization and isolation of rare T-cells with defined specificity. Multimer-guided T-cell sorting permits the in vitro culture of antigen-specific T-cells as lines or clones. Cytolytic T-cells capable of recognizing HLA–peptide complexes endogenously processed by tumor cells are selected for further expansion, since lysis of tumor cells in vitro is a prerequisite for effective tumor elimination in vivo. The expansion of tumor-reactive CD8+ T-cells yields cell numbers sufficient for adoptive transfer. Tumor-reactive T-cells retain the functional activity in terms of cytolysis after expansion, encouraging their use in the immunotherapy of cancer patients.

Key Words: Cytotoxic T-lymphocytes; human; antigens/peptides/epitopes; MHC; HLA; tumor immunity.

1. Introduction

Patients with advanced cancer have an impaired cellular immune system *(1)*. The rationale of adoptive T-cell therapy is based on the attempt to circumvent this preexisting tolerance by taking out the anergic, potentially tumor-reactive T-cells from the tolerizing environment and subsequently activating these T-cells ex vivo. Following the expansion of tumor-reactive T-cells in vitro, large numbers of T-cells can be adoptively transferred to the patient (for review *see* **ref. 2**). With this approach, a high frequency level of ex vivo activated tumor-reactive T-cells can be achieved in vivo, which might not be accomplished by vaccine strategies.

One limitation of this approach is that the number of antigen-specific T-cells in the peripheral blood is exceedingly low. Recently, a novel method of identifying antigen-

specific T-lymphocytes has been described *(3)*. Tetrameric MHC–peptide complexes, called *tetramers* or *multimers*, have been shown to bind stably and specifically to appropriate MHC-peptide-specific T-cells. This technique permits both detection and isolation of antigen-specific T-cells present at low frequencies *(4)*. If the natural T-cell frequency in the blood is too low to be detectable by multimers, the number of antigen-specific peripheral blood T-lymphocytes may be enhanced by repetitive stimulation with peptide-loaded autologous dendritic cells (DC) in vitro. Peptide-specific T-cells are visualized with fluorochrome-labeled HLA-peptide multimers and sorted with a fluorescence-activated cell sorter (FACS). Following multimer-guided sorting, T-cells are cultured as bulk or cloned by limiting dilution, both in the presence of irradiated allogeneic peripheral blood mononuclear cells (PBMC), B-lymphoblastoid cell lines (LCL), anti-CD3 monoclonal antibody, and interleukin (IL)-2 *(5)*. Following expansion, the specificity and the function of the sorted T-cells are confirmed by the recognition of HLA-matched, antigen-expressing tumor cells. The expansion of the tumor-reactive T-cells yields cell numbers sufficient for adoptive immunotherapy in tumor patients. The generation of Melan-A-specific melanoma-reactive CTL clones will be presented in order to illustrate the methods for the stimulation, isolation, cloning, and expansion of peptide-specific, tumor-reactive CTL clones (*see* **Fig. 1**).

2. Materials

2.1. Chemicals and Buffers

1. Phosphate-buffered saline (PBS; Gibco-BRL, Karlsruhe, Germany).
2. Ficoll separation solution, density 1.077 g/mL (Biochrom, Berlin, Germany).
3. Erythrocyte lysis buffer: 8.3 g NH_4Cl, 1 g $KHCO_3$, 0.0372 g EDTA in 1 L H_2O.
4. FACS buffer: PBS 0.1% bovine serum albumin (BSA; Sigma, Milwaukee, WI), pH 7.3.
5. Propidium iodide (PI; Sigma, Milwaukee, WI).
6. β_2-microglobulin (Sigma, Taufkirchen, Germany).
7. Chromium^{51} (Cr^{51}; ICN Biomedicals, Eschwege, Germany).
8. Nonidet P40 (NP40) buffer: PBS 1% NP40 (Sigma, St. Louis, MO).

2.2. Media and Supplements

1. RPMI 1640 (Gibco-BRL).
2. X-VIVO 15 (BioWhittaker, Walkersville, MD).
3. L-glutamine (Gibco-BRL).
4. Penicillin/streptomycin (Gibco-BRL).
5. Fetal calf serum (FCS; sera plus; Pan Biotech GmbH, Aldenbach, Germany).
6. Human serum albumin (HSA) solution: 0.9% NaCl solution with 20% HSA (20% Immuno; Baxter, Unterschleißheim, Germany).
7. Serum from healthy donors with blood group AB (AB serum; Valley Biomedical, Winchester, VA).
8. Monocyte medium: RPMI 1640 supplemented with 1% heat-inactivated AB serum, 2 m*M* L-glutamine, 100 U/mL penicillin, 100 µg/mL streptomycin.
9. DC medium: X-VIVO 15 supplemented with 1% heat-inactivated AB serum, 2 m*M* L-glutamine, 100 U/mL penicillin, 100 µg/mL streptomycin.
10. T-cell medium: RPMI 1640 supplemented with 10% heat-inactivated AB serum, 2m*M* L-glutamine, 100 U/mL penicillin, 100 µg/mL streptomycin.
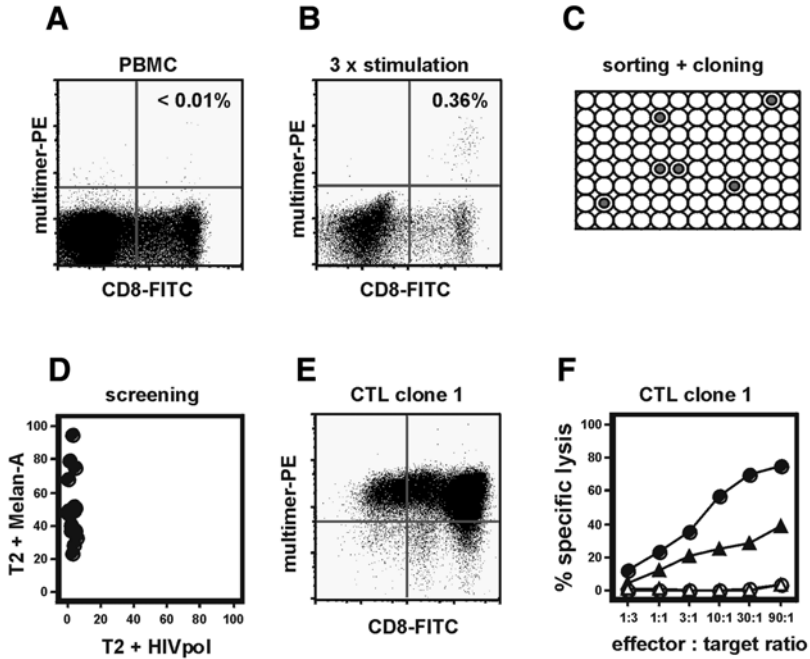
Fig. 1. Isolation, cloning, and expansion of melanoma-reactive cytotoxic T-lymphocytes recognizing the differentiation antigen Melan-A.

For the detection of HLA-A2-restricted Melan-A$_{27–35}$-specific T-cells in the peripheral blood, the HLA-peptide multimer consisting of the Melan-A$_{26–35}$A27L analog (ELAGIGILTV) *(9)* was used, which has a higher binding affinity to HLA-A2 and a higher immunogenicity than the natural nonapeptide Melan-A$_{27–35}$ (AAGIGILTV) *(10)*. Dot plots are shown for CD8 versus HLA-A2-peptide multimer staining **(A,B,E)**. Dot plots are gated on PI-negative cells. The percentages of CD8$^+$ multimer$^+$ T-cells gated on PI-negative cells are stated in the upper right quadrant **(A,B)**. A low frequency of circulating Melan-A-specific T-cells was detected in peripheral blood **(A)**. The frequency of multimer$^+$ T-cells increased after three stimulations with Melan-A$_{27–35}$-pulsed autologous dendritic cells **(B)**. Following sorting with fluorochrome-labeled HLA-peptide multimers, CD8$^+$ multimer$^+$ T-cells were cloned **(C)**. Proliferating T-cell clones (e.g., 6/96, C) were screened for Melan-A-specific lytic activity using ^{51}Cr-labeled T2 cells as target cells loaded with the relevant peptide Melan-A$_{27–35}$ respective an irrelevant peptide derived from the HIV reverse transcriptase (HIV$_{476–484}$) **(D)**. Following expansion of Melan-A-specific cytotoxic T-lymphocyte (CTL) clones, antigen-specificity was confirmed by HLA-A2-Melan-A multimer staining **(E)**. Staining of cultured CTL clones did not reach 100% of CD8$^+$ multimer$^+$ cells due to activated T-cells having downregulated the CD8 molecule and due to remaining feeder cells. Expanded CTL clones retained lytic function, as documented in a standard ^{51}Cr release assay **(F)**. The CTL clones lysed T2 cells loaded with the relevant peptide Melan-A$_{27–35}$ (●), but not T2 cells pulsed with the irrelevant peptide HIV$_{476–484}$ (○). Of importance, the CTL clone 1 was able to recognize endogenously processed peptides, as documented by lysis of an HLA-A2$^+$, Melan-A$^+$ melanoma cell line (▲). CTL clone 1 did not lyse an HLA-A2$^-$, Melan-A$^+$ melanoma cell line (△), confirming HLA-A2 as the restriction element.

11. Lymphoblastoid B-cell line (LCL) medium: RPMI 1640 supplemented with 10% heat-inactivated FCS, 2 m*M* L-glutamine, 100 U/mL penicillin, 100 μg/mL streptomycin.
12. Freezing medium: 20% HSA supplemented with 10% dimethylsulfoxide (DMSO; Serva GmbH).

2.3. Cytokines and Prostaglandin

1. Recombinant human granulocyte macrophage-colony stimulating factor (GM-CSF; Cell-Genix, Freiburg, Germany).
2. Recombinant human IL-1β (R&D Systems, Wiesbaden, Germany).
3. Recombinant human IL-2 (Chiron, Emeryville, CA).
4. Recombinant human IL-4 (R&D Systems).
5. Recombinant human IL-6 (R&D Systems).
6. Recombinant human IL-7 (R&D Systems).
7. Recombinant human IL-12 (R&D Systems).
8. Recombinant human IL-15 (Sigma, Milwaukee, WI).
9. Prostaglandin E_2 (PGE$_2$; Pharmacia, Erlangen, Germany).
10. Recombinant human tumor necrosis factor (TNF)-α (Roche AG, Grenzach-Wyhlen, Germany).

2.4. Monoclonal Antibodies

1. Anti-CD3 monoclonal antibody (OKT3; Janssen-CILAG, Neuss, Germany).
2. FITC-labeled mouse antihuman CD8 monoclonal antibody (clone 3B5; Caltag Laboratories, Burlingame, CA).

3. Methods

3.1. Generation of DC From Monocytes

DC are generated from peripheral blood monocytes according to the method published by Jonuleit et al. *(6)*:

1. Draw peripheral blood in a heparinized syringe.
2. Split blood in aliquots (15 mL of blood per 50-mL conical centrifuge tube).
3. Add 15 mL PBS to 15 mL blood and mix.
4. Carefully layer 15 mL ficoll under the blood/PBS mixture.
5. Centrifuge cells at 900*g* for 15 min at room temperature (RT) in a swing-out rotor centrifuge without brakes.
6. After centrifugation the PBMC form a buffy coat at the ficoll/plasma interface. Transfer PBMC located in the interphase carefully to a new 50-mL tube.
7. Fill the PBMC-containing tube with PBS to 40 mL, mix, and centrifuge at 600*g* for 10 min at RT.
8. Discard the supernatant and then resuspend all of the cell pellets with an appropriate amount of PBS in order to pool the PBMC in a 50-mL conical tube.
9. Centrifuge at 450*g* for 8 min at RT and discard the supernatant.
10. Resuspend the cell pellet in 10 mL erythrocyte lysis buffer and incubate for 10 min at RT.
11. Fill cell-containing tube with 30 mL of PBS. Then mix and count the PBMC.
12. Centrifuge at 350*g* for 7 min, discard the supernatant, and resuspend the PBMC in monocyte medium.
13. Seed PBMC in six-well flat-bottom plates at 1×10^7 cells/well in 3 mL monocyte medium and incubate for 2 h in a 37°C, 5% CO$_2$, humidified atmosphere.

14. Remove nonadherent cells by rinsing and adding fresh monocyte medium (3 mL/well).
15. Incubate for 10–20 h at a 37°C, 5% CO_2, humidified atmosphere.
16. Remove monocyte medium and add DC medium supplemented with 800 U/mL GM-CSF and 1000 U/mL IL- 4 (3 mL/well) (d 1).
17. Culture monocytes in a 37°C, 5% CO_2, humidified atmosphere.
18. Add 1 mL/well DC medium supplemented with 1600 U/mL GM-CSF and 1000 U/mL IL-4 on d 2, 4, and 6.
19. On d 7, harvest and pool nonadherent immature DC (*see* **Note 1**) in a 50-mL conical tube. Count the DC and centrifuge at 350*g* for 5 min at RT.
20. Resuspend the cell pellet and seed the DC in a new six-well plate at a concentration of 5×10^5 cells/well in 2 mL DC medium containing GM-CSF (800 U/mL) and IL-4 (500 U/mL).
21. Incubate in a 37°C, 5% CO_2, humidified atmosphere.
22. After 4 h, add 1 mL/well DC medium with the following supplements at final concentrations: IL-1β (10 ng/mL), TNF-α (10 ng/mL), IL-6 (1000 U/mL) and PGE_2 (1 μg/mL).
23. Culture for 2–3 d in a 37°C, 5% CO_2, humidified atmosphere.
24. On d 9–10, harvest the mature DC. The phenotype of mature DC is routinely checked by flow cytometry (CD14−, CD80+, CD83+, CD86+, and HLA-DR+).

3.2. Stimulation of T-Cells With Peptide-Pulsed DC

Autologous dendritic cells are incubated with peptides and used as antigen-presenting cells for stimulating autologous T-cells *(7)*.

3.2.1. First T-Cell Stimulation In Vitro

1. Incubate the freshly harvested mature DC with 10 μg peptide in 1 mL T-cell medium in a 15-mL conical tube. Incubating with peptide is also known as "pulsing."
2. Incubate for 2 h at RT and mix gently every 20 min.
3. Following peptide pulsing, wash DC three times with RPMI, count, and resuspend DC in T-cell medium.
4. Isolate PBMC from the same donor as the DC, either from fresh blood or from thawed frozen PBMC. Resuspend the PBMC in T-cell medium and determine the cell concentration.
5. Co-culture autologous peptide-pulsed DC and PBMC in a 96-well round-bottom plate at the following concentration: 5×10^3 DC and 1×10^5 PBMC per well (DC:PBMC ratio of 1:20). Culture DC and PBMC in 150 μL/well T-cell medium supplemented with 2 ng/mL IL-12 in a 37°C, 5% CO_2, humidified atmosphere.
6. On d 1, add 25 μL T-cell medium with 5 ng/mL IL-7 (final concentration) per well.
7. On d 2 and 5, add 25 μL T-cell medium with 20 U/mL IL-2 (final concentration) per well.

3.2.2. Restimulations of T-Cells In Vitro

The first restimulation is done in the same plate. For further restimulations, the cell cultures are pooled and seeded with 2×10^5 cells per well in fresh 96-well round-bottom plates. Weekly restimulations are done with a DC:PBMC ratio of 1:40.

1. Pulse fresh or thawed frozen DC with peptide, wash, and resuspend in T-cell medium (*see* **Subheading 3.2.1., step 1**).
2. For the first restimulation, remove 100 μL/well and add 5×10^3 DC in 50 μL of T-cell medium with 1 ng/mL IL-12 (final concentration) per well.

3. For further restimulations, pool T-cells, wash with T-cell medium, and plate 2×10^5 T-cells plus 5×10^3 peptide-pulsed DC in 150 µL/well; no IL-12 is added.
4. On d 1, add 25 µL T-cell medium with 5 ng/mL IL-7 (final concentration) per well.
5. On d 2 and 5, add 25 µL T-cell medium with 20 U/mL IL-2 (final concentration) per well.
6. HLA-peptide multimer staining may be performed 7–10 d after each restimulation.

3.3. HLA-Peptide Multimer Staining

3.3.1. Specificity Analysis of Stimulated T-Cells

Following repetitive T-cell stimulations with peptide-loaded DC, the frequency of peptide-specific T-cells is measured by HLA/peptide multimer (*see* **Note 2**) staining.

1. The staining procedure has to be performed on ice in the dark.
2. Use 5×10^5 T-cells as a negative control and 5×10^5 T-cells for positive staining.
3. Bring up 1×10^6 T-cells in 200 µL FACS buffer and then pipet 100 µL/well into two wells of a 96-well round-bottom plate.
4. Centrifuge the plate at 350*g* at 4°C, discard the supernatant, and resuspend the cell pellets in 50 µL FACS buffer.
5. Add 1.25 µL of multimer stock solution (1 mg/mL) to each cell-containing well for a 1:40 dilution, and then mix gently with the pipet.
6. Incubate the cells in the 96-well round-bottom plate for a minimum of 45 to a maximum of 120 min at 4°C.
7. Add 0.5 µL of anti-CD8-FITC mAb (*see* **Note 3**) to each well for a 1:100 dilution, resuspend, and incubate cells for 15 min at 4°C.
8. Wash the stained T-cells three times with 200 µL FACS buffer per well.
9. Resuspend T-cells in 500 µL FACS buffer containing 2 µg/mL PI.
10. Analyze by flow cytometry.

3.3.2. HLA-Peptide Multimer-Guided T-Cell Sorting

1. The staining procedure must be performed in sterile tubes.
2. Up to 2×10^7 stimulated cells are stained in 500 µL with a 1:20 to 1:40 dilution of multimer stock solution (1 mg/mL).
3. For sorting, resuspend cells at 1×10^7 cells/mL in FACS buffer.
4. Sort multimer$^+$ CD8$^+$ T-cells with a cell sorter into a sterile tube containing T-cell medium.

3.4. T-Cell Cloning

Following the sorting, peptide-specific T-cells are cloned by limiting dilution. T-cell clones are cultured in the presence of irradiated allogeneic LCL and PBMC (so-called feeder cells), IL-2, and anti-CD3 mAb.

1. Harvest allogeneic LCL. Wash and bring these cells up in 20 mL LCL medium. Irradiate LCL with 10 Gy and wash these cells twice with LCL medium; 1×10^5 irradiated LCL/well are required.
2. Isolate or thaw, and then pool and wash allogeneic PBMC from three different donors. Irradiate the pooled PBMC with 3 Gy in 20 mL of T-cell medium and then wash these cells twice with T-cell medium; 5×10^4 irradiated PBMC are required per well.
3. Seed the required amount of irradiated feeder cells in a 96-well round-bottom plate in 100 µL of T-cell medium supplemented with 50 U/mL IL-2 and 30 ng/mL anti-CD3 mAb per well.

4. Sorted T-cells are diluted in T-cell medium supplemented with 50 U/mL IL-2 and 30 ng/mL anti-CD3 mAb. Add diluted T-cells to feeder cells (100 μL/well). Seed T-cells in 96-well round-bottom plates at a concentration of 0.3 and 1 T-cell per well; prepare five plates per concentration.

5. Culture the T-cells together with the irradiated feeder cells in a 37°C, 5% CO_2, humidified atmosphere.

6. On d 7 and 14, remove 100 μL supernatant from each well and add 100 μL of fresh T-cell medium supplemented with 100 U/mL IL-2 (50 U/mL final concentration).

7. Check for clonal T-cell growth (*see* **Note 4**) by microscopy beginning on d 12.

8. Perform screening cytotoxicity assay between d 14 and 21.

3.5. Screening Cytotoxicity Assay

Lysis of chromium[51]-labeled target cells by T-cells is quantified by measuring the amount of chromium[51] released to the supernatant after the co-culture. Peptide-pulsed T2 cells can be used as target cells for analyzing lytic activity of HLA-A2-restricted peptide-specific T-cells. Maximum lysis is calculated by adding 1% NP40 to the target cells, and minimum lysis, also known as spontaneous Cr^{51} release, is calculated by measuring the amount of Cr^{51} released from untreated target cells.

1. Up to 5×10^5 T2 cells (*see* **Note 5**) are suspended in 100 μL of 37°C prewarmed FCS.

2. Add 100 μCi Cr^{51} and incubate for 90 min at 37°C. Mix gently every 20 min.

3. Wash Cr^{51}-labeled T2 cells twice with LCL medium and count the cells.

4. Incubate Cr^{51}-labeled T2 cells in 1 mL of LCL medium containing 10 μg/mL of either relevant or irrelevant peptide. 10 μg/mL β2-microglobulin is added to each tube. Incubate for 1 h at RT. Mix gently every 20 min.

5. Meanwhile prepare effector T-cells:
   a. Resuspend the CTL clones in the 96-well round-bottom culture plate.
   b. Transfer 50 μL of the resuspended T-cell clone from the culture plate into one well of a fresh 96-well v-bottom plate and transfer another 50 μL to a second well.
   c. Refill the culture plate containing CTL clones with 100 μL/well T-cell medium containing IL-2 (50 U/mL final concentration). Culture at 37°C (5% CO_2, humidified atmosphere) until antigen-specific T-cell clones are identified and can be expanded.

6. After peptide pulsing, wash T2 cells twice with LCL medium.

7. Resuspend peptide-pulsed Cr^{51}-labeled T2 cells in LCL medium and then add to the T-cell clones, which each had been divided into two wells of a 96-well v-bottom plate (*see* **step 5c**). Add T2 cells pulsed with the relevant peptide to the first and T2 cells pulsed with the irrelevant peptide to the second well (1×10^3 T2 cells in 150 μL/well).

8. Add 50 μL 1% NP40 buffer to each maximum control well containing 1×10^3 T2 cells (in total six wells). For the spontaneous release control, add 50 μL LCL medium to each well, containing 1×10^3 T2 cells (in total six wells).

9. Incubate for 4 h at 37°, 5% CO_2.

10. Following the incubation, 100 μL of the supernatant is collected from each well and transferred to tubes appropriate for the gamma counter. Cr^{51} released to the supernatant is measured with a gamma counter.

11. Calculate lysis:

$$\text{percent specific } Cr^{51} \text{ release} = \frac{(\text{experimental } Cr^{51} \text{ release} - \text{spontaneous } Cr^{51} \text{ release}) \times 100}{\text{maximum } Cr^{51} \text{ release} - \text{spontaneous } Cr^{51} \text{ release}}$$

3.6. Expansion of Antigen-Specific T-Cell Clones

Antigen-specific cytotoxic T-cell clones are expanded in the presence of irradiated allogeneic feeder cells, anti-CD3 mAb, and IL-2 *(5)*. This approach leads to a 100- to 500-fold expansion of T-cells after 2 wk of culture.

1. The required amount of LCL are harvested and washed. LCL are transferred to a 50-mL tube with 20 mL LCL medium and irradiated with 10 Gy. 5×10^6 LCL are needed per flask.
2. Thaw, pool, and then wash PBMC (*see* **Note 6**) from three different donors and irradiate with 3 Gy in 20 mL T-cell medium. Calculate 2.5×10^7 PBMC for each tissue culture flask (25 cm^2).
3. After the irradiation, wash the feeder cells twice. Count the washed cells.
4. Pool and resuspend the feeder cells in 25 mL T-cell medium supplemented with 30 ng/mL anti-CD3 mAb per flask.
5. Harvest T-cells from one clone and add to the flask.
6. Place the culture flask lid up in the incubator (37°C, 5% CO$_2$, humidified atmosphere).
7. Add 50 U/mL IL-2 (final concentration) on d 1.
8. On d 3, 5, 8, 11, and 14, remove 15 mL supernatant without swirling the cells and add 15 mL T-cell medium supplemented with IL-2 (50 U/mL final concentration).
9. Starting on d 14, the T-cells are ready for analysis.
10. For further expansions, $1–2 \times 10^5$ T-cells are cultured with 2.5×10^7 irradiated PBMC and 5×10^6 LCL per tissue-culture flask.
11. T-cells can be frozen at $1–2 \times 10^6$/mL in freezing medium. Pelleted cells are resuspended in freezing medium and transferred into cryovials. Immediately afterwards, the cryovials are placed in a cryo freezing container and frozen at –80°C overnight.
12. Transfer the cryovials to liquid nitrogen.

3.7. Cytotoxicity Assay of Expanded T-Cell Clones

This cytotoxicity assay is performed in order to determine whether the expanded T-cell clones retain peptide-specific lytic activity and whether they are able to lyse tumor cell lines presenting the endogenously processed peptide antigen. The difference between the chromium release assay for screening CTL clones (*see* **Subheading 3.5.**) and the chromium release assay for testing the expanded T-cell clones are as followed:

1. Target cells other than T2 cells (e.g., tumor cells) are labeled for 1 h with 100 µCi Cr^{51}. Use 1×10^3 target cells per well.
2. Prepare T-cells for the following effector:target ratios by sequential dilution: 90:1, 30:1, 10:1, 3:1, 1:1, and 1:3 in a volume of 100 µL LCL medium.
3. Add Cr^{51}-labeled target cells in 100 µL/well LCL medium and resuspend carefully with T-cells.
4. Add 100 µL 1% NP40 buffer to maximum control wells and 100 µL LCL medium to minimum control wells.

4. Notes

1. If immature DC are not detached on d 7, the reason may be the cytokine concentration of IL-4. Different bioassays to determine the biological activity of cytokines are used by the companies and, therefore, international units may not be comparable.

2. An alternative to using HLA-peptide multimers for T-cell staining and isolation is the usage of reversible HLA-peptide multimers, so-called streptamers *(8)*. We are currently investigating the efficacy of reversible HLA-peptide multimers, which can be dissociated from the T-cells and, therefore, may prevent T-cells from HLA-peptide multimer-induced cell death. Streptamers are commercially available through the company IBA, Göttingen, Germany.

3. Some monoclonal antibodies against CD8 may interfere with the multimer binding and, therefore, lead to false-negative multimer staining. The herein recommended mAb anti-CD8 (clone 3B5; Caltag Laboratories, Burlingame, CA) does not interfere with multimers.

4. T-cells do not survive when feeder cells are infected with mycoplasma. Therefore, it is recommended to regularly check for mycoplasma infection (e.g., PCR).

5. Split or feed target cells one day before performing the chromium release assay in order to prevent high spontaneous Cr^{51} release. In addition, resuspend target cells in prewarmed FCS during Cr^{51} labeling to avoid non-specific cell death. High spontaneous Cr^{51} release may also be a sign of mycoplasma infection of target cells.

6. PBMC can be collected by leukapheresis if a high amount of PBMC is needed.

Acknowledgments

References

1 Lee, P. P., Yee, C., Savage, P. A., et al. (1999) Characterization of circulating T cells specific for tumor-associated antigens in melanoma patients. *Nat. Med.* **5,** 677–685.

2 Yee, C., Riddell, S. R., and Greenberg, P. D. (1997) Prospects for adoptive T cell therapy. *Curr. Opin. Immunol.* **9,** 702–708.

3 Altman, J. D., Moss, P. A., Goulder, P. J., et al. (1996) Phenotypic analysis of antigen-specific T lymphocytes. *Science* **274,** 94–96.

4 Busch, D. H., Philip, I. M., Vijh, S., and Pamer, E. G. (1998) Coordinate regulation of complex T cell populations responding to bacterial infection. *Immunity* **8,** 353–362.

5 Riddell, S. R., Watanabe, K. S., Goodrich, J. M., Li, C. R., Agha, M. E., and Greenberg, P. D. (1992) Restoration of viral immunity in immunodeficient humans by the adoptive transfer of T cell clones. *Science* **257,** 238–241.

6 Jonuleit, H., Kuhn, U., Müller, G., et al. (1997) Pro-inflammatory cytokines and prostaglandins induce maturation of potent immunostimulatory dendritic cells under fetal calf serum-free conditions. *Eur. J. Immunol.* **27,** 3135–3142.

7 Fleischer, K, Schmidt, B, Kastenmüller, W., et al. (2004) Melanoma-reactive class I-restricted cytotoxic T cell clones are stimulated by dendritic cells loaded with synthetic peptides, but fail to respond to dendritic cells pulsed with melanoma-derived heat shock proteins in vitro. *J. Immunol.* **172,** 162–169.

8 Knabel, M., Franz, T. J., Schiemann, M., et al. (2002) Reversible MHC multimer staining for functional isolation of T-cell populations and effective adoptive transfer. *Nat. Med.* **8,** 631–637.

 9. Valmori, D., Fonteneau, J. F., Lizana, C. M., et al. (1998) Enhanced generation of specific tumor-reactive CTL in vitro by selected Melan-A/MART-1 immunodominant peptide analogues. *J. Immunol.* **160,** 1750–1758.

10. Schneider, J., Brichard, V., Boon, T., Meyer zum Büschenfelde, K. H., and Wölfel, T. (1998) Overlapping peptides of melanocyte differentiation antigen Melan-A/MART-1 recognized by autologous cytolytic T lymphocytes in association with HLA-B45.1 and HLA-A2.1. *Int. J. Cancer* **75,** 451–458.

14

Tracking Adoptively Transferred Antigen-Specific T-Cells With Peptide/MHC Multimers

Norbert Meidenbauer and Andreas Mackensen

Summary

Advances in immunological monitoring provide the means to track tumor antigen-specific cytotoxic T-lymphocytes (CTL) in humans after adoptive transfer with greater specificity and sensitivity than before. Novel tools can be used not only to detect antigen-specific CTL, but also to evaluate the function and phenotype of individual T-cells. Peptide major histocompatibility complexes (MHC) class I multimeric complexes are proving invaluable as fluorescent reagents for tracking of antigen-specific T-cells. The multimeric complex is constructed of four synthetic and biotinylated peptide-loaded MHC molecules, which are linked by a fluorochrome-labeled streptavidin molecule. In contrast to "indirect" assays such as limiting dilution analysis (LDA) or ^{51}Cr release assays requiring in vitro stimulation, this method allows direct monitoring of very low numbers of peptide-specific T-cells without the need for in vitro sensitization. By combining the use of multimers with anticytokine antibodies, a more detailed picture of the tracked T-cell can be obtained. This chapter summarizes the application of these protocols to monitor ex vivo the frequency and functional activity of tumor-specific CTL after adoptive transfer. Furthermore, it details potential problems interfering with correct staining and provides guidance for interpretation of results.

Key Words: Adoptive immunotherapy; CTL; tumor immunity; antigens; cell trafficking; MHC multimers.

1. Introduction

T-cell therapy has attracted a great deal of interest in the treatment of viral infections *(1)*, EBV-associated lymphoma *(2)*, and relapse of hematologic diseases after allogeneic bone-marrow transplants. The persistence of adoptively transferred T-cells and reconstitution of virus-specific immunity was demonstrated in the absence of noticeable side effects *(1)*. These data provided compelling proof of principle for the clinical use of adoptive T-cell therapy.

Immunotherapy with autologous tumor-specific T-cells for solid tumors is much more difficult, since specific tumor-associated antigens (TAA) have been defined in

only a minority of tumors. In malignant melanoma, several TAA have been recently identified and used as targets for immunotherapy *(3)*.

A major drawback of this treatment modality was the fact that TAA-specific T-cells had to be selected from tumor-infiltrating lymphocytes (TIL), and often only a relatively low number of cells could be produced. Recently, adoptive T-cell therapy as a therapeutic option has regained interest by improved in vitro stimulation techniques, allowing the generation of high numbers of antigen-specific T-cells *(4)*. However, the knowledge about the fate of antigen-specific T-cells after transfer into patients with solid tumors is still very limited. Yee and colleagues reported on T-cell infiltration into both skin and tumor tissue after adoptive transfer of a Melan-A-specific CTL clone *(5)*. We have demonstrated recently that in vitro generated Melan-A-specific CTL survive intact in vivo for several weeks and localize preferentially to tumor *(6)*.

The in vitro and in vivo monitoring and quantitation of antigen-specific T-cell functions during the interaction with the cognate MHC/peptide ligand represent an essential tool for detailed analysis of specific immune responses. They include the measurement of cytokine secretion using monoclonal antibodies (mAbs) (ELISA, intracellular cytokine staining, or ELISPOT), flow-cytometric staining of surface molecules, and the analysis of the proliferative responses by ^{3}H-thymidine incorporation. To determine the cytolytic activity of T-cells, the ^{51}Cr-release assay performed over 4–5 h is recognized as the standard method.

This chapter summarizes a new approach to the analysis of T-cell-mediated functional activity, the MHC multimer technology. Multimers allow for direct visualization of antigen-specific T-cells by flow cytometry *(7)*. The multimeric complex is usually constructed of four synthetic and biotinylated peptide-loaded HLA molecules that are linked by a fluorochrome-labeled streptavidin molecule. The use of multimers has a major impact on immunology. It is possible to look at T-cell functions as well as the presence of the receptor. Furthermore, multimer staining may differentiate between high- and low-affinity T-cells, thus allowing purification of the most effective T-cells, which can be expanded in vitro and adoptively transferred to the patients. In contrast to "indirect" assays such as limiting dilution analysis (LDA), or ^{51}Cr-release assays requiring in vitro stimulation, this method allows direct monitoring of very low numbers of peptide-specific T-cells without the need for in vitro sensitization. The sensitivity of HLA class I multimers is usually 1/3000 CD8$^+$ T-cells. To define the functional activity of antigen-specific T-cells, multimers can be used together with antibodies targeted against surface markers or intracellular or surface-bound cytokines *(8,9)*.

HLA class II multimers have been more difficult to produce but have already been demonstrated to detect low frequencies of antigen-specific CD4$^+$ T-cells *(10)*.

In a recent study, we have used HLA class I multimers to demonstrate that Melan-A-specific CTL generated by in vitro stimulation with peptide-pulsed dendritic cells (DC) survive physiologically intact in vivo for several weeks *(6)*. Combination of multimer analysis with the cytokine secretion assay demonstrated unimpaired functional activity of the transferred T-cells in the peripheral blood for at least 24 h post infusion.

In this chapter we summarize the application of HLA class I multimers to track ex vivo the frequency and functional activity of tumor-specific CTL after adoptive transfer.

2. Materials

2.1. Generation of Antigen-Specific CTL Lines

1. Cells I (effector cells): Peripheral blood mononuclear cells (PBMC) were freshly isolated from heparinized peripheral blood of healthy donors or patients by Ficoll density gradient centrifugation.
2. Cells II (stimulator cells): Monocytes were enriched from PBMC either by counter-current elutriation or adherence.
3. Medium: Lymphocytes and monocytes were cultured in RPMI 1640 supplemented with 300 mg/L L-glutamine, 50 μM β-mercapthoethanol, 1 mM sodium pyruvate, 40 μg/mL streptomycin, 40 U/mL penicillin, 1X MEM vitamins, and 1X nonessential amino acids (= standard culture medium, M').
4. CD8$^+$ T-cell isolation kit: The CD8$^+$ T-cell isolation kit II (Miltenyi Biotec, Bergisch Gladbach, Germany), is an indirect magnetic labeling system for the isolation of untouched CD8$^+$ CTL from peripheral blood.
5. Cytokines. The following recombinant human cytokines and proteins are used for in vitro differentiation of DC at concentrations indicated in parentheses: interleukin (IL)-1β (10 ng/mL), IL-4 (500 U/mL), IL-6 (1000 U/mL), tumor necrosis factor (TNF)-α (10 ng/mL), transforming growth factor (TGF)-β (5 ng/mL) (all from CellGenix, Freiburg, Germany), granulocyte/macrophage colony-stimulating factor (GM-CSF) (500 U/mL) (Essex Pharma and Novartis Pharma, Basel, Switzerland), prostaglandin E$_2$ (PGE$_2$) (1 μg/mL) (Pharmacia & Upjohn, Erlangen, Germany).
6. The following HLA-A2 binding peptides were used: modified Melan-A$_{26-35}$ A27L (ELAGIGILTV) (designated as Melan-A$_{26-35L}$), natural Melan-A$_{26-35}$ (EAAGIGILTV), and gp100$_{280-288}$ (YLEPGPVTA) (Bachem Biochemica GmbH, Heidelberg, Germany). The identity of each peptide was confirmed by mass spectral analysis. The peptides were >98% pure as assessed by high-pressure liquid chromatography analysis. The endotoxin level was <0.1 endotoxin units/mL.
7. Human β_2-microglobulin (β2m) (10 μg/mL), (ICN, Eschwege, Germany).
8. T-cell growth factor (TCGF): preparation of TCGF was described previously *(11)*. TCGF was produced by stimulating 2.5×10^6/mL PBMC for 2 h with 5 μg/mL phytohemagglutinin (Murex, Dartford, England), 5 ng/mL phorbol myristate acetate (Sigma-Aldrich, Taufkirchen, Germany), and 5000 rad-irradiated EBV-transformed B-cells. The cells were then washed to remove the mitogens and resuspended in RPMI 1640 supplemented with 2.5% human AB serum. After 40 h of incubation, supernatants were harvested, passed through 0.2 μm filters, and stored at –70°C.

2.2. Multimer Staining

1. Cells I: PBMC were freshly isolated from heparinized peripheral blood of healthy donors or patients by Ficoll density gradient centrifugation. Immune monitoring after adoptive transfer is recommended before and at least at 1, 6, and 24 h or later after T-cell infusion.
2. Cells II (control cells): Antigen-specific control T-cell lines or clones *(4)*.
3. PE or APC-labeled HLA-A*0201 multimers that had been folded around ELAGIGILTV (Melan-A$_{26-35L}$), SLLMWITQC (NY-ESDA$_{157-165}$), YMDGTMSQV (Tyrosinase$_{369-377}$), IMDQVPFSV (gp100$_{209-217M}$), and SLYNTVATL (HIVgag) (e.g., synthesized by Beckman Coulter, Fullerton, CA).

4. Multimer washing buffer: phosphate-buffered saline (PBS) + 0.1% bovine serum albumin (BSA).
5. Five-milliliter polystyrene round-bottom tubes (Falcon).
6. Ninety-six-well V-bottom microtiter plates (Falcon).
7. FITC- or APC-labeled anti-CD3, anti-CD4, and anti-CD8 monoclonal antibodies (mAbs).
8. PerCP-labeled anti-CD14 mAb for monocyte exclusion.
9. FITC-labeled annexin-V (e.g., PharMingen, San Diego, CA).
10. Annexin-V buffer (PharMingen).
11. Paraformaldehyde (PFA), 0.5% (Merck, Darmstadt, Germany).

2.3. Interferon-Secretion Assay

1. Cells I (responder cells): Peripheral blood mononuclear cells (PMNC) freshly isolated from heparinized peripheral blood of healthy donors or patients by Ficoll density gradient centrifugation. Immune monitoring should be performed before T-cell transfer and at 24 h after T-cell infusion. Antigen-specific T-cell lines or clones *(4)* were used as positive controls.
2. Cells I (stimulator cells): autologous monocyte-derived DC pulsed with the appropriate peptide (30 μg/mL) and human β2m (10 μg/mL) in serum-free medium, were used as stimulators.
3. The following HLA-A2-binding peptides were used: modified Melan-A$_{26-35}$ A27L (ELAGIGILTV) (designated as Melan-A$_{26-35L}$), natural Melan-A$_{26-35}$ (EAAGIGILTV), and gp100$_{280-288}$ (YLEPGPVTA) (Bachem Biochemica GmbH).
4. Buffer: PBS containing 0.5% BSA and 2 mM EDTA, must be used ice cold.
5. Interferon (IFN)—γ secretion assay detection kit APC human (Miltenyi) containing:
   a. Cytokine catch reagent: anticytokine mAb conjugated to cell surface (CD45)-specific mAb (Miltenyi).
   b. Cytokine detection antibody: anticytokine mAb conjugated to PE or APC (Miltenyi).
6. Medium: any standard medium may be used, e.g., RPMI-1640 or Iscove containing 10% AB or autologous serum. Medium is required both ice cold and at 37°C. Do not use fetal calf serum (FCS) as this gives high nonspecific "background" responses.
7. Fifty-mL centrifuge tubes (Corning GmbH, Wiesbaden, Germany).
8. PE- or APC-labeled HLA-A*0201 multimers that had been folded around ELAGIGILTV (Melan-A$_{26-35L}$), YMDGTMSQV (Tyrosinase$_{369-377}$), IMDQVPFSV (gp100$_{209-217M}$), and SLYNTVATL (HIVgag) (Beckman Coulter).
9. Ninety-six-well round-bottom plates (Falcon) and 48-well flat-bottom plates (Corning).
10. Staphylococcal enterotoxin B (SEB) (Sigma-Aldrich).
11. Five-milliliter polystyrene round-bottom tubes (Falcon).
12. FITC- or APC-labeled anti-CD3, ant-CD4, and anti-CD8 mAbs.
13. PerCP-labeled anti-CD14 mAb for monocyte exclusion.
14. Propidium iodide (PI) or 7-AAD to exclude dead cells from the flow-cytometric analysis.
15. PFA, 0.5 %.

3. Methods

The methods described below outline (1) the in vitro generation of antigen-specific T-cells; (2) multimer staining for detection of antigen-specific T-cells; and (3) the combination of the multimer technology with a functional assay, as represented by the cytokine secretion assay.

3.1. In Vitro Generation of Antigen-Specific T-Cell Lines

Antigen-specific CTL lines were generated as described previously *(4,6)*.

1. CD8$^+$ T-lymphocytes are enriched from PBMC by depletion of CD4$^+$, CD11b$^+$, CD16$^+$, CD19$^+$, CD20$^+$, and CD56$^+$ cells with magnetic cell sorting using a midiMACS device (Miltenyi).
2. DC are generated from monocytes enriched by counter-current elutriation or adherence and then cultured with M' medium plus 2% autologous serum, supplemented with human GM-CSF, IL-4, and TGF-β. On d 6, fresh medium containing GM-CSF, IL-4, TNF-α, IL-6, IL-1β, and PGE$_2$ is added to the culture for an additional 48 h.
3. The DC are then harvested and pulsed for 2 h at 37°C with the appropriate peptide (30 μg/mL) and human β$_2$m (10 μg/mL) in serum-free M'-medium.
4. Co-culture $2–5 \times 10^4$ effector cells/well and 5×10^3 peptide-pulsed autologous DC/well in 96-well round-bottom plates in M' medium supplemented with 10% human AB serum and 1–2% TCGF *(12)*.
5. Medium exchange is performed twice a wk; effector cells are restimulated weekly with fresh peptide-pulsed DC.
6. After four cycles of stimulation, phenotypic and functional analysis of T-cells should be performed.

3.2. Tracking Antigen-Specific T-Cells
Using MHC Peptide Multimer Staining

Optimal temperature and incubation time should be determined for each multimer prior to analysis. To minimize nonspecific staining, each multimer has to be titered and used at the lowest concentration that showed a clearly distinguishable positive population in antigen-specific CTL lines. We recommend the use of in vitro generated antigen-specific CTL lines (the protocol has been described above in **Subheading 3.1.**) or antigen-specific T-cell clones (some of them are commercially available, e.g., ProImmune, Oxford, UK).

As with mAb staining, the intensity of multimer staining is dependent on the concentration of ligand in solution and not on the cell concentration or receptor density on the cells. This is due to the fact that ligand is present in enormous excess compared to the total number of receptor molecules. We therefore recommend conserving reagents by staining cells suspended in a minimal volume.

3.2.1. Multimer Staining

1. Typically we stain cells in 5-mL polystyrene round-bottom tubes.
2. Add PBMC or T-cells (5×10^6 in a volume of 150 μL) to the tube.
3. Centrifuge for 10 min at 400g (1600 rpm) and remove the supernatant.
4. Add multimer to the cell pellet and mix gently.
5. Coincubate cells with the multimer on a cell shaker. For the majority of the multimers, incubation time should be 30 min at room temperature (RT) (*see* **Note 1**).
6. Add mAbs for surface staining and incubate cells in the dark for 30 min at 4°C (*see* **Note 2**).
7. Wash twice and then fix the cells with 0.5% PFA, if not immediately analyzed.
8. For combination of multimer and annexin-V staining, wash cells once with flow buffer and once with annexin-V buffer (PharMingen) after incubation with surface mAbs.
9. Resuspend cells in 100 μL annexin buffer and add 1 μL annexin-V. After incubation of 20 min at RT in the dark, fix cells with 0.5% PFA.

10. We recommend the analysis of the following mAb/multimer panels for proper multimer staining of PBMC:
    a. CD3-FITC, multimer-PE, CD14-PerCP, CD8-APC;
    b. CD3-FITC, multimer-PE, CD14-PerCP, CD4-APC (control for specific staining because CD4+ T-cells should not stain with MHC class I multimers);
    c. CD3-FITC, PBS, CD14-PerCP, CD8-APC (exclusion of random events in the quadrant of interest);
    d. Annexin-V-FITC, multimer-PE, CD3-PerCP, CD8-APC;
    e. CD8-FITC, control multimer-PE, CD14-PerCP, CD3-APC (control of background staining of multimers);
    f. Isotype controls.

In most common flow-cytometry applications, the phenotypic markers of interest are expressed on 5% or more the cells to be analyzed. In contrast, as shown in **Figs. 1** and **2**, multimer+ T-cells are often present at frequencies below 1%, and thus multimer staining can be considered as a rare-event problem. As in all rare-event problems, a large denominator is required. For detection of multimer frequencies in the range of 1/1000 to 1/8000 it is advisable to routinely require >10^6 total events.

3.2.2. Exclusion of Cells and Other Known Sources of Unspecific Multimer Binding and Autofluorescence

In common with any other low-frequency analysis, to properly identify positively stained cells, positive staining (e.g., with CD3 and/or CD8) is required and exclusion of unwanted cells from analysis is vital. Multimer-positive events are evaluated within a Boolean gate including cells within an extended lymphoid light scatter gate and a CD3+ gate (**Fig. 1**). Furthermore, CD14+ monocytes, which do bind non-specifically with flurochrome-conjugated multimers, should be excluded (*see* **Fig. 1**).

Similarly, exclusion of the dead cells (which are present in even the most accurately gated lymphocyte population) using propridium iodide (PI) or 7-AAD will eliminate nonspecific background staining (data not shown).

3.2.3. Competition Between Multimer and Anti-CD3 mAb Binding

To determine the specificity of the multimer staining, we quantified the extent to which multimer binding competed with CD3 binding on CD8+ cells, using the formula described previously *(13)*:

$$\% \text{ competition} = \frac{\left(\text{CD3Mnl}_{CD3+CD8+multimer}\right) - \left(\text{CD3Mnl}_{CD3+CD8+multimer+}\right)}{\text{CD3Mnl}_{CD3+CD8+multimer-}} \tag{1}$$

where CD3Mnl is the log mean fluorescence intensity (MFI) of CD3 staining of the population designated by the subscript. The usefulness of this phenomenon was confirmed with multimers for several antigens *(6,13)* (*see also* **Fig. 3**), but multimers have been described that did not compete for CD3 binding *(14)*.

3.2.4. Example of In Vivo Tracking of Antigen-Specific CTL After Adoptive Transfer

Using the multimer technology, we assessed the frequency of circulating Melan-A-specific CTL in advanced melanoma patients during adoptive T-cell therapy *(6)*.
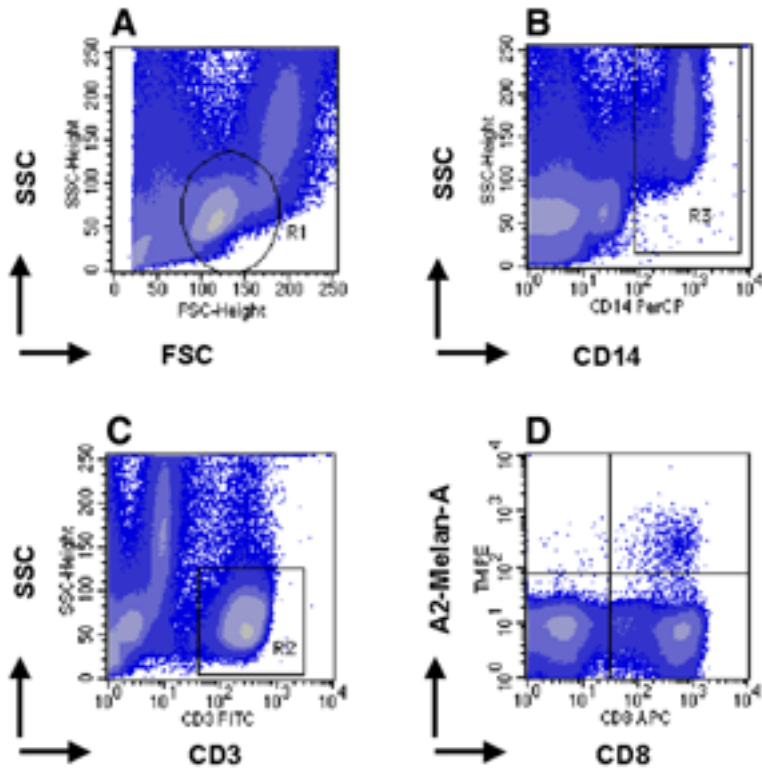
Fig. 1. Compound gating strategy used to identify tetramer+ CD8+ T-cells. PBMC from an HLA-A2.1+ melanoma patient were stained with Melan-A multimers followed by anti-CD14, anti-CD3, and anti-CD8 mAbs using four-color flow cytometry. To obtain a clearly discernible cluster of multimer+ cells (*see* upper right quadrant of **D**), a Boolean gate including cells within an extended lymphoid light scatter gate **(A)** and a generous CD3+ gate **(C)** and excluding CD14+ events **(B)** was used.

Melan-A-specific CTL were generated from HLA-A2.1+ patients by in vitro stimulation of CD8+ T-cells with DC pulsed with a mutated HLA-A2-binding Melan-A (ELAGIGILTV) peptide. PBMC obtained immediately before and 1 h, 24 h, and 14 d after transfer (i.e., immediately before the subsequent transfer) were stained with PE-conjugated Melan-A-multimer and APC-conjugated anti-CD8 mAb.

The multimer staining procedure and gating strategy for elimination of non-specific multimer-binding events, described in **Subheadings 3.2.1.** and **3.2.2.**, resulted in a clear population of specific multimer+/CD8+ T-cells (*see* **Fig. 2**).

As demonstrated in **Fig. 2**, the pre-infusion frequency of Melan-A-multimer+ cells within CD8+ peripheral blood lymphocytes (PBL) in the melanoma patient was <0.1% *(6)*. This particular melanoma patient received an i.v. infusion of a total number of 0.5 $\times$ 10^8 Melan-A-multimer+ CTL. One h after infusion, a marked increase in the frequency of Melan-A-multimer+/CD8+ T-cells up to 1.4% of total CD8 cells could be observed (**Fig. 2**). Between 24 h and 14 d post infusion, the frequency of Melan-A-TM+/CD8+ T-cells in this particular patient decreased to a level in the range of the pre-infusion value.
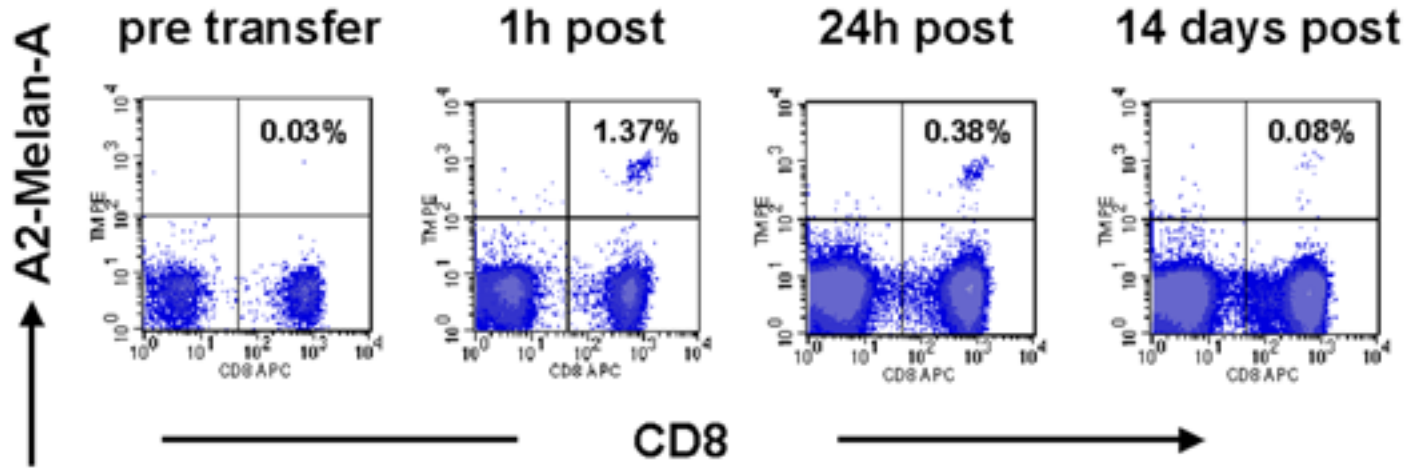
Fig. 2. Kinetics of the frequencies of Melan-A-multimer+ cells within CD8+ peripheral blood lymphocytes (PBL) in a melanoma patient after adoptive transfer of Melan-A-specific CTL. Peripheral blood mononuclear cells taken at the indicated time points following adoptive transfer were stained with PE-conjugated Melan-A-multimer and APC-conjugated anti-CD8 mAb. Dot plots are shown on gated CD3+, CD14- small lymphocytes (by forward and side scatter). Numbers in the upper right quadrants represent percentages of Melan-A-multimer+/CD8+ cells within total CD8+ PBL.
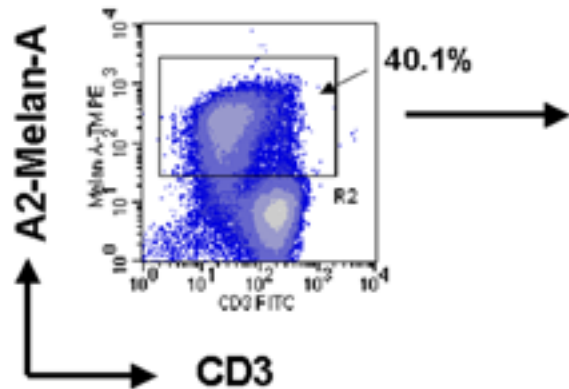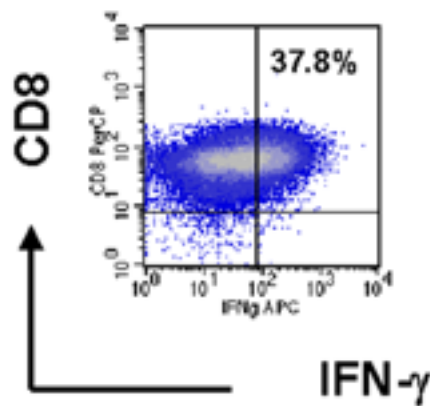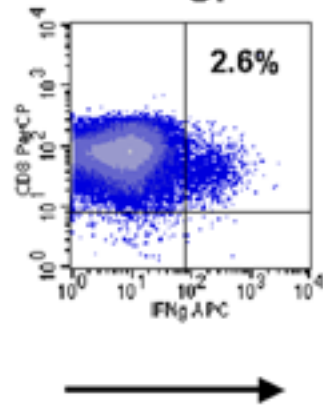
Fig. 3. IFN-γ secretion-based detection of Melan-A-specific CD8+ T-cells after in vitro stimulation with Melan-A peptide-pulsed DC. Melan-A-specific T-cells were incubated with autologous dendritic cells pulsed with the specific Melan A_{26-35L} peptide or irrelevant gp100 peptide. After 4 h, cells were labeled as described in protocol and then directly analyzed by flow cytometry. For analysis of IFN-γ secretion, cells were gated for CD3+ Melan-A-multimer+ cells (left dot plot). Please note the competition of CD3 binding in the multimer+ population compared to CD3 binding in the multimer- T-cell population (left dot plot). The right 2 dot plots show staining with APC-conjugated anti-IFN-γ mAb and PerCP-conjugated anti-CD8 mAb. Numbers in the upper right quadrants represent percentages of IFN-γ+/CD8+ cells within CD3+/Melan-A-multimer+ T-cells.
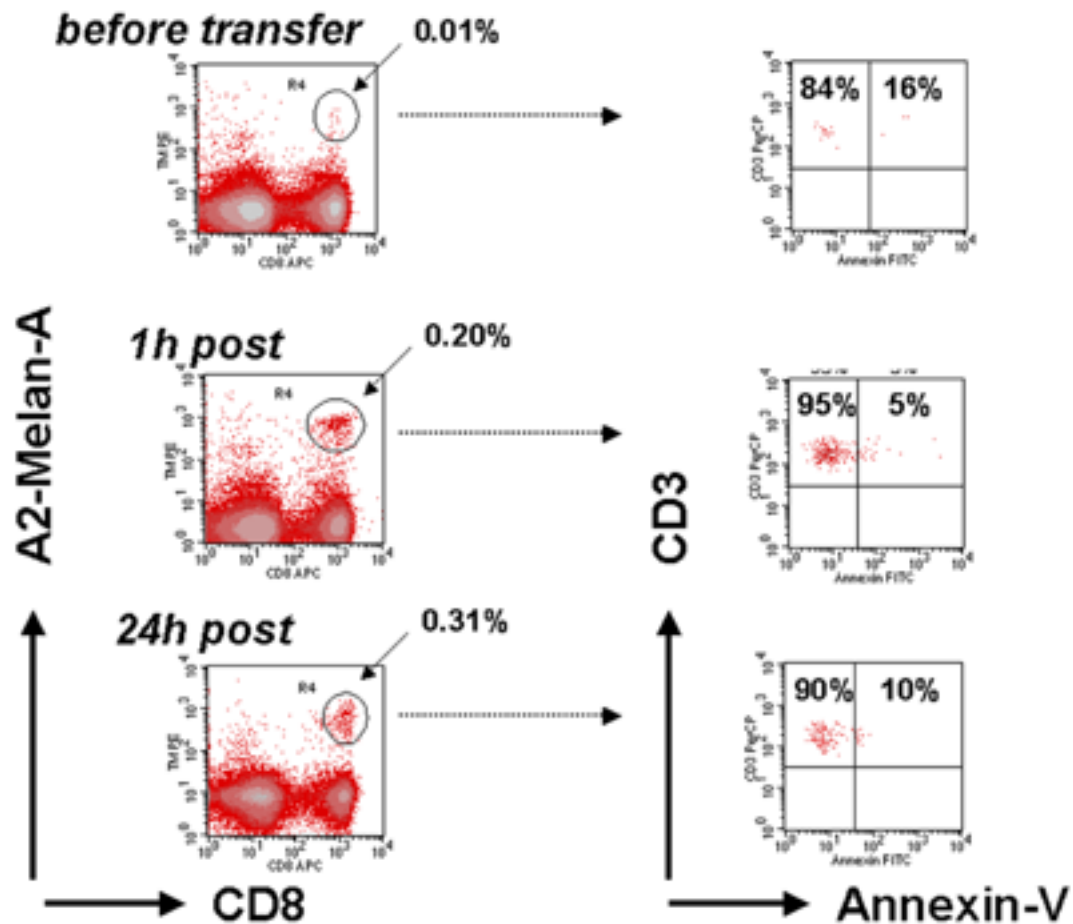
3.2.5. Combination of Annexin-V and Multimer Staining

Apoptosis of transferred antigen-specific T-cells has been described as an important mechanism for the failure of adoptive T-cell therapy in HIV disease *(15)*. Combination of annexin-V and multimer staining represents an interesting technical approach to answer this question. The frequency of apoptotic Melan-A-multimer+ T-cells in circulating patients PBL was analyzed before and after 1 h and 24 h after T-cell infusion. An example is shown in **Fig. 4**, demonstrating that the frequency of Melan-A-specific T-cells undergoing apoptosis was not significantly elevated. Please note that T-cells can die from apoptosis after multimer labeling (*see* **Note 3**).

3.3. Combination of Cytokine Secretion Assay
With Peptide/MHC Multimer Staining

One major disadvantage of multimer analysis is the lack of information about functional activity of the T-cells. This problem can be solved by combining the multimer technology with a functional assay, as represented by the cytokine secretion assay (e.g., provided by Miltenyi, Bergisch Gladbach, Germany) or intracellular staining for cytokines or other relevant functional proteins.

The combination of multimer staining with cytokine secretion was first described by Pittet and colleagues *(8)*. We have adopted this assay to monitor the function of adoptively transferred Melan-A-specific T-cells in patients with malignant melanoma *(6)*. T-cells are stimulated with the cognate peptide and secreted IFN-γ molecules are retained on the cell surface by a bispecific mAb against IFN-γ and CD45 (leukocyte marker) (*see* **Fig. 5**). A fluorochrome-labeled anti-IFN-γ mAb allows flow-cytometric analysis.

3.3.1. Protocol of the Combined Multimer/Cytokine Secretion Assay

1. Autologous or HLA-A2-matched DC are cultured and matured as described before.
2. Harvest DC from the culture, wash, and resuspend in complete medium (e.g., RPMI + 10% AB-serum), adjusted to 3×10^6/mL.
3. Add relevant and control peptide (final concentration: 30 μg/mL) and β2m (final concentration: 10 μg /mL), and incubate at 37°C for 45 min.
4. Before the end of the incubation, add responder cells (5×10^6 in a volume of 150 μL) to a 5-mL polystyrene round-bottom tube.

Fig. 4. *(opposite page)* Annexin-V staining of circulating Melan-A-multimer+/CD8+ gated T-cells after adoptive transfer. Apoptosis of transferred antigen-specific T-cells before and after 1 h and 24 h post T-cell infusion was detected by a combined approach of multimer and annexin-V staining. PBMC taken from melanoma patient at the indicated time points following adoptive transfer were stained with PE-conjugated Melan-A-multimer, APC-conjugated anti-CD8, PerCP-conjugated anti-CD3 mAbs, and FITC-conjugated annexin-V, respectively. For analysis of annexin-V, cells were gated for CD8+ Melan-A-multimer+ cells (left dot plot). The right dot plots show staining with FITC-conjugated annexin-V and PerCP-conjugated anti-CD3 mAb. Numbers in the upper right quadrants represent percentages of annexin-V+/CD3+ cells within CD8+/Melan-A-multimer+ T-cells.
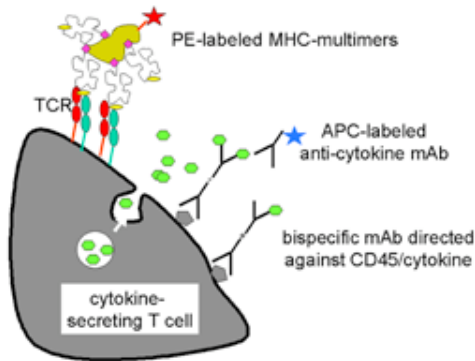
Fig. 5. Principles of the combined multimer and cytokine secretion analysis for detection of functionally active antigen-specific T-cells.

5. Wash responder cells (e.g., T-cells, PBMC) in PBS + 0.1% AB serum.
6. Centrifuge for 10 min at 400*g* (1600 rpm) and remove the supernatant.
7. Add multimer to the cell pellet and mix gently.
8. Co-incubate cells with the multimer on a cell shaker. For the majority of the multimers, incubation time should be 30 min at RT (*see* **Note 4**).
9. Wash pulsed DC, count, and resuspend in complete medium.
10. Wash stained responder cells and resuspend them in complete medium into 4 aliquots:
    a. Aliquot 1: Add DC pulsed with relevant peptide (ratio DC:responder cells = 1:3).
    b. Aliquot 2: Add DC pulsed with irrelevant peptide (ratio DC:responder cells = 1:3).
    c. Aliquot 3: Add SEB to get a final concentration of 50 µg/mL.
    d. Aliquot 4: nonstimulated sample. For PBMC we recommend 4×10^6 cells/aliquot, for purified T-cells 2×10^6 cells/aliquot in order to be able to acquire about 1×10^6 events/sample.
11. Incubate each aliquot of 500 µL in a 48-well plate for 2 h at 37°C.
12. Harvest the aliquots, wash with excess of cold buffer, and add cold complete medium (90 µL/1×10^6 cells) and cytokine catch reagent (anti-IFN-γ-catch-mAb [10 µL/1×10^6 cells]).
13. Mix well and incubate cells for 5 min on ice.
14. Add 10 mL warm complete medium/1×10^6 cells and incubate for 30 min at 37°C under slow continuous agitation/rotation, or mix every 5 min to avoid sedimentation of the cells.
15. Wash with cold buffer in excess, add cold complete medium (90 µL/1×10^6 cells) and cytokine-detection antibody (e.g., anti-IFN-γ detection mAb [10 µL/1×10^6 cells]) and additional staining reagent, such as anti-CD3 and/or anti-CD8 mAbs.
16. Mix well and incubate for 10 min on ice in the dark.
17. Wash cells with cold buffer in excess, centrifuge at 300*g* for 5 min at RT, remove supernatant.
18. Wash cells with cold buffer in excess, centrifuge at 300*g*. Resuspend cells in 500 µL of cold buffer and proceed with flow-cytometric analysis or perform fixation with PFA (1%).

3.3.2. Example for a Combination of the Cytokine Secretion
Assay With Peptide/MHC Multimer Staining
for Functional Analysis of Antigen-Specific CTL

CD8-purified T-cells from a melanoma patient were stimulated once a week with Melan-A$_{26–35L}$ peptide-pulsed DC. Seven days after the fourth stimulation (d 28), T-cells were incubated with autologous DC pulsed with the specific Melan A$_{26–35L}$ peptide or irrelevant gp100 peptide. Additional controls included unstimulated T-cells (negative control) or T-cells unspecifically stimulated with SEB (positive control). As shown in **Fig. 3**, 37.8% of Melan-A-multimer$^+$ T-cells secreted IFN-γ upon stimulation with Melan-A-pulsed autologous DC. Upon stimulation with the control peptide, gp100, there was no increase in the IFN-γ secretion compared to the unstimulated T-cells. Of note is a down-regulation of Melan-A-multimer staining upon specific stimulation, showing a reduction in the frequency of Melan-A-multimer$^+$ T-cells in the stimulated samples compared to unstimulated controls. This phenomenon has already been described and provides indirect evidence for the specificity of the generated T-cells *(6,16)*.

4. Notes

1. Temperature influences multimer binding: Whelan et al. examined the fine specificity of multimer staining using a well-characterized set of HIV epitope variants *(17)*. Peptide variants that elicit little or no functional cellular response from CTL stained these cells at 4°C but not at 37°C when incorporated into multimers. These results suggest that some studies reporting multimer incubations at 4°C could detect cross-reactive populations of CTL with minimal avidity for the multimer peptide, especially in the multimer-low population.

   The data are confirmed by our studies (**Fig. 6A**), demonstrating that incubation with Melan-A tetramers at 37°C improves the staining intensity of specific CTLs, resulting in improved separation of tetramer-high CD8$^+$ cells.

   However, this observation does not necessarily apply to all multimer specificities. As shown in **Fig. 6B**, NY-ESO-1 multimer staining at 4°C resulted in a brighter expression and higher percentage than staining at 37°C. Temperature had a minimal effect on the binding of peptides derived from MAGE10 *(18)*, gp100 *(19)*, and p53 *(20)*.

   In conclusion, the optimal temperature, concentration, and incubation time should be determined for each multimer. However, conditions that yield the highest percentage of multimer$^+$ events or the brightest multimer binding are not necessarily those that give the most biologically relevant information.

2. Sequence of staining with MHC peptide multimers and mAbs is critical: Denkberg et al. have demonstrated that T-cell receptor (TCR)-binding to multimers is coreceptor dependent *(19)*. They could show with a human CTL clone specific for a tumor-associated MHC-peptide complex that the binding of multimers to the TCR on these cells is completely blocked by antihuman CD8 mAbs. This blockage was mediated by anti-CD8 mAbs but not anti-CD3 mAbs. The blocking effect of the anti-CD8 Abs was attributable to directly inhibiting multimer binding and was not attributable to mAb-mediated TCR-CD8 internalization and down-regulation *(19)*. However, inhibition of multimer binding was not observed when cells were incubated with multimer followed by anti-CD8 mAb. There is ample evidence that binding of the MHC class I molecule to the CD8 coreceptor is not required for avid multimer binding, and indeed, may even increase the frequency of false-positive events.
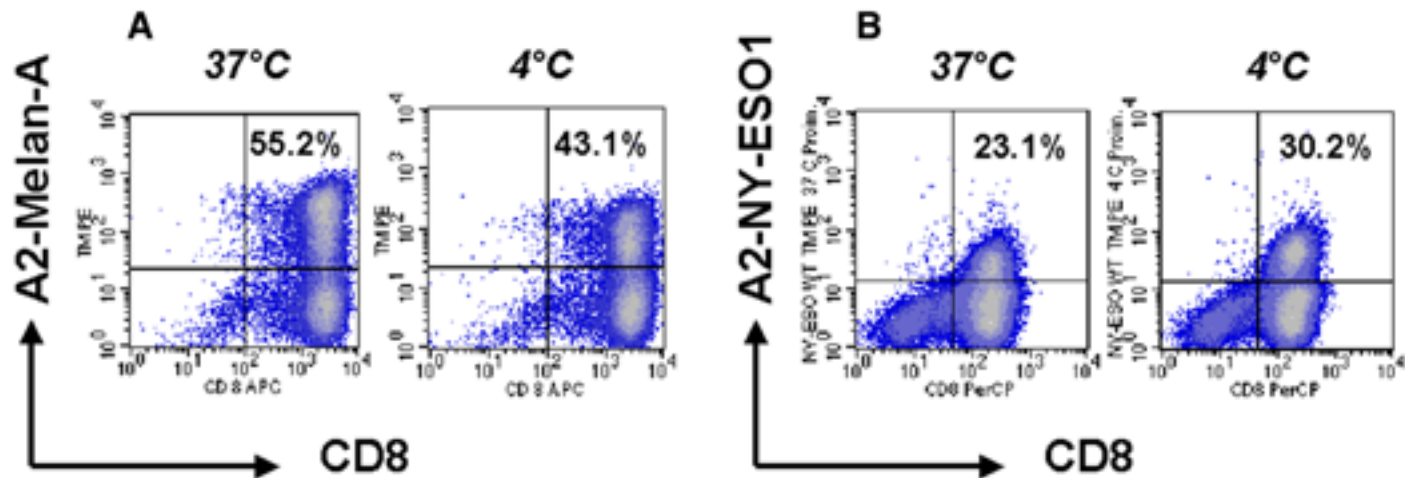
Fig. 6. Temperature influence multimer binding. Melan-A^{+} and NY-ESO-1^{+} CD8^{+} T-cell lines were generated by repetitive antigen-specific in vitro stimulation. The frequency of both CTL lines was determined by multimer staining. Melan-A[+] and NY-ESO-1^{+} CTL were stained directly with APC-conjugated anti-CD8 mAb and PE-conjugated Melan-A (**A**) or NY-ESO-1 (**B**) multimers, respectively, and incubated for 30 min either at 4°C or 37°C. Percentages of CD8^{+}/multimer^{+} T-cells are shown in the upper right quadrant of the dot plot.

MHC class I multimers developed and marketed by Beckman-Coulter Immunomics circumvent this potential problem by using a modified MHC class I molecule carrying a mutation in the α3-domain, which does not bind to the CD8 coreceptor.

We therefore recommend staining with multimer first, followed by antibodies.

3. Sequence of multimer staining and T-cell stimulation is critical: Upon stimulation with antigen, the TCR on the antigen-specific T-cells can be rapidly down-regulated. This dramatically reduces peptide-MHC multimer staining. Therefore, the peptide-MHC multimer labeling should be done prior to the stimulation with peptide. After staining with peptide/MHC multimer, cells are stimulated with the specific peptide for 2–3 h followed by the standard secretion assay procedure.

Depending on the type of multimer used, the peptide-MHC multimer may or may not stimulate cytokine secretion. If the multimer does not stimulate, then the controls may be carried out as normal—i.e., stain with multimer as for the stimulated samples, then incubate with no or control peptide. However, if the multimer does stimulate, an extra control should be included, where the cells are first cultured with no peptide or control peptide, and then incubated with multimer.

4. Reversible MHC multimer staining for functional isolation of antigen-specific T-cells: It has been shown that T-cells die from apoptosis or are functionally defective after multimer labeling *(21)*. An interesting technology of reversible staining appears to leave the T-cells intact, and could improve the quality of functional studies performed after multimer labeling *(22)*. The authors describe multimers constructed with a mutated streptavidin molecule that binds a short peptide sequence with a moderate affinity (Kd 10^{-6} M) and biotin with a high affinity (Kd 10^{-13} M). The streptavidin-peptide bonds of the multimer can be competitively disrupted by adding free biotin.

References

1 Walter, E. A., Greenberg, P. D., Gilbert, M. J., et al. (1995) Reconstitution of cellular immunity against cytomegalovirus in recipients of allogeneic bone marrow by transfer of T-cell clones from the donor. *N. Engl. J. Med.* **333,** 1038–1044.

2 Papadopoulos, E. B., Ladanyi, M., Emanuel, D., et al. (1994) Infusions of donor leukocytes to treat Epstein-Barr virus-associated lymphoproliferative disorders after allogeneic bone marrow transplantation. *N. Engl. J. Med.* **330,** 1185–1191.

3 Rosenberg, S. A. (2001) Progress in human tumour immunology and immunotherapy. *Nature* **411,** 380–384.

4 Oelke, M., Moehrle, U., Chen, J. L., et al. (2000) Generation and purification of CD8+ melan-A-specific cytotoxic T lymphocytes for adoptive transfer in tumor immunotherapy. *Clin. Cancer Res.* **6,** 1997–2005.

5 Yee, C., Thompson, J. A., Roche, P., et al. (2000) Melanocyte destruction after antigen-specific immunotherapy of melanoma. Direct evidence of t cell-mediated vitiligo. *J. Exp. Med.* **192,** 1637–1644.

6 Meidenbauer, N., Marienhagen, J., Laumer, M., et al. (2003) Survival and tumor localization of adoptively transferred Melan-A- specific T cells in melanoma patients. *J. Immunol.* **170,** 2161–2169.

7 Altman, J. D., Moss, P. A. H., Goulder, P. J. R., et al. (1996) Phenotypic analysis of antigen-specific T lymphocytes. *Science* **274,** 94–96.

8 Pittet, M. J., Zippelius, A., Speiser, D. E., et al. (2001) Ex vivo IFN-gamma secretion by circulating CD8 T lymphocytes: implications of a novel approach for T cell monitoring in infectious and malignant diseases. *J. Immunol.* **166,** 7634–7640.

9 Appay, V. and Rowland-Jones, S. L. (2002) The assessment of antigen-specific CD8+ T cells through the combination of MHC class I tetramer and intracellular staining. *J. Immunol. Methods* **268,** 9–19.

10 Kwok, W. W., Ptacek, N. A., Liu, A. W., and Buckner, J. H. (2002) Use of class II tetramers for identification of CD4+ T cells. *J. Immunol. Methods* **268,** 71–81.

11 Hercend, T., Meuer, S., Brennan, A., et al. (1983) Identification of a clonally restricted 90 kD heterodimer on two human cloned natural killer cell lines. Its role in cytotoxic effector function. *J. Exp. Med.* **158,** 1547–1560.

12 Mackensen, A., Carcelain, G., Viel, S., et al. (1994) Direct evidence to support the immunosurveillance concept in a human regressive melanoma. *J. Clin. Invest* **93,** 1397–1402.

13 Hoffmann, T. K., Donnenberg, V. S., Friebe-Hoffmann, U., et al. (2000) Competition of peptide-MHC class I tetrameric complexes with anti-CD3 provides evidence for specificity of peptide binding to the TCR complex. *Cytometry* **41,** 321–328.

14 Meidenbauer, N., Hoffmann, T. K., and Donnenberg, A. D. (2003) Direct visualization of antigen-specific T cells using peptide-MHC-class I tetrameric complexes. *Methods* **31,** 160–171.

15 Tan, R., Xu, X., Ogg, G. S., et al. (1999) Rapid death of adoptively transferred T cells in acquired immunodeficiency syndrome. *Blood* **93,** 1506–1510.

16 Nielsen, M. B., Monsurro, V., Migueles, S. A., et al. (2000) Status of activation of circulating vaccine-elicited CD8+ T cells. *J. Immunol.* **165,** 2287–2296.

17 Whelan, J. A., Dunbar, P. R., Price, D. A., et al. (1999) Specificity of CTL interactions with peptide-MHC class I tetrameric complexes is temperature dependent. *J. Immunol.* **163,** 4342–4348.

18 Dutoit, V., Rubio-Godoy, V., Doucey, M. A., et al. (2002) Functional avidity of tumor antigen-specific CTL recognition directly correlates with the stability of MHC/peptide multimer binding to TCR. *J. Immunol.* **168,** 1167–1171.

19 Denkberg, G., Cohen, C. J., and Reiter, Y. (2001) Critical role for CD8 in binding of MHC tetramers to TCR: CD8 antibodies block specific binding of human tumor-specific MHC-peptide tetramers to TCR. *J. Immunol.* **167,** 270–276.

20 Hoffmann, T. K., Loftus, D. J., Nakano, K., et al. (2002) The ability of variant peptides to reverse the nonresponsiveness of T lymphocytes to the wild-type sequence p53(264–272) epitope. *J. Immunol.* **168,** 1338–1347.

21. Xu, X. N. and Screaton, G. R. (2002) MHC/peptide tetramer-based studies of T cell function. *J. Immunol. Methods* **268,** 21–28.

22. Knabel, M., Franz, T. J., Schiemann, M., et al. (2002) Reversible MHC multimer staining for functional isolation of T-cell populations and effective adoptive transfer. *Nat. Med.* **8,** 631–637.

15

Gene Transfer of MHC-Restricted Receptors

**Helmut W. H. G. Kessels, Monika C. Wolkers,
and Ton N. M. Schumacher**

Summary

Adoptive therapy with allogeneic or tumor-specific T-cells has shown substantial clinical effects for several human tumors, but the widespread application of this strategy remains a daunting task. The antigen specificity of T-lymphocytes is solely determined by the T-cell receptor (TCR) α and β chains. Consequently, genetic transfer of TCR chains may form an alternative and potentially appealing strategy to impose a desirable tumor-antigen specificity onto cytotoxic or helper T-cell populations. In this strategy, autologous or donor-derived T-cell populations are equipped with a TCR of defined reactivity in short-term ex vivo cultures, and re-infusion of the redirected cells is used to supply T-cell reactivity against defined tumor-specific antigens.

We have previously described the genetic introduction of T-cell receptor genes into peripheral T-cells in mouse model systems. Here we discuss the requirements for the successful genetic modification of murine T-lymphocytes and the subsequent use of such genetically modified cells in in vivo models.

Key Words: T-cell receptor; gene therapy; adoptive transfer; immunotherapy; retroviral vectors.

1. Introduction

The immune system sometimes falls short in battling diseases because T-cells that can recognize the disease-associated antigens are reduced in number or activity. This deficiency of antigen-specific T-cell immunity can be the result of a more general immunodeficiency, be it acquired (e.g., AIDS, chemotherapy), or congenital. Alternatively, the absence of disease-specific T-cell reactivity can be due to a lack of immunogenicity of the affected cell type, as is the case for most nonviral tumors. In cases where the disease-specific T-cells are absent or reduced in number/activity, therapies that introduce the desired T-cell reactivity through adoptive transfer provide a conceptually attractive approach. The adoptive transfer of T-lymphocytes that contain T-cell receptors (TCR) that recognize tumor-specific targets has provided encouraging results for the treatment of melanoma *(1,2)*. Likewise, the antileukemic effect of HLA-

matched allogeneic bone-marrow transplantation is based on the transfer of novel T-cell reactivities, in this case specific for recipient minor histocompatibility antigens. The main drawback of adoptive therapy with defined T-cell populations is that it is difficult to produce sufficient quantities of antigen-specific T-cells for subsequent infusion. As an alternative to the adoptive transfer of T-cell immunity at the cellular level, T-cell immunity can also be transferred at the level of the T-cell receptor *(3,4)*. In this strategy, autologous or donor-derived T-cell populations are equipped with a TCR of defined specificity in short-term ex vivo cultures, and re-infusion of the redirected cells is used to supply T-cell reactivity against defined antigens. TCR gene therapy is currently developed in a number of preclinical models, and clinical trials for TCR gene therapy will likely commence within several years. Here we discuss the current technology for the genetic modification of T-lymphocytes with exogenous TCR and the in vitro and in vivo analysis of the resulting TCR-modified cell populations in murine preclinical models.

2. Materials

2.1. Production of Retrovirus

1. Phoenix-Eco packaging cell line.
2. Tissue-culture treated 3003 Petri dish (Falcon, BD).
3. FuGENE™ 6 transfection reagent (Roche Molecular Biochemicals).
4. pMX retroviral vector containing both the TCRα and TCRβ coding sequences, separated by an internal ribosomal entry site (IRES) (pMX-TCRα-IRES-TCRβ).
5. Iscove's modified Dulbecco's medium (Life Technologies BV, Scotland) supplemented with 5% fetal calf serum (FCS; BioWhittaker, Belgium), 0.5 μM β-mercaptoethanol (Merck, Germany), penicillin (100 U/mL), and streptomycin (100 μg/mL) (Boehringer Mannheim, Germany).
6. Saponin (Merck).
7. pCLEco (Imgenex).

2.2. Retroviral Infection of Mouse T-Lymphocytes

1. Mouse splenocytes.
2. Concanavalin A (Calbiochem).
3. Interleukin (IL)-7 (Santa Cruz).
4. Twenty-four-well cell-culture plates, flat bottom, tissue-culture treated (Costar).
5. Twenty-four-well cell-culture plates, flat bottom, non-tissue-culture treated (BD).
6. Recombinant human fibronectin fragment CH-296 (RetroNectin™; Takara, Otsu, Japan).
7. Bovine serum albumin (BSA) (Sigma).
8. Phosphate-buffered saline (PBS).
9. RPMI 1640 medium (Life Technologies BV, Scotland) supplemented with 8% FCS (BioWhittaker), penicillin (100 U/mL), and streptomycin (100 μg/mL) (Boehringer Mannheim).
10. Erylysis buffer: 155 mM NH_4Cl, 10 mM $KHCO_3$, 0.1 mM EDTA, pH 7.4.

2.3. Adoptive Transfer and Tracing of Genetically Modified Cells

1. Recipient mice.
2. Hank's buffered salt solution (HBSS, Gibco).
3. Allophycocyanin (APC)-labeled major histocompatibility complex (MHC) tetramers.

4. FITC- or PE-conjugated anti-TCRVα chain and anti-TCRVβ chain mAbs, PE- or APC-conjugated anti-CD8b.2 mAb, PE- or Cy5-conjugated anti-CD4 mAb, FITC-conjugated anti-interferon (IFN)-γ mAb (all mAbs from PharMingen), PE- or Cy5-conjugated F4/80 mAb (Serotec).
5. Propidium iodide (Sigma).
6. rhIL-2 (Chiron).
7. Cytofix/Cytoperm plus kit (PharMingen).
8. AutoMACS or varioMACS (Miltenyi) plus LS/LD columns, anti-PE micro beads (Miltenyi) (optional).
9. MACS buffer: PBS, 0.5% BSA, 2m*M* EDTA (optional).
10. PBA: 1X PBS, 0.5% BSA, and 0.02% sodium azide.
11. Ficoll (Merck).
12. FacsCalibur (Becton Dickinson, MountainView, CA), CellQuest software.
13. Antigenic stimulus (e.g., virus, tumor cells, vaccine).

3. Methods

The methods described below outline (1) the production of retroviruses that contain RNA that encodes the desired TCR chains; (2) the procedure to infect murine T-cells with TCR-encoding retroviruses and the in vitro analysis of the resulting cells; and (3) the transfer of transduced T-cells to recipient mice and the subsequent detection and functional characterization of TCR-transduced T-cells in these mice.

3.1. Production of Retrovirus

The production of retroviruses that, upon infection, provide T-cells with a new set of TCR genes is described and includes (1) a description of the retroviral vector and the conditions such a vector should meet for TCR gene transfer; and (2) a description of the procedure to generate retrovirus by transfection of producer cell lines.

3.1.1. Retroviral Plasmids

The pMX expression system is a Moloney leukemia virus (MLV)-based retroviral expression system developed by Kitamura *(5)*. A sequence encoding both the TCRα and the TCRβ chain separated by an IRES is inserted into the pMX vector between the viral long terminal repeats (LTRs). In this setting, expression of the transgene is driven by the MLV-LTR promoter. All current TCR transfer strategies make use of retroviral vector systems for gene transfer because retroviral integration into the host genome allows for the stable transmission of the transgene through cell division (*see* **Note 1**). This ensures that the transgene will remain resident in T-cells undergoing extensive proliferation upon activation. The pMX retroviral vector is a minimal retroviral expression vector that does not encode an antibiotic resistance marker or other markers to detect genetically modified cells, in order to minimize the immunogenicity of the retrovirally modified T-cells in in vivo experiments (*see* **Note 2**).

3.1.2. Transfection of Producer Cells

For the generation of retroviruses, we transiently transfect the retroviral packaging cell line Phoenix, created by the Nolan laboratory (*see* Website: http://www.stanford.edu/group/nolan/). This helper-defective packaging line is capable of producing all

the necessary trans proteins (gag, pol, and env) that are required for packaging, processing, reverse transcription, and integration of recombinant genomes. For the production of retroviruses, either the Phoenix-Ampho or Phoenix-Eco cell line can be used. The retroviral particles that are produced in these systems carry different envelope proteins (amphotropic vs ecotropic) and thereby determine the tropism of the resulting recombinant retrovirus. The ecotropic packaging system is capable of delivering genes to dividing murine or rat cells, whereas the amphotropic system is capable of delivering genes to dividing cells of most mammalian species, including human cells. Pseudotyping with other envelope proteins is possible and can lead to enhanced transduction efficiency, depending on the cell type that is targeted (*see* **Note 3**).

In our TCR gene-transfer experiments, where viruses are produced to infect mouse splenocytes, the Phoenix-Eco cell line is transiently transfected with the pMX-TCRα-IRES-TCRβ using the FuGENE 6 transfection reagent according to the manufacturer's protocol (FuGENE is a multi-component lipid-based transfection reagent that complexes with DNA and mediates transport of DNA into the cell during transfection). In short:

1. Twenty-five microliters FuGENE reagent is added to 800 μL serum-free Iscove's medium.
2. After a 5-min incubation at room temperature, 20 μg purified retroviral plasmid DNA is added. At this stage, 7.5 μg of pCLEco DNA can be added for improved virus titers *(6)*.
3. After a 15-min incubation at room temperature, the FuGENE/DNA suspension is added to a culture dish (10 cm diameter) containing Phoenix cells grown to approx 30% confluency in 10 mL Iscove's medium.
4. Twenty-four h after transfection, the medium of the Phoenix culture is replaced with 7 to 12 mL Iscove's medium, depending on the amount of virus needed.
5. Another 24 h later, at the peak of virus production, the retroviral supernatant is collected and spun (425*g*, 10 min) to remove all producer cells.

The retroviral supernatant is directly used for the transduction procedure. The supernatants can also be stored at –70°C, although virus titers may drop as a result of the freeze-thaw cycle.

The efficiency of transfection of producer cells is often determined by flow cytometry in cases where proteins are generated that are expressed at the cell surface, or in case a fluorescent marker gene is used. However, TCR gene products are not transported to the cell surface in virus producer cell lines due to the absence of CD3 components, and we therefore use an alternative assay to monitor transfection efficiency (Calogero et al., unpublished). In this protocol, TCRα or TCRβ chain expression is determined by intracellular antibody staining. The transfected Phoenix cells are collected and permeabilized with 1 mg/mL saponin, which permeabilizes both plasma and internal membranes. The cells are washed and stained with a fluorochrome-labeled TCR-specific antibody, and subsequently analyzed by flow cytometry. Transfection efficiencies can vary between 10 and 100% of Phoenix cells, depending on both the fitness of the Phoenix cell culture and purity of the DNA. High-level transduction of mouse T-cells is generally achieved only with retroviral supernatant of Phoenix cells transfected with greater than 40% efficiency. It is noted that depending on the experimental setup it can be desirable to generate stable transfectants of producer cell lines (*see* **Note 4**).

3.2. Retroviral Infection of Mouse T-Lymphocytes

Retroviruses can be used to stably transduce mouse T-cells with a desired TCR. The procedure to infect mouse T-cells with such retroviruses, and methods to test transgene expression are described under **Subheadings 3.2.2.** and **3.2.3.**

3.2.1. Generation of Spleen Cell Cultures

Moloney-based retroviruses can integrate into the genome only of dividing cells (*see* **Note 5**), and in line with this, the transduction efficiency of resting T-cells is negligible. To obtain actively dividing T-cells, mouse splenocytes are stimulated with concanavalin A (ConA) and IL-7 2 d prior to transduction. ConA is a lectin that activates T-cells by cross-linking membrane glycoproteins, and IL-7 is added to improve the survival of T-cells. For the isolation of splenocytes, a freshly removed spleen is dispersed by pressing the spleen through a cell strainer using a plunger. Erythrocytes are removed by resuspending the spleen cells in 3 mL erylysis buffer and incubating for 3 min on ice. The splenocytes are washed and resuspended in RPMI 1640 medium containing 2 µg/mL concanavalin A (ConA) and 1 ng/mL IL-7, and are cultured at 37°C for 48 h in tissue culture-treated 24-well plates at 3×10^6 cells per well. Total splenocytes rather than purified T-cells are used for ConA/IL-7 stimulation, as T-cell activation is dependent on the presence of non-T accessory cells. In addition, the presence of activated CD4$^+$ cells appears to benefit the survival of CD8$^+$ T-cells upon ConA activation. In experimental setups where it is desirable to use selected CD8$^+$ T-cell populations, such cell populations should be isolated subsequent to the transduction procedure (*see* **Subheading 3.3.1.**). In contrast, the depletion of CD8$^+$ T-cells before transduction does not affect the survival or transduction efficiency of CD4$^+$ T-cells.

3.2.2. Infection of Spleen Cell Cultures

1. Non-tissue-culture-treated 24-well plates are coated with 0.5 mL of 50 µg/mL recombinant human fibronectin fragment CH-296 at room temperature for 2 h.
2. The CH-296 solution is removed and replaced with 1 mL 2% bovine serum albumin in PBS for 30 min at room temperature, and plates are washed with PBS.
3. Two d after ConA stimulation, the splenocytes are plated on CH-296-coated plates (3×10^6 cells/well) in 0.5–1 mL of retroviral supernatant. The plates are subsequently centrifuged for 90 min at 425g (spin infection), after which the cells are cultured at 37°C.

3.2.3. In Vitro Analysis of Transgene Expression

Twenty-four to forty-eight h after transduction, transgene expression can be monitored. Maximal transgene expression is observed after 48 h, but analysis at an earlier time point may be preferred, as prolonged in vitro culture adversely affects the subsequent in vivo survival of modified T-cells *(7)*.

To detect whether T-cells express the introduced TCR, the cells can be stained with antibodies that are specific for the TCRVα and TCRVβ subfamily used by the introduced TCR, and analyzed by flow cytometry. This approach is not feasible for all T-cell receptors because the required Vα- and Vβ-specific antibodies may be lacking. An additional limitation of this approach is that even when expression of both the TCR

α and β chain can be detected, this does not provide definitive proof for expression of the correct TCR heterodimer, as it is (at least formally) possible that the observed staining reflects assembly of the exogenous TCR chains with endogenous TCR subunits (*see* **Note 6**). Transduced T-cells are preferably stained with soluble MHC-tetramers *(8)* in combination with CD8- or CD4-specific antibodies to provide direct proof for transgenic TCR expression. MHC class I tetramer staining is performed in PBA at room temperature for 15 min. MHC class II tetramer staining is performed in culture medium at 37°C for 3.0–3.5 h. Staining with (CD4- or CD8-specific) antibodies is performed during the last 20 min of tetramer staining. In case of MHC class II tetramer staining, cells are also stained with the macrophage marker F4/80 specific mAbs to reduce background staining *(9)*. Propidium iodide (1 µg/mL) is included prior to analysis to be able to exclude dead cells. In our hands, transduction efficiencies for both CD4+ and CD8+ T-cells as judged by TCR expression can vary between 5 and 40% of total T-cells. This likely forms an underestimate of the true frequency of modified T-cells, as some of the resulting T-cells express the introduced TCR at a level that is below the threshold for detection (*see* **Note 7**). Of the currently available systems for retroviral transfer, the typing of retroviral particles with the ecotropic receptor results in the highest transduction efficiency for mouse T-cells. Transduction of human T-cells (with a GFP marker gene) has been reported to be most efficient with the use of the MLV 10A1 receptor *(10)*, although in our hands transduction frequencies up to 60% have also been reached with the Phoenix-Ampho system (Jorritsma et al., unpublished observations).

3.2.4. In Vitro Analysis of Transgene Function

To test whether antigen recognition by the introduced TCR results in successful signaling and subsequent activation of T-cells, expression of cell-surface markers associated with T-cell activation (e.g., CD69, CD40L) can be determined by cell-surface staining. Alternatively, antigen-induced cytokine production (e.g., IFN-γ, IL-2, tumor necrosis factor [TNF]-α) or production of cytotoxic granule components (e.g., granzyme B) can be determined by intracellular staining. Because ConA-stimulated T-cells have a very limited lifespan in vitro (*see* **Note 9**), the in vitro analysis of transduced T-cells is preferably performed within 1–3 d after transduction.

Protocol for intracellular cytokine staining of CD8+ T-cells:

1. Incubate transduced cells for 5 h at 37°C in the presence of rhIL-2 (10 CU/mL), Brefeldin-A (1 µL/mL), and (different concentrations of) antigenic peptide.
2. After incubation, cells are surface stained with PE-conjugated anti-CD8b.2 mAb for 15 min on ice, washed, and incubated in Cytofix/Cytoperm solution for 20 min on ice.
3. After washing, the cells are stained with FITC-conjugated anticytokine mAb on ice for 20 min.
4. Cells are washed and resuspended in PBA, and analyzed by flow cytometry.

Because in most cases only a fraction of antigen-specific T-cells produce detectable levels of a given cytokine upon antigen encounter, the percentage of cells that is positively stained for this cytokine will provide an underestimate of the total percentage of transduced T-cells.

3.3. Adoptive Transfer and Tracing of Genetically Modified Cells

The functional capacity of redirected T-cells can be analyzed in vivo in mouse models of viral infection and tumor growth. The monitoring of redirected T-cell function in such models is described in **Subheadings 3.3.2.** and **3.3.3.**

3.3.1. Infusion of Genetically Modified Cells

T-cell transfer into mice combined with subsequent antigenic stimulation allows the examination of the in vivo behavior of redirected T-cells. Since a large fraction of spleen cells do not survive the procedure of retroviral transduction, dead cells are removed by a Ficoll step before infusion into mice, 1–3 d after transduction. Viable transduced spleen cells can be directly used for infusion, but in cases where purified CD4+ or CD8+ T-cell populations are preferred, CD4+ or CD8+ T-cells can either be isolated or depleted from the splenocyte population prior to adoptive transfer by magnetic cell separation (MACS).

To this purpose:

1. Stain the splenocyte population with PE-conjugated (CD4- or CD8-specific) antibodies following the Ficoll step for 15 min on ice in culture medium.
2. Cells are washed twice and anti-PE microbeads are added in culture medium according to the manufacturer's protocol (Miltenyi; anti-FITC and anti-APC MACS beads are also available).
3. Cells are washed twice in culture medium, resuspended in MACS-buffer, and loaded on a positive or negative selection column (LS or LD columns, respectively).
4. The desired cell fraction is collected and washed twice with HBSS.
5. The cells are resuspended in a small volume of HBSS, such that each mouse receives the desired amount of transduced cells in an injection volume of 200 μL.
6. The cell suspensions are transported on ice, and administered immediately by intravenous injection. Prior to injection, the recipient mice are fixated and exposed to ionizing radiation (IR) light for approx 3 min (time frame depending on the mouse strain), until dilation of the tail veins is visible (note: long exposure to IR light will cause dehydration of mice).

The number of redirected T-cells that needs to be infused to induce a significant immune response depends both on the quality of the introduced TCR and the antigenic challenge administered, but in most cases very small numbers of cells will suffice. For the influenza A/NT/60/68-specific F5 TCR, and for the chicken ovalbumin-specific OT-I TCR, infusion of only 10^3 to 10^5 TCR-transduced CD8+ T-cells yields a large population of redirected cells (3–30% of the total CD8+ T-cell population) upon influenza A infection, or upon tumor challenge with a transplantable tumor cell line that expresses the corresponding T-cell epitope.

3.3.2. Tracing of Genetically Modified Cells

T-cell maintenance or expansion can be determined either by flow-cytometry analysis of peripheral blood cells, which allows the longitudinal analysis of T-cell populations within individual mice, or by analysis of lymphoid or peripheral organs at specific time points. To collect peripheral blood T-cells for analysis:

1. Harvest approx 50 µL blood in 1 mL PBS/heparin solution.
2. Cells are spun, resuspended in 1 mL erylysis buffer, and incubated for 15 min on ice to remove erythrocytes.
3. After spinning for 5 min at 153*g*, the supernatant (containing the erythrocytes) is removed, and the cells are resuspended in PBA.
4. The staining procedure is performed as described below or in **Subheading 3.2.3.**

Lymphocytes may also be isolated from peripheral organs such as spleen, secondary lymphoid organs, lung, and liver. To prepare cell suspensions from spleen or secondary lymphoid organs, organs are dispersed by pressing through a cell strainer as described under **Subheading 3.2.1.** When necessary, erythrocytes are removed from organs by incubation in erylysis buffer for 2–3 min on ice. Isolation of lymphocytes from other organs is described elsewhere *(11)*. Redirected T-cell responses in peripheral blood or solid organs can be followed through the use of donor cells that express an allotype marker that differs from the recipient allotype, or by using retroviral vectors that carry a selection marker or reporter molecule (*see* **Note 2**). However, both allotype markers and retroviral markers can be regarded as non-self by the host immune system. Although the magnitude of the immune response induced by different markers varies *(12–15)*, immune responses directed against the redirected T-cells can result in a decreased efficiency of TCR gene transfer, especially when long-term reactivity is required.

To circumvent possible host rejection of redirected T-cells, a setting is preferred where the transduced cells are congenic (or autologous) and where retroviral marker genes are absent. Vα/Vβ or MHC tetramer staining may be used in such situations (*see* **Subheading 3.2.3.**). However, these techniques do not distinguish endogenous and exogenous T-cell responses. As an alternative strategy, TCR-transduced T-cells can be traced by monitoring dual Vβ expression. In contrast to the sizable population of T-cells that expresses two Vα chains, the vast majority (approx 99%) of human and mouse T-cells express only one Vβ chain *(16–18)*. Consequently, responses of TCR-modified T-cells can be followed by flow-cytometric analysis of T-cells that express the Vβ element used by the transgenic TCR in addition to one of the other Vβ elements. Lymphocytes are stained for 15 min at room temperature with a mixture of all available FITC-conjugated Vβ chains except the one that is used by the donor TCR (this mixture is referred to as Vβ pool). Co-staining is performed with a PE-conjugated antibody specific for the Vβ element used by the transgenic TCR, and APC-labeled anti-CD4 or anti-CD8 lineage markers. Before analysis by flow cytometry, PI is added for exclusion of dead cells from analysis. The percentage of TCR-transduced T-cells is determined by calculating the fraction of Vβ pool[+] T-cells that is also positive for the Vβ element of the transgenic TCR.

3.3.3. In Vivo Function of Genetically Modified Cells

Analysis of the in vivo function of genetically modified cells focuses on two separate issues: (1) The capacity of the modified cells to expand and home to the site of inflammation; and (2) the capacity of the modified cells to contribute to clearance of antigen-expressing cells.

Viral infection (e.g., influenza A infection) is a good means to analyze the basic function of redirected T-cells because it provides a strong antigenic stimulus. For TCR

with specificities other than influenza antigens, recombinant influenza strains can be generated that contain the desired T-cell epitope *(19)*. Influenza A infection is carried out intranasally. Upon anesthesia of the mice with diethylether, the viral mixture is dropped onto the nose in a volume of 50 µL HBSS. The mouse takes up the viral fluid while inhaling. The influenza infection can be performed the same d as the T-cell transfer, but may also be performed 1–3 d later.

Expansion of modified T-cells upon encounter with the antigen of interest can be followed as described in **Subheading 3.3.2.** The T-cell response may peak earlier than the endogenous T-cell response, either because the transferred T-cells have been activated prior to adoptive transfer or because of the increase in precursor frequency.

The effectiveness of transferred T-cells in clearing antigen-expressing cells may in theory be determined by quantifying the virus titer in the infected organ (i.e., in lung for the influenza A model). However, such assays are useful only in viral infection models where the contribution of T-cell immunity in viral clearance is significant, and in wild-type mice, immune control of influenza A infection is largely due to the humoral immune response. Consequently, control of influenza A infection by redirected T-cells can be assessed only in mice that lack the endogenous B-cell compartment, such as RAG-1-deficient mice *(20)*.

T-cell dependent models for tumor rejection (or autoimmunity) are better suited to analyze the contribution of redirected T-cells in clearing the antigen-expressing cell population. For transplantable tumor models (*see* **Note 10**), the effectiveness of T-cell therapy can be determined either in a prophylactic setting by injecting T-cells prior to tumor injection, or in a curative setting that involves T-cell transfer several days after tumor inoculation, when the tumor is measurable. Prior to inoculation, tumor cells are washed twice with HBSS and are injected subcutaneously, intravenously, or intraperitoneally, depending on the tumor model used. The growth of subcutaneous tumors can easily be followed by conventional caliper measurements. In order to monitor tumor growth in intraperitoneal or intravenous model systems, tumor cells may be modified by the introduction of a luciferase gene. Intraperitoneal injection of the luciferase substrate luciferin can then be used to monitor tumor growth in internal organs in a noninvasive fashion with a CCD camera (Jorritsma et al., unpublished).

4. Notes

1. Dr. Alain Fischer and coworkers have successfully used retroviral-based gene transfer for the treatment of children that suffer from severe combined immunodeficiency (SCID). SCID-X1 disorder is caused by mutations in a single gene, coding for the cytokine receptor common gamma (γc) chain. Restoration of gamma c expression in stem cells of these patients by gene transfer led to a near complete immune reconstitution. Unfortunately, the initial success of this gene therapy trial has been clouded by the occurrence of leukemic disorders in two of the treated patients *(21)*. Although still under investigation, insertional mutagenesis by the retroviral transgenes is likely to have been one of the critical factors in the observed cellular transformation. Whether the incidence of cellular transformation is dependent on the type of transgene used or/and the number of divisions that the transduced cells undergo will require further evaluation. Nonetheless, these serious side effects are likely to at least temporarily limit the use of retrovirus-mediated human gene therapy

trials to life-threatening conditions where alternative treatment options are lacking. In addition, the adverse events in the SCID-X1 trial provide a strong incentive for the continued development of gene-transfer systems in which the chances of cellular transformation due to insertional mutagenesis are reduced. Current candidates form systems for site-specific integration and gene-transfer systems that are maintained episomally.

2. To distinguish donor T-cells from the host T-cell population, extracellular allotype markers such as Ly5, Ly1, and Thy1, or intracellular biochemical markers such as glucose-phosphate-isomerase (Gpi) can be used. Ly5 (CD45) is often used as surface marker in cell transfer experiments, as all bone-marrow-derived cells (except erythrocytes and erythroblasts) express this molecule. The transferred donor cells (e.g., Ly5.1) can be distinguished from the host cells (e.g., Ly5.2) by staining tissue samples from the mice ex vivo with Ly5.1- or Ly5.2-specific antibodies. However, minor immunological disparities between donor and host cells can affect cell survival when allotype markers such as Ly5 are used in transplantation studies *(22)*. Alternatively, autologous T-cells may be equipped with an intracellular reporter molecule (e.g., GFP) or an antibiotic resistance marker (e.g., neomycin, hygromycin) through the inclusion of marker genes in the retroviral vector. However, expression of such intracellular markers in gene-modified T-cells has likewise been shown to make the transferred cells immunogenic to the host T-cell immune system *(12–14)*.

3. A large series of alternative envelopes has been developed in particular for the transduction of human cells. A Phoenix cell line called Phoenix-gp is available that expresses only gag-pol and that can be used for pseudotyping of retroviral virions by co-transfection of the gene encoding one of the alternative envelope proteins (e.g., gibbon ape leukemia virus envelope or vesicular stomatitis VSV-G protein). Producer cell lines that already carry one of the alternative envelopes are also available from a number of commercial and non-commercial sources. A recent study demonstrated that transduction of primary human CD8$^+$ and CD4$^+$ T-cells occurs with very high efficiency with retroviral vectors pseudotyped with the envelope of the amphotropic murine leukemia virus 10A1 (MLV-10A1) *(10,23)*. The superior efficiency of MLV-10A1 seen in this study could be correlated to the longer half-life of this pseudotype in comparison to A-MLV, and to the usage of both the A-MLV (Pit2) and the GaLV receptor (Pitl) for cell entry.

4. To facilitate the production of viral supernatants, and to increase viral titers, stable transfectants of producer cell lines can be generated by including a selection marker in the retroviral vector. Such markers may be included either between the viral LTRs or in the vector backbone. Only in the former case will the marker gene also be present in the retroviral genome and therefore be expressed in retrovirally transduced cells (*see* **Note 2**). Alternatively, the producer cell line can be co-transfected with a separate vector that only contains the selection marker. In this case, the vector that contains the marker gene should be present at substoichiometric amounts during transfection (10- to 20-fold lower) compared to the vector that contains the TCR, in order to increase the chance that the selected producer cells also contain the TCR construct of interest. The nuclear replication and retention functions of the Epstein-Barr virus have been used to maintain retroviral vectors episomally within retroviral packaging cell lines *(24)*. These hybrid EBV/retroviral vectors carry a selection marker and can be used to rapidly generate high-titered retroviral stocks. A disadvantage of these hybrid vector systems is that due to their size, recombination of vector sequences is sometimes observed during growth in *E. coli*.

5. The T-cell activation and proliferation required for retroviral transduction with Moloney-based vector systems may affect the viability and possibly immune competence of the

transduced cells. HIV-derived, lentiviral vectors have been put forward as an alternative, as these retroviral systems effectively infect resting T-cells. It is noted that also in this case stimulation of naïve T-cells with cytokines is required to obtain high transduction efficiencies *(25,26)*.

6. The introduction of TCR chains into mature T-cells will result in pairing of introduced chains with endogenous TCR chains. In cases where these mixed TCR dimers will be formed preferentially over the desired dimer of both exogenous chains, the transduced cells will express both TCRα and TCRβ on their surface, but may not possess reactivity towards the antigen of interest.

7. In the Moloney-based retroviral transduction system used by us, the surface expression level of the introduced TCR is about three- to fivefold lower than that of the endogenous TCR. This lower TCR expression may reduce the sensitivity of the resulting T-cells, although the magnitude of this effect is likely to be modest *(27)*. In addition, the lower expression level of the introduced TCR can in some cases complicate efforts to detect the TCR-modified cells. When necessary, the expression level of introduced TCR may be improved by using constructs that have an increased promoter activity or by enhancing transgene expression at the post-transcriptional level *(28)*. Surface expression of the desired TCR heterodimer is likely to also be reduced as a consequence of the formation of mixed TCR dimers between endogenous and exogenous TCR chains *(29)*, an issue that remains unresolved to date (*see* **Note 8**).

8. Pairing of introduced and endogenous TCR chains will lead to the formation of mixed TCR dimers with unanticipated specificities *(29)*, and may possibly lead to the generation of auto-reactive T-cells. Although no incidences of auto-immunity upon TCR gene transfer in a large number of mouse experiments have been observed to date (Wolkers et al., unpublished), the risk of autoimmunity due to inadvertent pairing is clearly TCR dependent and should be re-evaluated for every single TCR used. Efforts to remodel the interface of TCR α-β interaction in such a way that introduced TCR chains preferentially pair with each other, are currently being undertaken and may offer a solution to this problem. In addition, several groups have developed chimeric receptors for gene transfer into T-cells. These receptors consist of a single-chain antibody that is coupled to signaling modules that are normally present in the T-cell receptor (TCR) complex, or are composed of recombinant (e.g., single chain) T-cell receptors *(30)*. The rationale for the production of these receptors is that they can confer antigen-recognition potential to T-cells that is not complicated by the formation of mixed TCR dimers, and in the case of antibody-based receptors, can be MHC independent. While chimeric receptors form an appealing concept, the available data suggest that the current-generation chimeric receptor systems do not function as well as conventional T-cell receptors in redirecting T-cell immunity.

9. ConA-stimulated T-cells are not all that happy. Three d after ConA/IL-7 stimulation (1 d after transduction), approx 30–50% of splenocytes has died, while 6 d after stimulation (3 d after transduction), up to 90% of the cells are no longer viable. Both in vitro and in vivo studies with retrovirally transduced murine T-cells are therefore preferably performed shortly after the transduction procedure. This inconvenience is mouse-related; human T-cells have been shown to be much more robust and can be cultured for prolonged periods in vitro after being activated and transduced.

10. The tumor model systems used to date in TCR gene-transfer studies (and described here) rely on transplantable tumor cell lines, but it is clear that the concepts that will emerge from these studies will require further validation in spontaneous tumor models that much more closely mimic the human situation.

Acknowledgments

References

1 Dudley, M. E., Wunderlich, J. R., Robbins, P. F., et al. (2002) Cancer regression and autoimmunity in patients after clonal repopulation with antitumor lymphocytes. *Science* **298,** 850–854.

2 Yee, C., Thompson, J. A., Byrd, D., et al. (2002) Adoptive T cell therapy using antigen-specific CD8+ T cell clones for the treatment of patients with metastatic melanoma: in vivo persistence, migration, and antitumor effect of transferred T cells. *Proc. Natl. Acad. Sci. USA* **99,** 16,168–16,173.

3 Dembic, Z., Haas, W., Weiss, S., et al. (1986) Transfer of specificity by murine alpha and beta T-cell receptor genes. *Nature* **320,** 232–238.

4. Kessels, H. W., Wolkers, M. C., and Schumacher, T. N. (2002) Adoptive transfer of T-cell immunity. *Trends Immunol.* **23,** 5, 264–269.

5 Kitamura, T. (1998) New experimental approaches in retrovirus-mediated expression screening. *Int. J. Hematol.* **67,** 351–359.

6 Naviaux, R. K., Costanzi, E., Haas, M., and Verma, I. M. (1996) The pCL vector system: rapid production of helper-free, high-titer, recombinant retroviruses. *J. Virol.* **70,** 5701–5705.

7 Kolen, S., Dolstra, H., van de Locht, L., et al. (2002) Biodistribution and retention time of retrovirally labeled T lymphocytes in mice is strongly influenced by the culture period before infusion. *J. Immunother.* **25,** 385–395.

8 Altman, J. D., Moss, P. A., Goulder, P. J., et al. (1996) Phenotypic analysis of antigen-specific T lymphocytes. *Science* **274,** 94–96.

9 Schepers, K., Toebes, M., Sotthewes, G., et al. (2002) Differential kinetics of antigen-specific CD4+ and CD8+ T cell responses in the regression of retrovirus-induced sarcomas. *J. Immunol.* **169,** 3191–3199.

10 Uckert, W., Becker, C., Gladow, M., et al. (2000) Efficient gene transfer into primary human CD8+ T lymphocytes by MuLV-10A1 retrovirus pseudotype. *Hum. Gene Ther.* **11,** 1005–1014.

11 Masopust, D., Vezys, V., Marzo, A. L., and Lefrancois, L. (2001) Preferential localization of effector memory cells in nonlymphoid tissue. *Science* **291,** 2413–2417.

12 Riddell, S. R., Elliott, M., Lewinsohn, D. A., et al. (1996) T-cell mediated rejection of gene-modified HIV-specific cytotoxic T lymphocytes in HIV-infected patients. *Nat. Med.* **2,** 216–223.

13 Jung, D., Jaeger, E., Cayeux, S., et al. (1998) Strong immunogenic potential of a B7 retroviral expression vector: generation of HLA-B7-restricted CTL response against selectable marker genes. *Hum. Gene Ther.* **9,** 53–62.

14 Stripecke, R., Carmen Villacres, M., Skelton, D., Satake, N., Halene, S., and Kohn, D. (1999) Immune response to green fluorescent protein: implications for gene therapy. *Gene Ther.* **6,** 1305–1312.

15 Skelton, D., Satake, N., and Kohn, D. B. (2001) The enhanced green fluorescent protein (eGFP) is minimally immunogenic in C57BL/6 mice. *Gene Ther.* **8,** 1813–1814.

16 Davodeau, F., Peyrat, M. A., Romagne, F., et al. (1995) Dual T cell receptor beta chain expression on human T lymphocytes. *J. Exp. Med.* **181,** 1391–1398.

17 Padovan, E., Giachino, C., Cella, M., Valitutti, S., Acuto, O., and Lanzavecchia, A. (1995) Normal T lymphocytes can express two different T cell receptor beta chains: implications for the mechanism of allelic exclusion. *J. Exp. Med.* **181,** 1587–1591.

18 Balomenos, D., Balderas, R. S., Mulvany, K. P., Kaye, J., Kono, D. H., and Theofilopoulos, A. N. (1995) Incomplete T cell receptor V beta allelic exclusion and dual V beta-expressing cells. *J. Immunol.* **155,** 3308–3312.

19 Topham, D. J., Castrucci, M.R., Wingo, F.S., Belz, G.T., and Doherty, P.C. (2001) The role of antigen in the localization of naive, acutely activated, and memory CD8(+) T cells to the lung during influenza pneumonia. *J. Immunol.* **167,** 6983–6990.

20 Moskophidis, D. and Kioussis, D. (1998) Contribution of virus-specific CD8+ cytotoxic T cells to virus clearance or pathologic manifestations of influenza virus infection in a T cell receptor transgenic mouse model. *J. Exp. Med.* **188,** 223–232.

21 Hacein-Bey-Abina, S., von Kalle, C., Schmidt, M., et al. (2003) A serious adverse event after successful gene therapy for X-linked severe combined immunodeficiency. *N. Engl. J. Med.* **348,** 255–256.

22 van Os, R., Sheridan, T. M., Robinson, S., Drukteinis, D., Ferrara, J. L., and Mauch, P. M. (2001) Immunogenicity of Ly5 (CD45)-antigens hampers long-term engraftment following minimal conditioning in a murine bone marrow transplantation model. *Stem Cells* **19,** 80–87.

23 Gladow, M., Becker, C., Blankenstein, T., and Uckert, W. (2000) MLV-10A1 retrovirus pseudotype efficiently transduces primary human CD4+ T lymphocytes. *J. Gene Med.* **2,** 409–415.

24 Kinsella, T. M. and Nolan, G. P. (1996) Episomal vectors rapidly and stably produce high-titer recombinant retrovirus. *Hum. Gene Ther.* **7,** 1405–1413.

25 Unutmaz, D., KewalRamani, V. N., Marmon, S., and Littman, D. R. (1999) Cytokine signals are sufficient for HIV-1 infection of resting human T lymphocytes. *J. Exp. Med.* **189,** 1735–1746.

26 Cavalieri, S., Cazzaniga, S., Geuna, M., et al. (2003) Human T lymphocytes transduced by lentiviral vectors in the absence of TCR-activation maintain an intact immune competence. *Blood* **102(2),** 497–505.

27 Labrecque, N., Whitfield, L. S., Obst, R., Waltzinger, C., Benoist, C., and Mathis, D. (2001) How much TCR does a T cell need? *Immunity* **15,** 71–82.

28 Zufferey, R., Donello, J. E., Trono, D., and Hope, T. J. (1999) Woodchuck hepatitis virus posttranscriptional regulatory element enhances expression of transgenes delivered by retroviral vectors. *J. Virol.* **73,** 2886–2892.

29. Schumacher, T. N. (2002) T-cell-receptor gene therapy. *Nat Rev Immunol* **7,** 512–519.

30. Eshhar, Z. (1997) Tumor-specific T-bodies: towards clinical application. *Cancer Immunol. Immunother.* **45,** 131–136.

16

Immunotherapy With CTL Restricted by Nonself MHC

Liquan Gao, Anne-Marie Downs, and Hans J. Stauss

Summary

In the past years a number of target antigens recognized by cytotoxic T-lymphocytes (CTL) have been identified in human malignancies. In most cases, the CTL-recognized antigens did not arise from mutations, but were instead encoded by genes that were identical in normal and tumor cells. Gene expression in normal tissues may result in tolerance of high avidity CTL, leaving behind low avidity CTL that cannot provide effective immunity against tumors expressing the relevant target antigens. In this chapter we describe a strategy to circumvent immunological tolerance that can be used to generate high avidity CTL against self-proteins, including human tumor-associated antigens.

Key Words: Cytotoxic T-lymphocytes; tumor; immunotherapy; tolerance; allorestriction; avidity.

1. Introduction

One of the most significant advances in the field of tumor immunology has been the identification and characterization of tumor antigens that are recognized by CTL *(1–3)*. Whilst the expression of some tumor antigens is restricted solely to the tumor cell, many tumor antigens are also expressed in normal tissues *(4–6)*. Expression in the thymus is likely to cause deletion of high-avidity CTL specific for peptides presented by self-MHC class I molecules. As a result, low-avidity CTL will be released into the periphery. These low-avidity tumor antigen-specific CTL may be incapable of recognizing naturally processed antigen on the tumor cell surface and are thus ineffective in tumor rejection. Some high-avidity CTL may escape thymic deletion but are likely to be rendered unresponsive by antigen expression in the periphery. In this chapter we will describe a strategy that can be used to circumvent tolerance and to generate high-avidity CTL specific for tumor antigens that are also expressed in normal tissues.

As T-cell tolerance is self-MHC restricted, the T-cell repertoire is rendered tolerant to self-peptides presented by self-MHC class I molecules but not to peptides presented by allogeneic class I molecules *(7,8)*. It is therefore possible to generate high-avidity peptide-specific CTL from allogeneic donors *(9–12)*. The generation of such allo-

restricted CTL specific for tumor antigens provides a unique opportunity to circumvent tolerance and to produce high-avidity tumor-specific CTL for adoptive immunotherapy, despite the antigen being expressed on both normal and transformed cells *(9,13–16)*.

The frequency of allo-restricted CTL against a given peptide of interest is usually low. In order to isolate and expand these small numbers of CTL, cultures need to be manipulated in order to favor stimulation of peptide-specific CTL and avoid the expansion of allo-reactive CTL, which are present at a much higher frequency. In this chapter, we describe the culture conditions that support the isolation and expansion of low-frequency peptide-specific CTL isolated from allogeneic donors. We focus on the production of allogeneic CTL that are restricted by HLA-A2 class I molecules, because it is the most common class I allele in the Caucasian population. Thus, the protocol describes the isolation of peptide-specific, HLA-A2-restricted CTL from the peripheral blood of HLA-A2-negative healthy donors. The major steps in this process are summarized in **Fig. 1** and comprise (a) bulk stimulation of HLA-A2$^-$ peripheral blood mononuclear cells (PBMC) with TAP-deficient HLA-A2$^+$ antigen-presenting cells (APC) coated with HLA-A2-binding peptides; (b) limiting dilution plating to identify peptide-specific microcultures; and (c) expansion of microcultures and establishment of peptide-specific CTL lines.

2. Materials

2.1. Cells

1. Responder cells: PBMC (separated from buffy coat blood packs).
2. Stimulator cells:
   a. T2 (a TAP [transporter associated with antigen processing]-deficient, HLA-A2$^+$ EBV-transformed human B-cell line) *(17)*
   b. *Drosophila* cells transfected with HLA-A2, human β2-microglobulin, B7.1, and ICAM-1 molecules.
3. HLA-A2$^+$ cells that express the relevant antigen endogenously.
4. HLA-A2$^+$ cells that do not express the relevant antigen endogenously.
5. HLA-A2$^-$ cells that express the relevant antigen endogenously.

2.2. Media, Chemicals, and Apparatus

1. RPMI 1640 (Life Technology, UK).
2. Complete T-cell culture medium (CM): RPMI 1640 containing 10% fetal calf serum (FCS) (*see* **Note 1**), 100U/mL penicillin, 100 µg/mL streptomycin, and 2 m*M* L-glutamine.
3. Schneider's insect cell-culture medium (Invitrogen, UK) containing 5% heat-inactivated FCS.
4. Copper sulphate (Sigma, UK).
5. T75 tissue-culture flasks with filter caps (Helena Biosciences, UK).
6. T75 tissue-culture flasks with sealed caps (Nalgene Nunc, UK).
7. Lymphoprep (Axis Shield, Norway).
8. Dimethyl sulphoxide (DMSO) (Sigma-Aldrich, Poole, UK).
9. Cryovials (Nalgene Nunc).
10. Mouse anti-HLA-A2 monoclonal antibody HB-54 (American Type Culture Collection (ATCC), Manassas, VA) *(18)*.

Day 0: Initial stimulation
Stimulators: peptide-loaded Drosophila transfectants

↓

Day 5: Re-stimulate bulk culture
Stimulators: peptide-loaded T2

Day 12: Limiting dilution
Stimulators: peptide-loaded T2

↓

Day 26: Re-stimulate micro-cultures
Stimulators: peptide-loaded T2

↓

Day 31-32: Split-well analysis
Targets: T2 + irrelevant peptide
          T2 + relevant peptide

↓

**Day 33: Expand micro-cultures to
          48-well plate**
Stimulators: peptide-loaded T2

↓

**Day 40: Expand from 48-well
          to 24-well plate**
Stimulators: peptide-loaded T2

↓

Day 12: Re-stimulate bulk culture
Stimulators: peptide-loaded T2

↓

Day 19: Limiting dilution
Stimulators: peptide-loaded T2

↓

Day 33: Re-stimulate micro-cultures
Stimulators: peptide-loaded T2

↓

Day 38-39: Split-well analysis
Targets: T2 + irrelevant peptide
          T2 + relevant peptide

↓

**Day 40: Expand micro-cultures to
          48-well plate**
Stimulators: peptide-loaded T2

↓

**Day 47: Expand from 48-well
          to 24-well plate**
Stimulators: peptide-loaded T2

Validate CTL → **Cytotoxicity assay** ← Validate CTL
           → **Flow cytometry** ←

↓

Re-stimulate CTL every 7-12 days

Fig. 1. Flow-chart summarizing the process of generating human allo-restricted peptide-specific cytotoxic T-lymphocytes.

11. Mouse anti-HLA-A2 monoclonal antibody HB-117 (ATCC) *(19)*.
12. Sheep antimouse IgG-FITC (Sigma).
13. Phosphate-buffered saline (PBS).
14. Peptides:
    a. HLA-A2-binding relevant peptide of interest.
    b. HLA-A2-binding irrelevant control peptide.
15. Dithiothreitol (DTT) (Sigma).
16. Anti-CD4 monoclonal antibody QS4120 *(20)*.
17. Twenty-four-well tissue-culture plates (Nalgene Nunc).
18. Human recombinant interleukin (IL)-2 (Chiron, Amersterdam-Zuidoost, Netherlands).
19. Human IL-7 (R&D Systems, Abingdon, UK).
20. Round-bottom 96-well tissue-culture plates (Nalgene Nunc).
21. Two-mercaptoethanol (2-ME) (Sigma-Aldrich).
22. ^{51}Cr (sodium chromate aqueous solution) (Amersham, Bucks, UK).
23. One percent trifluoroacetic acid (TFA) (Sigma-Aldrich).
24. LP2 round-bottom tubes (Life Sciences International, UK).
25. Forty-eight-well tissue-culture plates (Nalgene Nunc).
26. Access to: irradiator, radiation facilities for ^{51}Cr work, and gamma counter.

3. Methods

The methods described below outline (1) the in vitro stimulation of HLA-A2$^-$ PBMC with peptide-loaded HLA-A2$^+$ APC; (2) re-stimulation of bulk cultures; (3) limiting dilution plating; (4) the identification of peptide-specific microcultures; and (5) the expansion and validation of peptide-specific microcultures.

3.1. In Vitro Stimulation of HLA-A2$^-$ PBMC With Peptide-Loaded HLA-A2$^+$ APC

CTL lines are generated by incubating PBMC of HLA-A2$^-$ donors with TAP-deficient HLA-A2$^+$ APC. The APC used are unable to present endogenous peptides and can efficiently present exogenously loaded peptides. The commonly used APC are *Drosophila* cells transfected with HLA-A2, human β2-microglobulin, B7.1, and ICAM-1 molecules, T2 cells (TAP-deficient and HLA-A2$^+$) and RMA-S-A2 cells (TAP-deficient murine cell line [RMA-S] transfected with the human HLA-A2 molecule) (*see* **Note 2**). For the initial stimulation, IL-7 is added to the cultures, and for further stimulations, recombinant IL-2 and autologous feeders are also added to the cultures (*see* **Note 3**).

How to set up the initial in vitro stimulation culture is described in **Subheadings 3.1.1.–3.1.4.** . This includes details about the culture of the cell lines used as APC (stimulators) (**Subheading 3.1.1.**), PBMC preparation (responders) (**Subheading 3.1.2.**), preparation of the peptides used (**Subheading 3.1.3.**), and setting up the stimulation cultures (**3.1.4.**).

3.1.1. Culture of Cell Lines To Be Used As Stimulators

All tissue-culture procedures should be performed in a class II tissue-culture cabinet.

3.1.1.1. T2 CELLS

T2 cells should be cultured in T75 tissue-culture flasks in Comple T-cell culture medium (CM), which should be warmed to 37°C prior to use. Split the cells approx twice a wk to a cell density of $1–5 \times 10^5$/mL. Culture the cells in an upright flask in a humidified 37°C incubator with 5% CO_2.

3.1.1.2. *DROSOPHILA* CELLS

Drosophila cells should be cultured in Schneider's insect cell-culture medium supplemented with 5% FCS. Split the cells approx twice a wk by re-seeding the cells to a density of $2–3 \times 10^5$/mL in a fresh T75 flask (with sealed cap). *Drosophila* cells should be incubated at 24°C (with atmospheric CO_2), and the flasks should be placed horizontally. *Drosophila* cells need to be induced with 100 m*M* copper sulphate 48 h prior to peptide loading to induce expression of the transfected HLA-A2 and co-stimulator molecules. After induction, wash cells three times with RPMI in order to remove the copper sulphate before peptide loading.

Screen all cell cultures for mycoplasma regularly.

3.1.2. PBMC Preparation

Described below is the separation of lymphocytes from buffy coat blood packs, the freezing of PBMC for use as feeders, and the staining of PBMC to identify HLA-A2⁻ PBMC.

3.1.2.1. SEPARATION OF LYMPHOCYTES FROM BUFFY COAT BLOOD PACKS

Lymphocytes are separated from buffy coat blood packs by lymphoprep density centrifugation.

1. Ensure blood packs are sterile by spraying with 70% ethanol.
2. Drain the blood (approx 50–80 mL) into a T75 tissue-culture flask.
3. Add an equal volume of room temperature RPMI (containing no additives) and mix well but gently.
4. Pipet 20 mL of lymphoprep (room temperature) into a 50-mL tube and gently apply 30 mL of diluted blood onto the lymphoprep surface.
5. Centrifuge for 20 min at 800*g* (room temperature) with the brake turned off.
6. Collect the interface fraction (approx 10 mL) into a 50-mL tube.
7. Add 40 mL cold RPMI (containing no additives) and centrifuge for 10 min at 800*g*.
8. Repeat this wash step twice.
9. Count the cells and resuspend in CM at a concentration of 5×10^7/mL.

3.1.2.2. FREEZING CELLS

Preparation of cryopreserved stocks of PBMC should be well planned in order to provide enough feeders for re-stimulation of bulk cultures, setting up of microcultures, and establishment of CTL lines.

Freeze:

1. Ten vials of 5×10^6 cells per vial for use as feeders during the early stages of CTL culture.
2. Ten vials of 1×10^7 cells per vial for use as feeders during later stages of CTL culture.
3. The remaining PBMC at 5×10^7 per vial for use as feeders for CTL expansion.

PBMC are cryopreserved in freezing solution containing 20% DMSO, 50% FCS, and 30% RPMI. The freezing solution should be chilled prior to use by storing on ice.

1. Add an equal volume of cold freezing solution to the cell suspension (therefore diluting freezing solution 1:2).
2. Place 1 mL of the cell suspension mixture into a prelabeled cryovial and place the vials on ice.
3. Place the cryovials in a freezing box and store at –80°C overnight.
4. The next d, transfer vials to liquid nitrogen.

3.1.2.3. DETECTION OF HLA-A2⁻ PBMC

HLA status is determined by staining the cells with antibodies that bind to HLA-A2. To determine HLA status, two antibodies are used for staining PBMC—HB-54 (anti-HLA-A2, B17) *(18)* and HB-117 (HLA-A2, A28) *(19)*. The antibodies are detected using secondary staining with antimouse IgG-FITC antibody. Only if *both* antibodies stain positive, are the PBMC from a buffy coat blood pack defined as HLA-A2⁺. If only one of the antibodies binds but not the other, the PBMC are defined as HLA-A2⁻. Only HLA–A2⁻ PBMC should be used as responders and feeders.

3.1.3. Preparation of Synthetic Peptides

Peptides are most commonly synthesized using fluorenylmethoxycarbonyl chemistry. Peptide purity is an important factor and should be greater than 90%. Some peptides can be diluted in PBS and should be diluted to a working stock concentration of 2 mM. Hydrophobic peptides should first be dissolved in DMSO, in a volume that will be one-tenth of the final volume, and then diluted in PBS to produce a working stock concentration of 2 mM. Peptides containing cysteines or methionines should be dissolved in neat DMSO first, in a volume that will be 10% of the final volume. DTT is then added to prevent oxidation and is added at a maximal final concentration of 5 mM (high concentrations of DTT can be toxic to T-cells and APC). Finally, PBS (pH 7.4) is added to produce a final peptide concentration of 2 mM. Peptides should be stored at –20°C in 200-µL aliquots.

3.1.4. In Vitro Stimulation (Day 0)

3.1.4.1. PEPTIDE-LOADING OF STIMULATOR CELLS

1. Induce the *Drosophila* transfectants with copper sulphate 24–36 h prior to setting up the in vitro stimulation (*see* **Subheading 3.1.1.**).
2. On d of setting up the stimulation, wash the required number of *Drosophila* cells three times with RPMI and resuspend the cells (up to 2×10^6) in 200 µL RPMI containing 5% boiled FCS (*see* **Note 4**).
3. Add 10 µL of 2 mM peptide to produce a final peptide concentration of 100 µM and mix well.
4. Incubate at 37°C for 2 h.
5. Wash cells once with RPMI.

3.1.4.2. SETTING UP THE STIMULATION CULTURE

1. Set up two wells on a 24-well tissue-culture plate in 2 mL CM containing the following: 2×10^6 HLA-A2⁻ PBMC (responders); 2×10^5 peptide-loaded *Drosophila* transfectants

(stimulators) (*see* **Note 5**); 2.5 ng/mL human IL-7; 10% mycoplasma-free QS4120 (anti-CD4 monoclonal antibody) *(20)* (*see* **Note 6**).

2. Culture the cells in a humidified incubator at 37°C with 5% CO_2.

3.2. Re-Stimulation of the Bulk Culture

The bulk CTL culture should be re-stimulated with fresh stimulators, feeders, and cytokines on d 5.

1. Re-suspend up to 2×10^6 T2 cells in 200 µL RPMI containing 5% boiled FCS. Add 10 µL of 2 m*M* peptide to produce a final peptide concentration of 100 µ*M* and mix well.
2. Incubate at 37°C for 2 h to peptide-load the T2 cells.
3. Irradiate the T2 cells with 80 Gy and wash once with RPMI.
4. Defrost autologous PBMC for use as feeders: thaw the cells quickly in a 37°C water bath and pipet gently into 10 mL of cold RPMI containing no additives (*see* **Note 7**). Centrifuge for 5 min at 400*g* and resuspend the cell pellet in cold RPMI (no additives) for irradiation. Irradiate the PBMC with 30 Gy, then spin and resuspend the cells in warm CM.
5. Harvest and count the T-cells from the bulk culture (*see* **Note 8**).
6. Place the following cell numbers and cytokines into a fresh 24-well tissue-culture plate (*see* **Note 9**) in 2 mL CM per well:
   a. 1×10^6 T-cells from the bulk culture.
   b. 2×10^5 peptide-loaded T2 cells (irradiated, 80 Gy).
   c. 2×10^6 autologous PBMC (irradiated, 30 Gy).
   d. 10 U/mL human IL-2.
   e. 2.5 ng/mL human IL-7.
7. Culture the cells in a humidified incubator at 37°C with 5% CO_2.

To confirm that the irradiation dose used is sufficient to prevent proliferation of the irradiated cells, always set up one well with irradiated cells only. Add an aliquot of 1×10^5 cells in 1 mL CM in a well of a 24-well tissue-culture plate and culture for 5 d at 37°C. If proliferation of the irradiated cells is observed, the CTL culture must be discontinued and restarted using a higher dose of irradiation.

3.3. Limiting Dilution and Re-Stimulation

This section describes the setting up of limiting dilution cultures (*see* **Subheading 3.3.1.**) and the subsequent re-stimulation of microcultures (*see* **Subheading 3.3.2.**).

3.3.1. Limiting Dilution Cultures

The aim of this procedure is to isolate peptide-specific microcultures. **Fig. 2** shows that without limiting dilution, it is difficult to detect peptide-specific CTL in bulk cultures. Limiting-dilution plating is performed after two and three rounds of bulk stimulation (*see* **Fig.1.**).

1. Harvest and count the T-cells from the bulk culture.
2. Using round-bottom 96-well tissue-culture plates, plate out three plates of 1 responder CTL per well and one plate with 10 responder CTL per well, in 100 µL CM. At this stage, while each well contains very low CTL numbers, CM should contain 5×10^{-5} *M* 2-ME.
3. Add 100 µL CM (containing 5×10^{-5} *M* 2-ME) per well, containing:
   a. 2×10^4 peptide-loaded T2 cells (irradiated, 80 Gy).
   b. 2×10^5 autologous PBMC (recovered from frozen and irradiated, 30 Gy).
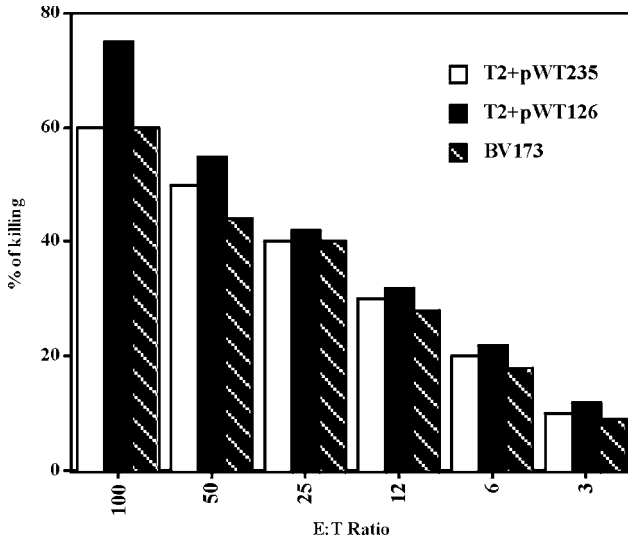
Fig.2. Cytotoxicity assay of a typical bulk culture. Cytotoxic T-lymphocytes (CTL) from a HLA-A2⁻ donor were stimulated with HLA-A2⁺ APC coated with pWT126 peptide. pWT126 and pWT235 *(13,21)* are peptides derived from the tumor-associated antigen Wilms' tumor 1 (WT1), which is a zinc finger transcription factor that is expressed at low levels in normal cells and overexpressed in several malignancies *(22–24)*. CTL from the pWT126-stimulated bulk culture were tested for killing ability after two rounds of stimulation and prior to limiting dilution. The graph shows the percentage of specific killing of T2 cells loaded with relevant (pWT126) and irrelevant (pWT235) peptide (both HLA-A2-binding) and a HLA-A2⁺ leukemia line that expresses WT1 endogenously (BV173). Effector to target cell (E:T) ratios ranged from 100:1 to 3:1. The data demonstrate that prior to limiting dilution there is a high level of HLA-A2 allo-reactivity but no peptide-specific killing of target cells.

    c. 20 U/mL human IL-2 (10 U/mL final concentration).
    d. 5 ng/mL human IL-7 (2.5 ng/mL final concentration).
  4. Re-stimulate the remaining bulk culture and perform a second limiting dilution one wk later. This is to increase the likelihood of isolating the desired CTL. All subsequent procedures then apply as for the first round of limiting-dilution plating.

3.3.2. Re-Stimulation of Microcultures in 96-Well Tissue-Culture Plates

Fourteen d after setting up the limiting-dilution plates, peptide-specific CTL are still in small numbers and need to be expanded by re-stimulating the cells. Remove 100 μL medium from each well and replace with the following in 100 μL CM (containing 5×10^{-5} *M* 2-ME):

1. 2×10^4 peptide-loaded T2 cells (irradiated, 80 Gy).
2. 2×10^5 autologous PBMC (recovered from frozen and irradiated, 30 Gy).
3. 20 U/mL human IL-2 (10 U/mL final concentration).
4. 5 ng/mL human IL-7 (2.5 U/mL final concentration).
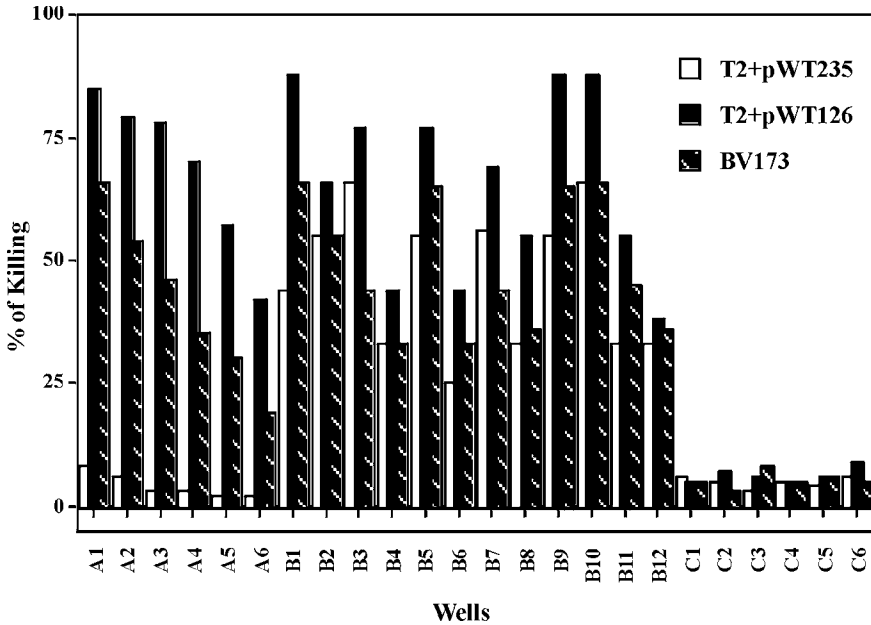
Fig. 3. A typical split-well analysis of 96-well microcultures (shown are 24 wells only). These microcultures were derived from limiting dilution of the bulk cultures described in **Fig. 2**. Wells A1–A6 show good killing of T2 cells loaded with the relevant peptide (pWT126) and BV173 cells. There is little background killing of T2 cells loaded with irrelevant peptide (pWT235). Wells B1–B12 show high levels of HLA-A2 allo-reactivity, while wells C1–C6 show no killing activity against any of the three targets.

3.4. Screening of Microcultures for Specificity (Split-Well Analysis)

The limiting-dilution plates are screened to determine the ability of the microcultures to kill target cells loaded with the relevant peptide. This is done using a chromium release cytotoxicity assay which is performed 5–6 d after the last stimulation, as this is when CTL killing activity peaks. A sample of CTL are removed from each of the microcultures and tested for their ability to kill T2 loaded with the relevant peptide and irrelevant control peptide. The process of screening limiting-dilution plates by this method is referred to as "split-well analysis" and is described in this section. **Fig. 3** shows a typical result of split-well analysis of 96-well microcultures.

1. Peptide load the T2 cells (targets) (*see* **Subheading 3.2.**) with 100 μ*M* relevant/irrelevant peptide for 1 h at 37°C.
2. Resuspend peptide-loaded T2 cells in 200 μL CM and add 50 μCi ^{51}Cr per 1×10^6 cells. Chromium-label slightly more cells than required to allow for loss of cells during subsequent washing steps. Incubate at 37°C for 1 h.

3. After labeling, wash the target cells three times with CM.

4. Count and resuspend target cells to 5×10^4/mL.

5. Thoroughly mix the CTL in each well of the limiting-dilution plates with a multichannel pipet.

6. Transfer 50 µL of CTL from each well into the corresponding wells of a fresh round-bottom 96-well plate and do the same for a second 96-well plate. Two plates are set up per limiting-dilution plate—one as a control to test the killing ability of the CTL against T2 loaded with irrelevant peptide (plate A) and the second to test the killing ability of T2 loaded with the relevant peptide (plate B).

7. Spin the plates containing the transferred cells at 340g for 3 min and discard all the supernatant by flicking the plate once (*see* **Note 10**).

8. Resuspend the cell pellets in 100 µL CM per well.

9. Add 100 µL (5×10^3) T2 cells loaded with irrelevant peptide to each well of the control plate A and 100 µL (5×10^3) T2 cells loaded with the relevant peptide to each well of plate B.

10. Set up eight wells to measure the spontaneous chromium release by adding 100 µL of chromium-labeled T2 cells and 100 µL of CM per well.

11. Set up eight wells to measure the maximum release by adding 100 µL of chromium-labeled T2 cells and 100 µL of 1% TFA per well.

12. Spin the plates at 340g for 3 min, then place into a humidified 37°C incubator with 5% CO_2 for 4 h.

13. Harvest 100 µL of supernatant from each well and place into a round-bottom LP2 tube.

14. Measure the radioactivity using a Wallac Gamma Counter (Wallac, UK).

The specific lysis is calculated by the equation:

$$\frac{(\text{experimental release} - \text{spontaneous release})}{\text{maximum release} - \text{spontaneous release}} \times 100 \tag{1}$$

If the specific lysis of the T2 cells loaded with the relevant peptide is greater than 10% of that of T2 loaded with irrelevant peptide, the well is defined as positive and will be expanded in the next step.

3.5. Expansion and Validation of Micro-CTL Cultures

This section describes the expansion of micro-CTL cultures from 96-well plate to 48-well plate and from 48-well plate to 24-well plate (**Subheading 3.5.1.**); the validation of expanded CTL, including details of the cytotoxicity assay (**Subheading 3.5.2.**); and the expansion and maintenance of validated CTL (**Subheading 3.5.3.**).

3.5.1. Expansion of Micro-CTL Cultures

The d following split-well analysis, transfer all CTL from each of the wells determined to be positive into a 48-well plate. Add 1 mL of CM containing:

1. 1×10^5 peptide-loaded T2 cells (irradiated, 80 Gy).

2. 1×10^6 autologous PBMC (recovered from frozen and irradiated, 30 Gy).

3. 10 U/mL human IL-2.

Seven days after expansion to 48-well plates, transfer wells which are proliferating to 24-well plates and re-stimulate. To do this, remove 0.5 mL of medium (trying not to
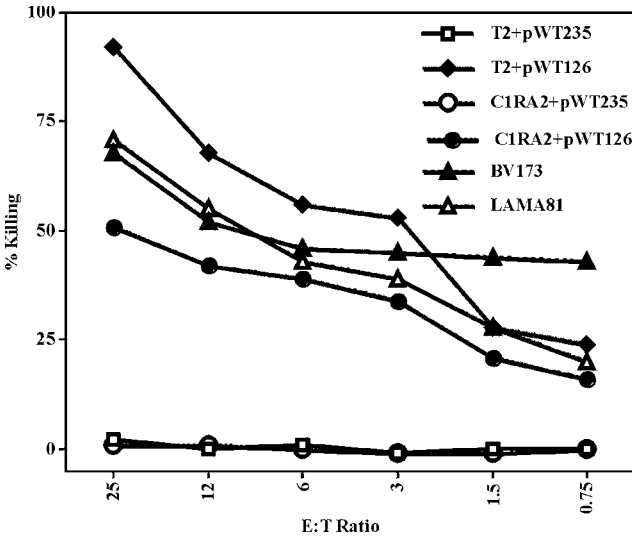
Fig. 4. Cytotoxicity assay demonstrating the specificity of high-avidity allo-restricted CTL generated against the pWT126 peptide. pWT126-specific cytotoxic T-lymphocytes (CTL) were isolated by limiting dilution of bulk cultures and expanded by stimulation with T2 cells coated with pWT126 peptide. Isolated CTL lines killed the TAP-deficient T2 target cells loaded with the relevant peptide (pWT126), C1R-A2 cells (HLA-A2+ and WT1−) loaded with the relevant peptide, and HLA-A2+ WT1+ leukemic cell lines BV173 and LAMA81. The CTL lines did not kill T2 cells or C1R-A2 cells loaded with the irrelevant HLA-A2-binding pWT235 control peptide.

remove any cells) from each well of the 48-well plate and discard. Transfer the remaining 0.5 mL containing CTL into a 24-well plate and add 1.5 mL CM containing:

1. 2×10^5 peptide-loaded T2 cells (irradiated, 80 Gy).
2. 2×10^6 autologous PBMC (recovered from frozen and irradiated, 30 Gy).
3. 10 U/mL human IL-2.

3.5.2. Validation of the CTL Lines

All CTL lines must be tested for their killing ability against a panel of peptide-coated targets and target cells expressing the antigen endogenously, using a cytotoxicity assay. It is important to use both sets of target cells, as low-avidity CTL may kill peptide-loaded targets efficiently but not targets expressing the antigen endogenously.

3.5.2.1. CYTOTOXICITY ASSAY

All proliferating CTL in 24-well cultures should be validated using the cytotoxicity assay on d 5 or 6 after re-stimulation. **Fig. 4** shows a typical result from a cytotoxicity assay in which high-avidity allo-restricted CTL generated against the pWT126 peptide were tested against a panel of targets. Details of the cytotoxicity assay are described in **Subheading 3.4.** The same procedure applies at this stage;

however, in order to obtain more information about the sensitivity of the expanded CTL, CTL are tested for their killing ability at a range of effector-to-target-cell ratios (E:T ratios). Start the E:T ratio at 25:1 (using 5×10^3 target cells) and perform double dilutions down a 96-well plate (i.e., eight dilutions). Target cells should include:

1. T2 cells loaded with the relevant peptide.
2. T2 loaded with irrelevant peptide.
3. HLA-A2$^+$ cells that express the relevant antigen endogenously.
4. HLA-A2$^+$ cells that do not express the relevant antigen endogenously.
5. HLA-A2$^-$ cells that do express the relevant antigen endogenously.

CTL lines that specifically kill HLA-A2$^+$ cells expressing the relevant antigen and T2 loaded with the relevant peptide and not the control cells (*see* **Fig. 4**) will be further expanded.

Phenotypic profiling is also carried out, in order to further validate the CTL lines. This is done by staining the CTL with fluorescence-labeled antibodies and analyzing by flow cytometry. For characterization of a CTL line, the most common antibodies to use are anti-CD3, anti-CD4, and anti-CD8. Anti-Vβ antibodies can be used to determine the T-cell receptor (TCR)-Vβ usage, and tetramer staining is also used to provide additional information regarding the specificity of the TCR. Tetramer staining should be performed on d 8–10 following re-stimulation.

3.5.3. Expansion and Maintenance of Allo-Restricted Peptide-Specific CTL

Large-scale expansion of peptide-specific allo-restricted CTL lines is technically straightforward but not always successful. CTL lines that have been repeatedly stimulated in culture do not expand as efficiently as recently established lines. We recommend performing one large-scale expansion of the CTL lines and to make sufficient numbers of freezings for later use. This should be done as soon as possible after the CTL lines have been expanded from 48-well to 24-well plate. In our experience, CTL grow much better in 24-well plates than flasks. Re-stimulate the CTL every 7–12 d, by adding the following in 2 mL CM per well:

1. 5×10^5 CTL.
2. 2×10^5 peptide-loaded T2 cells (irradiated, 80 Gy).
3. 2×10^6 autologous or HLA-A2$^-$ donor PBMC (recovered from frozen and irradiated, 30 Gy) (*see* **Note 3**).
4. 10 U/mL IL-2.

4. Notes

1. FCS (both heat-inactivated and non-heat-inactivated) from a range of suppliers should be batch tested prior to use in these experiments, to see which is most suitable for supporting the growth and proliferation of human T-cells. This can be done by stimulating a T-cell line in CM supplemented with the FCS being tested and measuring the proliferation on d 5 (by ^{3}H-thymidine incorporation) or by counting the T-cell numbers at time points up until d 10 after stimulation. Alternatively, a mixed lymphocyte reaction can be set up in CM containing the different batches of FCS and the proliferation measured on d 5.
2. Stimulators can be switched during stimulation of the bulk culture to minimize the generation and re-stimulation of CTL with unwanted peptide specificities. The most efficient

stimulator to use for the initial stimulation is the *Drosophila* transfectant. Stimulators for subsequent re-stimulations of the bulk culture can then be alternated between T2 and RMA-S-A2 cells up until limiting dilution and subsequent expansions, when T2 cells should be used.

3. It is better to use autologous feeders during the initial phase of CTL culture and limiting-dilution plating. Once the CTL line has been established and validated, third-party HLA-A2⁻ feeders can be used.

4. Boiled FCS is used in the culture medium during peptide loading. This includes peptide loading for stimulations and also for the cytotoxicity assay. FCS contains enzymes that may degrade the peptides, and therefore boiling the FCS may help to reduce this enzyme activity. To boil the FCS, it must first be diluted to 50% in RPMI (containing no additives) and then heated to 95°C for 10 min. The FCS can then be further diluted in RPMI (to 5%) for use in peptide loading.

5. *Drosophila* cells do not need to be irradiated, as they will die after a short period of time in CM at 37°C.

6. Addition of hybridoma culture supernatant that contains anti-human CD4 antibody has proved to be beneficial in inhibiting proliferation of the CD4⁺ population and favoring expansion of the desired CD8⁺ CTL population. However, the presence of some CD4⁺ cells is desirable. In the conditions described here, CD8⁺ clones have a limited lifespan in the absence of CD4⁺ T-cells, and therefore long-term CTL lines usually contain CD4⁺ cells.

7. When PBMC are defrosted, they must be resuspended in cold RPMI containing no additives, to prevent clumping and subsequent reductions in recoverable cell numbers.

8. CTL cultures are very sensitive to changes in environmental conditions. For this reason, do not leave cultures out of the incubator longer than necessary.

9. Do not reuse the same wells of tissue-culture plates for re-stimulation, as the cells do not grow well in the old wells. Also, tissue-culture plasticware may vary in terms of toxicity to cultures; therefore, use plasticware from the same supplier throughout.

10. The plates must be flicked only once in order to remove supernatant, as cells will be lost if the plates are flicked more than this.

References

1 van der Bruggen, P., Traversari, C., Chomez, P., et al. (1991) A gene encoding an antigen recognizedby cytolytic T-lymphocytes on a human melanoma. *Science* **254,** 1643–1647.

2 Kawakami, Y., Eliyahu, S., Delgado, C. H., et al. (1994) Identification of human melanoma antigen recognized by tumor infiltrating lymphocytes associated with in vivo tumor rejection. *Proc. Natl. Acad. Sci. USA* **91,** 6458–6462.

3 Finn, O. J. (1993) Tumor-rejection antigens recognized by T lymphocytes. *Curr. Opin. Immunol.* **5,** 701–708.

4 Theobald, M., Biggs, J., Dittmer, D., Levine, A. J., and Sherman, L. A. (1995) Targeting p53 as a general tumor antigen. *Proc. Natl. Acad. Sci. USA* **92,** 11,993–11,997.

5 De Visser, K. E., Schumacher, T. N., and Kruisbeek, A. M. (2003) CD8+ T cell tolerance and cancer immunotherapy. *J. Immunother.* **26,** 1–11.

6 Morris, E. C., Bendle, G. M., and Stauss, H. J. (2003) Prospects for immunotherapy of malignant disease. *Clin. Exp. Immunol.* **131,** 1–7.

7 Matzinger, P., Zamoyska, R., and Waldmann, H. (1984) Self tolerance is H-2 restricted. *Nature* **308,** 738–741.

8 Rammensee, H. G. and Bevan, M. J. (1984) Evidence from in vitro studies that tolerance to self antigens is MHC-restricted. *Nature* **308,** 741–744.

9 Sadovnikova, E. and Stauss, H. J. (1996) Peptide-specific cytotoxic T lymphocytes restricted by nonself major histocompatibility complex class I molecules: Reagents for tumor immunotherapy. *Proc. Natl. Acad. Sci. USA* **93,** 13,114–13,118.

10 Obst, R., Munz, C., Stevanovic, S., and Rammensee, H. G. (1998) Allo- and self-restricted cytotoxic T lymphocytes against a peptide library: evidence for a functionally diverse allorestricted T cell repertoire. *Eur. J. Immunol.* **28,** 2432–2443.

11 Munz, C., Obst, R., Osen, W., Stevanovic, S., and Rammensee, H. G. (1999) Alloreactivity as a source of high avidity peptide-specific human CTL. *J. Immunol.* **162,** 25–34.

12 Moris, A., Teichgraber, V., Gauthier, L., Buhring, H. J., and Rammensee, H. G. (2001) Cutting edge: characterization of allorestricted and peptide-selective alloreactive T cells using HLA-tetramer selection. *J. Immunol.* **166,** 4818–4821.

13 Gao, L., Bellantuono, I., Elsasser, A., Marley, S. B., Gordon, M. Y., Goldman, J. M., and Stauss, H. J. (2000) Selective elimination of leukemia CD34+ by CTL specific for WTI. *Blood* **95,** 2198–2203

14 Sadovnikova, E., Jopling, L. A., Soo, K. S., and Stauss, H. J. (1998) Generation of human tumor-reactive cytotoxic T cells against peptides presented by non-self HLA class I molecules. *Eur. J. Immunol.* **28,** 193–200.

15 Stauss, H. J. (1999) Immunotherapy with CTLs restricted by nonself MHC. *Immunol. Today* **20,** 180–183.

16 Mutis, T., Blokland, E., Kester, M., Schrama, E., and Goulmy, E. (2002) HLA class II restricted T-cell reactivity to a developmentally regulated antigen shared by leukemic cells and CD34+ early progenitor cells. *Blood* **100,** 547–552.

17 DeMars, R., Chang, C. C., Shaw, S., Reitnauer, P. J., and Sondel, P. M. (1984) Homozygous deletions that simultaneously eliminate expressions of class I and class II antigens of EBV-transformed B-lymphoblastoid cells. I. Reduced proliferative responses of autologous and allogeneic T cells to mutant cells that have decreased expression of class II antigens. *Hum. Immunol.* **11,** 77–97.

18 McMichael, A. J., Parham, P., Rust, N., and Brodsky, F. (1980) A monoclonal antibody that recognizes an antigenic determinant shared by HLA A2 and B17. *Hum. Immunol.* **1,** 121–129.

19 Parham, P. and Bodmer, W. F. (1978) Monoclonal antibody to a human histocompatibility alloantigen HLA-A2. *Nature* **276,** 397–399.

20 Healey, D., Dianda, L., Moore, J. P., et al. (1990) Novel anti-CD4 monoclonal antibodies separate human immunodeficiency virus infection and fusion of CD4+ cells from virus binding. *J. Exp. Med.* **172,** 1233–1242.

21 Bellantuono, I., Gao, L., Parry, S., Marley, S., Dazzi, F., Apperley, J., Goldman, J. M., and Stauss, H. J. (2002) Two distinct HLA-A0201-presented epitopes of the Wilms tumor antigen 1 can function as targets for leukemia-reactive CTL. *Blood* **100,** 3835–3837.

22 Oji, Y., Ogawa, H., Tamaki, H., et al. (1999) Expression of the Wilms' tumor gene WT1 in solid tumors and its involvement in tumor cell growth. *Jpn. J. Cancer Res.* **90,** 194–204.

23. Menssen, H. D., Bertelmann, E., Bartelt, S., et al. (2000) Wilms' tumor gene (WT1) expression in lung cancer, colon cancer and glioblastoma cell lines compared to freshly isolated tumor specimens. *J. Cancer Res. Clin. Oncol.* **126,** 226–232.

24. Scharnhorst, V., van der Eb, A. J., and Jochemsen, A. G. (2001) WT1 proteins: functions in growth and differentiation. *Gene* **273,** 141–161.

17

Designing TCR for Cancer Immunotherapy

Ralf-Holger Voss*, Jürgen Kuball*, and Matthias Theobald

*Both authors contributed equally to this work.

Summary

Reprogramming T-cell populations by T-cell receptor (TCR) gene transfer is a new therapeutic tool for adoptive tumor immunotherapy. Gene transfer of human leukocyte antigen (HLA)-transgenic mice-derived TCR into human T-cells allows the circumvention of tolerance to tumor-associated (self) antigens (TAA). This chapter reports on the identification of the α and β chains of the heterodimeric TCR derived from a mouse T-cell clone. The related DNA fragments are inserted into a retroviral vector for heterologous expression of the TAA-specific TCR in human T-cells. Polymerase chain reaction (PCR)-based cloning protocols are provided for the tailor-made customization of murine TCR. We describe the humanization and chimerization of such TCR as well as their expression in human T-cells.

Key Words: Cancer therapy; immunotherapy; T-cell receptor; high-affinity TCR; high-avidity T-cell; tolerance; human leukocyte antigen; major histocompatibility complex; HLA-A*0201 restriction; tumor-associated antigen; HLA-A2 transgenic mice; reverse transcription and polymerase chain reaction; rapid amplification of cDNA ends; single-chain TCR and single-chain Fv; retroviral transduction; packaging cell line 293T and phoenix-ampho; adoptive transfer of T-cells.

1. Introduction

1.1. T-Cell Receptors As Molecular Tools for Cancer Immunotherapy

Immunotherapy of cancer is becoming feasible by the recent break-through in both the understanding of the principles of molecular aspects of tumor immunology *(1)* and the development of biochemical techniques for the rapid identification, modification, and in vitro as well as in vivo reimplementation of biologically relevant molecules *(2)*. On a molecular basis, the T-cell receptor (TCR) represents the direct link between the effector T-cell and the target cell *(3)*. The TCR triggers a cascade of signaling events directed towards the interior of the T-cell after successfully recognizing the major histocompatibility complex (MHC)-buried peptide—in the case of cancer, the tumor-associated antigen (TAA) *(4)*. However, TAA-specific T-cells with TCR of sufficient affinity cannot frequently be recruited by immunization or are absent from the human T-cell repertoire due to mechanisms of self-tolerance *(5,6)*.

Thus, for a successful T-cell-based tumor immunotherapy, it is necessary to extend the T-cell repertoire of cancer patients by adoptively transferring activated T-cells harnessed with TAA-specific TCR of sufficient affinity *(7,8)*. The introduced TCR should fulfill the following biochemical criteria:

1. TCR affinity has to exceed a minimal threshold critical for the recognition of even very low amounts of tumor antigen on tumor cells *(9,10)*. T-cells of sufficient avidity are available against a small number of defined TAAs *(11)*. Once cloned, their TCR can be isolated and retrovirally imported into patients' T-cells and subsequently expanded in vitro, thereby preventing the cumbersome establishment of TAA-specific T-cell clones for adoptive transfer (**Fig. 1**). However, for most of the TAAs, either the avidity of specific T-cells is low or they are even absent from the repertoire. As a consequence, many laboratories have attempted to increase the quality of TAA-specific yet low-affinity TCR by different biotechnological approaches, such as yeast *(12)* or TCR display *(13)*. In iterative cycles of affinity sampling, high-affinity TCR are generated and filtered out to yield affinities in the nanomolar range. In addition, the generation of allo-peptide-reactive T-cells is a source for high-quality TCR, and is discussed elsewhere in this book *(7,14)*. As an alternative, the HLA-A2(K^b)-transgenic mouse model allows the generation of high-affinity TCR specific for human TAAs *(6,15)*. A2K^b-transgenic mice contain the human $\alpha1$ and $\alpha2$ domains of HLA-A*0201 and the mouse $\alpha3$ domain of H-2K^b, which allows the interaction of murine CD8 with the A2K^b transgene product. The peripheral T-cell repertoire of these transgenic mice has not been depleted of high-affinity TCR directed against human antigens, and therefore represents a diverse source of HLA-A2-restricted, high-avidity T-cells and their respective TCR (*[16]*, **Fig. 1**; this method will be described under **Subheading 3.1.**). However, a major disadvantage arises from the xenogenic mouse origin of the TCR, which may require their partial *(7)* or almost complete humanization to affect their potential immunogenicity in humans. The successful humanization of mouse antibodies as a prototype for immunoglobulin-like folded proteins *(17)* and their subsequent clinical benefit have been documented in a multitude of published trials (*[18]* and J. Saldanha's web-site: "Humanization by Design" [http://people.cryst.bbk.ac.uk/~ubcg07s/]). The structural homology of antibodies and T-cell receptors enables the embodiment of antibody-related characteristics in TCR constructs with respect to affinity maturation, humanization, and chimerization. A protocol for partial humanization of a mouse TCR will be described under **Subheading 3.3.1.**

   Not only to overcome the affinity barrier, "T-bodies" have been designed that make use of antibody-derived antigen-specific high-affinity variable domains covalently linked to invariant domains of different origin. Such T-bodies are ideally suited to produce high-avidity, MHC-independent T-cells *(19)*.

2. Exogenous TAA-specific TCR introduced into a T-cell face a significant proportion of endogenous TCR ($1–4 \times 10^4$ per cell, *[20]*). Thereby, the exogenous TCR have to compete with the endogenous TCR to become part of the functional TCR/CD3 complex, consisting of the heterodimeric TCR$\alpha\beta$ and the heterohexameric CD3 complex, formed during post-translational assembly in the endoplasmatic reticulum and subsequent transport to the cell surface *(21)*. Mouse TCR are of sufficient structural homology to be incorporated into the human CD3 complex *(7)* and to rescue surface expression in mutant T-cells *(22)*. Surprisingly, exogenous mouse TCR for different TAA specificities are prone to be more favorably incorporated into the human signaling complex as compared to an exogenous gp100-specific human TCR (unpublished results).

HUMAN TCRs
1) High-affinity human TCRs with specificity for TAA (rare event, no modification necessary).

2) Low affinity human TCRs with specificity for TAA (more frequent, affinity maturation required).

3) High-affinity TCR from allorestricted TAA-specific human T-cells.

TCR

TCR*

T-Cell

T-Cell TCR

TCR*

XENOGENIC TCRs
A2(K^b)-transgenic mice allow the generation of A2-restricted and human TAA-specific TCRs with sufficient affinity (abundant source, no affinity modification necessary but potentially partial or complete humanization).

Harnessing human T-cells with TAA-specific TCRs allows the direct reinfusion of activated TCR transduced T-cells without time consuming in vitro expansion.

Fig. 1. T-cell receptor (TCR) gene transfer into human T-cells for adoptive immunotherapy. TCR*: endogenous TCR.

   In case of partially humanized TCR harboring human constant domains, the assembly machinery is not able to dissect endogenous and exogenous TCR due to the invariant nature of the constant domains. Hence, combinatorial preferences, if they exist at all, can be solely assigned to the nature of the subfamily-specific variable domains. Although the major determinants for interchain pairing are believed to be located within the constant domains *(23)*, the stability of the TCR duplex may also be influenced by their favorable subfamily interchain pairing *(24–26)*. Nevertheless, it is not ultimately clarified to what extent structural constraints or thymic selection processes determine the combinatorial TCR diversity of an individual *(27)*. This restriction does not seem to pose any problems on the sufficient coverage of functional diversity, as only 2×10^6 clones, orders of magnitude less than the maximum theoretical size of 10^{15}, have been estimated in the spleen of immunocompetent mice *(28)*.

3. One potential problem is the undesired event of mixed chain pairing between endogenous and transferred TCR, which is likely to happen predominantly with the delivery of human or humanized TCR. First, self-reactive specificities could be generated, and second, the correct heterodimeric TCR-surface expression with specificity for the desired TAA will be decreased and may thus impair functional responsiveness. To avoid this event, the "single chain TCR concept" has been developed as an attractive alternative, which aims to covalently attach the variable α/β domains to each other via a flexible and thermodynamically stable linker *(29,30)*. This molecule can be chimerized with a constant domain that allows membrane anchoring and assembly with the CD3 complex *(31)*. To enhance signaling efficiency, these chimeric molecules have also been hooked up to the CD3-ζ chain as a substrate for proximal signaling functions, such as tyrosine phosphorylation by Syk/Fyn kinases *(32)*, or by fusion to the downstream molecules themselves *(33)*. Apart from the ITAM (immunoreceptor tyrosine-based activation motif)-containing cytoplasmic domain, CD3-ζ contributes its transmembrane and short ectodomain *(34)*, and is thus responsible for disulfide-bridge linkage-driven homodimerization. Double chain TCR (dcTCR) could be similarly modified in order to increase the probability of a TCR chain pairing with its desired antigen-specific counterpart: for this purpose, the CD3-ζ chain not only endows the chimeric dcTCRα/β-ζ construct with immediate signaling potency, but is also supposed to support preferential pairing due to the dimerization motif located inside its transmembrane domain *(35)*. As an alternative, point mutations that introduce novel amino acid interactions at the interface of the adjacent chains are able to manipulate the combinatorial preferences (unpublished data, *[36]*). The study of TCR crystal structures facilitates the selection of amino acid positions suited for manipulation of interchain pairing. This is further supported by the observations that both the human and mouse TCR backbones can be closely superimposed and that the amino acid sequences, in particular those of the constant domains, are highly conserved *(37)*. However, the primary structure of the transferred TCR chains has to be carefully modified in order to synergistically combine maintenance of function with the implementation of preferential pairing. This should be kept in mind to avoid any impairment of the signaling machinery by unreasonably omitting functionally relevant motifs or even domains that are indispensable for protein–protein interactions *(38)*, and secondary structural elements, such as glycosylation sites *(39)*, believed to stabilize the framework of the TCR/CD3 complex. Assembly with CD3 and the co-receptors CD4 or CD8 has to be taken into consideration *(40)*, as low- to intermediate-affinity TCR, the most prominent representatives of the TCR repertoire of an individual, require assistance by these co-receptors to surmount an intrinsic threshold for T-cell activation *(9,41)*.

2. Materials

1. 1 kb DNA ladder (New England Biolabs, Beverly, MA).
2. 100 bp DNA ladder (New England Biolabs).
3. 5'/3' RACE Kit (Roche, Basel, Switzerland).
4. Agarose DNA-grade (Biomol, Plymouth Meeting, PA).
5. Alkaline phosphatase, calf intestinal (CIP) (New England Biolabs).
6. Anti-CD3 antibody: Orthoclone OKT3™ (Janssen-Cilag, Neuss, Germany).
7. Calcium Phosphate Transfection System (Invitrogen, Carlsbad, CA, former Life Technologies, cat. no. 18306-019).
8. Dextrane sulfate (Sigma, St. Louis, MO).
9. Freund's adjuvant (Difco, Detroit, MI).
10. DMEM (Cambrex, Walkersville, MD).
11. Dulbecco's PBS (Cambrex).
12. Dynabeads® CD3/CD28 T-cell Expander (Dynal, Oslo, Norway).
13. Fetal calf serum (Cambrex).
14. Fugene 6 (Roche).
15. Geniticin (G418) (Sigma).
16. Gentamicin (Cambrex).
17. HEPES (Cambrex).
18. High Pure PCR Product Purification Kit (Roche).
19. Human AB serum (Bloodbank Clinical University Mainz, Germany).
20. Human CD8-PC5 (Beckman-Coulter, Miami, FL).
21. Interleukin-2 (Proleukin, Chiron, Emeryville, CA).
22. L-Glutamine (Cambrex).
23. Lipopolysaccharide (LPS) (Sigma).
24. Mastercycler Gradient (Eppendorf, Hamburg, Germany).
25. β-Mercaptoethanol (Sigma).
26. Murine Vβ6-antibody (Becton Dickinson, San Jose, CA).
27. Nonidet P-40, 10% (w/v) (Roche).
28. Oligonucleotides (MWG, Ebersberg, Germany).
29. Penicillin-Streptomycin (Cambrex).
30. Pfu DNA Polymerase (Stratagene, La Jolla, CA).
31. Platinum® Pfx DNA Polymerase (Invitrogen).
32. pcDNA3.1(–) (Invitrogen).
33. Plasmocin (Invivogen, San Diego, CA).
34. pNEB193 (New England Biolabs).
35. Polybrene (Sigma).
36. Puromycin (Sigma).
37. Restriction enzymes (New England Biolabs).
38. RNase-Inhibitor (Roche).
39. Rneasy Mini Kit (Qiagen,Valencia, CA).
40. RPMI without phosphate (PAA, Pasching, Austria).
41. RPMI (Cambrex).
42. T4 DNA Ligase (New England Biolabs).
43. T4 DNA Polymerase (New England Biolabs).
44. T4 Polynucleotide Kinase (New England Biolabs).
45. Titan™ One Tube RT-PCR System (Roche).
46. RetroNectin (TaKaRa, Shiga, Japan).

Chemicals, unless otherwise stated, were purchased from Sigma; 10X reaction buffers of the respective enzymes were provided by the supplier.

3. Methods

3.1. Generation of High-Avidity T-Cells
With Specificity for Human TAA in HLA-Transgenic Mice

A2K^b-transgenic mice are injected subcutaneously at the base of the tail with 100 µg of an A2-presented synthetic peptide and 150 µg of an I-A^b-binding synthetic T-helper peptide representing residues 128–140 of the hepatitis B virus core protein *(42)* emulsified in 150 µL of incomplete Freund's adjuvant. Seven days later, spleen cells (1 × 10^6/mL) of nonimmunized A2(K^b)-transgenic mice are activated by 25 µg/mL of LPS and 7 µg/mL of dextrane sulfate in an upright T75 tissue flask. After 3 d, LPS-activated spleen cells are irradiated (3000 rad). Ten days following immunization, spleen cells of primed mice are cultured with irradiated A2(K^b)-transgenic LPS-activated spleen-cell stimulators that are pulsed with the respective peptide at 5 µg/mL and human β$_2$-microglobulin at 10 µg/mL in complete RPMI medium (RPMI 1640 containing 10% [v/v] fetal calf serum, 25 m*M* HEPES, 2 m*M* glutamine, 5 × 10^{-5} *M* β-mercaptoethanol, and 50 µg/mL gentamicin, *[15]*). The resultant polyclonal T-cell lines are weekly restimulated in 2 mL in a 24-well plate with irradiated (20,000 rad) JA2 (Jurkat cells transfected with HLA-A*0201 cDNA) stimulators (0.5 × 10^6/well) that had been pulsed with 5 µg of the primary stimulating peptide, irradiated C57BL/6 spleen feeder cells (6 × 10^6/well), and 2–10% (v/v) of rat concanavalin A supernatant *(43)*. T-cells are cloned by limiting dilution.

3.2. Isolation and Cloning of Murine TCR

The α- and β-T-cell receptor chains (TCRα, TCRβ) are 280-310 amino acids in length. Each of the upstream 130 amino acids comprise the variable domains that form the TCRα/β heterodimeric complex and specifically recognize the MHC-presented antigen. The constant domains are invariant and can be classified as Cα, Cβ1, and Cβ2, the latter differing by a few non-silent base sequence alterations at the very end of the reading frame *(44)*. The variable regions are highly degenerated and can be classified into distinct subfamilies (IMGT, the international ImMunoGeneTics information system http://imgt.cines.fr; Initiator and coordinator: Marie-Paule Lefranc, Montpellier, France *[45–48]*). The signal peptide-encoding sequences vary as well. A time-consuming approach is the development of degenerate primers to cover as much as possible of the whole panel of more than 20 subfamily sequences of each TCR chain. This strategy has initially been designed for the identification of both TCR chains by RT-PCR, but finally led to success only in case of the TCRβ chain. Only a non-functional TCRα chain has been identified, originating from the leaky allelic exclusion mechanism for TCRα chains *(49)*. This α chain had a frameshift mutation within the CDR3 segment, generated by genetic rearrangements inside the TCRα locus during thymic maturation. The identification of this TCR domain likely resulted from the bias of the developed degenerate primer for the 5' sequence of the nonfunctional TCR reading frame. An RT-PCR protocol will be provided for the isolation of the invariant Cα and Cβ regions of TCRα/β (**Subheading 3.2.3.**).
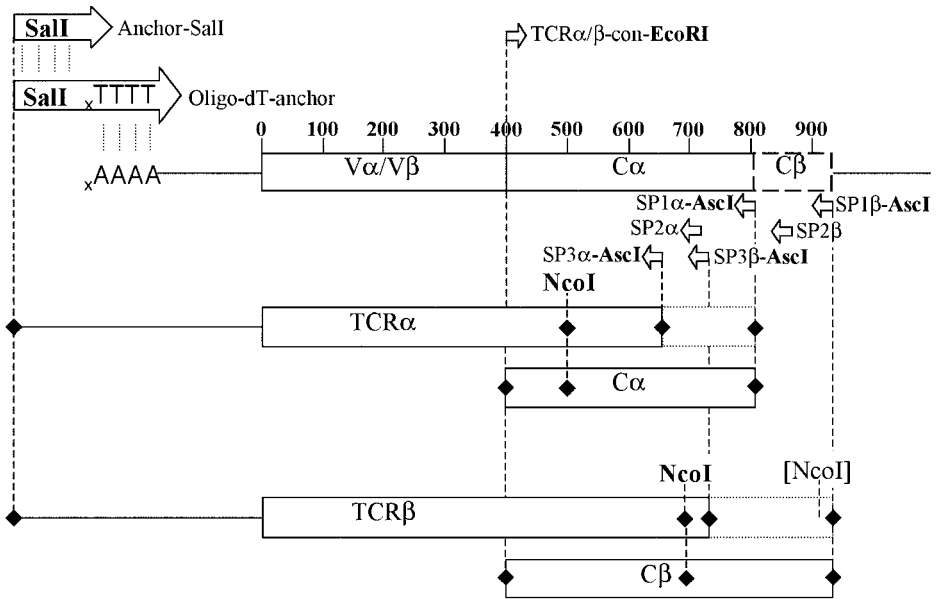
Fig. 2. Strategy for cloning full-length TCRα and TCRβ using 5'-RACE-PCR as illustrated for both chains in a superimposed fashion. Base sequence lengths of both TCR are indicated: the constant region of TCRβ is more than 100 bases longer (indicated by a dashed box Cβ) than Cα. The variable regions are almost identical in size (400 bases). The cloning procedure of each chain is composed of reverse transcription (primer SP1α/β-AscI), polyA tailing, and two subsequent nested 5'-RACE-PCRs (primer pair oligo-dT-anchor / SP2α/β and anchor-SalI/ SP3α/β-AscI). Relevant enzyme restriction sites, whether (AscI, EcoRI, SalI) or not (NcoI) being introduced by PCR primers, are highlighted. Their relative positions are indicated by dashed lines that end in rhombic symbols. The truncated TCR are cloned via SalI/AscI in pNEB193. In parallel, each full-length constant region is amplified by RT reaction (SP1α/β-AscI) and one-step PCR (primer pair TCRα/β-con-EcoRI/SP1α/β-AscI), and cloned via EcoRI/ AscI in pNEB193. Due to an extended overlap that harbors a common NcoI site, subcloning of an NcoI/AscI fragment finally complements (dotted boxes) the reading frame (RF) of each truncated TCRα/β. The NcoI site to be silenced at almost the 3'-end of the Cβ2 RF is indicated by square brackets.

Thus, a strategy had to be chosen to match all TCR chains of a T-cell clone. A straight-forward technique to isolate full-length coding sequences is the rapid amplification of cDNA ends (RACE-PCR ; **Fig. 2**): mRNA is transcribed in vitro into a complementary cDNA strand (primer SP1). The 3' moiety that ends up with the non-translated region of unknown base sequence is extended with a short homopolymeric "dA"-oligonucleotide by the terminal transferase reaction. This specific tail serves as template for a specific complementary oligonucleotide (primer "oligo-dT-anchor"), harboring several restriction sites at its 5' end, to enzymatically synthesize the second strand cDNA with a thermostable DNA polymerase. In combination with a reverse

primer (SP2) binding to the 3' end of the invariant region, but nested to SP1 to strengthen specificity, the double-stranded DNAs are amplified. The first PCR product may be further amplified by a nested second PCR ("Anchor" primer/SP3), albeit this will again truncate the sequence of the constant domain (**Note 1**) and will necessitate the independent cloning of the constant regions (**Subheading 3.2.3.**). A unique NcoI site in the overlapping region of both DNA fragments enables the rapid subcloning of full-length TCR. Using this approach, each TCR chain has been inserted into the expression vector pcDNA3.1(–) (Invitrogen) by SalI at its 5' and by BamHI at its 3' end. The protocol and the 5' primers have basically been used as outlined in the "5'/3'-RACE Kit" from Roche, whereas the 3' primers SP1–SP3 have been assigned to each TCRα/β chain individually.

3.2.1. RNA Preparation

The preparation of fully matured cytoplasmic mRNA has been performed as described in the protocol for the isolation of cytoplasmic RNA from the cytoplasm of animal cells of the Rneasy Mini Kit (Qiagen). To determine the functional reading frames of the TCR, the mRNA has to be fully processed by excising the non-coding intron sequences out of the exons. For this purpose, the detergent NP-40 has been used in order to solubilize exclusively the cell membrane and to separate the cytoplasmic content from the nuclei (*see* **Note 2**). 4–15×10^6 T-cells of a mouse T-cell clone have been lysed in 0.5% (w/v) of the nonionic detergent Nonidet-P-40 (NP-40; Roche) containing lysis buffer; formation of viscous solution by the release of chromosomal DNA is avoided. The yield of RNA has been optimized by raising the recommended time for solubilization from 5 min to 30 min on ice. On average, 4×10^6 murine T-cells produce 15 μg of RNA, which is sufficient for an experimental series of reverse transcription and PCR analysis. Raising the absolute T-cell number progressively improves RNA yield. RNA has been frozen in 5-μg aliquots and stored at –20°C for short-term analysis to assess PCR product specificity at five separate annealing temperatures in RT/RACE-PCR assays (*see* **Note 3**).

3.2.2. RACE-PCR

RACE-PCR includes the reverse transcription of mRNA into cDNA and subsequently the PCR amplification thereof to yield sufficient amounts of DNA for cloning and further characterization.

The following protocol has been applied to both the generation of the TCRα chain as well as the TCRβ chain. The RNA was prepared as described under **Subheading 3.2.1.** and diluted to 1–5 μg/10 μL RNase-free water. Reverse transcription was performed in 20 μL with 9 μL RNA, 4 μL 5X cDNA synthesis buffer (250 mM Tris-HCl pH 8.5 [20°C], 40 mM MgCl$_2$, 150 mM KCl, 5 mM DTT), 2 μL dNTP (stock: 10 mM each), 1 μL RNase-Inhibitor (40 U/μL from human Placenta [Roche]), 1 μL rev-TCRα-SP1-<u>AscI</u> (12.5 μM, 5'- A<u>GG CGC GCC</u> T**TC A**AC TGG ACC ACA GCC TCA GCG T -3') or rev-TCRβ-SP1-<u>AscI</u> (12.5 μM, 5'- A<u>GG CGC GCC</u> T**TC A**GG AAT T**Y**T TT**Y** T**Y**T TGA CCA T -3' wherein **Y** = C/T and **TCA** refers to the stop codon), 1 μL AMV-RT (20 U/μL), 2 μL RNase-free water (*see* **Note 4**). The TCR-specific reverse primers are identical to those that have been used to clone full length constant regions (**Subheading**

3.2.3.). Base composition and length of primers have to be considered for optimal temperature in RT reaction. This has been worked out for a PCR device as follows: the lid was equilibrated to 102°C; a "hold" step at 55°C enables positioning of 0.2-mL PCR tubes of the RT-assay, followed by a 60-min reverse transcription at 55°C, and 10 min 65°C RNase heat inactivation of AMV-RT. The samples were equilibrated to room temperature for subsequent purification to separate them from excess primers that would otherwise interfere with amplification steps. The purification was performed as described in the High Pure PCR Product Purification Kit (Roche).

The tailing of the first strand cDNA took place in a PCR device preceded by a short heat denaturation step to make the 3'-noncoding region accessible to terminal transferase: 19 μL of the purified cDNA was added to 2.5 μL tailing 10X reaction buffer (100 m*M* Tris-HCl pH 8.3 [20°C], 15 m*M* MgCl$_2$, 500 m*M* KCl), 2.5 μL dATP (2 m*M* dATP in Tris-HCl pH 8.3 [20°C]) at 94°C for 3 min and then rapidly cooled to 4°C to minimize rehybridization. The sample was prewarmed to 37°C before addition of 1 μL of terminal transferase (10 U/μL, hold step) and incubated for 20 min to allow for enzymatic synthesis of the homopolymeric deoxy-adenosine tail. A 10-min heat inactivation step at 70°C finishes the tailing reaction. 5-μL aliquots can be directly used for PCR amplification in a temperature-dependent annealing gradient (*see* **Note 5**). For this purpose, 5-μL aliquots of the tailing product were combined with 45 μL of a master mix composed of 180 μL redistilled water, 5 μL of the SalI-oligo-dT-anchor primer (5'- GAC CAC GCG TAT CGA TGT CGA CTT TTT TTT TTT TTT TTV -3' wherein V = A/C/G; stock: 37.5 μ*M*), which is complementary to the enzymatically appended oligo-dA tail, 5 μL of reverse TCR-specific primers, rev-TCRα-SP2 (5'- AGG TTC ATA TCT GTT TCA A -3'; stock 12.5 μ*M*) or rev-TCRβ-SP2 (5'- GGA TCT CAT AGA GGA TGG T -3', 12.5 μ*M*), 5 μL dNTP (10 m*M* each), 25 μL Pfu-DNA-polymerase reaction buffer (10X stock: 200 m*M* Tris-HCl [pH 8.8], 100 m*M* KCl, 100 m*M* [NH$_4$]$_2$SO$_4$, 20 m*M* MgSO$_4$, 1 % Triton X-100, 1 mg/mL BSA), and 5 μL Pfu-DNA polymerase (2.5 U/μL). The five vials evenly span the temperature gradient and were run on the thermal cycler Mastercycler Gradient (Eppendorf): After an initial denaturation step at 94°C for 120 s, 10 PCR cycles follow, consisting of denaturation for 30 s at 94°C, slow (1°C/s) annealing at 45°C ± 10°C, extension for 60 s at 72°C. This is followed by 25 cycles of denaturation for 30 s at 94°C, slow annealing at 45°C ± 10°C, extension for 60 s at 72°C in the eleventh cycle that will be prolonged by 20 s for each subsequent cycle to compensate for nucleotide depletion, and finally a 7-min extension step to blunt-end all 3' termini for efficient cloning. The extension temperature had to be raised to 72°C to meet the temperature optimum criteria of the high-fidelity Pfu-DNA polymerase (Stratagene).

In order to strengthen specificity and product yield, 1 μL of the PCR product was submitted to a second round of amplification with nested reverse primers: for TCRα, a primer harboring an AscI cloning site, rev-TCRα-SP3-AscI (5'- AGG CGC GCC TGG CGT TGG TCT CTT TGA A -3'); for TCRβ, rev-TCRβ-SP3-AscI (5'- AGG CGC GCC TGG CCA CTT GTC CTC CTC TGA A -3') in combination with the forward SalI-containing "anchor" primer (5'- GAC CAC GCG TAT CGA TGT CGA C -3') was used as described for the first PCR. One-fifth of the PCR product was analyzed on a 1.0% agarose gel (**Fig. 3**); the remainder was processed for cloning via SalI/AscI and NcoI/AscI to produce full-length TCR as outlined under **Subheading 3.2.4.**
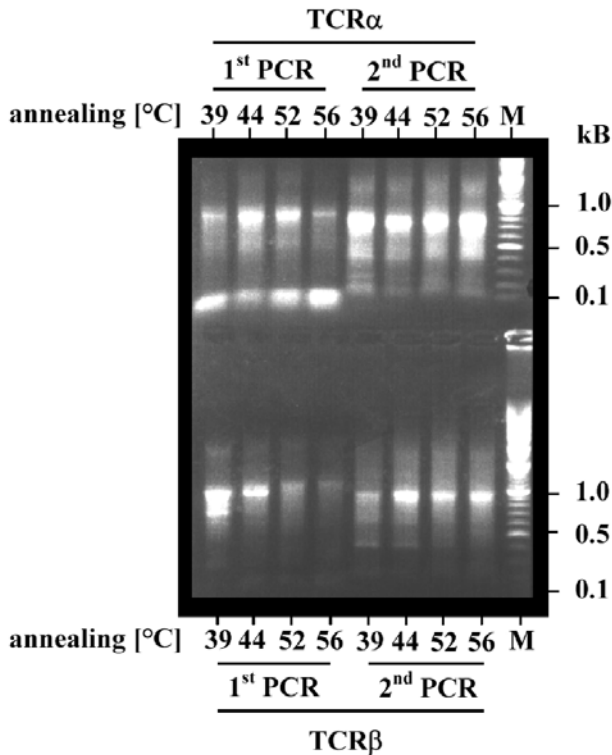
Fig. 3. RACE-PCR (1st PCR) and subsequent 3'-nested PCR (2nd PCR) for mouse TCRα and β chains as outlined in **Fig. 2**. The different annealing temperatures are indicated. The 1st PCR produced faint PCR bands, whereas the nested PCR of the 1st PCR product amplified trace amounts for virtually all temperatures. The PCR products were longer than the hypothetical length of the coding regions for TCRα and -β due to the integration of the 5'-non-coding regions.

3.2.3. Isolation of the Invariant TCRα and -β Regions by RT-PCR

RT-PCR basically consists of the reverse transcription of isolated mRNA to first strand cDNA and subsequent PCR amplification(s), provided that the flanking sequences of the gene of interest are known or can at least be covered by degenerate primers. The relevant components have been assembled in the Titan™ One Tube RT-PCR System (Roche).

The optimal production of PCR fragments has been further refined by five individual temperatures in the annealing step, as already specified for RACE-PCR. Therefore, a master mix has been pipetted (250 μL) that was aliquoted into five 0.2-mL PCR tubes and placed evenly among the temperature gradient (20°C) of a thermal cycler (Mastercycler gradient, Eppendorf). The one-step RT-PCR comprises two master

mixes: Mastermix 1 was pipetted in the following sequence: 90 μL RNAse free water (DEPC-treated and autoclaved twice), 5 μL dNTP (25m*M* stock), 2.5 μL for-Cβ1/2- or Cα-specific primer (100 pmol/μL stock, for sequences *see* below), 2.5 μL rev-Cβ1/2- or Cα-specific primer (100 pmol/μL stock), 12.5 μL DTT (100 m*M* stock), 2.5 μL RNase inhibitor (40U/μL stock), and 10 μL RNA (5 μg). The source of RNA was identical to the mouse T-cell clone preparation, as already mentioned (RACE-PCR). The components are mixed with RNase-free plasticware and stored on ice. The Mastermix 2 is composed of 10 μL RNase-free water, 50 μL 5X RT-PCR buffer, 60 μL MgCl$_2$ (25 m*M* stock), and 5 μL AMV-RT/Taq/Pwo-DNA-polymerase enzyme mix. The Mastermix 2 is homogenized as well, then mixed together with Mastermix 1, and aliquoted to 50 μL into individual PCR tubes.

The thermal cycler is programmed to continuously link reverse transcription with polymerase reaction: initially, the device is pre-equilibrated to the preferred temperature for the RT reaction (55°C, "hold" function). The five PCR tubes are placed among the temperature gradient in an 8 × 12-well format. Reverse transcription proceeds for 45 min and, after a 2-min heat-inactivation step, is followed by the PCR reaction. The default cycling program consists of 10 cycles of denaturation at 94°C for 30 s, annealing at 45 ± 10°C for 60 s, and extension at 68°C for 90 s. To compensate for nucleotide depletion, 25 cycles of denaturation at 94°C for 30 s, annealing at 45 ± 10°C for 60 s, and extension at 68°C for 90 s follows, prolonged by 4 s for each cycle. A final extension at 68°C for 7 min and cooling to 4°C ("hold" function) terminates the protocol.

RT-PCR with for-TCRβ-con-EcoRI (5'- G<u>GA ATT C</u>CG AGG ATC TGA GAA ATG TGA -3') and the degenerated rev-TCRβ-con-<u>AscI</u> (5'- A<u>GG CGC GCC</u> **T**TC **A**GG AAT **T**Y**T** TT**Y** T**Y**T TGA CCA T -3' wherein Y = C/T) to cover the constant regions Cβ1 and Cβ2 (*see* **Note 6**), elicited a strong PCR band of 0.5 kB without subsequent nested PCR. The constant TCRα segment has been isolated in parallel from the same RNA source with the primers for-TCRα-con-<u>EcoRI</u> (5'- G<u>GA ATT C</u>CC CAG AAC CCA GAA CCT GCT GTG TA -3') and rev-TCRα-con-<u>AscI</u> (5'- A<u>GG CGC GCC</u> **T**TC **A**AC TGG ACC ACA GCC TCA GCG T -3').

3.2.4. Cloning of TCR-Related PCR Products

Cloning of DNA fragments was performed according to common protocols and therefore is only summarized (explicit guidelines in *(50)*; **Note 7**): One-fifth of the (nested) PCR product was analyzed on a regular 1% (w/v) agarose gel in 0.5X TBE electrophoresis buffer. The PCR product was purified by the High Pure PCR Product Purification Kit (Roche) to eliminate excess primer and was spectroscopically quantified by UV light absorption at 260 nm. At least 2 μg were used for cloning into pNEB193 (NEB) by subsequent SalI (or EcoRI) and AscI restriction (NEB) of fragment and vector, dephosphorylation of the vector by calf intestinal phosphatase (CIP), and directional ligation of the fragment into the cut vector with T4 DNA polymerase. Transformation was performed with the CaCl$_2$-competent *Escherichia coli* strain XL1-Blue (Stratagene). Small-scale plasmid preparations of individual clones were prepared with the QIAprep Spin Miniprep Kit (Qiagen). TCR sequences have been confirmed in both directions by a commercial supplier.

3.2.5. Subcloning of TCR Fragments
to Yield Full-Length TCR Reading Frames

The outlined concept of RACE-PCR did not provide a complete coding sequence for the TCRα/β chains. The TCR clones comprising the almost full-length TCR (*see* **Subheading 3.2.2.**) and those encoding the constant domains (**3.2.3.**) share a common NcoI site inside their (residual) constant regions (**Fig. 2**). In the case of TCRα, simple subcloning of an NcoI/AscI-digested Cα fragment into the NcoI/AscI-cut vector harboring the truncated TCRα results in a full-length TCRα chain ready for functional expression studies. Cloning of TCRβ turned out to be a little more complex due to an additional internal NcoI site at almost the 3' end of the Cβ2 region; this was dealt with by partial enzyme restriction to produce predominantly a complete NcoI/AscI fragment instead of a truncated NcoI/NcoI fragment (*see* **Note 8**).

3.2.6. Subcloning of TCRα/β Genes
in Retroviral Expression Vectors

The full-length TCR have been introduced into the retroviral vector system pBullet by NcoI/BamHI ligation. This vector was kindly provided by Ralph Willemsen (Department of Clinical and Tumor Immunology, Daniel den Hoed Cancer Center, Rotterdam, The Netherlands; **refs.** *32,51,52*). The vector is ideally suited for transient transfection of the packaging cell line 293T and, depending on the envelope used, for reproducible transduction of species-specific T-cells.

The pBullet vector system belongs to the class of splicing vectors that make use of splice donor and acceptor sites to improve expression of the gene of interest *(53)*. An NcoI site located directly downstream of the splice acceptor element allows the insertion of the transgene into the same sequence context as compared to the wild-type retroviral envelope protein. This concept requires the integration of the start codon ATG into the NcoI-site CC<u>ATG</u>G.... Occasionally, this will modify the proximal amino acid as an integral part of the signal peptide.

The transgenes have been amplified by PCR and their 5' and 3' ends trimmed to NcoI and BamHI. In the case of NcoI, the internal NcoI sites of mouse TCR disable direct digestion; the vector was therefore cut with NcoI, filled to blunt end with T4-DNA polymerase, and subsequently BamHI digested and dephosphorylated *(50)*. The forward primer for PCR was designed at its 5' end in such a way as to amend the missing G... to the blunt-ended vector ...CCATG to restore NcoI ...CCATGG... in the recombinant vector. In addition, the 5' end was chemically (oligonucleotide synthesis) and/or enzymatically phosphorylated by T4-DNA-polynucleotide kinase (PNK, **ref.** *50*). This cloning procedure is similar to directional insertion via blunt/sticky end ligation (*see* **Note 9**).

3.3. Modification of TCR Constructs

3.3.1. Humanization of TCR

Each chain of the heterodimeric TCRα/β comprises two immunglobulin-like folded domains, of which the variable domain harbors the three CDR loops responsible for the

recognition of the peptide/MHC complex. The constant domain is invariant and primarily serves as distance holder to expose the variable domain to the peptide/MHC complex of the antigen-presenting cell (APC) and to enable the association to the CD3 complex and to the coreceptors CD4 or CD8. A disulfide bridge close to the transmembrane region covalently links both chains. A transmembrane region with a very short cytoplasmic tail provides membrane anchoring and accurate association with CD3 subunits. Charged pairs of residues inside the hydrophobic core of the TCR/CD3 complex direct the asymmetric assembly of the subunits *(54)*.

Although mouse and human TCR are of considerable sequence identity with respect to their constant domains, the usefulness of murine TCR in man may be limited by their potential immunogenicity. Both the high degree of sequence and structural homology and the invariant character of mouse constant domains permit their entire replacement by human Cα/β regions without interfering with TCR function. Humanization beyond that initial step of domain replacement ("deimmunization") requires several rounds of mutational refinements with regard to structural and functional aspects of TCR biology.

The variable and constant domains of either TCRα/β chain, each composed of a twisted anti-parallel β sheet, are linked by an extended loop and interact with each other via a few residues. The interactions of both the juxtaposed variable Vα and Vβ as well as the constant domains Cα and Cβ are complex, and the tight interactions of the Cα/Cβ pair in particular govern interchain affinity *(23)*. Vα/Cβ and Vβ/Cα interactions are almost absent and thus facilitate domain replacement.

On a genetic basis, an approach towards humanization took advantage of singular restriction sites located inside the loop sequence that joins the variable and constant domains to produce chimerized, so-called partially humanized TCR; in the case of the mouse TCRα chain, a conserved AlwNI-site CAGNNNCTG (wherein *N* = A/C/G/T), translationally located aminoterminally to the first Cα β-strand and embedded inside the conserved PEPA sequence, allows the domain exchange (**Fig. 4A**).

A full-length human constant Cα has been isolated irrespective of its subfamily specificity by coupled RT-PCR/nested PCR from the human Jurkat cell line. The RT-PCR protocol was identical to the isolation of huCα and huCβ, and has been slightly modified as described under **Subheading 3.2.3.** by increasing the annealing temperature to 55 ± 10°C (RT-PCR: primer pair for_huCαTCR: [5'- ATA TCC AGA ACC CTG ACC CT -3'] / rev_huCαTCR [5'- GGG AGC ACA GGC TGT CTT ACA -3']). For nested PCR, the RT-PCR protocol has been adopted, omitting the RT reaction and using the high-fidelity Pfu-DNA polymerase whose optimal extension temperature lies at 72°C (nested PCR: primer pair for_huCαTCR_<u>AlwNI</u> [5'- CAG AAC C<u>**CA GAA CCT G**</u>CC GTG TAC CAG CTG AGA GAC TCT A -3'] / rev_huCα_<u>BamHI</u> [5'- CG <u>GGAT CC</u>**T CA**G CTG GAC CAC AGC CGC AGC GTC ATG A -3']). In order to get a full-length constant region, the reverse primers for RT-PCR have been located at the 3'-noncoding region close to the stop codons of TCRα (as for TCRβ). By introducing two mutations into a primer suited for nested PCR, an AlwNI site has been designed at the corresponding position in the human as compared to the mouse residue sequence (**Fig. 4A**).

4A:

	β-strand Vα									Loop					β-strand Cα				
muTCRα	...G	A	G	T	R	L	K	V	I	A	H	I	**Q**	N	P	E	**P**	**A**	**V**	**Y**
	gga	gca	ggt	acc	aga	ctg	aag	gtt	ata	gca	cac	atc	cag	aac	*cca*	**gaa**	**cct**	*gct*	gtg	tac
	gga	caa	ggg	acc	atc	ttg	act	gtc	cat	cca	aat	atc	cag	aac	*cct*	**gac**	**cct**	*gcc*	gtg	tac
huTCRα	**G**	Q	**G**	**T**	I	**L**	T	V	H	P	N	**I**	**Q**	**N**	**P**	D	**P**	**A**	**V**	**Y...**

4B:

	β-strand Vβ									Loop					β-strand Cβ				
muTCRβ	...G	P	**G**	**T**	**R**	**L**	**T**	**V**	L	E	D	L	*R*	N	V	T	**P**	**P**	K	V
	ggt	ccc	ggc	acc	agg	ctc	acg	gtt	tta	ga*g*	**gat**	**ct**g	aga	aat	gtg	act	cca	ccc	aag	gtc
	ggg	ccg	ggc	acc	agg	ctc	acg	gtc	aca	ga*g*	**gac**	**ct**g	aaa	aac	gtg	ttc	cca	ccc	gag	gtc
huTCRβ	**G**	**P**	**G**	**T**	**R**	**L**	**T**	**V**	I	**E**	**D**	L	K	N	V	F	**P**	**P**	E	V...

Fig. 4. **(A)** Nucleotide and amino acid sequence alignment of a mouse MDM2(81–88)-specific and a human gp100(280–288)-specific TCRα at the related regions of domain replacement to exemplify the high degree of amino acid homology. Highly conserved amino acids are indicated in bold. GxG refers to the C-terminal consensus sequence of the CDR3 loop, and IQNPxPAVY to the start of the highly conserved Cα domain. Additionally, boxed residues delineate the amino acid sequence of the resulting chimerized molecule. Differing residues are underlined. The AlwNI restriction site CAGNNNCTG (italic for the recognized bases, bold for the whole sequence) is located close to the start of the Cα domain. Nucleotides that have to be changed in the PCR primer for complementarity to the mouse Vα region are underlined. **(B)** Nucleotide and amino acid sequence alignment of an A2.1-restricted mouse MDM2(81–88)-specific and a human gp100(280–288)-specific TCRβ. Abbreviations are as described in (A). EDL refers to the start of a loop connecting both domains, followed by the highly conserved Cβ domain. The BstYI restriction site PuGATCPy is located within the EDL consensus sequence. For cloning strategy refer to **Subheading 3.3.1.**

Due to internal AlwNI sites in the vector, DNA fragment ligation had to be performed: the cloned mouse TCR was digested with EcoRI/AlwNI and ligated to the AlwNI/BamHI-cut nested PCR product. The heteromultimerized products were separated from the unwanted homomultimers (generated as an artifact by "head to tail" multimerization) by redigestion with EcoRI/BamHI to yield the chimerized DNA fragment (*see* **Note 10**). The resulting 0.83-kB band was ligated into a cloning vector (**Subheading 3.2.4.**) and subsequently cloned via NcoI/BamHI into the retroviral pBullet vector (**Subheading 3.2.6.**).

The generation of the chimerized TCRβ chain has been designed the same way (**Fig. 4B**): a nonunique BstYI site "PuGATCPy" (Pu = purine-base/Py = pyrimidine-base) has been identified in the DNA sequence of the conserved "EDL" stretch in the intervening loop. The additional location of BstYI inside the constant domain of human TCR requires the blunt-end ligation of the nested PCR product to circumvent truncation: the BstYI fragment encoding the mouse variable domain has been blunt-ended by the T4-DNA polymerase fill reaction, and subsequently cut with EcoRI. The resulting EcoRI/[BstYI]-fragment has been blunt-ligated to the nested PCR fragment 5'- p-[BstYI]-huCβ-BamHI -3', thereby restoring the nonpalindromic BstYI recognition sequence: the T4-DNA polymerase reaction results in a "GGATC"-3'-end of muVβ that will complement with the 5'-"T"-end of PCR-amplified huCβ to a BstYI site (*see* **Note 11**). Before ligation, the blunt PCR product has to be enzymatically phosphorylated by T4 DNA-PNK (**Subheading 3.2.6.**). The mixed ligation product has to be recut with EcoRI/BamHI (for the same reasons as mentioned above) and cloned into appropriate expression vectors for functional studies (RT-PCR: for_huCβTCR [5'- TAG AGG ACC TGA ACA AGG TGT T -3'] / rev_huCβTCR [5'- AAC CAT GAC GGG TTA GAA GCT CCT A -3']; nested PCR: for_huCβTCR_[BstYI] [5'- <u>T</u>GA ACA AGG TGT TCC CAC CCG A -3']/ rev_huCβTCR_BamHI [5'- CG<u>G GAT CC</u>**T CA**G AAA TCC TTT CTC TTG ACC ATG GCC ATC A -3']). The related nucleotide sequences for human TCRα/β has been taken from Genbank of NCBI (National Center for Biotechnology Information, Bethesda, MD; Entrez nucleotide in http://www.ncbi.nlm.nih.gov/) and refers to the entry M12423 for TCRα in Jurkat and M15564 as a clonal representative of a TCRβ sequence that will be found in Jurkat cell line. There exist "a few sequence differences" (due to 2 Cβ alleles) when comparing multiple TCRβ sequences (e.g., to gp100(280–288)-specific TCRβ in **Fig. 4**) in this region relevant for primer design, but this does not impair the approach.

Due to the location of the restriction sites AlwNI and BstYI centered in the loops that link the variable and constant domains, they are found in all murine TCRs irrespective of their subfamily membership, including Cβ1 and Cβ2 domains. The humanization approach is affected by these restriction sites when additionally located inside the coding segments of the variable domains: this is likely to occur, in particular, with respect to the highly degenerate CDR3-loop segments. As a consequence, truncated variable regions have to be avoided by partial restriction.

More elaborate PCR techniques work with an intermediate megaprimer: in a first PCR, this strategy produces a large fragment of the gene to be fused (i.e., the mouse variable region) by utilizing an oligonucleotide that anneals to a short stretch of bases
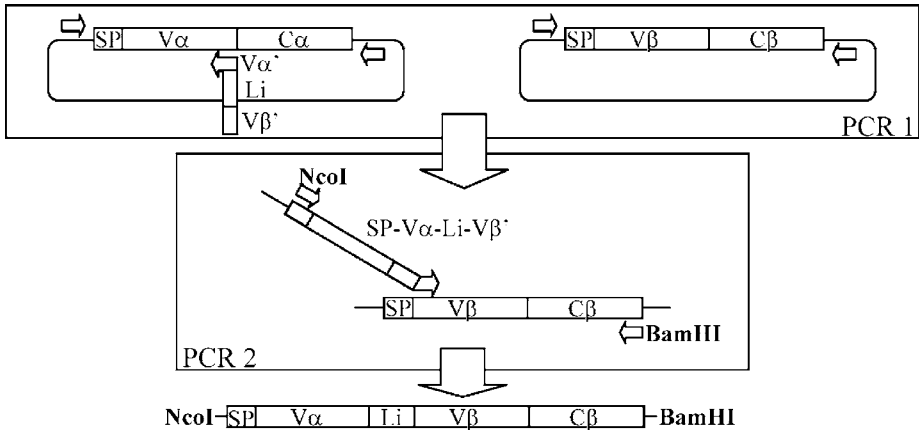
Fig. 5. Ligation PCR consists of two consecutive PCRs: the first PCR produces the double-stranded megaprimer (SP-Vα-Li-Vβ') that downstream is complementary to the 5'-end of the Vβ region (Vβ'). An aliquot of the 1st PCR product that already includes the 2nd template is transferred to the second PCR mix containing the nested primers. Intermediate purification is usually not necessary, as the nested primers are of sufficient specificity.

at the sequence of interest (i.e., the ample region between the variable and the constant region). The chosen position has to be of sufficient homology with the 5' end of the second gene fragment (i.e., the human constant region) to allow annealing of the megaprimer with its 3' end in a subsequent PCR. The advantages of this approach are its independence from restriction enzymes and its ability to simply join gene segments at a precise nucleotide and at any amino acid position (*see also* **Subheading 3.3.2.**).

3.3.2. Generation of Single-Chain TCR

Single-chain TCR (scTCR) are chimeric TCR consisting of the variable Vα and Vβ domains of an antigen-specific TCR covalently linked via a 15–20 amino acid sequence, the so-called linker, to bridge the C-terminal of the preceding Vα domain to the N-terminal of the Vβ domain. The linkage should provide sufficient length to maintain the sterical orientation between the domains and to allow for some kind of flexibility required for antigen recognition and signal transduction into the cytoplasm *(55)*. The linker has to be resistant against proteolysis *(29)*, and thus must have an amino acid composition that combines flexibility, solubility, thermodynamic stability, and a sustainment of defined oligomeric state *(30)*; a triplicate redundancy of the glycine-rich motif GlyGlyGlyGlySer proved to be effective for generating functional scTCR and scFv fragments of antibodies. The variable Vβ domain is followed by the Cβ domain to displace the antigen-recognition domains far enough from the polar lipid of the cell membrane. The linker has to be specifically inserted at the borders of the Vα and Vβ domains, thus at the end of the last β strand of Vα (*see also* **Figs. 4 & 5**) and the beginning of Vβ. The flanking base sequences are likely non-homologous

and can therefore be easily linked by a modified PCR that utilizes a chimeric primer consisting of identical base sequences for successful priming to the domains as templates. In addition, any arbitrary sequence, in our case the 218 linker sequence (*[29]*; NH$_2$-Gly Ser Thr Ser Gly Ser Gly Lys Pro Gly Ser Gly Glu Gly Ser Thr Lys Gly-COOH), can be inserted between the two sequence-related parts. Because the upstream Vα region is much smaller than the residual construct, it is more convenient to design the chimeric primer in reverse and use it in combination with a forward primer specific for the signal peptide sequence that precedes Vα. In this case, this leads to the production of conceivably the shortest megaprimer (**Fig. 5**). The first PCR product encodes the signal peptide of Vα, Vα, the artificial linker, and a short tail that specifically recognizes the 5' end of Vβ directly downstream of the signal peptide encoding sequence, as defined by the mouse TCR variable gene segment families (*[56]*; first PCR: for_pBullet [5'- GGA TAC ACG CCG CCC ACG TGA -3'] / rev_pBullet_IRES [5'- GAG GGA GTA CTC ACC CCA ACA -3']; chimeric primer: rev_Chim_218 [5'- TTT GGG TGT CTG AGT AAT GAT GCC ACC GCC CTT GGT GCT GCC CTC GCC GCT GCC GGG TTT GCC GCT ACC GGA AGT AGA GCC TGC TAT AAC CTT CAG TCT GGT ACC TGC -3']). A nested PCR using the double-stranded megaprimer and a nested primer as forward primer mix combined with a reverse primer specific for the 3' end of the Cβ region will yield a full-length scTCR of any desired amino acid sequence and linkage (*see* **Note 12**). Second PCR: megaprimer: first PCR product, comprising 5'- SP-Vα-Li-Vβ'-3'; primer: for_SP-Vα_[NcoI] (5'- GAA AGG CTG CTG TGC TCT CT -3') / rev_Cβ_BamHI (5'- CGG GAT CCG CTC AGG AAT TTT TTT TCT TGA CCA T -3'). Even minimal changes in the annealing temperature significantly influence the amount of PCR product. In case of trouble, base composition, GC content, and possible secondary structures that may form inside the chimeric primer have to be taken into consideration. The second PCR uses nested primers encoding enzyme restriction sites that turn the PCR product suitable for digestion and efficient cloning into expression vectors. We cloned the PCR product directly with NcoI/BamHI into the retroviral transfer vector pBullet *(32,51,52)*, which depends on NcoI site-specific insertion at the 5' end of the scTCR transgene. We have modified the ligation PCR method somewhat to conveniently yield scTCR in two consecutive PCRs. A primer pair that hybridizes to plasmid sequences flanking the templates amplifies them and turns them into more ideally suited PCR templates for the subsequent, nested PCR. As a prerequisite, both templates have to be embedded in the same band of vectors. Only 2 pmol of chimeric primer are added, in contrast to 50 pmol for the flanking primers, in order to improve specificity of the intermediate megaprimer product (*see* **Note 13**). For a sample at a particular annealing temperature, 1 μL (100 ng) of each plasmid encoding the templates to be chimerized are pipetted to 0.5 μL of the plasmid-specific forward and reverse primer (each 100 pmol/μL), 2 μL chimeric primer (1 pmol/μL), 0.5 μL dNTP (each 10 m*M*), 1 μL MgSO$_4$ (50 m*M*), 10X Pfx amplification buffer (Invitrogen), 10X Pfx enhancer solution, 33 μL sterile water, and 0.5 μL Pfx polymerase (2.5 U/μL). The cycling parameters were chosen to be 2 min at 94°C, followed by 34 cycles of denaturation for 30 s at 94°C, annealing for 45 s at 55 ± 10°C, extension for 60 s/kB template at 68°C, and
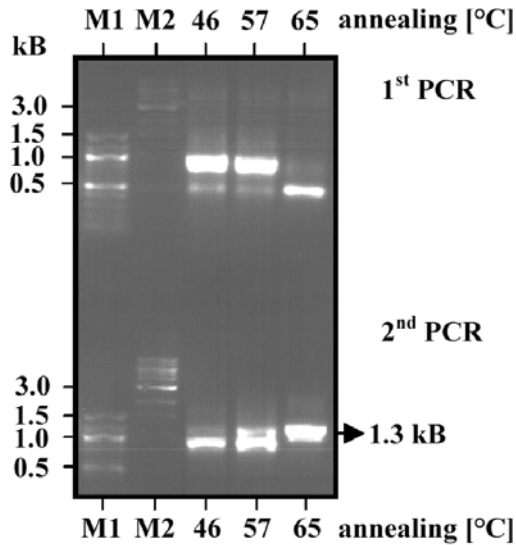
Fig. 6. Ligation PCR for MDM2-specific TCRα and TCRβ as templates to generate a scTCR with an 18-mer linker. One-fifth of each PCR has been loaded on a regular 1% agarose gel. In general, higher annealing temperatures (65°C) produce sufficient megaprimer (0.5 kB) for subsequent PCR to gain a full-length scTCR (1.3 kB). Although the first PCR does not produce even a faint band resulting from the scTCR construct, the second PCR visibly enhances amplification of tiny amounts of the scTCR construct. This gel photography was kindly provided by Simone Thomas (Theobald Laboratory, Department of Hematology and Oncology, Johannes Gutenberg University, Mainz, Germany). M1 = 100-bp marker, M2 = 1-kB marker (NEB).

final extension for 7 min at 68°C. For the nested PCR, template-specific primers were applied, which included blunt NcoI and BamHI restriction sites in the forward and reverse direction, respectively. The chimeric primer and the plasmid templates were replaced by water, and for each corresponding temperature, 1 µL of the first PCR product was added. Again, a temperature gradient was used for the same three independent temperatures (*see* **Note 14**). Cycling parameters were identical to the first PCR. Generally, higher annealing temperatures (>60°C) resulted in a unique ethidium bromide–stained band of almost 1.3 kB, specific for the scTCR (**Fig. 6**). Ligation took place as described under **Subheading 3.2.6.**

3.4. Heterologous Expression of Mouse TCR in Human T-Cells

3.4.1. Selection Markers for In Vitro Enrichment of TCR-Transduced T-Cells

For in vitro analysis of defined TCR-transduced T-cells and evaluation of subtle TCR modifications, it is essential to analyze pure TCR-transduced T-cell subpopulations. Therefore, TCR cassettes are linked by an internal ribosome entry site (IRES) to a resistance marker. The IRES element located between two genes allows the bicis-

tronic mRNA transcripts to be translated simultaneously. Because both the protein of interest and the antibiotic resistance protein are produced from a single transcript, it is more likely that a single cell will express either protein. Furthermore, cells will express high levels of the desired protein when an attenuated IRES is used that minimizes translation of the selection marker relative to the gene of interest and thus raises the selective pressure to survive. Hence, high doses of antibiotics will select for cells expressing higher levels of the gene of interest. We use the IRES-puro2 and -neo cassettes (BD-Clontech), which contain the IRES element of the encephalomyocarditis virus (ECMV). For this purpose, TCR transgenes are cloned upstream and the selection cassettes downstream of the IRES element (**Fig. 7**; *[57,58]*). For routine application, the IRES cassettes were integrated into the retroviral vector pBullet in order to insert and to select for any TCR chain (*see* **Note 15**). The insertion of the selection cassettes between the LTRs reduces exposure to the antibiotics to one week, subsequently ensuring stable transgene expression.

3.4.2. Transduction, Selection, and Expansion Procedure

The principal method relies on the transient transfection of the packaging cell line 293T and its derivative phoenix-ampho for rapid virus production. The transduction protocol differs somewhat from that of Ralph Willemsen *(32,51,52)* or Garry P. Nolan (*see* **Note 16**). The major advantage of this routine protocol is the reproducible yield of virus titers in the range of 1×10^6–1×10^7 GFU/mL (GFP forming units/mL), which is a critical threshold for successful transduction (*see* **Note 17**). One may keep in mind that each TCR chain is encoded on a separate plasmid **(Fig. 7)**. Poor transfection will drop the detection of transduced T-cells that have incorporated both transgenes at the same time. The original calcium phosphate transfection method was more sensitive to physicochemical changes (temperature, pH) than the Fugene transfection agent (Roche), which is based on a proprietary blend of lipids:

1. Day 1. 293T and phoenix-ampho cell lines (ATCC) will be coseeded, each at 1.2×10^6, in a T75 tissue flask (DMEM for 293T/phoenix-ampho [DMEM, 10% heat-inactivated FCS, 1X glutamine, 1X NEAA, 25 m*M* HEPES, 1X Pen/Strep]) (*see* **Note 18**).
2. Day 2. Medium will be removed and replaced (10 mL) by fresh DMEM 10% FCS. Four h later, 60 µL of Fugene 6 will be added to prewarmed (RT) 900 µL DMEM (without FCS) as well as 5 µg of each of the plasmids: pHit60, pCOLT-GALV (kindly provided by R. Willemsen; **refs.** *32,51,52*), and both, the TCRα/IRESpuromycin- as well as the TCRβ/IRESneomycin-recombinant plasmid. The mix will be incubated for 20 min and then slowly dropped into the medium of the gently swirled 293T/phoenix-ampho coculture (*see* **Note 19**).

   PBMCs will be seeded at 2×10^6/mL in 24-well plates (2 mL each well) and activated for 2 d with soluble anti-CD3 antibody at 20 ng/mL in huRPMI/10% (medium composition for human T-cells: RPMI, phosphate-free, 10% pooled and heat-inactivated [30 min, 55°C] human AB-serum, 1X glutamine, 25 m*M* HEPES, 1X Pen/Strep) (*see* **Note 20**).
3. Day 3. DMEM medium will be removed and replaced by 8 mL of huRPMI/10%.
4. Day 4. Retroviral supernatant of 293T/phoenix-ampho will be harvested and replaced the same way as on d 3, and centrifuged for 1 min (324*g*) to remove nonadherent 293T and phoenix-ampho cells. 4–8×10^6 of the pooled preactivated T-cells (depending on availability) will be suspended in 4–8 mL of retroviral supernatant (1×10^6 T-cells/mL)
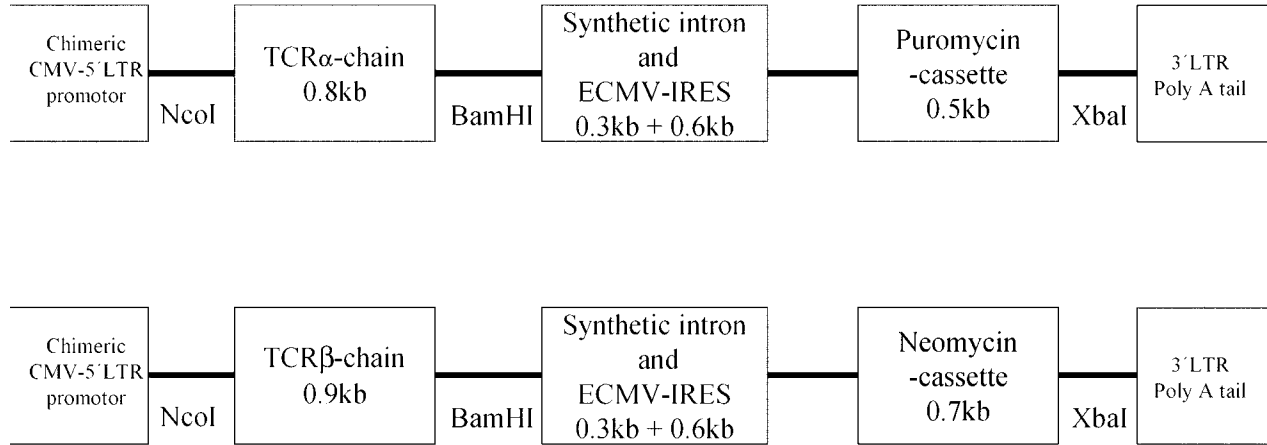
Fig. 7. Vector design. Insertion of the selection cassettes into retroviral vectors to generate bicistronic mRNAs for coupled translation of TCRα/puromcin-N-acetyl-transferase and TCRβ/neomycin phosphotransferase. CMV = cytomegalovirus; ECMV-IRES = internal ribosomal entry site of the encephalomyocarditis virus; kb = kilobases; LTR = long terminal repeats. Synthetic intron refers to an mRNA-stabilizing element (BD/Clontech). Cloning sites are indicated. The polyA signal is located in the 3' LTR.

adding Polybrene (4 μg/mL) and IL2 (40–100 U/mL) and seeded in one well of a 6-well plate (Becton Dickinson Falcon, Cat. No. 353046), centrifuged at 30°C for 60 min (1300*g*), and co-incubated overnight at 37°C in a humidified incubator (5% CO$_2$), thereby initiating the first cycle of retroviral transduction (*see* **Note 21**).

5. Day 5. T-cells will be separated from exhausted retroviral supernatant by centrifugation (324*g*, 5 min, 21°C) and suspended in freshly prepared supernatant. The second cycle is identical with the first one (*see* **Note 22**).
6. Day 6. T-cells will be removed from old retroviral supernatant and supplemented with fresh huRPMI/10% medium at an equal volume (4–8 mL). For sustained activation of T-cells, 2 μL CD3/28 beads/1 × 10^6 T-cells (Dynal) and 40–100 U IL2/mL will be added.
7. Day 8. For selection of transduced T-cells, 600–800 μg/mL (f.c.) geniticin will be added.
8. Day 12. Five μg/mL (f.c.) puromycin will be added.
9. Day 15. CD3/28 beads will be removed by magnetic depletion and cells will be cultured at 0.5 × 10^6/mL in fresh huRPMI/10%, weekly supplemented with 2 μL CD3/28 beads/ 1 × 10^6 cells and 40–100 U IL2/mL (up to twice a wk) (*see* **Note 23**).

This protocol allows rapid and efficient selection as well as expansion of TCR-transduced T-cells up to some orders of magnitude. The cell numbers are sufficient to isolate subpopulations (e.g., CD4$^+$/CD8$^+$) for further expansion and functional analyses (*see* **Fig. 8**). However, the expansion of T-cells by CD3/28 beads selectively promotes the expansion of CD28$^+$ T-cells. Also, CD8$^+$ T-cell growth is favored (400-fold expansion within 6 wk, unpublished results). As the expansion of CD8$^+$ T-cells correlates with the amount of CD4$^+$ T-cells in the culture, the expansion of T-cells without any other cell-based feeder system is limited. Depending on the individual donor, cells can be kept in culture for more than 3 mo. We recommend freezing an aliquot of freshly selected T-cells at that early time for convenient reculturing.

4. Notes

1. Alternatively, one might try to exploit the invariant nature of the 3'-noncoding regions for the primers SP1/2 and to position SP3 at the 3' end of the TCR reading frame. This would enable the isolation of the full-length TCR gene, in particular TCRα, which is represented by only one constant region gene locus.
2. Mouse T-cells will be restimulated weekly with excess of irradiated C57BL/6-derived spleen feeder cells and peptide-pulsed HLA-A2.1-transfected human Jurkat cells (JA2). This will not impede the sufficiently homogenous purification of the RNA pool. Nevertheless, the mouse T-cells have to be carefully counted and morphologically distinguished.
3. In case of insufficient T-cell numbers (growth, availability), one might try to scale down the input RNA since PCR is very sensitive.
4. Alternatively, control RNA and primer may be added as internal standards to control reverse transcription and subsequent PCRs (for details, *see* protocol "5'/3'-RACE Kit" [Roche]).
5. As the amount of the tailing product is not a limiting factor, it is strongly recommended to assay at least three different annealing temperatures in the range of 55–65°C. The optimal annealing temperature turned out to be in the elevated range, since this tends to minimize unspecific reactions without loss of the specific product. The same guideline applies to the second PCR—keep the temperature gradient unchanged and deliver each sample of the first PCR to the same temperature in the subsequent PCR. In case of trouble, one may try to fine tune a PCR product of one particular temperature of the first PCR on a tem-

before selection   **after selection**

A
Mock

B
GFP

C
Mu Wt TCR MDM2

D
Mu Chim TCR MDM2

huCD8 – PCy5

Vβ6 - FITC
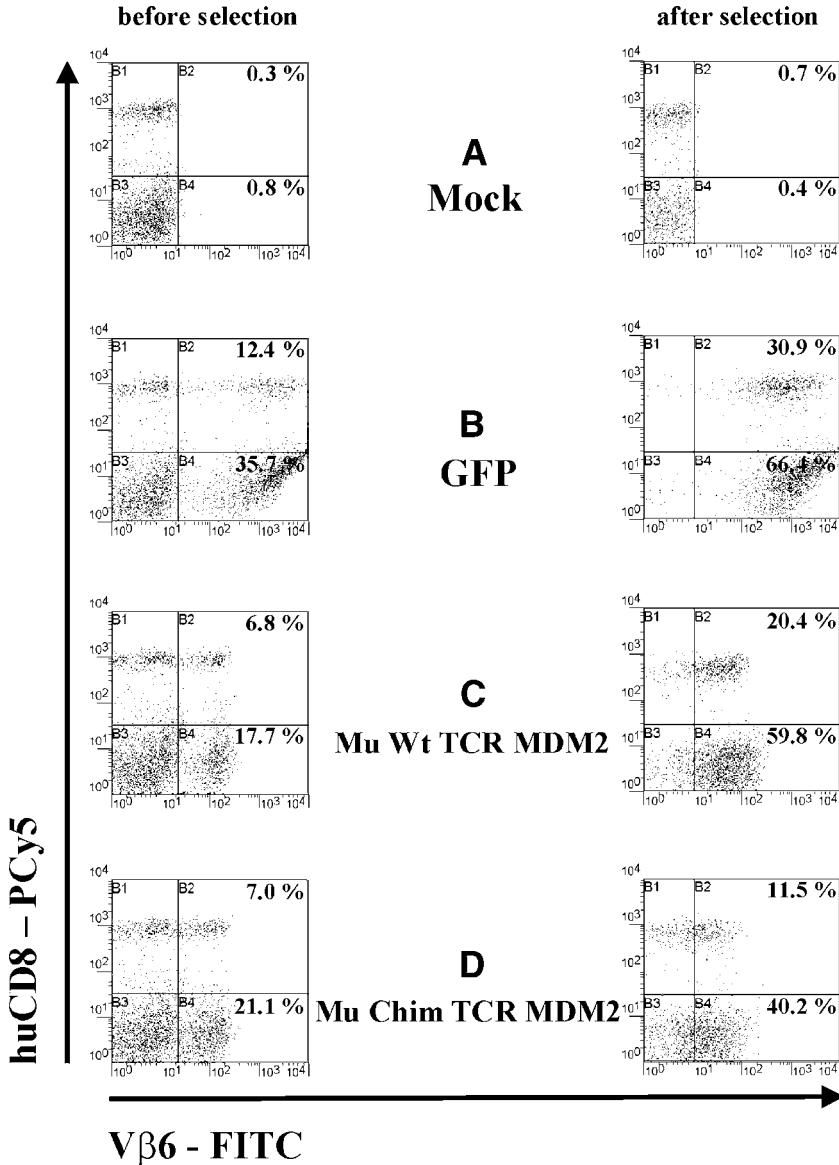
Fig. 8. Human T-cells transduced with empty vector (mock) **(A)**, green fluorescent protein (GFP) **(B)**, mouse wild-type MDM2-specific TCR (Mu Wt TCR MDM2) **(C)**, and chimeric MDM2-specific TCR with humanized constant domains (Mu Chim TCR MDM2) **(D)**. The left panel shows the bulk transduction efficiency 2 d after two consecutive transduction cycles and before geneticin/puromycin selection; the right panel shows the overall selection efficiency for all constructs 2 wks after cessation of the selective pressure. In general, TCR that were structurally modified, as exemplified for the partially humanized TCR **(D)** tend to be expressed at lower amounts according to anti-vβ6 or tetramer staining (not shown).

perature gradient in the second PCR. The setup of master mixes guarantees uniformity and comparability of the individual temperatures. As a general rule, the rise or decline of PCR bands within a temperature gradient is a reliable indicator for the optimal annealing temperature.

6. The introduction of multiple ambivalent base positions into PCR primers has to be considered carefully, because aberrant amino acid sequences may be generated due to possible permutations of adjacent base triplets—in this case, the three Y positions will only result in the two allowed motifs "LysArgLys" and "LysLysLys" of the C-terminal tail (Cβ1 and Cβ2), which might serve as ER retention signals during TCR recycling *(59)*.

7. There is a high degree of variability in choosing the appropriate ligation strategy: the restriction sites for cloning have to be scrutinized to avoid cutting inside the TCRα/β genes. When uncertain about the sequences of the variable gene regions, one may choose eight-base-pair cutters like Asc (NEB) to minimize the probability of undesired digestion, or select "A/T" cloning to prevent trouble with restriction sites. Altogether, however, it is of advantage to use restriction enzymes, because any construct can be easily subcloned or routinely checked by test digestion for accuracy.

8. More conveniently, the reverse primer for RT-PCR (**Subheading 3.2.3.**) amplification of the Cβ2 region could be extended to silence the NcoI site by a base mutation without changing the amino acid sequence. Mouse Cβ1 has no terminal NcoI site.

9. For routine cloning, it is much more comfortable to precede ligation by silencing any internal NcoI sites. NcoI/BamHI cloning allows higher ligation and transformation efficiency.

10. For optimal fragment ligation, either DNA fragment has to be quantified in analytical agarose gels to get an estimate of equivalent stoichiometry. The multimers can easily be distinguished from the heterodimer by molecular weight and should vanish after the EcoRI/BamHI cut.

11. The major drawback of this approach is the reduced ligation efficiency of blunt-ended DNA and the frequent generation of 5' overhangs by T4 DNA polymerase, which will reduce compatibility of the ligation educts. Strictly adhere to recommended blunt-end cloning protocols and screen more bacterial clones than usual.

12. One limitation is the synthetic length of the chimeric primer (120mers have been probed in our laboratory); each end of the chimeric primer that is complementary to its template should be of at least half the sequence length as compared to the DNA linker sequence. For example, the 18 amino acids of a linker will be encoded by 54 bases. As a consequence, the complementary sequences on both sides of the chimeric primer should comprise a minimum of 27 bases, resulting in a 108mer.

13. Raising the amount of the chimeric primer did not ameliorate both the amount and specificity of the final chimeric PCR product, as determined by extensive primer titration.

14. It is strongly recommended to assess PCR at three different annealing temperatures at once. A temperature gradient of 20°C overall, with an average temperature of 55°C, proved to be a useful vantage point.

15. For any cell line and antibiotics used, killing curves have to be determined in order to guarantee lethal doses. In the case of bulk IL-2 treated T-cells, 400 μg/mL geneticin and 2.5 μg/mL puromycin (f.c.) proved to kill the cells. During the 1 wk of treatment, the concentration is doubled to be fail-safe. The stock concentration of the antibiotics is corrected for biological activity and stored in frozen aliquots.

16. Useful hints/tutorials and protocols for reproducible transfection and transduction are given at the homepage of the Garry P. Nolan laboratory, which is mainly responsible for

the advanced 293T/phoenix-ampho retroviral transduction system (*see* Website: http://www.stanford.edu/group/nolan/). Material transfer agreement (MTA) forms for delivering the packaging cell lines can be downloaded; after being signed by the principal investigator, these have to be returned for ATCC orders. In our hands, the packaging cell lines have initially been expanded to the maximum and Plasmocin treated (Invivogen) before being frozen down in aliquots of 5×10^6 per vial. Cell morphology and adherence capability were checked routinely (protrusions that form cell/cell contacts as monolayers, no clumps, and striking granularity). Frequent passaging (2×10^6/T75 flask for 2.5 d) and confluence were avoided. Ideally, the cells were not taken in culture until 3 d before starting a new transduction experiment (at d 1). Extensive but careful (293T are semiadherent) washing with PBS before trypsinization is important to avoid the formation of clumps and to favor uniform adherence as a monolayer when seeded. The incubator and the sterile bench were routinely deactivated to minimize the risk of mycoplasma contamination, which would have a detrimental effect on transduction.

17. The retroviral particle-containing supernatant has been titrated by transduction of the susceptible cell line CF2TH *(52)* with 10-fold dilutions of a retroviral supernatant originating from a green fluorescent protein (GFP)-containing vector construct. The proportion of positive cells has been quantified by FACS in the green-emitting FITC channel upon excitation by 488 nm. One drawback of this transient technique is the significant drop in transduction efficiency of thawed cultures of recently transfected packaging cells. This necessitates the redundant transfection with the same vector constructs in cases where the experiment has to be repeated. Alternatively, one may attempt to establish stable packaging cell lines/clones. For high throughput of novel TCR constructs, however, the transient approach is sufficient and less time-consuming.

18. Prevent cells from confluence until virus supernatant harvest, as this will dramatically reduce virus titer and transduction efficacy. The addition of HEPES supports pH stability.

19. Ratio of Fugene (µL) to plasmid (µg) has to be titrated in order to increase transfection efficiency. In our hands, a ratio of 3:1 proved to be feasible for the simultaneous transfection of up to 4 plasmids (equals 20 µg). Adhere to the recommendations of the commercial supplier for handling of the transfection reagent.

20. RPMI depleted of phosphate not only improves transduction efficiency due to an increase of phosphate receptor expression as target for the GALV envelope *(60)*, but also improves performance, survival, and antigen specificity of transduced bulk T-cell cultures in vitro.

21. In our hands, the use of RectoNectin™ (TaKaRa) as a mediator for cell/virus-particle adherence improves transduction somewhat. For critical vector constructs, one may enhance expression of the transgene product by taking advantage of fibronectin-coated 6-well plates.

22. This procedure may be repeated as long as retroviral supernatant of exponentially growing packaging cells will be harvested. Once seeded, the packaging cells will become confluent at latest on d 5. In case of transient transfection, the schedule is therefore limited to two daily cycles. For a more convenient Monday-to-Friday protocol, the second cycle may be dispensable. The transfected cells can be stored at –80°C and thawed again in order to isolate new supernatant for further transductions, albeit with lower efficiency as long as they have not been confluent before freezing.

23. Achievable cell densities depend on their actual expansion potency. The older the culture, the more limited cell division is. Cell density should not fall below 0.5×10^6/mL and should not exceed 1.5×10^6/mL, as this would lead to unfavorable growth and the eventual death of the cell culture. These events favor the outgrowth of oligoclonal T-cell populations of uncertain specificities that differ from those of bulk cultures and may lead to a functional bias.

References

1 Yu, Z. and Restifo, N. P. (2002) Cancer vaccines: progress reveals new complexities. *J. Clin. Invest.* **110(3),** 289–294.

2 Kessels, H. W., Wolkers, M. C., and Schumacher, T. N. (2002) Adoptive transfer of T-cell immunity. *Trends Immunol.* **23(5),** 264–269.

3 Bankovich, A. J. and Garcia, K. C. (2003) Not just any T cell receptor will do. *Immunity* **18(1),** 7–11.

4 Kane, L. P., Lin, J., and Weiss, A. (2000) Signal transduction by the TCR for antigen. *Curr. Opin. Immunol.* **12(3),** 242–249.

5 Theobald, M., Biggs, J., Hernandez, J., Lustgarten, J., Labadie, C., Sherman, L. A. (1997) Tolerance to p53 by A2.1-restricted cytotoxic T lymphocytes. *J. Exp. Med.* **185(5),** 833–841.

6 Kuball, J., Schuler, M., Antunes, FE., et al. (2002) Generating p53-specific cytotoxic T lymphocytes by recombinant adenoviral vector-based vaccination in mice, but not man. *Gene Ther.* **9(13),** 833–843.

7 Stanislawski, T., Voss, R. H., Lotz, C., et al. (2001) Circumventing tolerance to a human MDM2-derived tumor antigen by TCR gene transfer. *Nat. Immunol.* **2(10),** 962–970.

8 Kessels, H. W., Wolkers, M. C., van den Boom, M. D., van der Valk, M. A., and Schumacher, T. N. (2001) Immunotherapy through TCR gene transfer. *Nat. Immunol.* **2(10),** 957–961.

9 Holler, P. D. and Kranz, D. M. (2003) Quantitative analysis of the contribution of TCR/pepMHC affinity and CD8 to T cell activation. *Immunity* **18(2),** 255–264.

10 Lanzavecchia, A., Lezzi, G., and Viola, A. (1999) From TCR engagement to T cell activation: a kinetic view of T cell behavior. *Cell* **96(1),** 1–4.

11 Rosenberg, S. A. (1999) A new era for cancer immunotherapy based on the genes that encode cancer antigens. *Immunity* **10(3),** 281–287.

12 Holler, P. D., Holman, P. O., Shusta, E. V., O'Herrin, S., Wittrup, K. D., and Kranz, D. M. (2000) In vitro evolution of a T cell receptor with high affinity for peptide/MHC. *Proc. Natl. Acad. Sci. USA* **97(10),** 5387–5392.

13 Kessels, H. W., van den Boom, M. D., Spits, H., Hooijberg, E., and Schumacher, T. N. (2000) Changing T cell specificity by retroviral T cell receptor display. *Proc. Natl. Acad. Sci. USA* **97(26),** 14,578–14,583.

14 Stauss, H. J. (1999) Immunotherapy with CTLs restricted by nonself MHC. *Immunol. Today* **20(4),** 180–183.

15 Theobald, M., Biggs, J., Dittmer, D., Levine, A. J., and Sherman, L. A. (1995) Targeting p53 as a general tumor antigen. *Proc. Natl. Acad. Sci. USA* **92(26),** 11,993–11,997.

16 Sherman, L. A., Hesse, S. V., Irwin, M. J., La Face, D., and Peterson, P. (1992) Selecting T cell receptors with high affinity for self-MHC by decreasing the contribution of CD8. *Science* **258(5083),** 815–818.

17 Katayama, C. D., Eidelman, F. J., Duncan, A., Hooshmand, F., and Hedrick, S. M. (1995) Predicted complementarity determining regions of the T cell antigen receptor determine antigen specificity. *EMBO J.* **14(5),** 927–938.

18 Breedveld, F. C. (2000) Therapeutic monoclonal antibodies. *Lancet* **355(9205),** 735–740.

19 Eshhar, Z. (1997) Tumor-specific T-bodies: towards clinical application. *Cancer Immunol. Immunother.* **45(3–4),** 131–136.

20 Labrecque, N., Whitfield, L. S., Obst, R., Waltzinger, C., Benoist, C., and Mathis, D. (2001) How much TCR does a T cell need? *Immunity* **15(1),** 71–82.

21 Carson, G. R., Kuestner, R. E., Ahmed, A., Pettey, C. L., and Concino, M. F. (1991) Six chains of the human T cell antigen receptor.CD3 complex are necessary and sufficient for processing the receptor heterodimer to the cell surface. *J Biol Chem.* **266(12),** 7883–7887.

22 Gouaillard, C., Huchenq-Champagne, A., Arnaud, J., Chen, C. L., and Rubin, B. (2001) Evolution of T cell receptor (TCR) alpha beta heterodimer assembly with the CD3 complex. *Eur J. Immunol.* **31(12),** 3798–3805.

23 Li, Z. G., Wu, W. P., and Manolios, N. (1996) Structural mutations in the constant region of the T-cell antigen receptor (TCR)beta chain and their effect on TCR alpha and beta chain interaction. *Immunology* **88(4),** 524–530.

24 Saito, T., Sussman, J. L., Ashwell, J. D., and Germain, R. N. (1989) Marked differences in the efficiency of expression of distinct alpha beta T cell receptor heterodimers. *J. Immunol.* **143(10),** 3379–3384.

25 Uematsu, Y. (1992) Preferential association of alpha and beta chains of the T cell antigen receptor. *Eur J. Immunol.* **22(2),** 603–606.

26 Burns, R. P., Jr., Natarajan, K., LoCascio, N. J., et al. (1998) Molecular analysis of skewed Tcra-V gene use in T-cell receptor beta-chain transgenic mice. *Immunogenetics* **47(2),** 107–114.

27 Vacchio, M. S., Granger, L., Kanagawa, O., et al. (1993) T cell receptor V alpha-V beta combinatorial selection in the expressed T cell repertoire. *J. Immunol.* **151(3),** 1322–1327.

28 Casrouge, A., Beaudoing, E., Dalle, S., Pannetier, C., Kanellopoulos, J., and Kourilsky, P. (2000) Size estimate of the alpha beta TCR repertoire of naive mouse splenocytes. *J. Immunol.* **164(11),** 5782–5787.

29 Whitlow, M., Bell, B. A., Feng, S. L., et al. (1993) An improved linker for single-chain Fv with reduced aggregation and enhanced proteolytic stability. *Protein Eng.* **6(8),** 989–995.

30 Robinson, C. R. and Sauer, R. T. (1998) Optimizing the stability of single-chain proteins by linker length and composition mutagenesis. *Proc. Natl. Acad. Sci. USA* **95(11),** 5929–5934.

31 Chung, S., Wucherpfennig, K. W., Friedman, S. M., Hafler, D. A., and Strominger, J. L. (1994) Functional three-domain single-chain T-cell receptors. *Proc. Natl. Acad. Sci. USA* **91(26),** 12,654–12,658.

32 Willemsen, R. A., Weijtens, M. E., Ronteltap, C., et al. (2000) Grafting primary human T lymphocytes with cancer-specific chimeric single chain and two chain TCR. *Gene Ther.* **7(16),** 1369–1377.

33 Fitzer-Attas, C. J., Schindler, D. G., Waks, T., and Eshhar, Z. (1998) Harnessing Syk family tyrosine kinases as signaling domains for chimeric single chain of the variable domain receptors: optimal design for T cell activation. *J. Immunol.* **160(1),** 145–154.

34 Johansson, B., Palmer, E., and Bolliger, L. (1999) The extracellular domain of the zeta-chain is essential for TCR function. *J. Immunol.* **162(2),** 878–885.

35 Bolliger, L. and Johansson, B. (1999) Identification and functional characterization of the zeta-chain dimerization motif for TCR surface expression. *J. Immunol.* **163(7),** 3867–3876.

36 Atwell, S., Ridgway, J. B., Wells, J. A., and Carter, P. (1997) Stable heterodimers from remodeling the domain interface of a homodimer using a phage display library. *J. Mol. Biol.* **270(1),** 26–35.

37 Garcia, K. C., Degano, M., Pease, L. R., et al. (1998) Structural basis of plasticity in T cell receptor recognition of a self peptide-MHC antigen. *Science* **279(5354),** 1166–1172.

38 Backstrom, B. T., Milia, E., Peter, A., Jaureguiberry, B., Baldari, C. T., and Palmer, E. (1996) A motif within the T cell receptor alpha chain constant region connecting peptide domain controls antigen responsiveness. *Immunity* **5(5),** 437–447.

39 Rudd, P. M., Elliott, T., Cresswell, P., Wilson, I. A., and Dwek, R. A. (2001) Glycosylation and the immune system. *Science* **291(5512),** 2370–2376.

40 Germain, R. N. (2002) T-cell development and the CD4-CD8 lineage decision. *Nat. Rev. Immunol.* **2(5),** 309–322.

41 Naeher, D., Luescher, I. F., and Palmer, E. (2002) A role for the alpha-chain connecting peptide motif in mediating TCR-CD8 cooperation. *J. Immunol.* **169(6),** 2964–2970.

42 Sette, A., Vitiello, A., Reherman, B., et al. (1994) The relationship between class I binding affinity and immunogenicity of potential cytotoxic T cell epitopes. *J. Immunol.* **153(12),** 5586–5592.

43 Irwin, M. J., Heath, W. R., and Sherman, L. A. (1989) Species-restricted interactions between CD8 and the alpha 3 domain of class I influence the magnitude of the xenogeneic response. *J. Exp. Med.* **170(4),** 1091–1101.

44 Gascoigne, N. R., Chien, Y., Becker, D. M., Kavaler, J., and Davis, M. M. (1984) Genomic organization and sequence of T-cell receptor beta-chain constant- and joining-region genes. *Nature* **310(5976),** 387–391.

45 Lefranc, M. P., Giudicelli, V., Ginestoux, C., et al. (1999) IMGT, the international Immuno-GeneTics database. *Nucleic Acids Res.* **27(1),** 209–212.

46 Ruiz, M., Giudicelli, V., Ginestoux, C., et al. (2000) IMGT, the international Immuno-GeneTics database. *Nucleic Acids Res.* **28(1),** 219–221.

47 Lefranc, M. P. (2001) IMGT, the international ImmunoGeneTics database. *Nucleic Acids Res.* **29(1),** 207–209.

48 Lefranc, M. P. (2003) IMGT, the international ImmunoGeneTics database. *Nucleic Acids Res.* **31(1),** 307–310.

49 Niederberger, N., Holmberg, K., Alam, S. M., et al. (2003) Allelic exclusion of the TCR alpha-chain is an active process requiring TCR-mediated signaling and c-Cbl. *J. Immunol.* **170(9),** 4557–4563.

50. Sambrook, J., Fritsch, E. F., and Maniatis, T. (1989) *Molecular Cloning. A Laboratory Manual*, 2nd Ed. Cold Spring Harbor Laboratory Press, Cold Spring Harbor, NY.

51 Weijtens, M. E., Hart, E. H., and Bolhuis, R. L. (2000) Functional balance between T cell chimeric receptor density and tumor associated antigen density: CTL mediated cytolysis and lymphokine production. *Gene Ther.* **7(1),** 35–42.

52 Weijtens, M. E., Willemsen, R. A., Hart, E. H., and Bolhuis, R. L. (1998) A retroviral vector system "STITCH" in combination with an optimized single chain antibody chimeric receptor gene structure allows efficient gene transduction and expression in human T lymphocytes. *Gene Ther.* **5(9),** 1195–1203.

53. Tuan, R. S. (1997) *Recombinant Gene Expression Protocols.* 1st Ed. Human Press Inc., Totowa, NJ.

54 Call, M. E., Pyrdol, J., Wiedmann, M., and Wucherpfennig, K. W. (2002) The organizing principle in the formation of the T cell receptor-CD3 complex. *Cell* **111(7),** 967–979.

55 Rudd, P. M., Wormald, M. R., Stanfield, R. L., et al. (1999) Roles for glycosylation of cell surface receptors involved in cellular immune recognition. *J. Mol. Biol.* **293(2),** 351–366.

56 Arden, B., Clark, S. P., Kabelitz, D., and Mak, T. W. (1995) Mouse T-cell receptor variable gene segment families. *Immunogenetics* **42(6),** 501–530.

57 Gurtu, V., Yan, G., and Zhang, G. (1996) IRES bicistronic expression vectors for efficient creation of stable mammalian cell lines. *Biochem. Biophys. Res. Commun.* **229(1),** 295–298.

58 Mizuguchi, H., Xu, Z., Ishii-Watabe, A., Uchida, E., and Hayakawa, T. (2000) IRES-dependent second gene expression is significantly lower than cap-dependent first gene expression in a bicistronic vector. *Mol. Ther.* **1(4),** 376–382.

59. Jackson, M. R., Nilsson, T., and Peterson, P. A. (1990) Identification of a consensus motif for retention of transmembrane proteins in the endoplasmic reticulum. *EMBO J.* **9(10),** 3153–3162.

60. Bunnell, B. A., Muul, L. M., Donahue, R. E., Blaese, R. M., and Morgan, R. A. (1995) High-efficiency retroviral-mediated gene transfer into human and nonhuman primate peripheral blood lymphocytes. *Proc. Natl. Acad. Sci. USA* **92(17),** 7739–7743.

18

Isolation and Expansion of Tumor-Specific CD4+ T-Cells by Means of Cytokine Secretion

Christian Becker

Summary

A major objective of immune analysis in the setting of cancer, cancer vaccination, and therapy is to accurately characterize and isolate functional T-cells elicited by a tumor. Secretion of cytokines is an important function of activated effector and memory T-cells. The cytokine secretion assay (CSA) directly assesses T-cells secreting cytokines after a short restimulation in vitro. Cells can be stained for surface markers enabling characterization of subsets. Viable cytokine-secreting T-cells can be isolated for expansion and further functional testing or adoptive transfer. Since the method is not restricted to any antigen or major histocompatibility complex (MHC) haplotype, it enables us to detect CD8+ as well as CD4+ T-cells reacting against a wide vary of tumor-associated antigens, ranging from particular known tumor antigens to whole tumor cells and crude tumor lysates. Thus, the method provides a valuable tool to analyze and isolate functional tumor-responsive T-cells according to one of their effector functions.

Key Words: T-lymphocyte; immunoassay; T-cell differentiation; CD4+ T-helper cell; tumor immunity; cytokine secretion assay.

1. Introduction

Considerable evidence suggests a central role of CD4+ T-cells in T-cell-mediated tumor immunity *(1–6)*. In naïve hosts, tumor-specific CD4+ T-cells exist in very low frequencies. During the course of an immune response against a tumor, these cells may expand and acquire effector function. Yet, expanded effector and memory populations remain small, and functional testing of these cells has been tedious and indirect. The cytokine secretion assay (CSA) *(7,8)* overcomes these limitations by assessing a prominent effector function of CD4+ T-helper cells: cytokine secretion.

Basically, only T-cells that have previously progressed towards an effector memory phenotype respond with cytokine production to temporary ex vivo peptide/antigen restimulation. To detect these cells, single-cell suspensions will be briefly stimulated in vitro, and surface-coated with an antibody specific for the secreted cytokine of interest.

The cells are activated for a short period of time and labeled afterwards with a secondary cytokine-specific antibody for cytometric analysis and cell sorting. The secreted cytokine binds preferentially to the affinity matrix on the secreting cells.

CSA has been used in tumor immunology to isolate human- and mouse-tumor-reactive CD8^{+} T-cells from peripheral blood (*9–11*) and tumor-infiltrating lymphocytes (TILs) from tumor patients *(12)* or from immunized mice *(12)*. This chapter describes a protocol for the isolation and expansion of murine interleukin (IL)-2- and interferon (IFN)-γ-secreting CD4^{+} T-cells induced by tumor immunization in vivo.

2. Materials

2.1. Media, Buffers, and Reagents

1. Stimulation buffer: IMDM (Invitrogen, Carlsbad, CA) + 0.5% MS (mouse serum).
2. Washing buffer: PBS 1X, 4°C.
3. Secretion buffer: IMDM + 10% FCS, 37°C.
4. Culture medium: IMDM + 10% FCS, 1ng/mL rmIL-7 (R&D Systems, Minneapolis, MN) + Gentamycin.
5. Propidium iodide (PI) (Sigma-Aldrich, St. Louis, MO).

2.2. Antibodies

1. Cytokine secretion assay detection kit (Miltenyi, Bergisch Gladbach, Germany) consisting of:
   a. Cytokine catch reagent (anti-cytokine antibody conjugated to cell surface antibody).
   b. Cytokine detection antibody conjugated to phycoerythrin (PE) (antibody against the same cytokine as the cytokine catch antibody, but binding to a different epitope).
2. For stimulation: anti-CD28 (37.51, BD PharMingen, San Diego, CA), anti-CD3 (145-2C11, BD Pharmingen).
3. For phenotypic characterization/sorting: FITC-conjugated anti-CD4, APC-conjugated anti-CD45R/B220 (BD PharMingen).

2.3. Devices

1. Fluorescence-activated cell sorter (i.e., MoFlo, Dako Cytomation, Carpinteria, CA, or other) with sample cooling system.
2. Sample mixer (i.e., MX1, Dynal, Brown Deer, WI).
3. Cell strainer, 70 µm, nylon (Falcon).
4. Sample mixer (i.e., Dynal) .
5. Fifty-milliliter centrifuge tubes (i.e., Corning GmbH, Wiesbaden, Germany).
6. Twenty-four-well plates (i.e., Corning).

3. Methods

3.1. Isolation of Murine-Tumor-Specific CD4^{+} T-Cells From Mice Immunized With Irradiated Tumor Cells

This protocol has been established for the isolation and expansion of hemagglutinin (HA)-peptide-specific IFN-γ- or IL-2-secreting CD4^{+} T-cells induced by immunization of BALB/c mice with irradiated HA-transfected tumors (*see* **Fig. 1**). It may need optimization when applied to other tumor antigens or T-cells secreting other cytokines.

1. Isolate spleens from mice 3 wks after the last immunization with tumor cells (*see* **Note 1**), place into IMDM without serum (*see* **Note 2**) and prepare single-cell suspensions by mincing with toothed forceps. After erythrocyte lysis, remove cell debris by passing the cell suspension through a cell strainer. Resuspend cells in complete IMDM medium with 0.5% mouse serum at a cell density of 1×10^7 cells/mL.

2. Stimulate at least 1×10^7 cells per well in a 24-well plate with 10 µg/mL peptide for 4–6 h under standard culture conditions. Additionally, always set up controls without peptide and with spleen cells from mock-immunized mice (PBS-injected or injected with a tumor not expressing the antigen of interest, sex and age matched) with and without peptide. Add 0.2 µg/mL anti-CD28 antibody (i.e., 37.51, BD Pharmingen) to all samples to provide co-stimulation (*see* **Note 3**). While cells are stimulated, prewarm IMDM/FCS medium at 37°C.

3. Re-collect cells from wells and wash twice with ice-cold IMDM to remove previously produced cytokines that might result in cross-staining.

4. Labeling with catch matrix: Resuspend cells in 80 µL ice-cold IMDM/FCS per 10^7 cells, put on ice, and add 20 µL cytokine catch antibodies per 10^7 cells. Leave on ice for 7 min.

5. Cytokine secretion period: Transfer samples (in labeling buffer) into tubes with pre-warmed 37°C IMDM/FCS medium (use 50 mL medium for 5×10^7 cells) and put tube(s) on sample mixer at 37°C. Slowly tumble/mix tube(s) for 45 min. During this incubation, cells will secrete cytokines, and these will bind to the cytokine catch matrix on the cells. Diluting the cells avoids cross-staining of nonproducing cells.

6. Spin down cells at 4°C and wash cells three times with 5 mL ice-cold PBS. Keep cells on ice or at 4°C from now on to avoid loss of cytokine staining.

7. Secondary cytokine staining: Resuspend cells in 80 µL ice-cold IMDM/FCS per 10^7 cells, put on ice, and add 20 µL cytokine-staining antibodies per 10^7 cells. Additionally, label cells with anti-CD4 FITC and anti-B220 Allophycocyanine (APC) antibodies (BD Pharmingen). Leave on ice for 10 min.

8. Wash twice with ice-cold PBS. Resuspend cells to 1×10^7 cells/mL in ice-cold PBS, add PI (propidium iodide, 5 µg/mL, Sigma), and subject to fluorescence-activated cell sorting (*see* **Note 3**).

9. Sorting (*see* **Fig. 2**): Set up an FSC/SSC dot plot and draw a gate on small lymphocytes [R1] (recently activated memory T-cells are not significantly larger than resting T-cells). Analyze R1-gated cells in a secondary Pulse Width/FSC dot plot to gate out doublets. Create a new gate [R1 and R2] and analyze cells in a third FL5/FL4 dot plot. Draw a gate on FL5⁻ cells to gate <u>out</u> cells with higher auto-fluorescence [gate R5]. Create a combined gate [R1 and R2 and not R5] on the gate list and analyze in a fourth FL4/FL2 dot plot, and gate <u>out</u> FL4 (B220⁺) high cells (B220-APC-labeled B-lymphocytes) [gate R3]. Finally create a gate [R1 and R2 and R3 and not R5] and analyze in a fifth Fl1/Fl2 dot plot. Use the final dot plot to gate on FL1- and FL2-positive cells [R4] (cytokine-secreting CD4+ T-cells) for sorting. Sort at least 20,000 cells using the combined gating strategy [R1 and R2 and R3 and R4 and not R5].

10. After sorting, spin down tube with sorted cells and re-suspend in 200 µL complete medium with IL-7. CD4+/IFN-γ+ or CD4+/IL-2+ cells can be cultivated under these conditions for up to 7 d without any visible loss of viability.

11. Cell numbers achieved by the CSA may be insufficient for functional testing, and further expansion of the cells may thus be inevitable: For in vivo expansion, cells are transferred into T-cell deficient, syngeneic recipient mice (RAG⁻/⁻ or SCID). Under these conditions, cells expand into memory-type cells with improved effector function. Aspirate well with
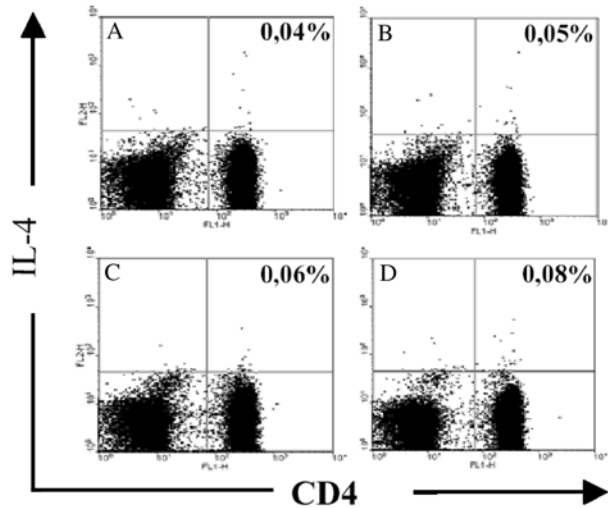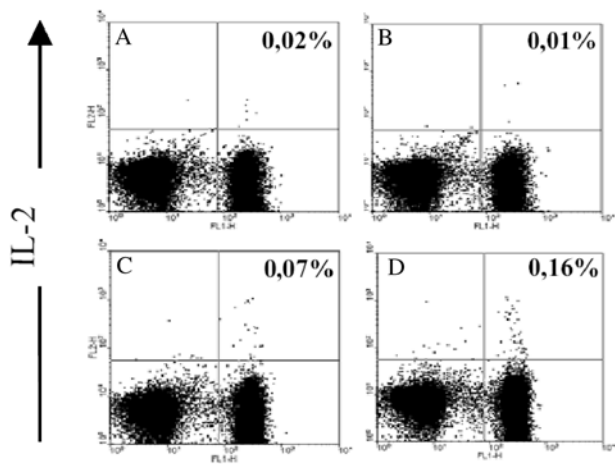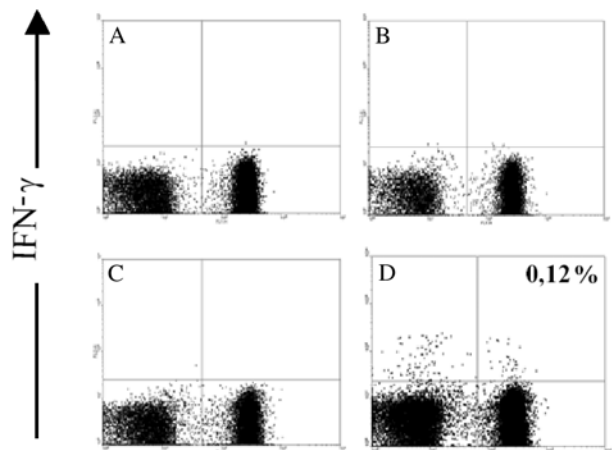
syringe (Omnifix-F, 1 mL, 0.33 × 12 mm needle) and directly inject into the tail vein of a mouse. Analyze and isolate cells from mice after at least 50 d of expansion in vivo (population size depends on the number of transferred cells) (*see* **Fig. 3**). For an alternative in vitro expansion procedure, *see* **Note 4**.

4. Notes

1. Irradiation dosage, cell numbers, and time schedule for protective tumor immunization must be predetermined for each tumor individually by immunization/challenge experiments. For sorting of cytokine-secreting T-cells, use animals that have completely rejected the tumor challenge. Basically, memory CD4+ T-cells (isolated 3 wk after immunization) are more rugged than recently activated effector T-cells and ride out the isolation procedure much better. The assay can be performed with cells from a single spleen. Other tissues (such as tumor-draining lymph nodes) should be pooled from several immunized mice to achieve sufficient cell numbers for sorting.

   The cytokine secretion assay does not distinguish between cells of high and low recognition efficiency. Cytokine production (i.e., IFN-γ by CD4+ T-cells) is not a direct measure of other functions (i.e., cytotoxicity), since these may be regulated independently.

2. Carefully avoid xenogeneic sera and protein in media throughout cell preparation and stimulation, as these will activate undesired T-cell specificities. However, during the secretion phase of the assay, FCS-containing media may be used. Generally, enrichment efficiency of antigen-specific cytokine-secreting cells depends on the amount of unrelated background activity in the sample. Controls should be set up to evaluate this background, and specific cells should be isolated only when background activity is low (e.g., on the level of peptide-stimulated cells from naïve mice). Basically, the IFN-γ secretion assay shows much less background activity than IL-2 and IL-4 secretion assays. When starting experiments, also add a positive control (i.e., stimulated with anti-CD3 and anti-CD28 [1 µg/mL each or stimulate cells with the superantigen staphylococcal enterotoxin B (Sigma) 1 µg/mL]). Generally, the assay is best for detection and isolation of cytokine-secreting populations up to 2% of the total population.

3. Although faster, magnetic enrichment of cytokine-producing cells is not recommended. First, magnetic separation leads to many undesired cytokine-positive cells as well as cytokine-negative cells in the positive fraction (i.e., B-cells that react with PE). Second, magnetic enrichment was found to be only 10- to 15-fold for mouse cells. Most important, the positive fraction usually contains cell debris that negatively influences the viability of the isolated population. Keep the sample cooled during sorting, as the cytokine-holding antibody matrix will easily come off at room temperature.

Fig. 1. *(opposite page)* Cytokine secretion of HA-peptide-reactive CD4+ T-cells induced by immunization of BALB/c mice with irradiated HA-expressing tumor cells. Spleen cells from individual mice isolated 3 wk after the last immunization with irradiated, HA-expressing tumor cells were stimulated in vitro with 10 µg/mL HA-peptide (SFERFEIFPKE, I-E^d-restricted hemagglutinin epitope from influenza Mount Sinai strain A/PR/8/34) for 6 h (**D**) or left unstimulated (**C**). Spleen cells from PBS-injected control littermates, either peptide stimulated (**B**) or unstimulated (**A**), served as controls. For co-stimulation, all cultures were supplemented with 0.2 µg/mL anti-CD28 antibody. Stimulated cells were subjected to the IFN-γ-, IL-2-, or IL-4-secretion assay. Subsequently, cells were counterstained with anti-CD4-FITC and anti-B220-APC antibodies and PI, and analyzed by FACS. 30,000 cell gated on B220−/PI− cells are shown.
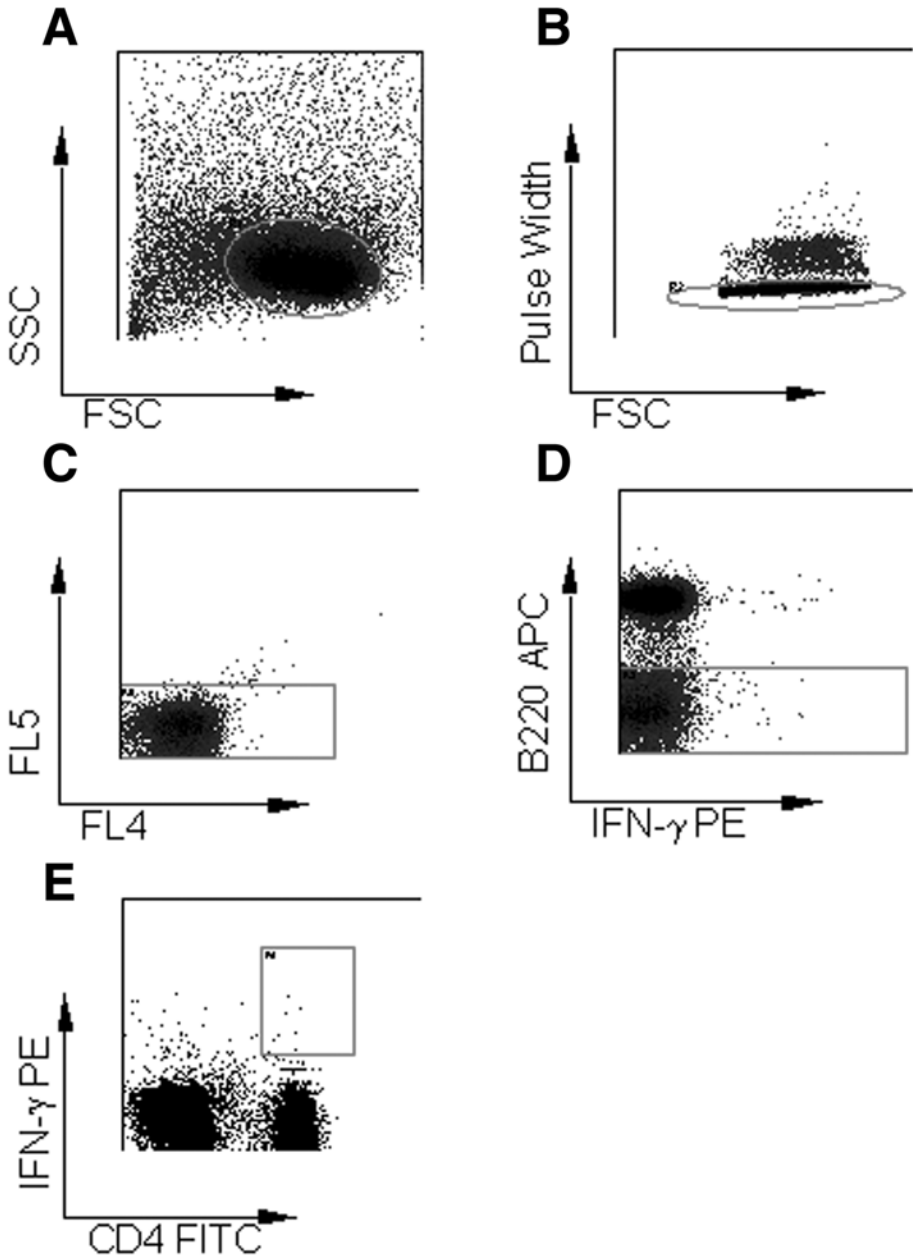
Fig. 2. Sorting strategy: Illustration of the sorting dot plots and gates as described under Methods. **(A)** Lymphocyte gate. **(B)** Doublet discrimination. **(C)** Autofluorescence. **(D)** Gating out B cells. **(E)** CD4+/cytokine+ gate.
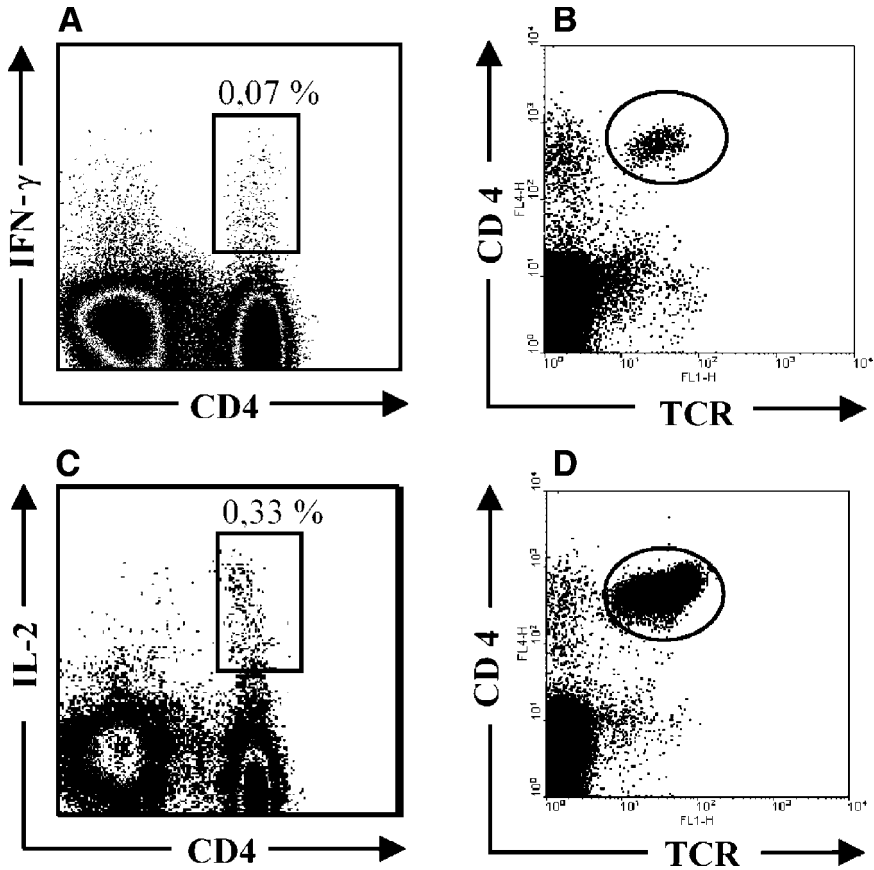
Fig. 3. Sorting and in vivo expansion of IFN-γ- and IL-2-secreting CD4⁺ HA-peptide-specific T-cells. CD4⁺ T-cells were induced and activated in vitro as described, and cytokine-producing CD4⁺ T-cells sorted out as shown in **Fig. 2** on a MoFlo FACS sorter. Ten thousand sorted cells from **(A)** and 20,000 cells from **(C)** were injected into the tail vein of individual BALB/c RAG⁻ᐟ⁻ mice 24 h after sort. One wk later, mice were immunized with irradiated HA-expressing cells from an unrelated tumor. Four wk later, spleen cells of adoptively transferred mice were analyzed for CD4⁺/T-cell receptor (TCR)⁺ cells.

4. Keep in mind that all expansion procedures will alter the phenotype and function (although not the specificity) of the cells. Alternatively, sorted cells may be expanded in vitro. Wash cells after 48 h with medium and stimulate with freshly prepared syngeneic dendritic cells. To prepare dendritic cells for in vitro expansion, spleen cells from naïve, syngeneic mice are incubated with anti-CD11c beads followed by magnetic sorting (MACS). The isolated DC are immature but acquire the mature phenotype after overnight culture in granulocyte/macrophage colony-stimulating factor (GM-CSF)-conditioned (R&D Systems) medium. Use approx 10- to 20-fold more dendritic cells than sorted T-cells. Under these conditions,

cells will expand independent of their specificity *(13)*. Expansion can be further amplified by adding IL-7 (1 ng/mL) to the cultures.

References

1. Goedegebuure, P. S. and Eberlein, T. J. (1995) The role of CD4+ tumor-infiltrating lymphocytes in human solid tumors. *Immunol. Res*. **14,** 119–131.
2. Hung, K., Hayashi, R., Lafond-Walker, A., Lowenstein, C., Pardoll, D., and Levitsky, H. (1998) The central role of CD4+ T cells in the antitumor immune response. *J. Exp. Med.* **188,** 2357–2368.
3. Marzo, A. L., Kinnear, B. F., Lake, R. A., et al. (2000) Tumor-specific CD4+ T cells have a major "post-licensing" role in CTL mediated anti-tumor immunity. *J. Immunol.* **165,** 6047–6055.
4. Surman, D. R., Dudley, M. E., Overwijk, W. W., and Restifo, N. P. (2000) Cutting edge: CD4+ T cell control of CD8+ T cell reactivity to a model tumor antigen. *J. Immunol.* **164(2),** 562–565.
5. Ossendorp, F., Mengede, E., Camps, M., Filius, R., and Melief, C. J. (1998) Specific T helper cell requirement for optimal induction of cytotoxic T lymphocytes against major histocompatibility complex class II negative tumors. *J. Exp. Med.* **187(5),** 693–702.
6. Nishimura, T., Nakui, M., Sato, M., et al. (2000) The critical role of Th1-dominant immunity in tumor immunology. *Cancer Chemother. Pharmacol.* **46(Suppl),** S52–61.
7. Manz, R., Assenmacher, M., Pflüger, E., Miltenyi, S., and Radbruch, A. (1995) Analysis and sorting of live cells according to secreted molecules relocated to a cell-surface affinity matrix. *Proc. Natl. Acad. Sci. USA* **92,** 1921–1925.
8. Brosterhus, H., Brings, S., Leyendeckers, H., et al. (1999) Enrichment and detection of live antigen-specific CD4 + and CD8 + T cells based on cytokine secretion. *Eur. J. Immunol.* **29,** 4053–4059.
9. Oelke, M., Moehrle, U., Chen, J. L., et al. (2000) Generation and purification of CD8 + Melan-A-specific cytotoxic T lymphocytes for adoptive transfer in tumor immunotherapy. *Clin. Cancer Res.* **6,** 1997–2005.
10. Oelke, M., Kurokawa,T., Hentrich, I., et al. (2000) Functional characterization of CD8+ antigen-specific cytotoxic T lymphocytes after enrichment based on cytokine secretion: comparison with the MHC-tetramer technology . *Scand. J . Immunol.* **52,** 544–549.
11. Pittet, M. J., Zippelius, A., Speiser, D. E., et al. (2001) Ex vivo IFN-γ secretion by circulating CD8 T lymphocytes: implications of a novel approach for T cell monitoring in infectious malignant diseases. *J. Immunol.* **166,** 7634–7640.
12. Becker, C., Pohla, H., Frankenberger, F., et al. (2001) Adoptive tumor therapy with T lymphocytes enriched through an IFN-γ capture assay. *Nat. Med.* **7(10),** 1159–1162.
13. Ge, Q., Palliser, D., Eisen, H. N., and Chen, J. (2002) Homeostatic T cell proliferation in a T cell–dendritic cell coculture system. *Proc. Natl. Acad. Sci. USA* **99,** 2983–2988.

19

Methods for the Ex Vivo Characterization of Human CD8+ T Subsets Based on Gene Expression and Replicative History Analysis

Nathalie Rufer, Patrick Reichenbach, and Pedro Romero

Summary

The generation of an antigen-specific T-lymphocyte response is a complex multi-step process. Upon T-cell receptor-mediated recognition of antigen presented by activated dendritic cells, naive T-lymphocytes enter a program of proliferation and differentiation, during the course of which they acquire effector functions and may ultimately become memory T-cells. A major goal of modern immunology is to precisely identify and characterize effector and memory T-cell subpopulations that may be most efficient in disease protection. Sensitive methods are required to address these questions in exceedingly low numbers of antigen-specific lymphocytes recovered from clinical samples, and not manipulated in vitro. We have developed new techniques to dissect immune responses against viral or tumor antigens. These allow the isolation of various subsets of antigen-specific T-cells (with major histocompatibility complex [MHC]-peptide multimers and five-color FACS sorting) and the monitoring of gene expression in individual cells (by five-cell reverse transcription-polymerase chain reaction [RT-PCR]). We can also follow their proliferative life history by flow-fluorescence *in situ* hybridization (FISH) analysis of average telomere length. Recently, using these tools, we have identified subpopulations of CD8+ T-lymphocytes with distinct proliferative history and partial effector-like properties. Our data suggest that these subsets descend from recently activated T-cells and are committed to become differentiated effector T-lymphocytes.

Keywords: Cytolytic T-lymphocytes (CTL); memory; effector; tumor immunity; T-cell differentiation; melanoma; immunoassay; senescence; fibroblasts; gene expression; single-cell RT-PCR; polyA cDNA amplification; replicative history; telomere length; flow-FISH; *in situ* hybridization; nuclei.

1. Introduction

In both cancers, such as melanoma, and chronic viral infections, such as HIV, antigen-specific CD8+ T-cell responses often develop, but their therapeutic effects are limited. Therefore, issues such as CD8+ T-cell subset (memory or effector) composition and a full understanding of their functional properties in well-defined clinical situations are

particularly pertinent. In this regard, metastatic melanoma lends itself to this type of analysis. On one hand, this type of skin cancer has proven to be one of the most immunogenic among human tumors. On the other hand, a relatively high number of molecularly defined antigens that are recognized by both MHC class I and class II T-lymphocytes have been identified in the last 13 y *(1)*. Some of these antigens have been targeted for specific immunotherapy. For instance, more than 23 phase I–II clinical studies using peptide-based cancer vaccines have been reported since 1995 (reviewed in *[2]*). In addition to vaccination, tumor antigens are targeted in other approaches such as adoptive transfer therapy *(3,4)* or passive transfer of specific monoclonal antibodies *(5)*.

Cytolytic T-lymphocyte (CTL)-defined tumor antigens have received great attention and are at the forefront of the development of cancer vaccines. Some of them include MAGE-A3 *(6)*, NY-ESO-1 *(7)*, gp100 *(8,9)*, and Melan-A/MART-1 *(10)*. A major focus of cancer vaccine development is the quantitative and qualitative monitoring of the tumor antigen-specific CTL response in vaccinated patients *(2)*. This type of analysis has been greatly facilitated by the development in the 1990s of techniques to identify single T-cells producing cytokines in response to challenge with antigen *(11,12)* and of fluorescent MHC/peptide multimers *(13)*. Despite this important progress, monitoring of single-antigen-specific CTL remains difficult because of the incomplete understanding of human CD8$^+$ T-cell biology and also because most of tumor antigen-specific CTL occur in accessible compartments, such as peripheral blood, at frequencies below the detection limit of current immunoassays. One fortunate exception is the CD8$^+$ T-cell response to an immunodominant HLA-A2 restricted peptide derived from the melanocyte/melanoma-associated antigen Melan-A/MART-1 *(14)*. We have observed that the majority of healthy individuals have detectable numbers of HLA-A2/Melan-A/MART-1 peptide multimer$^+$ CD8 T-lymphocytes in the circulating lymphocyte compartment. Remarkably, these cells are phenotypically and functionally naive despite their high frequency *(10)*. This was explained by the existence of a high level of thymic output of Melan-A/MART-1-specific CD8 T-cells *(15)*. Importantly, this large repertoire is activated in HLA-A2 patients with metastatic melanoma, whose tumors drive the expression of high levels of the Melan-A/MART-1 antigen. In this setting, Melan-A/MART-1-specific T-lymphocytes acquire phenotypic and functional characteristics of antigen-experienced CD8$^+$ T-lymphocytes and can be found not only in peripheral blood but also among the lymphocytes infiltrating solid tumors or in lymph node metastasis *(10)*.

We are currently characterizing the functional diversity of Melan-A/MART-1-specific CD8$^+$ T-lymphocytes that can be found either in blood or in tumor-infiltrated lymph nodes (TILNs) from melanoma patients. The five-cell RT-PCR is an elegant approach to study the function of isolated tumor-specific T-cells in patients in whom only limited amounts of blood and of metastatic tumor material are available. This allows us to analyze the expression level of genes involved in effector or regulatory functions. Moreover, the precise characterization of the gene expression pattern (by five-cell cDNA amplification RT-PCR) and of the replicative history (flow-FISH analysis of average telomere length) of tumor antigen-specific T-lymphocytes provide valuable insights in dissecting the maturation pathways of effector and memory T-cells in
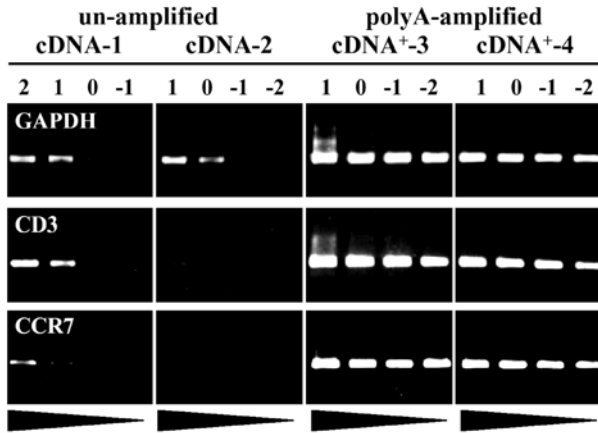
Fig. 1. Gene expression analysis of four samples processed either without (cDNA-1, cDNA-2) or with (cDNA⁺-3, cDNA⁺-4) the amplified poly(A) reverse transcription-polymerase chain reaction protocol. The starting cDNA (isolated from 10^2 or 10 cells) and polyA-amplified cDNA (isolated from 10 cells) was prepared using 10-fold serial dilutions as indicated (Log_{10} of the reciprocal of the dilution value). Expression of GAPDH, CD3, and CCR7 mRNAs is depicted.

the Melan-A model. Understanding the position of these subsets in the process of CD8⁺ T-cell differentiation and their role in immune responses will help us to improve vaccination strategies for melanoma patients.

We have used a modified RT-PCR protocol that relies on the detection of specific cDNAs after global amplification of expressed mRNAs *(16,17)*. Because the method yields sufficient cDNA in material harvested from as few as five isolated T-lymphocytes, it allows the analysis of gene expression in small purified T-cell subpopulations. **Figure 1** shows the levels of detection of target mRNAs among four samples processed either without or with the poly(A)-amplified cDNA RT-PCR protocol. Typically, low to undetectable levels of expression of glyceraldehyde phosphate dehydrogenase (GAPDH), CD3, and CCR7 mRNAs are found in cDNA samples that were not poly(A) amplified. In contrast, amplified poly(A) cDNA allows the detection of all genes of interest even when using a 10^3-fold dilution (or corresponding to 10^{-2} cells) and gives robust PCR signals (**Fig. 1**). A recent study showed that this method could detect CD3ε transcripts in 60 to 90% of extracts from single CD3⁺ cells *(18)*. More recently, using the same five-cell cDNA amplification protocol, we described the properties of CD8⁺ T-lymphocyte subsets with functional features that are intermediate between naive and effector T-cells. Indeed, these subsets express increasing levels of mediators of effector CD8⁺ T-lymphocyte functions such as granzyme B, perforin, interferon (IFN)-γ, tumor necrosis factor (TNF)-α, and CD94 *(19)*.

Telomeres are specialized structures found at the eukaryotic chromosomal ends. They are composed of repeating oligonucleotide units, and their length progressively decreases with age and with population doublings in vitro. The evolution of telomere

length has been extensively monitored mainly in two types of human cells—fibroblasts and lymphocytes. Indeed, in human T-lymphocytes, telomeres shorten by approx 30–60 base pairs with every cell division. It is in principle possible to calculate the number of divisions that a particular lymphocyte has undergone, provided one knows the initial telomere length. The latter information is rather difficult to obtain. However, it is still possible to compare telomere lengths between different lymphocyte populations and infer the average number of cell divisions that separate the populations with shorter telomeres from those with the longer telomeres.

In a population of cells, the average telomere length per cell would be an indicator of the number of divisions that the cell has undergone relative to the reference population. This requires an assay that allows one to measure the content of telomeric DNA in individual cells. We have developed a flow-cytometry method using quantitative fluorescence *in situ* hybridization (flow-FISH) with labeled peptide nucleic acid (PNA) probes *(20,21)* for this purpose. This probe hybridizes to denatured telomere repeats in fixed cells. Comparison of flow-FISH measurements with the results of conventional telomere-length measurements by Southern blot analysis ($R = 0.9$) showed that the amount of label (intensity of fluorescence signal) is a measure of the average length of telomere repeats. Since the assay requires only 10^5 cells, the flow-FISH technique permits comparison of telomere lengths in individual cells belonging to different subpopulations. Consistent differences in telomere length in CD8^{+} T-cell subsets were identified. The telomere length of memory T-cells or of HLA-A*0201-influenza-specific T-lymphocytes in normal adults is significantly shorter than that of naive T-cells, thus supporting the notion that the telomere length reflects the replicative history of T-lymphocytes *(20–23)*.

2. Materials

2.1. Five-Cell cDNA Amplification and RT-PCR

1. 0.1 *M* DTT (DiThioThreitol; Fluka, Buchs, Switzerland; at –20°C).
2. Lysis buffer: for 1 mL of lysis buffer, add 8 µL of 10 mg/mL, –20°C tRNA (Roche Diagnostics Gmbh, Mannheim, Germany), 30 µL of 100% Triton X-100 (Fluka), 40 µL of 0.1 *M* DTT, and 922 µL of dd-H_2O. Prepare aliquots of 1 mL and store at –20°C.
3. Oligo-dT primer, 20-mer (stock-solution at 1 µg/µL at –20°C; prepare a working solution at 100 ng/µL with dd-H_2O and store at –20°C).
4. dNTP (Invitrogen, Paisley, UK): prepare aliquots at 10 m*M* and store at –20°C.
5. Moloney murine leukemia virus reverse transcriptase (M-MLV RT), 200 U/µL (Invitrogen).
6. Recombinant RNAsin ribonuclease inhibitor (RNAsin), 40 U/µL (Promega, Madison, WI).
7. Glycogen (Roche Diagnostics Gmbh): 20 mg/mL of aliquots at –20°C.
8. Ethanol, 100% (room temperature [RT], protected from light) and ice-cold 70% (–20°C).
9. NH_4-acetate, 7.5 *M* ($C_2H_7NO_2$; Fluka).
10. dATP (Amersham Pharmacia, Piscataway, NJ): aliquots of 10 m*M* at –20°C.
11. Terminal deoxynucleotidyl transferase enzyme (TdT, Promega), 25 U/µL.
12. Oligo-dT Iscove primer, 61-mer (HPCL purified, 1µg/µL in aliquots at –20°C), 5'-CAT GTC GTC CAG GCC GCT CTG GGA CAA AAT ATG AAT TCT TTT TTT TTT TTT TTT TTT TTT T-3'.
13. KCl, 1 *M*; Tris-HCl (pH 8.8), 1 *M*; $MgCl_2$, 1 *M* (Fluka).

14. PCR buffer, 5X (final 1.5 m*M* and 2 m*M* MgCl₂): 250 m*M* KCl, 50 m*M* Tris-HCl (pH 8.8), 0.5 mg/mL BSA (bovine serum albumine; CalBioChem, San Diego, CA; 100 mg/mL, filter and store at 4°C), and 7.5 m*M* or 10 m*M* MgCl₂. Aliquot 5X PCR buffer and store at –20°C.
15. *Taq* DNA recombinant polymerase Platinum (Invitrogen; 5 U/μL).
16. Mineral oil (Eurobio, Les Ullis, France).

2.2. Flow-FISH Analysis of Average Telomere Length

1. Bovine serum albumin (BSA; CalBioChem, 100 mg/mL = 10% (w/v); filter and store at 4°C).
2. Ultrapure deionized formamide (Invitrogen). To deionize 500 mL of formamide, use 25 g of resin (AgR 501-X8 (D); BioRad Laboratories), stir for 2 h at RT, filter twice, aliquot, and keep at –20°C. As formamide is highly toxic, the chemical hood should be used for all manipulations.
3. Telomere-specific FITC-conjugated (C₃TA₂)₃ peptide nucleic acid (PNA) probe (Applied Biosystems, Rotkreuz, Switzerland). Dilute the telomere-specific PNA probe at 1 mg/mL in 1/1 *N/N'* dimethylformamide/H₂O (HPLC grade, Fluka). Aliquot to the equivalent volume of 20 μL and store at –20°C. For use, dilute in 1X TE buffer pH 8.0 (10 m*M* Tris, 1 m*M* EDTA) at the working concentration of 30 μg/mL, and store up to several months at 4°C.
4. Tris-HCl, 1 *M*, pH 7.1.
5. Formamide for washes (Sigma-Aldrich Chemie, Gmbh, Steinheim, Germany).
6. Ten percent (w/v) Tween-20 (Sigma).
7. RNase T1 (Roche Diagnostics Gmbh): dilute 1:5 in 1X PBS (10⁵ U/mL), heat at 80°C for 20 min to inactivate DNAse, aliquot, and store at 4°C.
8. Propidium iodide (Sigma): dilute at 10 μg/mL in 1X PBS and store at 4°C.
9. Quantum 24p Fluorescein Microbeads Standards (Bangs Laboratories, Fishers, IN).
10. Cell lysis buffer, 5X: 40 m*M* Tris-HCl (pH 7.5), 20 m*M* MgCl₂, 1.28 *M* sucrose, and 4% Triton X-100, store at 4°C.
11. Thirty percent sucrose solution: 8 m*M* Tris-HCl (pH 7.5), 4 m*M* MgCl₂, 30% sucrose, and 0.05% Na-azide, store at 4°C.

3. Methods

3.1. Five-Cell cDNA Amplification and RT-PCR

The basic principle of the five-cell global cDNA amplification protocol requires that the target sequences to be amplified be flanked by known sequences to which the amplification primers can anneal and initiate polymerization (**Fig. 2**). One end is initially defined through a cDNA reaction using reverse transcriptase and an oligo(dT) primer that will prime via the poly(A) tail present at the 3' end of most mRNA molecules. The other end is then created by the addition of an homopolymer d(A) sequence to the 3'-OH end of the first cDNA using terminal deoxynucleotidyl transferase. Global PCR amplification of the dA/dT flanked cDNAs is carried out using a single modified oligo(dT) primer as previously described by Brady and Iscove *(16)*. Priming of the cDNA during global RT-PCR is initiated via annealing of the d(T) region of the 61-mer oligonucleotide primer (named oligo-dT Iscove hereafter) to the homopolymeric d(A) regions present at the termini of the cDNA molecules. We have included a purification step before adding the poly d(A) tails, in order to get rid of free dNTPs that may interfere during the tailing reaction.
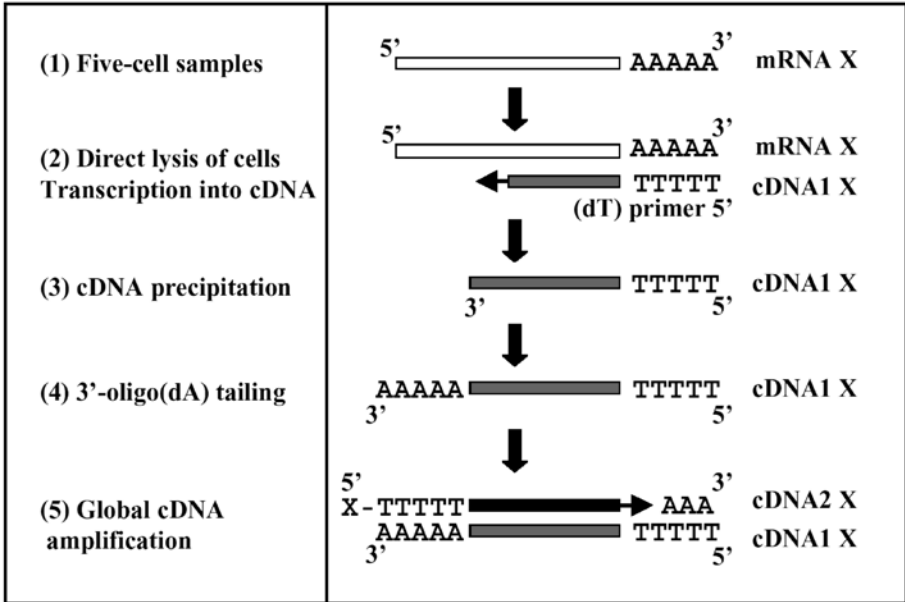
Fig. 2. Basic principles and outlines of the five-cell global cDNA amplification protocol. Adapted from Brady and Iscove *(16)*.

Taken together, the methods described below outline (1) the five-cell sorting of cytolytic CD8+ T-lymphocyte subsets of interest by flow cytometry; (2) the simultaneous lysis of five-cell aliquots and the transcription of total mRNA into cDNA; (3) the cDNA precipitation; (4) the 3'-oligo(dA) tailing of precipitated cDNA; (5) the global cDNA amplification by RT-PCR; and (6) the characterization of gene expression patterns in T-cell subsets by RT-PCR using specific primers.

3.1.1. Cell Preparation and Flow Cytometry

CD8+ T-cells are purified in two rounds of positive sorting by magnetic beads and a MiniMACS device (Miltenyi Biotech, Bergish Gladbach, Germany). The resulting cells are >98% CD3+CD8+. Cells are stained with appropriate monoclonal antibodies in 20 m*M* PBS containing 0.2% BSA and 50 µ*M* EDTA for 20 min at 4°C and washed. To avoid contamination of small populations by more abundant subsets, 10×10^3 cells of each subset of interest are first isolated by flow-cytometry-based cell sorting (FACS-Vantage SE, using CellQuest software, Becton Dickinson, San Diego, CA). A representative example shows the purity of naive(CD45RA+CCR7+CD27+), pre-effector (CD45RA+CCR7-CD27+), and effector (CD45RA+CCR7-CD27-) CD8+ T-lymphocyte subsets following flow-cytometry sorting (**Fig. 3**). Each subset (corresponding to >95% of the sort window) is then resorted directly into 96-well V-bottom plates (five cells per well) containing 15 µL of a lysis/cDNA mix solution.
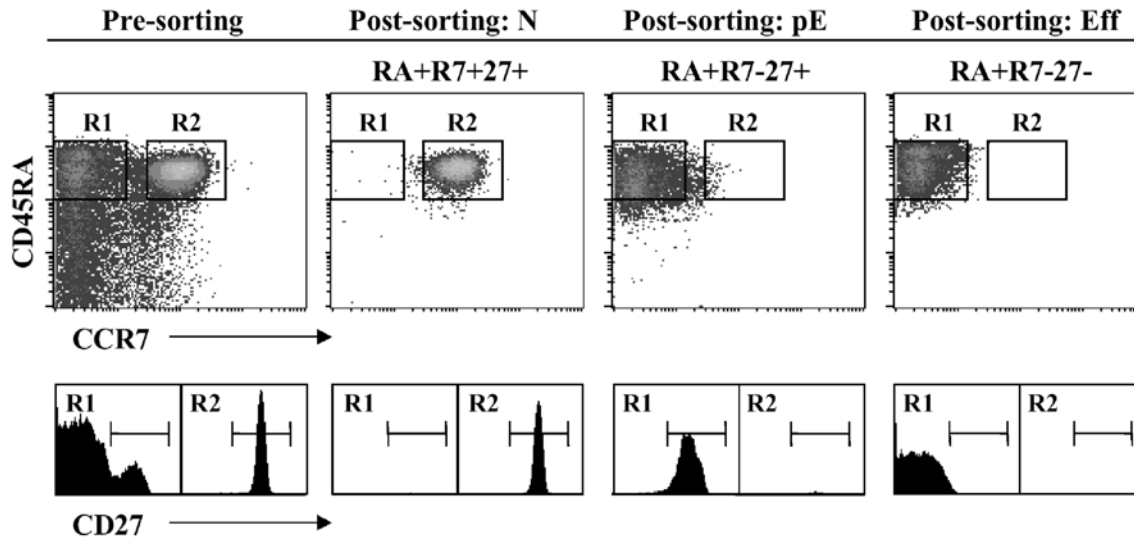
Fig. 3. Isolation of CD8^{+} T-lymphocyte subsets by flow cytometry for the five-cell cDNA amplification protocol. First, CD8^{+} T-lymphocytes were purified by magnetic beads and a MiniMACS device. Second, 10^4 T-cells of naive (N; RA^{+}CCR7^{+}27^{+}), of pre-effector (pE; RA[+]CCR7[-]27[+]), and of effector (E; RA[+]CCR7[-]27[-]) subsets were sorted by flow cytometry. Immediate reanalysis of the various sorted subpopulations revealed more than 95% purity. Third, five-cell aliquots of these highly purified subsets were resorted directly into 96-well V-bottom plates containing the lysis/cDNA mix solution and further processed. Sorting regions used are indicated as R1 or R2.

3.1.2. Cell Lysis and cDNA Synthesis

1. The lysis/cDNA mix solution is freshly prepared while cells are being sorted. This solution is composed of 6.3 µL of lysis buffer, 3 µL of 5X reverse transcriptase (RT) buffer (comes along with the MMLV-RT enzyme), 1.5 µL of DTT (0.1 *M*; final 10 m*M*), 0.75 µL of dNTPs (10 m*M*; final 0.5 m*M*), 0.25 µL of oligo-dT (100 ng/µL; final 1.67 ng/mL), 0.2 µL of RNAsin (40 U/µL; final 8 U), 0.4 µL of MMLV-RT (200 U/µL; final 80 U) and of 2.6 µL of dd-H$_2$O. The total volume is 15 µL per 96-well and per five-cell sorted aliquot.
2. After flow-cytometry sorting of a set of five-cell aliquots, the 96-well V-bottom plates are covered carefully with a plastic adhesive cover (Catalys AG, Wallisellen, Switzerland). To allow the transcription of total mRNA into cDNA, the 96-well plates are incubated 60 min at 37°C and plates are spun down once (300*g*, 3 min).
3. The contents of each well are then transferred into 0.5-mL PCR tubes, and the M-MLV reverse transcriptase is heat-inactivated at 90°C for 3 min.
4. Tubes are placed on ice for a few min, centrifuged, and stored at –20°C, or at –80°C for longer periods of time (*see* **Note 1**).

3.1.3. cDNA Precipitation

1. For further processing, the cDNA is precipitated overnight at –80°C after addition of 7.5 µL of 7.5 *M* NH4-acetate, 45 µL of 100% ethanol using 2 µL of 10 mg/mL glycogen as a carrier.
2. Aliquots of 20 mg/mL of glycogen are kept at –20°C and the dilution 1:2 with dd-H$_2$O is prepared freshly just before use.
3. Following overnight precipitation, tubes are centrifuged at 4°C for 20 min (13,000*g*) and the supernatant is carefully removed with a pipet. Neat white-to-transparent pellets should be seen at the bottom of the tubes.
4. Pellets are washed in 150 µL of ice-cold 70% ethanol, vortexed, and centrifuged at 4°C for 10 min (13,000*g*). The ethanol is removed and pellets are dried 1–2 h at RT.

3.1.4. Homopolymeric 3'-Oligo(dA) Tailing

To evaluate mRNA expression in a small number of cells (1–10 cells), the following method was adapted from previously published protocols *(16,17)*:

1. First, to promote 3'-oligo(dA) tailing of cDNA, the dried pellets are suspended in 5 µL of tailing solution containing 0.25 µL of dATP (10 m*M*; final 0.5 m*M*), 0.05 µL of terminal deoxynucleotidyl transferase (TdT; 25 U/µL; final 1.25 U), 1 µL of 5X tailing buffer (comes along with the TdT enzyme) and 3.7 µL of dd-H$_2$O.
2. Second, processed samples are incubated at 37°C for 30 min (in a water bath) and the tailing reaction is then heat inactivated at 90°C for 3–5 min.
3. Tubes are then placed onto ice, briefly centrifuged (13,000*g*), and samples are ready for global cDNA amplification RT-PCR.

3.1.5. Global cDNA Amplification by RT-PCR

1. The PCR mix is prepared on ice and contains 10 µL of 5X PCR buffer (final 2 m*M* MgCl$_2$), 1 µL of oligo-dT Iscove (1 µg/µL; final 20 ng/µL), 1 µL of dNTP (10 m*M*; final 0.2 m*M*), 2.5 µL of Triton X-100 (10%; final 0.5%), 1 µL of *Taq* Platinum (5 U/µL; final 5 U) and 29.5 µL of dd-H$_2$O.
2. Into each tube containing 5 µL of dA-tailed cDNA, 45 µL of PCR mix is added, as well as 2 drops of mineral oil.

Table 1
Primer Sequences for Human CD8+ T-Lymphocytes

Name of gene	Primer sequence-forward 5'→ 3'	Primer sequence-reverse 5'→ 3'
GAPDH	GGACCTGACCTGCCGTCTAG	CCACCACCCTGTTGCTGTAG
CD3	CGTTCAGTTCCCTCCTTTTCTT	GATTAGGGGGTTGGTAGGGAGTG
CD8alpha	AACCACAGGAACCGAAGACGT	GGACTTGCTCCCTCAAAAGGA
CD27	ACGTGACAGAGTGCCTTTTCG	TTTGCCCGTCTTGTAGCATG
CCR7	CCAGGCCTTATCTCCAAGACC	GCATGTCATCCCCACTCTG
Granzyme B	GCAGGAAGATCGAAAGTGCGA	GCATGCCATTGTTTCGTCCAT
Perforin	TTCACTGCCACGGATGCCTAT	GCGGAATTTTAGGTGGCCA
IFN-γ	GCCAACCTAAGCAAGATCCCA	GGAAGCACCAGGCATGAAATC
TNF-α	CTGCCTTGGCTCAGACATGTT	CAGTTGGTCACCAAATCAGCA
CD94	GTGGGAGAATGGCTCTGCAC	TGAGCTGTTGCTTACAGATATAACGA

3. Tubes are placed into a PCR machine (BioLabo Scientific Instruments, Chatel-St-Denis, Switzerland) at 94°C for 3 min to activate the *Taq* Platinum, and followed by 5 cycles of PCR (50 s at 94°C; 2 min at 37°C; 9 min at 72°C), 35 cycles (50 s at 94°C; 90 s at 60°C; 8 min at 72°C), and 1 cycle (8 min at 72°C). This cDNA is now called globally amplified cDNA or cDNA+. It can be stored at –20°C for up to 6 mo or at –80°C for longer periods of time (*see* **Note 2**).

3.1.6. Second Step PCR Reaction

The final step is to test the quality of the globally amplified cDNA. To avoid any PCR contamination, the PCR mixes are prepared in a clean but different laboratory area the one(s) used during **steps 3.1.2. to 3.1.5.**

One μL of amplified cDNA is then subjected to a second round of PCR amplification (38–40 cycles, 30 s at 94°C; 45 s at 58°C; 1 min at 72°C, followed by 1 cycle, 8 min at 72°C) in 20 μL volumes of 4 μL of 5X PCR buffer (final 1.5 mM MgCl$_2$), 0.4 μL of dNTP (10 mM; final 0.2 mM), 0.4 μL of specific primers designed to amplify mRNA sequences of interest (100 ng/μL; final 2 ng/μL), 0.1 μL of *Taq* Platinum (5 U/μL; final 0.5 U) and 13.7 μL of dd-H$_2$O. Typically, we are using either H$_2$O or the Daudi B-cell line for the negative PCR control, while 10^3 peripheral blood mononuclear cells (PBMC) from a healthy individual are used as positive PCR control. We have tested the following primers for the gene expression analysis of human CD8+ T-lymphocytes (**Table 1**). For all primers, with the exception of the primer-pair for IFN-γ amplification (1.25 mM MgCl$_2$), 1.5 mM MgCl$_2$, and the annealing temperature of 58°C are used. The expected PCR products are visualized after electrophoresis on a 1.2% agarose gel as shown in **Fig. 4**.

In a recent study, we have characterized and described the properties of a "pre-effector" CD8+ T-lymphocyte subset, RA+CCR7−27+, in human peripheral blood *(19)*. By using five-cell RT-PCR, we found that all samples of CD8+ cells analyzed in the present study gave a CD3-specific PCR product. All naive T-cell samples but none of the aliquots of effector T-cells yielded a detectable CCR7-specific product (**Fig. 5**).
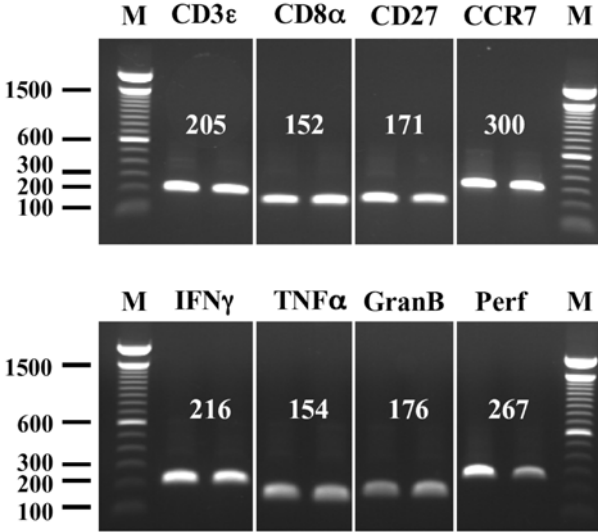
Fig. 4. Examples of specific reverse transcription-polymerase chain reaction (RT-PCR) reactions on samples processed following the five-cell global cDNA amplification protocol. The PCR products are visualized after electrophoresis on a 1.2% agarose gel, and the expected size for each set of primers is indicated. M: 100- to 1500-bp ladder. GranzB; granzyme B. Perf; perforin.
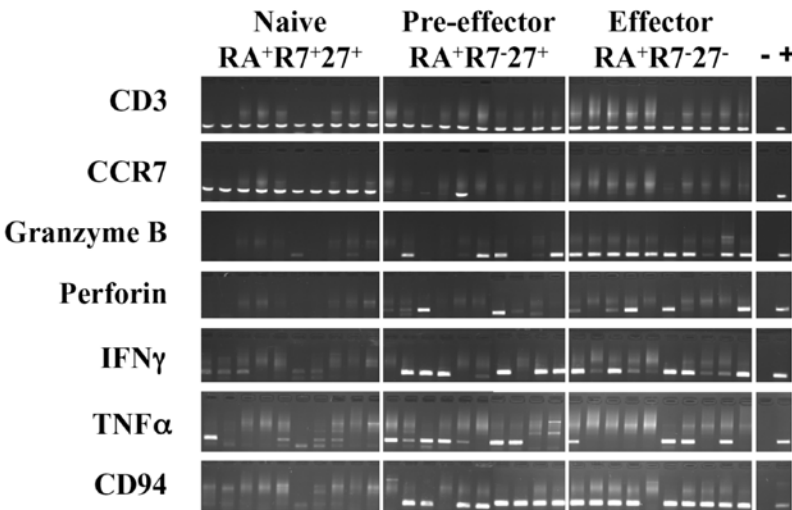
Fig. 5. Gene expression analysis was performed on naive (N; RA$^+$CCR7$^+$27$^+$), pre-effector (pE; RA$^+$CCR7$^-$27$^+$) and effector (E; RA$^+$CCR7$^-$27$^-$) T-cell subsets using the global cDNA amplification protocol. Data from 10 independent five-cell aliquots as well as negative (–) and positive (+) controls are depicted. The set of primers used in this experiment is described in detail in **Subheading 3.1.6.** Reprinted with permission from **ref. 19**.

As expected, naive CD8⁺ T-lymphocytes, which are not cytolytic and do not produce cytokines, did not contain detectable granzyme B, perforin, FasL, IFN-γ, or NK-receptor CD94 mRNA, and only rarely gave a TNF-α signal. In contrast, these mRNA transcripts were found in most (granzyme B, CD94) or in a significant fraction of effector T-lymphocyte aliquots. Transcript analysis of RA⁺CCR7⁻27⁺ pre-effector T-cells revealed the presence of all effector-function-associated mRNAs in a significant fraction of five-cell aliquots from this population. Among RA⁺CCR7⁻27⁺ cell aliquots there is no obvious correlation between the presence of PCR products corresponding to different effector-function-associated genes. For instance, one sample gave PCR products for granzyme B, IFN-γ, and CD94, while another was positive for FasL, TNF-α, and CD94 (**Fig. 5**). At this stage, we cannot decide whether this observation reflects a stochastic element in the PCR-based amplification from very small transcript numbers, cell biological heterogeneity among RA⁺CCR7⁻27⁺ T-cells, or heterogeneity of gene expression among individual cells from a homogeneous population *(24)*. We conclude that, unlike naive cells, a proportion of RA⁺CCR7⁻27⁺ T-cells express genes associated with cytolytic T-cell effector functions, and we refer to this subset as pre-effector T-lymphocytes.

3.2. Flow-FISH Analysis of Average Telomere Length

The estimation of telomere length in individual cells by flow FISH has been initially described in 1998 by two separate groups *(20,25)*. In a recent review, Lauzon et al. provide a complete description of both protocols with particular emphasis placed on their similarities and their differences *(26)*. The flow-FISH technique described below is based on the original publication by Rufer and colleagues *(20,21)* and outlines (1) the quantitative telomere fluorescence in situ hybridization; (2) the acquisition and the analysis of telomere fluorescence by flow cytometry; and (3) the adaptation of flow FISH to carry out telomere length measurement in nuclei obtained from fibroblasts and various cell lines (unpublished data). The flow-FISH method has been recently standardized to obtain highly accurate and reproducible results *(27)*, and some critical aspects of this technique are discussed.

3.2.1. Quantitative Fluorescence In Situ Hybridization

1. FACS-sorted human CD8⁺ T-lymphocytes of the desired subpopulation (2×10^5 cells) are placed in 1.5-mL V-bottom tubes (Eppendorf, Hamburg, Germany) and washed in 1X PBS (w/o Ca⁺⁺ and Mg⁺⁺) containing 0.1% (w/v) BSA.
2. Typically, 1×10^5 cells are resuspended in 100 μL of hybridization mixture containing 70% of ultrapure deionized formamide, 20 m*M* Tris (pH 7.1), 1% (w/v) BSA with either no probe (unstained control) or with 0.3 μg/mL telomere-specific FITC-conjugated $(C_3TA_2)_3$ PNA probe for stained samples.
3. Samples are subjected to heat denaturation of DNA for 10 min at 84°C in a water-bath followed by hybridization for 2 h at RT in the dark (*see* **Note 3**).
4. Cells are then spun down and the supernatant is aspirated (leave 100 μL of liquid at the bottom of the tubes, as formamide is quite viscous and compact cell pellets cannot be clearly observed).
5. To remove excess and non-specifically bound telomere-PNA probe, samples are washed twice with 1 mL of wash buffer containing 70% formamide, 10 m*M* Tris (pH 7.1), 0.1%

BSA, and 0.1% Tween-20 at RT. The last washing step is performed with a wash solution containing 1X PBS, 0.1% BSA, and 0.1% Tween-20. After each wash step, cells are spun down at 16°C for 7 min at 3000 rpm (1800*g*) for the formamide washes and at 2000 rpm (800*g*) for the PBS wash.

6. Following the last wash, cells are resuspended in 300 μL of 1X PBS containing 0.1% BSA, 1000 U/mL RNAse T1, and 0.02 μg/mL propidium iodide and transferred into FACS tubes (*see* **Note 4**).
7. Cells are incubated for at least 30 min at RT prior to analysis.

3.2.2. Flow-Cytometric Analysis

The analysis of telomere fluorescence by gating on single cells (2n; FCS/FL3; R1), excluding doublets, and gating on the lymphocyte population (FCS/SSC; R2) is done using Cell Quest (Becton Dickinson). A representative example is shown in **Fig. 6**. To correct for the auto-fluorescence of the cells in FL1, cells incubated in the hybridization stage in the absence of the FITC-labeled telomere-PNA probe are used. The telomere fluorescence of lymphocytes is calculated by subtracting the fluorescence of unstained controls from the telomere fluorescence measured in cells hybridized with the FITC-labeled telomere-PNA probe (**Fig. 6A**; Δ). To correct for daily shifts in the linearity of the flow cytometer, fluctuations in the laser intensity and optical alignment and to allow expression of results in standard fluorescence units, a mixture of four populations of FITC-labeled fluorescent beads is used. This mix of four populations of beads, each having a fluorescence corresponding to different known amounts of molecular equivalents of soluble fluorochrome (MESF), is suspended in 1X PBS–0.1% BSA and run in each experiment (**Fig. 6B**). The mean fluorescence for each of the four different fluorescence peaks is used to establish a calibration curve and to convert telomere fluorescence values into MESF values, allowing comparison among experiments. To estimate the telomere length (in kbp) from telomere fluorescence in MESF values, we use the following calibration curve: kbp = MESF $(10^{-3}) \times 0.5$ (**Fig. 6B**) (*see* **Note 5**). Recently, we measured the telomere length in CD8$^+$ T-lymphocyte subsets representing discrete stages of differentiation *(23)*. Telomere shortening appears to occur progressively, correlating with the stage of T-cell differentiation (**Fig. 6C**). Thus, highly differentiated effector-type T-cells display the profile corresponding to the shortest telomeres, with lengths (5.2 kb) equivalent to those observed in antigen-experienced CD8$^+$ T-cells from elderly individuals *(21)*. In contrast, naive and memory T-cell subsets still exhibited relatively long telomeres, with lengths of 9.1 kb and 6.8 kb respectively.

3.2.3. Flow-FISH on Nuclei of Fibroblasts

One of the major limitations of flow-FISH technology is its unique applicability to cells that do not contain large cytoplasm, such as lymphocytes or monocytes. To enable accurate measurement of telomere length in fibroblasts and various immortalized cell lines (i.e., HeLa, CaCo2, HTC75), we have recently adapted the flow-FISH technique to work with the nuclei of such cells (unpublished data). Cells grown on a monolayer are harvested by using trypsin treatment, and all procedures to lyse cells and isolate their nuclei are performed as follows:

1. Wash cells to be harvested once with 1X PBS.
2. Add 0.25% trypsin (Invitrogen) to the cell monolayer.
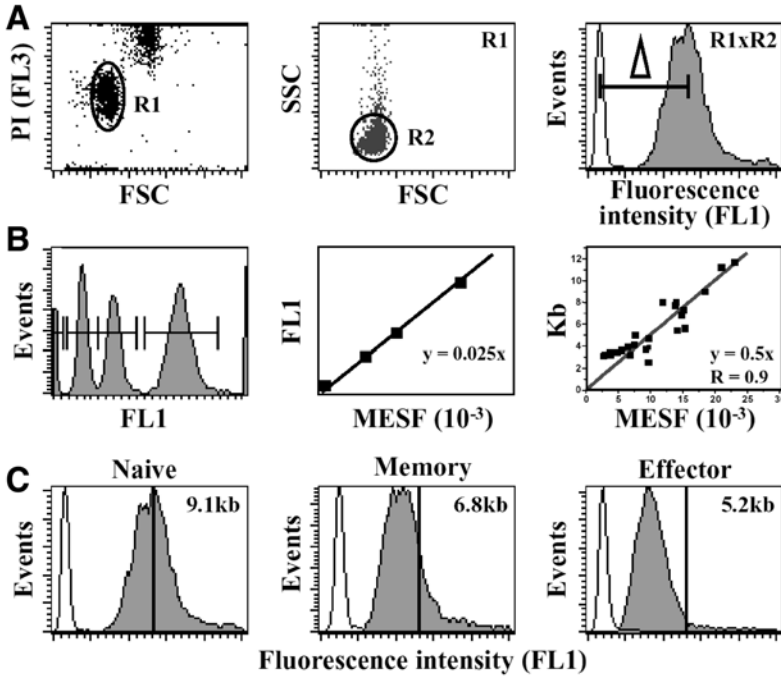
Fig. 6. **(A)** Flow-FISH analysis of the naive T-cell subset from an adult blood donor. Cells following in situ hybridization were gated on FL3 (PI) and forward scatter (FSC) and then on side scatter (SSC) vs FSC (R1 × R2) to obtain the fluorescence histogram (FL1; shaded histogram) derived from FITC-$(C_3TA_2)_3$-labeled PNA probe. As background control, the equivalent cell sample hybridized without the telomeric PNA probe is depicted (white histogram). Note that the fluorescent signal in the FL1 channel is acquired on the linear scale. The specific telomere fluorescence of cells is calculated by subtracting the mean background fluorescence from the mean fluorescence obtained with the telomere probe (Δ). **(B)** To allow the expression of results in standard fluorescence units or molecules of equivalent soluble fluorochromes (MESF × 10^{-3}), a mixture of four populations of FITC-labeled beads is acquired and a standardized linear regression line is generated (i.e., $y = 0.025x$). We have previously compared the telomere fluorescence of 25 different lymphocyte samples measured by flow-FISH to the telomere length (in kb) obtained from Southern blot analysis *(20)*. The slope of the obtained calibration curve is used to estimate the telomere length in kb from telomere fluorescence in MESF (× 10^{-3}) values ($y = 0.5x$, $R = 0.9$). **(C)** Example of telomere fluorescence analysis on sorted naive, memory, and effector CD8+ T-cell subsets. Note that there is a progressive telomere shortening as cells differentiate into effector-type of cells.

3. Wait until cells detach from the culture well.
4. Add 10% FBS-containing medium (i.e., DMEM) to stop enzymatic reaction, and transfer the suspension to a centrifuge tube in ice.
5. Wash the culture plate with 10 mL of cold PBS and add to the centrifuge tube.
6. Recover cells by centrifuging at 300*g* for 5–10 min at 4°C and discard supernatant.

7. Wash cells once again with cold PBS, discard supernatant, and resuspend to a final concentration of 1×10^6–5×10^6 in one volume of cold PBS (1 mL).

8. Add one volume of ice-cold cell lysis buffer (1 mL) and three volumes of ice-cold distilled water (3 mL).

9. Mix by inverting the tubes several times and incubate for 10 min on ice.

10. Prepare new series of tubes containing 2.5 volumes of an ice-cold 30% sucrose solution (2.5 mL).

11. Carefully add on the top of this sucrose cushion, the five volumes of the cell lysis buffer containing the lysed cells (5 mL).

12. Centrifuge at 2000*g* for 10 min at 4°C and remove the supernatant (which contains the cytoplasm of lysed cells).

13. Carefully resuspend the pellet containing the cell nuclei in cold PBS and count them. The recovery of nuclei from the starting intact cell population is 50 to 80%.

Nuclei from lysed cells such as fibroblasts and in vitro established cell lines are now ready to be used for telomere length measurements by flow FISH as described in **Subheading 3.2.1.** Since we have performed all experiments with 4×10^5 nuclei, the volume of the hybridization mixture is doubled (200 μL instead of 100 μL). Moreover, isolated nuclei are more fragile than intact cells. Therefore, isolated nuclei should be kept on ice, and all steps using pipets should be done with care. Do not vortex nuclei containing samples, even after they have been fixed with 70% formamide. Keep in mind that clumps and aggregates are more likely to form on fixed nuclei than on whole fixed cells. Telomere length analysis is then performed as described in **Subheading 3.2.2.**

To verify whether the same calibration slope ($y = 0.5x$) could be used for the analysis of telomere fluorescence values obtained from nuclei of human cells, 22 different nuclei preparations from fibroblasts and various cell lines were isolated and characterized separately by Southern blot (**Fig. 7A**) and flow-FISH (**Fig. 7B**). Southern blotting is the gold standard for measurement of telomere length *(28,29)*, but requires large numbers of cells and is relatively laborious. Briefly, the DNA is extracted from cells and digested by frequent cutting restriction enzymes such as RsaI and HinfI. These digested DNA fragments are run on an agarose gel and hybridized to a P^{32}-labeled $(C_3TA_2)_3$ telomeric probe. The blot is exposed to photographic film, and the telomere length is estimated from the resulting autoradiograph by densitometric analysis. Results from flow-FISH measurements (**Fig. 7B**) correlated with results from conventional telomere length analysis by Southern blot (**Fig. 7C**; $R = 0.86$). Furthermore, the slope for the calibration curve obtained with nuclei of fibroblasts and various cell lines was very similar to the previously described calibration curve using intact small-size cells (kbp = MESF × 0.5) *(20)*. Finally, we have characterized telomere length dynamics of in vitro cultured fibroblasts in relation to cell divisions. Progressive telomere shortening was observed by both Southern blot and flow-FISH analysis as fibroblasts were ageing in culture (**Fig. 7**).

4. Notes

1. Five-cell cDNA amplification and RT-PCR. We have developed a single-step procedure for cell lysis and cDNA synthesis, since our standard goal is to start with limited cell
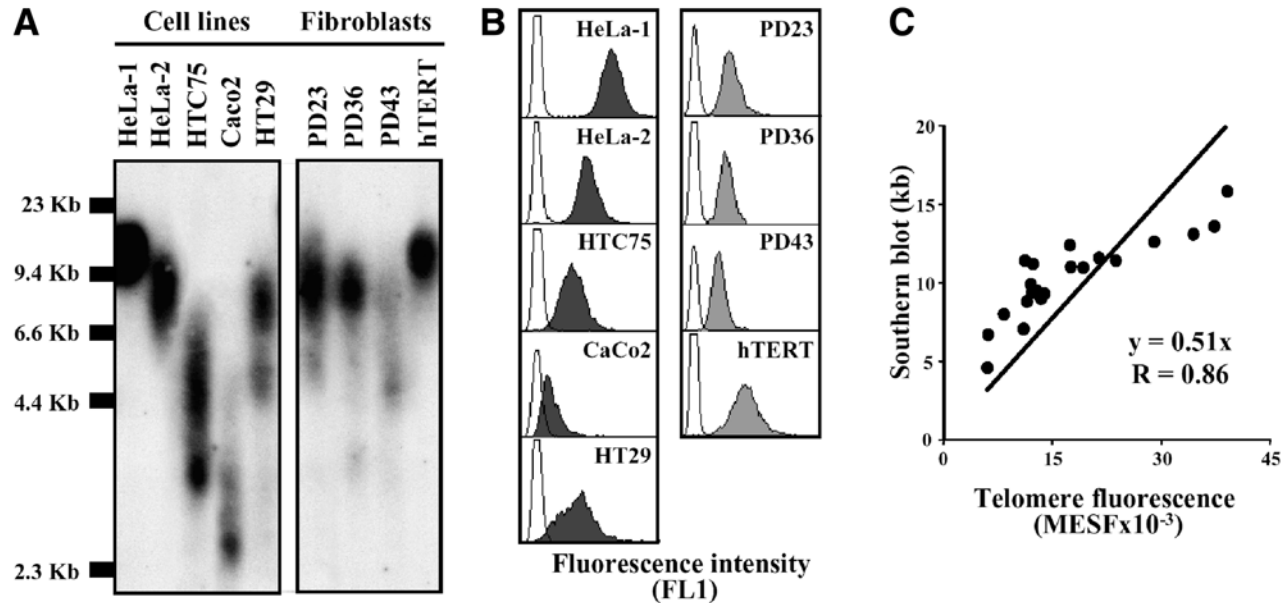
Fig. 7. Isolated nuclei from various cell lines (i.e., HeLa, HTC75, CaCo2, and HT29) as well as from fibroblasts at various time-points of in vitro culture (PD23, PD36, and PD43) and from hTERT-expressing fibroblasts were subjected to **(A)** Southern blot analysis of telomere repeat arrays and **(B)** flow-FISH analysis of average telomere length. **(C)** The telomere fluorescence (in MESF 10^{-3}) was proportional to the terminal restriction fragment values (in kbp) with a high correlation coefficient ($R = 0.86$). Note that the slope of the calibration curve described for nuclei of cells is similar to that of the previously described calibration curve obtained on intact cells *(20)*. PD, population doublings; MESF, molecules of equivalent soluble fluorochromes.

numbers (1–10 cells). This direct experimental step relies on Triton X-100 to lyse the outer cellular membrane, as well as on the presence of an RNAse inhibitor to protect the RNAs from degradation. Using such a strategy has the following consequences. First, cDNA strands are synthesized from the 3' poly(A) tails of mRNAs. Second, the length of synthesized first-strand cDNAs is estimated to vary between 100 and 2500 bp. Based on these facts, we designed our primers of interest (*see* **Table 1**) in such a way that they are located within the first 1000 bp following the 3'-polyA end of the mRNA sequence, and whenever possible between two exons. However, since most mRNAs have 3'-UTR sequences that largely exceed 1 kb of length, it is almost impossible to design primers located between two exons (with the exception of GAPDH, granzyme B, and CD8α primers). We have recently reported that specific PCR products nicely correlated with the levels of protein expression, and have concluded that the presence of genomic DNA was hardly detected using our selected primers *(19)*. As shown in **Fig. 4**, only naive T-cell samples yielded a detectable CCR7-specific product correlating with CCR7 cell-surface expression. Faint contaminant PCR bands—i.e., TNF-α and IFN-γ—were observed only in some rare cases among samples of naive T-cell origin. Thus, it is quite unlikely that these bands represent contaminant genomic DNA. Altogether, the fact that no genomic DNA is detected in our five-cell assay may be explained by the low number of genomic copies present within the 5-cell samples, and by their dilution following the global cDNA amplification procedure (10 copies per 50 μL).

2. The concentration of $MgCl_2$ in the global cDNA amplification RT-PCR appears to be a critical factor, and it was optimized at 2 m*M* (data not shown). More generally, the procedure is delicate and any departure from the outlined method, including changes in the commercial sources of the reagents, should be carefully evaluated using reference positive and negative controls. The original oligo(dT) Iscove primer is a 61-mer and contains an *Eco*RI restriction site prior to the dT stretch *(16)*. Beside these features, the unique sequence was chosen arbitrarily by Brady and colleagues *(16)*. We tested a truncated 43-mer of the same primer sequence (5'-CTG GGA CAA AAT ATG AAT TCT TTT TTT TTT TTT TTT TTT TTT T-3') and could observe neither major qualitative nor quantitative differences in the performance of the two primers. Successful global cDNA amplification generates samples containing a heterogeneous collection of 3'-cDNA fragments representing all transcribed poly(A) mRNAs. The loading of 5 μL of the amplified cDNA sample on a 1.2% agarose gel migrates as a relatively strong ethidium bromide-stained smear ranging from 100 to 2500 bp in length.

3. Flow-FISH analysis of average telomere length. There are two key aspects in the flow-FISH technique. First, we use directly labeled PNA probes instead of DNA or RNA probes. PNA probes are synthetic mimics of single-strand DNA with bases attached to an uncharged peptide-like backbone. The PNA probe hybridizes to complementary DNA in low ionic strength solutions that do not favor re-annealing of the target strands. Thus, PNA-DNA interactions are more stable than DNA-DNA or DNA-RNA interactions under hybridization conditions (reviewed in **ref. *30***). Second, the heating and formamide treatment allow the PNA probes, which are present during the denaturation step, to get into the cells without their prior permeabilization. In contrast to us, Hultdin and colleagues *(25)* employed the standard in situ hybridization method of fixation followed by permeabilization, with the Caltag Fix and Perm kit™. Our strategy avoids problems associated with excessive fixation, such as the potential accessibility of the PNA probe to penetrate the cell.

For the flow-FISH technique, DNA needs to be completely denatured to single strands within the cell, and the optimal denaturation temperature and time should not result in

disintegration of the cells or of the nuclei. The denaturation step takes place with the cells suspended in 70% formamide-based hybridization solution at 84°C for 10 min. For T-lymphocytes, there is a progressive increase in telomere fluorescence signals as the denaturation temperature is increased, reaching a plateau at 86°C (data not shown). At higher temperature (90°C) or longer time periods (>15 min) *(27)*, the overall telomere fluorescence signals decreased due to the loss of cells or of DNA. Finally, the optimal denaturation temperature and time also depends on the volume of hybridization solution. The technique described here is based on the use of low numbers of isolated T-lympho-cyte subsets (a maximum of 10^5 cells) and thus on low volumes (100–200 µL) of hybrid-ization mixture. If higher cell numbers are used (i.e., 5×10^5 cells), the final volume of 300 µL as well as a denaturation temperature ranging between 85 and 87°C for 15 min has been recommended *(27)*. Finally, the hybridization time represents another parameter that can be modified. Since the hybridization of the telomere-PNA probes requires more than 60 min to reach the plateau of telomere fluorescence (data not shown) *(27)*, we propose performing the hybridization with 0.3 µg/mL of PNA probe at RT and in the dark for 90–120 min.

4. Although formamide is relatively toxic and requires handling in a fume hood, the three washing steps are critical in order to dilute the excess of the PNA probe. Various washing protocols, including the use of 1X PBS instead of formamide, have been tested by Baerlocher and coworkers *(27)*, unfortunately without providing telomere fluorescence signals equivalent to those observed with the classical protocol. Propidium iodide (PI) staining is widely used for the distinction of single cells from doublets as well as for the discrimination of cells in G0/G1 vs in S phase. Because telomere replication takes place in early S phase, it is important to gate on the 2n population of cells as determined by PI staining (*see* **Fig. 6A**). Moreover, the PI emission spectrum overlaps to some extent with that of FITC in FL1, and using lower concentrations of the dye reduces interference with the telomere-PNA FITC measurements (data not shown). Thus, we use for 10^5, 2×10^5, and 4×10^5 cells, respectively, 0.02, 0.04, and 0.06 µg/mL of PI. Others have proposed resuspending cells in LDS 751 at a concentration of 0.01 µg/mL *(27)*.

5. Since the flow-FISH method involves many steps where relatively minor errors can trans-late into large shifts in fluorescent readout, we have focused our technique on monitoring intra- and inter-experimental errors by using calibration beads as well as frozen cell samples such as lymphoma cells or PBMC. First, FITC-labeled beads are run in each experiment, and the resulting calibration curve is used to correct for daily fluctuations in the laser intensity, alignment, and linearity. Second, in order to analyze the day-to-day variation in flow-FISH results, aliquots of the same frozen lymphoma cells were ana-lyzed in each experiment over a 6-mo period (data not shown) *(21)*. In 38 experiments, the mean (± s.d.) fluorescent value was 12.2 ± 1.8 MESF ($\times 10^{-3}$), with a coefficient of variation (CV) of 15 %. Variation between multiple samples of the same cell type in the same experiment was <5%, and variation between experiments using the same frozen control cells ranged between 10 and 20%. Recovery of hybridized cells varied in different experiments from 20 to 80%, with a higher range corresponding to freshly isolated cells with a high viability (>90%) and the lower range corresponding to previously frozen cells. In contrast, Hultdin et al. *(25)* used an internal control such as 1301 (T-cell lympho-blastic leukemia cell line) cells, known to possess extremely long telomeres (>25 kb). 1301 cells are mixed with each experimental cell sample, and the telomere fluorescence value is calculated as a ratio between the telomere signal of the experimental sample and of the 1301 T-cells.

Acknowledgments

References

1 Van Der Bruggen, P., Zhang, Y., Chaux, P., et al. (2002) Tumor-specific shared antigenic peptides recognized by human T-cells. *Immunol. Rev.* **188,** 51–64.

2. Speiser, D., Pittet, M. J., Rimoldi, D., et al. (2003) Evaluation of melanoma vaccines with molecularly defined antigens by ex vivo monitoring of tumor-specific T cells. *Seminars in Cancer Biology* **13,** 461–472.

3 Dudley, M. E. and Rosenberg, S. A. (2003) Adoptive-cell-transfer therapy for the treatment of patients with cancer. *Nat. Rev. Cancer* **3,** 666–675.

4 Ho, W. Y., Blattman, J. N., Dossett, M. L., Yee, C., and Greenberg, P. D. (2003) Adoptive immunotherapy: engineering T cell responses as biologic weapons for tumor mass destruction. *Cancer Cell* **3,** 431–437.

5. Waldmann, T. A., Levy, R., and Coller, B. S. (2000) Emerging therapies: spectrum of applications of monoclonal antibody therapy. *Hematology (Am. Soc. Hematol. Educ. Program)* **2000,** 394–408.

6 Marchand, M., Punt, C. J., Aamdal, S., et al. (2003) Immunisation of metastatic cancer patients with MAGE-3 protein combined with adjuvant SBAS-2: a clinical report. *Eur. J. Cancer* **39,** 70–77.

7 Scanlan, M. J., Gure, A. O., Jungbluth, A. A., Old, L. J., and Chen, Y. T. (2002) Cancer/testis antigens: an expanding family of targets for cancer immunotherapy. *Immunol. Rev.* **188,** 22–32.

8 Rosenberg, S. A., Yang, J. C., Schwartzentruber, D. J., et al. (2003) Recombinant fowlpox viruses encoding the anchor-modified gp100 melanoma antigen can generate antitumor immune responses in patients with metastatic melanoma. *Clin. Cancer Res.* **9,** 2973–2980.

9 Smith, J. W., 2nd, Walker, E. B., Fox, B. A., et al. (2003) Adjuvant immunization of HLA-A2-positive melanoma patients with a modified gp100 peptide induces peptide-specific CD8+ T-cell responses. *J. Clin. Oncol.* **21,** 1562–1573.

10 Romero, P., Valmori, D., Pittet, M. J., et al. (2002) Antigenicity and immunogenicity of Melan-A/MART-1 derived peptides as targets for tumor reactive CTL in human melanoma. *Immunol. Rev.* **188,** 81–96.

11 Ghanekar, S. A. and Maecker, H. T. (2003) Cytokine flow cytometry: multiparametric approach to immune function analysis. *Cytotherapy* **5,** 1–6.

12 Pittet, M. J., Zippelius, A., Speiser, D. E., et al. (2001) Ex vivo IFN-gamma secretion by circulating CD8 T lymphocytes: implications of a novel approach for T cell monitoring in infectious and malignant diseases. *J. Immunol.* **166,** 7634–7640.

13 Altman, J. D., Moss, P. A. H., Goulder, P. J. R., et al. (1996) Phenotypic analysis of antigen-specific T lymphocytes. *Science* **274,** 94–96.

14 Kawakami, Y., Eliyahu, S., Sakaguchi, K., et al. (1994) Identification of the immunodominant peptides of the MART-1 human melanoma antigen recognized by the majority of HLA-A2-restricted tumor infiltrating lymphocytes. *J. Exp. Med.* **180,** 347–352.

15 Pittet, M. J., Zippelius, A., Valmori, D., Speiser, D. E., Cerottini, J. C., and Romero, P. (2002) Melan-A/MART-1-specific CD8 T cells: from thymus to tumor. *Trends Immunol.* **23,** 325–328.

16 Brady, G. and Iscove, N. N. (1993) Construction of cDNA libraries from single cells. *Methods Enzymol.* **225,** 611–623.

17 Sauvageau, G., Lansdorp, P. M., Eaves, C. J., et al. (1994) Differential expression of homeobox genes in functionally distinct CD34+ subpopulations of human bone marrow cells. *Proc. Natl. Acad. Sci. USA* **91,** 12,223–12,227.

18 Bigouret, V., Hoffmann, T., Arlettaz, L., et al. (2003) Monoclonal T-cell expansions in asymptomatic individuals and in patients with large granular leukemia consist of cytotoxic effector T cells expressing the activating CD94:NKG2C/E and NKD2D killer cell receptors. *Blood* **101,** 3198–3204.

19 Rufer, N., Zippelius, A., Batard, P., et al. (2003) Ex vivo characterization of human CD8+ T subsets with distinct replicative history and partial effector functions. *Blood* **102,** 1779–1787.

20 Rufer, N., Dragowska, W., Thornbury, G., Roosnek, E., and Lansdorp, P. M. (1998) Telomere length dynamics in human lymphocyte subpopulations measured by flow cytometry. *Nat. Biotechnol.* **16,** 743–747.

21 Rufer, N., Brummendorf, T. H., Kolvraa, S., et al. (1999) Telomere fluorescence measurements in granulocytes and T lymphocyte subsets point to a high turnover of hematopoietic stem cells and memory T cells in early childhood. *J. Exp. Med.* **190,** 157–167.

22 Zippelius, A., Pittet, M. J., Batard, P., et al. (2002) Thymic selection generates a large T cell pool recognizing a self-peptide in humans. *J. Exp. Med.* **195,** 485–494.

23 Papagno, L., Spina, C. A., Marchant, A., et al. (2004) Immune activation and CD8+ T-cell differentiation towards senescence in HIV-1 infection. *PLoS* **2(2),** e20.

24 Levsky, J. M., Shenoy, S. M., Pezo, R. C., and Singer, R. H. (2002) Single-cell gene expression profiling. *Science* **297,** 836–840.

25 Hultdin, M., Gronlund, E., Norrback, K., Eriksson-Lindstrom, E., Just, T., and Roos, G. (1998) Telomere analysis by fluorescence in situ hybridization and flow cytometry. *Nucleic Acids Res.* **26,** 3651–3656.

26 Lauzon, W., Sanchez Dardon, J., Cameron, D. W., and Badley, A. D. (2000) Flow cytometric measurement of telomere length. *Cytometry* **42,** 159–164.

27 Baerlocher, G. M., Mak, J., Tien, T., and Lansdorp, P. M. (2002) Telomere length measurement by fluorescence in situ hybridization and flow cytometry: tips and pitfalls. *Cytometry* **47,** 89–99.

28 Harley, C. B., Futcher, A. B., and Greider, C. W. (1990) Telomeres shorten during ageing of human fibroblasts. *Nature* **345,** 458–460.

29. Allsopp, R. C., Vaziri, H., Patterson, C., et al. (1992) Telomere length predicts replicative capacity of human fibroblasts. *Proc. Natl. Acad. Sci. USA* **89,** 10,114–10,118.

30. Lansdorp, P. M., Poon, S., Chavez, E., et al. (1997) Telomeres in the haemopoietic system. *Ciba Found. Symp.* **211,** 209–218; discussion 19–22.

20

Regulatory T-Cells in Antitumor Therapy

Isolation and Functional Testing of CD4+CD25+ Regulatory T-Cells

Helmut Jonuleit and Edgar Schmitt

Summary

Naturally occurring CD4+CD25+ T regulatory cells originate from the thymus and play a central role regarding the maintenance of peripheral tolerance by suppression of autoreactive T-cell populations. However, T regulatory cells can have beneficial as well as harmful effects. On the one hand, they prevent a variety of autoimmune and inflammatory diseases; but on the other hand, they concomitantly inhibit antitumor immune reactions by suppressing tumor-specific T-cell responses. Therefore, these ambivalent properties of T regulatory cells require detailed investigation especially with respect to a potential therapeutic exploitation of these cells. A prerequisite for such analyses is the isolation of pure T regulatory cells and the establishment of functional tests for the analysis of their suppressive properties, since no specific markers for CD4+CD25+ T regulatory cells are known so far. In this chapter, techniques applying immunomagnetic beads have been used to establish an efficient method for isolation of human as well as murine regulatory T-cells. A combination of positive and negative selection steps using immunomagnetic beads of different sizes yields preparations of functional, active CD4+CD25+ regulatory T-cells with high purity. Additionally, co-culture assays for functional characterization of isolated CD4+CD25+ regulatory T-cells are described that are able to detect their suppressive properties for conventional CD4+ T-cells with high sensitivity.

Key Words: CD4+CD25+ T-cells; regulatory T-cells; tolerance; T-cell suppression; regulation.

1. Introduction

The immune system distinguishes between self and nonself structures, but also between harmful and innocuous foreign antigens, to prevent unessential and self-destructive immune responses. To maintain tolerance against self as well as protective immunity against pathogens, sophisticated and highly balanced immune mechanisms have evolved to generate antigen-specific effector cell responses as well as antigen-specific tolerance induction.

The idea of specific suppressor T-cell populations that counteract harmful autoaggressive immune responses in the periphery was first described in the 1970s by

Gershon et al. *(1)*. However, at that time neither the cells nor the hypothetical soluble suppressor factors responsible for the observed effects could be identified. In 1995, Sakaguchi et al. described a subpopulation of CD4$^+$ T helper cells, characterized by a constitutive expression of the interleukin (IL)-2 receptor α-chain (CD25), that is essential to control autoaggressive immune responses in mice *(2)*. After subsequent in vitro studies by several groups, this population is now referred to as CD4$^+$CD25$^+$ T regulatory cells. This distinct T-cell population was originally described in mice. Meanwhile, comparable T regulatory cell populations, with identical phenotype and functional activities, have been defined more recently in rats and humans *(3–8)*. They represent 5–10% of total peripheral CD4$^+$ T-cells. Freshly isolated, CD4$^+$CD25$^+$ T regulatory cells do not proliferate after allogeneic or polyclonal stimulation, but suppress the activation and cytokine release of conventional CD4$^+$ and CD8$^+$ T-cells in an antigen-nonspecific and cell contact-dependent manner *(3,8–10)*. Currently, no specific markers for regulatory T-cells are known, but under noninflammatory conditions they comprise the vast majority of all CD25$^+$CD4$^+$ T-cells. T regulatory cells can be isolated from naïve as well as from tolerized donors, and this chapter is focused on methods that can be utilized for isolation and functional characterization of human and murine CD4$^+$CD25$^+$ T regulatory cells.

2. Materials

2.1. Isolation and Testing of Human Regulatory T-Cells

1. Isolation buffer: PBS 1X (w/o Ca^{2+}, Mg^{2+}), 0.5% human serum albumin (HSA, i.e., Human-Albumin Kabi 20%, Octapharma, Langenfeld, Germany), 3 m*M* EDTA, 4°C.
2. Washing buffer: PBS 1X (w/o Ca^{2+}, Mg^{2+}), 1 m*M* EDTA, 4°C.
3. Depletion buffer: MEM + 5% FCS, 4°C.
4. Culture medium: X-VIVO 15 (BioWhittaker, Walkersville, MD).
5. For isolation: anti-CD25-FITC (M-A251, BD PharMingen, San Diego, CA).
6. For stimulation: anti-CD3 (OKT-3, ATCC), anti-CD28 (CD28.2, BD PharMingen).
7. For phenotypical characterization: FITC- or phycoerythrin (PE)-conjugated anti-CD3, anti-CD4, anti-CD25, anti-CD45RO, anti-CTLA-4 (Coulter/Immunotech, Marseille, France).
8. CD4-MACS-Multisort-Kit (Miltenyi, Bergisch-Gladbach, Germany).
9. CD25 microbeads (Miltenyi).
10. Anti-FITC Multisort Kit (Miltenyi).
11. Anti-phycoerythrin (PE) microbeads (Miltenyi, optional for isolation of T regulatory cell subsets).
12. Dynabeads M450: CD8, CD14, CD19, CD25 (Dynal, Hamburg, Germany).
13. MACS Separator (Miltenyi).
14. MACS Separation Columns LS (Miltenyi).
15. Magnetic Particle Concentrator for Dynabeads (Dynal).
16. Sample mixer (i.e., MX1, Dynal).

2.2. Isolation and Testing of Murine Regulatory T-Cells

1. Erythrocyte lysis: Gey's lysis buffer: 8.29g NH$_4$Cl, 1g KHCO$_3$, 0.0372g EDTA, pH 7.29; add to 1 L of H$_2$O and filtrate with 0.2 μm.
2. GM buffer: PBS 1X (w/o Ca^{2+}, Mg^{2+}), 0.5% BSA, 0.01% NaN$_3$, 5m*M* EDTA.
3. PBS 1X (w/o Ca^{2+}, Mg^{2+}), 10% FCS, 4°C.

4. PBS 1X (w/o Ca^{2+}, Mg^{2+}), 0.5% BSA, 4°C.
5. Culture medium: IMDM + 5% FCS + 1 mM NaPyr + 2 mM Gln.
6. Isolation: anti-CD25 (7D4), biotinylated (BD PharMingen).
7. Depletion: anti-CD25 (PC61, BD PharMingen), biotinylated with biotinamidocaproate *N*-hydroxysuccinimide (Sigma, St. Louis, MO).
8. Isolation: anti-CD4 (H129.19), biotinylated (BD PharMingen).
9. Stimulation: anti-CD3 (145-2C11), anti-CD28 (37.51), both purified using protein G sepharose (Pharmacia, New York, NY).
10. Phenotypical characterization: FITC- or phycoerythrin (PE)-conjugated anti-CD4 and anti-CD25 (BD PharMingen).
11. Streptavidin (SA) beads (Miltenyi).
12. Anti-phycoerythrin (PE) beads (Miltenyi).
13. Dynabeads M450:
    a. CD8 (Lyt2) beads, 4×10^8 beads/mL (Dynal) .
    b. Pan-B (B220) beads, 4×10^8 beads/mL (Dynal) .
    c. Anti-MAC 1 beads (CD11b): generated by binding 230 µg anti-MAC-1 mAb (M7/70.15.11.5) to 4×10^8/mL beads (Dynal, M-450 Epoxy).
14. Streptavidin, phycoerythrin labeled (SA-PE, Dianova, Hamburg, Germany).
15. MACS Separation Columns, LS (Miltenyi).
16. Cell strainer, 70 µm, nylon (Falcon).
17. MACS Separator (Miltenyi).
18. Magnetic Particle Concentrator for Dynabeads (Dynal).
19. Sample mixer (MX1, Dynal).

3. Methods

The methods described below outline the isolation and functional testing of human CD4$^+$CD25$^+$ T regulatory cells *(5,11)* and T regulatory cell subsets as well as the isolation and a functional assay for murine regulatory T-cells.

3.1. Isolation and Functional Analysis of Human Regulatory T-Cells

The isolation procedure starts with peripheral blood mononuclear cells (PBMC) isolated by standard gradient centrifugation from normal buffy coats of healthy volunteers. However, it is also possible to use PBMC isolated from whole peripheral blood or leukapheresis products (*see* **Note 1**). Importantly, positively selected CD4$^+$CD25$^+$ T-cell subsets have to be used in functional assays immediately after isolation, or at least have to be preactivated for subsequent functional analysis.

3.1.1. Multisort Positive Selection of CD4$^+$CD25$^+$ T-Cells

The basic scheme for isolation of human CD4$^+$CD25$^+$ regulatory T-cells is shown in **Fig. 1**.

3.1.2. Isolation of CD4$^+$ T-Cells (First Step)

1. Before isolation, PBMC are washed two times with 50 mL washing buffer.
2. Afterwards, CD4$^+$ T-cells can be directly isolated using the CD4-MACS Multisort Kit according to the instructions of the manufacturer. However, to prevent contamination (i.e., activated monocytes, which also express small amounts of CD4), do not use more than 4 µL beads per 10^7 PBMC for isolation of CD4$^+$ T-cells (*see* **Note 2**). For selection procedure, use the isolation buffer.
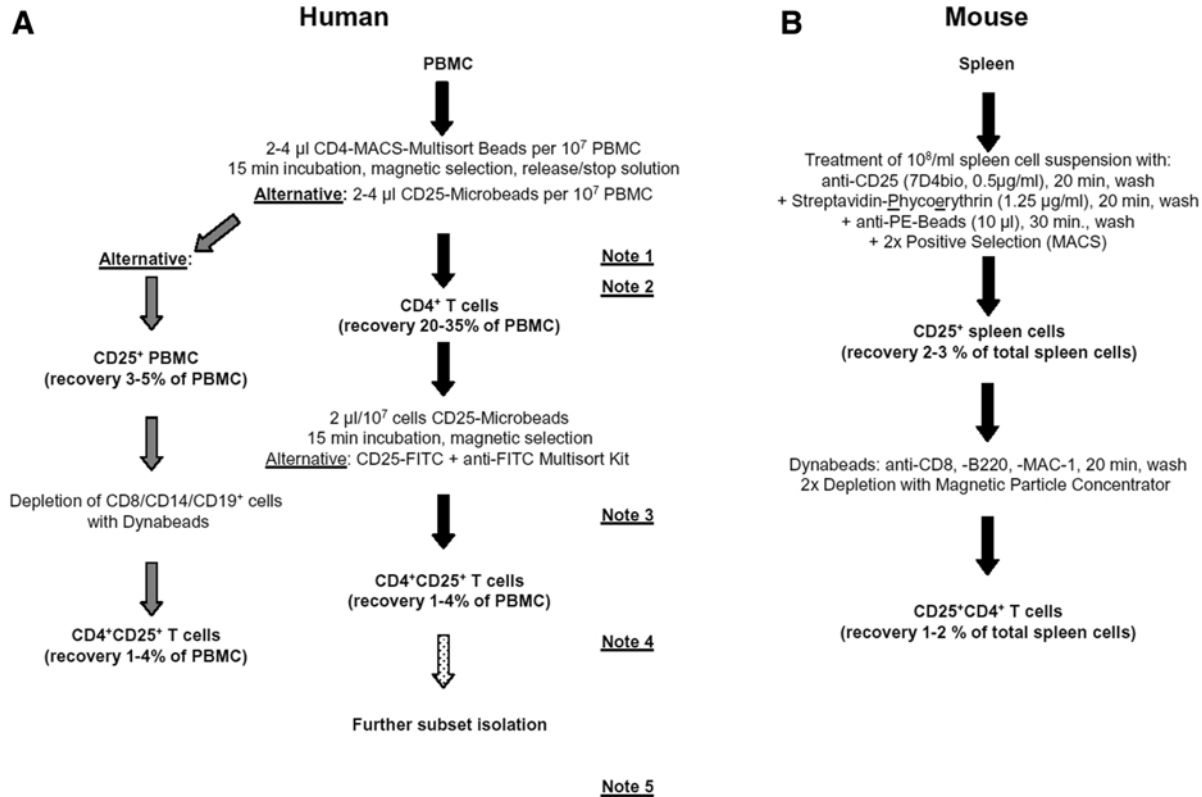
Fig. 1. Overview of the isolation techniques for human (**A**) and murine (**B**) CD4$^+$CD25$^+$ regulatory T-cells. Human preparations start with ficoll histopaque-isolated peripheral blood mononuclear cells (PBMC). This method can be used for isolation of regulatory T-cells from peripheral blood, buffy coats, or leukapheresis products. The example for isolation of murine CD4$^+$CD25$^+$ T-cells starts with a spleen cell suspension. However, the method is also useful for single-cell suspensions isolated from other murine organs (i.e., lymph nodes).

3.1.3. Isolation of CD4⁺CD25⁺ T-Cells (Second Step)

1. After detaching from CD4-Multisort Microbeads, isolate the CD25⁺ fraction using CD25 micobeads (2 µL beads per 10^7 CD4⁺ cells) (*see* **Notes 1** and **2**).
2. This method results in a purity of >97% CD4⁺CD25⁺ T-cells. However, the CD25 microbeads can not be detached. Therefore, it is not possible to use microbeads for the subsequent isolation of T regulatory cell subsets (*see* **Note 3**).

3.1.4. Alternative Isolation of CD4⁺CD25⁺ T-Cells

Alternatively, the CD25⁺ T-cell subset can be isolated by the combination of anti-CD25-FITC monoclonal antibodies (mAb) and the anti-FITC Multisort Kit (*see* **Note 5**).

1. After detaching of CD4-Multisort Microbeads, incubate the T-cells for 15 min with anti-CD25-FITC (10–20 µg per 10^8 CD4⁺ T-cells).
2. Wash two times with washing buffer.
3. Select positively with anti-FITC Multisort Microbeads (3 µL/10^7 CD4⁺ T-cells) according to the manufacturer's instructions.
4. After detaching, this preparation can be used for isolation of distinct CD4⁺CD25⁺ T-cell subsets (i.e., CD45RO⁺ vs CD45RO⁻ cells using anti-CD45RO-PE in combination with anti-PE microbeads).

3.1.5. Combination of Positive and Negative Selection for Isolation of CD4⁺CD25⁺ T-Cells

Alternatively, CD4⁺CD25⁺ T-cells can be isolated from PBMC by a combination of positive selection with microbeads (Miltenyi) and depletion of contaminating cells with Dynabeads (Dynal, *see* **Note 4**).

3.1.5.1. Positive Selection of CD25⁺ PBMC

1. Washed PBMC are incubated with CD25 microbeads (2 µL/10^7 PBMC) for 20 min at 4°C in isolation buffer (1×10^8/mL).
2. Afterwards, the cells are washed two times in PBS.
3. The CD25⁺ fraction is isolated using a MACS separator (Miltenyi) according to the instructions of the manufacturer.

3.1.5.2. Depletion of CD4-Negative Cells With Dynabeads

The positively selected CD25⁺ fraction contains 65–80% CD4⁺ T-cells and 20–35% contaminating CD19⁺ B-cells, CD8⁺ T-cells, and a few CD14⁺ monocytes. The contaminating cells can be depleted with Dynabeads. The following amounts of beads are used: CD19 Dynabeads: 2 beads/cell, CD8 Dynabeads: 3 beads/cell, CD14 Dynabeads: 1 bead/cell.

1. Wash the collected Dynabeads two times in 15-mL tubes with depletion buffer using the magnetic particle concentrator (Dynal).
2. Add the CD25⁺ PBMC fraction (5×10^7/mL) in depletion buffer and incubate the suspension for 20 min at 4°C on a shaker (sample mixer, Dynal).
3. Deplete contaminating cells according to the manufacturer's instructions by the use of the magnetic particle concentrator.
4. Repeat this Dynabeads depletion once for higher purity of CD4⁺CD25⁺ T-cells (>98% after two rounds of depletion).

3.1.6. Positive Isolation of Conventional CD4+ T-Cells (CD25 Depleted)

Co-expression of CD4 and CD25 is not sufficient for characterization of human regulatory T-cells. CD4+CD25+ regulatory T-cells are defined by their functional activity to suppress the activation of conventional T-cells. Therefore, to prevent experimental artifacts, analysis of functional activities of freshly isolated CD4+CD25+ T-cell preparations is mandatory. Several protocols for isolation of conventional CD4+ T-cells are useful and well established. In the following, we briefly describe one easy method for isolation of CD25-depleted CD4+ T helper cells.

1. For direct isolation of CD4+ T-cells, CD4 microbeads (Miltenyi, 2–4 µL/10^7 PBMC) can be used according to the manufacturer's instructions.
2. Contaminating CD4+CD25+ T-cells can be depleted in a second step by using CD25 Dynabeads (0.5 beads/cell). This depletion procedure is carried out as described under **Subheading 3.1.5.2.** and results in highly purified CD4+CD25− T helper cells (>98%).

3.1.7. Functional Analysis of Human Freshly Isolated CD4+CD25+ T-Cell Preparations

CD25 is a helpful surface marker for isolation of regulatory T-cells. However, CD25 is not specific for regulatory T-cells. This marker is also expressed on conventional CD4+ and CD8+ T-cells soon after activation. Therefore, control of the suppressive activities of human CD4+CD25+ T-cell preparations in suitable functional assays is extremely important for human regulatory T-cell preparations. In the following, two assays will be described *(12)*.

3.1.7.1. Allogeneic Mixed Leukocyte Reaction (MLR)

For an optimal stimulation of freshly isolated T-cell populations in an antigen-specific (alloantigen) manner, mature dendritic cells (DC) from allogeneic donors generated by standard methods can be used *(13)*.

1. Freshly isolated CD4+ as well as CD4+CD25+ T-cell subsets (1×10^5/well) are cultured in the presence of allogeneic DC in 96-well plates (200 µL/well, DC:T-cell ratio 1:10 or 1:20) in X-VIVO 15 (RPMI + 5% FCS can also be used).
2. After 4 d of incubation, T-cell proliferation is measured; for an additional 16 h, cells are pulsed with ^{3}H-TdR (37 kBq/well), and incorporated radioactivity is measured by using a liquid scintillation counter.
3. Co-cultures of CD4+ and CD4+CD25+ T-cells activated with allogeneic DC have to be performed to analyze the suppressive activity of CD4+CD25+ T-cells on the proliferation of conventional CD4+ T-cells. Therefore, a constant number of CD4+ T-cells is co-cultured with different numbers of CD4+CD25+ T-cells (ratio 1:1 to 1:4), and both T-cell populations are activated with a constant ratio of allogeneic DC.

3.1.7.2. Polyclonal Stimulation With Anti-CD3 and Anti-CD28 mAb

As an alternative to allogeneic stimulation:

1. Activate polyclonally constant numbers of conventional CD4+ T-cells (1×10^5/well) with anti-CD3 (1 µg/mL, OKT-3) and CD28 mAb (2 µg/mL, CD28.2) in the presence of varying numbers of CD4+CD25+ T-cells (ratio 1:1 to 1:4).

2. T-cell proliferation is measured after 3 d of culture and an additional 16 h pulse with ^{3}H-TdR (37 kBq/well).

Typical results of this standard assays for suppressive activity of freshly isolated human CD4$^+$CD25$^+$ regulatory T-cells are shown in **Figure 2.**

3.2. Isolation and Functional Analysis of Murine Regulatory T-Cells

Spleens from different strains of mice can be used as a source for primary CD4$^+$ and CD4$^+$CD25$^+$ T-cells. Single-cell suspensions of spleen cells are subjected to erythrocyte lysis (lysis buffer) and subsequently the debris is removed by passing through a cell strainer. Cell number is determined, and after centrifugation at 600*g* for 10 min, cells are suspended in cold (4°C) GM buffer in a final concentration of 1×10^8 cells/mL.

3.2.1. Isolation of Murine CD25$^+$CD4$^+$ T Regulatory Cells
3.2.1.1. Positive Selection of CD25$^+$ Cells by MACS

1. Spleen cells are stained with biotinylated anti-CD25 mAb (7D4) in a concentration of 0.5 µg/mL and incubated for 20 min at 4°C.
2. Cells are washed twice with GM buffer and suspended in cold GM buffer (1×10^8 cells/mL).
3. Afterwards, streptavidine-phycoerithrine (PE), in a dilution of 1/400, is added, and cells are incubated for an additional 20 min at 4°C.
4. Cells are washed twice with GM buffer and diluted in cold GM buffer (5×10^8 cells/mL). Anti-PE beads (50 µL) are added to 1 mL cell suspension (5×10^8 cells/mL) and cells are incubated for 30 min on a shaker at room temperature. The suspension is filled up to 5 mL with GM buffer and rinsed through a cell strainer to remove cell clusters.
5. Afterwards, the cell suspension is loaded slowly on top of a MACS Separation Column (LS) that is fixed in a MACS separator, and CD25$^+$ cells are positively enriched according to the manufacturer's instructions.
      Repeat this positive selection step once. Finally the cells are washed and suspended in 1 mL of PBS + 0.5% BSA. (*see* **Note 6**).

3.2.1.2. Depletion of CD4$^-$ Cells by Dynabeads

The resulting cell population consists of 70–80% CD25$^+$CD4$^+$ T-cells and 20–30% contaminating cells, mainly B-cells, CD8$^+$ T-cells, and macrophages. These contaminating cell types are depleted using Dynabeads directed against B220, CD8, and MAC-1 (*see* **Notes 7** and **8**).

1. Add the cell suspension in a fourfold excess regarding the estimated numbers of the contaminating cell types, and incubate on a shaker for 20 min at room temperature (RT).
2. Depletion is performed using a magnetic particle concentrator according to the manufacturer's instructions.
3. Repeat this depletion step once.
4. Finally, the cells are washed and suspended in culture medium. Typically, this procedure yields a highly pure (>97%) population of murine CD25$^+$CD4$^+$ T regulatory cells (**Fig. 1B**).

3.2.2. Preactivation of Murine CD25$^+$CD4$^+$ T Regulatory Cells

Freshly isolated CD25$^+$CD4$^+$ T regulatory cells cannot inhibit the activation of differentiated T helper cells, indicating that they have a limited suppressive capacity.

A

**Freshly isolated <u>human</u>
CD4⁺CD25⁺ T cells**
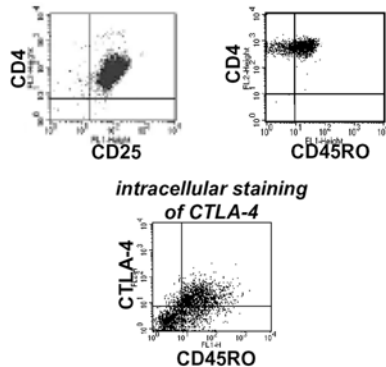
Functional analysis of CD4⁺CD25⁺ T cell preparations

Stimulation with allogeneic DC

- 1 x 10⁵ T cells/well
- 1 x 10⁴ mature allogeneic DC/well
- 4 days + 16 h ³H-Tdr

Stimulation with anti-CD3/CD28

- 1 x 10⁵ T cells/well
- 1μg/ml anti-CD3 + 2μg/ml anti-CD28
- 2 days + 16 h ³H-Tdr

*intracellular staining
of CTLA-4*
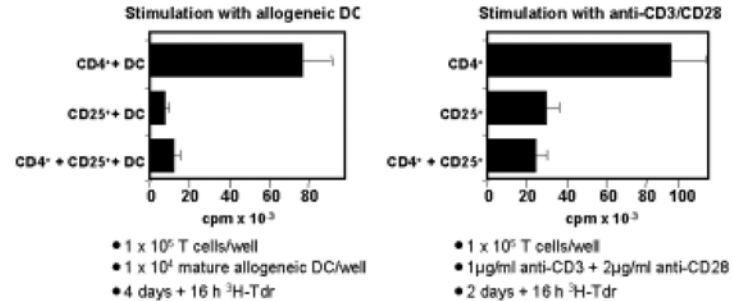
B

**Freshly isolated <u>murine</u>
CD4⁺CD25⁺ T cells**

Stimulation with anti-CD3

- 1 x 10⁵ T cells/well
- 1 x 10⁴ A20 APC/well
- 1.5 μg/ml anti-CD3
- 3 days + 16 h ³H-Tdr

**IL-4 Production of Th2 cells
Inhibition by <u>pre</u>CD25⁺ T cells**

- 1 x 10⁶ T cells/ml
- 1 x 10⁵ A20 APC
- 3 μg/ml anti-CD3
- 2 days
- Detection of IL-4 by ELISA
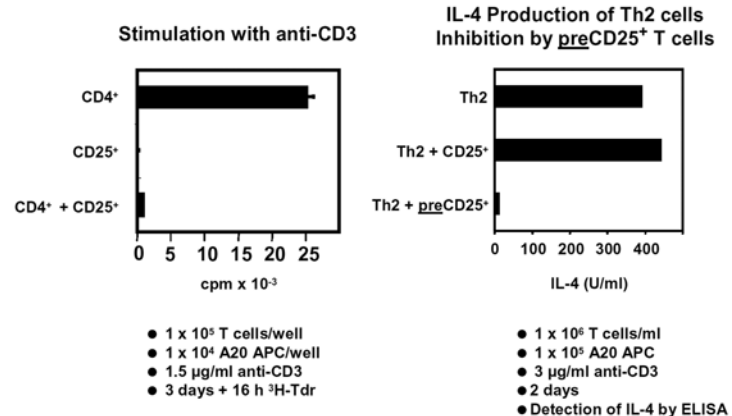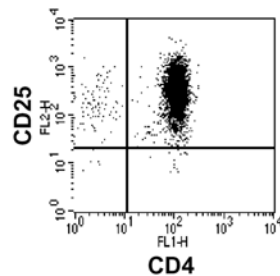
On the other hand, preactivated CD25+CD4+ T regulatory cells exert a potent suppressive activity and also inhibit differentiated T helper cells (**Fig. 2B**). Thus, preactivation is indispensable for the generation of highly suppressive CD25+CD4+ T regulatory cells.

Preactivation of CD25+CD4+ T regulatory cells is performed using a combination of plate-bound anti-CD3 mAb and anti-CD28 mAb.

1. Twenty-four-well culture plates are coated with anti-CD3 mAb (145-2C11, 5 µg/mL, diluted in PBS) at 37°C.
2. After 30 min, the wells are washed (PBS), secondarily coated with anti-CD28 mAb (37.51, 10 µg/mL, diluted in PBS), and incubated for additional 30 min at 37°C.
3. After an intensive wash (PBS, three times) of coated plates, the CD25+CD4+ T regulatory cells are stimulated on these plates in culture medium, harvested after 48 h, and used as preactivated CD25+CD4+ T regulatory cells.

3.2.3. Isolation of Murine Conventional CD4+ T-Cells (CD25 Depleted)

So far there is no unique marker defined for murine CD25+CD4+ T regulatory cells, and CD25 is also highly expressed by activated conventional T-cells. Thus, murine CD25+CD4+ T regulatory cells have to be characterized using a bioassay. In the following, we briefly describe one easy method for isolation of CD25-depleted CD4+ conventional T-cells for the functional analysis of regulatory T-cells.

3.2.3.1. DEPLETION OF CD25+ T-CELLS

1. Spleen cells are stained with biotinylated anti-CD25 mAb (PC61; 0.5 µg/mL) and incubated for 20 min at 4°C.
2. Cells are washed twice with cold GM buffer and suspended in cold GM buffer (1×10^8/mL).
3. Add streptavidine beads (Miltenyi), dilute 1/20, and incubate for 20 min at 4°C. Fill up the suspension to 5 mL with GM buffer and rinse the cells through a cell strainer to remove cell clusters.
    Load this suspension slowly on top of a MACS Separation Column (LS) that is fixed in a MACS separator, and deplete the CD25+ cells according to the manufacturer's instructions.

Fig. 2. *(opposite page)* Examples of phenotypic and functional characterization of human **(A)** and murine **(B)** CD4+CD25+ T regulatory cells. Phenotypically, freshly isolated human T regulatory cells express CD4 and CD25 homogeneously. The majority of T-cells also express CD45RO and intracellulary CTLA-4. The marker CD45RO can be used for further purification of human T regulatory cells as described in the methods section. CTLA-4 will be upregulated and expressed on the surface after activation of CD4+CD25+ T regulatory cells in vitro. On the right side, two examples for functional analysis of freshly isolated human CD4+CD25+ T-cells are shown. After allogeneic as well as after polyclonal stimulation, proliferation of CD4+CD25+ T regulatory cells themselves is marginal. Nevertheless, in co-culture they suppress the activation of conventional T-cells dose dependently.

Murine Th2 cells are generated by stimulating CD4+ T-cells in the presence of interleukin (IL)-4 and anti-interferon (IFN)-γ mAb for 6 d. Restimulation of these cells leads to a considerable production of IL-4 (detected by an ELISA) that cannot be suppressed by freshly isolated CD25+ T regulatory cells but by preactivated CD25+ T regulatory cells (preCD25+).

3.2.3.2. POSITIVE SELECTION OF CD4⁺ T-C-ELLS

1. The CD25-depleted cell suspension is stained with biotinylated anti-CD4 mAb (H129.19; 0.5 µg/mL) and incubated for 15 min at 4°C.
2. Cells are washed twice with GM buffer and suspended in cold GM buffer (1×10^8/mL). Afterwards, streptavidine beads (Miltenyi, dilution 1/40) are added and incubated for 15 min at 4°C.
3. Fill up the suspension to 5 mL with GM buffer and rinse the cells through a cell strainer to remove cell clusters.
4. Load this suspension slowly on top of a MACS Separation Column (LS) that is fixed in a MACS separator, and positively enrich the CD4⁺ T-cells according to the manufacturer's instructions.
5. Repeat this positive selection step.
6. Finally, the cells are washed and suspended in culture medium.

3.2.3.3. FUNCTIONAL ANALYSIS OF MURINE CD25⁺CD4⁺ T REGULATORY CELLS

1. CD4⁺ T-cells (1×10^6/mL), depleted of CD25⁺ T-cells (anti-CD25 mAb: PC61) and isolated by two rounds of positive selection using a MACS column, are polyclonally activated by anti-CD3 mAb (1–3 µg/mL) in the presence of mitomycin C-treated A20 B-tumor cells (1×10^5/mL) as accessory cells (*see* **Note 9**). Simultaneously, the CD25-depleted CD4⁺ T-cells are activated in the presence of CD25⁺CD4⁺ T regulatory cells (ratio 1:1); only the purified CD25⁺CD4⁺ T regulatory cells are activated.
2. After 4 d, ³H-TdR (18.5 kBq/well) is added for 18 h and thymidine uptake of the T-cells is monitored by liquid scintillation counting.

    As shown in **Fig. 2B**, CD4⁺ T-cells undergo a strong proliferation, whereas CD25⁺CD4⁺ T regulatory cells alone and the combination of CD4⁺ T-cells and CD25⁺CD4⁺ T regulatory cells exhibit no or only a minimal thymidine incorporation, indicating the strong suppressive capacity of CD25⁺CD4⁺ T regulatory cells.

4. Notes

1. CD4 and CD25 are nonspecific surface markers for regulatory T-cells, and the ratio of CD25⁺ cells in peripheral blood depends on the immune status of the individual donor. Therefore, percentages of CD4⁺CD25⁺ T-cells vary among individual donors. To prevent artificial preparation of conventional (preactivated) CD25⁺ T-cells, the ratio of CD25⁺ PBMC should be analyzed before isolation, and only PBMC preparations that contain less than 5% CD25⁺ cells should be used for isolation of CD4⁺CD25⁺ regulatory T-cells.
2. The described technique is optimized for isolation of human CD4⁺CD25⁺ regulatory T-cells with high purity. Use of higher concentrations of antibodies or beads for isolation might enhance the recovery but decreases the purity. If large numbers of CD4⁺CD25⁺ regulatory T-cells are required, use the combination of positive and negative selection as described under **Subheading 3.1.5.** This technique results in higher recoveries compared to positive selection using Multisort beads. Note that the enzymatic release of microbeads is necessary if the separated cells will be used for additional steps of magnetic cell sorting. However, this enzymatic release decreases the recovery by 25%.
3. CD25 microbeads are very efficient for isolation of CD25⁺ T-cells with high purity. However, it is difficult to stain positively selected CD25⁺ T-cells with anti-CD25 mAb (most of the CD25 epitopes are engaged by microbeads). Therefore, for phenotypical control of the purity of CD25⁺ separated cells, anti-CD25 mAb (FITC- or PE-conjugated) can be

mixed with CD25 microbeads (ratio of microbeads to anti-CD25 mAb = 3:1) before separation. By this technique, the cells will be stained directly during the separation procedure.

4. The described technique is optimized for high purity of CD4$^+$CD25$^+$ T-cells and not for the highest recovery of positive cells. The mean recovery of CD4$^+$CD25$^+$ T-cells is 50% of total marker-positive cells, depending on the individual donor and the method of isolation. As described earlier, the use of Multisort beads reduces the recovery significantly but results in preparations of high purity. The combination of positive selection with CD25 microbeads and depletion of contaminations by Dynabeads is a compromise between recovery and purity of CD4$^+$CD25$^+$ T-cells, and this technique reduces the costs compared to the Multisort positive selection.

5. Preparations of human CD4$^+$CD25$^+$ T-cells contain regulatory T-cells as well as conventional (preactivated) T helper cells, and the ratio of contamination varies from donor to donor. For higher purity of CD4$^+$CD25$^+$ regulatory T-cells, the CD45RA$^+$ contaminating cells (10–25%) can be depleted by anti-CD45RA mAb in combination with anti-mouse-IgG Dynabeads (Dynal) directly after positive selection step using CD25 microbeads. Alternatively, the CD45RO$^+$ fraction can be positively selected using CD45RO microbeads (Miltenyi). However, for positive separation, use Multisort-selected cells only. This step enhances the purity of isolated regulatory T-cells. Preparations isolated by anti-CD25-FITC mAb plus anti-FITC Multisort beads also offers the possibility of separating distinct subsets of human CD4$^+$CD25$^+$ regulatory T-cells by positive selection with microbeads (i.e., β_7-integrin$^+$ vs β_7-integrin$^-$ regulatory T-cells using β_7-PE mAb plus anti-PE-microbeads).

6. Spleen cells should be incubated in as small as possible a volume of buffer (e.g., 2×10^9 spleen cells in 2 mL). A second step of CD25 positive selection leads to a considerable enrichment of CD25$^+$ cells, whereas a third step does not, but results in a substantial loss of cells.

7. The CD25$^+$CD4$^+$ T-cells are usually contaminated with 20–30% other cell types, mainly B-cells, CD8$^+$ T-cells, and macrophages. These cells can be depleted using Dynabeads, since the Magnetic Particle Concentrator from Dynal does not affect the microbeads from Miltenyi, so that microbead-loaded CD25$^+$CD4$^+$ T-cells are not retarded in the concentrator.

8. Based on the assumption that the contaminating cell population comprises about 30% of total CD25$^+$ cells and consists of 50% B-cells, 25% CD8$^+$ T-cells, and 25% macrophages, the cell numbers of the different T-cell types are calculated and the specific Dynabeads (anti-CD8, -B220, -MAC-1) are used at a ratio of 4 Dynabeads:1 cell.

9. For the functional analysis of the CD25$^+$CD4$^+$ T-cells, it is important to use only limited concentrations of anti-CD3 mAb, roughly in the range of 1–3 μg/mL. In the presence of higher concentrations of anti-CD3 mAb, the suppressive capacity of the CD25$^+$CD4$^+$ T-cells will not be sufficient to inhibit the proliferation of the co-cultured conventional CD4$^+$ T-cells. The same holds true in case anti-CD28 mAb are used as an additional costimulator.

Acknowledgments

References

1. Gershon, R. K. (1975) A disquisition on suppressor T cells. *Transplant. Rev.* **26,** 170–185.
2. Sakaguchi, S., Sakaguchi, N., Asano, M., Itoh, M., and Toda, M. (1995) Immunologic self-tolerance maintained by activated T cells expressing IL-2 receptor alpha-chains (CD25). Breakdown of a single mechanism of self-tolerance causes various autoimmune diseases. *J. Immunol.* **155,** 1151–1164.
3. Jonuleit, H., Schmitt, E., Stassen, M., Tuettenberg, A., Knop, J., and Enk, A. H. (2001) Identification and functional characterization of human CD4(+)CD25(+) T cells with regulatory properties isolated from peripheral blood. *J. Exp. Med.* **193,** 1285–1294.
4. Dieckmann, D., Plottner, H., Berchtold, S., Berger, T., and Schuler, G. (2001) Ex vivo isolation and characterization of CD4(+)CD25(+) T cells with regulatory properties from human blood. *J. Exp. Med.* **193,** 1303–1310.
5. Ng, W. F., Duggan, P. J., Ponchel, F., et al. (2001) Human CD4+ CD25+ cells: a naturally occurring population of regulatory T cells. *Blood* **98,** 2736–2744.
6. Seddon, B. and Mason, D. (2000) The third function of the thymus. *Immunol. Today* **21,** 95–99.
7. Seddon, B. and Mason, D. (1999) Peripheral autoantigen induces regulatory T cells that prevent autoimmunity. *J. Exp. Med.* **189,** 877–882.
8. Thornton, A. M. and Shevach, E. M. (1998) CD4+CD25+ immunoregulatory T cells suppress polyclonal T cell activation in vitro by inhibiting interleukin 2 production. *J. Exp. Med.* **188,** 287–296.
9. Suri-Payer, E., Amar, A. Z., Thornton, A. M., and Shevach, E. M. (1998) CD4+CD25+ T cells inhibit both the induction and effector function of autoreactive T cells and represent a unique lineage of immunoregulatory cells. *J. Immunol.* **160,** 1212–1218.
10. Piccirillo, C. A. and Shevach, E. M. (2001) Cutting edge: control of CD8+ T cell activation by CD4+CD25+ immunoregulatory cells. *J. Immunol.* **167,** 1137–1140.
11. Jonuleit, H., Schmitt, E., Kakirman, H., Stassen, M., Knop, J., and Enk, A. H. (2002) Infectious tolerance: human CD25(+) regulatory T cells convey suppressor activity to conventional CD4(+) T helper cells. *J. Exp. Med.* **196,** 255–260.
12. Jonuleit, H., Schmitt, E., Schuler, G., Knop, J., and Enk, A. H. (2000) Induction of interleukin 10-producing, nonproliferating CD4(+) T cells with regulatory properties by repetitive stimulation with allogeneic immature human dendritic cells. *J. Exp. Med.* **192,** 1213–1222.
13. Jonuleit, H., Kuhn, U., Müller, G., et al. (1997) Pro-inflammatory cytokines and prostaglandins induce maturation of potent immunostimulatory dendritic cells under fetal calf serum-free conditions. *Eur. J. Immunol.* **27,** 3135–3142.

21

Monoclonal Antibody-Based Strategies in Autoimmunity and Transplantation

Lucienne Chatenoud

Summary

Monoclonal antibodies are homogeneous sets of immunoglobulins with well-defined specificity and biochemical characteristics. They were introduced into clinical practice in the early 1980s, and since then their use has rapidly expanded.

Most of the side effects observed with first-generation murine (mouse or rat) antibodies have been successfully overcome with the advent of humanized (chimeric or CDR-grafted) and more recently fully human antibodies. Our aim is to review the major steps in the development of therapeutic monoclonal antibodies in the fields of transplantation and autoimmunity, and discuss the salient features of antibodies presently used in the clinic—notably anti-T-cell and anticytokine antibodies. The discussion will also focus on the unique capacity of some monoclonal antibodies to induce immune tolerance.

Key Words: Monoclonal antibody; immune tolerance; immunosuppression; autoimmune diseases; transplantation.

1. Introduction

Major human diseases are recognized to have an autoimmune origin, placing autoimmunity as the third major cause for morbidity and mortality in developed countries after cancer and atherosclerosis. Moreover, the frequency of autoimmune diseases is steadily increasing. Organ and bone-marrow transplantation represent the only therapeutic possibility for a variety of life-threatening conditions. It is now clear that the fundamental immune mechanisms underlying both autoimmune diseases and allograft rejection are similar. In both, the immune response exploits functionally distinct cellular subsets (macrophages, dendritic cells, B-cells, effector and regulatory T-cells) that interact through an intricate network of membrane receptors and soluble mediators (cytokines and chemokines). For several years, in both situations, therapeutic approaches were essentially based on immunosuppression, which is non-specific—in other words, is unrelated to the antigens involved. The mainstays of such non-specific immunosupression are small molecules (corticosteroids, azathioprine, methotrexate, cyclophos-

phamide, cyclosporin, FK506, mycophenolate mofetil, rapamycin), whose activities are targeted to intracellular processes. Their major drawback is their relative ineffectiveness in the long term, with the likely risk of recurrence of the pathogenic immune process once the drug is withdrawn, necessitating indefinite drug administration with the attendant problems of recurrent infection and drug toxicity.

One radical solution would be to discover ways in which the immune system can be selectively immunosuppressed just to those antigens unique to the target tissue, avoiding the hazards of long-term nonspecific immunosuppression. Operationally, this means the establishment of immunological tolerance in a mature immune system— that is, a state of lasting antigen-specific unresponsiveness in the absence of generalized immunosuppression. More than 20 yr of experience in using immunosuppressive monoclonal antibodies both in the experimental and clinical fields have clearly demonstrated their unique advantages over conventional immunosuppressants, to combine both an extremely efficacious immunosuppressive potency and, under particular circumstances, a tolerance-promoting ability. Thus, antibodies or genetically engineered molecules specific for distinct functionally relevant T-cell receptors (i.e., CD4, CD3, CD80, CD86, CD40 ligand [CD40L], adhesion receptors, or adhesins) were shown to induce immune tolerance to foreign-tissue alloantigens and to autoantigens.

Our aim will be to review the present state of the art on the use of monoclonal antibodies in autoimmunity and transplantation, presenting both the specificities that are part of the routine clinical armamentarium as well as those that are presently under development. In doing so, we shall also address the mode of action of these biological agents, which constitute very effective tools aimed at controlling deleterious immune responses to allografts and preventing or even treating established autoimmune diseases through their capacity to restore self-tolerance.

2. Uniqueness of Monoclonal Antibodies As Drugs

Several characteristics relying on both molecular and pharmacological properties of monoclonal antibodies clearly distinguish them from conventional chemicals. Some of these features are significant advantages, while others constitute important problems that have frequently hampered more rapid development and transfer to the clinic. The factors that will be discussed are listed as pros and cons in **Table 1**.

2.1. Pharmacological and Biological Versatility

As opposed to conventional chemicals, which mostly act through the removal and/ or functional inhibition of their targets, monoclonal antibodies present a wide spectrum of pharmacological and biological activities that impact the capacity to redirect immune responses. Thus, depending on their fine specificity, monoclonal antibodies can: (1) neutralize soluble mediators such as cytokines and chemokines, which play an essential role in orchestration of immune responses and immune cell recruitment; (2) physically remove target cells (i.e., the use of either nonmanipulated monoclonal antibodies or toxin or radioisotope-labeled antibodies) thus raising the concern of the turnover of the depleted cell population; (3) inhibit or block the functional capacity of target cells without physically eliminating them; and (4) function as pharmacological agonists that signal through specialized immune cell receptors and their asso-

Table 1
Uniqueness of Monoclonal Antibodies As Drugs

Pro	Con
• Pharmacological versatility	• Cumbersome and expensive production
• Fine specificity for any target	• Need for extensive quality controls
• Rapidity of clinical development	(biochemical, virology...)
• Long half-life for humanized and human	• Sensitization
monoclonal antibodies	

ciated intracellular pathways to trigger immunoregulatory T-cells that are able to control the pathogenic activity of autoreactive or alloreactive lymphocyte effectors.

2.1.1. Cytokine Neutralization

In order to neutralize the biological effect of cytokines, one must effectively interfere with their binding to specific receptors. This can be achieved by different means, including the use of cytokine-specific antibodies, soluble cytokine receptors *(1–3)*, antagonists of cytokine receptors (as in the case if interleukin [IL]-1) *(4)*, and genetically engineered immunoadhesins, including two soluble receptor fragments linked to an immunoglobulin constant frame *(5,6)*.

Pathological conditions that may benefit from therapeutic strategies aimed at cytokine neutralization are, first, diseases associated with overproduction of pro-inflammatory cytokines, i.e., tumor necrosis factor (TNF), IL-1, and IL-6, and, secondly, pathological situations involving an immunologically mediated target tissue damage in which cytokines driving T helper 1 (Th1) (i.e., interferon [IFN]-γ, IL-12) or Th2 responses (i.e., IL-4, IL-10) exert a central immunoregulatory role.

Concerning proinflammatory cytokines, the use of agents that neutralize TNF was, as we shall discuss in detail below, a major breakthrough in the clinical management of some autoimmune diseases, such as rheumatoid arthritis and psoriasis, as well as in immune-mediated disease such as inflammatory bowel disease *(7)*.

Concerning the blockade of immunoregulatory cytokines, the case of IFN-γ is of particular interest, given the compelling data obtained from animal models and the present ongoing phase II trial in inflammatory bowel disease *(8–10)*. In explaining the therapeutic effect of anti-IFN-γ antibodies, one should consider not only their capacity to dampen Th2 responses, but also their ability to block the IFN-γ-mediated upmodulation of major histocompatibility complex (MHC) class I and class II antigen expression. In fact, this capacity of IFN-γ to promote "aberrant" class II MHC antigens on cells that do not normally express them (astrocytes, keratinocytes, thyroid, and pancreatic islet cells) represents a major triggering factor in autoimmune diseases *(11,12)*. In human allograft recipients, acute rejection was often associated with the de novo expression of class II HLA antigens on cells within the allograft, such as kidney tubular cells or myocytes *(13,14)*. Such de novo MHC class II antigen expression increases the antigenicity of the graft and the suceptibility of such cells to specific cytotoxic T-cell effectors.

2.1.2. Cellular Depletion

Following the in vivo injection of polyclonal anti-T-cell antibodies, cell lysis mainly occurred through complement-dependent lysis in the circulation or cell opsonization and removal in the liver and the spleen by reticuloendothelial cells *(15,16)*.

On the other hand, with cell-directed monoclonal antibodies, the mechanisms involved in antibody-mediated cell destruction in vivo are more varied and complex. Actually, not only the antibody isotype (i.e., the capacity of the Fc antibody portion to interact with Fc receptors to mediate antibody-dependent cell cytotoxicity [ADCC] and to activate complement) but also its fine specificity can influence the lytic capacity. Thus, it is not sufficient to select the adequate immunoglobulin constant domain to achieve the desired in vivo depleting or nondepleting effect *(17,18)*. First-generation mouse and rat monoclonal antibodies to cell antigens mostly expressed, when injected into humans, a rather poor lytic capacity. This was due to the now well-characterized membrane-bound factors that inhibit activation of human complement in a species-restricted manner. The situation of course evolved with the advent of humanized, chimeric, or complementarity determining region (CDR)-grafted monoclonal antibodies, and more recently of fully human monoclonals.

However, it is interesting to discuss at this point that, independently from their isotype, some monoclonal antibody specificities, for reasons still ill defined, are highly depleting. This is the case for antibodies to CD52 (i.e., CAMPATH-1 antigen) a small glycosylphosphatidylinositol (GPI)-linked protein abundantly expressed on B-cells, T-cells, and monocytes that were extensively used in bone-marrow transplantation and hematologic malignancies *(17)*. Using DNA technology, sets of recombinant monoclonal antibodies with identical specificities but different constant regions were probed for the sequences that determine antibody function, and ranked in human complement-mediated lysis and ADCC with regard to efficiency *(18)*. These studies showed first that both the fine specificity (independently from the isotype) and the density of distribution of the target antigen-influenced lytic capacity of cell-binding monoclonal antibodies. Secondly, among given sets of monoclonal antibodies sharing the same specificity (i.e., variable region), a hierarchy in terms of lytic capacity could be established that in the case of human immunoglobulins is as follows: IgG1>IgG2 >IgG3>>IgG4.

For obvious reasons, a cell antigen that easily undergoes antigenic modulation, namely the disappearance of a receptor from the cell membrane upon binding of a specific ligand (in this case the monoclonal antibody), will be a poor target for lysis. This is the case for T-cell antigen receptors (CD3-TCR) (*see* **Subheading 2.1.3.**). The lytic potential may, in this case, be significantly improved using univalent antibodies that avoid antigenic modulation *(19,20)*.

Among mechanisms involved in cell lysis and linked to monoclonal antibody fine specificity, one must mention redirected T-cell lysis occurring upon the bridging of cytotoxic T-cells to the target *(21)* and, in particular, for antibodies to CD3 and CD4 faced with activated T-cells, the induction of apoptosis, or programmed cell death *(22)*.

Finally, one may add here immunotoxins that are conjugates between a toxin (diphteria toxin or ricin) and a monoclonal antibody or a cytokine *(23,24)*. The toxin is

specifically directed to the target cell through the antibody or the cytokine, and kills the target following internalization.

The immunological effects of cell depletion will closely depend on the cellular selectivity of the monoclonal antibody (i.e., generally affecting leukocytes [antibodies to CD52], T-cells [antibodies to CD3], T-cell subsets [antibodies to CD4, CD8], or only activated T-cells [antibodies CD25]) and on the renewal rate of the target cellular population. Pools of short-lived lymphocytes will rapidly reappear after short-term depletion. Conversely, recovery of recirculating long-lived T-cells will take several wk in the mouse and several mo in man. In this context, the data using depleting monoclonal antibodies to CD4 is both intriguing and deserves a word of clinical caution. Thus, the chimeric (humanized) antibody to CD4 MT-512 (human IgG1), used in both transplanted and autoimmune patients, induced, especially when administered at high doses (700 mg cumulative dosage), extremely pronounced and prolonged (up to 60% from baseline for over 18–30 mo) peripheral CD4+ cell depletion *(25)*.

2.1.3. Functional Inhibition

Among the mechanisms accounting for antibody-mediated inhibition of cell function are (a) antibody-mediated cell coating or "blindfolding," interfering with cell-to-cell interactions; (b) antigenic modulation of a functionally relevant target cell receptor; and (c) induction of cell unresponsiveness (anergy) through modulation of activation signals delivered.

The relevance of antibody-mediated cell coating was initially described with polyclonal anti-lymphocyte antibodies, since the induced lymphocytopenia did not appear as the only factor mediating their therapeutic effect. In fact, T-cells that reappeared after treatment were functionally impaired both in vitro and in vivo. Monoclonal antibodies to human, mouse, and rat CD4 have been described expressing both immunosuppressive and tolerogenic capacities that are nondepleting and coat their cell target *(26–30)*. It is likely that CD4 coating, given the contribution of CD4 to TCR/CD3-mediated signaling, not only interferes with lymphocyte binding to MHC class II on antigen-presenting cells, but also triggers therapeutically relevant negative signals *(31–36)*. Thus, independent ligation of CD3 and CD4 in vitro, as it may occur in vivo following injection of monoclonal antibodies to CD4, significantly decreases proliferative responses and lymphokine production induced by stimulation with soluble antigens, alloantigens, and polyclonal stimulants.

Some cell-directed antibodies also induce antigenic modulation—the redistribution of their ligands or receptors on the cell surface. The antigen–antibody complex will eventually form a "cap" at a pole of the cell and disappear upon internalization or shedding *(37)*. Such loss of expression of a functionally relevant membrane receptor will render the target cell functionally inactive. This is well documented for antibodies to CD3 *(37–39)*. Depletion is only partial in both mice and humans at usual doses. In terms of phenotype, cells undergoing antigenic modulation are CD3-TCR-CD4+ or CD3-TCR-CD8+. The phenomenon is reversible within 8–12 h once the antibody is cleared from the surrounding medium. Cells undergoing CD3 antibody-mediated antigenic modulation are unresponsive to in vitro antigen-specific or mitogen stimulation

(37,39), a pattern that correlates well with the significant clinical immunosuppressive effect of CD3 antibodies.

As previously mentioned, sustained T-cell activation upon engagement of CD3-TCR needs the simultaneous delivery of costimulatory signals through specialized receptors, such as CD28, CTLA-4, CD40L, ICOS interacting with their ligands B7.1, B7.2, CD40, ICOSL at the surface of antigen-presenting cells. Several in vitro models using both murine and human clones showed that occupancy of the TCR alone, in the absence of adequate costimulation, induced a state of unresponsiveness termed *anergy (40,41)*. The role of anergic cells in physiological or induced immune tolerance is still a matter of debate. However, one cannot exclude that monoclonal antibodies targeting some of the receptors listed above exert their in vivo therapeutic effect at least in part through T-cell anergy.

2.1.4. Triggering of Immunoregulatory T Cells

Although less well defined in cellular and molecular terms, another crucial in vivo effect of some anti-T-cell monoclonal antibodies is the triggering of "immuno-regulatory" pathways leading in the long term to the establishment of an "operational" immune tolerance relying on T-cell immune deviation and/or dominant or infectious tolerance, depending on the models.

The unique tolerogenic capacity of antibodies to CD4 has been known for a long time, since antibodies to CD4 injected into mice did not trigger an antiglobulin response, as was the case with the majority of rodent monoclonal antibodies against other T-cell antigens *(42,43)*. Moreover, specific tolerance could be induced into normal adult euthymic animals if soluble antigens were administered under the cover of depleting or non-depleting antibodies to CD4 *(42,43)*. Such immune tolerance was maintained through the delivery of the antigen alone, at regular intervals, in the absence of any further monoclonal antibody treatment. These findings using antibodies to CD4 were rapidly extended to tissular antigens such as alloantigens (especially using antibodies to CD4 and CD8 in association) and autoantigens *(26,28,44,45)*. In parallel, compelling evidence has been accumulated to show that targeting of other T-cell receptors, and in particular of CD3 and costimulatory receptors, was also very effective in inducing tolerance in both transplantation and autoimmune settings *(29,44,46–55)*.

In terms of mechanisms, the immune tolerance induced in several of these models is "active" or "dominant," i.e., mediated by subsets of CD4$^+$ immunoregulatory or suppressor T-cells that control pathogenic effectors. It can be transferred to naïve recipients upon transfusion of such CD4$^+$ immunoregulatory subsets, and can be maintained only in the presence of the tolerogenic antigen *(29,44,46–56)*. The precise phenotype of these regulatory T-cells varies depending on the model; some of them express the α chain of the IL-2 receptor (CD25), as "naturally" occurring suppressor T-cells shown to maintain physiological tolerance do, whereas others appear to emerge from peripheral CD4$^+$CD25$^-$ T-cells *(29,57–63)*. The same variability applies to their cytokine dependency: only in some models a role for immunoregulatory cytokines (i.e., IL-4 or TGF-β) has been demonstrated *(55,64)*. Several groups are presently involved in the characterization of genes or molecules selectively expressed by such regulatory T-cells that may lead to a more precise understanding of their mode of action *(27,65)*.

2.2. Monoclonal Antibodies Can Be Produced Against Almost Any Target

New protein targets are continuously emerging from genomics and proteomics. One of the main aims of these approaches is to discover new drug classes targeting these new molecules. This has proven difficult, however, for conventional small molecules, in spite of the accessibility to large libraries, because of the need in each case for good and reliable bioassays.

The monoclonal antibody approach has the major advantage of initially avoiding such bioassays. One may directly produce monoclonals against a new protein once it has been adequately expressed, and test the pharmacological (functional) properties of the antibodies in conventional in vitro and in vivo assays—namely, various immune functions in the case of antibodies targeting molecules related to the immune system. In fact, it has become a common practice of many pharmaceutical companies to produce monoclonals against newly discovered molecules, notably using the very versatile phage assay techniques. In this way, functionally relevant antibodies can be produced against molecules whose physiological and physiopathological roles are unknown.

As a meaningful example, one may quote the case of TNF. Despite all the experimental suggestions arguing for a central role for TNF in the pathophysiology of rheumatoid arthritis, only anti-TNF monoclonal antibodies and fusion proteins provided the tools to effectively and specifically neutralize its biological activity. Until then, all conventional anti-inflammatory agents had failed to provide such a radical effect.

2.3. Factors That Impact on Clinical Development

2.3.1. Less Toxicity

Due to their very strict target specificity (with the exception of rare and unexpected undesirable cross-reactions), therapeutic monoclonal antibodies usually do not express side effects unrelated to their pharmacological recognition of the initial target molecule. This is a major advantage over small chemicals that very often display pharmacological activities (some of which lead to significant side effects) unrelated to the target responsible for the relevant pharmacological effect. Thus, in the case of immunosuppressive agents, many drugs inhibit the proliferation of many cell types other than lymphocytes, notably other white blood cells, and many of them show direct toxicity for non-lymphoid organs, as in the case of cyclosporin nephrotoxicity.

Finally, the possibility of assessing the toxicity of monoclonal antibodies is often limited by their species specificity.

2.3.2. High-Scale Production

This still represents a real problem for the clinical development of monoclonal antibodies. Only a few centers worldwide are able to produce high amounts of good manufacturing practice (GMP)-grade antibodies for clinical trials. Due to present regulations, this in fact implies exclusive in vitro production using adapted bioreactors to grow validated cell lines harboring validated expression vectors that allow the production of the antibodies from their coding genes. The various steps needed to go from the initial antibody to the adequate cell line producing it in vitro in high amounts are all cumbersome and costly.

Once these steps are taken, the purification procedures are simple *per se*, though they are submitted to extensive quality-control tests at each of their steps, evaluating not only the physicochemical characteristics of the antibody but also its safety, notably to exclude the presence of any viral contamination of the final product.

2.4. The Problem of Sensitization

Monoclonal antibodies that were initially used therapeutically were of xenogeneic origin, mainly mouse or rat anti-human antibodies. Even in rodents, antibodies were also most often xenogeneic hamster and rat anti-mouse antibodies. Administration of such xenogeneic antibodies regularly led to the appearance of an antimonoclonal humoral response, often endowed with a potent neutralizing activity. Studies initially performed with human antibodies and subsequently with rodent ones have allowed a better definition of the pattern of the antiglobulin response. Various methods have been proposed to circumvent the problem.

Antimonoclonal globulins express two major specificities that are antiisotypic and antiidiotypic *(42,66,67)*. Antiidiotypic antibodies represent the majority if not the totality of neutralizing antibodies. Their detection is based on ELISAs and immunofluorescence assays testing for their capacity to inhibit the binding of the monoclonal antibody to the target cell *(66)*. Studies performed on immunized patients and monkey affinity purified antiidiotypic antibodies showed that the response is oligoclonal *(68)*. Antiisotypic antibodies are essentially nonneutralizing *(69)*. Thus, the neutralizing potential of the humoral response to monoclonal antibodies relies more on its specificity than on the overall amount of antibodies produced, since only a few specific clones were recruited. Serum sickness was not observed because the amounts of immune complexes formed were insufficient to elicit a generalized reaction. The antimonoclonal humoral response may also include IgE antibodies (associated with the potential risk of anaphylaxis), but in practice this has appeared to be an extremely rare observation *(70,71)*. Thus, from the clinical point of view, sensitization essentially posed the problem of the abrogation of the therapeutic efficacy of the monoclonal antibody.

In practice, the adjunction of adequate dosages of chemical immunosuppressants to the monoclonal antibody significantly decreased the frequency and intensity of sensitization *(72)*.

Although this approach has been quite useful, in order to get more complete protection from sensitization, a common trend has been to generate humanized antibodies, or more recently human monoclonal antibodies.

2.4.1. Humanized Antibodies

Humanized chimeric or CDR-grafted monoclonal antibodies were produced in the attempt to reduce the amount of xenogeneic determinants *(73)*. Chimeric antibodies present intact variable regions (Fab) from the parental rodent antibody, coupled to human immunoglobulin constant regions. These chimeric immunoglobulins were initially derived from chemical procedures and subsequently by molecular engineering. In the case of recombinant CDR-grafted antibodies, the rodent CDRs (i.e., the hypervariable regions specifically interacting with the antigen) are inserted into human heavy-

and light-chain immunoglobulin frameworks. These two approaches allow the selection of the desired human Fc fragment that will impact the final antibody effector capacities (complement fixation, opsonization, and ADCC) and, in the case of CD3 antibodies *(46,74,75)*, mitogenic capacity (discussed later in more detail).

The risk of a deleterious antiidiotypic response still occurring with these humanized antibodies is a valid concern. In fact the clinical data available so far show that chimeric and reshaped humanized antibodies are immunogenic in some patients, but only when the monoclonal is administered alone (in the absence of associated immunosuppressants) and after more than two to three repeated antibody courses *(76)*. However, it is the general experience that the association to conventional immunosuppressants, even in low doses, significantly decreases the incidence of sensitization *(7,77,78)*. From a fundamental point of view, these data are the first indication of the crucial role of the monoclonal antibody Fc fragments in the induction of the antiidiotypic response.

In the particular case of CD3 antibodies, as previously discussed, humanization has offered the double advantage of circumventing the problems linked to sensitization and the mitogenicity that is responsible for the cytokine-related flu-like syndrome, which is a major side effect *(46)*. Thus in the first few hours after anti-CD3 administration, a massive but transient systemic release of several cytokines is observed (TNF, IFNγ, IL-2, IL-3, IL-4, IL-6, IL-10, granulocyte/macrophage colony-stimulating factor [GM-CSF]), which induces high fever, chills, and headache together with repeated episodes of vomiting and diarrhea; patients become prostrated through massive fluid and electrolyte loss *(46,79,80)*. A minor proportion of patients may develop more severe and potentially life-threatening conditions such as severe respiratory distress (related to pulmonary edema in patients with significant fluid overload), neurotoxicity, and hypotension, but only after the first injection *(46,79,80)*. As we already mentioned, this mitogenic capacity is due to the ability of the Fc portion of CD3 antibodies to interact with monocyte Fc receptors *(46)*. Thus, by mutating or aglycosylating *(46,74,75)* the Fc portion of engineered humanized nonmitogenic CD3, antibodies have been obtained. Results from pilot trials are very encouraging, since they confirmed that they were well tolerated as well as having the capacity to reverse ongoing kidney allograft rejection.

2.4.2. Human Antibodies

Three approaches have recently been made available to produce human therapeutic monoclonal antibodies.

The first one consists of the use of mice whose endogenous immunoglobulin genes have been knocked out and that have been made transgenic for human constant and variable immunoglobulin encoding genes. Almost all the B-cells in these animals express human immunoglobulin chains and produce human antibodies. The number of human immunoglobulin encoding sequences introduced proved sufficient to allow the generation of a significant diversity. This method has the advantage of simplicity (once the transgenic mice are available) and of the production of high-affinity antibodies using an in vivo antigen-driven selection upon immunization.

An alternative approach is phage display using cDNA libraries expressed on filamentous phages, allowing a rapid, fully in vitro selection of antibodies with high specificity *(81)*.

The third approach consists in establishing human-mouse chimeras. Irradiated mice are reconstituted with bone-marrow cells from SCID mice. Human lymphocytes from presensitized donors are then injected into the reconstituted mice, where they are boosted with defined antigens and used for fusion with myeloma cells *(82)*.

3. A Wide Array of Specificities Already Available

Among the vast panel of monoclonal antibodies interfering with immune cells' cooperation pathways, the ones of particular interest for therapeutic purposes are listed in **Table 2**. These mainly include: monoclonal antibodies directed at receptors and coreceptors involved in antigen recognition, such as CD3, CD4, and MHC molecules; costimulatory molecules; receptors exclusively expressed on activated T-cells (such as CD25); cell adhesion receptors; and cytokines.

The case of antibodies to CD52 (a small GPI-anchored protein expressed at the surface of human B cells and T-cells as well as monocyte/macrophages whose function is still ill-defined), is also interesting, since they have been extremely potent at promoting long-term acceptance of organ allografts as well as prolonged remission of established, and otherwise intractable, autoimmune diseases such as multiple sclerosis, vasculitis, and rheumatoid arthritis *(83–86)*.

4. Special Ability to Induce Immune Tolerance

The experiments of R. Billingham, L. Brent, and P. Medawar were the first to establish that immunological tolerance was an acquired state *(87)*. The authors showed that mouse neonates injected with allogeneic cells accepted skin grafts sharing the same haplotype as the cells injected at birth indefinitely, as adults. Importantly, this tolerant state was specific, since the animals could reject third-party allogeneic skin *(87)*. At variance with what was initially thought, central deletion of alloreactive T-cells is not the only mechanism explaining neonatal tolerance. Peripheral tolerance mechanisms also operate to sustain the unresponsiveness. Thus, lymphoid cells from treated animals can transfer tolerance to adult syngeneic recipients *(88)*. A Th2-type immune deviation has also been evidenced in tolerant animals, since upon specific activation, alloreactive T-cells produce low IFN-γ but high IL-4 levels *(89,90)*. Moreover, neonatal tolerance is abrogated when IL-4-neutralizing antibodies or IL-12 are administered in combination with the allogeneic cells at birth *(89,90)*.

Among the strategies attempted to recreate in adult hosts an immune environment "permissive" to tolerance induction, those using polyclonal or monoclonal antibodies seem to hold great promise for foreseeable future clinical applications. The groundbreaking experiments performed by Monaco and Woods in the 1960s showed that a combination of anti-lymphocyte (ALS) treatment and posttransplantation donor bone-marrow infusion could induce specific unresponsiveness to skin allografts *(91,92)*.

Table 2
Targets of Therapeutic Monoclonal Antibodies and Fusion Proteins [a]

Target	Efficacy in experimental transplantation	Use in clinical transplantation	Efficacy in experimental autoimmunity	Use in clinical autoimmunity
CD2	+/−	Organ Tx	ND	ND
CD3	+++	Organ Tx	+++	IDD
CD4	+++	Organ Tx	+++	RA, PS, MS, SLE, Vasculitis
CD4+CD8	+++	ND	+++	ND
CD20	ND	PTLD	ND	RA, MS, SLE
CD25	++	Organ Tx	++	Uveitis
B7.1, B7.2 (use of CTLA4-Ig)	++	ND	++	RA, PS, SLE
CD40L	++	Organ Tx	++	SLE
CD52	ND	Bone marrow, Organ Tx	ND	RA, MS
LFA-1 ICAM-1	++	Organ Tx	+++	ND
VLA-4	ND	ND	++?	MS
MHC Class I	ND	ND	+	ND
MHC Class II	+	ND	+	ND
TNF	+++ experimental GVHD	ND	+++	RA, IBD, PS
IFN-γ	ND	ND	+++	IBD ongoing
IL-1	ND	ND	++	RA

[a] Experimental and clinical applications.
ND, not done; RA, rheumatoid arthritis; MS, multiple sclerosis; IBD, inflammatory bowel disease; PS, psoriasis; Tx, transplantation; IDD, insulin dependent diabetes; SLE, systemic lupus erythematosus; GVHD, graft-vs-host disease; PTLD, posttransplant lymphoproliferative disease.

Since then, various groups have reproduced and extended these findings, showing that:

1. Tolerance to vascularized and nonvascularized allografts was not only induced by ALS but also by different monoclonal antibodies or fusion proteins interfering with T-cell surface receptors or their ligands—i.e., CD3, CD4, and CD8, costimulation receptors such as CD28, CTLA-4, and CD40 ligand *(29,44,46–56)*.
2. Several of these biological immunosuppressants (i.e., ALS, CD3 immunotoxin, CD4 antibodies, CD40 ligand antibodies alone or associated to CTLA-4 Ig) reproduced the same result in larger animals such as monkeys, which are valuable preclinical models *(50,51,54,93–96)*.
3. Donor bone marrow was not indispensable in both the rodent and monkey models *(50,51,96,97)*.
4. Some anti-T-cell monoclonal antibodies also represent invaluable tools to restore self-tolerance in established autoimmunity *(46)*.

At present, the precise cellular and molecular mechanisms underlying this immune tolerance are not fully elucidated. What is known, however, is that in nearly all the models we mentioned, tolerance is not deletional—i.e., not based on the physical elimination of the alloreactive or autoreactive effector T-cells. Instead, the tolerant hosts frequently show potent T-cell-mediated regulatory mechanisms that effectively control, downmodulate, or suppress the pathogenic activity of alloreactive or autoreactive effectors. Tolerance, once induced, is frequently dominant or "infectious" (the term initially coined by Gershon *[98]*) and can be acquired by nontolerant T-cells in the absence of further immunosuppression *(26,99)*. In some transplantation models, it was also shown that the tolerance can also spread to additional antigenic determinants, provided that all determinants are presented together on the same antigen-presenting cell, a phenomenon termed *linked suppression (100)*. The underlying principle is that tolerance to one antigen in one tissue allograft will facilitate tolerance to other alloantigens on other transplants, provided that the determinants are presented by the same antigen-presenting cell; in other words, that there is, at least partly, alloantigen sharing between the different grafts *(100)*.

Despite the fact that most studies concerning tolerance induction to organ allografts have focused on antibodies to CD4, other specificities also deserve interest—for instance, antibodies to CD3, the combination of antibodies to LFA-1 and ICAM-1, and antibodies to CD25 (especially in rat transplant models). Combined administration of LFA-1 and ICAM-1 to mice resulted in permanent engraftment of fully mismatched vascularized heart allografts, but also specific tolerance to donor-type skin allografts *(101)*. In a mouse heart and skin allograft model, the simultaneous but not independent blockade of the CD28 and CD40 costimulatory pathways promoted long-term, although not indefinite, allograft survival and, importantly, also inhibited the development of chronic vascular rejection in the grafted hearts *(102)*. Non-human primates treated with antibodies to CD40 ligand also significantly prolonged survival of fully mismatched renal allografts *(54)*. Unfortunately, attempts to transfer this strategy to the clinic were unsuccessful because of severe thromboembolic complications due to the expression of CD40L on platelets.

Based on the Th1/Th2 paradigm *(103)*, several authors attempted to explain most of these phenomena by an exclusive immune deviation from a Th1 allo or auto-destructive response to a Th2 nondestructive or even protective response. The data from some models of CD4 antibody-induced tolerance to cardiac and renal allografts were in support of this assumption, but this was far from a general conclusion *(99,104)*. As a whole, results obtained using different transplantation and autoimmunity models argue for a significant heterogeneity of immunoregulatory T-cells operational in sustaining the long-term effects. As discussed above, their precise phenotype and their cytokine dependency also varies depending on the model (i.e., CD4$^+$CD25$^+$, CD4$^+$CD25$^-$ T-cells *(29,55,57–64)*.

5. Efficacy in Advanced Disease

Unlike transplantation, in which tolerance-inducing drugs may be given at the time of the organ implantaion, any such treatment for clinical autoimmune disease can hap-

pen only at the time of diagnosis, when the immune system is already primed and once the target tissue has already undergone significant damage. Even at such a late stage, some monoclonal antibodies (in particular antibodies to CD3) have been shown to be very promising tools to restore self-tolerance in established autoimmunity. Initial data were obtained in non-obese diabetic (NOD) mice, which are a good model for human auto-immune insulin-dependent diabetes. In NOD mice, disease spontaneously develops by 4 mo of age and is preceded, starting at 3 wks of age, by a progressive infiltration of the islets of Langerhans with mononuclear cells (i.e., insulitis).

Diabetogenic T-cells that transfer acute diabetes into immunoincompetent syngeneic recipients are present in high frequency in the spleen of diabetic NOD mice, and include both CD4$^+$ (essentially IFN-γ-producing Th1 cells) and CD8$^+$ lymphocytes *(105–110)*. In parallel to these effector cells, co-transfer experiments have identified subsets of immunoregulatory T-cells (in the spleen and the thymus of prediabetic animals) that express CD25 and/or L-selectin (CD62L) mediating "active tolerance," namely, exerting an active control or a down-regulatory effect on diabetogenic lymphocytes or their precursors that fully prevents the transfer of disease by diabetogenic cells *(61,62,111–113)*.

A low-dose CD3 treatment (5 to 20 µg for 5 consecutive d) administered to overtly diabetic NOD mice (i.e., presence of glycosuria and glycemia = 4g/L) induced permanent disease remission in 60–80% of mice *(46,47,114)*. The remission was long lasting, and the effect was not related to generalized long-standing immunosuppression, because 8 to 10 wk after treatment all mice responded normally to exogenous antigens. The long-term effect was specific to β-cell-associated antigens, since mice showing remission after CD3 antibody treatment did not destroy syngeneic islet grafts as untreated diabetic NOD females normally did, even though they were not immunocompromised as shown by their capacity to rapidly reject allogeneic skin grafts *(46,47)*. Nonmitogenic F[ab']2 fragments of 145 2C11 were as effective as the whole mitogenic antibody in promoting permanent remission of overt diabetes *(46,47,114)*. Interestingly, in contrast with the major therapeutic effect observed in diabetic mice, at an advanced stage in the disease, CD3 antibody treatment was totally ineffective for disease prevention when applied to young prediabetic NOD mice *(46,114)*. Concerning the mechanisms mediating the therapeutic effect, one may distinguish two distinct consecutive phases. The first is temporary, elapses during the time of antibody treatment, and is associated with complete clearance of the insulitis. The second is long-lasting, correlating with the presence of a non-destructive pancreatic infiltrate (i.e., peripheral insulitis) and of CD4$^+$CD25$^+$/CD62L$^+$ immunoregulatory T-cells, whose numbers and functional capacity are increased as compared to those observed in diabetic untreated NOD mice *(46,47,61,62,64,114)*. More recent data have shown the central role of transforming growth factor (TGF-β) in this state of CD3 antibody-induced T-cell-mediated active tolerance. In particular, neutralizing antibodies to TGF-β fully prevent disease remission when administered concomitantly with CD3 antibodies *(46,64)*.

These experimental data paved the way for clinical trials that are presently in progress using non-mitogenic engineered antibodies to human CD3 *(74,115)* to preserve a functional insulin-secreting β cell mass in patients presenting recent-onset

insulin-dependent diabetes. The recent data from the first Phase I pilot clinical trial are very promising, and show that a significant preservation of β cell functional capacity can be observed at a 1-yr follow-up after treatment of only a few days applied within 6 wk of the first diagnosis *(116)*. A Phase II randomized placebo-controlled trial is presently in progress in Europe that includes a total of 80 patients. The results of this study will be available before the end of this 2004.

6. Monoclonal Antibodies and Fusion Proteins in Phase II/III Clinical Trials

6.1. CD3 Antibodies

The clinical use of CD3 antibodies essentially developed in solid-organ transplantation. Between 1981 and 1985, a first pilot trial including a few patients, immediately followed by a large, randomized, multicenter trial, clearly established the efficacy of OKT3 in reversing early acute renal allograft rejection episodes *(117–119)*, a use for which the antibody was rapidly licensed both in the United States and Europe. The dose regimen was based on the data from the pilot trial, in which escalating doses were applied *(117–119)*. Thus, 5 mg/d were administered for 10 to 15 consecutive d. The general practice was also to decrease the dosages of other concurrent medications during OKT3 treatment.

The use of OKT3 rapidly expanded from the treatment of early acute rejection to that of rejection episodes unresponsive to conventional high-dose corticosteroids and polyclonal anti-lymphocyte globulins, also termed *rescue* treatment. Various studies with large numbers of patients have demonstrated the efficacy of the antibody in this setting as well *(120–122)*. In addition, the interesting results obtained in renal transplantation also encouraged the use of the antibody for liver and heart transplant rejection. In both situations, OKT3 was essentially developed as a rescue treatment *(120,123–125)*.

OKT3 has also been used in several centers as an "induction" therapy, namely, as a first line treatment to prevent or delay the advent of acute rejection episodes and to improve long-term allograft survival. Moreover, particularly in renal transplantation, the use of OKT3 in the early post-transplant period was of interest to avoid complications linked to cyclosporin nephrotoxicity. Various controlled, single-center studies demonstrated the efficacy of OKT3 in this setting when compared to control regimens, some of which included polyclonal anti-T-cell antibodies *(126–128)*. In this context, OKT3 was administered for 10–14 consecutive days (starting on the day of transplant) in association with corticosteroids, azathioprine, and cyclosporin. In most cases, cyclosporin was applied starting a few days before the end of the antibody therapy. This is a clinically relevant issue, since the data from the European registry suggest that long-term allograft survival is significantly reduced when cyclosporin treatment is introduced concomitantly and not consecutively to OKT3 *(129)*.

OKT3 induction therapy was also applied with success in liver transplantation *(130–133)*.

Despite these results, OKT3 is not adopted any more as a routine prophylactic treatment, because of the risk of sensitization, which could preclude the use of the antibody for a steroid-resistant rejection, and secondly, because of the occurrence of the flu-like

syndrome that, as compared to ATG or conventional triple therapy with cyclosporin, could complicate the management of the patients *(46,79,80,132,134,135)*.

The future will be the use of humanized nonmitogenic CD3 antibodies that are already available. They have been used in transplantation in pilot clinical trials for the treatment of established renal allograft rejection episodes *(136,137)*. Results confirmed that these antibodies were well tolerated and that, despite the low numbers of patients included, the therapeutic effectiveness (reversal of rejection) was comparable to that observed with OKT3 *(136,137)*. These antibodies are also presently used in the autoimmunity setting, to treat patients with recent-onset insulin-dependent diabetes *(46,116)*.

6.2. CD25 Antibodies

As compared to OKT3, clinical experience with other murine monoclonal antibodies was limited and never reached the point of large-scale distribution, though encouraging results were reported. This was the case for antibodies to CD25 or LFA-1 *(138–142)*.

Here again, the panorama rapidly evolved with the advent of humanized antibodies. Some years ago, two humanized antibodies to CD25 (one chimeric [basiliximab/ Simulect®] and one CDR-grafted [daclizumab/ Zenapax®]), which are very well tolerated and are effective as part of induction regimens to prevent organ allograft rejection, were approved for use as induction therapies in organ transplantation *(77,78,143,144)*. Treatment with CD25 antibodies is started at the time of transplant for a limited number of injections (i.e., covering a 2- to 3-wk therapeutic window) on a background double therapy (cyclosporin and azathioprine) or triple therapy (cyclosporin, azathioprine, and corticosteroids). With the two antibodies, a significant reduction was observed in the incidence of biopsy-proven acute rejection as compared to placebo-treated patients. Results from Phase III trials showed that graft survival at 3 yr was not different in antibody- vs placebo-treated patients; pooled patient survival was >91–93% in both groups, and the incidence of posttransplant lymphoproliferative disease (PTLD) was comparable. These conclusions were recently confirmed in a meta-analysis of eight randomized controlled trials (total of 1858 patients) *(145)*. Studies with follow-ups longer than 3 yr may be needed to see statistical differences in graft and patient survival.

Recent data also indicated that humanized CD25 antibodies could also be beneficial for the treatment of established rejection *(145)*. These data are of particular interest since they argue for a greater efficacy of humanized CD25 antibodies as compared to the parent murine molecules. Thus, mouse CD25 antibodies were without effect for treatment of established rejection. This may also explain that humanized CD25 antibodies appear potentially interesting for the treatment of some severe autoimmune diseases, such as uveitis *(146,147)*.

6.3. CD4 Antibodies

As already discussed, a significant amount of data have accumulated showing the remarkable capacity of monoclonal antibodies to CD4 to suppress immune responses to soluble and tissular antigens, i.e., alloantigens and autoantigens *(26–30,148,149)*.

In humans, CD4 is expressed not only at the surface of a subset of lymphocytes but also on monocytes, macrophages, Langerhans cells, eosinophils, endothelial cells of hepatic sinusoids, sperm, and brain cells. The first pilot trials used mouse antibodies to human CD4 applied to patients presenting long-standing rheumatoid arthritis, psoriasis, inflammatory bowel disease, and uveitis *(150–157)*. The treatment was well tolerated. Only rare cases of mild side effects after the first injection (linked to minor cytokine release) have been reported *(150–157)*. The antibodies essentially induced partial and transient disappearance of circulating CD4+ cells. Coating of CD4+ cells was also observed, along with dose-dependent saturation of CD4 binding sites *(150–157)*. When present, antigenic modulation affected only a minor proportion of CD4 receptors. The results were encouraging in terms of therapeutic effectiveness, but in most cases the effects were brief *(150–156)*.

The drawback in all these trials was the sensitizing effect of the murine monoclonals, which justified trials of humanized CD4 antibodies. Several of the published studies focused on the use of the chimeric cM-T412 antibody (human IgG1). In rheumatoid arthritis, results from open studies seemed encouraging, especially when cumulative doses ranging from 350 to 700 mg were used *(158–161)*. There were no major signs of acute toxicity reported; some authors describe self-limited adverse events such as fever associated with myalgia, malaise, and asymptomatic hypotension, which appear to correlate with transient elevations of serum IL-6 *(158,160,161)*. Mild sensitization was reported in a majority of the patients *(158,160,161)*. However, the major problem was that the therapeutic effect could not be confirmed in the context of a large randomized, double-blind, placebo-controlled study including patients with early rheumatoid arthritis *(159)*. Also of concern was the significant and long-lasting CD4+ cell depletion (up to 60% from baseline for over 18–30 mo) *(25)* noted with cM-T412, contrary to what had initially been reported with the parental mouse M-T151 anti-CD4 antibody *(154)*. It has been proposed that apoptosis could mediate, at least in part, this massive depletion *(162)*.

The cM-T412 antibody has also been used in patients with multiple sclerosis, but here again without any evident clinical effect *(163)*.

The non-depleting humanized antibody to CD4 OKT4cdr4A (the CDR-grafted version of OKT4A) was used in patients presenting with severe psoriasis; one open pilot study and a placebo-controlled one were conducted, both of which provided promising data *(157,164)*.

Results from open pilot studies suggested that CD4 antibody therapy in combination (i.e., with antibodies to CD52) could be effective to treat severe forms of vasculitis *(84,85)*. One may hope that controlled studies will be actively promoted in cases with such indications to definitely prove the validity of the approach.

6.4. Antibodies to TNF

The introduction into clinical practice of humanized antibodies to TNF was a major step in the development of novel therapeutic strategies for treatment of rheumatoid arthritis. This was the consequence of the pioneer experimental and clinical work conducted by the groups of M. Feldmann and T. Maini. The first crucial in vitro finding was that neutralizing antibodies to TNF significantly decreased the production of most

of the pro-inflammatory cytokines (i.e., IL-1, IL-6, IL-8, GM-CSF) normally found in in vitro cultures of cells infiltrating synovial membranes from rheumatoid arthritis patients *(7,165)*. The in vivo relevance of this hypothesis was validated in two experimental settings. Mice expressing a human TNF transgene develop chronic arthritis that may be fully prevented by treatment with antibodies to TNF *(7,165)*. In addition, in a model of collagen type II-induced arthritis, in which the animals develop an erosive form of chronic arthritis, CD4 antibodies can prevent disease but are ineffective once the inflammatory and destructive process is established *(7,165)*. At variance with this, neutralizing antibodies to murine TNF applied once the disease has started are able to decrease the severity of objective and histopathological symptoms (e.g., swollen joints, bone erosions) *(7,165)*. Another unexpected but potentially relevant observation was that in established arthritis, combining a sub-optimal dose of antibody to TNF, which had no significant effect *per se*, with CD4 antibody therapy greatly improved limb involvement and helped heal paw-swelling and joint erosion. Furthermore, optimal anti-TNF combined with the CD4 antibody significantly improved the results obtained with anti-TNF alone *(166)*. Thus, in this model, anti-TNF and anti-CD4 are synergistic in ameliorating established disease. One interpretation of these results is that in order to sensitize the system to the effect of T-cell-directed immunointervention, it is mandatory to neutralize the inflammation that is the hallmark of self-perpetuating ongoing autoimmunity. In terms of strategy, this could be relevant for most autoimmune diseases, not only for established arthritis.

The results of the first randomized placebo-controlled double-blind study showing the effectiveness of the chimeric neutralizing antibody to TNF cA2 (human IgG1), now termed infliximab (and subsequently marketed as Remicade), for the treatment of long-standing rheumatoid arthritis were reported in 1994 *(167)*. They fully confirmed the data from the initial phase I/II open trial showing no acute toxicity and significant therapeutic benefits, as assessed by the clinical and laboratory parameters, lasting for several weeks after the end of treatment. Some of the patients having disease relapse underwent two or more cycles of retreatment; disease flare-ups were sensitive to retreatment, but the mean duration of the induced remissions progressively diminished, probably due to the appearance of antiallotypic sensitization *(76)*. Presently trials are being conducted that associate these molecules to methotrexate in an attempt to obtain longer-lasting clinical remissions *(7,168,169)*. Part of the beneficial effect of combining with methotrexate is probably due to a reduction of the immunogenicity of the anti-TNF antibody, as confirmed by the reduced response to the chimeric antibody in patients receiving the combined therapy *(7,168,169)*. These results were then confirmed in a subsequent Phase III study. Importantly, data from this trial showed that anti-TNF therapy was effective in protecting against joint destruction; arrest of damage was observed in more than 50% of patients by 6 mo after beginning treatment and lasted for the 2 yr of the study. There was also evidence of repair in a significant proportion of patients *(170,171)*. Based on these results, infliximab was approved for use, in combination with methotrexate, both in the United States and Europe. In the attempt to obtain a better clinical benefit, especially in terms of the duration of the remissions, trials have been conducted enrolling patients with recent onset disease (at about 6 mo from first symptoms and 2 mo from formal diagnosis). Recently reported results appear very promising.

With the disclosure of the very promising results using the cA2/ infliximab antibody, other biological agents targeting TNF were developed. Another chimeric anti-TNF monoclonal antibody named CDP571 was also shown to be clinically effective *(172)*. Two fusion proteins linking the TNF receptor molecules p55 or p75 to a human IgG constant frame (lenercept or etanercept/Enbrel®) also showed effectiveness in clinical rheumatoid arthritis *(173–175)*. However, only etanercept had an active clinical development and has been approved both in the United States and Europe. Other interesting candidates are on their way, among which the fully human D2E7 antibody (adalimumab) showed good efficacy in both Phase II and III trials *(176,177)*.

Antibodies to TNF were also used with success for treatment of severe Crohn's disease and are presently also approved for this indication *(178,179)*. Although the pathophysiology of this disease remains unclear, there is evidence for the significant role played by inflammatory cytokines *(180)*. The therapeutic benefit obtained upon TNF antibody treatment correlated with a decrease in IFN-γ production by mononuclear cells infiltrating the lamina propria *(181)*.

More recently, there were also interesting data reported from trials using TNF blocking agents in juvenile rheumatoid arthritis *(182)*, ankylosing spondylitis *(183)*, psoriatic arthritis *(184)*, and psoriasis *(185)*.

One side effect reported, especially in patients undergoing repeated treatments with infliximab, was the increased incidence of tuberculosis *(186)*. This is one reason why combination therapy with drugs aimed at neutralizing TNF and IL-1 has recently been disapproved by the Food and Drug Administration.

6.5. Antibodies to CD52

CD52 is a low molecular weight (12 amino acids) GPI-anchored protein expressed at the surface of human B-cells, T-cells, as well as monocytes/macrophages. The first rat antibody to CD52, Campath-1H, was characterized in 1983 and was initially used to deplete mature T-cells from bone-marrow transplants. A fully reshaped humanized version, Campath-1H (human IgG1), was derived by genetic engineering *(73)* and is available for clinical use as alemtuzumab. It has been extensively used in vivo to treat CD52$^+$ hematologic malignancies and in vitro to purge bone-marrow transplants to prevent graft-vs-host disease. Campath-1H is highly depleting in vivo; CD4$^+$ cells do not return to normal for several consecutive months. Upon the first injection, Campath-1H triggers an acute self-limited cytokine release that is the cause of a transient flu-like syndrome.

Campath-1H has been applied in patients with rheumatoid arthritis. At 3 and 6 mo of treatment, an improvement in the Paulus score was observed in about half of the patients *(187)*. Another indication in which Campath-1H seems to be very effective is severe systemic vasculitis *(84–86)*. The antibody was initially applied to rare forms of vasculitis, the pathogenesis of which is thought to involve mainly T-cell-mediated mechanisms. Subsequently, patients with Wegener's granulomatosis have also been treated with success. Particularly impressive in this clinical context were the long-term remissions that were obtained when combining antibodies to CD52 and to CD4 *(84–86)*.

Very promising results have been obtained in multiple sclerosis *(188–190)*. The initial trials included patients with relapsing/remitting disease evolving over many years and unresponsive to conventional treatments. Data from 8-yr follow-up are available. In a vast majority of the patients, a stabilization of clinical symptoms has been observed over 6–12 mo. Over the long-term follow-up, a marked decrease in the appearance of new lesions in the central nervous system as assessed by nuclear magnetic resonance (NMR) scanning was evidenced that seemed to correlate with the observed long-lasting and significant peripheral depletion of CD4+ T-lymphocytes *(188–190)*. An unexpected side effect of the treatment was the appearance of Graves' disease in a significant proportion of the patients successfully treated for their multiple sclerosis *(190)*. Multicenter trials are presently ongoing, including patients with more recent onset disease.

As a whole, Campath-1H seems quite unique in its capacity to promote long-lasting remission of life-threatening autoimmune diseases that are unresponsive to conventional treatments. Results from ongoing trials will help to draw more definitive conclusions.

Of particular interest are also the data reported by the group of R. Calne with the CD52 antibody Campath-1H in transplantation *(83)*. Campath 1H was administered to 31 renal allograft recipients at a dose of 20 mg (i.v.) on d 0 and 1 after transplant. The patients were maintained on low-dose monotherapy with cyclosporin started 72 h after transplant. At 15–28 mo of follow-up, 29 patients presented with functioning grafts. Six rejection episodes were scored that were responsive to conventional steroid therapy. More recently, two pilot studies attempted a similar strategy using Campath-1H and rapamycin monotherapy *(191,192)*. The data are interesting, but larger studies are needed to draw definitive conclusions.

6.6. Antibodies to VLA-4

Integrins are adhesion molecules of fundamental importance to the recruitment of leucocytes in inflammation. The α4β1 integrin VLA-4 is a leucocyte ligand for endothelial vascular cell adhesion molecule-1 (VCAM-1), fibronectin, and osteopontin. The interaction between VLA-4, expressed at the surface of activated lymphocytes and monocytes, with its ligand, VCAM-1, is essential for cell migration into inflamed parenchyma. Based on promising data obtained in experimental models of VLA-4 blockade, a specific humanized monoclonal antibody, natalizumab, was tested in randomized placebo-controlled trials. A first indication was multiple sclerosis *(193)*. A total of 213 patients presenting relapsing–remitting or relapsing secondary progressive multiple sclerosis received natalizumab or placebo treatment every 28 d for 6 mo. Results showed a marked reduction in the number of new brain lesions, as assessed by gadolinium-enhanced magnetic resonance imaging, in natalizumab- vs placebo-treated patients over the 6-mo observation period *(193)*. The same antibody was applied in Crohn's disease *(194)*. Here again, a placebo-controlled randomized trial was conducted including a total of 248 patients presenting with moderate to severe disease. Two infusions of the antibody were administered 4 wk apart. Patients who received natalizumab had higher remission rates than the placebo group, and a significant

improvement in Crohn's Disease Activity Index. The quality of life improved in natalizumab-treated patients, and no major adverse events were reported *(194)*.

6.7. Biological Ligand of CD2: the LFA-3Ig Fusion Protein

The human LFA-3/human IgG1 fusion protein (alefacept) binds to CD2 at the surface of T-lymphocytes. Controlled multicenter studies were conducted using this agent in patients with chronic plaque psoriasis. Depending on the trial, one or two 12-wk courses of alefacept were administered once a wk (7.5 to 15 mg/injection). In all cases, the drug was well tolerated and at least a 75% reduction of the disease score (PASI index) was observed at 2 wk from the last dose that in a significant proportion of the patients lasted for 7 mo *(194,195)*. Based on these positive results, alefacept has been approved by regulatory authorities for this indication. The immunological monitoring of the patients evidenced a selective reduction of memory-effector CD45R0$^+$ cells in the circulation, while lymphocytes expressing a naïve phenotype were spared *(195)*. These reductions in memory T-cell counts correlated with measurements of disease activity, which fits the assumption that pathogenic T-cells are included among memory T-lymphocytes *(194)*.

6.8. Antibodies to CD20

Rituximab (Rituxan®) is a human-mouse chimeric monoclonal antibody specific for CD20, a B-cell CD20 antigen. It causes rapid and specific B-cell depletion. Rituximab was approved in the United States in 1997 and in Europe in 1998 (MabThera®) to treat severe refractory CD20-positive B-cell non-Hodgkin's lymphoma. The use of this antibody has now been extended as first-line therapy and maintenance therapy to lymphoma and stem-cell transplantation procedures.

More recent studies are also evaluating the use of rituximab in autoimmune disorders, such as rheumatoid arthritis, immune thrombocytopenic purpura, autoimmune hemolytic anemia, systemic lupus erythematosus, and multiple sclerosis *(196–200)*. In rheumatoid arthritis, the treatment appears safe and associated with major improvement. Based on these results, a phase II controlled trial is presently in progress.

From a more fundamental point of view, these results highlight the pathogenic role of B-cells in rheumatoid arthritis.

7. Future Perspectives

The progress achieved on therapeutic monoclonal antibodies over the last decade is remarkable. They are already well established in several clinical settings, fulfilling needs that had not been met with conventional chemical immunosuppressants. One may assume in view of the numerous antibodies and fusion proteins presently under development, especially humanized and fully human molecules, that their importance will rapidly expand both in transplantation and in autoimmunity.

Today, monoclonal antibodies represent the most promising approach for tolerance induction in animal models (both induction of tolerance to alloantigens in transplantation and restoration of self-tolerance in autoimmune diseases). One may reasonably hope that these spectacular results will be rapidly transferred to the clinic. Moreover, understanding the molecular basis of these unique tolerogenic properties would clear

the way for the development of chemicals or recombinant receptor agonists and/or antagonists that would mimic the desired therapeutic effect.

References

1 Fanslow, W. C., Sims, J. E., Sassenfeld, H., et al. (1990) Regulation of alloreactivity in vivo by a soluble form of the interleukin-1 receptor. *Science* **248,** 739–742.

2 Jacobs, C. A., Lynch, D. H., Roux, E. R., et al. (1991) Characterization and pharmacokinetic parameters of recombinant soluble interleukin-4 receptor. *Blood* **77,** 2396–2403.

3 Ozmen, L., Gribaudo, G., Fountoulakis, M., Gentz, R., Landolfo, S., and Garotta, G. (1993) Mouse soluble IFN gamma receptor as IFN gamma inhibitor. Distribution, antigenicity, and activity after injection in mice. *J. Immunol.* **150,** 2698–2705.

4 Dinarello, C. A. (1991) Interleukin-1 and interleukin-1 antagonism. *Blood* **77,** 1627–1652.

5 Peppel, K., Crawford, D., and Beutler, B. (1991) A tumor necrosis factor (TNF) receptor-IgG heavy chain chimeric protein as a bivalent antagonist of TNF activity. *J. Exp. Med.* **174,** 1483–1489.

6 Lesslauer, W., Tabuchi, H., Gentz, R., et al. (1991) Recombinant soluble tumor necrosis factor receptor proteins protect mice from lipopolysaccharide-induced lethality. *Eur. J. Immunol.* **21,** 2883–2886.

7 Feldmann, M. (2002) Development of anti-TNF therapy for rheumatoid arthritis. *Nat. Rev. Immunol.* **2,** 364–371.

8 Skoglund, C., Scheynius, A., Holmdahl, R., and Van Der Meide, P. H. (1988) Enhancement of DTH reaction and inhibition of the expression of class II transplantation antigens by in vivo treatment with antibodies against gamma-interferon. *Clin. Exp. Immunol.* **71,** 428–432.

9 Nicoletti, F., Meroni, P. L., Landolfo, S., et al. (1990) Prevention of diabetes in BB/Wor rats treated with monoclonal antibodies to interferon-gamma. *Lancet* **336,** 319.

10 Bach, J. F. (1993) Strategies in immunotherapy of insulin-dependent diabetes mellitus. *Ann. N. Y. Acad. Sci.* **696,** 364–376.

11 Pujol-borrell, R., Todd, I., Doshi, M., et al. (1987) HLA class II induction in human islet cells by interferon-gamma plus tumour necrosis factor or lymphotoxin. *Nature* **326,** 304–306.

12 Sarvetnick, N., Liggitt, D., Pitts, S. L., Hansen, S. E., and Stewart, T. A. (1988) Insulin-dependent diabetes mellitus induced in transgenic mice by ectopic expression of class II MHC and interferon-gamma. *Cell* **52,** 773–782.

13 Hall, B. M., Bishop, G. A., Duggin, G. G., Horvath, J. S., Philips, J., and Tiller, D. J. (1984) Increased expression of HLA-DR antigens on renal tubular cells in renal transplants: relevance to the rejection response. *Lancet* **2,** 247–251.

14 Fuggle, S. V., Mcwhinnie, D. L., and Morris, P. J. (1987) Precise specificity of induced tubular HLA-class II antigens in renal allografts. *Transplantation* **44,** 214–220.

15 Greaves, M. F., Tursi, A., Playfair, J. H., Torrigiani, G., Zamir, R., and Roitt, I. M. (1969) Immunosuppressive potency and in vitro activity of antilymphocyte globulin. *Lancet* **1,** 68–66.

16 Martin, W. J. and Miller, J. F. (1968) Cell to cell interaction in the immune response. IV. Site of action of antilymphocyte globulin. *J. Exp. Med.* **128,** 855–885.

17 Bindon, C. I., Hale, G., and Waldmann, H. (1988) Importance of antigen specificity for complement-mediated lysis by monoclonal antibodies. *Eur. J. Immunol.* **18,** 1507–1514.

18 Isaacs, J. D., Clark, M. R., Greenwood, J., and Waldmann, H. (1992) Therapy with monoclonal antibodies. An in vivo model for the assessment of therapeutic potential. *J. Immunol.* **148,** 3062–3071.

19. Abbs, I. C., Clark, M., Waldmann, H., Chatenoud, L., Koffman, C. G., and Sacks, S. H. (1994) Sparing of first dose effect of monovalent anti-CD3 antibody used in allograft rejection is associated with diminished release of pro-inflammatory cytokines. *Therapeutic Immunology* **1,** 325–331.

20 Routledge, E. G., Lloyd, I., Gorman, S. D., Clark, M., and Waldmann, H. (1991) A humanized monovalent CD3 antibody which can activate homologous complement. *Eur. J. Immunol.* **21,** 2717–2725.

21 Wong, J. T. and Colvin, R. B. (1991) Selective reduction and proliferation of the CD4+ and CD8+ T cell subsets with bispecific monoclonal antibodies: evidence for inter-T cell-mediated cytolysis. *Clin. Immunol. Immunopathol.* **58,** 236–250.

22 Wesselborg, S., Janssen, O., and Kabelitz, D. (1993) Induction of activation-driven death (apoptosis) in activated but not resting peripheral blood T cells. *J. Immunol.* **150,** 4338–4345.

23 Kronke, M., Depper, J. M., Leonard, W. J., Vitetta, E. S., Waldmann, T. A., and Greene, W. C. (1985) Adult T cell leukemia: a potential target for ricin A chain immunotoxins. *Blood* **65,** 1416–1421.

24 Walz, G., Zanker, B., Brand, K., et al. (1989) Sequential effects of interleukin 2-diphtheria toxin fusion protein on T-cell activation. *Proc. Natl. Acad. Sci. USA* **86,** 9485–9488.

25 Moreland, L. W., Pratt, P. W., Bucy, R. P., Jackson, B. S., Feldman, J. W., and Koopman, W. J. (1994) Treatment of refractory rheumatoid arthritis with a chimeric anti-CD4 monoclonal antibody. Long-term followup of CD4+ T cell counts. *Arthritis Rheum.* **37,** 834–838.

26 Qin, S., Cobbold, S. P., Pope, H., Elliott, J., Kioussis, D., Davies, J., and Waldmann, H. (1993) "Infectious" transplantation tolerance. *Science* **259,** 974–977.

27 Cobbold, S. P., Nolan, K. F., Graca, L., et al. (2003) Regulatory T cells and dendritic cells in transplantation tolerance: molecular markers and mechanisms. *Immunol. Rev.* **196,** 109–124.

28 Waldmann, H. and Cobbold, S. (2001) Regulating the immune response to transplants. a role for CD4+ regulatory cells? *Immunity* **14,** 399–406.

29 Bushell, A., Karim, M., Kingsley, C. I., and Wood, K. J. (2003) Pretransplant blood transfusion without additional immunotherapy generates CD25+CD4+ regulatory T cells: a potential explanation for the blood-transfusion effect. *Transplantation* **76,** 449–455.

30 Bushell, A., Morris, P. J., and Wood, K. J. (1995) Transplantation tolerance induced by antigen pretreatment and depleting anti-CD4 antibody depends on CD4+ T cell regulation during the induction phase of the response. *Eur. J. Immunol.* **25,** 2643–2649.

31 Bank, I. and Chess, L. (1985) Perturbation of the T4 molecule transmits a negative signal to T cells. *J. Exp. Med.* **162,** 1294–1303.

32 Emmrich, F., Kanz, L., and Eichmann, K. (1987) Cross-linking of the T cell receptor complex with the subset-specific differentiation antigen stimulates interleukin 2 receptor expression in human CD4 and CD8 T cells. *Eur. J. Immunol.* **17,** 529–534.

33 Jabado, N., Le Deist, F., Fisher, A., and Hivroz, C. (1994) Interaction of HIV gp120 and anti-CD4 antibodies with the CD4 molecule on human CD4+ T cells inhibits the binding activity of NF-AT, NF-kappa B and AP-1, three nuclear factors regulating interleukin-2 gene enhancer activity. *Eur. J. Immunol.* **24,** 2646–2652.

34 Jabado, N., Pallier, A., Jauliac, S., Fischer, A., and Hivroz, C. (1997) gp160 of HIV or anti-CD4 monoclonal antibody ligation of CD4 induces inhibition of JNK and ERK-2 activities in human peripheral CD4+ T lymphocytes. *Eur. J. Immunol.* **27,** 397–404.

35 Jabado, N., Pallier, A., Le Deist, F., Bernard, F., Fischer, A., and Hivroz, C. (1997) CD4 ligands inhibit the formation of multifunctional transduction complexes involved in T cell activation. *J. Immunol.* **158,** 94–103.

36 Jauliac, S., Mazerolles, F., Jabado, N., et al. (1998) Ligands of CD4 inhibit the association of phospholipase Cgamma1 with phosphoinositide 3 kinase in T cells: regulation of this association by the phosphoinositide 3 kinase activity. *Eur. J. Immunol.* **28,** 3183–3191.

37 Chatenoud, L. and Bach, J. F. (1984) Antigenic modulation: a major mechanism of antibody action. *Immunol. Today* **5,** 20–25.

38 Hirsch, R., Eckhaus, M., Auchincloss, J. R., Sachs, D. H., and Bluestone, J. A. (1988) Effects of in vivo administration of anti-T3 monoclonal antibody on T cell function in mice. I. Immunosuppression of transplantation responses. *J. Immunol.* **140,** 3766–3772.

39. Chatenoud, L. and Bach, J. F. (1982) The use of monoclonal antibodies for the follow-up of transplanted patients. *Heart Transplant.* **2,** 47–51.

40 Schwartz, R. H. (1990) A cell culture model for T lymphocyte clonal anergy. *Science* **248,** 1349–1356.

41 Schwartz, R. H. (1996) Models of T cell anergy: is there a common molecular mechanism? [*see* comment] *J. Exp. Med.* **184,** 1–8.

42 Benjamin, R. J., Cobbold, S. P., Clark, M. R., and Waldmann, H. (1986) Tolerance to rat monoclonal antibodies. Implications for serotherapy. *J. Exp. Med.* **163,** 1539–1552.

43 Gutstein, N. L., Seaman, W. E., Scott, J. H., and Wofsy, D. (1986) Induction of immune tolerance by administration of monoclonal antibody to L3T4. *J. Immunol.* **137,** 1127–1132.

44 Cobbold, S. P., Adams, E., Marshall, S. E., Davies, J. D., and Waldmann, H. (1996) Mechanisms of peripheral tolerance and suppression induced by monoclonal antibodies to CD4 and CD8. *Immunol. Rev.* **149,** 5–33.

45 Cobbold, S. P., Adams, E., Graca, L., and Waldmann, H. (2003) Serial analysis of gene expression provides new insights into regulatory T cells. *Semin. Immunol.* **15,** 209–214.

46 Chatenoud, L. (2003) CD3-specific antibody-induced active tolerance: from bench to bedside. *Nat. Rev. Immunol.* **3,** 123–132.

47 Chatenoud, L., Thervet, E., Primo, J., and Bach, J. F. (1994) Anti-CD3 antibody induces long-term remission of overt autoimmunity in nonobese diabetic mice. *Proc. Natl. Acad. Sci. USA* **91,** 123–127.

48 Nicolls, M. R., Aversa, G. G., Pearce, N. W., et al. (1993) Induction of long-term specific tolerance to allografts in rats by therapy with an anti-CD3-like monoclonal antibody. *Transplantation* **55,** 459–468.

49 Pearson, T. C., Madsen, J. C., Larsen, C. P., Morris, P. J., and Wood, K. J. (1992) Induction of transplantation tolerance in adults using donor antigen and anti-CD4 monoclonal antibody. *Transplantation* **54,** 475–483.

50 Thomas, F. T., Ricordi, C., Contreras, J. L., et al. (1999) Reversal of naturally occuring diabetes in primates by unmodified islet xenografts without chronic immunosuppression. *Transplantation* **67,** 846–854.

51 Thomas, J. M., Neville, D. M., Contreras, J. L., et al. (1997) Preclinical studies of allograft tolerance in rhesus monkeys: a novel anti-CD3-immunotoxin given peritransplant with donor bone marrow induces operational tolerance to kidney allografts. *Transplantation* **64,** 124–135.

52 Niimi, M., Pearson, T. C., Larsen, C. P., et al. (1998) The role of the CD40 pathway in alloantigen-induced hyporesponsiveness in vivo. *J. Immunol.* **161,** 5331–5337.

53 Larsen, C. P., Elwood, E. T., Alexander, D. Z., et al. (1996) Long-term acceptance of skin and cardiac allografts after blocking CD40 and CD28 pathways. *Nature* **381,** 434–438.

54 Kirk, A. D., Burkly, L. C., Batty, D. S., et al. (1999) reatment with humanized monoclonal antibody against CD154 prevents acute renal allograft rejection in nonhuman primates [see comments]. *Nat. Med.* **5,** 686–693.

55 Bushell, A., Niimi, M., Morris, P. J., and Wood, K. J. (1999) Evidence for immune regulation in the induction of transplantation tolerance: a conditional but limited role for IL-4. *J. Immunol.* **162,** 1359–1366.

56 Plain, K. M., Chen, J., Merten, S., He, X. Y., and Hall, B. M. (1999) Induction of specific tolerance to allografts in rats by therapy with non-mitogenic, non-depleting anti-CD3 monoclonal antibody: association with TH2 cytokines not anergy. *Transplantation* **67,** 605–613.

57 Wood, K. J., Luo, S., and Akl, A. (2004) Regulatory T cells: potential in organ transplantation. *Transplantation* **77,** S6–8.

58 Karim, M., Kingsley, C. I., Bushell, A. R., Sawitzki, B. S., and Wood, K. J. (2004) Alloantigen-induced CD25+CD4+ regulatory T cells can develop in vivo from CD25-CD4+ precursors in a thymus-independent process. *J. Immunol.* **172,** 923–928.

59 Graca, L., Le Moine, A., Cobbold, S. P., and Waldmann, H. (2003) Antibody-induced transplantation tolerance: the role of dominant regulation. *Immunol. Res.* **28,** 181–191.

60 Graca, L., Thompson, S., Lin, C. Y., Adams, E., Cobbold, S. P., and Waldmann, H. (2002) Both CD4(+)CD25(+) and CD4(+)CD25(-) regulatory cells mediate dominant transplantation tolerance. *J. Immunol.* **168,** 5558–5565.

61 Chatenoud, L., Salomon, B., and Bluestone, J. A. (2001) Suppressor T cells—they're back and critical for regulation of autoimmunity! *Immunol. Rev.* **182,** 149–163.

62 Bach, J. F. and Chatenoud, L. (2001) Tolerance to islet autoantigens and type I diabetes. *Annu. Rev. Immunol.* **19,** 131–161.

63 Hall, B. M., Pearce, N. W., Gurley, K. E., and Dorsch, S. E. (1990) Specific unresponsiveness in rats with prolonged cardiac allograft survival after treatment with cyclosporine. III. Further characterization of the CD4+ suppressor cell and its mechanisms of action. *J. Exp. Med.* **171,** 141–157.

64 Belghith, M., Bluestone, J. A., Barriot, S., Megret, J., Bach, J. F., and Chatenoud, L. (2003) TGF-β dependent mechanisms mediate restoration of self-tolerance induced by antibodies to CD3 in overt autoimmune diabetes. *Nature Medicine* **9,** 1202–1208.

65 Zelenika, D., Adams, E., Humm, S., et al. (2002) Regulatory T cells overexpress a subset of Th2 gene transcripts. *J. Immunol.* **168,** 1069–1079.

66 Chatenoud, L., Baudrihaye, M. F., Chkoff, N., Kreis, H., Goldstein, G., and Bach, J. F. (1986) Restriction of the human in vivo immune response against the mouse monoclonal antibody OKT3. *J. Immunol.* **137,** 830–838.

67 Chatenoud, L. (1986) The immune response against therapeutic monoclonal antibodies. *Immunol. Today* **7,** 367–368.

68. Chatenoud, L., Jonker, M., Villemain, F., Goldstein, G., and Bach, J. F. (1986) The human immune response to the OKT3 monoclonal antibody is oligoclonal. *Science* **232,** 1406–1408.

69 Baudrihaye, M. F., Chatenoud, L., Kreis, H., Goldstein, G., and Bach, J. F. (1984) Unusually restricted anti-isotype human immune response to OKT3 monoclonal antibody. *Eur. J. Immunol.* **14,** 686–691.

70 Abramowicz, D., Crusiaux, A., and Goldman, M. (1992) Anaphylactic shock after retreatment with OKT3 monoclonal antibody. *N. Engl. J. Med.* **327,** 736.

71 Abramowicz, D., Crusiaux, A., Niaudet, P., Kreis, H., Chatenoud, L., and Goldman, M. (1996) The IgE humoral response in OKT3-treated patients - Incidence and fine specificity. *Transplantation* **61,** 577–581.

72 Hricik, D. E., Mayes, J. T., and Schulak, J. A. (1990) Inhibition of anti-OKT3 antibody generation by cyclosporine-—results of a prospective randomized trial. *Transplantation* **50,** 237–240.

73 Riechmann, L., Clark, M., Waldmann, H., and Winter, G. (1988) Reshaping human antibodies for therapy. *Nature* **332,** 323–327.

74 Bolt, S., Routledge, E., Lloyd, I., et al. (1993) The generation of a humanized, non-mitogenic CD3 monoclonal antibody which retains in vitro immunosuppressive properties. *Eur. J. Immunol.* **23,** 403–411.

75 Alegre, M.L., Peterson, L.J., Xu, D., et al. (1994) A non-activating "humanized" anti-CD3 monoclonal antibody retains immunosuppressive properties in vivo. *Transplantation* **57,** 1537–1543.

76 Elliott, M. J., Maini, R. N., Feldmann, M., et al. (1994) Repeated therapy with monoclonal antibody to tumour necrosis factor alpha (cA2) in patients with rheumatoid arthritis. *Lancet* **344,** 1125–1127.

77 Nashan, B., Moore, R., Amlot, P., Schmidt, A. G., Abeywickrama, K., and Soulillou, J. P. (1997) Randomised trial of basiliximab versus placebo for control of acute cellular rejection in renal allograft recipients. CHIB 201 International Study Group [published erratum appears in *Lancet* 1997 **350(9089),** 1484]. *Lancet* **350,** 1193–1198.

78 Vincenti, F., Kirkman, R., Light, S., et al. (1998) Interleukin-2-receptor blockade with daclizumab to prevent acute rejection in renal transplantation. Daclizumab Triple Therapy Study Group [*see* comments]. *N. Engl. J. Med.* **338,** 161–165.

79 Chatenoud, L., Ferran, C., Legendre, C., et al. (1990) In vivo cell activation following OKT3 administration. Systemic cytokine release and modulation by corticosteroids. *Transplantation* **49,** 697–702.

80 Abramowicz, D., Schandene, L., Goldman, M., et al. (1989) Release of tumor necrosis factor, interleukin-2, and gamma-interferon in serum after injection of OKT3 monoclonal antibody in kidney transplant recipients. *Transplantation* **47,** 606–608.

81 Marks, J. D., Hoogenboom, H. R., Bonnert, T. P., Mccafferty, J., Griffiths, A. D., and Winter, G. (1991) By-passing immunization. Human antibodies from V-gene libraries displayed on phage. *J. Mol. Biol.* **222,** 581–597.

82 Lubin, I., Segall, H., Marcus, H., et al. (1994) Engraftment of human peripheral blood lymphocytes in normal strains of mice. *Blood* **83,** 2368–2381.

83 Calne, R., Moffatt, S. D., Friend, P. J., et al. (1999) Campath IH allows low-dose cyclosporine monotherapy in 31 cadaveric renal allograft recipients. *Transplantation* **68,** 1613–1616.

84 Mathieson, P. W., Cobbold, S.P., Hale, G., et al. (1990) Monoclonal-antibody therapy in systemic vasculitis. *N. Engl. J. Med.* **323,** 250–254.

85 Lockwood, C. M., Thiru, S., Isaacs, J. D., Hale, G., and Waldmann, H. (1993) Long-term remission of intractable systemic vasculitis with monoclonal antibody therapy. *Lancet* **341,** 1620–1622.

86 Lockwood, C. M., Thiru, S., Stewart, S., et al. (1996) reatment of refractory Wegener's granulomatosis with humanized monoclonal antibodies [*see* comments]. *QJM* **89,** 903–912.

87 Billingham, R. E., Brent, L., and Medawar, P. B. (1953) Actively acquired tolerance to foreign cells. *Nature* **172,** 603–606.

88 Roser, B. J. (1989) Cellular mechanisms in neonatal and adult tolerance. *Immunol. Rev.* **107,** 179–202.

89 Donckier, V., Flamand, V., Desalle, F., et al. (1998) IL-12 prevents neonatal induction of transplantation tolerance in mice. *Eur. J. Immunol.* **28,** 1426–1430.

90 Donckier, V., Wissing, M., Bruyns, C., et al. (1995) Critical role of interleukin 4 in the induction of neonatal transplantation tolerance. *Transplantation* **59,** 1571–1576.

91. Monaco, A. P., Wood, M. L., and Russell, P. S. (1966) Studies on heterologous antilymphocyte serum in mice. III. Immunological tolerance and chimerism produced across the H2-locus with adult thymectomy and antilymphocyte serum. *Ann. N. Y. Acad. Sci.* **129,** 190–209.

92 Wood, M. L., Monaco, A. P., Gozzo, J. J., and Liegeois, A. (1971) Use of homozygous allogeneic bone marrow for induction of tolerance with antilymphocyte serum: dose and timing. *Transplant. Proc.* **3,** 676–679.

93 Thomas, F. T., Carver, F. M., Foil, M. B., et al. (1983) Long-term incompatible kidney survival in outbred higher primates without chronic immunosuppression. *Ann. Surg.* **198,** 370–378.

94 Thomas, J. M., Carver, F. M., Foil, M. B., Hall, W. R., Adams, C., and Fahrenbruch, G. B. (1983) Renal allograft tolerance induced with ATG and donor bone marrow in outbred rhesus monkeys. *Transplantation* **36,** 104–106.

95 Thomas, J., Alqaisi, M., Cunningham, P., et al. (1992) The development of a posttransplant TLI treatment strategy that promotes organ allograft acceptance without chronic immunosuppression. *Transplantation* **53,** 247–258.

96 Hamawy, M. M. and Knechtle, S. J. (1998) Strategies for tolerance induction in nonhuman primates. *Curr. Opin. Immunol.* **10,** 513–517.

97 Qin, S. X., Wise, M., Cobbold, S. P., et al. (1990) Induction of tolerance in peripheral T cells with monoclonal antibodies. *Eur. J. Immunol.* **20,** 2737–2745.

98 Gershon, R. K. and Kondo, K. (1971) Infectious immunological tolerance. *Immunology* **21,** 903–914.

99 Cobbold, S. and Waldmann, H. (1998) Infectious tolerance. *Curr. Opin. Immunol.* **10,** 518–524.

100 Davies, J. D., Leong, L. Y., Mellor, A., Cobbold, S. P., and Waldmann, H. (1996) T cell suppression in transplantation tolerance through linked recognition. *J. Immunol.* **156,** 3602–3607.

101 Isobe, M., Yagita, H., Okumura, K., and Ihara, A. (1992) Specific acceptance of cardiac allograft after treatment with antibodies to ICAM-1 and LFA-1. *Science* **255,** 1125–1127.

102 Larsen, C. P. and Pearson, T. C. (1997) The CD40 pathway in allograft rejection, acceptance, and tolerance. *Curr. Opin. Immunol.* **9,** 641–647.

103 Mosmann, T. R. and Coffman, R. L. (1989) TH1 and TH2 cells: different patterns of lymphokine secretion lead to different functional properties. *Annu. Rev. Immunol.* **7,** 145–173.

104 Nickerson, P., Steurer, W., Steiger, J., Zheng, X., Steele, A. W., and Strom, T. B. (1994) Cytokines and the Th1/Th2 paradigm in transplantation. *Curr. Opin. Immunol.* **6,** 757–764.

105 Bendelac, A., Carnaud, C., Boitard, C., and Bach, J. F. (1987) Syngeneic transfer of autoimmune diabetes from diabetic NOD mice to healthy neonates. Requirement for both L3T4+ and Lyt-2+ T cells. *J. Exp. Med.* **166,** 823–832.

106 Wicker, L. S., Miller, B. J., and Mullen, Y. (1986) Transfer of autoimmune diabetes mellitus with splenocytes from nonobese diabetic (NOD) mice. *Diabetes* **35,** 855–860.

107 Yagi, H., Matsumoto, M., Kunimoto, K., Kawaguchi, J., Makino, S., and Harada, M. (1992) Analysis of the roles of CD4+ and CD8+ T cells in autoimmune diabetes of NOD mice using transfer to NOD athymic nude mice. *Eur. J. Immunol.* **22,** 2387–2393.

108 Haskins, K., Portas, M., Bergman, B., Lafferty, K., and Bradley, B. (1989) Pancreatic islet-specific T-cell clones from nonobese diabetic mice. *Proc. Natl. Acad. Sci. USA* **86,** 8000–8004.

109 Katz, J. D., Benoist, C., and Mathis, D. (1995) T helper cell subsets in insulin-dependent diabetes. *Science* **268,** 1185–1188.

110 Healey, D., Ozegbe, P., Arden, S., Chandler, P., Hutton, J., and Cooke, A. (1995) In vivo activity and in vitro specificity of CD4+ Th1 and Th2 cells derived from the spleens of diabetic NOD mice. *J. Clin. Invest.* **95,** 2979–2985.

111 Herbelin, A., Gombert, J. M., Lepault, F., Bach, J. F., and Chatenoud, L. (1998) Mature mainstream TCR alpha beta(+)CD4(+) thymocytes expressing L-selectin mediate ''active tolerance'' in the nonobese diabetic mouse. *J. Immunol.* **161,** 2620–2628.

112 Lepault, F. and Gagnerault, M. C. (2000) Characterization of peripheral regulatory CD4(+) T cells that prevent diabetes onset in nonobese diabetic mice. *J. Immunol.* **164,** 240–247.

113 Lepault, F., Gagnerault, M. C., Faveeuw, C., Bazin, H., and Boitard, C. (1995) Lack of L-selectin expression by cells transferring diabetes in NOD mice: insights into the mechanisms involved in diabetes prevention by Mel-14 antibody treatment. *Eur. J. Immunol.* **25,** 1502–1507.

114 Chatenoud, L., Primo, J., and Bach, J. F. (1997) CD3 antibody-induced dominant self tolerance in overtly diabetic NOD mice. *J. Immunol.* **158,** 2947–2954.

115 Alegre, M. L., Collins, A. M., Pulito, V. L., et al. (1992) Effect of a single amino acid mutation on the activating and immunosuppressive properties of a "humanized" OKT3 monoclonal antibody. *J. Immunol.* **148,** 3461–3468.

116 Herold, K. C., Hagopian, W., Auger, J. A., et al. (2002) Anti-CD3 monoclonal antibody in new-onset type 1 diabetes mellitus. *N. Engl. J. Med.* **346,** 1692–1698.

117 Cosimi, A. B., Burton, R. C., Colvin, R. B., et al. (1981) Treatment of acute renal allograft rejection with OKT3 monoclonal antibody. *Transplantation* **32,** 535–539.

118 Cosimi, A. B., Colvin, R. B., Burton, R. C., et al. (1981) Use of monoclonal antibodies to T-cell subsets for immunologic monitoring and treatment in recipients of renal allografts. *N. Engl. J. Med.* **305,** 308–314.

119. Ortho Multicenter Transplant Study Group (1985) A randomized clinical trial of OKT3 monoclonal antibody for acute rejection of cadaveric renal transplants. *N. Engl. J. Med.* **313,** 337–342.

120 Goldstein, G., Kremer, A. B., Barnes, L., and Hirsch, R. L. (1987) OKT3 monoclonal antibody reversal of renal and hepatic rejection in pediatric patients. *J. Pediatr.* **111,** 1046–1050.

121 Hricik, D. E., Zarconi, J., and Schulak, J. A. (1989) Influence of low-dose cyclosporine on the outcome of treatment with OKT3 for acute renal allograft rejection. *Transplantation* **47,** 272–277.

122 Norman, D. J., Barry, J. M., Bennett, W. M., et al. (1988) The use of OKT3 in cadaveric renal transplantation for rejection that is unresponsive to conventional anti-rejection therapy. *Am. J. Kidney Dis.* **11,** 90–93.

123 Colonna Jo, D., Goldstein, L. I., Brems, J. J., et al. (1987) A prospective study on the use of monoclonal anti-T3-cell antibody (OKT3) to treat steroid-resistant liver transplant rejection. *Arch. Surg.* **122,** 1120–1123.

124 Woodle, E. S., Thistlethwaite Jr, J. R., Emond, J. C., et al. (1991) OKT3 therapy for hepatic allograft rejection. Differential response in adults and children. *Transplantation* **51,** 1207–1212.

125 Gilbert, E. M., Dewitt, C. W., Eiswirth, C. C., et al. (1987) Treatment of refractory cardiac allograft rejection with OKT3 monoclonal antibody. *Am. J. Med.* **82,** 202–206.

126 Frey, D. J., Matas, A. J., Gillingham, K. J., et al. (1992) Sequential therapy—a prospective randomized trial of MALG versus OKT3 for prophylactic immunosuppression in cadaver renal allograft recipients. *Transplantation* **54,** 50–56.

127 Debure, A., Chkoff, N., Chatenoud, L., et al. (1988) One-month prophylactic use of OKT3 in cadaver kidney transplant recipients. *Transplantation* **45,** 546–553.

128 Abramowicz, D., Goldman, M., De Pauw, L., Vanherweghem, J. L., Kinnaert, P., and Vereerstraeten, P. (1992) The long-term effects of prophylactic OKT3 monoclonal antibody in cadaver kidney transplantation—a single-center, prospective, randomized study. *Transplantation* **54,** 433–437.

129 Opelz, G. (1995) Efficacy of rejection prophylaxis with OKT3 in renal transplantation. Collaborative Transplant Study. *Transplantation* **60,** 1220–1224.

130 Farges, O., Ericzon, B. G., Bresson-hadni, S., et al. (1994) A randomized trial of OKT3-based versus cyclosporine-based immunoprophylaxis after liver transplantation. Long-term results of a European and Australian multicenter study. *Transplantation* **58,** 891–898.

131 Millis, J. M., Mcdiarmid, S. V., Hiatt, J. R., et al. (1989) Randomized prospective trial of OKT3 for early prophylaxis of rejection after liver transplantation. *Transplantation* **47,** 82–88.

132. Eason, J. D. and Cosimi, A. B. (1999) Biologic immunosuppressive agents. In: *Transplantation*. Ginns, L., Cosimi, A., and Morris, P., eds. Blackwell Science, Malden, MA, pp. 196–224.

133 Robbins, R. C., Oyer, P. E., Stinson, E. B., and Starnes, V. A. (1992) The use of monoclonal antibodies after heart transplantation. *Transplant. Sci.* **2,** 22–27.

134 Chatenoud, L., Ferran, C., Reuter, A., et al. (1989) Systemic reaction to the anti-T-cell monoclonal antibody OKT3 in relation to serum levels of tumor necrosis factor and interferon-gamma. *N. Engl. J. Med.* **320,** 1420–1421.

135 Cosimi, A. B. (1987) Clinical development of Orthoclone OKT3. *Transplant. Proc.* **19,** 7–16.

136 Friend, P. J., Hale, G., Chatenoud, L., et al. (1999) Phase I study of an engineered aglycosylated humanized CD3 antibody in renal transplant rejection. *Transplantation* **68,** 1632–1637.

137 Woodle, E. S., Xu, D., Zivin, R. A., et al. (1999) Phase I trial of a humanized, Fc receptor nonbinding OKT3 antibody, huOKT3gamma1(Ala-Ala) in the treatment of acute renal allograft rejection. *Transplantation* **68,** 608–616.

138 Le Mauff, B., Hourmant, M., Rougier, J. P., et al. (1991) Effect of anti-LFA1 (CD11a) monoclonal antibodies in acute rejection in human kidney transplantation. *Transplantation* **52,** 291–296.

139 Maraninchi, D., Mawas, C., Stoppa, A. M., et al. (1989) Anti LFA1 monoclonal antibody for the prevention of graft rejection after T cell-depleted HLA-matched bone marrow transplantation for leukemia in adults. *Bone Marrow Transplant.* **4,** 147–150.

140 Soulillou, J. P., Cantarovich, D., Le Mauff, B., et al. (1990) Randomized controlled trial of a monoclonal antibody against the interleukin-2 receptor (33B3.1) as compared with rabbit antithymocyte globulin for prophylaxis against rejection of renal allografts. *N. Engl. J. Med.* **322,** 1175–1182.

141 Kriaa, F., Hiesse, C., Alard, P., et al. (1993) Prophylactic use of the anti-IL-2 receptor monoclonal antibody LO-Tact-1 in cadaveric renal transplantation: results of a randomized study. *Transplant. Proc.* **25,** 817–819.

142 Kirkman, R. L., Shapiro, M. E., Carpenter, C. B., et al. (1991) A randomized prospective trial of anti-Tac monoclonal antibody in human renal transplantation. *Transplantation* **51,** 107–113.

143 Waldmann, T. A. and O'Shea, J. (1998). The use of antibodies against the IL-2 receptor in transplantation. *Curr. Opin. Immunol.* **10,** 507–512.

144 Bumgardner, G. L., Hardie, I., Johnson, R. W., et al. (2001) Results of 3-year phase III clinical trials with daclizumab prophylaxis for prevention of acute rejection after renal transplantation. *Transplantation* **72,** 839–845.

145 Adu, D., Cockwell, P., Ives, N. J., Shaw, J., and Wheatley, K. (2003) Interleukin-2 receptor monoclonal antibodies in renal transplantation: meta-analysis of randomised trials. *BMJ* **326,** 789.

146 Nussenblatt, R. B. (2002) Bench to bedside: new approaches to the immunotherapy of uveitic disease. *Int. Rev. Immunol.* **21,** 273–289.

147 Guex-Crosier, Y., Raber, J., Chan, C. C., et al. (1997) Humanized antibodies against the alpha-chain of the IL-2 receptor and against the beta-chain shared by the IL-2 and IL-15 receptors in a monkey uveitis model of autoimmune diseases. *J. Immunol.* **158,** 452–458.

148 Shizuru, J. A., Taylor-Edwards, C., Banks, B. A., Gregory, A. K., and Fathman, C. G. (1988) Immunotherapy of the nonobese diabetic mouse: treatment with an antibody to T-helper lymphocytes. *Science* **240,** 659–662.

149 Wofsy, D. and Seaman, W. E. (1987) Reversal of advanced murine lupus in NZB/NZW F1 mice by treatment with monoclonal antibody to L3T4. *J. Immunol.* **138,** 3247–3253.

150 Horneff, G., Burmester, G. R., Emmrich, F., and Kalden, J. R. (1991) Treatment of rheumatoid arthritis with an anti-CD4 monoclonal antibody. *Arthritis Rheum.* **34,** 129–140.

151 Wendling, D., Wijdenes, J., Racadot, E., and Morel-Fourrier, B. (1991) Therapeutic use of monoclonal anti-CD4 antibody in rheumatoid arthritis. *J. Rheumatol.* **18,** 325–327.

152 Morel, P., Revillard, J. P., Nicolas, J. F., Wijdenes, J., Rizova, H., and Thivolet, J. (1992) Anti-CD4 monoclonal antibody therapy in severe psoriasis. *J. Autoimmun.* **5,** 465–477.

153 Emmrich, J., Seyfarth, M., Fleig, W. E., and Emmrich, F. (1991) Treatment of inflammatory bowel disease with anti-CD4 monoclonal antibody. *Lancet* **338,** 570–571.

154 Reiter, C., Kakavand, B., Rieber, E. P., Schattenkirchner, M., Riethmuller, G., and Kruger, K. (1991) Treatment of rheumatoid arthritis with monoclonal CD4 antibody M-T151. Clinical results and immunopharmacologic effects in an open study, including repeated administration. *Arthritis Rheum.* **34,** 525–536.

155 Goldberg, D., Chatenoud, L., Morel, P., et al. (1990) Preliminary trial of an anti-CD4 monoclonal antibody (MoAb) in rheumatoid arthritis (RA). *Arthritis Rheum.* **33,** S153.

156. Goldberg, D., Morel, P., Chatenoud, L., et al. (1991) Immunological effects of high dose administration of anti-CD4 antibody in rheumatoid arthritis patients. *J. Autoimmun.* **4,** 617–630.

157 Bachelez, H., Flageul, B., Dubertret, L., et al. (1998) Treatment of recalcitrant plaque psoriasis with a humanized non-depleting antibody to CD4. *J. Autoimmun.* **11,** 53–62.

158 Moreland, L. W., Bucy, R. P., Tilden, A., et al. (1993) Use of a chimeric monoclonal anti-CD4 antibody in patients with refractory rheumatoid arthritis. *Arthritis Rheum.* **36,** 307–318.

159 Van Der Lubbe, P. A., Dijkmans, B. A., Markusse, H. M., Nassander, U., and Breedveld, F. C. (1995) A randomized, double-blind, placebo-controlled study of CD4 monoclonal antibody therapy in early rheumatoid arthritis. *Arthritis Rheum.* **38,** 1097–1106.

160 Van Der Lubbe, P. A., Reiter, C., Breedveld, F. C., et al. (1993) Chimeric CD4 monoclonal antibody cM-T412 as a therapeutic approach to rheumatoid arthritis. *Arthritis Rheum.* **36,** 1375–1379.

161 Van Der Lubbe, P. A., Reiter, C., Miltenburg, A. M., et al. (1994) Treatment of rheumatoid arthritis with a chimeric CD4 monoclonal antibody (cM-T412): immunopharmacological aspects and mechanisms of action. *Scand. J. Immunol.* **39,** 286–294.

162 Choy, E. H., Adjaye, J., Forrest, L., Kingsley, G. H., and Panayi, G. S. (1993) Chimaeric anti-CD4 monoclonal antibody cross-linked by monocyte Fc gamma receptor mediates apoptosis of human CD4 lymphocytes. *Eur. J. Immunol.* **23,** 2676–2681.

163 van Oosten, B. W., Lai, M., Hodgkinson, S., et al. (1997) Treatment of multiple sclerosis with the monoclonal anti-CD4 antibody cM-T412: results of a randomized, double-blind, placebo-controlled, MR-monitored phase II trial. *Neurology* **49,** 351–357.

164 Gottlieb, A. B., Lebwohl, M., Shirin, S., et al. (2000) Anti-CD4 monoclonal antibody treatment of moderate to severe psoriasis vulgaris: results of a pilot, multicenter, multiple-dose, placebo-controlled study. *J. Am. Acad. Dermatol.* **43,** 595–604.

165 Brennan, F. M. and Feldmann, M. (1992) Cytokines in autoimmunity. *Curr. Opin. Immunol.* **4,** 754–759.

166 Williams, R. O., Mason, L. J., Feldmann, M., and Maini, R. N. (1994) Synergy between anti-CD4 and anti-tumor necrosis factor in the amelioration of established collagen-induced arthritis. *Proc. Natl. Acad. Sci. USA* **91,** 2762–2766.

167 Elliott, M. J., Maini, R. N., Feldmann, M., et al. (1994) Randomised double-blind comparison of chimeric monoclonal antibody to tumour necrosis factor alpha (cA2) versus placebo in rheumatoid arthritis. *Lancet* **344,** 1105–1110.

168 Maini, R. N., Breedveld, F. C., Kalden, J. R., et al. (1998) herapeutic efficacy of multiple intravenous infusions of anti-tumor necrosis factor alpha monoclonal antibody combined with low-dose weekly methotrexate in rheumatoid arthritis [see comments]. *Arthritis Rheum.* **41,** 1552–1563.

169 Feldmann, M. and Maini, T. (2001) Anti-TNF alpha therapy of rheumatoid arthritis: what have we learned? *Annu. Rev. Immunol.* **19,** 163–196.

170 Maini, R., St Clair, E. W., Breedveld, F., et al. (1999) Infliximab (chimeric anti-tumour necrosis factor alpha monoclonal antibody) versus placebo in rheumatoid arthritis patients receiving concomitant methotrexate: a randomised phase III trial. ATTRACT Study Group. *Lancet* **354,** 1932–1939.

171 Lipsky, P. E., van der Heijde, D. M., St Clair, E. W., et al. (2000) Infliximab and methotrexate in the treatment of rheumatoid arthritis. Anti-Tumor Necrosis Factor Trial in Rheumatoid Arthritis with Concomitant Therapy Study Group. *N. Engl. J. Med.* **343,** 1594–1602.

172 Rankin, E. C., Choy, E. H., Kassimos, D., et al. (1995) The therapeutic effects of an engineered human anti-tumour necrosis factor alpha antibody (CDP571) in rheumatoid arthritis. *Br. J. Rheumatol.* **34,** 334–342.

173 Furst, D. E., Weisman, M., Paulus, H. E., et al. (2003) Intravenous human recombinant tumor necrosis factor receptor p55-Fc IgG1 fusion protein, Ro 45-2081 (lenercept): results of a dose-finding study in rheumatoid arthritis. *J. Rheumatol.* **30,** 2123–2126.

174 Moreland, L. W., Baumgartner, S. W., Schiff, M. H., et al. (1997) reatment of rheumatoid arthritis with a recombinant human tumor necrosis factor receptor (p75)-Fc fusion protein [*see* comments]. *N. Engl. J. Med.* **337,** 141–147.

175 Moreland, L. W., Margolies, G., Heck, Jr., L. W., et al. (1996) Recombinant soluble tumor necrosis factor receptor (p80) fusion protein: toxicity and dose finding trial in refractory rheumatoid arthritis. *J. Rheumatol.* **23,** 1849–1855.

176 Kempeni, J. (1999) Preliminary results of early clinical trials with the fully human anti-TNFalpha monoclonal antibody D2E7. *Ann. Rheum. Dis.* **58(Suppl 1),** I70–72.

177 den Broeder, A., van de Putte, L., Rau, R., et al. (2002) A single dose, placebo controlled study of the fully human anti-tumor necrosis factor-alpha antibody adalimumab (D2E7) in patients with rheumatoid arthritis. *J. Rheumatol.* **29,** 2288–2298.

178 Van Dullemen, H. M., Van Deventer, S. J., Hommes, D. W., et al. (1995) Treatment of Crohn's disease with anti-tumor necrosis factor chimeric monoclonal antibody (cA2). *Gastroenterology* **109,** 129–135.

179 Ghosh, S., Goldin, E., Gordon, F. H., et al. (2003) Natalizumab for active Crohn's disease. *N. Engl. J. Med.* **348,** 24–32.

180 Van Deventer, S. J. (1997) Tumour necrosis factor and Crohn's disease *Gut* **40,** 443–448.

181 Plevy, S. E., Landers, C. J., Prehn, J., et al. (1997) A role for TNF-alpha and mucosal T helper-1 cytokines in the pathogenesis of Crohn's disease. *J. Immunol.* **159,** 6276–6282.

182 Lovell, D. J., Giannini, E. H., Reiff, A., et al. (2000) Etanercept in children with polyarticular juvenile rheumatoid arthritis. Pediatric Rheumatology Collaborative Study Group. *N. Engl. J. Med.* **342,** 763–769.

183 Brandt, J., Haibel, H., Cornely, D., et al. (2000) Successful treatment of active ankylosing spondylitis with the anti-tumor necrosis factor alpha monoclonal antibody infliximab. *Arthritis Rheum.* **43,** 1346–1352.

184 Mease, P. J., Goffe, B. S., Metz, J., VanderStoep, A., Finck, B., and Burge, D. J. (2000) Etanercept in the treatment of psoriatic arthritis and psoriasis: a randomised trial. *Lancet* **356,** 385–390.

185 Chaudhari, U., Romano, P., Mulcahy, L. D., Dooley, L. T., Baker, D. G., and Gottlieb, A. B. (2001) Efficacy and safety of infliximab monotherapy for plaque-type psoriasis: a randomised trial. *Lancet* **357,** 1842–1847.

186 Gomez-Reino, J. J., Carmona, L., Valverde, V. R., Mola, E. M., and Montero, M. D. (2003) Treatment of rheumatoid arthritis with tumor necrosis factor inhibitors may predispose to significant increase in tuberculosis risk: a multicenter active-surveillance report. *Arthritis Rheum.* **48,** 2122–2127.

187 Isaacs, J. D., Watts, R. A., Hazleman, B. L., et al. (1992) Humanised monoclonal antibody therapy for rheumatoid arthritis. *Lancet* **340,** 748–752.

188 Moreau, T., Thorpe, J., Miller, D., et al. (1994) Preliminary evidence from magnetic resonance imaging for reduction in disease activity after lymphocyte depletion in multiple sclerosis [published erratum appears in *Lancet* 1994 **344(8920),** 486]. *Lancet* **344,** 298–301.

189 Coles, A. J., Wing, M. G., Molyneux, P., et al. (1999) Monoclonal antibody treatment exposes three mechanisms underlying the clinical course of multiple sclerosis. *Ann. Neurol.* **46,** 296–304.

190 Coles, A. J., Wing, M. G., Smith, S., et al. (1999) Pulsed monoclonal antibody treatment and autoimmune thyroid disease in multiple sclerosis. *Lancet* **354,** 1691–1695.

191 Knechtle, S. J., Pirsch, J. D., Fechner, J. H., et al. (2003) Campath-1H induction plus rapamycin monotherapy for renal transplantation: results of a pilot study. *Am. J. Transplant.* **3,** 722–730.

192 Kirk, A. D., Hale, D. A., Mannon, R. B., et al. (2003) Results from a human renal allograft tolerance trial evaluating the humanized CD52-specific monoclonal antibody alemtuzumab (CAMPATH-1H). *Transplantation* **76,** 120–129.

193 Miller, D. H., Khan, O. A., Sheremata, W. A., et al. (2003) A controlled trial of natalizumab for relapsing multiple sclerosis. *N. Engl. J. Med.* **348,** 15–23.

194 Lebwohl, M., Christophers, E., Langley, R., Ortonne, J. P., Roberts, J., and Griffiths, C. E. (2003) An international, randomized, double-blind, placebo-controlled phase 3 trial of intramuscular alefacept in patients with chronic plaque psoriasis. *Arch. Dermatol.* **139,** 719–727.

195 Krueger, G. G. (2003) Clinical response to alefacept: results of a phase 3 study of intravenous administration of alefacept in patients with chronic plaque psoriasis. *J. Eur. Acad. Dermatol. Venereol.* **17 Suppl 2,** 17–24.

196 Rastetter, W., Molina, A., and White, C. A. (2004) Rituximab: expanding role in therapy for lymphomas and autoimmune diseases. *Annu. Rev. Med.* **55,** 477–503.

197 Shaw, T., Quan, J., and Totoritis, M. C. (2003) B cell therapy for rheumatoid arthritis: the rituximab (anti-CD20) experience. *Ann. Rheum. Dis.* **62(Suppl 2),** ii55–59.

198 Silverman, G. J. and Weisman, S. (2003) Rituximab therapy and autoimmune disorders: prospects for anti-B cell therapy. *Arthritis Rheum.* **48,** 1484–1492.

199. Leandro, M. J., Edwards, J. C., and Cambridge, G. (2002) Clinical outcome in 22 patients with rheumatoid arthritis treated with B lymphocyte depletion. *Ann. Rheum. Dis.* **61,** 883–888.

200. De Vita, S., Zaja, F., Sacco, S., De Candia, A., Fanin, R., and Ferraccioli, G. (2002) Efficacy of selective B cell blockade in the treatment of rheumatoid arthritis: evidence for a pathogenetic role of B cells. *Arthritis Rheum.* **46,** 2029–2033.

22

Producing Bispecific and Bifunctional Antibodies

Dipankar Das and Mavanur R. Suresh

Summary

Bispecific antibodies are artificially engineered monoclonal antibodies (MAbs) that consist of two distinct binding sites and are capable of binding two different antigens noncovalently. They can be produced by chemical cross-linkage, genetic engineering, or somatic hybridization. This chapter describes a rapid method using somatic fusion to generate hybrid hybridomas (quadromas). Two fluorescence-labeled hybridoma cell lines were fused with polyethylene glycol (PEG) to generate the quadroma. Generation of a quadroma secreting bsMAb against biotin and HRPO is described, along with a benzhydroxamic acid-agarose affinity chromatography procedure to purify the bsMAb–HRPO complex. This bsMAb can be used for ultrasensitive ELISA detection of biotinylated antigens. Essentially a similar method can be used for fusing any two hybridomas for therapeutic applications.

Bifunctional antibodies are colinear molecules with one or more paratopes linked with diagnostic or therapeutic molecules. There are some limitations of therapeutic monoclonal antibodies in the clinic that can be overcome by engineering smaller and more effective antibody fragments. Here we describe a stepwise procedure for developing a bifunctional ScFv (bfScFv). We constructed a bfScFv from a hybridoma cell line using PCR strategies. The VL and VH gene segments are linked with a 45-bp linker and fused with a biotin mimic sequence at the 3' end. This engineered bifunctional antibody fragment gene could be expressed and the protein purified on a large scale in *Escherichia coli* as inclusion bodies. Such bifunctional antibody molecules could have useful applications in the area of immunodiagnostics and immunotherapy. Similar strategies can be used to incorporate a second single-chain antibody or any nonantibody entity such as a cytokine for therapeutic applications.

Key Words: Bispecific antibodies; FITC; TRITC; polyethylene glycol (PEG) fusion; ELISA; bifunctional antibodies; ScFv; PCR; inclusion bodies; refolding.

1. Introduction

In the 1950s, cancer immunotherapy and radioimmunotherapy emerged as a new strategy based on polyclonal antibody preparations *(1)*. The heterogeneous nature of polyclonals was a major limitation. With the development of the hybridoma technology for producing monoclonal antibodies (MAbs) by Kohler and Milstein *(2)* in

1975, it became possible to make large quantities of pure, identical antibodies against a particular antigen. This landmark discovery has revolutionized the use of MAb in the area of immunodetection and immunotherapy of cancers, infectious, and other diseases. In the last 30 yr, with the rapid developments in recombinant DNA technology, facile preparation of recombinant antibodies has been achieved *(3,4)*. This technology allowed the design flexibility to alter size, configuration, valency, effector functions, and species-specific domains in the construction of MAbs. These include whole chimeric, humanized antibodies and their small antibody reductants, such as Fab, F(ab')2, and single-chain variable (ScFv) and domain antibodies. A single-chain antibody molecule consists of the two variable domains (VH and VL) of an antibody molecule joined together by a designed artificial polypeptide linker such that the antigen-binding site is retained in a single co-linear protein *(5,6)*. Bispecific antibodies (bsMAb) are artificially engineered immunoglobulins incorporating two distinct binding specificities, and were first generated by chemical methods *(7)*. A bispecific antibody incorporates two distinct paratopes, which are capable of binding two different epitopes or antigens noncovalently. In contrast, a bifunctional antibody (bfMAb) refers to the colinear molecules that have one or more paratopes linked to a diagnostic or therapeutic non-antibody entity *(8)*. With the specificity of antigen binding coupled with unique functionalities, applications range from immunohistochemistry, ultrasensitive immunodetection, radioimmunotherapy, radioimmunodiagnosis, and immunotherapy to targeted drug delivery. Bispecific monoclonal antibodies have been extensively studied in both diagnostic *(9,10)* and therapeutic areas *(11–19)*. These types of nanoprobes can be made by chemical fusion, somatic fusion, or genetic engineering methods *(20)*.

In this chapter, we will describe in a stepwise fashion how to develop (a) bispecific MAb for diagnostic applications using quadromas (hybrid hybridoma); and (b) bifunctional ScFv (bfScFv) for therapeutic applications using recombinant antibody technology.

2. Materials

2.1. Quadroma Development

1. Mouse IgG1 antibiotin hybridoma cell line (P54).
2. Rat IgG2a antihorseradish peroxidase (HRPO) hybridoma cell line (YP4).
3. Fluorescein isothiocyanate (FITC; Sigma, St. Louis, MO).
4. Tetramethyl rhodamine isothiocyanate (TRITC; Sigma).
5. DMEM medium (Gibco-BRL, Roockville, MD).
6. Fetal bovine serum (FBS; Gibco-BRL).
7. Penicillin, streptomycin, and glutamine (PSG; Gibco-BRL).
8. Ninety-six-well sterile tissue-culture plate (Nunc, Naperville, IL).
9. Ninety-six-well ELISA plate (Nunc).
10. Goat antimouse horseradish peroxidase (GAM-HRPO; Sigma).
11. 10% BSA (dialyzed in 1X PBS, pH 7.3).
12. 3,3',5,5'-Tetra-methyl benzidine (TMB) peroxidase substrate (Kirkegaard & Perry Laboratories, Gaithersburg, MD).
13. Polyethylene glycol (PEG; Hybrimax, Sigma).

14. Benzhydroxamic acid agarose (BHA; Upfront Chromatography, Copenhagen, Denmark).
15. Dimethyl sulfoxide (DMSO, Sigma).
16. 0.22 μ*M* syringe filter (Millipore, Bedford, MA).

2.2. Bifunctional Single-Chain Variable-Fragment Antibody Development

1. Anti-WEE (western equine encephalitis) producing hybridoma (11D2) cell lines (Defence Research and Development Canada, Medicine Hat, AB, Canada).
2. DMEM cell-culture medium (Gibco-BRL).
3. Fetal bovine serum (FBS, Gibco-BRL).
4. Penicillin, streptomycin, and glutamine (PSG, Gibco-BRL).
5. TRizol® reagent (Gibco-BRL).
6. Oligonucleotide primers.
7. PCR machine (Robocycler 40, Stratagene, La Jolla, CA).
8. 100 m*M* dNTPs (Pharmacia, New York, NY).
9. RNasin (Promega, Madison, WI).
10. Diethyl pyrocarbonate (DEPC, Sigma).
11. Agarose (Gibco-BRL).
12. TAE, 50X: 242 g Tris base, 57.1 mL glacial acetic acid, 100 mL 0.5 *M* EDTA (pH 8.0) per 1 L water.
13. Ethidium bromide (EtBr, Sigma).
14. DNA mol wt markers, T4 DNA ligase, Superscript II, restriction enzymes (Gibco-BRL).
15. *E. coli* strain TOP 10 F' (Invitrogen, Carlsbad, CA).
16. *E. coli* strain BL21 (DE3) (Novagen, Madison, WI).
17. Expression vector pET22b+ (Novagen).
18. Isopropyl β-D-thiogalacto pyranoside (IPTG, Gibco-BRL).
19. Lysozyme (Sigma).
20. Prestained protein mol wt markers, Biorad protein assay reagent (Bio-Rad, Hercules, CA).
21. Vent DNA polymerase (New England Biolabs [NEB], Beverly, MA).
22. L-arginine (Sigma).
23. Urea (Sigma).
24. Sarcosyl (Sigma).
25. Carbenicillin (Sigma).
26. SOC medium: 2% tryptone, 0.5% yeast extract, 10 m*M* NaCl, 2.5 m*M* KCl, 10 m*M* MgCl$_2$, 10 m*M* MgSO$_4$, 20 m*M* glucose.
27. QIAprep plasmid DNA isolation kit (Qiagen, Valencia, CA).
28. QIAquick gel extraction kit (Qiagen).
29. Lysis buffer: 50 m*M* Tris-HCl (pH 8.0), 200 m*M* NaCl, 1 m*M* EDTA.
30. Refolding buffer: 50 m*M* Tris-HCl (pH 8.0), 0.4 *M* L-arginine.
31. Dialysis membrane (MWCO: 12,000–14,000 Da).
32. Petri dish.
33. Luria Bertani (LB) medium: 1% tryptone, 0.5% yeast extract, 0.5% NaCl, pH 7.3.
34. TMB peroxidase substrate (Kirkegaard & Perry Laboratories Inc).
35. 10% BSA; dialyzed in 1X PBS, pH 7.3.
36. Streptavidin horseradish peroxidase (St-HRPO) (Sigma).
37. PBST: PBS with 0.1% Tween-20, pH 7.3.
38. ELISA plate (Nunc).

3. Methods

3.1. Quadroma Development

Somatic fusion for the development of bispecific MAb involves (1) fusion of two established hybridomas, generating a quadroma *(9,21)*; and (2) fusion of one established hybridoma (instead of a nonsecreting myeloma) with lymphocytes derived from a mouse immunized with a second antigen generating a trioma *(22)*. Here we will describe the stepwise protocol for the development of a quadroma from two well-established, fluorescence-labeled hybridomas *(23,24)*. The method described below includes the different steps of (1) cell labeling; (2) PEG fusion; (3) FACS; (4) screening for quadromas; (5) affinity purification of bsMAb; and (6) characterization of bsMAb.

3.1.1. Cell Labeling

1. Prepare the fluorescent dye (FITC and TRITC) solution as a 1 mg/mL stock in DMSO and sterile filter with a 0.22-μm syringe filter.
2. Wash separately 2×10^7 hybridoma cells of P54 and YP4 in 10 mL serum-free DMEM (SFDMEM) medium three times at 800 rpm ($114g$) for 5 min at room temperature. Resuspend the P54 cells in 10 mL SFDMEM medium, pH 7.4, and the YP4 cells in 10 mL SFDMEM medium, pH 6.8. Calculate the viability of P54 and YP4 hybridoma cells by the trypan blue exclusion method prior to fusion. Ideally, viability should be approx 90–95% (*see* **Note 1**).
3. Label the P54 cells with TRITC solution (final concentration of 2 μg/mL in SFDMEM, pH 7.4) and the YP4 cells with FITC solution (final concentration of 1 μg/mL in SFDMEM, pH 6.8) *(25)*.
4. Incubate cells with the respective fluorescent dyes for 30 min at 37°C with gentle shaking (*see* **Note 2**).
5. Wash with SFDMEM medium to remove any free fluorescent dye.
6. Resuspend in 10 mL of SFDMEM medium.

3.1.2. PEG Fusion

1. Mix 5 mL of TRITC-labeled P54 cells (10^7 cells) with 5 mL of FITC-labeled YP4 cells (10^7 cells) and centrifuge at 800 rpm ($114g$) for 5 min at room temperature.
2. Decant the supernatant completely and resuspend the cells in remaining medium (50–100 μL) (*see* **Note 3**).
3. Fuse approx 10^7 cells from the TRITC-labeled P54 hybridoma with the same number of cells from the FITC-labeled YP4 hybridoma by using 500 μL of 50% (w/v) polyethylene glycol (PEG) solution for 2 min in a CO_2 incubator (**Fig. 1**) (*see* **Note 4**).
4. Centrifuge the cells at 800 rpm ($114g$) for 5 min at room temperature to remove PEG and resuspend in 15 mL of DMEM medium with 10–15% FBS.
5. Wash the cells three times in 15 mL DMEM with 10–15% FBS and finally suspend in 10 mL of DMEM medium with 10–15% FBS (*see* **Note 5**).
6. Transfer the cells to a 25-cm² tissue-culture flask and incubate for 1 h at 37°C with 5% CO_2 in a standard tissue-culture incubator.

3.1.3. FACS

1. Perform flow cytometric cell sorting using Epics Elite Cell Sorter (Coulter Corporation, Hialeah, FL) or a similar instrument.
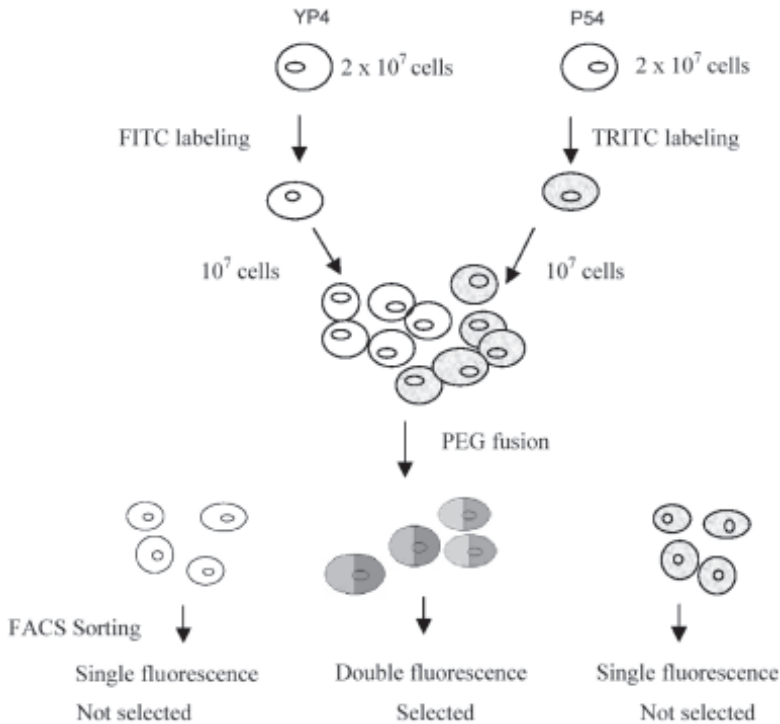
Fig. 1. Outline of PEG fusion.

2. Sort cells with dual fluorescence and clone one to two cells per well in a 96-well tissue-culture plate (*see* **Note 6**).
3. Culture the sorted cells at 37°C with 5% CO_2 for 1–3 wk and monitor for the appearance of clones.
4. Screen the resulting putative quadromas for bispecific monoclonal antibody secretion after 10–20 d as described below in **Subheading 3.1.4.**

3.1.4. Screening for Quadromas Secreting Bispecific Antibodies

1. Coat NUNC microtiter plates with biotin-BSA (1 μg/well, in 100 μL of PBS using a stock of 10 μg/mL) overnight at 4°C *(10,26)*.
2. Wash the plate three times with 200 μL of PBST (PBS with 0.1% Tween-20).
3. Block free binding sites with 200 μL of 1% BSA at 37°C for 1 h.
4. Dilute (1:10, 1:100, and 1:1000) various cell-culture supernatants with 1% BSA in PBS. Add 100 μL to the antigen-coated well along with 50 μL of 10 μg/mL HRPO in 1% BSA per well, and incubate for 1 h at 37°C (*see* **Note 7**).
5. Wash the plate three times with PBST and add 100 μL of TMB peroxidase substrate to each well.
6. Select positive quadromas secreting bsMAb after 15–45 min of color development by measuring OD at 650 nm using an ELISA plate reader.

7. This bridge ELISA measures only the bsMAb activity, by binding to the solid-phase antigen with one paratope (antibiotin) and in solution to the other.
8. Select strongly positive clones and subclone by limiting dilution three successive times to get the best-producing quadroma (*see* **Note 8**).

3.1.5 Affinity Co-Chromatography of bsMAb

1. Harvest the quadroma supernatant containing the bsMAb at 1500 rpm (403*g*) for 7 min at room temperature to remove the cells.
2. Add ammonium sulphate to 50% saturation to the supernatant and precipitate the bsMAb. Resuspend the pellet in a minimum volume of PBS and dialyze against PBS, pH 7.0 *(27)*.
3. Combine approx 150 mg of crude bsMAb with 10 mg of HRPO in PBS, pH 7.0, and incubate for 20 min at 37°C.
4. Load HRPO-bsMAb complex to a 15-mL benzhydroxamic acid–agarose (BHA) (1.25 × 30 cm column) matrix and adjust flow rate to 20 mL/ h *(28)* (*see* **Note 9**).
5. Wash the column with six to eight column volumes of PBS and elute bound protein as a preformed HRPO–bsMAb complex in 2-mL fractions with 0.1 *M* borate buffer, pH 9.0.
6. Check eluted fractions for bsMAb activity on an antigen-coated plate (*see* **Note 10**).
7. Pool the most active fractions and dialyze against PBS, pH 7.3.

3.1.6 Characterization of bsMAb Activity

1. Perform a two-step bridge ELISA with 96-well microtiter plates. This is based on the activity of the bsMAb capable of bridging the two antigens.
2. Coat wells with biotin-BSA (1 μg/well, in 100 μL of PBS using a stock of 10 μg/mL) overnight at 4°C.
3. Wash the plate three times with 200 μL of PBST. Block free binding sites with 200 μL of 1% BSA and incubate for 30 min to 1 h at 37°C.
4. Wash the plate with PBST, add 100 μL different dilutions of bsMAb–HRPO complex in PBS, and incubate for 1 h at 37°C.
5. Wash thrice with PBST, incubate the plate with 100 μL/well of TMB peroxidase substrate.
6. Take the OD at 650 nm within 15–30 min in a microplate reader to determine the titer of the bsMAb activity.
7. Test purity of the affinity-purified material by SDS-PAGE and estimate protein concentration by the Bradford method.

3.2. Bifunctional Single-Chain Variable-Fragment Antibody Development

3.2.1. Bifunctional ScFv Cloning by Recombinant DNA Technology

The initial cloning of specific variable immunoglobulin regions (VH and VL) is done by PCR strategies. The Kabat database is a valuable source for design of primers and sequence predictions *(29)*. Designed PCR primers have been used to anneal many VH and VL genes in segments encoding their FR1 and FR4 framework region sequences *(30)*. At the 5' end of VH and VL, one may use primers for FR1, whereas at the 3' end, PCR primers for the constant region are appropriate. Following the elucidation of the nucleotide sequence (by manual or automated sequencers), one can engineer appropriate restriction sites in a second PCR reaction. The amplification of VH and VL with desired restriction site(s) is followed by linking or assembly of VH and VL with a peptide linker using an overlapping PCR procedure. Here we outline the design of 11D2-biotin mimic

bifunctional ScFv fragment, consisting of VL domain linked by a 15-amino-acid linker to the VH domain for eventual expression. The protocol for the isolation and cloning of bifunctional ScFv is a modification of a previously described method *(31)*.

3.2.2. Cloning of ScFv

All DNA manipulations are performed according to standard cloning procedures *(32)*.

3.2.2.1. TOTAL RNA ISOLATION AND cDNA SYNTHESIS

1. Centrifuge 11D2 hybridoma cells (5–6 × 10^{6}cells/mL) at 1500 rpm (403g) for 7 min at 20°C and remove the supernatant.
2. Lyse hybridoma cells by adding 1 mL of TRizol reagent and pass the cell lysate several times through a 1-mL pipet.
3. Incubate the lysed sample for 5 min at 15–30°C to allow complete dissociation of nucleoprotein complex.
4. Add 0.2 mL of chloroform, mix well by shaking vigorously, and incubate at 15–30°C for 2–3 min.
5. Centrifuge the sample at 12,000g for 15 min at 2–8°C.
6. Remove the RNA-containing aqueous phase, avoiding interface material.
7. Add 0.5 mL isopropyl alcohol to the aqueous phase and incubate at 15–30°C for 10 min.
8. Pellet the RNA by centrifugation at 12,000g for 10 min at 2–8°C.
9. Wash the RNA pellet with 75% ethanol and centrifuge at 7500g for 5 min at 2–8°C (*see* **Note 11**).
10. Briefly dry the RNA pellet (5–10 min) and dissolve in RNase free water by incubating at 55 to 60°C for 10 min.
11. Read A$_{260}$/A$_{280}$ of 1:100 dilution of the RNA (*see* **Note 12**).
12. Aliquot and store RNA at –70°C (*see* **Note 13**).
13. Synthesize the first strand of cDNA by mixing 2 µg total RNA, 100 pmoles specific primers (PL for light chain and PH for heavy chain), 200 units SuperscriptII (RNase H reverse transcriptase) in a total volume of 20 µL containing 50 mM Tris (pH 8.3), 75 mM KCl, 3 mM MgCl$_2$, 10 mM DTT, 0.5 mM dNTPs, and 1 unit RNasin (**Fig. 2A**) (*see* **Note 14**).
14. Incubate the reaction at 42°C for 1 h.
15. Generate VL or VH by mixing 1 µL of cDNA reaction mixture, 0.5 µM each primer (P1 and P2 for VL, P3 and P4 for VH), 200 µM dNTPs, and 1 unit vent DNA polymerase in 20 mM Tris (pH 8.8), 10 mM (NH$_4$)$_2$SO$_4$, 2 mM MgSO$_4$, and 0.1% Triton X-100 (**Fig. 2B**) (*see* **Note 15**).
16. Set the PCR cycle at 94°C/55°C/72°C, 45 s/45 s/45 s for 25 cycles. At the beginning of the first cycle, incubate for 3 min at 94°C, and at the end of the last cycle, incubate for 7 min at 72°C.
17. Analyze PCR products by 1% agarose/TAE gel electrophoresis prestained with EtBr (0.25 µg/mL) (*see* **Note 16**).
18. Purify amplified PCR products in 1% agarose/TAE gel by using QIAquick gel extraction kit.

3.2.2.2. ASSEMBLY OF VH AND VL GENES WITH LINKER

1. Perform assembly of ScFv by mixing equimolar amounts of VL, linker oligonucleotide (P5), VH, 200 µM dNTPs, 1 unit vent DNA polymerase, and 5 µL 10X PCR buffer in a 50 µL volume (**Fig. 2C**) (*see* **Note 17**).
2. Set the PCR at 94°C/55°C/72°C, 45 s/45 s/45 s for 10 cycles.

A

11D2 hybridoma cell line

↓ Total RNA preparation

————————————AAAAA   ————————————AAAAA

↓ 1st strand cDNA synthesis, RT-PCR

————————————AAAAA   ————————————AAAAA
←——   ←——
PL   PH

↓

————————   ————————
1st strand cDNA of VL   1st strand cDNA of VH
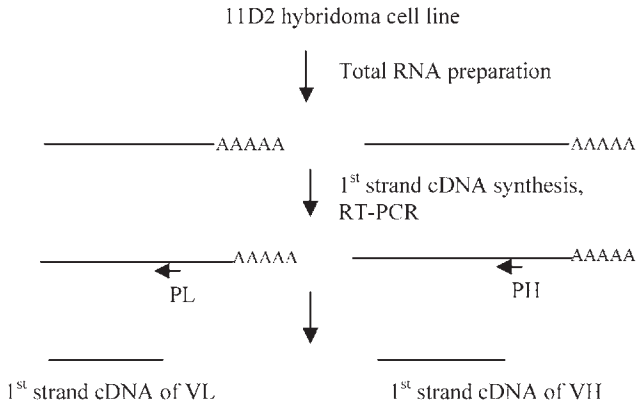
PL: 5' CTC ATT CCT GTT GAA GCT CTT GAC 3'
PH: 5' CTC AAT TTT CTT GTC CAC CTT GGT GC 3'

B

P1   P3
→   →
VL   P2   CL   VH   P4   CH1

↓ PCR Amplification of VL   ↓ PCR Amplification of VH

————————   ————————
VL   VH
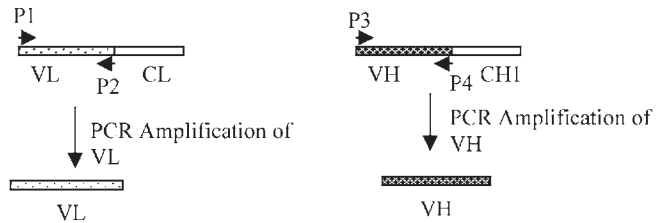
P1: 5' ATT AAT TCG **GAT CCC** GAC ATT GTG CTG ACA CAG TCT CCT 3'
P2: 5' AGC CCG TTT TAT TTC CAA CTT GGT 3'
P3: 5' GAG GTG CAG CTG GTG GAG TCT GGG 3'
P4: 5' C TAG AAA GCT **GGC GGC CGC** TGA GGA GAC GGT GAC CGT GGT CCC 3'

Fig. 2. **(A)** First strand cDNA synthesis. **(B)** Amplification of VL and VH.

3.2.2.3. Reengineering of ScFv to ScFv-Biotin Mimic Tag

1. Transfer a small aliquot of assembled ScFv (1 μL) to a new PCR mixture containing 0.5 μ*M* of P1 and P6 primers, 200 μ*M* dNTPs, 1 unit vent DNA polymerase and 5 μL 10X PCR buffer in a 50-μL volume (**Fig. 2D**) and continue amplification at 94°C/60°C/72°C, 45 s/45 s/45 s for 25 more cycles. At the beginning of the first cycle, incubate for 3 min at 94°C, and at the end of the last cycle, incubate for 7 min at 72°C *(33)* (*see* **Note 18**).

C
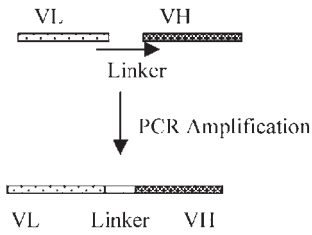
Linker (P5) : 5' ACC AAG TTG GAA ATA AAA CGG GCT **GGA GGT GGC GGA TCA GGA GGC GGA GGT TCT GGC GGA GGT GGG AGT** GAG GTG CAG CTG GTG GAG TCT GGG 3'

D
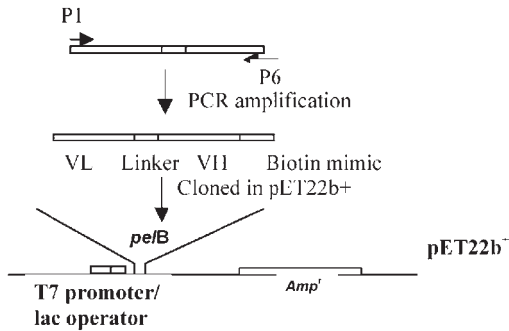
Biotin mimic: 5' CCA TGC CAT CCG CAG TTC CCA CGA TGT TAT GCG 3'
             Pro   Cys   His   Pro   Gln   Phe   Pro   Arg   Cys   Tyr   Ala

P6: 5' ATG ATG ATG **GTC GAC** *TCA* CGC ATA ACA TCG TGG GAA CTG CGG ATG GCA TGG G**GC GGC CGC** TGA GGA GAC GGT GAC CGT GGT CCC 3'

Fig. 2. **(C)** Assembly of VL and VH. **(D)** Incorporation of Biotin Mimic tag.

2. Analyze the amplified product by 1% agarose/TAE gel and purify bifunctional ScFv band from the gel by QIAquick gel extraction kit.
3. Digest the purified bifunctional ScFv fragment with *BamH*I and *Sal*I.
4. Digest *E. coli* expression vector pET22b+ with *BamH*I and *Sal*I, and purify from gel as described above (*see* **Note 19**).

3.2.2.4. LIGATION AND TRANSFORMATION

1. Analyze both purified insert (bifunctional ScFv) and vector by 1% agarose/TAE gel.
2. Perform ligation of bifunctional ScFv with vector by mixing 2 μL 10X ligase buffer, 50 ng vector DNA, 50 ng insert DNA, 1 unit T4 DNA ligase in a 20-μL volume.
3. Incubate the ligation mixture at room temperature for 1 h or at 14°C overnight.
4. Increase the ligation mixture volume up to 50 μL with sterile water and inactivate T4 DNA ligase at 65°C for 10 min.
5. Add 500 μL *n*-butanol to precipitate the DNA and isolate by centrifugation at 12,000*g* for 10 min at room temperature. Redissolve precipitated DNA in 5 μL sterile water.
6. Use 2 μL of the redissolved ligation mixture to transform 40 μL freshly prepared Top10F' *E. coli* competent cells by electroporation (*E. coli* Pulser, Bio-Rad) (*see* **Note 20**).
7. Add 1 mL SOC medium and incubate at 37°C in incubator shaker for 1 h.
8. Plate 100 μL of the culture in LB plate containing 100 μg/mL carbenicillin and incubate in a 37°C incubator for 16 h (overnight).

3.2.2.5. SCREENING OF RECOMBINANT CLONES
AND TRANSFORMATION IN *E. COLI* EXPRESSION HOST

1. Pick single colonies and grow overnight at 37°C in 2–3 mL LB medium containing 100 μg/mL carbenicillin.
2. Isolate DNA from individual recombinant clones by QIAprep plasmid DNA isolation kit. Digest plasmid DNA by *BamH*I + *Sal*I enzymes and analyze by 1% agarose/TAE gel electrophoresis.
3. Select correctly oriented clones by restriction digestion fragment mapping for expression studies.
4. Transform plasmid containing the 11D2-biotin mimic ScFv in *E. coli* BL21 (DE3) competent cells by heat shock method (*see* **Note 21**).
5. Inoculate an overnight fresh colony of *E. coli* BL21 (DE3) transformants into 5 mL LB medium containing 100 μg/mL carbenicillin and shake at 250 rpm in a 37°C incubator until OD at 600 nm reaches 0.4–0.5 (*see* **Note 22**).
6. Induce bacterial culture by adding 1 m*M* IPTG and allow to grow at 30°C for 3 h.
7. Harvest the bacterial culture by centrifugation at 4000*g* for 10 min at 4°C and isolate total cell protein by treating 1 mL bacterial pellet with sample buffer (50 m*M* Tris (pH 6.8), 100 m*M* DTT, 2% SDS, 0.1% bromophenol blue, 10% glycerol) at 95°C for 5 min.
8. Analyze total cell protein by SDS-PAGE (**Fig. 3A**) using 10% polyacrylamide geland proceed according to Laemmli *(34)* with a Mini Protean II apparatus (Bio-Rad).
9. Stain protein gels with Coomassie Brilliant Blue R-250 (0.25 g of Coomassie Brilliant Blue R250 in 45 mL of methanol, 10 mL of acetic acid, and 45 mL of water) and destain with 10% acetic acid and 30% methanol. Visually look for the expected protein band at approx 32 kDa upon induction with IPTG and its corresponding absence in uninduced culture.

3.2.2.6. WESTERN BLOT ANALYSIS OF EXPRESSED 11D2-BIOTIN MIMIC SCFV

1. Electrophoretically separate total cell protein on SDS-PAGE using 10% polyacrylamide gel and transfer onto an ECL Hybond nitrocellulose membrane *(35)* using Trans blot apparatus (Bio-Rad) following manufacturer's instructions.
2. Block the membrane with 5% skim milk in PBST for 2 h.
3. Wash the membrane four times with PBST and react with streptavidin-HRPO (1:1,000 in 1% dialyzed BSA) for 1 h.
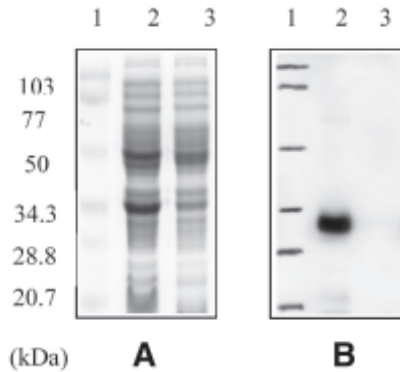
Fig. 3. Total cell protein of induced and uninduced bacterial culture sepdartated on SDS-PAGE and stained with Coomassie Brillant Blue (**A**). Western Blot probed with streptavidin-HRPO (**B**). Lane 1: St. mol wt markers; lane 2: induced with IPTG; lane 3: uninduced.

4. Finally, wash the membrane four times with PBST and perform enhanced chemiluminescent (ECL)-based detection (**Fig. 3B**) according to manufacturer's instructions (Amersham Pharmacia, Piscataway, NJ).

3.2.2.7. SEQUENCE ANALYSIS

1. Conduct DNA sequencing analysis of the functional clone.
2. Compare the deduced DNA sequence with Kabat Database (*see* Website: http://immuno. bmc.nwu.edu).

3.2.3. Protein Extraction

The steps described here in **Subheadings 3.2.3.1.** and **3.2.3.3.** outline the stepwise procedure for isolation of soluble protein and insoluble protein from 250 mL induced *E. coli* culture.

3.2.3.1. SOLUBLE PROTEIN

1. Suspend the bacterial pellet in 5% of culture volume of periplasmic extraction buffer (50 m*M* Tris [pH 8.0], 20% sucrose, 1 m*M* EDTA [pH 8.0]) and incubate on ice for 45 min with occasional shaking.
2. Centrifuge the suspension at 11,000*g* for 15 min at 4°C and collect supernatant as periplasmic soluble protein.
3. Resuspend the pellet in 5 mL of lysis buffer, 0.1 mg/mL lysozyme, and incubate for 30 min on ice with occasional shaking.
4. Homogenize the suspension by sonication (6 × 10 s) and centrifuge at 11,000*g* for 15 min at 4°C. Collect the supernatant as the cytoplasmic soluble protein and the pellets as the insoluble fraction.
5. Use the insoluble fraction to isolate inclusion bodies of the expressed protein.
6. Analyze the cytoplasmic and periplasmic soluble proteins by SDS-PAGE.
7. Perform Western blot as described earlier in **Subheading 3.2.2.6.**

3.2.3.2. Isolation of Inclusion Bodies

1. Resuspend the insoluble fraction in 3–5 mL lysis buffer, incubate at room temperature for 15 min, and repeat sonication (6 × 10 s) (*see* **Note 23**).
2. Adjust the sample to 2% sodium deoxycholate and mix well by inversion.
3. Incubate the sample at room temperature for 30 min and centrifuge at 11,000*g* for 30 min at 4°C.
4. Remove the supernatant and further wash pellet twice at 11,000*g* for 20 min at 4°C with 3 mL lysis buffer.
5. Estimate the purity of the inclusion bodies by SDS-PAGE using 10% polyacrylamide gel under reducing conditions.

3.2.4. Protein Refolding

Here we describe different steps of how to perform proper refolding that yields significant amounts of soluble functional protein (*see* **Note 24**).

3.2.4.1. Refolding of the 11D2-Biotin Mimic ScFv

1. Solubilize inclusion bodies by suspending in 100 mL 2% sarcosyl, 50 m*M* Tris (pH 10.0), and stirring at room temperature for 2 h.
2. Perform air oxidation by continued stirring of the sample in the presence of 50 μ*M* CuSO$_4$ for 20 h at room temperature.
3. Add solid urea to the sample to make a final concentration of 6 *M*. Remove sarcosyl from the sample by absorption twice with 10% Dowex 1X8. Prepare Dowex 1X8 200–400 mesh (Bio-Rad) by sequential washings in 1 *M* NaOH, water, 4 *M* acetic acid, water, 50 m*M* Tris (pH 10.0), and equilibrate in 6 *M* urea, 50 m*M* Tris (pH 8.0) *(36)*.
4. Upon removal of the sarcosyl, determine the protein concentration by the Bradford assay *(37)* (*see* **Note 25**).
5. Adjust solubilized denatured protein to 100 μg/mL in refolding buffer and dialyze over a period of 3 d with three changes.
6. Finally, dialyze the sample against 50 m*M* Tris-HCl (pH 8.0) for 48 h at 4°C.
7. Upon completion of dialysis, remove any aggregates by centrifugation at 8000*g* for 10 min at 4°C and determine protein concentration by Bradford method.

3.2.5. Characterization

The refolded and purified ScFv can be tested for its activity toward the WEE antigen by ELISA.

3.2.5.1. ELISA

1. Direct solid phase ELISA is performed by coating WEE antigen on a Nunc Maxisorb ELISA plate.
2. Coat wells at 4°C overnight with inactivated WEE antigen *(38)* (400 ng/well) or 1% dialyzed BSA as negative control in PBS.
3. Wash the plate three times with 200 μL of PBST and block with 200 μL of 1% BSA for 2 h at room temperature.
4. Subsequently wash the plate as described above and react with different concentrations of refolded 11D2-biotin mimic ScFv or irrelevant antibody as negative control (100 μL/well) for 2 h at room temperature.

5. Wash the plate and incubate 1 h with St-HRPO (1:1000 in 1% dialyzed BSA, 100 μL/well) or GAM-HRPO (1:10,000 in 1% dialyzed BSA, 100 μL/well) for negative control (*see* **Note 26**).

6. Following a final wash with PBST, develop the color by adding 100 μL of TMB peroxidase substrate to each well and read OD at 650 nm within 20–30 min using an ELISA plate reader.

3.2.6. Factors Influencing In Vitro Refolding

The mechanism of refolding of antibodies is similar to that of other proteins containing disulfide bonds *(39–41)*. The disulphide bond formation is promoted while minimizing aggregate formation. Urea and guanidine-HCl are the most commonly used denaturants to solubilize the inclusion bodies. However, it has been reported that treatment with mild detergent can also be used to solubilize inclusion body protein *(36,42)*. In addition, reducing agents such as β-mercaptoethanol or dithiothreitol (DTT) are used to reduce inter- or intra-chain disulphide bonds that might have formed during lysis of the bacteria and during solubilization of the inclusion bodies. In some cases, promotion of the correct disulfide bond formation is enhanced by the presence of metal ions or inclusion of redox coupling reagents, made of a mixture of reduced and oxidized thiol groups *(43)*. It has been recognized that protein folding, formation of disulphide bonds, and proper association of different domains are very much dependent on folding conditions *(44,45)*. Every protein species is unique in nature, and a refolding protocol for each needs to be optimized. There is no universal renaturation protocol that can be used for all recombinant proteins *(46)*.

4. Notes

1. Prepare 50 mL of SFDMEM medium with two different pH values of 6.8 and 7.4. Filter sterilize the medium and resuspend respective cell lines in two different media. pH of the medium is important for proper labeling by the fluorescent dye.

2. This cell-labeling protocol was similar to a previously described method *(25)*, with some modifications.

3. Remove medium by aspiration and mix gently to resuspend the cells.

4. This is a modified fusion protocol using PEG. Instead of electrofusion, we optimized the condition for generation of quadroma using PEG fusion, which is less time consuming and more efficient.

5. Do not spin the fused cells more than 800 rpm (114*g*), as cells are loosely attached to each other. Subsequent washing steps are also performed at 800 rpm (114*g*).

6. Keep proper controls (unlabeled, singly labeled cells) to select the dual fluorescence cells.

7. Testing neat and diluted supernatant is essential to mitigate inhibition by monospecific antibodies. It is very common to see higher ELISA activity in the diluted vs neat supernatants.

8. Quadromas are fused products of two hybridomas. The high ploidy levels of these cells require recloning more times to isolate a good cell line that is stable.

9. HRPO with a heme cavity in its substrate binding site has affinity for BHA. If a specific affinity ligand is not readily available, an immunopurification strategy using sepharose linked with specific heavy- or light-chain reactive antibodies (Sigma) can be used to purify only the bispecific molecules.

10. Purification of bsMAb-HRPO complex by BHA agarose will also co-purify monospecific antibodies directed towards HRPO. However, the co-purified contaminants and free excess HRPO should be of little concern, as they will not bind to the target antigen and will be eliminated in any subsequent wash steps.

11. All mRNA isolation reagents were prepared with 0.1% DEPC-treated autoclaved water.

12. A_{260} of 1 is equivalent to 40 µg/mL of RNA. Good quality RNA yields A_{260}/A_{280} of 1.8–2.0.

13. RNA can be stored at –70°C in DEPC-treated water.

14. Instead of total RNA, mRNA can be used for first strand cDNA synthesis. Poly A+-containing transcripts can be purified from total RNA by oligo (dT) beads, which are commercially available.

15. It is not necessary to precipitate cDNA. Samples from the RT reaction mixture can be used directly as template for PCR. Degenerate primers for VH and VL can be generated according to *(47–51)*.

16. EtBr is carcinogenic. Wear gloves and take precautions during agarose gel electrophoresis.

17. Measure A_{260} of the PCR-purified DNA. A_{260} of 1 is equivalent to 50 µg/mL of DNA. Linker oligo is designed in such a way that there are 24-base overlaps both at the 3' end of VL and the 5' end of VH.

18. Biotin mimic oligo is synthesized according to *(33)* and cloned at the 3' end of ScFv by PCR.

19. Digest isolated PCR products and vector DNA with restriction endonucleases suitable for cloning.

20. Electroporation was done in a 0.1-cm cuvette at 180 kV.

21. Preparation of chemical-competent cells of *E. coli* BL21 (DE3) and transformation were done according to *(32)*.

22. It has been observed that the pET22b+ expression vector in *E. coli* BL21 (DE3) cells can be unstable. Therefore, instead of expressing the ScFv from a frozen glycerol stock of transformed *E. coli* BL21 (DE3) cells, transformation of the *E. coli* BL21 (DE3) cells may have to be performed by the heat-shock method just prior to scaling up for expression.

23. Alternative method to isolate the inclusion bodies from *E. coli* is the use of a French Press.

24. In our protocol, urea was used to denature the inclusion bodies, but 4–6 *M* guanidine hydrochloride can also be used. We have discussed different issues in **Subheading 3.3.5.**, which should be considered during refolding of inclusion bodies.

25. For protein estimation, use the Bradford dye-binding assay, because it is very fast, sensitive, and easy to use.

26. Ensure that stock streptavidin-HRPO is diluted in extensively dialyzed BSA to remove traces of free biotin, which dampens the signal.

Acknowledgments

References

1. White., C. A., Weaver, R. L., and Grillo-Lopez, A. J. (2001) Antibody-targeted immunotherapy for treament of malignancy. *Annu. Rev. Med.* **52,** 125–145.

2. Kohler, G. and Milstein, C. (1975) Continuous cultures of fused secreting antibody of redefined specificity. *Nature* **256,** 495–497.

3. Winter, G. and Milstein, C. (1991) Man-made antibodies. *Nature* **349,** 293–299.
4. Pluckthun, A. and Pack, P. (1997) New protein engineering approaches to multivalent and bispecific antibody fragments. *Immunotechnology* **3,** 83–105.
5. Bird, R. E., Hardman, K. D., Jacobson, J. W., et al. (1988) Single-chain antigen-binding proteins. *Science* **242,** 423–426.
6. Huston, J.S., Levinson, D., Mudgett-Hunter, M., et al. (1988) Protein engineering of antibody binding sites: recovery of specific activity in an anti-digoxin single-chain Fv analogue produced in *Escherichia coli. Proc. Natl. Acad. Sci. USA* **85,** 5879–5883.
7. Nisonoff, A. and Rivers, M. M. (1961) Recombination of a mixture of univalent antibody fragments of different specificity. *Arch. Biochem. Biophys.* **93,** 460–462.
8. Kriangkum, J., Xu, B., Nagata, L. P., Fulton, R. E., and Suresh, M. R. (2001) Bispecific and bifunctional single chain recombinant antibodies. *Biomol. Eng.* **18(2),** 31–40.
9. Suresh, M. R., Cuello, C., and Milstein, C. (1986) Advantages of bispecific hybridomas in one-step immunocytochemistry and immunoassays. *Proc. Natl. Acad. Sci. USA* **83,** 7989–7993.
10. Cao, Y., Christian, S., and Suresh, M. R. (1998) Development of bsMAb anti-biotin x anti-HRPO as a universal immunoprobe for detecting biotinylated macromolecules. *J. Immunol. Methods* **220,** 85–91.
11. Van Ojik, H. H. and Valerius, T. (2001) Preclinical and clinical data with bispecific antibodies recruiting myeloid effector cells for tumor therapy. *Crit. Rev.Oncol. Hematol.* **38,** 47–61.
12. Withoff, S., Helfrich, W., de Leij, L. F. M. H., and Molema, G. (2001) Bi-specific antibody therapy for the treatment of cancer. *Curr. Opin. Mol. Ther.* **3,** 53–62.
13. Talac, R. and Nelson, H. (2000) Current perspectives of bispecific antibody-based immunotherapy. *J. Biol. Regul. Homeost. Agents* **14,** 175–181 .
14. van Spriel, A. B., van Ojik, H. H., and van De Winkel, J. G. (2000) Immunotherapeutic perspective for bispecific antibodies. *Immunol. Today* **21,** 391–397.
15. Kroesen, B. J., Helfrich, W., Molema, G., and de Leij, L. (1998) Bispecific antibodies for treatment for of cancer in experimental animal models and man. *Adv. Drug. Deliv. Rev.* **31,** 105–129.
16. Wang, H., Liu, Y., Wei, L., and Guo, Y. (2000) Bi-specific antibodies in cancer therapy. *Adv. Exp. Med. Biol.* **465,** 369–380.
17. Koelemij, R., Kuppen, P. J., van de Velde, C. J., Fleuren, G. J., Hagenaars, M., and Eggermont, A. M. (1999) Bispecific antibodies in cancer therapy, from the laboratory to the clinic. *J. Immunotherapy* **22,** 514–524.
18. Segal, D. M., Weiner, G. J., and Weiner, L. M. (1999) Bispecific antibodies in cancer therapy. *Curr. Opin. Immunol.* **11,** 558–562.
19. Cao, Y. and Lam, L. (2003) Bispecific antibody conjugates in therapeutics. *Adv. Drug. Deliv. Reviews***55,** 171–197.
20. Cao, Y. and Suresh, M. R. (1998) Bispecific antibodies as novel bioconjugates. *Bioconjugate Chemistry* **9 (8),** 635–644.
21. Milstein, C. and Cuello, A. C. (1983) Hybrid hybridomas and their use in immunohistochemistry. *Nature* **305,** 537–540.
22. Nolan, O. and Kennedy, O. R. (1990) Bifunctional antibodies: concept, production and applications. *Biochem. Biophys. Acta* **1040,** 1–11.
23. Karawajew, L., Behrsing, O., Kaiser, G., and Micheel, B. (1988) Production and ELISA application of bispecific monoclonal antibodies against fluorescein isothiocyanate (FITC) and horseradish peroxidase (HRP). *J. Immunol Methods* **111,** 95–99.

24. Karawajew, L., Micheel, B., Behrsing, O., and Gaestel, M. (1987) Bispecific antibody-producing hybrid bybridomas selected by a fluorescence activated cell sorter. *J. Immunol Methods* **96,** 265–270.

25. Kreutz, F. T., Xu, D. Z., and Suresh, M. R. (1998) A new method to generate quadromas by electrofusion and FACS sorting. *Hybridoma* **17,** 267–273.

26. Gupta, S. and Suresh, M. R. (2002) Affinity chromatography and co-chromatography of bispecific monoclonal antibody immunoconjugates. *J. Biochem. Biophys. Methods* **51,** 203–216 .

27. Husereau, D. R. and Suresh, M. R. (2001) A general affinity method to purify peroxidase-tagged antibodies. *J. Immunol. Methods* **249 (1–2)**, 33–41.

28. de Ropp, J. S., Mandal, P. K., and La Mar, G. N. (1999) Solution 1H NMR investigation of the heme cavity and substrate binding site in cyanide-inhibited horseradish peroxidase. *Biochemistry* **38,** 1077–1086.

29. Kabat, E. A., Wu, T. T., Perry, H. M., Gottesman, K. S., and Foeller, C. (1991) *Sequences of Proteins of Immunological Interest*, 5th Ed., U.S. Department Health and Human Services, Public Health Service, National Institute of Health, Publication No. 81-3242.

30. Orlandi, R., Gussow, D. H., Jones, P. T., and Winter, G. (1989) Cloning immunoglobulin variable domains for expression by the polymerase chain reaction. *Proc. Natl. Acad. Sci. USA* **86,** 3833–3837.

31. Xu, B., Kriangkum, J., Nagata, L. P., Fulton, R. E., and Suresh, M. R. (1999) A single chain Fv specific against western equine encephalitis virus. *Hybridoma* **18(4),** 315–323.

32. Sambrook, J., Fritsch, E. F., and Maniatis, T. (1989) *Molecular Cloning: A Laboratory Manual*. Cold Spring Harbor Laboratory Press, Cold Spring Harbor, NY.

33. Luo, D., Geng, M., Schultes, B., et al. (1998) Expression of a fusion protein of scFv-biotin mimetic peptide for immunoassay. *J. Biotechnol.* **65,** 225–228.

34. Laemmli, U.K. (1970) Cleavage of structural proteins during the assembly of the head of bacteriophage T4. *Nature* **277,** 680–685.

35. Towbin, H., Staehelin, T., and Gordon, J. (1979) Electrophoretic transfer of proteins from polyacrylamide gels to nitrocellulose sheets. *Proc. Natl. Acad. Sci. USA* **76,** 4350–4354.

36. Kurucz, I., Titus, J. A., Jost C. R., and Segal. D. M. (1995) Correct disulfide pairing and efficient refolding of detergent-solublilized single chain Fv proteins from bacterial inclusion bodies. *Molecular Immunology* **32 (17/18)**, 1443–1452.

37. Bradford, M. M. (1976) A rapid and sensitive method for the quantitation of microgram quantities of protein utilizing the principle of dye binding. *Anal. Biochem.* **72,** 248–254.

38. Long, M. C., Jager, S., Mah, D. C. W., et al. (2000) Construction and characterization of a novel recombinant single-chain variable fragment antibody against western equine encephalitis virus. *Hybridoma* **19(1),** 1–13.

39. Rudolph, R. (1990) Renaturation of recombinant disulfide -bonded protein from "inclusion bodies." In: *Modern Methods in Protein and Nucleic Acid Research*. Tschesche, H., ed., Walter de Druyter, Berlin, Germany, pp. 149–171.

40. Buchner, J. and Rudolph, R. (1991) Renaturation, purification and characterization of recombinant Fab-fragments produced in *Escherichia coli. Biotechnology* **9(2),** 157–162.

41. Buchne, J., Pastan, I., and Brinkmann, U. (1992) A method for increasing the yield of properly folded recombinant fusion proteins: single-chain immunotoxins from renaturation of bacterial inclusion bodies. *Anal. Biochem.* **205(2)**, 263–270.

42. Lacks, S. A. and Springhorn, S. S. (1980) Renaturation of enzymes after polyacrylamide gel electrophoresis in the presence of sodium dodecyl sulphate. *J. Biol. Chem.* **255,** 7467–7473.

43. Saxena, V. P. and Wetlaufer, D. B. (1970) Formation of three-dimensional structure in proteins. I. Rapid nonenzyme reactivation of reduced lysozyme. *Biochemistry* **9(25),** 5015–5023.

44. Suttnar, J., Dyr, J. E., Hamsikova, E., Novak, J., and Vonka, V. (1994) Procedure for refolding and purification of recombinant proteins from *Eschrichia coli* inclusion bodies using a strong anion exchanger. *J. Chromatogr. B* **656,** 123–126.

45. Wei, C., Tang, B., Zhang, Y., and Yang, K. (1999) Oxidative refolding of recombinant prochymosin. *Biochem. J.* **340,** 345–351.

46. Verma, R., Boleti, E., and George, A. J. T. (1998) Antibody engineering: Comparison of bacterial, yeast, insect and mammalian expression system. *J. Immunol. Methods* **216,** 165–181.

47. Clark, A.M. (2002) Standard protocols for the construction of Fab libraries. In: *Methods in Molecular Biology, vol. 178: Antibody Phage Display: Methods and Protocols.* O'Brien, P. M., and Aitken, R., eds. Humana, Totowa, NJ, pp. 39–58.

48. Dziegiel , M., Nielsen, L, K., Adersen, P. S., Blancher, A., Dickmeiss, E., and Engber, J. (1995) Phage display used for gene cloning of human recombinant antibody against the erythrocyte surface antigen, rhesus D. *J. Immunol. Methods* **182(1)**, 7–19.

49. Marks, J. D., Tristem, M., Karpas, A., and Winter, G. (1991) Oligonucleotide primers for polymerase chain reaction amplification of human immunoglobulin variable genes and design of family-specific oligonucleotide probes. *Eur. J. Immunol.* **21(4),** 985–991.

50. Kettleborough, C. A., Saldanha, J., Ansell, K. H., and Bendig, M. M. (1993) Optimization of primers for cloning libraries of mouse immunoglobulin genes using the polymerase chain reaction. *Eur. J. Immunol.* **23(1),** 206–211.

51. Burton, D. R. and Barbas, C. F. (1994) Human antibodies from combinatorial libraries. *Adv. Immunol.* **57,** 191–280.

23

Antibody–Cytokine Fusion Proteins for the Therapy of Cancer

Gustavo Helguera and Manuel L. Penichet

Summary

In recent years the development of tumor-specific recombinant antibodies fused to immuno-stimulatory cytokines such as interleukin-2 (IL-2), interleukin-12 (IL-12), and granulocyte/mac-rophage colony-stimulating factor (GM-CSF) has provided a promising novel approach to cancer immunotherapy. The combined properties of specific targeting of antibodies and the immune stimulation of cytokines results in high cytokine concentration in the tumor microenvironment, and as a consequence, in an improved tumoricidal activity of the antibody and/or in a secondary effective immune response against the tumor. In the present chapter we describe strategies for the construction, expression, and in vitro characterization of antibody–cytokine fusion proteins, with particular emphasis on antibody/IL-2 fusion proteins.

Key Words: Antibody engineering; antibody therapy; antibody; cancer; constant region; cytokine; expression vector fusion protein; IgG3; HER2/*neu*; immunocytokine; immunoglobulin; immunoligand; immunotherapy; interleukin-2; tumor targeting; variable region.

1. Introduction

Progress in genetic engineering and expression systems has led to the development of tumor-specific antibodies fused to immunostimulators, such as the cytokines interleukin (IL)-2, IL-12, and granulocyte/macrophage colony-stimulating factor (GM-CSF) *(1,2)*. The goal of using these tumor-specific antibodies is to concentrate the cytokines in the tumor microenvironment and enhance the tumoricidal activity of the antibody and/or the host immune response against the tumor while limiting the severe toxicity associated with high doses of cytokines. These antibody–cytokine fusion proteins, also called *immunocytokines* or *immunoligands (1,3)*, have shown significant antitumor activity in mice bearing tumors leading to clinical trials *(4–11)*.

Antibodies or immunoglubulins (Igs) are hetero-tetramers comprised of two identical light chain (L chain) and heavy chain (H chain) polypeptides held together by disulfide bonds (H_2L_2) (**Fig. 1**). The antigen-binding variable region (V-region) is formed by the amino-terminal domains of both the H (V_H) and L chain (V_L). The other domains of the H and L chains show much less variability and constitute the constant region (C-region).
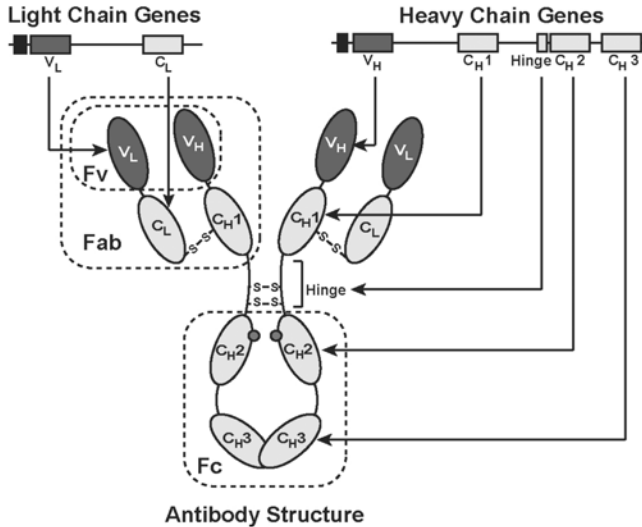
Fig. 1. Schema of an immunoglobulin G (IgG) molecule and the genes that encode its H and L chains. The genes encoding for IgG are represented on the top of the figure. Boxes represent exons encoding for discrete domains. The central line represent introns that are present in the primary transcript but not in the mature mRNA. Both H and L chains contain hydrophobic leader sequences (indicated by the black exon) necessary for their processing and secretion. The H chain is divided into four discrete functional domains (V_H, C_H1, C_H2, and C_H3), while the L chain consists of two domains (V_L and C_L). The V region domains form the Fv region, which is responsible for antigen binding. The C-region domains are responsible of the effector functions of the antibody. The C_H2 domains present glycosylation sites (dark circles) that contribute to the functional properties of the antibody. The hinge region provides flexibility to the molecule. The fragments product of the papain enzyme cleavage are also indicated: two Fab (responsible for antigen binding) and one Fc (responsible of the effector functions).

Variations in the H chain C region characterize different isotypes and define five classes of human antibodies: IgA (α chain), IgD (δ chain), IgG (γ chain), IgE (ε chain), and IgM (μ chain). In humans, IgG is the most abundant immunoglobulin present in serum, with four subclasses: IgG1, IgG2, and IgG4, exhibiting a mol wt of approx 150 kDa, and IgG3, exhibiting a mol wt of approx 165 kDa *(12)*. Differences in the C_L region result in two L-chain isotypes, κ and λ. The domains after the hinge of the C region form the Fc region, which is responsible for the antibody-related effector functions such as antibody-dependent cellular cytotoxicity (ADCC) and complement-dependent cytotoxicity (CDC) *(4,5,13,14)*. The Fc region also binds the FcRn (Brambell receptor) that results in an extended half-life in serum *(15,16)*. The domain structure of antibodies facilitates protein engineering, allowing the separation of their different functional regions and the genetic fusion of nonantibody molecules in different positions of the antibody molecule (**Fig. 2**). The nonantibody partner can be fused at the carboxy-terminus (C-terminus)
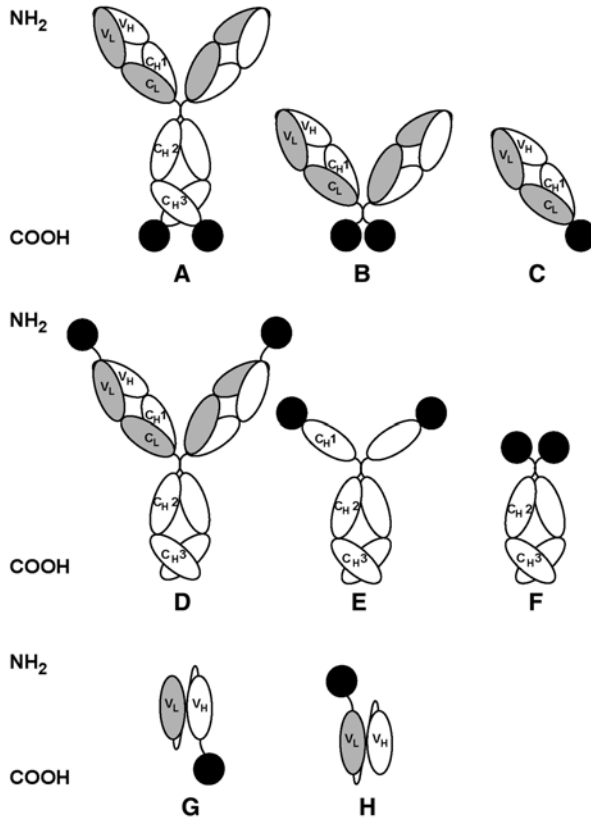
Fig. 2. Construction of antibody fusion proteins with the nonantibody partner or ligand fused to different regions of the H chain. Panels A, B, and C show C-terminus fusion proteins with the nonantibody partner (represented as a black circle) fused after the C_H3 domain (**A**), after the hinge (**B**), or after the C_H1 domain (**C**). Panels D, E, and F denote antibody fusion proteins with the ligand fused to the N-terminus of the complete H chain (**D**), the C_H1 domain (**E**), or immediately before the hinge (**F**). Panels G and H show scFv fragments with the ligand fused to the C-terminus (**G**) or N-terminus (**H**).

(**Fig. 2A,B,C**) or at the amino-terminus (N-terminus) of the H chain (**Fig. 2D,E,F**) or the L chain (not shown). In some cases, the nonantibody partner can be fused via a flexible linker, depending on the specific requirements of conformation, processing, or accessibility to the antigen or the cytokine receptor *(17–21)*. When the cytokine is fused to an intact antibody (**Fig. 2A,D**), the antibody–cytokine fusion protein can deliver both the biological activity associated with the genetically fused cytokine, and the antibody effector functions. Fusion of the ligand immediately after the hinge (H-ligand) (**Fig. 2B**) or to the C_H1 domain (C_H1-ligand) (**Fig. 2C**) results in a loss of antibody effector function. This may be useful when the Fc effector functions are unnecessary or harmful.

In addition, for many applications such as targeting well-established solid tumors, the small size of H-ligand and C_H1-ligand may be an advantage over the larger C_H3-ligand (3). The smallest antibody fragments, known as scFv fragments, are composed of the variable domains of H and L chains fused by a synthetic flexible linker peptide. Cytokines can also be fused to both the C- and N-terminus of scFv (**Fig. 2G,H**) (20,21). Alternatively, cytokines can replace the V_H domain or the V_H-C_H1 domains (**Fig. 2E,F**) of the antibody. Such molecules lose the ability to bind antigen but retain the antibody Fc effector properties and possess improved pharmacokinetics (22,23).

Multiple expression systems have been used for antibody production in bacteria, yeast, plants, baculovirus, insect cells, and mammalian cells (24–26). Each system has advantages and shortcomings, depending on the characteristics and expected use of the protein. Bacteria and yeast have been successfully used to express scFv antibody fragments, and complete functional antibodies have been expressed in plant and insect cells (24,25,27). However, mammalian cells have been the most effective in expressing full-length, functional recombinant antibodies and antibody fusion proteins, since these cells possess the machinery necessary for the correct assembly, post-translational modification, and secretion of these proteins (26).

In recent years, the field of antibody–cytokine fusion proteins has expanded to include a variety of cytokines fused to antibodies of different structures (1,2), making it virtually impossible to cover protocols about the construction, expression, and characterization of every antibody-cytokine fusion protein. Among this family of recombinant proteins, antibody/IL-2 fusion proteins have been the best characterized and most broadly used in successful antitumor experiments. In this chapter, we describe the methods for the construction, expression, and in vitro characterization of antibody fusion proteins, using as an example a well-studied human IgG3/IL-2 fusion protein developed in our laboratory (28) specific for the human tumor-associated antigen HER2/neu. However, it is important to stress that similar procedures can be applied to many combinations of antibodies and cytokines.

2. Materials

2.1. Construction of Antibody–Cytokine Fusion Proteins

2.1.1. Cloning of the V Region Sequence into the Antibody Expression Vectors

1. Mammalian expression vectors for human L- and H-chain C regions (pAG4622 and pAH4802) (34).
2. Primers 5' and 3' to amplify the DNA encoding for H- and L-chain V regions.
3. PCR equipment (PTC 100 Thermal Controller; M. J. Research, Watertown, MA).
4. *Taq*-DNA polymerase and reaction buffers (New England Biolabs, Beverly, MA).
5. TA cloning vector (Invitrogen, Carlsbad, CA).
6. Restriction endonucleases: *Eco*RV, *Nhe*I, *Sal*I, and reaction buffers (New England Biolabs).
7. T4 DNA ligase and reaction buffers (New England Biolabs).
8. Additional equipment and reagents for agarose gel electrophoresis, transforming *E. coli*, minipreps, restriction endonuclease digestion, and purification of DNA restriction fragments.

2.1.2. Construction of the Antibody–Cytokine Fusion Protein

1. Jurkat cells (American Type Culture Collection [ATCC], Rockville, MD).
2. Primers 5' and 3' to amplify the cDNA encoding for mature form of human IL-2.
3. Avian myeloblastosis virus (AMV) reverse transcriptase and reaction buffers (New England Biolabs).
4. Mammalian expression vectors for human L chain and H chain with desired V regions.
5. TA cloning vector (Invitrogen).
6. Intermediate cloning vector (pAT3462) *(29)*.
7. Restriction endonucleases: *Eco*RV, *Nhe*I, *Sal*I, *Bam*HI, *Ssp*I, *Nsi*I, *Eco*RI, *Pml*I, and reaction buffers (New England Biolabs).
8. T4 DNA ligase and reaction buffers (New England Biolabs).

2.2. Transfection into Expression Systems and Initial Characterization

2.2.1. Transfection into Mammalian Expression System

1. Mammalian expression vectors encoding for human L and H chains fused to the cytokine.
2. *Pvu*I restriction endonuclease and reaction buffers (New England Biolabs).
3. Recipients of transfection: murine myeloma cell lines such as Sp2/0-Ag14, P3X63 Ag8.653, or NS0/1 (ATCC).
4. Phosphate-buffered saline (PBS): 154 mM NaCl, 1.9 mM NaH$_2$PO$_4$, 8.1 mM Na$_2$HPO$_4$, pH 7.2.
5. Bio-Rad Gene Pulser Electroporator and 0.4-cm gap electroporation cuvet (Bio-Rad Laboratories, Hercules, CA).
6. Iscoves modified Dulbecco's medium (IMDM) (Irvine Scientific, Irvine, CA), supplemented with 2 mM L-glutamine, 10 U/mL penicillin, and 10 µg/mL streptomycin (Sigma Chemical, St. Louis, MO).
7. Growth medium: 10% calf serum (Atlanta Biologicals, Norcross, GA), 0.1 mg/mL gentamycin, 100 U/mL nystatin suspension (Sigma Chemical) in IMDM.
8. Selection medium: 10% calf serum, selection marker (histidinol or HXM) in IMDM.
9. One M histidinol in 0.1 M HEPES, pH 7.4 (Sigma Chemical).
10. HXM stock 30X: 3.75 mg/mL hypoxanthine, 225 µg/mL xanthine, and 90 µg/mL mycophenolic acid (Sigma Chemical).
11. Ninety-six-well tissue-culture flat-bottom plates (Falcon; Becton-Dickinson, Lincoln Park, NJ).

2.2.2. Enzyme-Linked Immunosorbent Assay (ELISA) Screening

1. Ninety-six-well flat-bottom microtiter plates (Immunolon II; Costar, Corning, NY).
2. Carbonate coating buffer: 0.015 M Na$_2$CO$_3$, 0.035 M NaHCO$_3$, pH 9.3.
3. Blocking buffer: 3% w/v BSA, 0.02% w/v sodium azide, in PBS.
4. Goat antihuman IgG (Zymed Laboratories, San Francisco, CA).
5. Goat antihuman κ antibody (free & bound) (Sigma Chemical).
6. Alkaline phosphatase (AP) goat antihuman κ L chain (Sigma Chemical).
7. Diethanolamine buffer: 9.6% v/v diethanolamine, 0.24 mM MgCl$_2$ (Sigma Chemical), pH 9.8.
8. AP substrate: 1 pellet *p*-nitrophenyl phosphate disodium (Sigma Chemical) dissolved in 5 mL diethanolamine buffer.
9. ELISA plate reader (MR700 Plate Reader; Dynatech Labs, Chantilly, VA).
10. Twenty-four-well tissue-culture plate (Falcon; Becton-Dickinson).

2.2.3. ^{35}S Biosynthetic Antibody Labeling and Immunoprecipitation

1. Petri dishes 60×15-mm (Falcon; Becton-Dickinson).
2. Twenty-four-well tissue-culture plate (Falcon; Becton-Dickinson).
3. Deficient Dulbecco's Modified Eagle Medium (DMEM) in L-glutamine, methionine, and cysteine (Cellgro; Mediatech, Herndon, VA), with 1:100 GlutaMAX (Gibco-BRL, Life Technologies, Rockville, MD).
4. Labeling medium: 0.1% (v/v) calf serum and EasyTag Labeling Mix composed of [^{35}S]-methionine + [^{35}S]-cysteine (NEN Life Science Products, Boston, MA) in deficient DMEM.
5. NDET: 1% v/v NP 40, 0.4% (w/v) deoxycholate, 66 mM EDTA, 10 mM Tris-HCl, pH 7.4.
6. 0.3% (w/v) Sodium dodecyl sulfate (SDS) in NDET.
7. Polyclonal antihuman IgG antibody, e.g., rabbit hyperimmune antihuman IgG *(30)*.
8. Sucrose pad: 30% (w/v) sucrose, 0.3% SDS in NDET.
9. Staph A: 10% (w/v) suspension of formaldehyde-fixed *Staphylococcus aureus* with membrane-bound protein A (IgGSorb, The Enzyme Center, Malden, MA), with 0.3% SDS in NDET.
10. Distilled H$_2$O.
11. SDS-PAGE sample buffer: 2% (w/v) SDS, 10% (w/v) glycerol, 0.008% (w/v) bromophenol blue, 25 mM Tris-HCl, pH 6.7.
12. β-mercaptoethanol.
13. Rainbow [^{14}C]-methylated protein mol wt marker (Pharmacia, UK).
14. J774.2 supernatant: sterile filtered supernatant of J774.2 cells (ATCC) grown in log phase with 10% v/v calf serum in IMDM.
15. Subcloning medium: 20% v/v calf serum and 10% v/v J774.2 supernatant in IMDM.
16. Ninety-six-well tissue-culture flat-bottom plates (Falcon; Becton-Dickinson).

2.2.4. Growing Cells in Roller Bottles

1. Petri dishes 100×20-mm (Falcon; Becton-Dickinson).
2. Fetalclone serum (HyClone, Logan, UT).
3. Tissue-culture roller bottle, 2 L (Falcon; Becton-Dickinson).
4. Cell production roller apparatus (Bellco Biotechnology, Vinland, NJ).
5. GlutaMAX-1 (Gibco, Invitrogen, France).
6. Whatman filter paper 1 (Whatman International, Maidstone, UK).

2.2.5. Purification, Quantification, and Storage

1. Protein A, recombinant; immobilized on 6% fast-flow beaded agarose (Sigma Chemical).
2. LKB IBF 11 mini-columns (Sepracor, Marlborough, MA).
3. Sodium azide in PBS, 0.02% (w/v).
4. Elution buffer A: 0.1 M citric acid-NaOH, pH 4.5. Elution buffer B: 0.1 M glycine-HCl, pH 2.5. Elution buffer C: 0.1 M glycine-HCl, pH 2.0.
5. Neutralization buffer: 2 M Tris-HCl, pH 8.0.
6. Centricon centrifugal filter concentrator (Millipore, Billerica, MA).
7. Dialysis buffer: 150 mM NaCl, 50 mM Tris-HCl, pH 7.8.
8. Dialysis tubing (Sigma Chemical).
9. Bicinchoninic acid-based protein assay (BCA protein assay; Pierce Chemical, Rockford, IL).

2.3. Further In Vitro Characterization of the Antibody Fusion Protein

2.3.1. Antigen Binding Studies

2.3.1.1. ELISA to Test Antibody–Cytokine Fusion Protein Antigen Binding

1. Purified antigen.
2. Same materials described in **Subheading 2.2.2.**

2.3.1.2. Flow Cytometry

1. Tumor cell line expressing antigen on its surface.
2. Flow cytometry buffer: 2% (v/v) calf serum, 0.02% (w/v) sodium azide in PBS.
3. Biotinylated goat antihuman IgG (Pharmingen, San Diego, CA).
4. Phycoerythrin (PE)-labeled streptavidin (Pharmingen).
5. Flow cytometer equipped with a blue laser excitation of 15 mW at 488 nm (FACScan; Becton-Dickinson, Mountain View, CA).

2.3.2. Study of the Cytokine Biological Activity

1. Ninety-six-well tissue-culture flat-bottom plates (Falcon, Becton-Dickinson).
2. CTLL-2 cell line (ATCC).
3. Recombinant human interleukin-2 (rhIL-2) (PeproTech, Rocky Hill, NJ).
4. [Methyl-^{3}H]-thymidine (ICN, Costa Mesa, CA).
5. Complete RPMI 10: RPMI 1640 (Gibco-BRL, Life Technologies), 10% (v/v) calf serum, 2 m*M* L-glutamine, 50 µM β-mercaptoethanol, 100 U/mL penicillin, and 100 µg/mL strep-tomycin sulfate.
6. Glass fiber filter 90 × 120-mm printed Filtermat (Wallac Oy, Turku, Finland).
7. Ninety-six-well-plate cell harvester (Tomtec, Hamden, CT).
8. EcoLume scintilliation medium (Amersham, Arlington Heights, IL).
9. Liquid scintillation counter (Microbeta 1450; Wallac Oy).

3. Methods

In this section we describe: (a) the construction of plasmids for expression of a human antibody fused to a cytokine; (b) transfection of the expression vector into myeloma expression systems, screening, scale-up culture, antibody fusion protein purification, and initial characterization; and (c) in vitro characterization of the antibody fusion protein antigen-binding properties and cytokine biological activity. Finally, we briefly mention some examples of in vivo studies using antibody-cytokine fusion proteins. As an example we present the anti-HER2/*neu* human IgG3/IL-2 antibody–cytokine fusion protein developed in our laboratory *(31)*.

3.1. Construction of Antibody–Cytokine Fusion Proteins

3.1.1. Cloning of the V-Region Sequence
into the Antibody-Expression Vectors

The production of functional antibodies requires the simultaneous expression of genes coding for both L and H chains. Several expression vectors encoding for L and H chains on separate plasmids are available for the construction of antibody–cytokine fusion proteins *(29,32–34)*. Alternatively, expression vectors containing the H and L chain in one plasmid have been described *(5,13,35,36)*. Although the single plasmid

has the advantage that co-transfection or sequential transfection is not required, large constructs may be difficult to manipulate *(26)*.

The first step to construct an antibody–cytokine fusion protein is to prepare the plasmids encoding the desired immunoglobulin isotype. **Figure 3** shows the expression vectors developed in Dr. Sherie Morrison's laboratory that contain the human κ C_L region (**Fig. 3A**), and the human γ1 (**Fig. 3B**) and human γ3 (**Fig. 3C**) C_H regions, respectively. The expression vectors are designed as cassettes and facilitate the cloning of PCR-amplified V_L and V_H regions in the corresponding C_L and C_H regions *(32,34)*.

V-region sequences targeting a tumor antigen can be obtained from hybridomas by RT-PCR using as template the mRNA and a set of primers that anneal to the DNA flanking regions encoding for the V regions *(32,34,37)*, from a phage display library *(38)* or from other sources. In the current example (anti-HER2/*neu* IgG3/IL-2), the DNA encoding the V_L and V_H domains of the humanized antibody hum4D5-8 *(39)*, also known as Herceptin (Trastuzumab), specific for the tumor-associated antigen HER2/*neu* was obtained from its developers at Genentech (San Francisco, CA) and cloned by PCR into the κ L chain and γ3 H chain PCR expression vectors.

The L-chain expression vector (**Fig. 3A**) contains the murine V_H promoter for expression in murine myeloma cells, the pBR322 origin of replication (*see* **Note 1**), the β-lactamase gene for selection in *Escherichia coli*, and the marker *gpt (40)*, which encodes xanthine-guanine phosphoribosyltransferase for selection in eukaryotic cells with HXM. The L-chain vector has the genomic sequences corresponding to the human κ C_L region and includes, flanking the region encoding for the V_L domain, the *Eco*RV-*Sal*I cloning sites allowing the direct replacement by a different V_L region *(34)*. The insertion of the V_L region into the L-chain expression vector requires standard methods of genetic engineering *(41)*. To begin, amplify by PCR the DNA encoding for the desired V-region sequence (in our case, anti-HER2/*neu* κ V_L chain), to generate an *Eco*RV blunt site at the 5' end and a *Sal*I at the 3' end *(32)*. **Table 1** shows the structure of the forward and reverse primers for PCR cloning of the V_L region. Ligate the PCR product to the TA cloning vector and sequence to identify potential errors. Then, digest the PCR clone and the κ L-chain expression vector using the *Eco*RV-*Sal*I restriction endonucleases. Isolate the digested V_L region fragment and the κ L-chain expression vector, purify, and ligate. Finally, verify by restriction analysis that the novel vector has the right structure.

The H-chain expression vectors have the same promoter, origin of replication, and prokaryotic selection marker as the L-chain vector. However, instead of *gpt*, the H-chain expression vectors have the eukaryotic selection marker *his* for resistance to histidinol *(42)*. **Figures 3B** and **C** show the vectors with the genomic sequence of the C_H region of IgG1 and IgG3, respectively. The vector has *Eco*RV and *Nhe*I restriction sites separated by a short fragment that allows the cloning of different V_H regions *(32)*. Antibody-cytokine fusion proteins have been successfully made with IgG1 *(4,5,13)*; however, in the current example, IgG3 was used because it has an extended hinge region. This long hinge region confers more flexibility and spacing to the fusion proteins, facilitating simultaneous binding to antigen and cytokine receptor *(3)*.
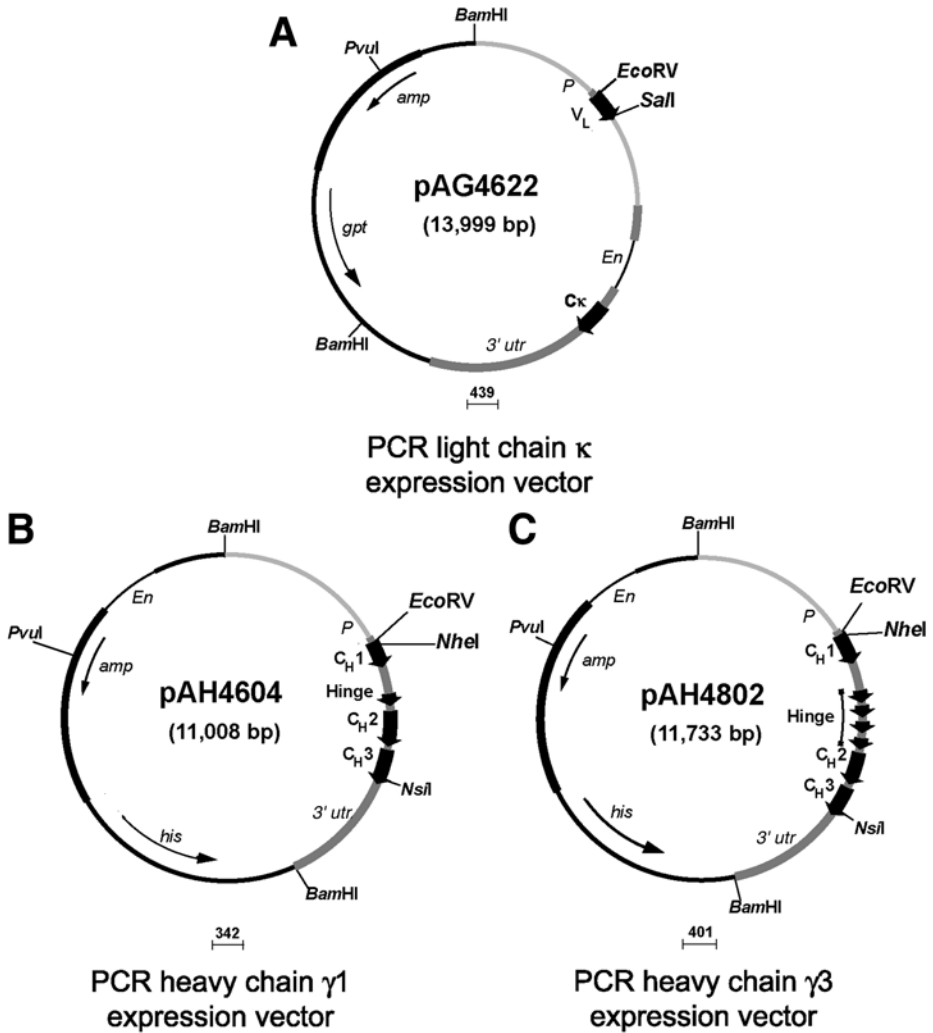
Fig. 3. Expression vectors for cloning V_L and V_H regions by PCR. (**A**) Scheme of the PCR κ L-chain expression vector. Thick black lines with arrows indicate the exons of human κ C_L region and a V_L sequence flanked by *Eco*RV-*Sal*I cloning sites. The point of the arrow indicates the direction of transcription. *P* refers to the promoter sequence, *En* the enhancer, *3'utr* the 3' untranslated region, *amp* the bacterial selective marker, and *gpt* the eukaryotic selective marker. (**B,C**) Maps of the PCR H-chain expression vectors γ1 and γ3, respectively. References are similar to panel A except that the thick black lines with arrows indicate the exons encoding for human C_H region, *his* refers to the eukaryotic selective marker, and V_H region is absent; only the cloning sites *Eco*RV-*Nhe*I are present.

Table 1
Structure of the Primers for Cloning the V$_L$ Region

PCR primer	Sequence structure
5' V$_L$ [a]	5'-GGG<u>GATAT</u>**CCACC**ATGNNN...3'
3' V$_L$ [b]	5'-AGC<u>GTCGAC</u>**TTAGC**NNN...3'

[a] The 5' V$_L$ sense primer contains the *Eco*RV site (underlined), the Kozak sequence (bold), the initiation codon (ATG), and part of the leader of the human or mouse L chain (NNN...).

[b] The 3' V$_L$ antisense primer include the *Sal*I site (underlined) and a short fragment of a splicing donor site (bold). Remember that the vectors used have the antibody genomic sequence. After the splicing site, include a fragment of the sequence complementary to the one that encode the J segment of the desired V$_L$ region (NNN...).

Table 2
Structure of the Primers for Cloning the V$_H$ Region

PCR primer	Sequence structure
5' V$_H$ [a]	5'-GGG<u>GATAT</u>**CCACC**ATGNNN...3'
3' V$_H$ [b]	5'-GGG<u>GCTAGC</u>NNN...3'

[a] The 5' V$_H$ sense primer has the *Eco*RV site (underlined), the Kozak sequence (bold), the initiation codon (ATG), and part of the leader of the human or mouse H chain (NNN...). Note that in the case of using a blunt site different than *Eco*RV, the restriction site will be lost once it is ligated to the expression vector.

[b] The 3' V$_H$ antisense primer includes the *Nhe*I site (underlined). After that sequence, include the sequence complementary to the one that encodes the J segment of the desired V$_H$ region (NNN...).

The procedure for cloning a V$_H$ region (in our case anti-HER2*/neu* V$_H$ region) into the PCR H chain γ3 expression vector is similar to the one described for the κ V$_L$ region. However, for the H-chain expression vector the cloning sites are *Eco*RV-*Nhe*I. The 3' primer requires an *Nhe*I site because the first two amino acids of the C$_H$1 domain of IgG3 and IgG1 are encoded in that site. **Table 2** shows the structure of the forward and reverse primers for PCR cloning of V$_H$ region.

3.1.2. Construction of the Antibody–Cytokine Fusion Protein

Using our expression vectors, the fusion of the antibody and the cytokine sequences requires the use of intermediate vectors. The nature of the intermediate steps required would depend on the antibody region to which the nonantibody partner will be fused. In the current example, the cytokine human IL-2 is fused at the 3' end of the anti-HER2*/neu* IgG3-C$_H$3. The cytokine cDNA can be obtained commercially (ATCC) or cloned from a known source. For example, PMA-stimulated Jurkat cells can be used

Table 3
Forward and Reverse Primers for Cloning of Mature Human IL-2

PCR primer	Sequence structure
5' (IL-2) [a]	5'- ACAA<u>CACGTG</u>CACCTACTTCAAGTTC-3'
3' (IL-2) [b]	5'- GCACT<u>GAATTC</u>**TCA**AGTCAGTGTTGA-3'

[a] The 5' (IL-2) sense primer includes the *Pml*I blunt site (underlined) and the first nucleotides of mature human IL-2 sequence.
[b] The 3' (IL-2) antisense primer includes the *Eco*RI site (underlined), the sequence complementary to the stop codon (TCA, in bold) and the last nucleotides of human IL-2 sequence.

to generate cDNA by reverse transcription using an oligo dT primer *(14)*. To clone the cDNA encoding human IL-2, amplify this cDNA by PCR using primers flanking the IL-2 coding sequence with appropriate restriction sites for subcloning (*see* **Table 3**). Clone the cytokine PCR product into TA cloning vector and sequence to identify potential errors. Using the restriction sites introduced during the PCR reaction (*Pml*I and *Eco*RI), subclone the IL-2 cDNA into the intermediate vector created for the fusion of the cytokine to the human IgG3-C_H3-3' end *(29)*. The digestion of the intermediate vector with *Ssp*I results in a blunt end one nucleotide after the last C_H3 codon, while the IL-2 cDNA fragment digested with *Pml*I results in a blunt end two base pairs before the first codon of mature IL-2. The ligation of the C_H3 blunt end *Ssp*I and the IL-2 *Pml*I result in a fusion protein linking the last amino acid of C_H3 to the first amino acid of mature IL-2 with a codon encoding a cysteine between them (**Fig. 4A**) (*see* **Note 2**). The product of this ligation is an intermediate vector with the IgG3-C_H3 domain of fused to the IL-2 and the 3' un-coding region (pAT3462/IL-2). The strategy for the construction of IL-2 fused to anti-HER2/*neu* IgG3 (vector pAH4802-V_H) is illustrated in **Fig. 4B**. In this case, the presence of multiple restriction sites makes a single ligation difficult, and a three-way ligation is required. Digestion of the vector pAH4802-V_H with *Nhe*I/*Nsi*I results in the fragment C_H γ3 (fragment 1). The digestion of pAH4802-V_H with *Nhe*I, and partial digestion *(43)* of the linearized vector with *Bam*HI result in fragment 2, containing the expression vector backbone with V_H (longest fragment). Digestion of the intermediate vector pAT3462/IL-2 with *Bam*HI/*Nsi*I produces fragment 3, which contains the DNA encoding for the last 20 amino acids of IgG3-C_H3 fused to IL-2 and the 3' un-translated region. The ligation of the three fragments yields the antihuman HER2/*neu* IgG3/IL-2 H-chain expression vector (*see* **Fig. 4B**).

Our expression vectors are developed as cassettes, making it straightforward to produce the same fusion proteins with variable regions of different affinities and/or specificities *(7,14,31)* or produce novel fusion proteins with the same variable regions but with a different nonimmunoglobulin partner *(19, 4–46)*. Another alternative is the creation of families of antibody fusion proteins with the nonantibody partner fused at different positions of the C_H region *(29)* or at the N-terminus of the V_H region via a flexible linker *(17,19,44)*.
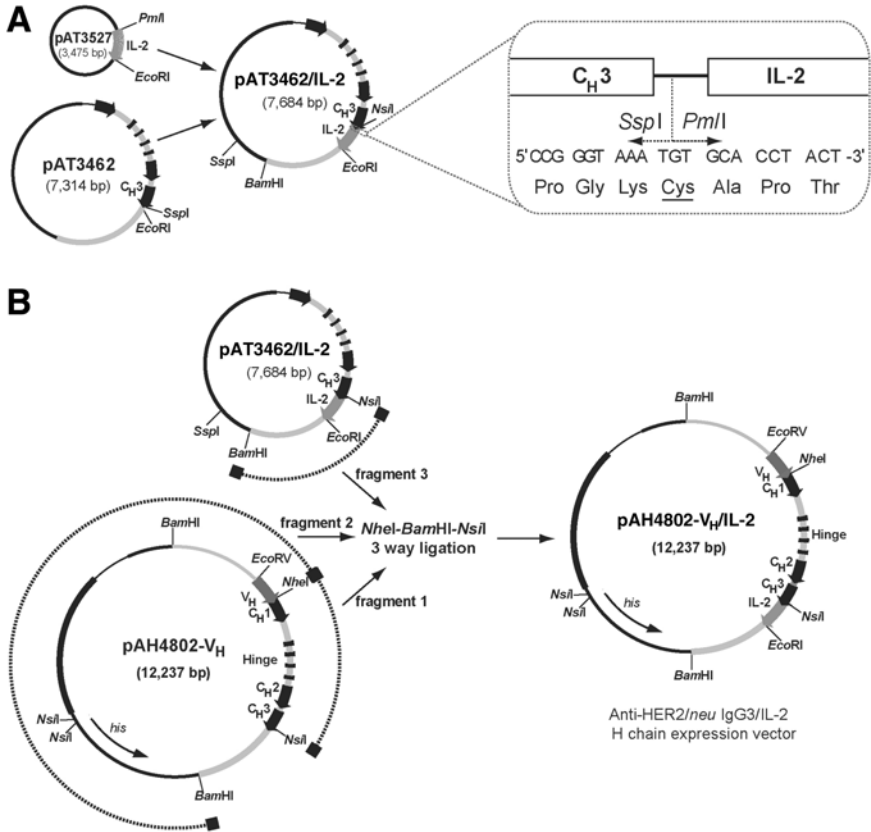
Fig. 4. Construction of anti-HER2/*neu* IgG3/IL-2 expression vector. Panel A shows the nucleotide and amino acid sequence of the γ3 C$_H$3/IL-2 fusion region. The ligation of the blunt sites *Ssp*I and *Pml*I results in a single amino acid (cysteine). Panel B show the strategy for the construction of the expression vector for anti-HER2/*neu* IgG3/IL-2. Three-way ligation of the fragments containing the DNA sequence encoding for the IgG3 constant regions from pAH4802 V$_H$ (fragment 1), the V$_H$ anti-HER2/*neu* and the expression vector backbone from pAH4802 V$_H$ (fragment 2), and the last 60 base pairs of γ3 C$_H$3 fused to IL-2 and the 3' untranslated region from vector pAT3462/IL-2 (fragment 3). A dotted line outside the plasmid indicates the fragment used in the three-way ligation.

3.2. Transfection into Expression Systems and Initial Characterization

The use of expression vectors with transcriptional control through immunoglobulin promoter requires the use of cell lines from the B-cell lineage, such as murine myeloma cells. This system has been used successfully in the production of several antibody–cytokine fusion proteins *(26)*. Alternatively, the human cytomegalovirus (CMV) promoter has been used for antibody production in both myeloma cell lines and mammalian cells from other lineages, including Chinese hamster ovary (CHO) cells *(5,47–49)*.

3.2.1. Transfection into Mammalian Expression System

Co-transfection of murine myeloma cell lines (Sp2/0-Ag14, P3X63Ag8.653, or NS0/1) with H- and L-chain expression vectors can result in successful producers *(44)*; however, we prefer to initially develop a L-chain producer as a recipient for transfection of different H-chain constructs. This procedure saves time and favors the development of cell lines expressing high levels of antibody fusion proteins *(19,28, 45)*. To begin, prepare the L-chain producer by transfecting the L-chain expression vector by electroporation (*see* **step 5**) and select stable transfectants by resistance to HXM. Screen by ELISA (*see* **Subheading 3.2.2.**), select the best L-chain producer, and use this stable cell line as a recipient for transfection with H-chain expression vectors.

1. Following standard genetic engineering techniques *(41)*, linearize 10 µg of the expression vectors with *Pvu*I. Confirm digestion with ethidium bromide agarose gel (*see* **Note 3**). Extract the DNA with phenol/chloroform (*see* **Note 4**). Precipitate with ethanol and air dry for 30 min. Resuspend in 50 µL cold sterile filtered PBS and keep at 4°C until transfection.
2. Count 2×10^6 cells/plate in log-phase growth of the myeloma cell lines (in case of H-chain transfection, use L-chain producers). For each transfection it is convenient to prepare five plates plus one negative control plate that is not transfected (*see* **Note 5**).
3. Pellet cells by centrifugation at 220*g* (*g* corresponds to gravity and is equivalent to "relative centrifugal force" or rcf) for 5 min at 4°C, pour off supernatant, and resuspend in 0.5 mL cold PBS.
4. Transfer the cells into the electroporation cuvet and add the linearized DNA.
5. Electroporate with a pulse of 960 µFd capacitance and 0.2 V pulse. Incubate on ice for 10 min.
6. Transfer to 10 mL 5% calf serum in IMDM at 4°C. Pellet the cells by centrifugation (220*g*, 5 min, 4°C) and pour off the supernatant.
7. Resuspend the transfected and control cells in 12.5 mL/plate growth medium. Dispense 125 µL/well in 96-well tissue-culture plates. Incubate at 37°C and 5% CO_2.
8. After 2 d, add 125 µL of selection medium to the transfected and control cells. For L-chain producers, use selection medium with HXM instead of histidinol. For P3X63Ag8.653 cells, the selection medium for H-chain transfectant is 5 m*M* histidinol or for L-chain transfectant is HXM: 125 µg/mL hypoxanthine, 7.5 µg/mL xanthine, and 3 µg/mL mycophenolic acid (*see* **Note 6**). Note that the final concentration of selection medium in the well is half.
9. Three d later, remove half of medium from the wells by aspiration and add 125 µL more of selection medium. The final concentration in the well of the drug used for selection after this final application is 75%.
10. After 10 to 14 d, the transfected clones should have visible colonies. The control plate should have no colonies; otherwise, you will have a high background of nonproducer clones in your transfectants. Do not let the cells become too dense (indicated when the medium turns yellow), since this may stress the cells and result in either selection for low-level producers or loss of the clone. Screen for the secreted antibody fusion proteins via ELISA.

3.2.2. ELISA Screening

1. Coat 96-well Immunolon II plate with 50 µL/well of 5 µg/mL goat antihuman IgG (for H-chain producers) or 5 µg/mL goat antihuman κ antibody (for L-chain producers) in

freshly made carbonate buffer using a multi-channel pipet *(32)*. The following steps are the same for screening both L-chain and H-chain producers.

2. Wash the plate wells four times with PBS and add 100 μL of blocking buffer to each well (*see* **Note 7**). For immediate use, leave at room temperature 30 min. For later use, leave at 4°C wrapped carefully to avoid evaporation.

3. Wash four times with PBS, apply 50 μL/well of supernatant from the samples to be screened, and incubate either 2 h at room temperature (RT) in rotator or overnight at 4°C. Include a positive (any supernatant from a good producer) and negative control (supernatant from untransfected cells).

4. Wash four times with PBS and incubate for 1 h at 37°C with AP-labeled goat antihuman κ according to manufacturer's instructions in 1% BSA in PBS.

5. Wash four times with PBS. Add freshly made AP substrate. Incubate at room temperature 30 min to 1 h and read the plates at 410 nm.

6. Compare the magnitude of the signal with the size of the clone, and identify a small clone with high signal strength. With this criterion, pick the five to eight best producers.

7. Carefully resuspend the cells and transfer to a 24-well plate with 0.5 mL 10% calf serum in IMDM to expand the clone. Transfer 2 to 6 d later to 60×15-mm Petri dishes (*see* **Note 8**).

3.2.3. ^{35}S Biosynthetic Antibody Labeling and Immunoprecipitation

This procedure is designed to determine the proper assembly, secretion, and mol wt of the antibody–cytokine fusion protein and to compare the productivity of different clones in order to select the optimal producer.

1. Count 10^6 cells from the clones that seem to be the best producers by ELISA. Pellet by centrifugation (5 min, 220g, 4°C) and remove the supernatant.

2. Wash the cells twice, resuspending in 2 mL of deficient DMEM, and pellet by centrifugation (5 min, 220g, 4°C).

3. Remove supernatant and add 1 mL of [^{35}S]-labeling medium containing 16 μCi/mL to each cell line (*see* **Note 9**).

4. Under sterile conditions, move the cells into 24-well plate and incubate overnight at 37°C in 5% CO_2. The supernatant should contain the secreted [^{35}S]-labeled antibody.

5. Resuspend the cells and transfer to 1.5-mL Eppendorf tube. Pellet by centrifugation (3 min, 1500g, RT).

6. Transfer the supernatant (secreted fraction) to a new 1.5-mL tube and add 0.5 mL of NDET to the pellet containing the cells (cytoplasmic fraction). Resuspend by pipetting up and down to lyse the cells. Pellet the cell lysate by centrifugation (5 min, 21,000g, 4°C) and transfer the supernatant to a new tube. Discard the pellet (*see* **Note 10**).

7. Add 2.5 μL of hyperimmune rabbit antihuman IgG to both sets of tubes (the secreted fraction and the cytoplasmic fraction). Incubate on ice for 1 h (*see* **Note 11**).

8. Add 100 μL of Staph A (mix the suspension well before using it). Incubate 5 min at RT. Pellet by centrifugation (1 min, 21,000g, RT) and remove supernatant.

9. Resuspend the immunoprecipitates with 0.5 mL 0.3% SDS in NDET. Layer samples on top of a 1.0-mL sucrose pad in a 1.5-mL Eppendorf tube. Pellet by centrifugation (1 min, 21,000g, RT). Discard supernatant.

10. Wash the precipitate, resuspending it in 300 μL 0.3% SDS in NDET and pellet by centrifugation (1 min, 21,000g, RT). Discard supernatant. Wash again (optional).

11. Resuspend the immunocomplex in 0.5 mL distilled H_2O to remove detergents, and pellet by centrifugation (1 min, 21,000g, RT). Drain well.

12. Add 50 μL of SDS-PAGE sample buffer, vortex, and incubate 2 min in boiling water to separate radiolabeled antibody from Staph A. Pellet by centrifugation and transfer the supernatant with the soluble radiolabeled antibody into a new tube.

13. For SDS-PAGE analysis, run half of the radiolabeled sample under nonreducing conditions on 5% phosphate gel and the other half under reducing conditions (30 min incubation at 37°C in the presence of 0.15 *M* β-mercaptoethanol) on 12% Tris-glycine gels *(50)* with radiolabeled mol wt marker. Dry the gels and expose for autoradiography to check the correct mol wt and assembly of the transfected proteins *(32,51)*. Always include as a negative control the untransfected cell line and (if available) a "good" producer as a positive control (*see* **Note 12**). As the productivity of the clone is proportional to the intensity of the signal, this will be a criterion for the selection of the best producer.

14. Once one cell line is selected, resuspend the cells and transfer it to 24-well plate to scale up.

15. It is necessary to subclone the cells by limiting dilution to assure the isolation of a pure clone. Take 100 μL of the log-phase cell culture and make serial dilutions in three tubes with 12.5 mL of subcloning medium. Plate the three different dilutions into 96-well tissue-culture plates, 125 μL/well. Incubate at 37°C and 5% CO_2. The next day, add 125 μL/well of subcloning medium, and incubate 7 to 10 d until colonies become visible. Screen the plates that have colonies by ELISA (*see* **Subheading 3.2.2.**) in less than 33% of the wells to minimize the chance of selecting a well with multiple colonies. Pick the best producer based on the criterion of small-size colony and high signal.

16. Expand the selected producer into roller bottles. Take a sample to prepare frozen stocks *(52)*.

3.2.4. Growing Cells in Roller Bottles

1. Take about 5×10^7 cells growing in 50 mL of medium (two 100×20-mm Petri dishes). Pellet by centrifugation for 5 min, 220*g*, at 4°C.

2. Resuspend in 100 mL of 10 % (v/v) Fetalclone serum in IMDM and seed into a 2-L roller bottle. It is not necessary to add the drug used for selection with subcloned cell lines. If a room with gas interchange is not available, briefly bubble the medium in the bottle with CO_2 and tighten the cap immediately. Put on a roller apparatus at 37°C (*see* **Note 13**).

3. Check the cells daily. When the medium turns orange-yellow due to the density of the cells, double the volume with IMDM alone. The cells often adhere to the sides of the flask and then grow in suspension.

4. Add IMDM up to 1 L to a final concentration of 1% Fetalclone serum. The full process can take 10 d to 4 wk, depending on the growth rate of the transfectant. As the cells continue to grow in roller bottles, the medium may be depleted of glutamine, resulting in lower antibody fusion protein yield. It is convenient then to add 35 mL of GlutaMAX-1 once the final volume of 1 L is reached.

5. If you wish to reuse the cells, harvest the supernatant just as the cells begin to look sick. Pellet by centrifugation as described in **step 6**. Add fresh medium with 1% Fetalclone serum and the cells. Harvest the supernatant as before. Alternatively, let the cells die; this will increase your yield of antibody.

6. Pellet the cells by centrifugation in 250-mL centrifuge bottles at 3500*g* for 10 min at 4°C.

7. Filter through Whatman 3MM paper or the equivalent before running through the chromatography column. To stabilize the supernatant, it is convenient to add 0.02% sodium azide, 2 m*M* EDTA, 10 m*M* PO_4 buffer and 0.45 *M* NaCl. Store at 4°C.

8. If after several preparations the cell line looses protein expression, it is convenient to subclone (*see* **Subheading 3.2.3., step 15**) to isolate again a good producer. To avoid this

problem, it is convenient to have a stock of good producers. Depending on the quality of the producers and the amount of protein required, the number of roller bottles required may differ. It is convenient to start with one or two roller bottles, determine the yield, and scale up if needed.

3.2.5. Purification, Quantification, and Storage

Different types of columns can be used for purification of antibody–cytokine fusion proteins, including protein A, protein G, or columns with the antigen *(53)*. Although human IgG3 does not bind protein A through its Fc fragment, the HER2/*neu* IgG3/IL-2 fusion protein that we have developed is able to bind protein A through its V region, since we use the V region of the humanized antibody hum4D5-8, also known as Herceptin (Trastuzumab; Genentech, San Francisco, CA) *(28,54)*.

1. Flow the roller bottle culture supernatants (up to 4 L) through a mini-column containing 1 mL protein A on 6% fast-flow beaded agarose by gravity. Repeat the procedure two to four times.
2. Prior to the elution, set up the 1.5-mL fraction tubes (Eppendorf tubes) with 150 µL of 2 *M* Tris-HCl (pH 8.0) to neutralize the eluates, and keep them on ice.
3. To collect the antibody fusion protein from the column, first wash the column with 10 mL of PBS with 0.02% sodium azide.
4. Elute the column with 2 mL buffer A, 4 mL buffer B, and 2 mL buffer C. In all cases (buffers A, B, and C) add up to 1 mL of buffer, collect the corresponding fraction, mix the tube gently to avoid bubbles and to neutralize the low pH, and repeat the procedure until the second mL of the buffer C passes through the column. Store the fraction tubes at 4°C.
5. After the elution of buffer C, wash the column again with 10 mL PBS with 0.02% sodium azide as in **step 2**. To store the column, fill with PBS with 0.02% sodium azide, seal with parafilm, and keep at 4°C.
6. Take 10 µL of each fraction, add sample buffer, and run an SDS-PAGE 5% phosphate gel under nonreducing conditions. Stain with Coomasie blue to detect the fractions with the band corresponding to the fusion protein. The fusion protein should be collected during the elution with buffer B (pH 2.5) (**Fig. 5**).
7. Repeat the procedure from **steps 1–6** until no more antibodies are collected. To assess the rate of antibody fusion protein depletion from the roller-bottle supernatants, take samples before proceeding to the elution and compare by quantitative ELISA (*see* **Note 14**).
8. Dialyze the eluted fractions using dialysis bags of appropriate molecular mass cut-off in a 2-L volume of dialysis buffer or PBS without sodium azide *(51)*. Change three times every 12 h. In case the concentration of eluted fractions is too low, concentrate using Centricon centrifugal filter concentrator with a molecular mass cut-off appropriate to the size of the antibody fusion protein prepared. Later proceed to dialysis.
9. Check the integrity of the protein before the quantification and storage by SDS-PAGE. Run the sample under nonreducing conditions on 5% phosphate gel, and under reducing conditions on 12% Tris-glycine gel (*see* **Subheading 3.2.3., step 13**). Stain with Coomasie Blue *(51)*. **Figure 6** shows a Coomasie blue-stained gel comparing the antibody alone with the antibody–cytokine fusion protein under nonreducing (**Fig. 6A**) and reducing conditions (**Fig. 6B**). The pattern should be similar to the autoradiography in **Subheading 3.2.3., step 13**.
10. Determine protein concentrations by bicinchoninic acid (BCA)-based protein assay using BSA as standard. As an alternative, use quantitative ELISA if available.
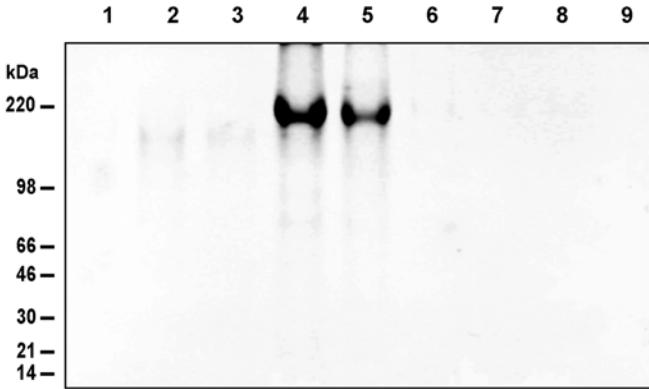
Fig. 5. Profile of anti-HER2/*neu* IgG3/IL-2 elution fractions from protein A column analyzed by SDS-PAGE under nonreducing conditions and stained by Coomasie blue. In the first fractions (1 to 3) at high pH, traces of bovine IgG can be found that correspond to a faint band at 150 kDa. With the elution at pH 2.5 (fractions 4 to 7), the 200-kDa band appears, which exhibits a mol wt corresponding to our antibody-cytokine fusion protein. At pH 2.0 (fractions 8 and 9), no protein is collected.
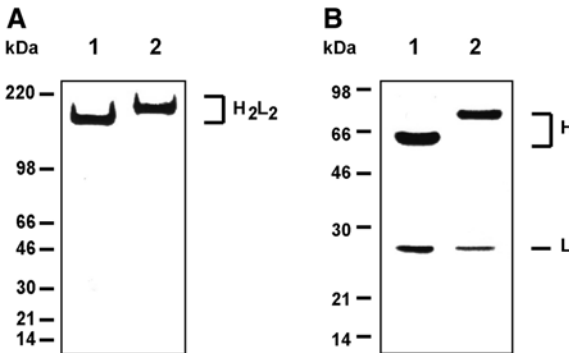
Fig. 6. SDS-PAGE analysis of anti-HER2/*neu* IgG3/IL-2. Secreted antibodies anti-HER2/*neu* IgG3 (lane 1) and anti-HER2/*neu* IgG3/IL-2 (lane 2) were purified from culture supernatants and analyzed by SDS-PAGE stained with Coomasie blue under nonreducing (**A**) and reducing (**B**) conditions. The estimated mol wt corresponds to 170 kDa for the antibody alone (**A,** lane 1) vs 200 kDa for the fully assembled antibody-cytokine fusion protein (**A,** lane 2) (H_2L_2). The 60-kDa size of the H chain alone (**B,** lane 1) shows an expected increase to 75 kDa, corresponding to the cytokine fused with the H chain (**B,** lane 2) (H), while no changes in mol wt are detected in the 25-kDa L-chain band (L).

11. The antibody fusion proteins can be stored in dialysis buffer or PBS at 4°C if they will be used in the short term (i.e., less than 6 mo). For longer storage, the fusion proteins can be aliquoted, snap frozen, and stored at –80°C *(52)*. In both cases (short and long term), a concentration of 1 mg/mL is recommended (*see* **Note 15**).

3.3. Further In Vitro Characterization of the Antibody Fusion Protein

Antibody–cytokine fusion proteins consist in two moieties: the antibody moiety that targets the tumor antigen, and the cytokine moiety that possess immunostimulatory activity. Their coexistence in the same molecule may affect the functional activity of each other. In fusion proteins that include complete antibodies, the Fab region must be tested for antigen binding while, depending on the isotype, the antibody Fc region can be tested using standard assays to study effector functions such as ADCC and CDC *(4,5,13,14,55)*. The fused cytokine also requires specific functional assays that are necessary to test its effective activity. Below we describe the procedures to study binding of the antibody to the antigen and the activity of the cytokine (IL-2).

3.3.1. Antigen-Binding Studies

3.3.1.1. ELISA ᴛᴏ Tᴇsᴛ Aɴᴛɪʙᴏᴅʏ–Cʏᴛᴏᴋɪɴᴇ Fᴜsɪᴏɴ Pʀᴏᴛᴇɪɴ Aɴᴛɪɢᴇɴ Bɪɴᴅɪɴɢ

The binding properties of the antibody may be affected by its fusion to the cytokine. ELISA is a convenient method to study the capacity of the antibody fusion protein to bind the antigen and estimate its comparative avidity in respect to the parental antibody (*see* **Note 16**). The current procedure corresponds to the binding of antihuman HER2/*neu* IgG3/IL-2 fusion protein to its antigen, the extracellular domain of HER2/*neu* (ECD-HER2), but can be adjusted to study antibody fusion proteins with different specificities.

1. Coat the 96-well Immunolon II plates with 50 µL of the antigen ECD-HER2, 1 µg/mL, in carbonate buffer, overnight at 4°C.
2. Block the plates according to **Subheading 3.2.2., step 2**.
3. Wash four times with PBS and apply serial dilutions of the antibody–cytokine fusion protein, the parental antibody as positive control, and a nonspecific isotype antibody as negative control (in our case, we use anti-DNS IgG3 antibody) in 50 µL PBS containing 1% BSA. Incubate overnight at 4°C.
4. Continue the protocol according to **Subheading 3.2.2., steps 4** and **5**.

3.3.1.2. Fʟᴏᴡ Cʏᴛᴏᴍᴇᴛʀʏ

The binding properties of the antibody–cytokine fusion protein to the antigen coated on a solid surface may not reflect effective binding to the antigen expressed on the surface of tumor cells. Flow cytometry can be used to determine effective binding of the antibody–cytokine fusion protein to cells expressing the target antigen on its surface (*see* **Note 17**). The same method can be adapted to study other antibody–cytokine fusion proteins.

1. Count 10^6 cells expressing the antigen on the surface (in this case, CT26-HER2/*neu*). Pellet cells by centrifugation at 220*g*, 5 min, at 4°C, pour off supernatant, resuspend in 1.0 mL of cold flow-cytometer buffer, and transfer to 1.5-mL tube. Keep the cells on ice through the procedure.
2. Pellet the cells by centrifugation (3 min at 1500*g* and RT) and remove the supernatant. Incubate with 1 µg of the antibody–cytokine fusion protein, anti-HER2/*neu* IgG3/IL-2, in 0.1 mL of flow-cytometry buffer for 2 h at 4°C. Shake gently every 15 min. Use anti-HER2/*neu* IgG3 *(44)* and isotype control (in our case, we use anti-DNS IgG3 antibody)

as positive and negative isotype controls, respectively. In addition, if available, the parental cell line not expressing the antigen should also be used as control to test binding specificity.

3. Wash the cells adding 1 mL of flow-cytometry buffer, mix, centrifuge for 3 min at 1500*g* at RT, and remove the supernatant. Repeat the washing step one more time and remove the supernatant.

4. Incubate for 30 min at 4°C with 0.5 µg of biotinylated goat antihuman IgG in a volume of 0.1 mL of flow-cytometry buffer. Shake gently every 15 min.

5. Wash the cells with 1 mL of flow-cytometry buffer, centrifuge for 3 min at 1500*g* and RT, and remove the supernatant. Incubate with PE-labeled streptavidin according to the manufacturer's instructions in a volume of 0.1 mL of flow-cytometry buffer for 30 min at 4°C in the dark. Shake gently every 15 min.

6. Wash the cells with 1 mL of flow-cytometry buffer, centrifuge for 3 min at 1500*g* and RT, and remove the supernatant. Resuspend in 0.2 mL flow-cytometry buffer to read immediately in flow cytometer. To store the cells for a period of days, resuspend the cells in 0.2 mL 2% paraformaldehyde, cover the tubes with aluminum foil, and keep at 4°C (*see* **Note 18**).

7. Perform analysis by flow cytometry with a FACScan equipped with a blue laser excitation of 15 mW at 488 nm (**Fig. 7**).

3.3.2. Study of the Cytokine Biological Activity

The cytokine bioactivity can be tested in vitro by the magnitude of the biological effect that the cytokine has on sensitive cell lines. Biological activities induced by cytokines include induction of cell proliferation, degranulation, and cytotoxicity, among others. A convenient type of test is the induction of cell proliferation dependent on the cytokines. Ideally, it requires the use of a cell line dependent on the cytokine being studied, as is the case of the murine macrophage cell line FDC-P1 for murine GM-CSF, or the murine cell lines CTLL-2 and HT-2 cells for human and murine IL-2 *(4,5,13,14,45)*. Here we describe a protocol to determine functional activity of IL-2 genetically fused to an antibody, using CTLL-2 proliferation assay.

1. Load into tissue-culture flat-bottom 96-well plates quadruplicate serial dilutions from 10 ng/mL to 0.01 ng/mL of rhuIL-2 (positive control), anti-HER2/*neu* IgG3/IL-2, and anti-HER2/*neu* IgG3 (negative control) in 50 µL complete RPMI 10 medium.

2. Seed with 50 µL of complete RPMI 10 medium containing 5×10^3 CTLL-2 cells (*see* **Note 19**). Incubate for 18 h at 37°C 5% CO_2 (*see* **Note 20**).

3. Pulse with 0.5 µCi/well [^{3}H]-thymidine in 25 µL complete RPMI 10 medium for 6 h (*see* **Note 21**).

4. Harvest with cell harvester through glass microfiber filter to collect the radiolabeled DNA (*see* **Note 22**).

5. Air-dry the filters and seal in envelope with EcoLume scintillation medium. Quantitate in a liquid scintillation counter.

6. Derive a linear regression from IL-2 control within the range where the growth is linearly dependent on IL-2 concentration. Determine sample activity by plotting points that fall within the linear range on the linear regression.

   In general, similar proliferation profile in rhuIL-2 and the IL-2 antibody-fusion protein has been observed; however, some cases reveal fusion proteins with lower activity than the free cytokine *(5,7,13,14)*.
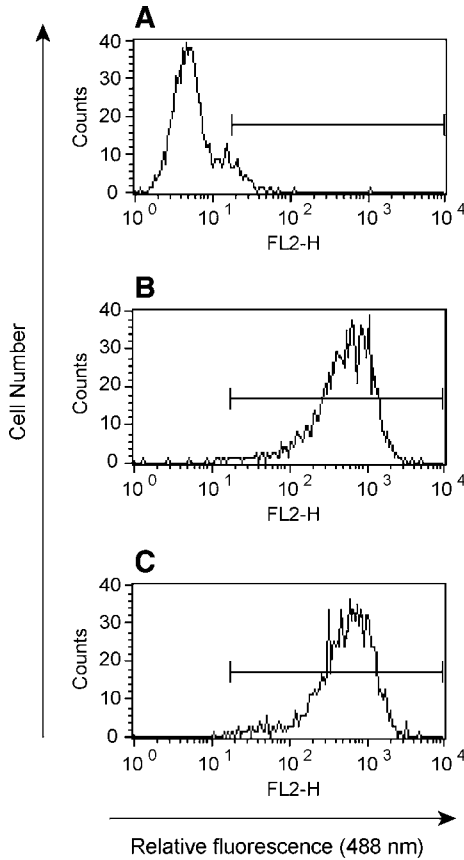
Fig. 7. Flow cytometry demonstrating binding of anti-HER2/*neu* IgG3/IL-2 to the HER2/*neu* expressed on the surface of CT26-HER2/*neu*. CT26-HER2/*neu* cells were incubated with anti-DNS human IgG3 (negative control) **(A)**, anti-HER2/*neu* human IgG3 (positive control) **(B)**, or anti-HER2/*neu* IgG3/IL-2 **(C)**, followed by biotinylated goat antihuman IgG and PE-labeled streptavidin. FL2-H indicates PE fluorescence.

3.4. In Vivo Assays for Antibody–Cytokine Fusion Proteins

Although in vivo studies are not the scope of this chapter, they are necessary to determine the effectiveness of the fusion proteins as cancer therapeutic tools. In general, these studies include half-life, biodistribution, tumor targeting, antitumor activity, and toxicity. A basic in vivo study required to understand the biological activity of the antibody-cytokine fusion protein is the pharmacokinetics. The half-life of antibodies in serum is in the range of d; the half-life of cytokines ranges from min to h *(56)*; for antibody-cytokine fusion proteins, the half-life is intermediate between that of the antibody and of the cytokine *(5,57,58)*. The biodistribution patterns indicate both the areas in which the antibody–cytokine fusion protein concentrates in the body

and whether it can effectively target tumors *(5,7,59)*. The antitumor activity is highly dependent on the model used, the targeting antigen, and the fused cytokine. Syngeneic tumor models are important to understand the immunological response triggered by treatment with the antibody–cytokine fusion proteins *(1,3)*. These tumor models can be local subcutaneous (s.c.) tumors *(4,7)* or metastases induced in lung or liver *(10)*. In general, the cell lines used to induce tumors express the antigen either naturally or artificially (transduction or transfection) and are able to grow in mice while maintaining the expression of the antigen *(7,8,10,46,60)*. Experiments can be designed to use the antibody–cytokine fusion protein directly to target the tumor *(4,7,10,61,62)* or as adjuvants of a tumor antigen vaccination *(6)*. In all cases, it is important to confirm that the treatment is more effective than the mixture of free antibody and cytokine or a nonspecific antibody–cytokine fusion protein *(1,3,10,58,62)*. It is necessary to study the mechanism responsible for antitumor activity, since the presence of the cytokine in the antibody may cause toxicity, and to conduct toxicology studies, which are critical if the antibody-cytokine fusion protein is intended to be used in clinical trials.

4. Notes

1. Because pBR322 is a low-copy-number plasmid, it is recommended to amplify the number of copies of the plasmid by adding chloramphenicol to the bacteria culture *(63)*. We use the *E. coli* strain HB101 to amplify our intermediate and expression vectors.
2. Fully functional antibody–cytokine fusion proteins, such as IgG1/IL-2 and IgG1/GM-CSF have been constructed with a peptide linker between the H-chain C-terminus and the cytokine *(4,5,13)*. IL-2 or GM-CSF has also been fused to the C-terminus of the C_H3 domain in the absence of a peptide linker, and the cytokine remains active *(14,45)*. However, it may be critical to include a flexible linker between the cytokine and the antibody when the nonantibody partner is fused to the N-terminus of the H chain, to facilitate antigen binding *(17,19,44,64)*.
3. CAUTION: Ethidium bromide is a strong mutagen and a possible carcinogen or teratogen. Wear a lab coat, chemical splash goggles, and nitrile gloves.
4. CAUTION: Phenol/chloroform is poisonous. Take precautions to avoid contact or ingestion. Chloroform is a suspected carcinogen. Perform all work in a chemical fume hood to avoid exposure by inhalation; wear protective clothes and gloves.
5. It is convenient to transfect different cell lines such as Sp2/0-Ag14, P3X63Ag8.653, or NS0/1 in parallel. Different antibody fusion proteins may be produced more successfully in one cell line than the other.
6. Previous to the transfection, it is convenient to make a titration curve in order to establish the minimum concentration of drug necessary to kill untransfected cells. Once the cell lines have been transfected, do not use more than one drug simultaneously, because the toxicity may be too high for the cell line to tolerate. In case of co-transfection, we have effectively selected clones using only the H-chain selection marker (histidinol).
7. CAUTION: Contains sodium azide, which is poisonous. It is a blocker of the cellular respiratory chain. Ingesting very small amounts can cause death. Avoid exposure by inhalation and skin contact. Wear protective clothes and gloves.
8. Nonadherent cell lines derived from Sp2/0-Ag14, P3X63Ag8.653, or NS0/1 myeloma cell lines can grow in Petri dishes; however, this is not the case for adherent cell lines such as CHO cells, which require the use of tissue-culture dishes to grow properly.

9. CAUTION: This procedure requires the use of ^{35}S and should be performed in Nuclear Regulatory Commission (NRC)-licensed sites by personnel trained in the use of this isotope.

10. We recommend analyzing both the cytoplasm and the secretions, especially the first time the transfection is made. The analysis of the cytoplasmic fraction allows the identification of antibody molecules during the synthesis process. The analysis of the supernatant fraction reveals whether the protein is being properly secreted and assembled. Most of the protein should be in the supernatant.

11. It is important to stress that the protein-A binding site for IgG is in the Fc region and that it is present in all wild-type human IgG except IgG3 *(65)*. For immunoprecipitation of IgG3 fusion proteins with Staph A, a prior incubation with a polyclonal rabbit antihuman IgG allows binding to protein A. In the case of L-chain producers, the L chain lacks a protein-A binding site; hence, co-immunoprecipitation with a rabbit antihuman Fab capable of binding the human L chain is required. To prepare these types of polyclonal antibodies, *see* **ref. *30***.

12. In our laboratory, for research use in mice, we define a "good" producer as the cell line able to secrete at least 1 µg/10^6 cells/24 h. However, for large-scale production of antibody–cytokine fusion proteins for clinical use, higher levels of antibody fusion protein production may be required.

13. Fetalclone serum is partially depleted of bovine IgG, which is convenient to avoid contamination with bovine IgG during the antibody fusion protein purification process. As an alternative, cells can be adapted to grow in serum-free media.

14. Quantitative ELISA can be used to determine the amount of antibody secreted by the transfectant. To perform a quantitative ELISA, follow the directions in **Subheading 3.2.2., steps 1–5**. In the same plate, prepare a calibration curve with serial dilution using an isotype quantified by BCA as standard (*see* **Subheading 3.2.5., step 10**).

15. Since freezing and thawing the antibody fusion protein may be harmful to both the antibody and the ligand, we recommend determining the antibody binding properties as well as the ligand specific activity of each new fusion protein before and after freezing. In addition, aggregates can also occur, resulting in a decrease of activity. To assess the presence of aggregates, analyze a sample using fast-performance liquid chromatography (FPLC) *(45)*.

16. Binding assays such as BIAcore or IAsys allow exact determination of affinity. With these assays, the kinetics of the antibody–cytokine fusion protein binding to the antigen can be studied in real time *(17)*. This technology can also be used to study the binding of the fused cytokine to its receptor *(66)*.

17. An alternative to flow cytometry to study the binding of antibody fusion protein to the surface of cells is cell ELISA *(67)*.

18. CAUTION: Paraformaldehyde is used in these procedures and is poisonous and a suspected carcinogen. It may cause heritable genetic damage and irreversible damage to sight, and is corrosive. Perform all work with in a chemical fume hood to avoid exposure by inhalation. Wear protective clothes, goggles, and gloves.

19. The process of thawing can be very traumatic for the CTLL-2 cells. The d after thawing, it may seem like all the cells have died. However, after 7 to 10 d with 20% calf serum in IMDM supplemented with 100 U/mL IL-2, the cells can be recovered. Once the density increases, decrease the calf serum to 5% and IL-2 to 5 to 10 U/mL.

20. For measurement of proliferation, alternatives to the use of radioisotope include the colorimetric methods MTT and MTS/PMS *(68,69)*. These methods detect cell meta-

bolic activity proportional to the cell number. The MTS/PMS assay Cell Titer 96 aqueous nonradioactive colorimetric assay (Promega, Madison, WI) is more sensitive than the [^{3}H]-thymidine incorporation in determining IL-2-induced CTLL-2 proliferation *(69)*. The higher sensitivity results from the fact that low concentrations of IL-2 are able to increase the metabolism of CTLL-2 cells without *de novo* DNA synthesis. If the MTS/PMS assay is used, the range of standard rhuIL-2 concentration for serial dilution has to be from 1 ng/mL to 0.001 ng/mL, one order of magnitude lower than for [^{3}H]-thymidine incorporation. Drawbacks of this method that may affect the final interpretation of the data include proportionally higher background levels, and increased MTS/PMS signal from dying cells *(69)*.

21. CAUTION: This procedure requires the use of ^{3}H and should be performed in NRC-licensed sites by personnel trained in the use of this isotope.

22. For your convenience, you may freeze the plate at –20°C to stop the proliferation and harvest up to 2 wk later. To thaw the plates, leave 45 min at RT or 10 min at 37°C.

Acknowledgments

References

1 Lode, H. N., Xiang, R., Becker, J. C., Gillies, S. D., and Reisfeld, R. A. (1998) Immunocytokines: a promising approach to cancer immunotherapy. *Pharmacol. Ther.* **80,** 277–292.

2 Helguera, G., Morrison, S. L., and Penichet, M. L. (2002) Antibody-cytokine fusion proteins: harnessing the combined power of cytokines and antibodies for cancer therapy. *Clin. Immunol.* **105,** 233–246.

3. Penichet, M. L., Shin, S. U., and Morrison, S. L. (1999) Fab fusion proteins: Immunoligands. In: *Antibody Fusion Proteins.* Chamow, S. M. and Ashkenazi, A., eds. John Wiley & Son, New York, NY, pp. 15–52.

4 Liu, S. J., Sher, Y. P., Ting, C. C., Liao, K. W., Yu, C. P., and Tao, M. H. (1998) Treatment of B-cell lymphoma with chimeric IgG and single-chain Fv antibody-interleukin-2 fusion proteins. *Blood* **92,** 2103–2112.

5 Hornick, J. L., Khawli, L. A., Hu, P., Lynch, M., Anderson, P. M., and Epstein, A. L. (1997) Chimeric CLL-1 antibody fusion proteins containing granulocyte-macrophage colony-stimulating factor or interleukin-2 with specificity for B-cell malignancies exhibit enhanced effector functions while retaining tumor targeting properties. *Blood* **89,** 4437–4447.

6 Dela Cruz, J. S., Lau, S. Y., Ramirez, E. M., et al. (2003) Protein vaccination with the HER2/neu extracellular domain plus anti-HER2/neu antibody-cytokine fusion proteins induces a protective anti-HER2/neu immune response in mice. *Vaccine* **21,** 1317–1326.

7 Penichet, M. L., Harvill, E. T., and Morrison, S. L. (1998) An IgG3-IL-2 fusion protein recognizing a murine B cell lymphoma exhibits effective tumor imaging and antitumor activity. *J. Interferon Cytokine Res.* **18,** 597–607.

8   Becker, J. C., Pancook, J. D., Gillies, S. D., Furukawa, K., and Reisfeld, R. A. (1996) T cell-mediated eradication of murine metastatic melanoma induced by targeted interleukin 2 therapy. *J. Exp. Med.* **183,** 2361–2366.

9   Becker, J. C., Varki, N., Gillies, S. D., Furukawa, K., and Reisfeld, R. A. (1996) Long-lived and transferable tumor immunity in mice after targeted interleukin-2 therapy. *J. Clin. Invest.* **98,** 2801–2804.

10 Xiang, R., Lode, H. N., Dolman, C. S., et al. (1997) Elimination of established murine colon carcinoma metastases by antibody-interleukin 2 fusion protein therapy. *Cancer Res.* **57,** 4948–4955.

11. Hank, J. A. A. M., Gan, J., Sternberg, A., et al. (2003) Clinical Administration of antibody-cytokine hu14.18-IL-2 induces IL-2-mediated immune activation. In: *Proceedings of the American Association for Cancer Research, 94th Annual Meeting.* 2nd Ed., Vol. 44, Washington, DC, p. 1156.

12. Janeway, C. A., Travers, P., Walport, M., and Schlomchick, M. (2001) *Immunobiology: the Immune System in Health and Disease.* 5th Ed. Garland, New York, NY.

13 Gillies, S. D., Reilly, E. B., Lo, K. M., and Reisfeld, R. A. (1992) Antibody-targeted interleukin 2 stimulates T-cell killing of autologous tumor cells. *Proc. Natl. Acad. Sci. USA* **89,** 1428–1432.

14 Harvill, E. T. and Morrison, S. L. (1995) An IgG3-IL2 fusion protein activates complement, binds Fc gamma RI, generates LAK activity and shows enhanced binding to the high affinity IL2-R. *Immunotechnology* **1,** 95–105.

15 Brambell, F. W., Hemmings, W. A., and Morris, I. G. (1964) A theoretical model of gamma-globulin catabolism. *Nature* **203,** 1352–1354.

16 Ward, E. S., Zhou, J., Ghetie, V., and Ober, R. J. (2003) Evidence to support the cellular mechanism involved in serum IgG homeostasis in humans. *Int. Immunol.* **15,** 187–195.

17 Challita-Eid, P. M., Abboud, C. N., Morrison, S. L., et al. (1998) A RANTES-antibody fusion protein retains antigen specificity and chemokine function. *J. Immunol.* **161,** 3729–3736.

18 McGrath, J. P., Cao, X., Schutz, A., et al. (1997) Bifunctional fusion between nerve growth factor and a transferrin receptor antibody. *J. Neurosci. Res.* **47,** 123–133.

19 Peng, L. S., Penichet, M. L., and Morrison, S. L. (1999) A single-chain IL-12 IgG3 antibody fusion protein retains antibody specificity and IL-12 bioactivity and demonstrates antitumor activity. *J. Immunol.* **163,** 250–258.

20 Lustgarten, J., Marks, J., and Sherman, L. A. (1999) Redirecting effector T cells through their IL-2 receptors. *J. Immunol.* **162,** 359–365.

21 Halin, C., Gafner, V., Villani, M. E., et al. (2003) Synergistic therapeutic effects of a tumor targeting antibody fragment, fused to interleukin 12 and to tumor necrosis factor alpha. *Cancer Res.* **63,** 3202–3210.

22 Moreland, L. W., Baumgartner, S. W., Schiff, M. H., et al. (1997) Treatment of rheumatoid arthritis with a recombinant human tumor necrosis factor receptor (p75)-Fc fusion protein. *N. Engl. J. Med.* **337,** 141–147.

23 Moreland, L. W., Schiff, M. H., Baumgartner, S. W., et al. (1999) Etanercept therapy in rheumatoid arthritis. A randomized, controlled trial. *Ann. Intern. Med.* **130,** 478–486.

24 Verma, R., Boleti, E., and George, A. J. (1998) Antibody engineering: comparison of bacterial, yeast, insect and mammalian expression systems. *J. Immunol. Methods* **216,** 165–181.

25 Potter, K. N., Li, Y., and Capra, J. D. (1993) Antibody production in the baculovirus expression system. *Int. Rev. Immunol.* **10,** 103–112.

26 Yoo, E. M., Chintalacharuvu, K. R., Penichet, M. L., and Morrison, S. L. (2002) Myeloma expression systems. *J. Immunol. Methods* **261,** 1–20.

27 Wright, A., Shin, S. U., and Morrison, S. L. (1992) Genetically engineered antibodies: progress and prospects. *Crit. Rev. Immunol.* **12,** 125–168.

28 Penichet, M. L., Dela Cruz, J. S., Shin, S. U., and Morrison, S. L. (2001) A recombinant IgG3-(IL-2) fusion protein for the treatment of human HER2/neu expressing tumors. *Hum. Antibodies* **10,** 43–49.

29 Shin, S. U., Friden, P., Moran, M., and Morrison, S. L. (1994) Functional properties of antibody insulin-like growth factor fusion proteins. *J. Biol. Chem.* **269,** 4979–4985.

30. Harlow, E. and Lane, D. (1989) Anti-immunoglobulin antibodies. In: *Antibodies: A Laboratory Manual.* 1st Ed. Cold Spring Harbor Laboratory, Cold Spring Harbor, NY, pp. 623–631.

31 Penichet, M. L., Dela Cruz, J. S., Challita-Eid, P. M., Rosenblatt, J. D., and Morrison, S. L. (2001) A murine B cell lymphoma expressing human HER2 / neu undergoes spontaneous tumor regression and elicits antitumor immunity. *Cancer Immunol. Immunother.* **49,** 649–662.

32. Morrison, S. L. (1994) Cloning, expression, and modification of antibody V regions. In: *Current Protocols in Immunology,* Vol. 1. Coligan, J. E., Kruisbeek, A. M., Margulies, D. H., Shevach, E. M., and Strober, W., eds. John Wiley & Sons, New York, NY, pp. 2.12.1–2.12.16.

33 Shin, S. U. and Morrison, S. L. (1990) Expression and characterization of an antibody binding specificity joined to insulin-like growth factor 1: potential applications for cellular targeting. *Proc. Natl. Acad. Sci. USA* **87,** 5322–5326.

34 Coloma, M. J., Hastings, A., Wims, L. A., and Morrison, S. L. (1992) Novel vectors for the expression of antibody molecules using variable regions generated by polymerase chain reaction. *J. Immunol. Methods.* **152,** 89–104.

35 Norderhaug, L., Olafsen, T., Michaelsen, T. E., and Sandlie, I. (1997) Versatile vectors for transient and stable expression of recombinant antibody molecules in mammalian cells. *J. Immunol. Methods* **204,** 77–87.

36 Preston, M. J., Gerceker, A. A., Reff, M. E., and Pier, G. B. (1998) Production and characterization of a set of mouse-human chimeric immunoglobulin G (IgG) subclass and IgA monoclonal antibodies with identical variable regions specific for Pseudomonas aeruginosa serogroup O6 lipopolysaccharide. *Infect. Immun.* **66,** 4137–4412.

37 Larrick, J. W., Danielsson, L., Brenner, C. A., Abrahamson, M., Fry, K. E., and Borrebaeck, C. A. (1989) Rapid cloning of rearranged immunoglobulin genes from human hybridoma cells using mixed primers and the polymerase chain reaction. *Biochem. Biophys. Res. Commun.* **160,** 1250–1256.

38. Powers, D. B. and Marks, J. (1999) Monovalent phage display of Fab and scFv fusions. In: *Antibody Fusion Proteins.* Chamow, S. M. and Ashkenazi, A., eds. John Wiley & Son, New York, NY, pp. 151–188.

39 Carter, P., Presta, L., Gorman, C. M., et al. (1992) Humanization of an anti-p185HER2 antibody for human cancer therapy. *Proc. Natl. Acad. Sci. USA* **89,** 4285–4289.

40 Mulligan, R. C. and Berg, P. (1981) Selection for animal cells that express the Escherichia coli gene coding for xanthine-guanine phosphoribosyltransferase. *Proc. Natl. Acad. Sci. USA* **78,** 2072–2076.

41 Sambrook, J., Fritsch, E. F., and Maniatis, T. (1989) Subcloning. In: *Molecular Cloning: A Laboratory Manual.* 2nd. Ed. Cold Spring Harbor Laboratory Press, Cold Spring Harbor, NY, pp. F.1–F.11.

42 Southern, P. J. and Berg, P. (1982) Transformation of mammalian cells to antibiotic resistance with a bacterial gene under control of the SV40 early region promoter. *J. Mol. Appl. Genet.* **1,** 327–341.

43. Sambrook, J., Fritsch, E. F., and Maniatis, T. (1989) Analysis and cloning of eukaryotic genomic DNA. In: *Molecular Cloning: A Laboratory Manual.* 2nd Ed. Cold Spring Harbor Laboratory Press, Cold Spring Harbor, NY, pp. 9.1–9.62.

44 Challita-Eid, P. M., Penichet, M. L., Shin, S. U., et al. (1998) A B7.1-antibody fusion protein retains antibody specificity and ability to activate via the T cell costimulatory pathway. *J. Immunol.* **160,** 3419–3426.

45 Dela Cruz, J. S., Trinh, K. R., Morrison, S. L., and Penichet, M. L. (2000) Recombinant anti-human HER2/neu IgG3-(GM-CSF) fusion protein retains antigen specificity and cytokine function and demonstrates antitumor activity. *J. Immunol.* **165,** 5112–5121.

46 Penichet, M. L., Challita, P. M., Shin, S. U., Sampogna, S. L., Rosenblatt, J. D., and Morrison, S. L. (1999) In vivo properties of three human HER2/neu-expressing murine cell lines in immunocompetent mice. *Lab. Anim. Sci.* **49,** 179–188.

47 Deans, R. J., Denis, K. A., Taylor, A., and Wall, R. (1984) Expression of an immunoglobulin heavy chain gene transfected into lymphocytes. *Proc. Natl. Acad. Sci. USA* **81,** 1292–1296.

48 Foecking, M. K. and Hofstetter, H. (1986) Powerful and versatile enhancer-promoter unit for mammalian expression vectors. *Gene* **45,** 101–105.

49 McLean, G. R., Nakouzi, A., Casadevall, A., and Green, N. S. (2000) Human and murine immunoglobulin expression vector cassettes. *Mol. Immunol.* **37,** 837–845.

50. Harlow, E. and Lane, D. (1989) Electrophoresis. In: *Antibodies: A Laboratory Manual.* 1st Ed. Cold Spring Harbor Laboratory, Cold Spring Harbor, NY, pp. 635–658.

51. Sambrook, J., Fritsch, E. F., and Maniatis, T. (1989) Commonly Used Techniques in Molecular Cloning. *In: Molecular Cloning: A Laboratory Manual.* 2nd Ed. Cold Spring Harbor Laboratory, Cold Spring Harbor, NY, pp. E.1–E.39.

52. Harlow, E. and Lane, D. (1989) Storing and purifying antibodies. In: *Antibodies: A Laboratory Manual.* 1st Ed. Cold Spring Harbor Laboratory, Cold Spring Harbor, NY, pp. 285–318.

53. Harlow, E. and Lane, D. (1989) Immunoaffinity purification. In: *Antibodies: A Laboratory Manual.* 1st Ed. Cold Spring Harbor Laboratory, Cold Spring Harbor, NY, pp. 511–551.

54 Meininger, D. P., Rance, M., Starovasnik, M. A., Fairbrother, W. J., and Skelton, N. J. (2000) Characterization of the binding interface between the E-domain of Staphylococcal protein A and an antibody Fv-fragment. *Biochemistry* **39,** 26–36.

55. Nelson, D. L., Kurman, C. C., and Serbousek, D. E. (1994) 51Cr release assay of antibody-dependent cell-mediated cytotoxicity (ADCC); In *Current Protocols in Immunology*, Vol. 2. Coligan, J. E., Kruisbeek, A. M., Margulies, D. H., Shevach, E. M., and Strober, W., eds. John Wiley & Sons, New York, NY, pp. 7.27.1–7.27.8.

56 Donohue, J. H. and Rosenberg, S. A. (1983) The fate of interleukin-2 after in vivo administration. *J. Immunol.* **130,** 2203–2208.

57 Kendra, K., Gan, J., Ricci, M., et al. (1999) Pharmacokinetics and stability of the ch14.18-interleukin-2 fusion protein in mice. *Cancer Immunol. Immunother.* **48,** 219–229.

58 Harvill, E. T., Fleming, J. M., and Morrison, S. L. (1996) In vivo properties of an IgG3-IL-2 fusion protein. A general strategy for immune potentiation. *J. Immunol.* **157,** 3165–3170.

59 Becker, J. C., Pancook, J. D., Gillies, S. D., Mendelsohn, J., and Reisfeld, R. A. (1996) Eradication of human hepatic and pulmonary melanoma metastases in SCID mice by antibody-interleukin 2 fusion proteins. *Proc. Natl. Acad. Sci. USA* **93,** 2702–2707.

60 Lode, H. N., Xiang, R., Dreier, T., Varki, N. M., Gillies, S. D., and Reisfeld, R. A. (1998) Natural killer cell-mediated eradication of neuroblastoma metastases to bone marrow by targeted interleukin-2 therapy. *Blood* **91,** 1706–1715.

61 Becker, J. C., Varki, N., Gillies, S. D., Furukawa, K., and Reisfeld, R. A. (1996) An antibody-interleukin 2 fusion protein overcomes tumor heterogeneity by induction of a cellular immune response. *Proc. Natl. Acad. Sci. USA* **93,** 7826–7831.

62 Sabzevari, H., Gillies, S. D., Mueller, B. M., Pancook, J. D., and Reisfeld, R. A. (1994) A recombinant antibody-interleukin 2 fusion protein suppresses growth of hepatic human neuroblastoma metastases in severe combined immunodeficiency mice. *Proc. Natl. Acad. Sci. USA* **91,** 9626–9630.

63. Sambrook, J., Fritsch, E. F., and Maniatis, T. (1989) Plasmid vectors. In: *Molecular Cloning: A Laboratory Manual.* 2nd Ed. Cold Spring Harbor Laboratory, Cold Spring Harbor, NY, pp. 1.1–1.110.

64 Chen, T. T., Tao, M. H., and Levy, R. (1994) Idiotype-cytokine fusion proteins as cancer vaccines. Relative efficacy of IL-2, IL-4, and granulocyte-macrophage colony-stimulating factor. *J. Immunol.* **153,** 4775–4787.

65. Harlow, E. and Lane, D. (1989) Bacterial cell wall proteins that bind antibodies. In: *Antibodies: A Laboratory Manual*. Cold Spring Harbor Laboratory, Cold Spring Harbor, NY, pp. 615–623.

66 Harvill, E. T. and Morrison, S. L. (1996) An IgG3-IL-2 fusion protein has higher affinity than hrIL-2 for the IL-2R alpha subunit: real time measurement of ligand binding. *Mol. Immunol.* **33,** 1007–1014.

67 Liu, Z., Gurlo, T., and von Grafenstein, H. (2000) Cell-ELISA using beta-galactosidase conjugated antibodies. *J. Immunol. Methods* **234,** P153–167.

68. McKenzie, A. N. J. and Zurawski, G. (1994) Measurement of Interleukin-13. In: *Current Protocols in Immunology*, Vol. 1. Coligan, J. E., Kruisbeek, A. M., Margulies, D. H., Shevach, E. M., and Strober, W., eds. John Wiley & Sons, New York, NY, pp. 6.18.1–6.18.5.

69. Gieni, R. S., Li, Y., and HayGlass, K. T. (1995) Comparison of [3H]-thymidine incorporation with MTT- and MTS-based bioassays for human and murine IL-2 and IL-4 analysis. Tetrazolium assays provide markedly enhanced sensitivity. *J. Immunol. Methods* **187,** 85–93.

24

Synthesis and Biological Evaluation
of a Paclitaxel Immunoconjugate

Ahmad Safavy and Kevin P. Raisch

Summary

Targeted cancer therapy is a promising strategy for the treatment of this disease. In this approach, a cytotoxic agent (CA), such as a drug or a radionuclide, is attached, usually covalently, to a "targeting" vehicle (TV), which in turn is capable of recognizing specific receptor motifs on the surface of the tumor cells. Once administered systemically, the construct would localize on the tumor through the TV moiety and would release the CA cargo, resulting in the destruction of the malignant tissue. Small-molecule peptides as well as monoclonal antibodies have been used as TVs. The synthesis, antigen binding, and cytotoxicity of a covalent conjugate of the anticancer drug paclitaxel (taxol) to the anti-epidermal growth factor receptor (EGFR) monoclonal antibody C225 (IMC-C225; Erbitux®, ImClone Systems, Somerville, NJ) are described in this chapter to illustrate the methods used for the construction and in vitro evaluation of these conjugates.

Key Words: Paclitaxel, taxol; C225; monoclonal antibody; immunoconjugates; targeted therapy; drug delivery; tumor targeting.

1. Introduction

Tumor-specific treatment of cancer has been greatly facilitated by the development of monoclonal antibodies (MAbs) and through the use of intact, fragmented, or chemically derived MAbs. In this strategy, cell-surface antigens, overexpressed by the cells of a malignant tissue, are targeted by the MAb molecules, which in turn *tag* the cell for elimination by the organism's immune system (intact MAb or fragments), or *deliver* an anticancer agent specifically to the site of the disease (immunoconjugates). Because of the tissue-specific nature of the delivery process, a high tumor-to-normal-tissue ratio would be expected in the target uptake of the CA, which may result in higher antitumor efficacy and lower systemic toxicity and side effects.

Paclitaxel (PTX) is the first of the important taxane antitumor drugs; it has shown activity against several types of human solid tumors *(1,2)*, and has been in clinical use since the early 1990s. The activity of this wide-spectrum drug against breast, ovarian, and prostate cancers is impressive: response rates (RRs) of 40% to 60% have been

reported for PTX in cancer patients, with significant RRs in anthracyclin-resistant disease *(3)*. In cisplatin-treated ovarian cancer patients, PTX has shown good RRs in a phase II study *(3)*. In phase II and III clinical trials with non-small-cell lung cancer patients, PTX demonstrated overall response rates of 10 to 36% *(4)*.

Although the therapeutic advantages of taxanes warranted further preclinical and clinical studies, some inherent shortcomings of these drugs could not be overlooked. Prohibitively low water solubility (approx 0.25 µg/mL) necessitated the addition of allergenic excipients to the clinical formulations. On the other hand, high systemic toxicity limited the level of the administered dose of these drugs. These, and the ultimate interest of the medicinal chemist in designing more potent anticancer drugs with concomitant preservation of the patient quality of life, have led to the design and development of soluble tumor-targeting taxane derivatives *(5)*.

The monoclonal antibody C225 is an anti-epidermal growth factor (EGF) receptor monoclonal antibody that is currently in clinical trials *(6–9)*. The EGF is a transmembrane protein of the tyrosine kinase growth factor family, and its receptor (EGFR) *(10–12)* is overexpressed in a number of human malignancies, including breast, ovarian, lung, and head and neck cancers *(13,14)*. This overexpression of EGFR in different human malignancies renders C225 an attractive model vehicle to study targeted delivery of anticancer agents.

A PTX-peptide conjugate was reported to evaluate the tumor-targeted strategy for this drug using a bombesin/gastrin-releasing peptide receptor-recognizing peptide *(15)*. An enhancement in the in vitro cytotoxic activity of PTX against H1299 human non-small-cell lung cancer cells was observed in controlled experiments, which was ascribed to the targeting mechanism of drug delivery by this conjugate. To further expand the development of water-soluble tumor-targeting taxanes, we conjugated PTX to C225 to build a model conjugate (**Fig. 1**) for evaluation of the potential of this drug-delivery system *(16)*. In this chapter we describe the details of the synthesis, purification, identification, and in vitro evaluation of the PTXC225 conjugate as a model protocol for preparation of paclitaxel-antibody covalent adducts.

2. Materials

Caution: The compounds and reagents listed below should be considered hazardous to living organisms. In addition to the specific indications given below, care must be taken in handling all of them. This may include, but may not be limited to, using protective gear and working in a contained and ventilated space.

1. Paclitaxel (Toxic! Avoid inhalation and contact with skin, eyes, and respiratory system).
2. Monoclonal antibody C225 (may be immunogenic and/or allergenic on ingestion or entering the circulation).
3. Phosphate buffer, 25 m*M*, pH 8.1.
4. Centricon-50 concentrator (Millipore, Bedford, MA).
5. Lowry reagents consisting of:
   a. 2% Na_2CO_3 in 0.1 *N* NaOH.
   b. 0.5% $CuSO_4 \cdot 5H_2O$ in 1% sodium potassium tartrate, adjusted to pH 7.0.
   c. Phenol Follin-Ciocalteau reagent (Sigma Chemical, St. Louis, MO) diluted 1:3 by distilled water.
6. Plate reader at 595 nm.
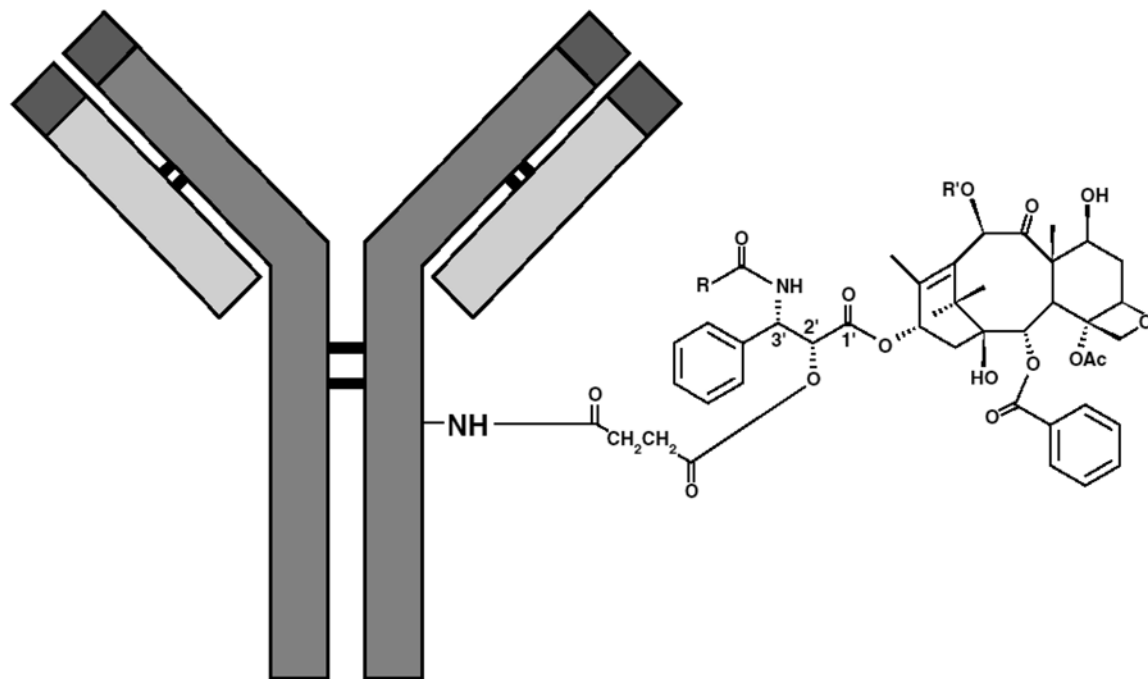
PTX-MAb

Fig. 1. Schematic representation of a paclitaxel-antibody conjugate. The linkage is through the 2'-hydroxy group of the drug. Reprinted with permission from **ref. 16**.

 7. Anhydrous succinic anhydride.
 8. Anhydrous pyridine (Aldrich Chemical, Milwaukee, WI).
 9. Silica gel-60, 230–400 mesh (Merck, Darmstadt, Germany).
10. Chloroform (HPLC grade).
11. Methanol (HPLC grade).
12. Low-pressure glass chromatography column.
13. Melting-point apparatus.
14. Anhydrous *N,N*-dimethyl formamide (DMF).
15. *N*-hydroxy succinimide (NHS).
16. 2-Ethoxy-1-ethoxycarbonyl-1,2-dihydroquinoline (EEDQ).
17. Dialysis tube or slide, 50,000 molecular-weight cut-off (MWCO).
18. Dulbecco's phosphate-buffered saline (DPBS).
19. A-431 human epidermoid cancer cells (CRL-1555, American Type Culture Collection [ATCC], Manassas, VA) (*see* **Note 1**).
20. Dulbecco's modified Eagle's medium (DMEM) (Invitrogen, Carlsbad, CA).
21. Phosphate-buffered saline (PBS): 2.7 mM KCl, 1.47 mM KH$_2$PO$_4$, 137 mM NaCl, 8 mM Na$_2$PO$_4$, pH 7.4.
22. Fetal bovine serum (FBS) (HyClone, Logan, UT).
23. L-glutamine (200 mM, Invitrogen).
24. Trypsin/EDTA solution: 0.03% w/v trypsin, 0.01% w/v EDTA, 0.1% w/v glucose, 220 μM KH$_2$PO$_4$, 168 μM Na$_2$HPO$_4$, 5.4 mM KCl, 137 mM NaCl, 0.006% w/v phenol red, pH 7.05.
25. Hemacytometer (Fisher Scientific, Pittsburgh, PA).
26. Coulter particle counter (Beckman Coulter, Fullerton, CA).
27. Tris-buffered saline with Tween-20 (TBS-T): 20 mM Tris-HCl (pH 7.5), 137 mM NaCl, 0.05% Tween-20.
28. EGF (20μg/mL stock) (Sigma Chemical) (dissolve EGF in 10 mM acetic acid with 0.1% BSA).
29. Lysis buffer: 0.025 M Tris-HCl (pH 7.5), 0.25 M NaCl, 0.005 M EDTA, 1% (v/v) NP-40, 0.001 M phenylmethylsulfonylfluoride (PMSF), 2 μg/mL aprotinin, 2 μg/mL leupeptin, 0.002 M Na orthovanadate, 0.05 M Na fluoride, and 0.03 M Na pyrophosphate (*see* **Note 2**).
30. Eppendorf tubes, 1.5-mL, sterilized by autoclaving.
31. BCA Protein Assay (Pierce, Rockford, IL).
32. SDS-PAGE apparatus (Bio-Rad, Hercules, CA).
33. Trans-Blot system (Bio-Rad).
34. Immobilon-P membrane (Millipore, Bedford, MA).
35. Mouse monoclonal anti-EGFR, clone F4 (Sigma Chemical).
36. Mouse monoclonal antiphosphotyrosine, PY99 (Santa Cruz Biotechnology, Santa Cruz, CA).
37. Sheep polyclonal antimouse IgG-HRP, NAV931 (Amersham Biosciences, Piscataway, NJ).
38. ECL Western Blotting Detection Kit (Amersham Biosciences).
39. BioMax X-ray film, 8 × 10 (Eastman Kodak, Rochester, NY).
40. BioMax film cassette (Eastman Kodak).
41. Photography darkroom.
42. X-ray film developing system.
43. Twenty-four-well cell-culture plates, 3524 (Corning, Corning, NY).
44. Isoton II diluent (Beckman Coulter).
45. Prism software (GraphPad Software, San Diego, CA).

46. Annexin V-FITC Apoptosis Detection Kit (BioVision Inc., Mountain View, CA).
47. Six-well cell-culture plates, 3516 (Corning Inc.).
48. Becton Dickinson FACSCalibur System (Becton-Dickerson, San Jose, CA).
49. CellQuest v. 3.1 software (Becton-Dickinson).

3. Methods

The methods shown in this chapter describe (1) preparation and purification of the side-chain-activated PTX (2'-*O*- paclitaxel succinate, PTXSX); (2) synthesis and purification of the PTXC225 conjugate; (3) identification of the PTXC225 conjugate by matrix-assisted LASER desorption/ionization time-of-flight mass spectrometry MALDI-TOF MS; (4) cell growth inhibition screening on the conjugate; and (5) apoptosis induction assay.

3.1. Preparation and Purification of 2'-O-Paclitaxel Succinate (PTXSX)

Since the antitumor activity of PTX is therapeutically significant only if the drug is available in its native (i.e., chemically unbound) form, potential delivery strategies may be those utilizing a *prodrug* mechanism. In this two-tier approach, the drug is first delivered to the tumor as a covalent adduct to a TV followed by the timely cleavage of PTX inside or in the close vicinity of the tumor to exert its cytotoxic effect.

Due to the special structure of PTX and the type and accessibility of chemical functionalities of the molecule, it was anticipated that esterification of one of the hydroxy groups would be a logical plan. In an attempt to generate water-soluble taxanes, Deutsch et al. had reported the synthesis of 2'-*O*-succinate of PTX in 1985 *(17)*. Also, drug-release kinetics results from early work in our laboratory identified this PTX derivative as a suitable candidate for the design of targeting peptide PTX prodrugs *(15)*. Thus, commercially available PTX and succinic anhydride were first dried in a high-vacuum desiccator over phosphorus pentoxide for 12 h and at room temperature. The dried PTX (1 eq) was then dissolved in anhydrous pyridine, and succinic anhydride (6 eq) was added in solid form and in several portions. The resulting solution was incubated under argon in a sealed flask and at room temperature for 6 h.

Distillation of the solvent in vacuum afforded the solid product PTXSX that was purified by column chromatography. In the procedure of Deutsch et al., a water/acetone crystallization process had been used to purify this product. To achieve better yields of recovery, we used silica gel (SiO$_2$) column chromatography for this purification. In this procedure, 20 g of SiO$_2$ per g of the crude PTXSX was used in a standard glass chromatography column with chloroform as solvent for column packing and product loading. A methanol gradient of 0–15% in chloroform was used to elute the product. This procedure afforded near-quantitative yields of recovery and high product purities. The identity of the PTXSX was established by comparing the melting point and nuclear magnetic resonance spectroscopy characteristics of this product to those reported in the literature *(17)* (*see* **Note 1**).

3.2. Synthesis of PTXC225

Introduction of the succinyl group to PTX generates a single carboxyl group as a specific site for the antibody conjugation. A logical technique for conjugation of

Table 1
Experimental [a] Molar Drug-to-Antibody Ratios (D:A)
for PTXC225 Conjugates Prepared Under Different Conditions [b]

Reaction	PTXSX:C225 [c]	D:A (PBS [d])	D:A (carb [e])
1	1.1	0	0
2	5.1	1.2 ± 0.6	0
3	10.1	2.2 ± 0.2	1.1 ± 0.3
4	20.1	4.5 ± 1.1	2.7 ± 1.7

[a] Measured from MR = MWconjugate - MWC225/ MWPTXSX using MALDI-measured MWs.

[b] Reprinted with permission from **ref. *16***.

[c] Reactant molar ratios

[d] Phosphate-buffered saline, 25 m*M*, pH 8.1

[e] Carbonate buffer, 25 m*M*, pH 9.1

this carboxyl group to the antibody, without interfering with other functions in the molecule, would be through activated ester (AE) formation *(18)*. In this strategy, the endogenous amine groups of the antibody are selectively targeted for binding. Although carboxylic AEs are known to react with hydroxy groups to form carboxylic esters, this transformation occurs only in the presence of a nucleophilic catalyst such as *N,N*-dimethyl 4-aminopyridine *(19)*.

In the presence of both amine and hydroxyl groups, and in the absence of a catalyst, an amide bond is preferentially formed within a typical reaction time. This property of the AE chemistry excluded the possibility of intramolecular self-condensation of PTX.

To design a reproducible protocol for this coupling, the yields of product recovery and the number of substituted drugs per C225 (the PTX:MAb ratio) were studied under different conditions such as reaction times, stoichiometry, solvents, and temperatures (**Table 1**).

Coupling of PTX-SX to the antibody was highly reagent selective. We examined several coupling reagents routinely used in peptide synthesis for amide bond formation *(20)*, and the progress and the extent of the reaction were followed by MALDI-TOF MS (*see* **Subheading 4.3.**). Work in our *(15)* and other laboratories *(21)* has shown that MALDI-TOF MS is a reliable and direct tool for the evaluation of conjugation reactions involving small molecules and antibodies or other large proteins (*see* **Subheading 4.3.**). Of the several different reagents used, only the EEDQ/NHS combination proved effective for this coupling. No significant increase in C225 MW was noticed with other reagents when monitored by mass spectrometry. Thus, the PTXSX (1 eq) was activated by the addition of NHS (1.1 eq) and EEDQ (1.2 eq) in dry DMF (125 µL/µmol PTXSX) at 0°C for 1 h. The DMF solution of the PTXSX activated ester (containing 10 eq of PTXNHS) was then added at 0°C to the solution of C225 (1 eq) in 25 m*M* (pH 8.1) PBS (300 µL/mg C225) with gentle stirring. Stirring was continued at this temperature for 1 h, at which time the formation of the conjugate was confirmed by MALDI-TOF MS. The final product PTXC225 was purified by dialysis in a cellulose membrane with a MW cut-off of 50 kDa and in DPBS (4 × 2 L).

The antibody content of the purified solution was measured by the standard method of Lowry *(22)* (*see* **Note 2**).

3.3 Identification of the PTXC225 Conjugate

A direct and unambiguous identification of the PTX-MAb conjugate is critical. An error in the measurement of the PTX:MAb ratio would result in errors in the calculation of the in vitro and in vivo doses, leading in turn to further complications such as false-negative therapeutic indices or false-positive toxicities. Access to a direct method of measurement of this ratio, therefore, will have obvious advantages *(21)*.

The use of MALDI-TOF MS provides direct MW analysis, which yields a clear measure of the degree of substitution in real time *(23)* and has been used in the conjugation of small molecules to antibodies. In the development of a protocol for the synthesis of unprotected hydroxamic acids (HA)-MAb conjugates, we reported the application of MALDI-TOF MS to the optimization of the reaction conditions and direct measurement of the HA:MAb ratio for the bifunctional chelating agent trisuccin *(24)*.

The PTXC225 described here, as well as other PTX-MAb conjugates not shown, were identified, and their drug-to-antibody (D:MAb) molar ratios were determined by the use of MALDI-TOF MS technique. Once the MWs are measured, the D:MAb is readily calculated through Eq. 1.

$$D:MAb = \frac{MW_{PTXC225} - MW_{C225}}{MW_{PTXSX}} \tag{1}$$

where $MW_{PTXC225}$ is the molecular weight of the purified final product conjugate, and MW_{C225} and MW_{PTXSX} are those of the unconjugated C225 and PTXSX, respectively.

A typical increase in the MW of the MAb as a result of PTX conjugation is shown in **Fig. 2**. In this conjugate, a measured molecular weight increase of 2925 Da refers to a PTX:C225 ratio of 3 as calculated by Eq. 1.

The PTX-C225 coupling was studied under different conditions before selecting the conditions described above. The results are shown in **Table 1**.

3.4. Tumor Cell Line and Maintenance

The A-431 cell line is maintained in Dulbecco's modified Eagle's medium (DMEM) containing 10% fetal bovine serum (FBS), supplemented with 2 m*M* L-glutamine and incubated at 37°C in 5% CO_2 (*see* **Note 3**).

Cells are subcultured (split) every 5–7 d, at a ratio of 1:6.

1. The culture medium is removed, and the cell monolayer is washed once with 5–10 mL PBS (*see* **Note 4**).
2. The cells are removed from the surface of the tissue-culture flask by adding trypsin/EDTA solution (use 1 mL for a T-25 flask or 3 mL for a T-75 flask).
3. The cells are incubated for 5–15 min at 37°C.
4. After the cells are released from the surface, the suspension is diluted using culture medium three times the trypsin/EDTA volume.
5. One-sixth of the cells are transferred to a new flask, and the remaining cells are counted for use in the following experiments (*see* **Note 5**).
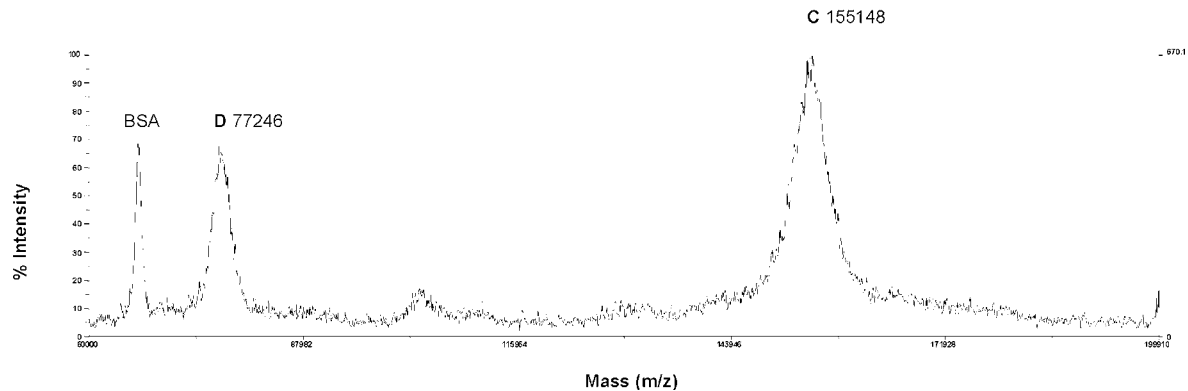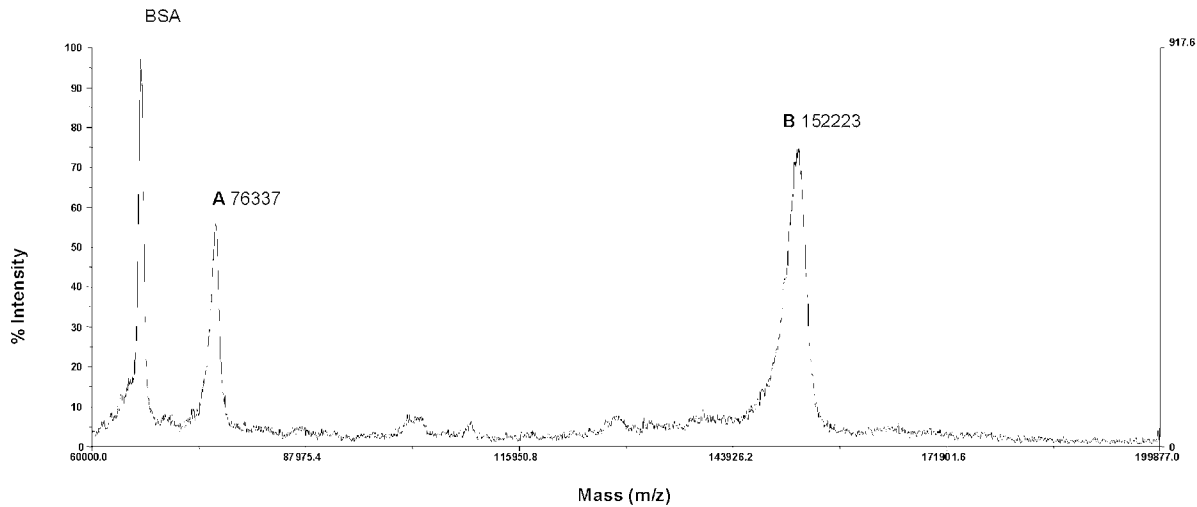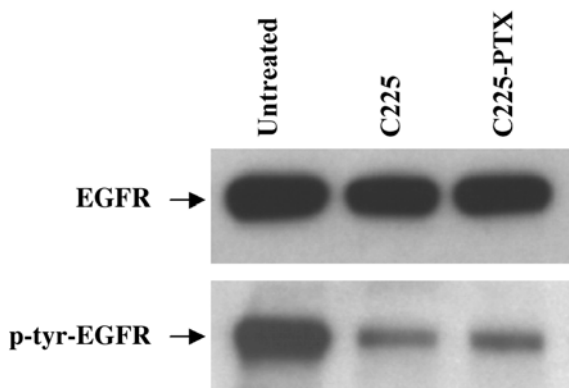
Fig. 3. Immunoblot assay to demonstrate the inhibition of EGFR kinase activity. **(Top)** A 24-h exposure of A-431 cells to C225 or PTXC225 had no effect on the receptor levels. **(Bottom)** EGF-activated EGF tyrosine kinase activity was reduced to the same extent by both C225 and PTXC225. The immunoblots were screened with either *anti*-EGFR **(top)** or *anti*-phosphotyrosine **(bottom)** antibodies. Antibody-free cells were used as controls. Sample cells were treated with equimolar concentrations of C225 and PTXC225. Reprinted with permission from **ref. *16***, copyright 2003 American Chemical Society.

3.5. Measurement of EGFR Expression and Receptor

3.5.1. Phosphorylation

In order to determine whether conjugation of PTX to C225 does not interfere with the ability of the antibody to bind to the corresponding antigen (i.e., EGFR), the conjugate's ability to block EGF-induced EGFR tyrosine kinase activity is examined by an immunoblot assay as shown in **Fig. 3** *(16)*.

1. A-431 cells are seeded in 6-well plates at a density of 100,000 cells/well in 3 mL culture medium per well and are allowed to grow for 48 h.
2. The cells are treated at a concentration of 1 µg/mL with C225 or PTXC225 for 24 h and are exposed to 10 n*M* (60 ng/mL) EGF for 5 min at 37°C (*see* **Note 6**).
3. The cell-culture plates are immediately placed on ice and the cell monolayers are washed three times with ice-cold PBS.
4. The cellular proteins are solubilized in the lysis buffer for 10–15 min on ice (*see* **Note 7**).
5. Enough lysis buffer is used to cover the surface of the cells, i.e., 400 µL of buffer per well in a 6-well tissue-culture plate.

Fig. 2. *(opposite page)* MALDI-TOF mass spectra of C225 **(B)** and PTXC225 conjugate **(C)**. The MW increase confirms the addition of PTX. BSA (MW 66 kDa) is used as a MW calibrator. Peaks A and D are the doubly charged molecular ions showing the half-MWs of B and C, respectively. Reprinted with permission from **ref. *16***, copyright 2003 American Chemical Society.

6. Four hundred μL of the cellular lysate are collected into a sterilized 1.5-mL Eppendorf tube.
7. The cellular lysate is clarified by centrifugation at 12,000g, for 15 min at 4°C, and is transferred into a 1.5-mL Eppendorf tube for storage at –20°C.
8. The protein concentration is quantitated in the clarified cellular lystates using a BCA protein assay kit. The lysis buffer is used as a blank and for diluting the protein standards (*see* **Note 8**).
9. Equal amounts of protein (5 μg) are loaded per lane and separated by 10% SDS-PAGE. Separated proteins are then transferred to Immobilon-P membrane using a Trans-Blot system (as described by the manufacturer).
10. The immunoblot is blocked in 10% milk-tris-buffered saline with Tween-20 (TBS-T), for 1 h at room temperature, or overnight at 4°C.
11. The blocking step and all the subsequent incubations and washes are done using a rocker or shaker with slow agitation:
12. The blocking buffer is removed, and primary antibody, anti-EGFR, or anti-phosphotyrosine is diluted 1:2000 in 3% milk-TBS-T. The blot is incubated at room temperature for 2 h or overnight at 4°C.
13. The primary antibody is removed and the blot is washed at room temperature with TBS-T (three times for 5–10 min each).
14. The secondary antibody, anti-mouse IgG-HRP antibody, is diluted 1:2000 in TBS-T and incubated with the blot for 1 h at room temperature.
15. The blot is washed three times at room temperature (5–10 min each wash) with TBS-T.
16. The blot is developed using the ECL Western Blot detection system according to the manufacturer's protocol.
17. The blot is wrapped in a single layer of plastic wrap and the package is placed in the film cassette. The film is then applied to a blot in the darkroom and is developed after being exposed to the blot for 1 min and 3 min. Based on the results, longer or shorter exposure times must be determined to obtain the optimal exposure.
18. To reprobe the immunoblot with a different primary antibody, the immunoblot is incubated in 7 *M* guanidine hydrochloride for 30 min at room temperature followed by washing four times with sterile H$_2$O. The immunoblot is blocked and probed as described above.

3.6. In Vitro Cell Proliferation Assay

A cell-proliferation assay is used to study the cytotoxic effect of PTXC225 to A-431 cells. Equal molar concentrations of the conjugate, C225 alone, PTX alone, or the combination of the two unconjugated molecules, are compared (*see* **Note 9**) *(16)*.

3.6.1. Determination of IC$_{50}$ Dose

Prior to analyzing PTXC225 in cell proliferation and apoptosis assays, the IC$_{50}$ dose must be determined. The IC$_{50}$ dose is the concentration of the agent resulting in 50% cell growth inhibition as compared to the untreated control cells. To be statistically significant, the IC$_{50}$ dose should be the average of at least three independent experiments:

1. A-431 cells are seeded in 24-well plates at a density of 10,000 cells/well in 1 mL culture medium and allowed to grow for 48 h.
2. On d 0, the cells are treated with PTXC225 in varying concentrations (1–10 n*M*) for 24 h. Filter-sterilized PTXC225 is diluted in culture medium to a concentration of 1 μ*M*.

One to ten µL of this solution is then dispensed into each well containing 1 mL of the culture medium to obtain a drug concentration of 1–10 n*M*.

3. After adding the drug, the plate is rocked for 1–2 min to completely mix the drug into the culture medium. The plate is then incubated at 37°C for 24 h.

4. The drug is removed on d 1 by aspiration, and each well is washed once with 1 mL PBS. The PBS is aspirated off, and 1 mL drug-free medium is added to each well. The plate is incubated at 37°C for an additional 3 d.

5. The cells are counted on d 4 by aspirating the culture medium from each well, washing once with 1 mL PBS/well, and adding 0.5 mL of trypsin-EDTA/well. After the cells are released from the surface, the 0.5 mL of trypsinized cells is diluted into 9.5 mL Isoton II and is counted using a Coulter particle counter: The untreated cells are normalized to 100%, to which base the percent-survival of each treated group is compared. Analyses are done using Prism software.

6. The IC_{50} dose is determined by plotting the normalized cell counts versus the drug dose and computing the dose that inhibits 50% of cell proliferation using a linear quadratic equation.

3.6.2. Determination of Cytotoxicity

1. A-431 cells are seeded in a 24-well plate at a density of 10,000 cells/well in 1 mL culture medium and allowed to grow for 48 h at which time (d 0) the cells are treated with C225 (3.2 n*M*), PTX (6.4 n*M*), C225 + PTX (0.32 n*M* + 0.64 n*M*), or PTXC225 conjugate (3.2 n*M*) for 24 h. All drugs are diluted in culture medium to a concentration of 1 µ*M* and filter sterilized. The wells are spiked with the corresponding agents and are incubated with rocking at 37°C.

2. The drug is removed on d 1 by aspiration, and each well is washed once with 1 mL PBS followed by the addition of 1 mL drug-free medium, and incubation at 37°C for an additional 3 d.

3. The cells are counted on d 4 and normalized to the percentage of untreated cells as described above in **Subheading 3.6.1., step 5**.

3.7. Measurement of Apoptotic Cell Death

Detection of early stages of apoptosis was determined using an annexin V-FITC apoptosis detection kit as described previously by Safavy et al. *(16)*:

1. A-431 cells are seeded in 6-well plates at a density of 40,000 cells/well in 3 mL culture medium per well and allowed to grow for 48 h.

2. On day 0, A-431 cells are treated with each agent for 24 h as described in **Subheading 3.6.2.**: PTX (6.4 n*M*), C225 (3.2 n*M*), PTX + C225 (6.4 n*M* + 3.2 n*M*), or PTXC225 conjugate (3.2 n*M*).

3. The drug is removed after 24 h by aspiration, and each well is washed once with 3 mL PBS per well followed by the addition of 3 mL drug-free medium to each well. The plate is incubated at 37°C for an additional 3 d.

4. On d 4, the culture medium is collected into a 12×75 mm tube, and a 1-mL PBS wash is added to each respective tube containing the culture medium.

5. The cell monolayer is removed by adding 0.5 mL typsin-EDTA and incubating the cells at 37°C. The trypsinized cells are added to the respective tube containing culture medium and PBS wash.

6. The cells are separated from the medium by centrifugation at 400*g* for 5 min.

7. The cells are washed once with 3 mL ice-cold PBS.

8. After centrifugation, the PBS is removed and the cells are incubated in binding buffer containing annexin V-FITC and PI as described by the manufacturer's protocol.
9. The data is collected using a Becton-Dickinson FACSCalibur system and analyzed using CellQuest v.3.1 software.

4. Notes

1. Due to the possibility of damaging the drug activity, heating of the PTX during the drying process should be avoided. We found that removing moisture over P_2O_5 at room temperature and in high vacuum is sufficient.

    The purity and dryness of the pyridine used is also very important. This highly hygroscopic liquid may be purified by storage over sodium hydroxide followed by distillation from barium oxide. Storage over 4 Å molecular sieve under dry argon or nitrogen is recommended.

2. It was found during the course of this study that conjugation of up to three PTX molecules per molecule of the antibody completely preserves the solubility of the MAb in aqueous media at concentrations normally used for in vitro and in vivo experiments. For this work, we used conjugate solutions within a C225 concentration range of 0.25–2.2 mg/mL. Furthermore, we have prepared completely soluble PTXC225 solutions for therapeutic experiments in animal models containing up to 10 mg/mL of the conjugate. Conjugate solubility, however, seemed to be limited by the PTX:C225 ratio. Conjugates with a PTX:C225 of >3 caused either immediate or delayed loss of the protein in the form of a heavy precipitate. At the same time, a PTX:C225 of 2 seemed to be sufficient for effective cell killing as indicated by the in vitro cytotoxicity experiments described in **Subheading 3.2**.

3. A-431 cells were used in this protocol, because they are a very well studied EGFR-overexpressing cell line *(24)*. However, while many other cell lines can be used, the initial cell-plating numbers may have to be adjusted according the growth characteristics of each particular cell line.

4. All cell-culture manipulations are carried out inside a biological hood. Culture medium and buffers containing glucose are 0.22-µm filter sterilized, and all other buffers are sterilized by autoclaving. Antibodies, antibody-drug conjugates, and chemotherapy drugs are 0.22-µm filter sterilized prior to use.

5. For cell counting, a particle counter by Beckman Coulter is very helpful due to the volume of samples to be counted. To set up the Beckman Coulter counter, first count the cells using a hemacytometer, following the manufacturer's protocol. The cell suspension may have to be diluted 1:10 or 1:100 in PBS in order to have an accurate count. After the number of cells per milliliter have been determined, five identical dilution vials are set up for the Beckman Coulter counter. Each vial can be used for three or four cell counts. Cells are counted at a low-threshold setting. Between cell counts, the lower threshold is adjusted up or down and the cells are counted again. Adjusting the lower threshold and cell counting is continued until the counter has accurately counted the same number of cells/mL as determined by the hemacytometer. This lower threshold setting should be recorded if it is to be used for counting this cell line. The lower threshold setting must be determined for each cell line used in these experiments.

6. EGF is added quickly to each well in a biological hood and mixed into the culture medium by gently making a figure-eight motion with the tissue-culture plates. Then the plate is incubated at 37°C for no more than 5 min. Reports have indicated that between 5 and 10 min after exposure to a high concentration of EGF, the EGF receptor begins to be internalized and degraded.

7. All the ingredients for the lysis buffer are to be mixed together except for the inhibitors leupeptin, Na-orthovanadate, aprotinin, and PMSF. The buffer should be autoclaved and stored at 4°C. On the d the lysis buffer is to be used, add the inhibitors to an aliquot of the buffer and PMSF, and store on ice.

8. Optimally, protein concentrations should be determined on the cellular lysates prior to storage at –20°C. However, this may not be practical if lysates are collected at different time points. Therefore, the cellular lysates can be quickly thawed at 37°C, and then placed on ice until used for the protein assay. If a precipitate is visible after thawing, the incubation of the lysates should be continued at 37°C followed by vortexing until the precipitate becomes soluble.

9. Due to solubility of PTX in aqueous solutions, the stock solution of the drug is prepared in high-purity DMSO. The amount of free PTX should be calculated from the measured PTX:C225 in the conjugate. A PTX:C225 of 2 translates into 6.4 n*M* of free PTX at a conjugate concentration of 3.2 n*M* with respect to C225.

References

1. Rowinsky, E. K. and Donehower, R. C. (1995) Paclitaxel (taxol). *N. Engl. J. Med.* **332,** 1004–1014.
2. Donehower, R. C., Rowinsky, E. K., Grochow, L. B., Longnecker, S. M., and Ettinger, D. S. (1987) Phase I trial of taxol in patients with advanced cancer. *Cancer Treat. Rep.* **71,** 1171–1177.
3. Khayat, D., Antoine, E. C., and Coeffic, D. (2000) Taxol in the management of cancers of the breast and the ovary. *Cancer Invest.* **18,** 242–260.
4. Goldspiel, B. R. (1997) Clinical overview of the taxanes. *Pharmacotherapy* **17,** 110S–125S.
5. Safavy, A. (2001) Taxane derivatives for targeted therapy of cancer. US patent no. 6.191.290.
6. Sridhar, S. S., Seymour, L., and Shepherd, F. A. (2003) Inhibitors of epidermal-growth-factor receptors: a review of clinical research with a focus on non-small-cell lung cancer. *Lancet Oncol.* **4,** 397–406.
7. Kies, M. S. and Harari, P. M. (2002) Cetuximab (Imclone/Merck/Bristol-Myers Squibb). *Curr. Opin. Investig. Drugs* **3,** 1092–1100.
8. Goldstein, N. I., Prewett, M., Zuklys, K., Rockwell, P., and Mendelsohn, J. (1995) Biological efficacy of a chimeric antibody to the epidermal growth factor receptor in a human tumor xenograft model. *Clin. Cancer Res.* **1,** 1311–1318.
9. Naramura, M., Gillies, S. D., Mendelsohn, J., Reisfeld, R. A., and Mueller, B. M. (1993) Therapeutic potential of chimeric and murine anti-(epidermal growth factor receptor) antibodies in a metastasis model for human melanoma. *Cancer Immunol. Immunother.* **37,** 343–349.
10. Thompson, D. M. and Gill, G. N. (1985) The EGF receptor: structure, regulation and potential role in malignancy. *Cancer Surv.* **4,** 767–788.
11. Schlessinger, J. (1988) The epidermal growth factor receptor as a multi-functional allosteric protein. *Biochem.* **27,** 3119–3123.
12. Carpenter, G. and Cohen, S. (1979) Epidermal growth factor. *Ann. Rev. Biochem.* **48,** 193–216.
13. Pathak, M. A., Matrisian, L. M., Magun, B. E., and Salmon, S. E. (1982) Effect of epidermal growth factor on clonogenic growth of primary human tumor cells. *Int. J. Cancer* **30,** 745–750.

14 Singletary, S. E., Baker, F. L., Spitzer, G., et al. (1987) Biological effect of epidermal growth factor on the in vitro growth of human tumors. *Cancer Res.* **47,** 403–406.

15 Safavy, A., Raisch, K. P., Khazaeli, M. B., Buchsbaum, D. J., and Bonner, J. A. (1999) Paclitaxel derivatives for targeted therapy of cancer: toward the development of smart taxanes. *J. Med. Chem.* **42,** 4919–4924.

16 Safavy, A., Bonner, J. A., Waksal, H., et al. (2003) Synthesis and biological evaluation of paclitaxel-C225 conjugate as a model for targeted drug delivery. *Bioconjug. Chem.* **14,** 302–310.

17 Deutsch, H., Glinski, J., Hernandez, M., et al. (1989) Synthesis of congeners and prodrugs: water soluble prodrugs of taxol with potent antitumor activity. *J. Med. Chem.* **32,** 788–792.

18 Wilbur, D. S. (1992) Radiohalogenation of proteins: An overview of radionuclides, labeling methods, and reagents for conjugate labeling. *Bioconjug. Chem.* **3,** 433–470.

19 Neises, B. and Steglich, W. (1978) Simple method for the esterification of carboxylic acids. *Angew. Chem. Int. Enl.* **17,** 522–523.

20. Lloyd-Williams, P., Albericio, F., and Giralt, E. (1997) *Chemical Approaches to the Synthesis of Peptides*. CRC, Boca Raton, FL.

21. Siegel, M. M., Hollander, I. J., Hamann, P. R., et al. (1991) Matrix-assisted uv-laser desorption/ionization mass spectrometric analysis of monoclonal antibodies for the determination of carbohydrate, conjugated chelator, and conjugated drug content. *Anal. Chem.* **63,** 2470–2481.

22. Lowry, O. H., Rosebrough, N. J., Farr, A. L., and Randall, R. J. (1951) Protein measurement with the folin phenol reagent. *J. Biol. Chem.* **193,** 265–275.

23. Fenselau, C. (1997) MALDI MS and strategies for protein analysis. *Anal. Chem.* **69,** 661A–665A.

24. Saleh, M. N., Raisch, K. P., Stackhouse, M. A., et al. (1999) Combined modality therapy of A-431 human epidermoid cancer using anti-EGFr antibody C225 and radiation. *Cancer Biother. Radiopharm.* **14,** 451–463.

25 ⎯⎯⎯⎯⎯⎯⎯⎯⎯⎯⎯⎯⎯⎯⎯⎯⎯⎯⎯⎯⎯⎯⎯⎯⎯⎯

Cytotoxic Tumor Targeting
With scFv Antibody-Modified Liposomes

Cornelia Marty and Reto A. Schwendener

Summary

Specific targeting of liposome-formulated cytotoxic drugs or antigens to receptors expressed selectively on target cells represents an effective strategy for increasing the pharmacological efficacy of the delivered molecules. We have developed a feasible technique to selectively attach antibodies and fragments thereof, but also small-mol-wt ligands such as peptides, carbohydrates, or any molecules that recognize and bind target antigens or receptors to the surface of small unilamellar liposomes. Our concept is based on the site-specific functionalization of the ligands to be attached to the liposomes by thiol groups. These thiol groups can easily be introduced to antibodies or peptides by addition of cysteines, preferably at sites that do not interfere with the receptor binding domains. Optimally, the site-specific modification is introduced at the C-terminal end of the ligand, separated by an inert spacer sequence located between the thiols and the specific part of the ligand. The thiol-reactive molecules on the liposome surface are maleimides that are linked to phospholipids composing the liposome bilayer membrane. We illustrate the coupling method of a functionalized single-chain antibody fragment with binding specificity to ED-B fibronectin, an isoform of fibronectin exclusively expressed in tumor tissues, to long circulating small unilamellar poly(ethylene glycol) liposomes.

Key Words: Ligand-mediated liposome targeting; site-directed ligand modification; ligand functionalization; liposomes; immunoliposomes; thiol-maleimide coupling; cysteine modification; single-chain antibody fragment; peptides; targeted tumor therapy; vaccines.

1. Introduction

Antibody or small-molecule ligand-mediated targeting of liposome-encapsulated anticancer or antiangiogenic drugs to receptors expressed selectively on tumor and/or tumor endothelial cells represents an effective strategy for increasing the therapeutic efficacy of the liposomal drugs. Small unilamellar ligand-targeted liposomes are intended to increase the specificity of interaction with target cells and to increase the amount of drug delivered to these cells *(1,2)*. We have developed a feasible technique to attach antibodies and fragments thereof, but also small-mol-wt ligands such as peptides, carbohydrates, or any molecules that selectively recognize and bind to

target antigens or receptors, to the surface of small unilamellar liposomes (SUV) *(3)*. The random introduction of reactive groups to a protein—e.g., via amino group modification—leads to uncontrollable attachment and random orientation of the attached molecules on the liposome surfaces, causing decrease of binding efficiency. By introducing reactive groups at a distinct site on the ligand molecule, the orientation on the liposome surface can be defined. Our concept is based on the site-specific functionalization of the ligands to be attached to the liposomes by thiol groups. These thiol groups can easily be introduced onto antibodies or peptides by addition of cysteines, preferably at sites that do not interfere with the receptor binding domains. Optimally, the site-specific modification is introduced at the C-terminal end of the ligand, separated by an inert spacer sequence located between the thiols and the specific part of the ligand. The thiol-reactive molecules on the liposome surface are maleimides that are linked to phospholipids composing the liposome bilayer membrane. We illustrate the coupling method of a functionalized single-chain antibody fragment (scFv) with binding specificity to ED-B fibronectin, an isoform of fibronectin exclusively expressed in tumor tissues, to long circulating small unilamellar poly(ethylene glycol)-liposomes (PEG-liposomes).

2. Materials

2.1. Liposome Preparation and Modification

1. Soy phosphatidylcholine (SPC) (L. Meyer GmbH, Hamburg, Germany).
2. Cholesterol Fluka (Buchs, Switzerland) (*see* **Note 1**).
3. D,L-α-tocopherol (Merck, Darmstadt, Germany).
4. 2-Dipalmitoyl-sn-glycero-3-phosphatidylethanolamine (DPPE) (Sygena, Liestal, Switzerland).
5. Methoxy-poly(ethylene glycol)-phosphatidylethanolamine (PE-PEG-OMet) (Sygena).
6. Amino-poly(ethylene glycol)-phosphatidylethanolamine (PE-PEG-NH$_2$) (Shearwater Polymers, Enschede, The Netherlands).
7. 3,3'-dioctadecyloxacarbocyanine perchlorate (DiO) (Molecular Probes, Leiden, The Netherlands).
8. Phosphate buffer (PB): 13 m*M* KH$_2$PO$_4$, 54 m*M* NaHPO$_4$, pH 7.4.
9. Sulfosuccinimidyl *N*-(4-carboxycyclohexylmethyl)maleimide (sulfo-SMCC) (Pierce, Rockford, IL).
10. Round-bottom flasks (25–250 mL).
11. Sodium cholate.
12. Rotatory evaporator, e.g., Rotavap (Buechi AG, Flawil, Switzerland).
13. Mini-Lipoprep instrument (Harvard Apparatus Limited, Edenbridge, Kent, UK).
14. Lipex™ extruder (Lipex Biomembranes, Vancouver, Canada).
15. Nuclepore membranes of defined pore sizes: 0.4, 0.2, 0.1 µm (Whatman, Maidstone, Kent, UK).
16. Dialysis tubing, 10,000 mol wt Cut off.
17. Fluorescence spectrometer.

2.2. Antibody Coupling

1. HBSE buffer: 10 m*M* HEPES, 150 m*M* NaCl, 9.1 m*M* EDTA, pH 7.5.
2. Tributylphosphine (Fluka, Buchs, Switzerland).

3. Metrizamide (Sigma , St. Louis, MO).
4. Ultracentrifuge tubes (Beckmann).
5. Ultracentrifuge.

2.3. In Vitro Binding of scFv-Liposomes to Tumor Cells

1. Cell-culture medium (DMEM; Gibco-BRL, Basel, Switzerland) supplemented with 10% fetal bovine serum (FBS), 1% L-glutamine, 1% nonessential amino acids, 1 mM sodium pyruvate, 100 U/mL penicillin, and 0.1 mg/mL streptomycin (all from Gibco-BRL).
2. Phosphate buffered saline (PBS): 137 mM NaCl, 2.68 mM KCl, 8.09 mM Na$_2$HPO$_4$, 1.76 mM KH$_2$PO$_4$, pH 7.4.
3. Glass cover slips (20-mm diameter).
4. Collagen I from rat tails (Sigma) or extracted from rat tails (*see* **Note 2**).
5. Glycerin 10%.
6. Fluorescence microscope.

3. Methods

The methods described below outline (1) the preparation of liposomes by detergent dialysis and filter extrusion; (2) the liposome modification with maleimide molecules; (3) the attachment of functionalized scFv antibody fragments to liposomes via thiol-to-maleimide coupling; (4) the separation of liposomes from unbound scFv fragments; and (5) the in vitro binding of scFv-modified liposomes to cancer cells.

3.1. Liposome Preparation

In the past 30 yr a large number of methods of liposome preparation have been developed and refined. For comprehensive information, we refer to the corresponding literature. We use the two methods described below because of their ease and versatility, as well as the high quality of the liposomes they produce.

3.1.1. General Liposome Compositions

Liposomes can be composed of a large selection of phospholipids and additional lipophilic compounds, such as cholesterol, poly(ethylene glycol) lipids (PEG), and antioxidants. Depending on the intended application of the liposomes, different lipid compositions have to be selected. The "state-of-the-art" liposomes used for intravenous applications—e.g., liposomes carrying cytotoxic antitumor drugs—are those composed of lipids containing hydrophilic carbohydrates or polymers, usually a poly(ethylene glycol)-modified phopholipid. Such PEG- or "stealth" liposomes evade fast absorption in the mononuclear phagocyte system *(1)*. Liposome formulations carrying antigens intended as vaccines are administered by subcutaneous or intradermal injection and do not require PEG modification, since the targets are phagocytosing cells—macrophages and dendritic cells localized at the site of injection *(4)*. The lipid compositions used for the preparation of conventional scFv-liposomes and pegylated scFv-liposomes are given in **Table 1**.

3.1.2. Model Calculations of Numbers of Liposomes and Reactive Groups

Based on experimentally determined mean hydrodynamic diameters of the liposomes (*see* **Note 3**) and from assumptions on vesicle geometry parameters made by

Table 1
Lipid Composition in Milligrams per Milliliter of the Liposome Types A, B, C, D

Type	Liposomes	SPC [a]	Cholesterol	DPPE	DPPE-PEG-Omet	DPPE-PEG-NH$_2$
A	Conventional control liposomes	40 mg 100 mol% 52 μmol	4 mg 20 mol% 10 μmol			
B	Conventional liposomes for modification	40 mg 100 mol% 52 μmol	4 mg 20 mol% 10 μmol	2.52 mg 7 mol% 3.5 μmol		
C	Control PEG liposomes	40 mg 100 mol% 52 μmol	4 mg 20 mol% 10 μmol		9.8 mg 7 mol% 36.0 μmol	
D	PEG liposomes for modification	40 mg 100 mol% 52 μmol	4 mg 20 mol% 10 μmol			9.8 mg 7 mol% 3.5 μmol

[a] The compositions of the lipid mixtures are always calculated by taking the main lipid component (SPC, or other lipids) as 100% in moles. The additional components are given as mole percents referred to the main lipid. To lipid mixtures containing unsaturated fatty acids antioxidants such as D,L-α-tocopherol are added at 0.1–0.2 mol% (*see* **Note 3**).

Table 2
Calculated Numbers of Liposomes As a Function
of Experimentally Measured Mean Diameters

Mean diameter (nm)	Phospholipid molecules per liposome	Liposomes per 1 mg phospholipid ($\times E^{13}$)	Trapped volume per 1 mg phospholipid (microliters)
25	4,250	18.400	0.52
50	19,930	3.930	1.60
80	54,000	1.450	2.90
100	86,070	0.911	3.80
120	125,500	0.625	4.70
200	357,500	0.219	8.20

Huang and Mason *(5)*, it is possible to approximate liposome numbers per volume and, e.g., the numbers of amino groups available on one liposome of a given composition and mean diameter. In **Table 2**, examples of calculations based on mean liposome sizes of 25 to 200 nm are listed. For example, a liposome with a mean diameter of 50 nm contains about 20,000 SPC molecules, based on the volume of one SPC molecule of 1.253 nm^3. Thus, the same given amount of lipid in mg/mL yields more than four times more liposomes with a diameter of 50 nm (1.6×10^{15}/mL) than liposomes having a diameter of 100 nm (3.6×10^{14}/mL; *see* **Table 2**).

A graphic plot of the liposome diameters (nm) vs the numbers of liposomes formed with 1 mg phospholipid/mL yields an exponential curve. After further transformations the following equation is obtained:

$$\text{Number of liposomes/mL} = a \times d^b \times c$$

where $a = 1.594 \times 10^{17}$ (per nm/mg), $b = -2.118$, c = phospholipid concentration of the liposome solution (mg/mL), and d = mean diameter of the prepared liposomes (nm).

Under the assumption that all other additional membrane-forming molecules occupy the same volume of 1.253 nm^3 in the bilayer, and that all molecules are evenly distributed in both lipid monolayers, liposomes containing, for example, 2 mol% amino groups with a mean diameter of 50 nm carry approx 400 amino groups distributed over the bilayer membrane. Hence, 200 amino groups are located on the outer monolayer surface, available for chemical modification. Consequently—as shown in **Table 3** for liposomes of 40 mg SPC/mL (*see* **Table 1**) and diameters of 50 and 100 nm, and considering losses during production—the vesicles are composed of different numbers of lipid molecules and reactive groups. A liposome containing 7 mol% amino groups and having a diameter of 50 nm carries on average 640 amino groups on its surface, whereas on a larger liposome of 100 nm, approx 2800 amino groups are available for modification.

3.1.3. Liposome Preparation by Dialysis

Small unilamellar vesicles (SUV) of 50–200 nm mean size can be prepared using the detergent dialysis method *(6)*. This method is based on the controlled removal of

Table 3
Calculation of Reactive Groups on Liposomes Prepared As Listed in Table 1

Diameter (nm)	NH$_2$-groups (mol%)	Initial concentration (NH$_2$-groups/mL)	Calculated numbers (NH$_2$-groups/lip)[a]	Yield after modification (maleimide groups/mL) [b]	Yield after modification (maleimide groups/lip) [c]
50 ± 15	2	3.1×10^{17}	200	1.6×10^{17}	120
	7	1.0×10^{18}	640	5.1×10^{17}	400
100 ± 15	2	3.1×10^{17}	850	1.6×10^{17}	510
	7	1.0×10^{18}	2800	5.1×10^{17}	1670

[a] lip, liposome.

[b] Yield calculation: [initial lipid concentration] $\times 0.95 \times 0.6 \times 0.9 = 0.513$ (based on yields of liposome preparation [95%], yield of sulfo-SMCC modification calculated from lipid-NH$_2$-group labeling with BODIPY [60%] and loss or dilution of lipid during dialysis [90%]).

[c] Corresponding to a sulfo-SMCC modification efficiency of 60 % at a 5X molar excess of sulfo-SMCC (*see* **Subheading 3.1.6.**).

detergent from mixed lipid/detergent micelles. The compositions of the lipid mixtures are calculated by taking the main bilayer-forming lipid component (SPC, or other lipids) as 100% in moles. The additional components are calculated as mole percents referred to the main lipid:

1. For liposome preparation, a given lipid mixture (SPC, 40 mg/mL; cholesterol, 4 mg/mL, 20 mol%; DPPE, 2.5 mg, 7 mol%; D,L-α-tocopherol, 0.2 mg, 1 mol%; *see* **Table 1**) is dissolved in methanol/methylene chloride (1:1 v/v) in a round-bottom flask (*see* **Notes 4** and **5**).
2. Sodium cholate (*see* **Note 6**) at a ratio of total lipids, including all lipophilic molecules, to detergent of 0.6 moles is added.
3. This mixture is evaporated at 40°C to dryness (30–60 min) using a rotatory evaporator.
4. The dry lipid/detergent film is dispersed in PB and left 30–60 min at room temperature for equilibration.
5. Dialyze the formed mixed lipid/detergent micelles against 3–5 L of PB (volume ratio = 1 to 1000) for 12–15 h at room temperature, e.g., using a Mini-Lipoprep instrument (*see* **Notes 7** and **8**).

3.1.4. Liposome Preparation by High-Pressure Filter Extrusion

SUVs can also be prepared by sequential filter extrusion of multilamellar liposome dispersions in PB through Nucleopore membranes (Sterico, Dietikon, Switzerland) of 0.4, 0.2, 0.1, and 0.05 µm pore diameter with a Lipex™ extruder (Lipex Biomembranes Inc., Vancouver, Canada) *(7)*. Using this method, lipid films without detergents are prepared as described in **Subheading 3.1.3.** and dispersed in PB, followed by sequential extrusion through Nucleopore membranes of decreasing pore sizes (*see* **Notes 9** and **10**).

3.1.5. Fluorescence Labeling of Liposomes and scFv Antibodies

The lipophilic dye DiO is used for the labeling of liposomes. DiO dissolved in methanol/methylene chloride (1:1, v/v) is added at 0.2–0.4 mg/mL (0.2–0.4 mol%) to the organic lipid mixture. To determine the initial lipid concentration, aliquots of the lipid dispersion are taken before dialysis or extrusion. These aliquots and those taken after liposome preparation are measured in a fluorescence spectrometer for the determination of the lipid concentrations after liposome preparation. Functionalized antibodies or peptides can be trace labeled with fluorescent dyes such as Alexa Fluor or BODIPY succinimidyl ester (Molecular Probes), allowing unspecific amino-group labeling with dyes of different fluorescence properties.

3.1.6. Introduction of Maleimide Groups onto Liposome Surfaces

The liposomes are modified with the bifunctional coupling reagent sulfo-SMCC to introduce maleimide groups onto their surface.

1. The liposome types B or D that contain amino groups introduced with corresponding lipids (*see* **Table 1**) in 0.5 mL PB are incubated under gentle stirring with 0.6 mg crystalline sulfo-SMCC corresponding to a fivefold molar excess relative to the reactive amino groups, for 30–60 min at 30°C.
2. Nonreacted sulfo-SMCC is removed by dialysis using a tube with 10,000 mol-wt cutoff (*see* **Notes 11–14**).
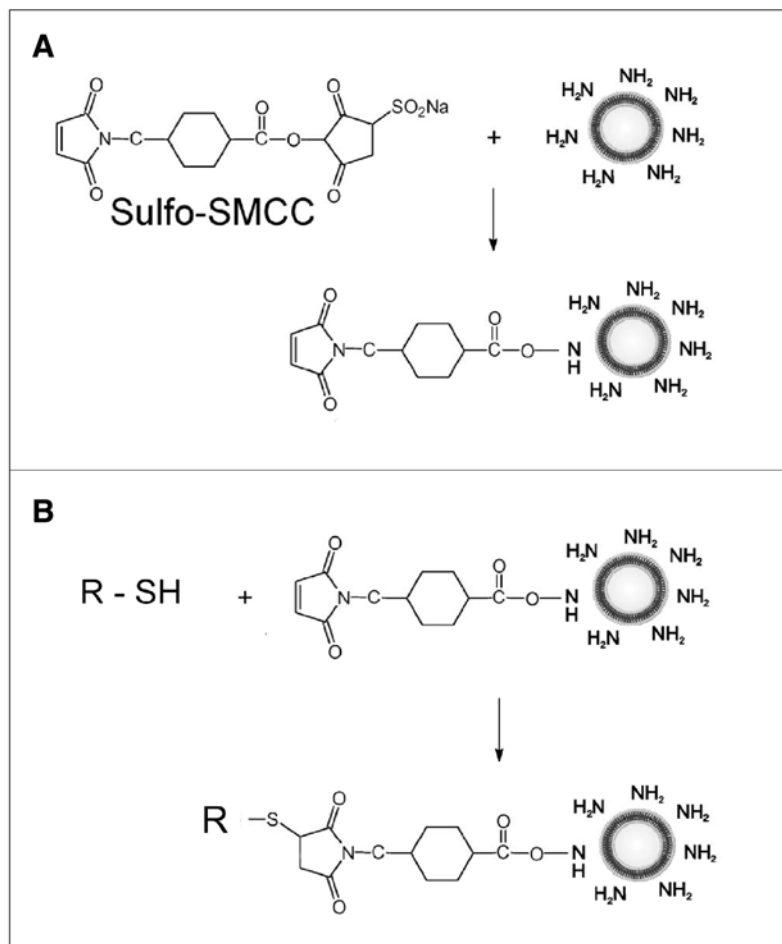
Fig. 1. **(A)** Introduction of maleimide groups to the surface of amino-group-containing conventional or PEG-liposomes. **(B)** Covalent coupling of thiol-functionalized molecules R-SH (scFv antibody fragments, peptides, and so on) to maleimide liposomes.

3.1.7. Coupling of scFv Antibody Fragments to Maleimide-Modified Liposomes

For the method of cloning, protein expression in *Pichia pastoris*, and purification of functionalized scFv antibody fragments, we refer to our publication *(8)*. Briefly, an original anti-ED-B-fibronectin scFv antibody was engineered by functionalization at its C-terminal end by the introduction of a hydrophilic spacer (GGSSGGSSGS) and the terminal cysteine -Cys-Gly-Cys-Ser-Cys sequence (*see* **Note 15**). The scheme of the scFv-liposome coupling is shown in **Fig. 1**.
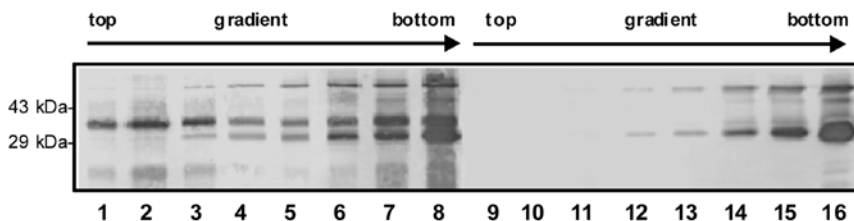
Fig. 2. Separation of scFv-liposomes from unbound scFv antibody molecules. Western blot analysis of aliquots taken from top to bottom of a metrizamide gradient: lanes 1–8, probes from an incubation of scFv-liposomes (positive reaction); lanes 9–16, probes from an incubation of scFv with unmodified control liposomes (negative control). Lanes 1–3 and 9–11 correspond to fractions containing liposomes.

Due to the presence of the introduced cysteines, the scFv antibodies form dimers in solution. Thus, coupling to the liposomes has to be effected in the presence of reducing agents (*see* **Note 16**). The purified scFv antibody dimer (0.5 mg/mL) in HBSE buffer is reduced in the presence of a 2 m*M* final concentration of tributylphosphine (TBP) for 4 h at 20–25°C (room temperature) under an argon or nitrogen atmosphere. Maleimide-modified and fluorescence-labeled liposomes (types B or D, conventional or "stealth") in 100 μL HBSE are incubated with 100 μg reduced scFv antibody in 200 μL HBSE for 10–20 h at 20–25°C (room temperature) in the presence of 2 m*M* TBP under argon or nitrogen atmosphere (*see* **Note 17**). Nonreacted maleimide groups can be blocked by addition of an excess of cysteine, followed by further incubation (e.g., 5- to 10-fold molar excess cysteine relative to the maleimide concentration, 2 h incubation). The modified liposomes are separated from nonreacted scFv on a metrizamide gradient as described in **Subheading 3.2.**

3.2. Separation of scFv-Liposomes From Nonreacted scFv on a Metrizamide Gradient

Nonreacted scFv fragments are separated from the scFv-liposomes by flotation on a discontinuous metrizamide gradient.

1. The liposome–scFv reaction solution (200 μL) is mixed with 100 μL metrizamide (60% in HBSE [w/v]) in ultracentrifuge tubes (5 mL, nitrocellulose) and overlaid with 2 mL metrizamide (10% in HBSE [w/v]) followed by HBSE as a top layer.
2. The density gradient is centrifuged for 7 h at 85,000*g* and 4°C using a swing-out rotor in an ultracentrifuge.
3. Fractions of 400 μL are carefully removed from the bottom to the top of the tubes by cautious insertion of a capillary tube or Pasteur pipet and analyzed for protein content on a non-reducing 14% SDS-PAGE gel followed by Western blot analysis (*see* **Note 18**).
   As shown in **Fig. 2**, fractions containing scFv-coupled liposomes (lanes 1–3) give a 33 kDa band on a Western blot, corresponding to the mol wt of the scFv antibody monomer plus the attached PEG-lipid. Nonreacted scFv monomers and dimers remain at the bottom of the metrizamide gradient (lanes 5–8 and 14–16). Incubation of unmodified
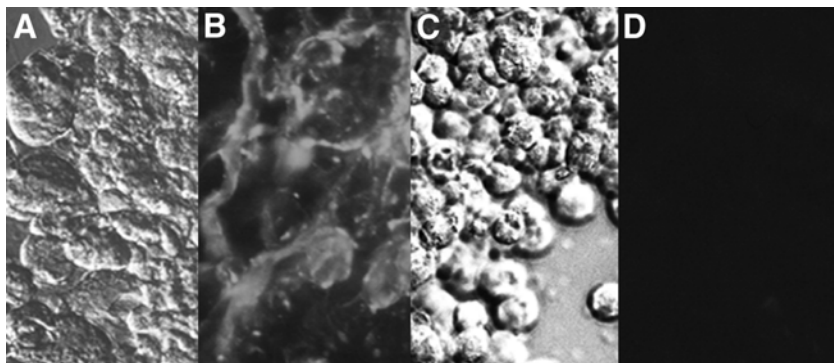
Fig. 3. Binding of α-ED-B scFv-PEG-immunoliposomes to human colon carcinoma cells Caco-2 (E-DB fibronectin positive) and Co-115 (E-DB fibronectin negative) cultured on collagen-I-coated cover slips. Phase contrast image **(A)** and immunofluorescence **(B)** showing binding of DiO-labeled α-ED-B scFv-PEG-immunoliposomes to ED-B-positive Caco-2 cells. On the ED-B-negative Co-115 cells shown in phase contrast **(C)** and by immunofluorescence **(D)**, binding was not detectable. Unmodified DiO-labeled control liposomes did not bind to both cell types (not shown).

control liposomes with the scFv antibody (lanes 9–16) results in no protein detection in the liposome fractions (lanes 9–11).

4. To remove the metrizamide, the pooled liposome fractions are dialyzed against PB using a 10,000-mol-wt cut-off dialysis tube (volume ratio = 1 to 1000).

3.3. Binding of scFv-Liposomes to Tumor Cells In Vitro

An example of how the binding properties of the prepared scFv-liposomes can be evaluated in vitro is given below (*see* **Fig. 3**).

1. Human colon carcinoma cells Caco-2 (ED-B fibronectin positive) and Co-115 (ED-B fibronectin negative) are cultured in complete DMEM medium. Glass cover slips (15–20 mm diameter) are placed into 12-well tissue-culture plates and coated with 100 μL rat-tail collagen I (10 mg/mL) and incubated for 30 min at 37°C.
2. Caco-2 and Co-115 cells (3×10^5 cells/well) are plated on the cover slips and cultured for 72 h in a humidified 5% CO_2 atmosphere at 37°C.
3. Then the washed cells (PBS) are incubated with 100 μL DiO-labeled α-ED-B scFv-liposomes corresponding to $9–10 \times 10^{13}$ liposomes or 12.5–31.5 μg scFv, respectively, in PBS for 30 min at 4°C.
4. After another washing step, the cover slips are removed, treated with 10% glycerine, placed on a microscope slide, and analyzed on a fluorescence microscope (Leica DLMB). As negative controls, the cells are incubated with unmodified fluorescence-labeled liposomes (liposome types A, C; *see* **Table 1** and **Note 19**).

4. Notes

1. Cholesterol (e.g., from Fluka, purum quality, >95%) should be recrystallized from methanol. Cholesterol of lower quality should be avoided, since liposome membrane stability can be reduced.

2. Rat-tail collagen can be extracted from fresh rat tails according to the method developed by Ellsdale *(9)*.

3. Mean hydrodynamic diameters of vesicles (liposomes, nanospheres, nanobeads) can be determined with dynamic laser light-scattering instruments, e.g., the NICOMP 380 particle sizer (Particle Sizing Systems, Santa Barbara, CA).

4. For steric reasons, the maximal amount of total PEG-lipids that can be incorporated into a lipid bilayer is 7 mol%. Within this amount, the contents of PE-PEG-Omet and PE-PEG-NH$_2$ can be varied—e.g., 5 mol% PE-PEG-Omet and 2 mol% PE-PEG-NH$_2$, depending on the required degree of amino group modification.

5. Other lipid compositions with synthetic lipids or hydrogenated SPC (HSPC) are often used, especially for liposome formulations intended for parenteral applications (long circulating or "stealth" liposomes). Several analytical methods to follow loss of lipids during the preparation and modification steps are available. Radioactively labeled lipids (^{3}H-DPPC, ^{14}C-DPPC) or cholesterol (^{3}H-cholesterol), or ^{3}H-cholesteryl hexadecyl ether (NEN Life Science Products, Boston, MA), or lipophilic fluorescent dyes (e.g., lipophilic BODIPY derivatives, Molecular Probes) are added at appropriate amounts to the initial lipid mixtures.

6. The preparation of liposomes from mixed detergent/lipid micelles can also be done with other detergents, such as *n*-alkyl-glucosides ($n = 6 – 9$), octyl-thioglucoside, or *N*-octanoyl-*N*-methylglucamin (MEGA-8, Fluka). Interestingly, the choice of detergent influences the size of the resulting liposomes. Thus, liposomes prepared from *n*-octyl-glucoside/lipid micelles have an average size of 180 nm, whereas those made with *n*-hexyl-glucoside are 60 nm in diameter *(10)*.

7. When synthetic lipids are used, the dialysis has to be performed above the corresponding transition temperature T$_c$ of the lipid. Hence, when for example dipalmitoylphosphatidyl choline (DPPC) is used as main liposome-forming lipid, a temperature above its T$_c$ of 41°C has to be chosen. Additional membrane-forming components (cholesterol and so on) depress the T$_c$ by several degrees.

8. The use of common dialysis tubes for the preparation of liposomes is not recommended because formation of concentration gradients in the tubes leads to uncontrolled detergent removal, resulting in nonhomogeneous liposome preparations. Controlled detergent removal—e.g., using a Mini-Lipoprep instrument or, for the production of large volumes of liposomes, a capillary dialyzer method *(11)*—is very important to obtain homogeneous and reproducible small unilamellar liposomes of defined mean diameters.

9. The major differences between detergent dialysis and filter extrusion are the following: Dialysis is a very gentle method, recommended when labile and unstable molecules are incorporated into liposomes. Furthermore, we made the observation that lipophilic dyes (e.g., Texas-red-DPPE) are strongly absorbed by Nucleopore membranes using the extrusion method, whereas in detergent dialysis, such dyes are quantitatively incorporated into the liposomes.

10. The detachment of the lipid mixtures from the glass walls of the round-bottom flasks can be accelerated by addition of small glass beads (2–3 mm diameter) and vigorous shaking. The encapsulation efficiency of hydrophilic molecules into the trapped volume of the liposomes is significantly increased by using the freeze-thaw method, as described by Mayer *(12)*. Using synthetic lipids, temperatures above the corresponding T$_c$ also have to be applied to the extrusion process.

11. The concentration of maleimide groups linked to the liposome surface can be determined by using either a fluorescent thio-reagent or, e.g., radiolabeled cysteine or methionine.

Alternatively, the maleimide groups are saturated with an excess of cysteine followed by determination of unbound cysteine with the Ellman's reagent *(13)*.

12. A large selection of bifunctional coupling reagents for amino-group modification is available from Pierce, Rockford, IL.

13. As an alternative to the coupling of bifunctional maleimide reagents, such as sulfo-SMCC, to amino groups on the liposomes, the maleimide-PEG-lipid molecule distearoyl-PEG-maleimide (DSPC-PEG-Mal) can be purchased from Avanti Lipid Products, Alabaster, AL.

14. Another alternative to the specific coupling method described here is the so-called post-insertion method *(1)*. Briefly, thiol-modified ligands are coupled to DSPC-PEG-Mal micelles in buffered aqueous solutions. After removing nonreacted ligand molecules by dialysis, the modified micelles are incubated with preformed liposomes, whereby the DSPC-PEG-maleimide-ligand molecules are efficiently transferred to the outer lipid layer of the liposomes.

15. The number of cysteines introduced into the ligand molecule can vary from one to three or more. Site-specific thiol modification with a single C-terminal cysteine—e.g., as used for the attachment of peptides to liposomes—is also effective *(9)*. Ideally, the coupling reaction of a thiolated ligand with maleimide-modified liposomes should be performed at a molar excess of ligand. However, the limited availability of large quantities of recombinant proteins or the high costs of synthetic peptides do not permit working with ideal reaction conditions.

16. The reduction of dimers can be achieved by using reducing agents containing thiol groups themselves, such as β-mercaptoethanol or dithiothreitol. However, the thiol groups of the reducing agent compete directly with those of the scFv antibodies for attachment to maleimide groups on the liposomes. Therefore they have to be removed after reduction and before liposome coupling. This problem can be circumvented by using the trialkyl-phosphine reagents tributylphosphine (TBP) or tris(2-carboxy-ethyl)phosphine (TCEP) for reduction *(14)*. Thus, we use TBP at a 2 m*M* final concentration for reduction of the scFv-dimers, and we recommend maintaining the reducing conditions during the coupling reaction to the liposomes.

17. It is recommended to use screw-cap glass vials with small magnetic stirring bars for the coupling reactions. Incubation time can vary from 2 to 24 h, depending on the properties (size, solubility) of the molecule to be attached to the liposomes.

18. Instead of separating the modified liposomes from nonreacted ligand molecules by metrizamide centrifugation, unbound scFv can be removed by dialysis using high-mol-wt cut-off dialysis tubes. Lately, metrizamide has been difficult to obtain. Thus, it can be replaced by Ficoll PM70 (Amersham Biosciences, Uppsala, Sweden) at the same concentrations as metrizamide. We recommend the Spectra/Por DispoDialyzers, which offer a wide selection of mol wt cut-offs ranging from 100 to 300,000 Daltons (Spectrum Laboratories).

19. Depending on the properties of the cells expressing target receptors for ligand-modified liposomes, flow cytometry can be used for the detection of liposome-cell binding.

Acknowledgments

References

1 Sapra, P. and Allen, T. M. (2003) Ligand-targeted liposomal anticancer drugs. *Progr. Lipid Res.* **42,** 439–462.

2 Allen, T. M. (2002) Ligand-targeted therpeutics in anticancer therapy. *Nat. Rev. Cancer* **2,** 750–762.

3 Marty, C., Ballmer-Hofer, K., Neri, D., Klemenz, R., Schott, H., and Schwendener, R. A. (2002) Cytotoxic targeting of F9 teratocarcinoma tumours with anti-ED-B fibronectin scFv antibody modified liposomes. *Br. J. Cancer* **87,** 106–112.

4 Ludewig, B., Barchiesi, F., Pericin, M., Zinkernagel, R. M., Hengartner, H., and Schwendener, R. A. (2000) In vivo antigen loading and activation of dendritic cells via a liposomal peptide vaccine mediated protective antiviral and antitumor immunity. *Vaccine* **19,** 23–32.

5 Huang, C. and Mason, J. T. (1978) Geometric packing constraints in egg phosphatidylcholine vesicles. *Proc. Natl. Acad. Sci. USA* **75,** 308–310.

6 Rubas, W., Supersaxo, A. Weder, H. G., et al. (1986) Treatment of murine L1210 leukemia and melanoma B16 with lipophilic cytosine arabinoside prodrugs incorporated into unilamellar liposomes. *Int J. Cancer* **37,** 149–154.

7 Mayer, L. D., Hope, M. J., and Cullis, P. R. (1986) Vesicles of variable sizes produced by a rapid extrusion procedure. *Biochim. Biophys. Acta* **858,** 161–168.

8 Marty, C., Scheidegger, P., Ballmer-Hofer, K., Klemenz, R., and Schwendener, R. A. (2001) Production of functionalized single-chain Fv antibody fragments binding to the ED-B domain of the B-isoform of fibronectin in *Pichia pastoris. Protein Expr. Purif.* **21,** 156–164.

9 Ellsdale, T. and Bard, J. (1972) Collagen substrata for studies on cell behaviour. *J. Cell. Biol.* **54,** 626–637.

10 Schwendener, R. A., Asanger, M., and Weder, H. G. (1981) The preparation of large bilayer liposomes: controlled removal of n-alkyl-glucoside detergents from lipid/detergent micelles. *Biochem. Biophys. Res. Commun.* **100,** 1055–1062.

11. Schwendener, R. A. (1986) The preparation of large volumes of homogeneous, sterile liposomes containing various lipophilic cytostatic drugs by the use of a capillary dialyzer. *Cancer Drug Delivery* **3,** 123–129.

12 Mayer, L. D., Hope, M. J., Cullis, P. R., and Janoff, A. S. (1985) Solute distributions and trapping efficiencies observed in freeze-thawed multilamellar vesicles. *Biochim. Biophys. Acta* **817,** 193–196.

13 Eyer, P., Worek, F., Kiderlen, D., et al. (2003) Molar absorption coefficients for the reduced Ellman reagent: reassessment. *Anal. Biochem.* **312,** 224–227.

14. Console, S., Marty, C., Garcia-Echeverria, C., Schwendener, R. A., and Ballmer-Hofer, K. (2003) Antennapedia and HIV TAT "protein transduction domains" promote endocytosis of high Mr cargo upon binding to cell surface glycosaminoglycans. *J. Biol. Chem.* **278(37),** 35,109–35,114.

15. Burmeister Getz, E., Xiao, M., Chakrabarty, T., Cooke, R., and Selvin, P. R. (1999) A comparison between the sulfhydryl reductants tris(2-carboxyethyl)phosphine and dithiothreitol for use in protein biochemistry. *Anal. Biochem.* **273,** 73–80.

26

Intravenous Immunoglobulin Treatment for Fibrosis, Atherosclerosis, and Malignant Conditions

Ilan Krause and Yehuda Shoenfeld

Summary

We describe our experience with intravenous immunoglobulin (IVIg) treatment in fibrotic conditions and our results and experience with the effect of IVIg therapy to prevent metastases in malignancy. We have delineated the mechanisms by which IVIg can affect atherosclerosis (i.e., effect on MMP-9, antiidiotypes to anti-OxLDL), which led to reduced atherosclerosis in animal models. The effect of IVIg on skin fibrosis was assessed in a murine model of scleroderma-like disease. Collagen expression was decreased in the skin of mice treated with mouse IVIg, associated with decreased type I collagen gene expression, and accompanied by inhibition of transforming growth factor (TGF)β and interleukin (IL)-4 secretion by splenocytes. We also described a favorable response to IVIg treatment in patients with either systemic sclerosis or myelofibrosis. The administration of IVIg to mice inoculated with melanoma or sarcoma cells induced a statistically significant inhibition of metastatic lung foci and prolongation of survival time. IVIg was found to stimulate the production of IL-12, an anti-tumor and anti-angiogenic cytokine. Positive staining of the cytoplasm, cell membrane, and nuclear membrane of several types of malignant tumors by IVIg was immunohistochemically demonstrated.

Key Words: intravenous immunoglobulins; fibrosis; atherosclerosis; malignancy.

1. Introduction

Recently, we were able to treat a large number of patients (>200) with various autoimmune conditions by IVIg. Herein, we review our experience with IVIg treatment in fibrotic conditions and describe our results and experience with the effect of IVIg therapy to prevent metastases in malignancy.

2. Therapy of Atherosclerosis With IVIg

The last decade has seen a revolution in our attitude toward the etiology and pathogenesis of atherosclerosis (AS). In addition to the conventional risk factors (e.g., smoking, diabetes, obesity, and so on), infections as well as inflammatory and immune involvements were found to be involved in the causation of AS. Accelerated athero-

sclerosis was also reported in many classical autoimmune rheumatic diseases, i.e., systemic lupus erythematodes (SLE), rheumatoid arthritis (RA), vasculitis, and others *(1–5)*.

The autoimmune aspects of AS have been delineated and seem to involve both the humoral and the cellular arms of the immune system, entailing a passive transfer; experiments with activated lymphocytes in naïve mice led to accelerated atherosclerosis. In contrast to many of the classical autoimmune diseases, several autoantigens/autoantibodies seem to be implicated, i.e., HSP65, OxLDL, β2GPI *(4,6)*, Lp(a), PT, antiendothelial cell antibodies (AECA), and more to come *(6,7)*.

As an immune/autoimmune mediated disease, AS is subject to immunomodulation with anti-CD40, IVIG, cytokines, chemokines, and other immunomodulators *(8)*. We have delineated the mechanisms by which IVIg can affect AS—effect on MMP-9 *(9)*, antiidiotypes to anti-OxLDL *(10)*. It seems that all the above mentioned immunomodulations led to reduced atherosclerosis in animal models. It is conceivable that in the near future, such novel therapeutic approaches (i.e., anti tumor necrosis factor [TNF]-α) will be incorporated into the routine therapy of subjects with atherosclerosis (i.e., restenosis prevention after angioplasty), and specifically when associated with rheumatic autoimmune diseases *(11)*.

3. IVIg in Fibrosis

Deposition of collagen, laminin, fibrinogen, and other molecules is fundamental to the process of inflammation and healing. However, the accumulation of excessive amounts of these extracellular proteins may lead to malfunction of vital organs, resulting in myelofibrosis, cirrhosis, pulmonary fibrosis, extraperitoneal fibrosis, or skin thickening. Systemic sclerosis (SSc) is an autoimmune connective-tissue disease characterized by microvascular damage, extracellular matrix deposition, and fibrosis, involving mainly the skin, lungs, and gastrointestinal tract. No effective therapy has so far been described for the diffuse fibrotic changes. Blank et al. *(12)* assessed the effect of IVIg on skin fibrosis in tight-skin (Tsk/+) mice. The Tsk/+ mouse represents a murine model of scleroderma-like disease with heritable fibrosis resembling the skin fibrosis seen in human SSc patients. The excessive fibrosis in these mice is the result of increased synthesis and accumulation of collagen in the skin. Tsk/+ mice received IVIg beginning at the age of 4 wk, administered twice weekly for 4 wks. Control mice were infused with 2% maltose. Collagen expression was decreased in the skin of Tsk/+ mice treated with IVIg compared with that in control mice. The decreased collagen expression after exposure to IVIg was associated with decreased type I collagen gene expression. The reduction in skin fibrosis upon IVIg treatment was accompanied by inhibition of TGFβ and IL-4 secretion by splenocytes. Levy et al. *(13)* were the first to report a response of SSc patients to treatment with IVIg. Three patients with progressive and rapidly deteriorating disease (mainly affecting the skin) were planned to receive six monthly courses of high-dose IVIg (2 g/kg). Two of the three patients received six IVIg courses as planned, and no adverse effects or disease progression occurred during the therapy. The third patient received three courses, after which he developed renal failure and later died of sepsis. All three patients had a large decrease

in their skin score after the treatment compared to that before the treatment. It seems, therefore, that IVIg may have a role in the treatment of SSc patients with rapidly deteriorating skin disease, and possibly other target organs fibrosis. Recently we have expanded our experiments to an additional 14 patients *(14)*.

Myelofibrosis has been reported as a rare cause of pancytopenia in patients with autoimmune diseases. Aharon et al. *(15)* described a 54-yr-old female patient who was admitted with severe anemia subsequently found to be due to marrow fibrosis. During the course of her hospitalization, the diagnosis of SLE was established. The patient was treated with high-dose steroids, but improvement of her clinical symptoms as well as normalization of her peripheral blood count were achieved only after high-dose therapy with IVIg was instituted. Along with the improvement in the peripheral blood parameters, normalization of the bone-marrow architecture was recorded on a repeated bone-marrow biopsy. We suggest that IVIg therapy may be considered in extreme cases of bone-marrow suppression in SLE.

4. Antimetastatic Effects of IVIg (Patent Nos. 5.562.902 and 5.965.130)

There is a bi-directional relationship between autoimmunity and cancer. Malignant conditions are frequently associated with autoimmune phenomena. Examples include: an increased incidence of Eaton–Lambert myasthenia-like syndrome in patients with small-cell carcinoma of the lung; thymoma in patients with myasthenia gravis; different types of epithelial or lymphoproliferative malignancies in patients with autoimmune hemolytic anemia, thrombocytopenia, or neutropenia; and melanoma associated with vitiligo. Conversely, there is an increased risk of cancer in autoimmune conditions, as exemplified by the emergence of ovarian carcinoma in patients with dermatomyositis, lymphoproliferative diseases in patients with rheumatoid arthritis, SLE and Sjogren's syndrome, lung cancer in scleroderma patients, and thyroid papillary carcinoma in patients with autoimmune thyroid diseases. The cancer may appear at the time of diagnosis of the autoimmune disease or several years later *(16)*. Since the two diseases are similarly treated, we studied the efficacy of IVIg as a treatment for malignant conditions: The administration of IVIg to mice inoculated intravenously with melanoma or sarcoma cells induced a statistically significant inhibition of metastatic lung foci and prolongation of survival time. Similar results were seen with SCID mice inoculated with SK-28 human melanoma cells *(17)*. In a different model, a lower number of melanoma recurrences and prolongation of survival time were demonstrated in the IVIg-treated groups. In vitro studies revealed that IVIg was found to stimulate the production of IL-12, an antitumor and antiangiogenic cytokine. Moreover, it enhanced natural killer (NK) cell activity, thus explaining its beneficial effect in SCID mice (which lack B- and T-cells but possess NK cells) *(18)*. The results indicate that IVIg acts as an anti-tumor agent, and may be considered as a potential therapy for the prevention of tumor spread in humans. In another experiment, we studied the effect of purified IVIg on MMP-9 secretion and mRNA expression by in vitro differentiated human monocytic cells. Degradation of the extracellular matrix (ECM) is essential for progression and metastasis of cancer cells. The ECM-degrading enzymes, matrix metalloproteinases (MMPs), are produced mainly by intratumor monocytes/macroph-

ages. MMPs, particularly MMP-9, are reported to be of crucial significance for both growth and tumor invasiveness. Inhibition of the expression of MMP-9 may prevent tumor development. We found that IVIg dose-dependently and significantly reduced the amount of secreted MMP-9 and its mRNA expression. $F(ab)_2$, but not Fc fragments, led to suppressed MMP-9 activity *(9)*. However, competitive experiments demonstrated that Fc, but not $F(ab)_2$ fragments, reversed the IVIg-induced inhibitory effects. Our results suggest that the whole IgG molecule may be needed for pertinent IVIg-induced MMP-9 down-regulation. Our study points to an additional new mechanism whereby IVIg may play a beneficial role in the prevention of tumor spread in humans. We also tried to determine whether $F(ab)_2$ prepared from IVIg binds to cellular structures of different tumor tissues. Direct immunohistochemistry using a streptavidin peroxidase staining method was performed on biopsy samples of 18 different tumor tissues. Positive staining of the cytoplasm, cell membrane, and nuclear membrane of several types of malignant tumors by $F(ab)_2$ from IVIg was immunohistochemically demonstrated. Nuclear staining of tumor cells by IVIg was rare. IVIg bound to different tumors of epithelial origin, especially colon carcinoma, breast carcinoma, and squamous cell carcinoma of the lung. Malignant tumors of mesenchymal origin such as leiomyosarcoma have also demonstrated positive staining by IVIg *(19)*. Hence, IVIg contains antibodies to the cytoplasm, nuclear membrane, and cell membrane of different malignant tumors, especially of epithelial origin. This binding might provide a basis for the assumption that IVIg treatment of cancer patients may induce antibody-dependent cell-mediated cytotoxicity response against tumors, and implies that it can be potentially beneficial as adjuvant treatment of malignant diseases. Merimsky et al. *(20)* observed a patient with a malignant peripheral nerve sheath tumor (MPNST) who was treated with IVIg for multiple sclerosis. Her MPNST course was remarkably longer and more indolent than expected; she achieved a disease-free interval (DFI) of 30 mo. Seven other patients who were not treated by IVIg had a relatively aggressive course (median DFI 3 mo). These results led us to examine the effect of IVIg on the growth of sarcoma in vitro and in vivo in an experimental model of MCA-bearing mice. When added to MCA-105 sarcoma cell cultures, IVIg produced a dose-dependent inhibitory effect on $[H^3]$-thymidine incorporation *(18)*. The results demonstrate that the anti-proliferative activity results from an apoptotic effect of IVIg on the tumor cells. In a second set of experiments, we evaluated the capability of IVIg, when administered orally or subcutaneously, to inhibit the growth of MCA-105 sarcoma lung metastases. A decrease in the mean lung weight was observed in the mice that were treated by subcutaneous or oral administration, the latter being more effective. The results point to a potential role for IVIg in the treatment of MPNST and other soft-tissue sarcomas. Recently, we reported about a patient with superficial spreading melanoma with liver and lung metastases *(21)*. The patient refused chemotherapy and was treated with monthly high-dose IVIg (2g/kg). Six mo after the initiation of IVIg therapy, the liver metastases regressed significantly, while the lung metastases remained the same. After about 9 mo from the initiation of IVIg therapy, new subcutaneous and bony metastases appeared, which continued to grow in the next 6 mo, although there was no significant change in the lung and hepatic lesions. The

patients died in a septic state 14 mo after the start of IVIg. This is the first report pointing to the probable efficiency of high-dose IVIg in cases of unresponsive widespread metastases of melanoma, and points to the implantation of the safe IVIg in some patients with tumor metastases.

References

1 Shoenfeld, Y. (2000) Atherosclerosis and the immune system: is atherosclerosis an autoimmune disease? *Sem. Clin. Immunol.* **1,** 5–6.

2 Shoenfeld, Y., Sherer, Y., and Haratz, D. (2001) Atherosclerosis as an infectious, inflammatory and autoimmune disease. *Trends in Immunol.* **22,** 293–295.

3. Shoenfeld, Y., Haratz, D., and Jacob, G. (2000) Heat shock protein 60/50, beta2-glycoprotein I and Oxidized LDL as players in murine atherosclerosis. *J. Autoimmunity* **15,** 199–202.

4 Sherer, Y. and Shoenfeld, Y.. (2003) Antiphospholipid antibodies: are they pro-atherogenic or an epiphenomenon of atherosclerosis? *Immunobiol.* **207,** 13–16.

5 George, J., Afek, A., Gilburd, B., Shoenfeld, Y., and Harats, D. (2001) Cellular and humoral immune responses to heat shock protein 65 are both involved in promoting fatty-streak formation in LDL-receptor deficient mice. *J. Am. Coll. Cardiol.* **38,** 900–905.

6 George, J., Harats, D., Gilburd, B., et al. (2000) Adoptive transfer of β2-glycoprotein I-reactive lymphocytes enhances early atherosclerosis in LDL receptor-deficient mice. *Circulation* **102,** 1822–1827.

7 Harats, D., Yacov, N., Gilburd, B., Shoenfeld, Y., and George, J. (2002) Oral tolerance with heat shock protein 65 attenuates *Mycobacterium tuberculosis*-induced and high-fat-diet-driven atherosclerotic lesions. *J. Am. Col. Cardiol.* **7,** 1333–1338.

8 Sherer, Y. and Shoenfeld, Y. (2002) Immunomodulation for treatment and prevention of atherosclerosis. *Autoimmune Rev.* **1,** 21–27.

9 Shapiro, S., Shoenfeld, Y., Gilburd, B., Sobel, E., Lahat, N. (2002) Intravenous gamma globulin inhibits the production of matrix metalloproteinase-9 in macrophages. *Cancer* **95,** 2032–2037 .

10 Wu, R., Shoenfeld, Y., Sherer, Y., et al.(2003) Anti-idiotypes to oxidized LDL antibodies in intravenous immunoglobulin preparations—possible immunomodulation of atherosclerosis. *Autoimmunity* **36,** 91–97.

11 Doria, A., Shoenfeld, Y., Wu, R., et al. (2003) Risk factors for subclinical atherosclerosis in patients with systemic lupus erythematosus. *Ann. Rheum. Dis.* **62,** 1071–1077.

12 Blank, M., Levy, Y., Amital, H., et al. (2002) Concise communication: the role of intravenous] immunoglobulin therapy in mediating skin fibrosis in tight skin mice. *Arth. Rheumat.* **46,** 1689–1690.

13 Levy, Y., Sherer, Y., Langevitz, P., et al. (2000) Skin score decrease in systemic sclerosis patients treated with intravenous immunoglobulin—a preliminary report. *Clin. Rheumatol.* **19,** 207–211.

14 Amital, H., Rewald, E., Levy, Y., et al. (2003) Fibrosis regression induced by intravenous gammaglobulin treatment. *Ann. Rheum. Dis.* **62,** 175–177.

15 Aharon, A., Levy, Y., Bar Dayan, Y., et al. (1997) Successful treatment of early secondary myelofibrosis in SLE with IVIG. *Lupus* **6,** 408–411.

16 Shoenfeld, Y. and Gershwin, E. M., eds. (2000) *Cancer and Autoimmunity*. Elsevier, Amsterdam, The Netherlands.

17. Shoenfeld, Y. and Fishman, P. (1999) Gamma-globulin inhibits tumor spread in mice. *Int. Immunol.* **11,** 1247–1251.

18 Fishman, P., Bar-Yehuda, S., and Shoenfeld, Y.(2002) IVIG to prevent tumor metastases (review). *Int. J. Oncol.* **21,** 875–880.

19 Bar-Dayan, T., Barshack, I., Blank, M., et al. (1999) Antibodies to the cytoplasm, cell membrane and nuclear membrane of malignant neoplasms in pooled normal human polyspecific immunoglobulin G. *Int. J. Oncol.* **15,** 1091–1096.

20. Merimsky, O., Meller, I., Inber, M., Bar-Yehuda, S., Shoenfeld, Y., and Fishman, P. (2002) A possible role for IVIG in the treatment of soft tissue sarcoma: a clinical case and an experimental model. *Int. J. Oncol.* **20,** 839–843.

21. Shoenfeld, Y., Levy, Y., and Fishman, P. (2001) Shrinkage of melanoma metastases following high dose intravenous immunoglobulin treatment. *IMAJ* **3,** 698–699.

Study of T-Cell Costimulatory Blockade In Vivo at a Single-Cell Level

Minh Diem Vu and Xian Chang Li

Summary

The critical role of costimulatory signals in T-cell activation and the complexity of T-cell costimulatory pathways involved make a detailed understanding of this system a challenging task. By taking advantage of the unique chemical properties of CFSE, we and others have developed an in vivo model that allows quantitative analysis of T-cell activation at a single-cell level. This model involves labeling of donor T-cells with the tracking dye CFSE and adoptively transferring into lethally irradiated allogeneic hosts. T-cells proliferating in the host mice can be explicitly analyzed upon recovery. By using mice deficient for certain costimulatory molecules as a source of donor cells or by treating the host mice with reagents that block certain costimulatory pathways, this CFSE model is extremely useful in studying the role of T-cell costimulatory signals in activation, survival, and effector differentiation of alloreactive T-cells in vivo.

Key Words: Costimulation; T-cell activation; alloimmunity; transplantation; in vivo assay; CFSE.

1. Introduction

T-cells are essential in allograft rejection. Thus, blocking T-cell activation remains a key strategy in preventing transplant rejection. In essence, T-cell activation requires at least two signals. Signal 1 is delivered by the T-cell receptor (TCR) upon recognition of the alloantigens, and signal 2 is provided by a set of cell-surface structures collectively called "costimulatory molecules." Both signals drive robust T-cell activation and development of T-cell effector function. In fact, stimulation of T-cells via the T-cell receptor in the absence of costimulatory signals often induces an anergic state or apoptotic cell death *(1–8)*. Thus, T-cell costimulatory molecules are of central importance in T-cell activation. Consequently, blocking T-cell costimulatory signals has attracted tremendous attention in tolerance induction.

Among the T-cell costimulatory molecules identified, CD28 and CD154 (CD154 is also called CD40 ligand, or CD40L) are the classical and also most extensively studied

ones *(9–12)*. However, cell-surface molecules with costimulatory properties are not confined to CD28 and CD154, and multiple alternative costimulatory molecules have been discovered *(13)*. For example, upon TCR stimulation, signals delivered by ICOS, OX40 (CD134), 4-1BB (CD137), CD30, CD27, and CD70 can costimulate T-cell activation, cytokine production, and effector cell function *(14–19)*. Thus, understanding precisely the individual and collective roles of such diverse costimulatory molecules in regulating activation of alloreactive T-cells becomes critically important in transplantation research. We and others have developed an in vivo model that allows quantitative analysis of T-cell activation at a single-cell level by taking advantage of a tracking dye called carboxyfluorescein succinimidyl ester (CFSE) *(20–25)*. In this chapter, CFSE-labeled T-cells proliferating in the allogeneic hosts are used to illustrate the model and the means by which T-cell activation in vivo and the impact of costimulatory blockade on T-cell activation are analyzed.

2. Materials

1. CFSE (Molecular Probes, Portland, OR).
2. Hank's balanced salt solution (HBSS) (BioWhittaker, Walkersville, MD).
3. Phosphate-buffered saline (PBS) (BioWhittaker).
4. Fetal bovine serum (FBS) (BioWhittaker).
5. Bovine serum albumin (BSA) (Sigma, St. Louis, MO).
6. Red blood cell lysing buffer (Sigma).
7. Surgical instruments for small animals.
8. Petri dishes (Corning, Bedford, MA).
9. Lymphocyte preparation kit (Sigma).
10. Nylon cell strainer, 70 µm (BD Biosciences, Bedford, MA).
11. Animal irradiator (Gammacell Exactor, Kanata, Ontario, Canada).
12. FACS machine equipped with CellQuest™ software (BD Biosciences, Mountain View, CA).
13. Paraformaldehyde (Sigma).
14. Staining mAbs: CyChrome anti-mouse CD4 (clone GK1.5), CyChrome anti-mouse CD8α (clone 53-6.7), PE-anti-mouse IL-2 (clone JES6-5H4), isotype control antibodies, and PE-annexin V (PharMingen, San Diego, CA).
15. Cytofix/Cytoperm™ kit (PharMingen).
16. Annexin V binding buffer (PharMingen).
17. C57BL/6 (H-2b) and DBA/2 (H-2d) mice (Jackson Laboratory, Bar Harbor, ME).
18. Murine CTLA4-Ig fusion protein.
19. Anti-CD154 mAb (MR1, hamster IgG, American Type Culture Collection [ATCC], Manassas, VA).
20. PMA and ionomycin (Sigma).
21. Penicillin and streptomycin (Sigma).

3. Methods

Technically, the in vivo CFSE assay consists of the following five steps: (1) labeling of donor lymphocytes with CFSE; (2) adoptively transferring CFSE-labeled cells into an allogeneic host; (3) recovery of CFSE-labeled donor cells from the host mice after a given period of time; (4) cell staining in vitro after recovery; (5) flow cytometry and data acquisition/analysis (**Fig. 1**) (*see* **Note 1**).
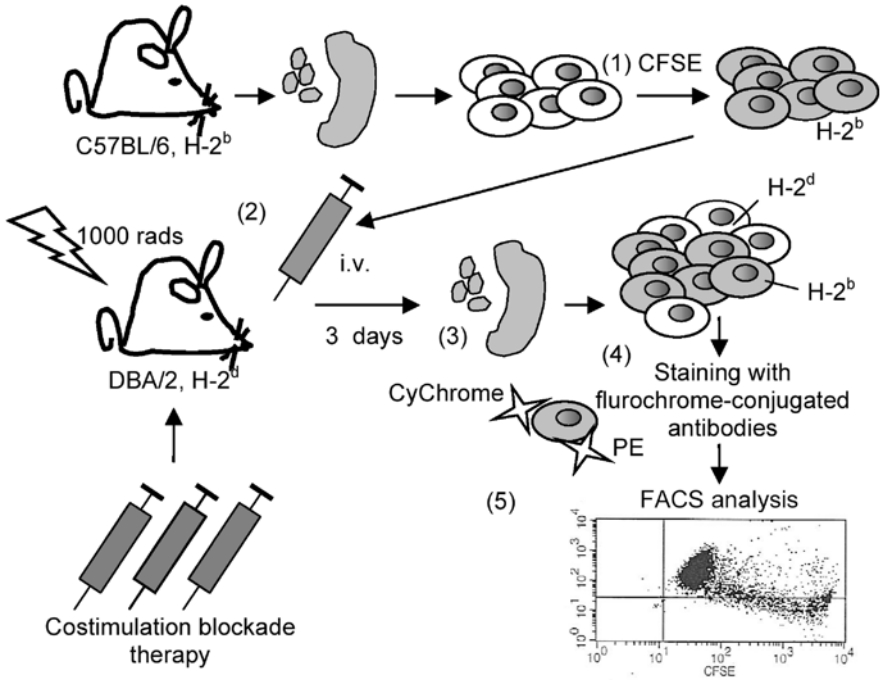
Fig. 1. A cartoon illustration of the in vivo CFSE model. Key steps include (1) labeling of donor cells with CFSE; (2) adoptive transferring of CFSE-labeled cells into irradiated hosts; (3) cell recovery; (4) in vitro staining; and (5) data acquisition and analysis.

3.1. Labeling of Donor Lymphocytes With CFSE

3.1.1. Chemical Properties of CFSE

The precursor of fluorescent CFSE dye is carboxyfluorescein diacetate succinimidyl ester (CFDASE), which is nonfluorescent, nonpolar, but highly lipophilic *(26,27)*. When CFDASE is added to cell suspensions, CFDASE passively diffuses through cell membranes, and upon esterase hydrolysis in the cytoplasm of live cells, CFDASE is converted to fluorescent CFSE. CFSE covalently binds to cytoplasmic proteins to form a stable complex *(22,23)*. When CFSE-labeled cells divide, the CFSE contents segregate equally between the two daughter cells. Therefore, the fluorescent intensity of labeled cells halves after each consecutive cell division, which allows tracking the division history of activated T-cells.

3.1.2. Donor Lymphocyte Preparation

Lymphocytes were prepared from the spleen and the peripheral lymph nodes of donor C57BL/6 (H-2b) mice. A detailed description of this method has been reported in **ref. 28**.

1. Sedated mice are sacrificed by cervical dislocation, and all the lymph nodes in the cervical, auxiliary, popliteal, and inguinal areas and the spleen are harvested and placed into a sterile Petri dish containing cold HBSS.
2. Single-cell suspension is prepared by gently disrupting the lymphoid tissues and pressing them through a 200-µm metal mesh.
3. Cells are then transferred from the Petri dish into 15-mL centrifuge tubes and centrifuged in Sorvall RTH250 rotor at 1200 rpm (300g) for 5 min at 4°C.
4. After centrifugation, the supernatant was discarded, leaving behind only the cell pellet. Red blood cells in the cell preparation are removed using red blood cell lysing buffer *(29)*. For this purpose, gently disrupt the cell pellet, and then add 10 mL of lysing buffer (room temperature).
5. Five min later, the tubes are centrifuged at 1200 rpm (300g) for 5 min to pellet the lymphocytes.
6. Cells are washed once in cold HBSS and resuspended in HBSS for cell counting and CFSE labeling.

3.1.3. CFSE Labeling

CFSE is prepared in DMSO at 5 m*M*, stored at –20°C, and used as stock solutions. Labeling of lymphocytes with CFSE consists of the following steps (*see* **Note 2**):

1. Resuspend cells in serum-free HBSS at 2×10^7 cells/mL in a 50-mL centrifuge tube.
2. Prepare an equal volume of CFSE in serum-free HBSS at 10 µ*M* using another 50-mL tube.
3. Gently mix the cell suspension and the CFSE solution, so the final cell concentration for labeling is 1×10^7/mL and the final CFSE concentration is 5 µ*M*.
4. Incubate the cells at room temperature for 6 min with gentle mixing.
5. After 6 min, stop the labeling reaction by adding FBS (10% of total volume).
6. Pass the cell suspension through a 70-µm nylon cell strainer to remove cell debris and cell clumps.
7. Wash cells twice in HBSS, resuspend cells in HBSS for counting and injection.

3.2. Adoptive Transfer of CFSE-Labeled Cells into Allogeneic Hosts

3.2.1. Irradiation of Host Mice

DBA/2 (H-2d) mice are given 1000 rads lethal irradiation with a GammaCell Exactor (Kanata, Ontario, Canada) 4 to 5 h before cell transfer.

3.2.2. Transfer of CFSE-Labeled Cells into the Irradiated Hosts

1. Resuspend CFSE-labeled cells in HBSS.
2. Restrain the host mice in an animal restrainer.
3. Inject 60 to 80×10^6 cells in a total volume of 0.5 mL into each host via the tail vein (*see* **Note 3**).

3.2.3. Treatment of Host Mice With Costimulatory Blockade Reagents

The host mice can be treated with CTLA4-Ig to block the B7/CD28 costimulatory pathway, anti-CD154 mAb (MR1) to block the CD40/CD154 costimulatory pathway, or a combination of both. Mice treated with isotype control antibody are included as a control. The reagents are given at 0.5 mg i.p. daily for 3 d starting at the time of cell transfer.

3.3. Recovery of CFSE-Labeled Donor Cells From the Host Mice

Three d after adoptive cell transfer, the host mice are killed, spleen and peripheral lymph nodes are harvested separately, and single-cell suspensions are prepared as described in **Subheading 3.2.** (*see* **Notes 4 and 5**). For cells from the host spleen, red blood cells are lysed using the red blood cell lysing buffer as described. Cells are then washed once in cold PBS containing 0.5% BSA (PBS/BSA), counted, and resuspended in PBS/BSA for staining.

3.4. Cell Staining After Recovery From the Hosts

3.4.1. Cell-Surface Staining

1. Resuspend cells in PBS/BSA at 1×10^7/mL and aliquot 100 μL into individual 1.5-mL Eppendorf tubes (1×10^6 cells/100 μL/tube).
2. Add 1 μg CyChrome-anti-mouse CD4 or 1 μg CyChrome-antimouse CD8 mAb into each tube. For 3-color staining, PE-conjugated mAbs against other cell-surface markers, for example, CD25, CD44, CD69, and so on can be added at the same time. Cells stained with CyChrome-conjugated or PE-conjugated isotype-matched control antibodies are included as controls.
3. Incubate the cells on ice for 20 min.
4. Wash cells twice in PBS/BSA after the incubation and fix the cells in 1% paraformaldehyde (prepared in PBS) for FACS analysis.

3.4.2. Staining for Intracellular Cytokines

1. Resuspend cells in RPMI-1640 medium supplemented with 10% FBS and 1% penicillin/streptomycin at 5×10^6 cells/mL.
2. Briefly stimulate the cells in vitro with PMA (50 ng/mL) and ionomycin (500 ng/mL) at 37°C for 4 h.
3. In the last 2 h of in vitro stimulation, add GolgiStop™ (PharMingen) at 1 μg/mL into the culture.
4. Harvest the cells and proceed to surface staining with CyChrome-anti-CD4 and CyChrome-anti-CD8 as described.
5. After cell-surface staining, cells are incubated in Cytofix/Cytoperm solution at 4°C for 10 min.
6. Wash the cells twice in Perm/Wash™ solution, aliquot cells into 1.5-mL Eppendorf tubes (1×10^6 cells/100 μL/tube), add PE-anti-IL-2, PE-anti-interferon (IFN)-γ, or PE-anti-tumor necrosis factor (TNF)-α, and incubate on ice for 30 min. PE-conjugated isotype-control antibodies are included as controls.
7. Wash the cells twice in Perm/Wash solution and resuspend the cells in Perm/Wash solution for FACS analysis.

3.4.3. Staining for Apoptotic Cell Death

1. Resuspend cells in Ca^{2+}-rich annexin V binding buffer at 1×10^6 cells/100 μL/tube in 1.5-mL Eppendorf tubes.
2. Add 5 μL of PE-conjugated annexin V into each tube and incubate at room temperature for 30 min.
3. Wash the cells once in annexin V binding buffer and resuspend the cells in the binding buffer for analysis.
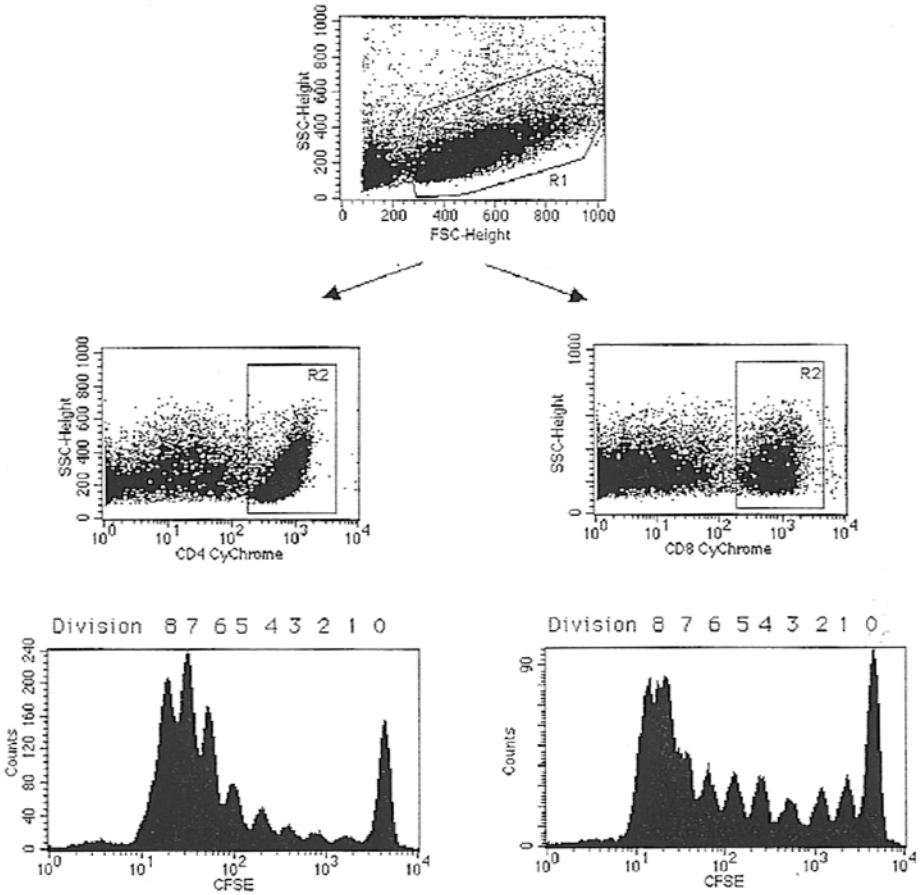
Fig. 2. Typical FACS parameters and setup for in vivo CFSE assay. FSC and SSC are used to identify and to gate lymphocyte population. CD4+ or CD8+ T-cells are gated based on subset staining, and their division history is revealed by the dilution of CFSE.

3.5. Flow Cytometry and Data Acquisition/Analysis

3.5.1. Data Acquisition

1. All samples are acquired using FACS equipped with CellQuest™ software (*see* **Note 6**).
2. The FACS should be set up based on the following parameters in order to identify the total cellular events, different T-cell subsets, and their CFSE profile: (1) FSC vs SSC dot plot; (2) FL3 (CyChrome staining) vs SSC dot plot; (3) FL1 (CFSE) vs FL2 (PE staining) dot plot; (4) FL1 (CFSE) histogram (**Fig. 2**).
3. For samples with three-color staining, pay special attention to parameter compensation, particularly the FL1 (i.e., CFSE), as the CFSE has a wide range of fluorescent intensity.
4. Collect a minimum of 500,000 events from each sample for better graphic representation.

3.5.2. Data Analysis

The following analyses can be readily accomplished using the CFSE model: (1) division frequency of T-cells and T-cell subsets can be precisely calculated; (2) activated T-cells at distinct division cycles can be phenotyped; (3) effector programs of activated T-cells can be systemically compared; (4) apoptotic cell death of activated T-cells at distinct division cycles can be precisely analyzed.

1. Calculation of division frequency: distinct division cycles of T-cells, CD4+ or CD8+ T-cell subsets are identified by their CFSE profiles and individually gated. The absolute number of daughter cells in each cell division is given by the CellQuest software, the number of precursors that have divided and given rise to the absolute number of daughter cells is extrapolated using the formula: $y/2^n$; in which y = absolute number of cells in each cell cycle and n = number of cell divisions. For example, 16 daughter cells in the third cell division are the progeny of two precursors, each of which have divided three times ($16/2^3$ = 2). The division frequency in the responding T-cell population is then calculated by dividing the total number of precursors by the total number of CFSE positive cells collected *(24)*.

2. Analysis of effector functions: total T-cells or CD4+ or CD8+ subsets are gated, their division history (i.e., CFSE profile, FL1) is plotted against intracellular cytokine staining (FL2), and a quadrant mark can be set up based on control staining using PE-isotype control antibody. Thus, the relative expression of effector cytokines in T-cells at distinct division cycles can be clearly appreciated. By gating onto individual division cycles, the absolute % of cytokine positive cells can be calculated and plotted (**Fig. 3**).

3. Phenotyping of dividing T-cells: within a given T-cell subset, the phenotypic changes following cell-cycle transitions can be analyzed. Similar to intracellular cytokine analysis, the division history of T-cells or CD4+ or CD8+ T-cells is identified by their CFSE profile (FL1) and plotted against surface staining with PE-conjugated specific antibodies (FL2). Thus, the phenotypic changes upon cell-cycle progression can be analyzed (**Fig. 4**). The same method can be used to identify apoptotic cell death based on staining with PE-annexin V (**Fig. 5**).

4. Notes

1. Depending on the questions asked and the T-cell subset examined, this CFSE model allows the integration of several variables. First, the CFSE-labeled donor cells can be prepared from genetic knockout mice—for example, CD28 knockout, CD154 knockout, or CD28/CD154 double knockout mice, and so on. Second, the host mice can be treated with a variety of therapeutic reagents, e.g., monoclonal antibodies or recombinant fusion proteins against different costimulatory pathways at the time of injecting CFSE-labeled allogeneic cells. Thus, T-cell activation in vivo in response to such treatments can be appreciated and compared. Third, the host mice can be prepared by lethal irradiation, or one can simply use genetically immunodeficient mice, such as scid mice or Rag-deficient mice. Also, F1 mice that share partial major histocompatibility complex (MHC) haplotype with donor mice can be used as the hosts. Apparently, either type of hosts has certain advantages and disadvantages, and therefore, proper experimental controls should be included in all experiments.

2. CFSE, like any other chemical, can be toxic to cells, and its toxicity is dose dependent and cell-type dependent. We noticed that the final CFSE concentration of 5 μM consistently produces excellent labeling for T-cells without any detectable side effect. How-
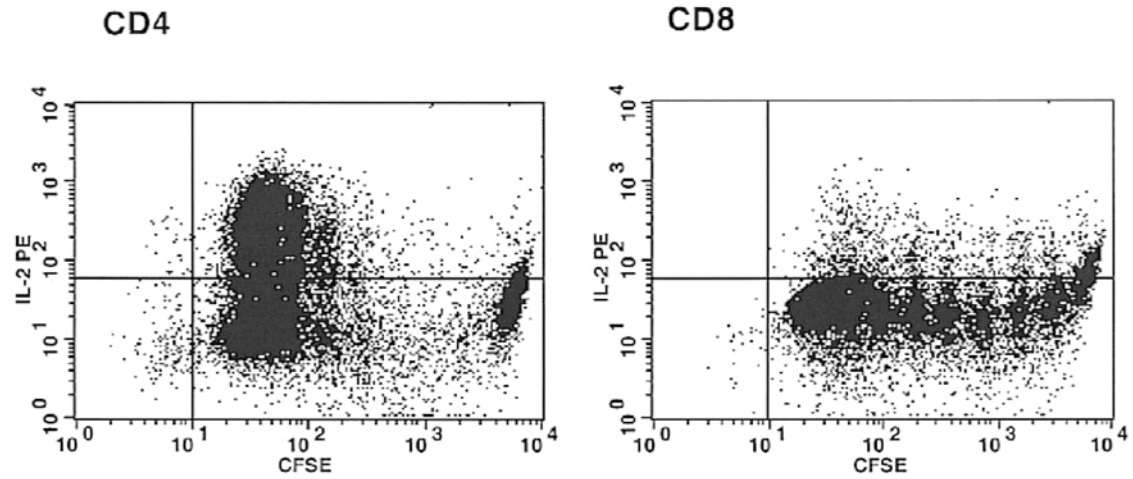
Fig. 3. Analysis of cytokine expression in the context of cell division. Donor cells were recovered from the host mice and stained for intracellular cytokine expression using PE-conjugated cytokine-specific mAb. CD4⁺ T-cells were identified by CyChrome-anti-CD4 staining, and their division history was revealed by the dilution of the CFSE dye. Cytokine expression in distinct division cycles was plotted and analyzed.
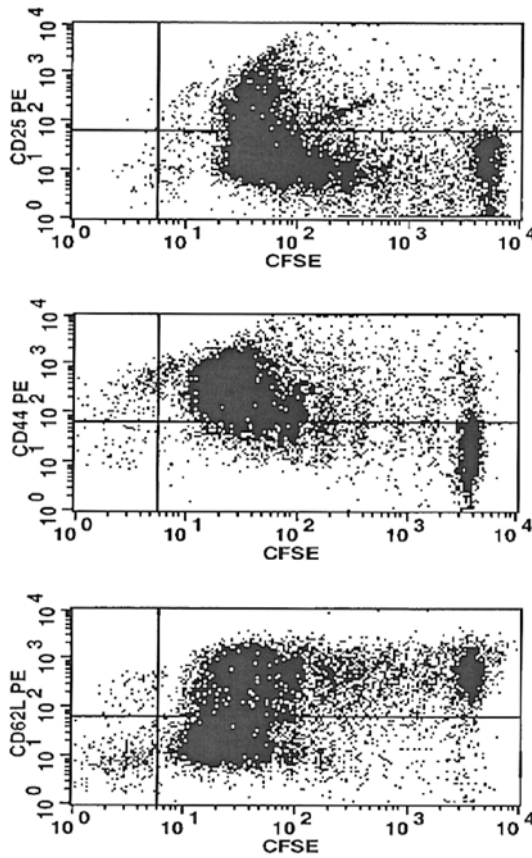
Fig. 4. Phenotypic characterization of dividing T-cells. Donor cells were recovered from the host mice and stained with PE-anti-CD25, PE-anti-CD44, and PE-anti-CD62L. CD4⁺ T-cells were identified by CyChrome-anti-CD4 staining and their division history was revealed by the dilution of the CFSE dye. Expression of such activation markers in distinct division cycles was plotted and analyzed.

ever, higher CFSE concentrations often result in greater cell loss during the labeling process. It is likely that higher CFSE concentrations may also interfere with T-cell function. Thus, care should be taken when labeling different types of cells with CFSE.

3. Transferring T-cells into lymphopenic mice can also induce homeostatic expansion of transferred cells. However, homeostatic expansion requires (1) empty hosts; (2) small number of T-cells transferred; and (3) a longer period of time (>7 d). Thus, the number of donor cells injected into the irradiated hosts is important to prevent homeostatic expansion from occurring. We recommend transferring 60 to 80×10^6 CFSE-labeled donor cells and performing the analysis 3 d after adoptive cell transfer. Cell proliferation under such conditions is driven primarily by the host alloantigens *(8)*.
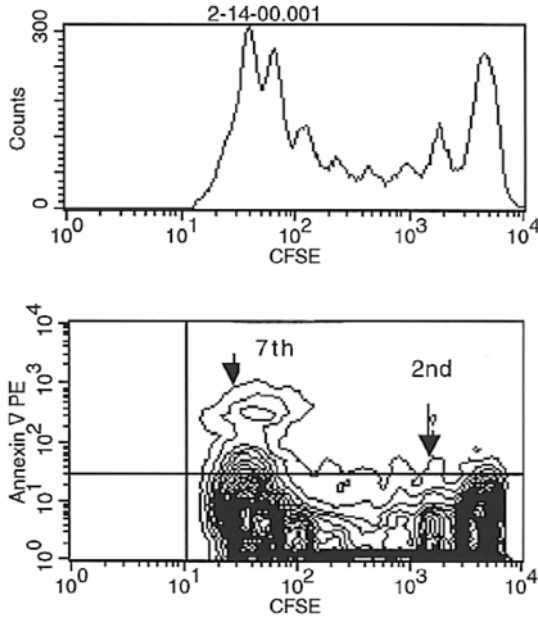
Fig. 5. Cell division and activation induced cell death. Donor cells were recovered from the host mice and stained with PE-annexin V. CD4$^+$ T-cells were identified by CyChrome-anti-CD4 staining and their division history was revealed by the dilution of the CFSE dye. Apoptotic cell death in distinct division cycles was plotted and analyzed.

4. In the model described, a 3-d period of in vivo stimulation represents the best window of opportunity to have a panoramic view of cell-division history in vivo, and up to eight cell divisions can be clearly identified at this time point. Longer than 3 d of in vivo stimulation often results in polarized cell-division profiles, i.e., a profile with two major peaks (divided cells and undivided cells), leaving little in between.

5. In vivo T-cell response is often compartmentalized. For example, T-cells activated in the host spleen may exhibit certain distinct characteristics other than those in the host lymph nodes *(30,31)*. Such differences may be due to distinct homing properties of T-cell subsets to different lymphoid compartments, or due to differences in the quality of stimulation in different lymphoid tissues. Thus, the host spleen and peripheral lymph nodes should be examined and compared separately.

6. Multi-color flow cytometry can be complex, especially with a CFSE fluorescent intensity across a wide spectrum. Thus, special attention should be paid to the following points: (1) proper adjustment of compensation parameters; (2) acquisition of adequate cell numbers, especially for analyzing rare cell subsets (e.g., $0.5–1.0 \times 10^6$ events); (3) when identification of donor-derived and host-derived cells appears confusing, it is helpful to incorporate additional markers such as donor MHC haplotype staining in order to be certain.

Acknowledgments

References

1 Jenkins, M. K., Pardoll, D. M., Mizuguchi, J., Quill, H., and Schwartz, R. H. (1987) T-cell unresponsiveness in vivo and in vitro: fine specificity of induction and molecular characterization of the unresponsive state. *Immunol. Rev.* **95,** 113–135.

2 Schwartz, R. H. (1990) A cell culture model for T lymphocyte clonal anergy. *Science* **248(4961),** 1349–1356.

3 Matzinger, P. (1999) Graft tolerance: a duel of two signals. *Nat. Med.* **5,** 616–617.

4 Gimmi, C. D., Freeman, G. J., Gribben, G. J., Gray, G., and Nadler, L. M. (1993) Human T-cell clonal anergy is induced by antigen presentation in the absence of B7 costimulation. *Proc Natl Acad Sci USA* **90(14),** 6586–6590.

5 Greenwald, R. J., Boussiotis, V. A., Lorsbach, R. B., Abbas, A. K., and Sharpe, A. H. (2001) CTLA-4 regulates induction of anergy in vivo. *Immunity* **14(2),** 145–155.

6 Wells, A. D., Walsh, M. C., Bluestone, J. A., and Turka, L. A. (2001) Signaling through CD28 and CTLA-4 controls two distinct forms of T cell anergy. *J. Clin. Invest.* **108(6),** 895–904.

7 Frauwirth, K. A., Alegre, M. L., and Thompson, C. B. (2000) Induction of T cell anergy in the absence of CTLA-4/B7 interaction. *J. Immunol.* **164(6),** 2987–2993.

8 Li, Y., Li, X. C., Zheng, X. X., Wells, A. D., Turka, L. A., and Strom, T. B. (1999) Blocking both signal 1 and signal 2 of T-cell activation prevents apoptosis of alloreactive T cells and induction of peripheral allograft tolerance. *Nat. Med.* **5(11),** 1298–1302.

9 Azuma, M., Cayabyab, M., Buck, D., Phillips, J. H., and Lanier, L. L. (1992) CD28 interaction with B7 costimulates primary allogeneic proliferative responses and cytotoxicity mediated by small, resting T lymphocytes. *J. Exp. Med.* **175(2),** 353–360.

10 Larsen, C. P., Elwood, E. T., Alexander, D. Z., et al. (1996) Long-term acceptance of skin and cardiac allografts after blocking CD40 and CD28 pathways. *Nature* **381(6581),** 434–438.

11 Kirk, A. D., Harlan, D. M., Armstrong, N. N., et al. (1997) CTLA4-Ig and anti-CD40 ligand prevent renal allograft rejection in primates. *Proc. Natl. Acad. Sci. USA* **94(16),** 8789–8794.

12 Cayabyab, M., Phillips, J. H., and Lanier, L. L. (1994) CD40 preferentially costimulates activation of CD4+ T lymphocytes. *J. Immunol.* **152(4),** 1523–1531.

13 Croft, M. (2003) Costimulation of T cells by OX40, 4-1BB, and CD27. *Cytokine Growth Factor Rev.* **14(3–4),** 265–273.

14 Hutloff, A., Dittrich, A. M., Beier, K. C., et al. (1999) ICOS is an inducible T-cell costimulator structurally and functionally related to CD28. *Nature* **397(6716),** 263–266.

15 Mallett, S., Fossum, S., and Barclay, A. N. (1990) Characterization of the MRC OX40 antigen of activated CD4 positive T lymphocytes-a molecule related to nerve growth factor receptor. *EMBO J.* **9(4),** 1063–1068.

16 de Jong, R., Loenen, W. A., Brouwer, M., et al. (1991) Regulation of expression of CD27, a T cell-specific member of a novel family of membrane receptors. *J. Immunol.* **146(8),** 2488–2494.

17 Kim, Y. J., Pollok, K. E., Zhou, Z., et al. (1993) Novel T cell antigen 4-1BB associates with the protein tyrosine kinase p56lck1. *J. Immunol.* **151(3),** 1255–1262.

18 Del Prete, G., De Carli, M., D'Elios, M. M., et al. (1995) CD30-mediated signaling promotes the development of human T helper type 2-like T cells. *J. Exp. Med.* **182(6),** 1655–1661.

19 Kobata, T., Agematsu, K., Kameoka, J., Schlossman, S. F., and Morimoto, C. (1994) CD27 is a signal-transducing molecule involved in CD45RA+ naive T cell costimulation. *J. Immunol.* **153(12),** 5422–5432.

20 Demirci, G., Gao, W., Zheng, X. X., Malek, T. R., Strom, T. B., and Li, X. C. (2002) On CD28/CD40 ligand costimulation, common gamma-chain signals, and the alloimmune response. *J. Immunol.* **168(9),** 4382–4390.

21 Lyons A.B. (2000) Analysing cell division in vivo and in vitro using flow cytometric measurement of CFSE dye dilution. *J. Immunol. Methods* **243(1–2), 147–154.**

22 Lyons, A. B. (1999) Divided we stand: tracking cell proliferation with carboxyfluorescein diacetate succinimidyl ester. *Immunol. Cell Biol.* **77(6),** 509–515.

23 Lyons, A. B. and Parish, C. R. (1994) Determination of lymphocyte division by flow cytometry. *J. Immunol. Methods* **171(1),** 131–137.

24 Wells, A. D., Gudmundsdottir, H., and Turka, L. A. (1997) Following the fate of individual T cells throughout activation and clonal expansion. *J. Clin. Invest.* **100(12),** 3173–3183.

25 Fulcher, D. and Wong, S. (1999) Carboxyfluorescein succinimidyl ester-based proliferative assays for assessment of T cell function in the diagnostic laboratory. *Immunol. Cell Biol.* **77(6),** 559–564.

26 Weston, S. A. and Parish, C. R. (1990) New fluorescent dyes for lymphocyte migration studies. *J. Immunol. Methods* **133(1),** 87–97.

27 Parish, C. R. (1999) Fluorescent dyes for lymphocyte migration and proliferation studies. *Immunol. Cell Biol.* **77(6),** 499–508.

28. Kruisbeek, A. M. (2000) In vitro assays for mouse lymphocyte function, In: *Current Protocols in Immunology*. Coligan, J. E., Kruisbeek, A. M., Margulies, D. H., Shevack, E. M., and Strober, W. (eds). National Institutes of Health, Wiley, New York, NY, pp. 3.1.1–3.1.5.

29 van Oss, C. J., Bronson, P. M., Dinolfo, E. A., and Chadha, K. C. (1981) Two methods for the removal of erythrocytes from buffy coats for the production of human leukocyte interferon. *Immunol. Commun.* **10(6),** 549–555.

30. Drake, D. R. 3rd. and Braciale, T. J. (2003) Not all effector CD8+ T cells are alike. *Microbes Infect.* **5(3),** 199–204.

31. Cron, R. Q., Gajewski, T. F., Sharrow, S. O., Fitch, F. W., Matis, L. A., and Bluestone, J. A. (1989) Phenotypic and functional analysis of murine CD3+,CD4–,CD8– TCR-gamma delta-expressing peripheral T cells. *J. Immunol.* **142(11),** 3754–3762.

28

Stem Cell Transplantation

Graft-Mediated Antileukemia Effects

William J. Hogan and Hans Joachim Deeg

Summary

Graft-mediated antileukemia (GVL) activity is a major factor contributing to the success of allogeneic hematopoietic stem transplantation (aHCT). Recent advances have permitted the establishment of GVL activity without the need for a myeloablative conditioning regimen, thereby permitting even older and sicker patients to avail of potentially curative therapy. Use of adoptive immunotherapy by combining reduced intensity conditioning and donor leukocyte infusion (DLI) has resulted in strategies that can be exploited to maximize GVL effects while minimizing toxicity. These advances, combined with new molecularly targeted agents, creates new possibilities to develop less toxic, curative therapy for a greater number of patients. This review summarizes pertinent information regarding the evidence in favor of GVL effects, the impact of disease type and mechanisms of GVL.

Key Words: GVHD; GVL effect; hematopoietic cell transplantation; minor antigens.

1. Introduction

Initial efforts to cure cancer were directed exclusively at chemotherapy or radiotherapy dose escalation. As toxicity to normal host hematopoietic cells was dose-limiting, allogeneic transplantation was seen as a way to permit further intensification of therapy. However, after cytotoxic therapy, malignant cells die with first-order kinetics, making cure an unachievable goal of dose escalation in most situations *(1)*. In addition, more intensive regimens are associated with more pronounced non-hematologic toxicity, reducing the net benefit of additional anti-leukemic effects *(2)*. Recent advances in the field of transplantation biology include efforts to reduce transplant-related mortality (TRM) by tailoring the conditioning regimen to the patient with targeted dosing of cytotoxic drugs *(3)* or by replacing myeloablative conditioning with much less intense regimens that rely predominantly on immunological effects of transplanted donor cells to eradicate malignant cells *(4–6)*. Advantages of reduced inten-

sity or minimally ablative conditioning regimens include reduction in organ toxicity attributable to the conditioning regimen, such as mucositis, bacterial infection, and venoocclusive disease of the liver, in addition to decreased transfusion requirements. There is also some evidence that the incidence of acute graft-vs-host disease (GVHD) might be decreased *(7)*. One possible explanation for this finding is that the less intense conditioning causes less of a cytokine storm, thereby reducing the contribution of one of the major putative factors in the pathogenesis of this disorder. These approaches have allowed older or less robust patients to be considered for allogeneic transplantation with curative potential, a critical issue, as the median ages of diagnoses for many hematological malignancies are in the sixth to seventh decades.

2. Evidence of a Graft-vs-Leukemia (GVL) Effect in Human Patients

During allogeneic transplantation, donor hematopoietic progenitor cells and immunoreactive leukocytes are transferred to the recipient and establish donor-derived hematopoiesis. As previously observed in rodent models, it was appreciated that donor cells also had unwanted effects, mediating a stereotypical syndrome, initially dubbed secondary disease, now known as graft-vs-host disease. Subsequent observations suggested, however, that this undesirable complication could be associated with a beneficial graft-vs-leukemia effect *(8–10)*. These observations included (1) the inverse correlation between GVHD and leukemia recurrence from retrospective single-institution and registry studies *(11)*; (2) the occurrence of leukemic remissions during episodes of acute and chronic GVHD *(12)*; (3) the ability to purposefully induce such remissions by the withdrawal of immunosuppression *(13,14)*; (4) the higher risk of relapse in recipients of either syngeneic or autologous grafts compared to human leukocyte antigens (HLA)-matched (but minor antigen disparate) donors *(15,16)*; (5) the increased risk of relapse associated with T cell depleted (TCD) grafts *(17–19)*; and, most convincingly, (6) the ability of donor lymphocyte infusions to induce sustained remissions after relapse following transplantation *(20)*.

2.1. Remissions Associated With GVHD
or Withdrawal of Immunosuppression

Barnes et al. *(21)* predicted the possibility of a GVL effect as early as 1956, and subsequent observations, including analyses of retrospective data from transplant registries, supported this hypothesis *(8–14)*. Sullivan et al. *(11)* analyzed data from 1202 patients with acute myeloid leukemia (AML), acute lymphocytic leukemia (ALL), or chronic myeloid leukemia (CML) receiving allogeneic marrow from HLA-identical siblings. Among patients with AML and ALL transplanted in relapse and surviving in remission to day +150 (thereby being at risk for chronic GVHD), the probability of subsequent relapse was 74% in those who did not develop GVHD compared to 34% in patients with chronic GVHD ($p < 0.001$). Actuarial survival was 25% and 62%, respectively ($p < 0.009$). Among patients with CML in accelerated phase or blast crisis, the probability of relapse after day +150 was 65% in patients without GVHD and 36% in those with acute and chronic GVHD ($p < 0.017$). Horowitz et al. reported data on 2254 patients receiving HLA-identical sibling bone-marrow transplants for AML

in first remission, ALL in first remission, and CML in first chronic phase *(17)*. For T-cell-replete grafts, lower relapse rates were observed in patients who developed acute (relative risk 0.68, $p = 0.03$), chronic (relative risk 0.43, $p = 0.01$), and both acute and chronic (relative risk 0.33, $p = 0.0001$) GVHD compared to those without GVHD, suggesting that GVHD was associated with durable anti-leukemic effects.

2.2. Outcomes With Syngeneic vs HLA-Identical Sibling Donors

Gale et al. reported International Bone Marrow Transplant Registry (IBMTR) data comparing outcomes in 103 identical-twin transplants to 1030 concurrent HLA-identical sibling transplants matched for prognostic factors *(16)*. Three-year probabilities of relapse were greater after identical-twin transplants for patients with ALL (36% vs 26%), AML (52% vs 16%), and CML (40% vs 7%). Increased relapse risks in AML and CML persisted after adjusting for GVHD (relative risk 3.1 and 5.5, respectively). This finding was consistent with prior reports of a greater relapse rate in patients with syngeneic donors (relative risk 2.58, $p = 0.008$) compared to those with HLA-identical siblings without GVHD *(17)*, suggesting that GVL effects may occur without clinically apparent GVHD. The advantage presented by a decreased risk of relapse in HLA-identical siblings was offset to some degree by more transplant-related mortality.

2.3. Outcomes After T-Cell Depleted Grafts

TCD was introduced in an effort to reduce the incidence and severity of GVHD. While successful in achieving this aim, this procedure resulted in an increased risk of disease relapse and graft failure, particularly in patients with myeloid leukemias. Apperley et al. *(18)* reported on patients with CML in chronic phase, receiving either unmanipulated ($n = 106$) or TCD ($n = 102$) donor bone marrow. The probability of remaining in remission after receiving a T-cell-replete graft (97% at 6 yr) was superior to a TCD graft (67% at 3 yr). There was an increased risk of early (8 vs 0 patients) and late graft failure (10 vs 0 patients) in the TCD graft recipients. These findings are consistent with IBMTR data on patients with CML, which demonstrated that recipients of HLA-identical, T-cell-replete grafts who did not develop GVHD were seven times less likely to relapse than those who received TCD grafts without developing GVHD. Even those recipients of TCD grafts who developed GVHD had a higher risk of relapse than those who received a T-cell-replete graft without GVHD *(17)*. These observations provided additional evidence to support the hypothesis that the immunobiology of GVL effects and GVHD are distinct at some level, providing hope that it may ultimately be possible to promote the development of a GVL effect while preventing GVHD.

2.4. Adoptive Immunotherapy With Donor Lymphocyte Infusions

Observations suggesting the presence of GVL effects were confirmed with the successful use of donor-derived lymphocytes to achieve remissions in patients with relapsed hematological malignancies *(20)*. Initial studies combined interferon (IFN)-α with donor lymphocyte infusion (DLI) *(20)*; however, it was subsequently shown that the combination was not superior to DLI alone *(22)*. More recent data suggest that the

composition of DLI is important in determining outcome, with a suggestion that the risk of severe GVHD can be reduced without compromising efficacy by limiting the T-cell (CD3$^+$) content of the infusion (23). DLI results in complete remissions (CRs) in a high percentage of patients with relapsed chronic-phase CML; however, CRs are observed less frequently in other situations, including advanced CML and acute leukemia.

Treatment-related mortality has been reported to be 7 to 9% for DLI from related donors, and up to 44% for alternative donor transplants (24–26). GVHD and transient or irreversible marrow hypoplasia are the major complications of DLI (27). The reported incidence of acute (21–70%) and chronic GVHD (26–60%) appears to depend on several factors, including interval between hematopoietic cell transplantation (HCT) and DLI, disease type, cell dose and infusion schedule, and the development of post-DLI marrow hypoplasia (22,24,25,27–30). While the occurrence of GVHD has been highly correlated with response in some studies (27), recent reports suggest that both the T-cell dose and the infusion schedule may be important in determining outcome, as a schedule of dose escalation may minimize the risk of severe GVHD while preserving GVL effects. Raiola (24) reported that after HLA-matched related DLI, the incidence of grades II–IV acute GVHD was 1%, 6%, and 23% for CD3$^+$ cell doses per infusion of 1×10^6, 1×10^7, and 1×10^8/kg respectively. Grade IV acute GVHD was only seen after 1×10^8 CD3$^+$ cells per kg for related donors but occurred with infusions of 1×10^7 CD3$^+$ cells per kg from alternative donors. Dazzi (31) compared a single large dose of donor lymphocytes (bulk dose regimen, BDR) with an escalating dose regimen (EDR). Although the probability of achieving cytogenetic remission did not differ significantly between the two groups, the incidence of GVHD was much lower using EDR (10% vs 44%, $p = 0.01$). After correcting for cell dose, the incidence and severity of acute and chronic GVHD were both significantly lower for recipients treated by EDR. Factors predicting response after DLI included the type and phase of disease, chemotherapy responsiveness, and the development of GVHD or marrow hypoplasia (24,30). Bone-marrow aplasia occurred in approx 11–18% of patients and was more likely in patients with predominant host hematopoiesis and hematologic relapse (22,27).

3. Disease Specificity of Graft-vs-Malignancy Effects

3.1. CML

With the introduction of DLI as a strategy to eradicate residual or relapsed disease after HCT, it was noted that certain malignancies, such as CML, were particularly sensitive to this therapeutic approach, while responses were less common in other diseases. Overall, complete responses are observed in 60–80% of CML patients who receive DLI without preceding chemotherapy (24,26). Response rates vary according to the amount of residual disease and response to prior chemotherapy, and may be as high as 100% in patients with isolated molecular relapse, 89% for cytogenetic relapse, 75–79% with chronic-phase relapse, compared to 12–36% of patients with accelerated-phase or blast-crisis CML (22,24,26). Other pre-DLI characteristics predictive of complete response in CML patients are post-transplant chronic GVHD, time interval

between BMT and DLI less than 2 yr, and development of GVHD after DLI. Overall, the probability of remaining in CR after a response has been suggested to be as high as 85%; however, this may also be dependent on disease status at time of DLI *(24–26)*. Dazzi reported that the probability of survival for patients who achieve molecular remissions was significantly better than for those who failed to do so (95% vs 53% at 3 yr after DLI, $p = 0.0001$) *(32)*. Extrapolation of these findings to the initial transplant approach has led to the increasing use of reduced-intensity or nonmyeloablative conditioning followed by HCT and exploitation of the allogeneic effect in the treatment of CML. While this modality has not been compared to conventional myeloablative HCT in a randomized fashion, there are encouraging signs that it may be a safe and effective alternative. Or et al. *(33)* reported data on 24 patients (median age 35 yr) with CML in first chronic phase conditioned with fludarabine, busulfan, and antithymocyte globulin (ATG). With median follow-up of 42 mo, 21 of 24 patients (88%) remained alive and disease free, suggesting that myeloablative conditioning is not necessary to cure diseases that are particularly susceptible to GVL effects.

3.2. AML/MDS

DLI alone is somewhat less effective for patients with relapsed AML, with CR rates ranging from 15 to 38% *(22,25,26)*. One study of 23 patients with AML undergoing unrelated donor DLI reported a remission rate of 42%, with responders having a 1-y disease-free survival probability of 23% *(29)*. DLI administered during isolated molecular relapse or combined with chemotherapy have been suggested as ways to improve results *(34,35)*. Small studies have reported CRs in 25–45% of patients with myelodysplastic syndrome, and responses in polycythemia vera (PV) have also been reported *(22,25,26)*.

3.3. ALL

Although the observation that acute and chronic GVHD are associated with reduced relapse rates for patients with ALL suggested that this disease might be amenable to manipulation of the immune system, the results with DLI have been disappointing *(36–38)*. CR rates after DLI alone for patients with hematological relapse have been reported to be 0–25% *(22,25,26)*. Collins et al. *(39)* evaluated patients from 27 transplant centers with persistent or recurrent ALL who received DLI with or without preceding chemotherapy. Two of 15 patients who received no pre-DLI chemotherapy achieved CR, lasting 1112 and >764 d, respectively. Of 25 patients who received DLI in the nadir after chemotherapy, 5 entered remission (median 83 d; range 42–193 d). Seven patients who did not respond initially received a second DLI; however, none of these patients attained durable remissions. Eighteen of 37 evaluable patients (49%) developed acute GVHD, and 5 of 20 (25%) evaluable patients developed chronic GVHD. Actuarial overall survival was 13% at 3 yr. In those patients who do respond to DLI, the duration of response tends to be less than for myeloid malignancies *(22)*. Despite these disappointing results, there is some evidence to suggest that sustained responses may be possible if DLI is administered at the time of molecular relapse *(24)*.

3.4. Myeloma

Anecdotal reports initially suggested a graft-vs-myeloma (GVM) effect *(40–44)*. Lokhorst subsequently reported on 27 patients, 25 of whom had a prior partially TCD graft *(30)*. Of the 13 patients who received pre-induction chemotherapy, 8 responded, but there were no complete responses. Overall, 14 of 27 patients (52%) responded to DLI, with 6 complete remissions (22%). Five responses occurred after dose escalation, and responses were more likely with chemotherapy-sensitive disease and a T-cell dose $>1 \times 10^8$/kg. Median overall survival for the entire group was 18 mo. Other reports have also suggested that responses occur in approx 25–50% of patients *(26)*.

3.5. Lymphoid Malignancies

Several studies have provided evidence suggesting a role for allogeneic cells in the treatment of lymphomas and chronic lymphocytic leukemia (CLL) *(4,45–49)*. Khouri et al. *(50)* reported on outcomes of 20 patients with relapsed follicular or small-cell lymphocytic lymphoma undergoing reduced intensity conditioning followed by HCT. The conditioning regimen consisted of fludarabine and cyclophosphamide with or without rituximab, and GVHD prophylaxis consisted of tacrolimus and methotrexate. At the time of HCT, 12 patients were in CR, all other patients achieved CR after HCT. At follow-up (median 21 mo), no patient had relapsed, and the actuarial probability of disease-free survival at 2 yr was 84%. Branson et al. *(51)* also described the use of DLI after progression or relapse following a reduced-intensity regimen based on fludarabine, melphalan, and alemtuzumab (CAMPATH) for patients with refractory or relapsed lymphoid malignancies. DLI was associated with a response in 6 of the 12 patients (50%) with progressive or relapsed disease. One patient with mantle-cell lymphoma achieved CR with DLI alone, while two patients with Hodgkin disease (HD) achieved CR with a combination of chemotherapy and DLI. One patient with HD and one with multiple myeloma (MM) remained progression free at 9 and 12 mo after DLI, while another patient with MM achieved partial response (PR) but died from GVHD and CMV infection 7 mo after DLI. In another study by Marks et al., 8 of 13 patients with persistent or relapsed follicular lymphoma had complete responses to DLI, suggesting that low-grade lymphoid malignancies are more susceptible to GVL effects *(27)*.

Reports suggesting graft-vs-tumor effects in HD led to a matched case control study by the European Group for Blood and Marrow Transplantation (EBMT) comparing outcomes after allogeneic HCT ($n = 45$) to outcomes after autologous HCT ($n = 45$) for patients with relapsed HD *(52)*. Patients were matched for age, gender, disease status, conditioning regimen, and time from diagnosis to HCT. TRM was very high in the allogeneic group, with 4-yr actuarial probabilities of survival, progression-free survival (PFS), and TRM of 25%, 15%, and 48% compared to 37%, 24%, and 27% after autologous HCT. However, there was an association between grades II–IV acute GVHD with lower relapse rates after allogeneic HCT, consistent with a graft-vs-Hodgkin's-disease effect. Overall, it did not appear that there was a major advantage to myeloablative allogeneic HCT; however, subsequent studies have suggested that there is a continuing risk of relapse or secondary AML/MDS more than a decade after autologous HCT; both complications are less likely after alloge-

neic HCT *(53)*. The advent of nonmyeloablative regimens has raised the possibility that less toxic approaches might be more successful, and it has even been suggested that patients with heavily pretreated HD may be so immunosuppressed that they might benefit from DLI without preceding HCT; however, this remains to be proven *(54,55)*.

3.6. Solid Tumors

While the majority of reports describing graft-vs-malignancy (GVM) effects relate to hematopoietic malignancies, this phenomenon has also been observed with certain solid tumors, especially renal cell cancer and occasionally breast or ovarian cancer *(56–64)*. Although there have been reports of graft-vs-malignancy effects in sarcomas *(64)* and tumors originating from prostate *(61)*, colon *(62)*, and lung *(63)*, responses have generally not been consistent or dramatic enough to suggest clinical benefit. Childs et al. *(57)* reported on 19 patients with metastatic renal-cell carcinoma receiving peripheral blood stem cell grafts from HLA-identical or single-antigen-mismatched siblings after reduced-intensity conditioning. Efforts to induce graft-vs-tumor effects included early withdrawal of postgrafting immunosuppression and use of DLI if necessary. There were complete responses in three patients and PRs in seven patients, resulting in a 53% overall response rate. Two patients died of non-relapse mortality and eight died of progressive disease. Rini et al. *(58)* also reported on a reduced-intensity conditioning regimen using cyclophosphamide and fludarabine for renal cell carcinoma. Of 12 patients who had follow-up to 180 d, 9 had sustained donor engraftment and 4 died of TRM. Four patients had partial remissions. Bregni et al. *(59)* reported on seven patients with renal-cell carcinoma who were treated with a reduced-intensity regimen consisting of thiotepa, cyclophosphamide, and Flu. Four partial remissions were observed; at the time of reporting, only one patient was alive with ongoing PR at 208 d, one was alive with progression, and two had died of transplant-related problems. Nevertheless, the presence of occasional dramatic responses in some patients with bulky metastatic renal-cell carcinoma provides hope that an adoptive immunotherapy approach might be further refined to improve outcomes in a disease with no other effective therapy.

Murine studies have suggested that breast carcinoma might be susceptible to graft-vs-tumor effects *(65,66)*. Bregni et al. *(59)* treated six patients with breast cancer with a reduced-intensity conditioning regimen followed by allogeneic HCT, and reported PRs in two patients, one of whom remained alive and in PR until the time of reporting at d 417, while the other patient died in PR from GVHD at 490 d. Bay et al. *(60)* reported on five patients with ovarian cancer receiving allogeneic transplantation from HLA-matched siblings. One patient received a myeloablative conditioning regimen, while the other four received non-myeloablative regimens. One recipient of a nonmyeloablative regimen died soon after transplantation from progressive disease. The remaining four patients developed GVHD associated with tumor regression. One patient died of GVHD at 127 d; two of the remaining patients received DLI, resulting in GVHD in both patients and GVM effect in one patient.

A number of factors have resulted in considering patients with malignant melanoma for adoptive immunotherapy approaches. These include (1) the observation that

spontaneous regressions have occasionally been reported, suggesting that in certain circumstances this tumor may be responsive to immunotherapy; (2) the identification of melanoma-specific tumor antigens; (3) the fact that eradication of normal melanocytes would not be expected to result in significant organ toxicity; and (4) the absence of another effective therapy. Childs et al. *(67)* reported the results of nonmyeloablative HCT on 15 patients with refractory metastatic melanoma. Four patients experienced a partial remission; however, this appeared to be temporally associated with the conditioning regimen. No clear GVM effect was seen after withdrawal of immunosuppression or institution of DLI. At the time of reporting, 1 patient remained alive (median survival 86 d), 12 had died from progressive melanoma, and 2 died from TRM.

3.7. Posttransplantation Lymphoproliferative Disorders

Infectious and malignant complications are commonly encountered after HCT due to delayed immune reconstitution. There is encouraging preliminary evidence to suggest that adoptive immunotherapy might be of value in the prevention and treatment of these complications. Despite advances in monitoring and therapy, cytomegalovirus (CMV) infection remains a major source of morbidity and even mortality after HCT. The recognition of the importance of T-cells in controlling CMV led to the adoptive transfer of T-cell clones to restore antiviral immunity *(68–70)*. This technique is also being evaluated for the prevention and treatment of diseases mediated by adenovirus and Epstein–Barr virus (EBV) *(71–74)*. EBV is instrumental in the development of posttransplantation lymphoproliferative disease (PTLD). This is an unusual neoplasm that usually arises in B-lymphocytes of donor origin after HCT and those of recipient origin after solid-organ transplantation. These neoplastic cells proliferate in the absence of an effective T-cell response, and reconstitution of EBV-specific T-cell immunity by adoptive immunotherapy often results in durable remissions *(75–79)*.

4. Mechanisms of GVL

Perhaps the greatest challenge in hematopoietic cell transplantation today is understanding the mechanisms that underlie GVL effects and GVHD. While these two processes generally occur in concert, there is tantalizing evidence to suggest that there might be sufficient differences between them to exploit in an immunotherapy strategy (**Fig. 1**). Although the underlying immunobiology of GVL effects is not yet fully understood, there is evidence to suggest that a number of mechanisms may be operative. For an individual, the extent of GVL may depend on several factors, including the quantity or quality of polymorphic differences between the donor and host, the type of malignancy, source of stem cells, and concomitant immunosuppression or infection.

4.1. Effector Cells

It is generally accepted that T-cells play a major role in generating GVL responses; however, other cells almost certainly provide important contributions. Certain malignant cells, such as CML blasts, may be able to act as antigen-presenting cells to donor T-cells, thereby facilitating an effective immune response. It is also increasingly recognized that natural killer cells may play a role, particularly in the HLA-C mismatched setting.
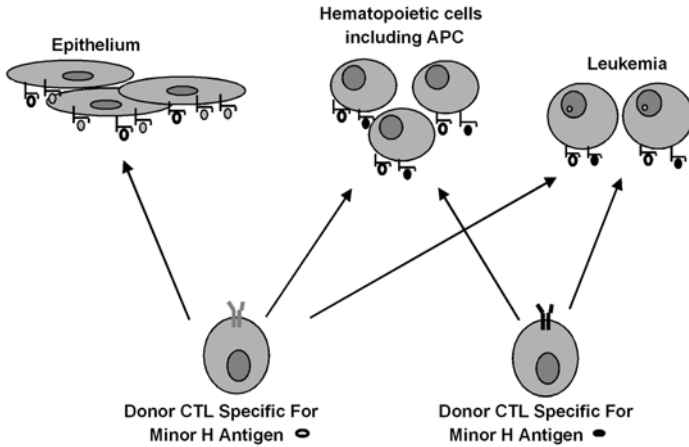
Fig. 1. Tissue-specific expression of minor histocompatibility antigens may permit selective graft-vs-leukemia activity.

4.1.1. T-Cells

Several lines of evidence suggest a major role for T-cells in the generation of GVL. Donor T-cells have been shown to be essential for GVL in murine models of leukemia *(80)*. Further studies in severe combined immunodeficiency mice with established human leukemia growth suggested that the role of T-cells in eradicating tumor cells is also important in humans *(81)*. The identification of CD4+ and CD8+ T-cell clones directed specifically against leukemic cells, and retrospective studies demonstrating increased relapse rates after TCD hematopoietic cell transplantation, provide additional support in favor of a major role for T-cells in mediating GVL effects in humans *(17,82–85)*.

There is debate regarding the relative importance of specific T-cell subsets in the immunobiology of GVL effects and GVHD. Evidence in support of a predominant role for CD4+ cells include murine studies where either CD8+-depleted marrow or CD4+-supplemented marrow was transplanted. Despite a low incidence of GVHD, leukemia-free survival appeared to be preserved in some strain combinations *(86)*. Clinical studies of CD8+-depleted hematopoietic grafts or DLI also appear to have anti-leukemic activity with less GVHD, reinforcing the contribution of the CD4+ population in generating GVL reactions *(87–89)*. Claret et al. analyzed the T-cell receptor (TCR) repertoire in four patients with relapsed CML who achieved a complete remission (3/4 without GVHD) after infusion of CD4+ lymphocytes from HLA-identical sibling donors *(90)*. Before DLI, all four patients were found to have a restricted TCR Vβ repertoire in peripheral T-cells, while after DLI, new Vβ clones were identified coincident with cytogenetic responses, suggesting the possibility of selective T-cell eradication of leukemic cells. Although CD4+ T-cells from transplant recipients have been shown to lyse leukemia cells, alloreactivity towards nor-

mal host cells is well described, suggesting a role for CD4^{+} cells in mediating both GVL effects and GVHD *(91,92)*. In other models, CD8^{+} cells appear to be the primary mediators of GVL, with CD4^{+} cells facilitating clonal expansion of CD8^{+} cells *(93,94)*. It is likely that at some level, GVH and GVL activities can be separated despite the existence of some effector cells that exhibit both activities, and it has been suggested that selective TCD methods might be feasible *(82)*.

4.1.2. Antigen-Presenting Cells

To optimize GVL potency, the malignant cell should act as both a stimulator and a target for donor effector mechanisms *(95)*. Dendritic cells represent the most effective antigen-presenting cells, with the ability to process and express antigenic peptides and initiate cell-mediated and humoral immune responses. In certain malignancies, such as CML, the leukemic clone is derived from a pluripotent hematopoietic cell with the potential to generate leukemic dendritic cells. These and other antigen-presenting cells harbor the chimeric BCR/abl fusion protein and may present leukemia-specific antigens to donor T-cells via class I or II major histocompatability complex (MHC) antigens *(96)*. This may be part of the explanation for better responses to DLI in CML, and augmentation of this ability may provide a means to achieve even greater success *(97,98)*.

4.1.3. Natural Killer Cells

Many tumors do not present tumor-specific antigens and have down-regulated class I MHC, thereby avoiding recognition by T-cells *(99)*. This means that T-cell-mediated GVL reactions are rendered either ineffective or less specific, relying on recognition of minor antigen targets expressed on both malignant and normal host cells. Natural killer (NK) cells do not depend on specific antigen recognition for target-cell lysis, rendering them very interesting from a tumor immunology perspective. While there has long been optimism that NK cells might provide a valuable contribution to successful tumor immunotherapy, this goal has been slower to realize *(100)*. To date, most strategies utilizing NK cells in the treatment of malignancies have employed ex vivo generation of lymphokine-activated killer (LAK) cells or activated NK cells, or in vivo administration of cytokines to activate NK cells against autologous cancer cells. In general these studies have been somewhat disappointing, limited by lack of efficacy or excessive toxicity, or both *(101–106)*. However, the recent identification and characterization of cell-surface receptors including killer cell immunoglobulinlike receptors (KIRs), C-type lectins, and natural cytotoxicity receptors (NCRs) have provided encouragement that the properties of NK cells can finally be exploited *(107)*. There is a wealth of new information becoming available, elucidating the activating and inhibitory pathways mediated through an array of NK receptors, promising a more sophisticated approach than previous non-specific intervention using cytokines such as interleukin (IL)-2. Whereas evidence to suggest that NK cells may contribute to antileukemic effects in the HLA-matched setting is limited, a potent GVL effect of NK cells is more convincing in the haplo-identical setting *(100,108–113)*. In this allogeneic situation, KIR mismatches facilitate leukemic cell lysis without GVHD *(114,115)*.

4.2. Antigenic Targets

Antigenic targets for GVL effects comprise two main categories: (1) antigenic differences that occur as a result of polymorphisms between donor and host (minor histocompatability antigens); and (2) tumor-specific antigens. Effective eradication of malignant cells may depend on an immune response directed against either or both of these targets.

4.2.1. Minor Histocompatability Antigens

Minor histocompatability antigens (mHA) are alloantigens capable of eliciting an allogeneic T-cell response between HLA-matched individuals and occur due to the presence of polymorphic peptides *(116)*. Minor antigen disparities are presumably the basis for the difference in relapse rates between recipients of hematopoietic grafts from syngeneic and HLA-matched sibling donors. Multiple minor antigens, derived from both autosomal and sex chromosomes, have already been described *(117–123)*. Polymorphisms in proteins may result in either a previously unencountered peptide or, alternatively, differential antigen processing, either of which may lead to presentation of a neo-antigen *(124,125)*. Such antigens may be restricted to certain tissues, such as hematopoietic cells, or be expressed by a multitude of tissue types, fueling enthusiasm that an allogeneic effect could be directed against malignant hematopoeitic cells in a relatively specific fashion *(126,127)*. One can imagine that either GVL or GVHD could be seen alone or in combination, depending on the distribution of mHA for a given donor–host combination. The eradication of malignant cells in the absence of clinical GVHD, noted in some patients after HCT or DLI, has provided additional encouragement that this approach may ultimately be successful. These findings have fostered a major effort to characterize immunodominant mHAs to be used as targets for immunotherapy.

4.2.2. Tumor Antigens

As malignant cells are derived from autologous cells, it is not entirely surprising that many "tumor antigens" are actually self-antigens, which are overexpressed in malignant cells. In a recent review, Pardoll describes four different categories of tumor antigens *(128)*. These include:

1. Unique antigens created as a result of a mutation. These include bcr-abl, PML/RARα, ETV6-AML, DEK-CAN, and activating mutations such as p21ras or inactivating mutations in cyclin-dependent kinase 4 (CDK4) *(129–140)*.
2. Viral antigens such as human papilloma virus 16 E6 and E7, which are expressed on most cervical cancers. Other oncogenic viruses, such as hepatitis B and C and EBV, may also provide useful tumor antigens.
3. Tissue-specific differentiation antigens. Proteinase 3 is a serine protease with several known polymorphisms found in high concentrations in the primary granules of acute and chronic myeloid blasts. Cytotoxic T lymphocytes (CTL) recognizing an octameric HLA-A2-restricted peptide (PR1) derived from proteinase 3 are capable of specific killing of myeloid leukemic cells. Such CTL occur spontaneously after allogeneic HCT and may be at least partially responsible for the curative potential of allogeneic transplantation in this disease *(141–143)*. Clave et al. *(144)* demonstrated that peptides derived from a specific

polymorphic site bind to the HLA-A2 molecule. In HLA-A2-expressing patients with myeloid leukemia undergoing HCT from HLA-identical donors, no relapses occurred in a group of 4 patients who had at least one allele absent in their donor, whereas 7 of the 15 remaining patients relapsed, raising the possibility of an appropriate target for T-cell immunotherapy. Other examples include the occurrence of T-cell responses directed against normal melanocytes, resulting in vitiligo, an observation that has been noted after immunotherapy for melanoma, or rarely after HCT. Putative antigens include tyrosinase, tyrosinase-related protein-1 (TRP-1), TRP-2, gp 100, and MART1/melan-A *(128,145,146)*

4. Tumor-selective antigens. This group includes antigens that are expressed at very low levels in normal tissues but are up-regulated in tumors. WT1 encodes a transcription factor expressed in embryogenesis and is rarely encountered in normal adult tissue. It is overexpressed in many types of leukemia and can elicit CTL responses that lyse leukemia cells in some circumstances *(147,148)*.

4.3. Effector Mechanisms

Even after appropriate recognition and clonal expansion by the donor immune system, GVL effects will occur only if malignant cells are susceptible to the effector mechanisms employed. Such mechanisms include direct lysis via the secretion of perforin and granzymes from cytotoxic cells, or induction of apoptosis via fas ligand (FasL) *(95,149–151)*. However, reduced susceptibility of malignant cells to these pathways have been reported *(152,153)*. In a murine model, Schmaltz et al. examined the relative contributions the perforin and FasL pathways in mediating GVHD and GVL effects *(154)*. In this model, donor T-cells mediated GVHD activity primarily through the FasL effector pathway, and GVL effects through the perforin pathway, suggesting a possible point of intervention to augment GVL effects while minimizing GVHD. Some T-cell clones demonstrate strong cytotoxic activity that is not mediated by either the FasL or perforin pathway *(155)*. Recently additional effector mechanisms have been identified, including tumor necrosis factor (TNF)-related apoptosis-inducing ligand (TRAIL), a member of the TNF superfamily. It participates in NK cell-mediated antitumor activity, and is also expressed on T-cells. In murine studies, TRAIL-expressing T-cells demonstrated greater anti-tumor activity but not more GVHD than TRAIL-deficient T-cells, suggesting another possible means to accentuate GVL effects without GVHD *(156,157)*.

Effector cells also depend on cytokines to mediate some of their anti-tumor effects. Cytokine gene polymorphisms can result in genetically fixed differences in cytokine responses to stimuli such as lipopolysaccharide (LPS). Investigation of cytokine gene polymorphisms has not yet been explored in detail with respect to how they might influence GVL activity; however, it has been proposed that certain polymorphisms are associated with the severity of acute (TNF, IL-10, IFN-γ) and chronic GVHD (IL-6) after allogeneic HCT *(158–161)*. Cytokine gene polymorphisms are also suggested to influence rejection after solid-organ transplantation *(162–165)*, raising the possibility that they may also be important in mediating GVL activity.

5. Conclusions

The GVM effects of allogeneic HCT make this therapeutic modality the most effective treatment for a range of malignancies. Recent progress has permitted older

and less robust patients to take advantage of this curative therapy by reducing transplant-related complications and mortality associated with high-intensity conditioning regimens. As adoptive immunotherapy using nonmyeloablative conditioning and DLI become established as a standard therapeutic intervention, further advances in our understanding of transplantation immunobiology have suggested potential strategies that might be exploited to maximize GVL effects while minimizing toxicity. These include the use of targeted dosing of cytotoxic agents, the combination of autologous HCT with delayed allografting using minimally myelosuppressive conditioning, and the development of more effective nonmyeloablative conditioning and postgrafting immunosuppression regimens. Appropriate dosing and intervention have enhanced the safety and effectiveness of DLI. Strategies to reproducibly separate the toxicity of GVHD from the beneficial GVL effect are under intense investigation; however, this important goal has yet to be fully realized in the clinical setting.

References

1. Porter, D. L. and Antin, J. H. (1999) The graft-versus-leukemia effects of allogeneic cell therapy. [Review]. *Annu. Rev. Med.* 50, **369–386.**
2. Clift, R. A., Buckner, C. D., Appelbaum, F. R., et al. (1990) Allogeneic marrow transplantation in patients with acute myeloid leukemia in first remission: a randomized trial of two irradiation regimens. *Blood* **76,** 1867–1871.
3. Deeg, H. J., Storer, B., Slattery, J. T., et al. (2002) Conditioning with targeted busulfan and cyclophosphamide for hemopoietic stem cell transplantation from related and unrelated donors in patients with myelodysplastic syndrome. *Blood* **100,** 1201–1207.
4. McSweeney, P. A., Niederwieser, D., Shizuru, J. A., et al. (2001) Hematopoietic cell transplantation in older patients with hematologic malignancies: replacing high-dose cytotoxic therapy with graft-versus-tumor effects. *Blood* **97,** 3390–3400.
5. Slavin, S., Nagler, A., Naparstek, E., et al. (1998) Nonmyeloablative stem cell transplantation and cell therapy as an alternative to conventional bone marrow transplantation with lethal cytoreduction for the treatment of malignant and nonmalignant hematologic diseases. *Blood* **91,** 756–763.
6. Giralt, S., Estey, E., Albitar, M., 'et al. (1997) Engraftment of allogeneic hematopoietic progenitor cells with purine analog-containing chemotherapy: harnessing graft-versus-leukemia without myeloablative therapy. *Blood* **89,** 4531–4536.
7. Mielcarek, M., Martin, P. J., Leisenring, W., et al. (2003) Graft-versus-host disease after nonmyeloablative versus conventional hematopoietic stem cell transplantation. Available online at First Edition Paper link, *see* Website: http://www.bloodjournal.org/. *Blood* 102(2), 756–762.
8. Weiden, P. L., Storb, R., Tsoi, M. S., Graham, T. C., Lerner, K. G., and Thomas, E. D. (1976) Infusion of donor lymphocytes into stable canine radiation chimeras: implications for mechanism of transplantation tolerance. *J. Immunol.* **116,** 1212–1219.
9. Weiden, P. L., Sullivan, K. M., Flournoy, N., Storb, R., and Thomas, E. D. (1981) Antileukemic effect of chronic graft-versus-host disease: contribution to improved survival after allogeneic marrow transplantation. *New Engl. J. Med.* **304,** 1529–1533.
10. Weiden, P. L., Flournoy, N., Thomas, E. D., et al. (1979) Antileukemic effect of graft-versus-host disease in human recipients of allogeneic-marrow grafts. *New Engl. J. Med.* **300,** 1068–1073.

11. Sullivan, K. M., Weiden, P. L., Storb, R., et al. (1989) Influence of acute and chronic graft-versus-host disease on relapse and survival after bone marrow transplantation from HLA-identical siblings as treatment of acute and chronic leukemia. *Blood* **73,** 1720–1728.

12. Odom, L. F., August, C. S., Githens, J. H., et al. (1978) Remission of relapsed leukaemia during a graft-versus-host reaction. A "graft-versus-leukaemia reaction" in man? *Lancet* **2,** 537–540.

13. Collins, R. H., Jr., Rogers, Z. R., Bennett, M., Kumar, V., Nikein, A., and Fay, J. W. (1992) Hematologic relapse of chronic myelogenous leukemia following allogeneic bone marrow transplantation: apparent graft-versus-leukemia effect following abrupt discontinuation of immunosuppression. *Bone Marrow Transplant.* **10,** 391–395.

14. Higano, C. S., Brixey, M., Bryant, E. M., et al. (1990) Durable complete remission of acute nonlymphocytic leukemia associated with discontinuation of immunosuppression following relapse after allogeneic bone marrow transplantation. A case report of a probable graft-versus-leukemia effect. *Transplantation* **50,** 175–177.

15. Fefer, A., Sullivan, K. M., Weiden, P., et al. (1987) Graft versus leukemia effect in man: the relapse rate of acute leukemia is lower after allogeneic than after syngeneic marrow transplantation. *Prog. Clin. Biol. Res.* **244,** 401–408.

16. Gale, R. P., Horowitz, M. M., Ash, R. C., et al. (1994) Identical-twin bone marrow transplants for leukemia. *Ann. Intern. Med.* **120,** 646–652.

17. Horowitz, M. M., Gale, R. P., Sondel, P. M., et al. (1990) Graft-versus-leukemia reactions after bone marrow transplantation. *Blood* **75,** 555–562.

18. Apperley, J. F., Mauro, F. R., Goldman, J. M., et al. (1988) Bone marrow transplantation for chronic myeloid leukaemia in first chronic phase: importance of a graft-versus-leukaemia effect.[erratum; *Br. J. Haematol.* **70(2),** 261]. *Br. J. Haematol.* **69,** 239–245.

19. Marmont, A. M., Horowitz, M. M., Gale, R. P., et al. (1991) T-cell depletion of HLA-identical transplants in leukemia. *Blood* **78,** 2120–2130.

20. Kolb, H. J., Mittermuller, J., Clemm, C., et al. (1990) Donor leukocyte transfusions for treatment of recurrent chronic myelogenous leukemia in marrow transplant patients. *Blood* **76,** 2462–2465.

21. Barnes, D. W. H., Corp, M. J., Loutit, J. F., and Neal, F. E. (1956) Treatment of murine leukaemia with X-rays and homologous bone marrow. Preliminary communication. *Br. Med. J.* **2,** 626–627.

22. Kolb, H. J., Schattenberg, A., Goldman, J. M., et al. (1995) Graft-versus-leukemia effect of donor lymphocyte transfusions in marrow grafted patients. European Group for Blood and Marrow Transplantation Working Party Chronic Leukemia. *Blood* **86,** 2041–2050.

23. Guglielmi, C., Arcese, W., Dazzi, F., et al. (2002) Donor lymphocyte infusion for relapsed chronic myelogenous leukemia: prognostic relevance of the initial cell dose. *Blood* **100,** 397–405.

24. Raiola, A. M., Van Lint, M. T., Valbonesi, M., et al. (2003) Factors predicting response and graft-versus-host disease after donor lymphocyte infusions: a study on 593 infusions. *Bone Marrow Transplant.* **31,** 687–693.

25. Shiobara, S., Nakao, S., Ueda, M., et al. (2001) Donor leukocyte infusion for Japanese patients with relapsed leukemia after allogeneic bone marrow transplantation: indications and dose escalation. *Ther. Apheresis* **5,** 40–45.

26. Collins, R. H., Jr., Shpilberg, O., Drobyski, W. R., et al. (1997) Donor leukocyte infusions in 140 patients with relapsed malignancy after allogeneic bone marrow transplantation. *J. Clin. Oncol.* **15,** 433–444.

27. Marks, D. I., Lush, R., Cavenagh, J., et al. (2002) The toxicity and efficacy of donor lymphocyte infusions given after reduced-intensity conditioning allogeneic stem cell transplantation. *Blood* **100,** 3108–3114.

28. de Lima, M., Bonamino, M., Vasconcelos, Z., et al. (2001) Prophylactic donor lymphocyte infusions after moderately ablative chemotherapy and stem cell transplantation for hematological malignancies: high remission rate among poor prognosis patients at the expense of graft-versus-host disease. *Bone Marrow Transplant.* **27,** 73–78.

29. Porter, D. L., Collins, R. H., Jr., Hardy, C., et al. (2000) Treatment of relapsed leukemia after unrelated donor marrow transplantation with unrelated donor leukocyte infusions. *Blood* **95,** 1214–1221.

30. Lokhorst, H. M., Schattenberg, A., Cornelissen, J. J., et al. (2000) Donor lymphocyte infusions for relapsed multiple myeloma after allogeneic stem-cell transplantation: predictive factors for response and long-term outcome. *J. Clin. Oncol.* **18,** 3031–3037.

31. Dazzi, F., Szydlo, R. M., Craddock, C., et al. (2000) Comparison of single-dose and escalating-dose regimens of donor lymphocyte infusion for relapse after allografting for chronic myeloid leukemia. *Blood* **95,** 67–71.

32. Dazzi, F., Szydlo, R. M., Cross, N. C., et al. (2000) Durability of responses following donor lymphocyte infusions for patients who relapse after allogeneic stem cell transplantation for chronic myeloid leukemia. *Blood* **96,** 2712–2716.

33. Or, R., Shapira, M. Y., Resnick, I., et al. (2003) Nonmyeloablative allogeneic stem cell transplantation for the treatment of chronic myeloid leukemia in first chronic phase. *Blood* **101,** 441–445.

34. Au, W. Y., Lie, A. K., Lee, C. K., Liang, R., and Kwong, Y. L.. (1999) Donor lymphocyte infusion induced molecular remission in relapse of acute myeloid leukaemia after allogeneic bone marrow transplantation. *Bone Marrow Transplant.* **23,** 1201–1203.

35. Lee, J. H., Lee, K. H., Kim, S., et al. (2001) Combination chemotherapy of intermediate-dose cytarabine, idarubicin, plus etoposide and subsequent mobilized donor leukocyte infusion for relapsed acute leukemia after allogeneic bone marrow transplantation. *Leukemia Res.* **25,** 305–312.

36. Zikos, P., Van Lint, M. T., Lamparelli, T., et al. (1998) Allogeneic hemopoietic stem cell transplantation for patients with high risk acute lymphoblastic leukemia: favorable impact of chronic graft-versus-host disease on survival and relapse. *Haematologica* **83,** 896–903.

37. Appelbaum, F. R. (1997) Graft versus leukemia (GVL) in the therapy of acute lymphoblastic leukemia (ALL). [Review] *Leukemia* **11(Suppl 4),** S15–17.

38. Passweg, J. R., Tiberghien, P., Cahn, J. Y., et al. (1998) Graft-versus-leukemia effects in T lineage and B lineage acute lymphoblastic leukemia. *Bone Marrow Transplant.* **21,** 153–158.

39. Collins, R. H., Jr., Goldstein, S., Giralt, S., et al. (2000) Donor leukocyte infusions in acute lymphocytic leukemia. *Bone Marrow Transplant.* **26,** 511–516.

40. Zomas, A., Stefanoudaki, K., Fisfis, M., Papadaki, T., and Mehta, J.. (1998) Graft-versus-myeloma after donor leukocyte infusion: maintenance of marrow remission but extramedullary relapse with plasmacytomas. *Bone Marrow Transplant.* **21,** 1163–1165.

41. Tricot, G, Vesole, DH, Jagannath, S, Hilton, J, Munshi, N, and Barlogie, B. (1996) Graft-versus-myeloma effect: proof of principle. *Blood* **87,** 1196–1198.

42. Alyea, E., Weller, E., Schlossman, R., et al. (2001) T-cell-depleted allogeneic bone marrow transplantation followed by donor lymphocyte infusion in patients with multiple myeloma: induction of graft-versus-myeloma effect. *Blood* **98,** 934–939.

43. Verdonck, L. F., Lokhorst, H. M., Dekker, A. W., Nieuwenhuis, H. K., and Petersen, E. J. (1996) Graft-versus-myeloma effect in two cases. *Lancet* **347,** 800–801.

44. Bertz, H., Burger, J. A., Kunzmann, R., Mertelsmann, R., and Finke, J. (1997) Adoptive immunotherapy for relapsed multiple myeloma after allogeneic bone marrow transplantation (BMT): evidence for a graft-versus-myeloma effect. *Leukemia* **11,** 281–283.

45. Mehta, J., Powles, R., Singhal, S., Iveson, T., Treleaven, J., and Catovsky, D. (1996) Clinical and hematologic response of chronic lymphocytic and prolymphocytic leukemia persisting after allogeneic bone marrow transplantation with the onset of acute graft-versus-host disease: possible role of graft-versus-leukemia. *Bone Marrow Transplant.* **17,** 371–375.

46. Rondon, G., Giralt, S., Huh, Y., et al. (1996) Graft-versus-leukemia effect after allogeneic bone marrow transplantation for chronic lymphocytic leukemia. *Bone Marrow Transplant.* **18,** 669–672.

47. Dreger, P. and Montserrat, E. (2002) Autologous and allogeneic stem cell transplantation for chronic lymphocytic leukemia. [Review]. *Leukemia* **16,** 985–992.

48. Sohn, S. K., Baek, J. H., Kim, D. H., et al. (2000) Successful allogeneic stem-cell transplantation with prophylactic stepwise G-CSF primed-DLIs for relapse after autologous transplantation in mantle cell lymphoma: a case report and literature review on the evidence of GVL effects in MCL. [Review]. *Am. J. Hematol.* **65,** 75–80.

49. Khouri, I. F., Keating, M., Korbling, M., et al. (1998) Transplant-lite: induction of graft-versus-malignancy using fludarabine-based nonablative chemotherapy and allogeneic blood progenitor-cell transplantation as treatment for lymphoid malignancies. *J. Clin. Oncol.* **16,** 2817–2824.

50. Khouri, I. F., Saliba, R. M., Giralt, S. A., et al. (2001) Nonablative allogeneic hematopoietic transplantation as adoptive immunotherapy for indolent lymphoma: low incidence of toxicity, acute graft-versus-host disease, and treatment-related mortality. *Blood* **98,** 3595–3599.

51. Branson, K., Chopra, R., Kottaridis, P. D., et al. (2002) Role of nonmyeloablative allogeneic stem-cell transplantation after failure of autologous transplantation in patients with lymphoproliferative malignancies. *J. Clin. Oncol.* **20,** 4022–4031.

52. Milpied, N., Fielding, A. K., Pearce, R. M., Ernst, P., and Goldstone, A. H. (1996) Allogeneic bone marrow transplant is not better than autologous transplant for patients with relapsed Hodgkin's disease. European Group for Blood and Bone Marrow Transplantation. *J. Clin. Oncol.* **14,** 1291–1296.

53. Akpek, G., Ambinder, R. F., Piantadosi, S., et al. (2001) Long-term results of blood and marrow transplantation for Hodgkin's lymphoma. *J. Clin. Oncol.* **19,** 4314–4321.

54. Carella, A. M., Cavaliere, M., Lerma, E., et al. (2000) Autografting followed by nonmyeloablative immunosuppressive chemotherapy and allogeneic peripheral-blood hematopoietic stem-cell transplantation as treatment of resistant Hodgkin's disease and non-Hodgkin's lymphoma. *J. Clin. Oncol.* **18,** 3918–3924.

55. Porter, D. L., Stadtmauer, E. A., and Lazarus, H. M. (2003) 'GVHD': graft-versus-host disease or graft-versus-Hodgkin's disease? an old acronym with new meaning. *Bone Marrow Transplant.* **31,** 739–746.

56. Eibl, B., Schwaighofer, H., Nachbaur, D., et al. (1996) Evidence for a graft-versus-tumor effect in a patient treated with marrow ablative chemotherapy and allogeneic bone marrow transplantation for breast cancer. *Blood* **88,** 1501–1508.

57. Childs, R., Chernoff, A., Contentin, N., et al. (2000) Regression of metastatic renal-cell carcinoma after nonmyeloablative allogeneic peripheral-blood stem-cell transplantation. *New Engl. J. Med.* **343,** 750–758.

58. Rini, B. I., Zimmerman, T., Stadler, W. M., Gajewski, T. F., and Vogelzang, N. J. (2002) Allogeneic stem-cell transplantation of renal cell cancer after nonmyeloablative chemo-

therapy: feasibility, engraftment, and clinical results.[comment]. *J. Clin. Oncol.* **20,** 2017–2024.

59. Bregni, M., Dodero, A., Peccatori, J., et al. (2002) Nonmyeloablative conditioning followed by hematopoietic cell allografting and donor lymphocyte infusions for patients with metastatic renal and breast cancer. *Blood* **99,** 4234–4236.

60. Bay, J. O., Fleury, J., Choufi, B., et al. (2002) Allogeneic hematopoietic stem cell transplantation in ovarian carcinoma: results of five patients. *Bone Marrow Transplant.* **30,** 95–102.

61. Peccatori, J. Ciceri, F., Bernardi, M., et al. (2002) Evidence of allogeneic graft-versus-tumor effect in prostate and ovarian cancer. *Haematologica* **87(Suppl 1),** 12–14.

62. Zetterquist, H., Hentschke, P., Thorne, A., et al. (2001) A graft-versus-colonic cancer effect of allogeneic stem cell transplantation. *Bone Marrow Transplant.* **28,** 1161–1166.

63. Moscardo, F., Martinez, J. A., Sanz, G. F., et al. (2000) Graft-versus-tumour effect in non-small-cell lung cancer after allogeneic peripheral blood stem cell transplantation. *Br. J. Haematol.* **111,** 708–710.

64. Pedrazzoli, P., Da Prada, G. A., Giorgiani, G., et al. (2002) Allogeneic blood stem cell transplantation after a reduced-intensity, preparative regimen: a pilot study in patients with refractory malignancies. *Cancer* **94,** 2409–2415.

65. Morecki, S., Moshel, Y., Gelfend, Y., Pugatsch, T., and Slavin, S. (1997) Induction of graft vs. tumor effect in a murine model of mammary adenocarcinoma. *Int. J. Cancer* **71,** 59–63.

66. Morecki, S., Yacovlev, E., Diab, A., and Slavin, S. (1998) Allogeneic cell therapy for a murine mammary carcinoma. Cancer Research. **58,** 3891–3895.

67. Childs, R. W., Bradstock, K. F., Gottlieb, D., Kefford, R., and Barrett, J. (2000) Non-myeloablative allogeneic stem cell transplantation as immunotherapy for metastatic melanoma: results of a pilot study. *Blood* **96(Part 2),** 353b. .

68. Foster, A. E., Gottlieb, D. J., Marangolo, M., et al. (2003) Rapid, large-scale generation of highly pure cytomegalovirus-specific cytotoxic T cells for adoptive immunotherapy. *J. Hematother. Stem Cell Res.* **12,** 93–105.

69. Walter, E. A., Greenberg, P. D., Gilbert, M. J., et al. (1995) Reconstitution of cellular immunity against cytomegalovirus in recipients of allogeneic bone marrow by transfer of T-cell clones from the donor. *New Engl. J. Med.* **333,** 1038–1044.

70. Riddell, S. R., Watanabe, K. S., Goodrich, J. M., Li, C. R., Agha, M. E., and Greenberg, P. D. (1992) Restoration of viral immunity in immunodeficient humans by the adoptive transfer of T cell clones. *Science* **257,** 238–241.

71. Gottschalk, S., Edwards, O. L., Sili, U., et al. (2003) Generating CTLs against the subdominant Epstein-Barr virus LMP1 antigen for the adoptive immunotherapy of EBV-associated malignancies. *Blood* **101,** 1905–1912.

72. Hamel, Y., Blake, N., Gabrielsson, S., et al. (2002) Adenovirally transduced dendritic cells induce bispecific cytotoxic T lymphocyte responses against adenovirus and cytomegalovirus pp65 or against adenovirus and Epstein-Barr virus EBNA3C protein: a novel approach for immunotherapy. *Hum. Gene Ther.* **13,** 855–866.

73. Regn, S., Raffegerst, S., Chen, X., Schendel, D., Kolb, H. J., and Roskrow, M.. (2001) Ex vivo generation of cytotoxic T lymphocytes specific for one or two distinct viruses for the prophylaxis of patients receiving an allogeneic bone marrow transplant. *Bone Marrow Transplant.* **27,** 53–64.

74. Hromas, R., Cornetta, K., Srour, E., Blanke, C., and Broun, E. R. (1994) Donor leukocyte infusion as therapy of life-threatening adenoviral infections after T-cell-depleted bone marrow transplantation. *Blood* **84,** 1689–1690.

75. Rooney, C. M., Smith, C. A., Ng, C. Y., et al. (1998) Infusion of cytotoxic T cells for the prevention and treatment of Epstein-Barr virus-induced lymphoma in allogeneic transplant recipients. *Blood* **92,** 1549–1555.

76. Emanuel, D. J., Lucas, K. G., Mallory, G. B., Jr., et al. (1997) Treatment of posttransplant lymphoproliferative disease in the central nervous system of a lung transplant recipient using allogeneic leukocytes. *Transplantation* **63,** 1691–1694.

77. Comoli, P., Labirio, M., Basso, S., et al. (2002) Infusion of autologous Epstein-Barr virus (EBV)-specific cytotoxic T cells for prevention of EBV-related lymphoproliferative disorder in solid organ transplant recipients with evidence of active virus replication. *Blood* **99,** 2592–2598.

78. Haque, T., Taylor, C., Wilkie, G. M., et al. (2001) Complete regression of posttransplant lymphoproliferative disease using partially HLA-matched Epstein Barr virus-specific cytotoxic T cells. *Transplantation* **72,** 1399–1402.

79. Restrepo, A., Albrecht, F., Raez, L. E., et al. (1999) Post-liver transplantation lymphoproliferative disorders with and without infusions of donor bone marrow cells. [Review] *Crit. Rev. Oncogen.* **10,** 239–245.

80. Truitt, R. L., Johnson, B. D., McCabe, C., and Weiler, M. B. (1997) Graft versus leukemia. In: *Graft- vs-Host Disease.* Ferrara, J. L. M, Deeg, H. J., and Burakoff, S. J., eds. Marcel Dekker, New York, NY, p. 385.

81. Malkovska, V., Cigel, F., and Storer, B. E. (1994) Human T cells in hu-PBL-SCID mice proliferate in response to Daudi lymphoma and confer anti-tumour immunity. *Clin. Exp. Immunol.* **96,** 158–165.

82. van Lochem, E., de Gast, B., and Goulmy, E. (1992) In vitro separation of host specific graft-versus-host and graft-versus-leukemia cytotoxic T cell activities. *Bone Marrow Transplant.* **10,** 181–183.

83. Sosman, J. A., Oettel, K. R., Smith, S. D., Hank, J. A., Fisch, P., and Sondel, P. M. (1990) Specific recognition of human leukemic cells by allogeneic T cells: II. Evidence for HLA-D restricted determinants on leukemic cells that are crossreactive with determinants present on unrelated nonleukemic cells. *Blood* **75,** 2005–2016.

84. Kondo, Y., Shiobara, S., and Nakao, S. (2001) Identification of T-cell clones showing expansion associated with graft-vs-leukemia effect on chronic myelogenous leukemia in vivo and in vitro. *Exp. Hematol.* **29,** 471–476.

85. Jiang, Y. Z., Kanfer, E. J., Macdonald, D., Cullis, J. O., Goldman, J. M., and Barrett, A. J. (1991) Graft-versus-leukaemia following allogeneic bone marrow transplantation: emergence of cytotoxic T lymphocytes reacting to host leukaemia cells. *Bone Marrow Transplant.* **8,** 253–258.

86. Korngold, R., and Sprent, J. (1987) T cell subsets and graft-versus-host disease. *Transplantation* **44,** 335–339.

87. Giralt, S., Hester, J., Huh, Y., et al. (1995) CD8-depleted donor lymphocyte infusion as treatment for relapsed chronic myelogenous leukemia after allogeneic bone marrow transplantation. *Blood* **86,** 4337–4343.

88. Nimer, S. D., Giorgi, J., Gajewski, J. L., et al. (1994) Selective depletion of CD8+ cells for prevention of graft-versus-host disease after bone marrow transplantation. A randomized controlled trial. *Transplantation* **57,** 82–87.

89. Alyea, E. P., Soiffer, R. J., Canning, C., et al. (1998) Toxicity and efficacy of defined doses of CD4(+) donor lymphocytes for treatment of relapse after allogeneic bone marrow transplant. *Blood* **91,** 3671–3680.

90. Claret, E. J., Alyea, E. P., Orsini, E., et al. (1997) Characterization of T cell repertoire in patients with graft-versus-leukemia after donor lymphocyte infusion. *J. Clin. Invest.* **100,** 855–866.

91 Faber, L. M., van Luxemburg-Heijs, S. A., Veenhof, W. F., Willemze, R., and Falkenburg, J. H. (1995) Generation of CD4+ cytotoxic T-lymphocyte clones from a patient with severe graft-versus-host disease after allogeneic bone marrow transplantation: implications for graft-versus-leukemia reactivity. *Blood* **86,** 2821–2828.

92 Jiang, Y. Z., and Barrett, A. J. (1995) Cellular and cytokine-mediated effects of CD4-positive lymphocyte lines generated in vitro against chronic myelogenous leukemia. *Exp. Hematol.* **23,** 1167–1172.

93 Truitt, R. L., and Johnson, B. D. (1995) Principles of graft-vs.-leukemia reactivity. [Review] *Biol. Blood Marrow Transplant.* **1,** 61–68.

94 Palathumpat, V., Dejbakhsh-Jones, S., and Strober, S. (1995) The role of purified CD8+ T cells in graft-versus-leukemia activity and engraftment after allogeneic bone marrow transplantation. *Transplantation* **60,** 355–361.

95 Barrett, A. J. (1997) Mechanisms of the graft-versus-leukemia reaction. [Review] *Stem Cells* **15,** 248–258.

96 Eisendle, K., Lang, A., Eibl, B., et al. (2003) Phenotypic and functional deficiencies of leukaemic dendritic cells from patients with chronic myeloid leukaemia. *Br. J. Haematol.* **120,** 63–73.

97 Eibl, B., Ebner, S., Duba, C., et al. (1997) Dendritic cells generated from blood precursors of chronic myelogenous leukemia patients carry the Philadelphia translocation and can induce a CML-specific primary cytotoxic T-cell response. *Genes Chromosomes Cancer* **20,** 215–223.

98 Dietz, A. B., Litzow, M. R., Bulur, P. A., and Vuk-Pavlovic, S.. (2001) Transgenic interleukin 2 secreted by CML dendritic cells stimulates autologous T(H)1 T cells. *Cytotherapy* **3,** 97–105.

99 Trinchieri, G. (1989) Biology of natural killer cells. [Review] *Adv. Immunol.* **47,** 187–376.

100 Hercend, T., Takvorian, T., Nowill, A., et al. (1986) Characterization of natural killer cells with antileukemia activity following allogeneic bone marrow transplantation. *Blood* **67,** 722–728.

101 Kruit, W. H., Goey, S. H., Lamers, C. H., et al. (1997) High-dose regimen of interleukin-2 and interferon-alpha in combination with lymphokine-activated killer cells in patients with metastatic renal cell cancer. *J. Immunother.* **20,** 312–320.

102 Law, T. M., Motzer, R. J., Mazumdar, M., et al. (1995) Phase III randomized trial of interleukin-2 with or without lymphokine-activated killer cells in the treatment of patients with advanced renal cell carcinoma. *Cancer* **76,** 824–832.

103 Okuno, K., Takagi, H., Nakamura, T., Nakamura, Y., Iwasa, Z., and Yasutomi, M. (1986) Treatment for unresectable hepatoma via selective hepatic arterial infusion of lymphokine-activated killer cells generated from autologous spleen cells. *Cancer* **58,** 1001–1006.

104 Kimura, H. and Yamaguchi, Y. (1995) Adjuvant immunotherapy with interleukin 2 and lymphokine-activated killer cells after noncurative resection of primary lung cancer. *Lung Cancer* **13,** 31–44.

105 Lim, S. H., Newland, A. C., Kelsey, S., et al. (1992) Continuous intravenous infusion of high-dose recombinant interleukin-2 for acute myeloid leukaemia—a phase II study. *Cancer Immunol. Immunother.* **34,** 337–342.

106 Meropol, N. J., Barresi, G. M., Fehniger, T. A., Hitt, J., Franklin, M., and Caligiuri, M. A. (1998) Evaluation of natural killer cell expansion and activation in vivo with daily subcutaneous low-dose interleukin-2 plus periodic intermediate-dose pulsing. *Cancer Immunol. Immunother.* **46,** 318–326.

107 Farag, S. S., Fehniger, T. A., Ruggeri, L., Velardi, A., and Caligiuri, M. A. (2002) Natural killer cell receptors: new biology and insights into the graft-versus-leukemia effect. [Review] *Blood* **100,** 1935–1947.

108 Ruggeri, L., Capanni, M., Casucci, M., et al. (1999) Role of natural killer cell alloreactivity in HLA-mismatched hematopoietic stem cell transplantation. *Blood* **94,** 333–339.

109 Zeis, M., Uharek, L., Glass, B., et al. (1997) Allogeneic MHC-mismatched activated natural killer cells administered after bone marrow transplantation provide a strong graft-versus-leukaemia effect in mice. *Br. J. Haematol.* **96,** 757–761.

110 Glass, B., Uharek, L., Zeis, M., Loeffler, H., Mueller-Ruchholtz, W., and Gassmann, W. (1996) Graft-versus-leukaemia activity can be predicted by natural cytotoxicity against leukaemia cells. *Br. J. Haematol.* **93,** 412–420.

111 Ruggeri, L., Capanni, M., Martelli, M. F., and Velardi, A. (2001) Cellular therapy: exploiting NK cell alloreactivity in transplantation. [Review] *Curr. Opin. Hematol.* **8,** 355–359.

112 Jiang, Y. Z., Barrett, A. J., Goldman, J. M., and Mavroudis, D. A. (1997) Association of natural killer cell immune recovery with a graft-versus-leukemia effect independent of graft-versus-host disease following allogeneic bone marrow transplantation. *Ann. Hematol.* **74,** 1–6.

113 Jiang, Y. Z., Cullis, J. O., Kanfer, E. J., Goldman, J. M., and Barrett, A. J. (1993) T cell and NK cell mediated graft-versus-leukaemia reactivity following donor buffy coat transfusion to treat relapse after marrow transplantation for chronic myeloid leukaemia. *Bone Marrow Transplant.* **11,** 133–138.

114 Aversa, F., Tabilio, A., Velardi, A., et al. (1998) Treatment of high-risk acute leukemia with T-cell-depleted stem cells from related donors with one fully mismatched HLA haplotype. *New Engl. J. Med.* **339,** 1186–1193.

115 Ruggeri, L., Capanni, M., Urbani, E., et al. (2002) Effectiveness of donor natural killer cell alloreactivity in mismatched hematopoietic transplants. *Science* **295,** 2097–2100.

116 Falkenburg, J. H., Marijt, W. A., Heemskerk, M. H., and Willemze, R. (2002) Minor histocompatibility antigens as targets of graft-versus-leukemia reactions. *Curr. Opin. Hematol.* **9,** 497–502.

117 Riddell, S. R., Murata, M., Bryant, S., and Warren, E. H. (2002) Minor histocompatibility antigens—targets of graft versus leukemia responses. *Intl. J. Hematol.* **2,** 155–161.

118 Goulmy, E. (1997) Human minor histocompatibility antigens: new concepts for marrow transplantation and adoptive immunotherapy. [Review] *Immun. Revs.* **157,** 125–140.

119 Wang, W., Meadows, L. R., den Haan, J. M., et al. (1995) Human H-Y: a male-specific histocompatibility antigen derived from the SMCY protein. *Science* **269,** 1588–1590.

120 Warren, E. H., Gavin, M. A., Simpson, E., et al. (2000) The human UTY gene encodes a novel HLA-B8-restricted H-Y antigen. *J. Immunol.* **164,** 2807–2814.

121 Vogt, M. H., van den Muijsenberg, J. W., Goulmy, E., et al. (2002) The DBY gene codes for an HLA-DQ5-restricted human male-specific minor histocompatibility antigen involved in graft-versus-host disease. *Blood* **99,** 3027–3032.

122 Vogt, M. H., Goulmy, E., Kloosterboer, F. M., et al. (2000) UTY gene codes for an HLA-B60-restricted human male-specific minor histocompatibility antigen involved in stem cell graft rejection: characterization of the critical polymorphic amino acid residues for T-cell recognition. *Blood* **96,** 3126–3132.

123 Vogt, M. H., de Paus, R. A., Voogt, P. J., Willemze, R., and Falkenburg, J. H. (2000) DFFRY codes for a new human male-specific minor transplantation antigen involved in bone marrow graft rejection. *Blood* **95,** 1100–1105.

124 Brickner, A. G., Warren, E. H., Caldwell, J. A., et al. (2001) The immunogenicity of a new human minor histocompatibility antigen results from differential antigen processing. *J. Exp. Med.* **193,** 195–206.

125 Pierce, R. A., Field, E. D., Mutis, T., et al. (2001) The HA-2 minor histocompatibility antigen is derived from a diallelic gene encoding a novel human class I myosin protein. *J. Immunol.* **167,** 3223–3230.

126 de Bueger, M., Bakker, A., Van Rood, J. J., Van der Woude, F., and Goulmy, E. (1992) Tissue distribution of human minor histocompatibility antigens. Ubiquitous versus restricted tissue distribution indicates heterogeneity among human cytotoxic T lymphocyte-defined non-MHC antigens. *J. Immunol.* **149,** 1788–1794.

127 Warren, E. H., Gavin, M., Greenberg, P. D., and Riddell, S. R. (1998) Minor histocompatibility antigens as targets for T-cell therapy after bone marrow transplantation. [Review] *Curr. Opin. Hematol.* **5,** 429–433.

128 Pardoll, D. M. (2002) Spinning molecular immunology into successful immunotherapy. [Review] *Nat. Rev. Immunol.* **2,** 227–238.

129 Clark, S. S., McLaughlin, J., Crist, W. M., Champlin, R., and Witte, O. N. (1987) Unique forms of the abl tyrosine kinase distinguish Ph1-positive CML from Ph1-positive ALL. *Science* **235,** 85–88.

130 Kurzrock, R., Blick, M. B., Talpaz, M., et al. (1986) Rearrangement in the breakpoint cluster region and the clinical course in Philadelphia-negative chronic myelogenous leukemia. *Ann. Intern. Med.* **105,** 673–679.

131 Ben-Neriah, Y., Daley, G. Q., Mes-Masson, A. M., Witte, O. N., and Baltimore, D. (1986) The chronic myelogenous leukemia-specific P210 protein is the product of the bcr/abl hybrid gene. *Science* **233,** 212–214.

132 Heisterkamp, N., Stam, K., Groffen, J., de Klein, A., and Grosveld, G. (1985) Structural organization of the bcr gene and its role in the Ph' translocation. *Nature* **315,** 758–761.

133 Fossum, B., Gedde-Dahl, T., 3rd, Breivik, J., et al. (1994) p21-ras-peptide-specific T-cell responses in a patient with colorectal cancer. CD4+ and CD8+ T cells recognize a peptide corresponding to a common mutation (13Gly→Asp). *Int. J. Cancer* **56,** 40–45.

134 Yotnda, P., Garcia, F., Peuchmaur, M., et al. (1998) Cytotoxic T cell response against the chimeric ETV6-AML1 protein in childhood acute lymphoblastic leukemia. *J. Clin. Invest.* **102,** 455–462.

135 Ohminami, H., Yasukawa, M., Kaneko, S., et al. (1999) Fas-independent and nonapoptotic cytotoxicity mediated by a human CD4(+) T-cell clone directed against an acute myelogenous leukemia-associated DEK-CAN fusion peptide. *Blood* **93,** 925–935.

136 Boer, J., Mahmoud, H., Raimondi, S., Grosveld, G., and Krance, R. (1997) Loss of the DEK-CAN fusion transcript in a child with t(6;9) acute myeloid leukemia following chemotherapy and allogeneic bone marrow transplantation. *Leukemia* **11,** 299–300.

137 Fornerod, M., Boer, J., van Baal, S., Morreau, H., and Grosveld, G. (1996) Interaction of cellular proteins with the leukemia specific fusion proteins DEK-CAN and SET-CAN and their normal counterpart, the nucleoporin CAN. *Oncogene* **13,** 1801–1808.

138. von Lindern, M., Fornerod, M., Soekarman, N., et al. (1992) Translocation t(6;9) in acute non-lymphocytic leukaemia results in the formation of a DEK-CAN fusion gene. [Review] [74 refs]. *Baillieres Clin. Haematol.* **5,** 857–879.

139 de The, H., Lavau, C., Marchio, A., Chomienne, C., Degos, L., and Dejean, A. (1991) The PML-RAR alpha fusion mRNA generated by the t(15;17) translocation in acute promyelocytic leukemia encodes a functionally altered RAR. *Cell* **66,** 675–684.

140 Kakizuka, A., Miller, W. H., Jr., Umesono, K., et al. (1991) Chromosomal translocation t(15;17) in human acute promyelocytic leukemia fuses RAR alpha with a novel putative transcription factor, PML. *Cell* **66,** 663–674.

141 Molldrem, J. J., Lee, P. P., Wang, C., et al. (2000) Evidence that specific T lymphocytes may participate in the elimination of chronic myelogenous leukemia. *Nat. Med.* **6,** 1018–1023.

142 Molldrem, J. J., Clave, E., Jiang, Y. Z., et al. (1997) Cytotoxic T lymphocytes specific for a nonpolymorphic proteinase 3 peptide preferentially inhibit chronic myeloid leukemia colony-forming units. *Blood* **90,** 2529–2534.

143 Molldrem, J., Dermime, S., Parker, K., et al. (1996) Targeted T-cell therapy for human leukemia: cytotoxic T lymphocytes specific for a peptide derived from proteinase 3 preferentially lyse human myeloid leukemia cells. *Blood* **88,** 2450–2457.

144 Clave, E., Molldrem, J., Hensel, N., Raptis, A., and Barrett, A. J. (1999) Donor-recipient polymorphism of the proteinase 3 gene: a potential target for T-cell alloresponses to myeloid leukemia. *J. Immunother.* **22,** 1–6.

145 Boon, T. and Old, L. J. (1997) Cancer tumor antigens. *Curr. Opin. Immunol.* **9,** 681–683.

146 Robbins, P. F. and Kawakami, Y. (1996) Human tumor antigens recognized by T cells. [Review] *Curr. Opin. Immunol.* **8,** 628–636.

147 Ohminami, H., Yasukawa, M., and Fujita, S. (2000) HLA class I-restricted lysis of leukemia cells by a CD8(+) cytotoxic T-lymphocyte clone specific for WT1 peptide. *Blood* **95,** 286–293.

148 Oka, Y., Elisseeva, O. A., Tsuboi, A., et al. (2000) Human cytotoxic T-lymphocyte responses specific for peptides of the wild-type Wilms' tumor gene (WT1) product. *Immunogenetics* **51,** 99–107.

149 Reddy, P., Teshima, T., Hildebrandt, G., et al. (2002) Interleukin 18 preserves a perforin-dependent graft-versus-leukemia effect after allogeneic bone marrow transplantation. *Blood* **100,** 3429–3431.

150 Brahmi, Z., Hommel-Berrey, G., Smith, F., and Thomson, B. (2001) NK cells recover early and mediate cytotoxicity via perforin/granzyme and Fas/FasL pathways in umbilical cord blood recipients. *Hum. Immunol.* **62,** 782–790.

151 Susskind, B., Shornick, M. D., Iannotti, M. R., et al. (1996) Cytolytic effector mechanisms of human CD4+ cytotoxic T lymphocytes. *Hum. Immunol.* **45,** 64–75.

152 Kunitomi, A., Hori, T., Maeda, M., and Uchiyama, T. (2002) OX40 signaling renders adult T-cell leukemia cells resistant to Fas-induced apoptosis. *Intl. J. Hematol.* **76,** 260–266.

153 Liu, J. H., Wei, S., Lamy, T., et al. (2002) Blockade of Fas-dependent apoptosis by soluble Fas in LGL leukemia. *Blood* **100,** 1449–1453.

154 Schmaltz, C., Alpdogan, O., Horndasch, K. J., et al. (2001) Differential use of Fas ligand and perforin cytotoxic pathways by donor T cells in graft-versus-host disease and graft-versus-leukemia effect. *Blood* **97,** 2886–2895.

155 Tanaka, Y., Takahashi, T., Nieda, M., et al. (2002) Generation of Fas-independent CD4+ cytotoxic T-cell clone specific for p190 minor bcr-abl fusion peptide. *Leukemia Res.* **26,** 317–321.

156 Schmaltz, C., Alpdogan, O., Muriglan, S. J., et al. (2003) Donor T cell-derived TNF is required for graft-versus-host disease and graft-versus-tumor activity after bone marrow transplantation. *Blood* **101,** 2440–2445.

157 Schmaltz, C., Alpdogan, O., Kappel, B. J., et al. (2002) T cells require TRAIL for optimal graft-versus-tumor activity. *Nat. Med.* **8,** 1433–1437.

158 Middleton, P. G., Taylor, P. R., Jackson, G., Proctor, S. J., and Dickinson, A. M. (1998) Cytokine gene polymorphisms associating with severe acute graft-versus-host disease in HLA-identical sibling transplants. *Blood* **92,** 3943–3948.

159 Nordlander, A., Uzunel, M., Mattsson, J., and Remberger, M. (2002) The TNFd4 allele is correlated to moderate-to-severe acute graft-versus-host disease after allogeneic stem cell transplantation. *Br. J. Haematol.* **119,** 1133–1136.

160 Dickinson, A. M., Cavet, J., Cullup, H., Wang, X. N., Sviland, L., and Middleton, P. G. (2001) GvHD risk assessment in hematopoietic stem cell transplantation: role of cytokine gene polymorphisms and an in vitro human skin explant model. *Hum. Immunol.* **62,** 1266–1276.

161 Cavet, J., Dickinson, A. M., Norden, J., Taylor, P. R., Jackson, G. H., and Middleton, P. G. (2001) Interferon-gamma and interleukin-6 gene polymorphisms associate with graft-versus-host disease in HLA-matched sibling bone marrow transplantation. *Blood* **98,** 1594–1600.

162 Warle, M. C., Farhan, A., Metselaar, H. J., et al. (2002) Cytokine gene polymorphisms and acute human liver graft rejection. *Liver Transplant.* **8,** 603–611.

163 Mazariegos, G. V., Reyes, J., Webber, S. A., et al. (2002) Cytokine gene polymorphisms in children successfully withdrawn from immunosuppression after liver transplantation. *Transplantation* **73,** 1342–1345.

164 Awad, M. R., Webber, S., Boyle, G., et al. (2001) The effect of cytokine gene polymorphisms on pediatric heart allograft outcome. *J. Heart Lung Transplant.* **20,** 625–630.

165. Poole, K. L., Gibbs, P. J., Evans, P. R., Sadek, S. A., and Howell, W. M. (2001) Influence of patient and donor cytokine genotypes on renal allograft rejection: evidence from a single centre study. *Transplant Immunol.* **8,** 259–265.

29

Influence of Radiation Protocols on Graft-vs-Host Disease Incidence After Bone-Marrow Transplantation in Experimental Models

Sebastian Schwarte and Matthias W. Hoffmann

Summary

Bone-marrow transplantation is an approved curative treatment for many hemato- and oncologic diseases. Nevertheless, the severe acute clinical course of graft-vs-host disease (GVHD) after allogeneic bone-marrow transplantation is frequently fatal, and is to date not curable. Acute GVHD must, therefore, be prevented from the start of the bone-marrow transplantation by immunosuppressive medication, causing sometimes serious side effects. Therefore, new preventive strategies are tested, starting with animal experiments. Often mice are chosen for this kind of trial, and the clinical protocol of bone-marrow transplantation is transferred into the experimental settings.

The first step to induce an acute GVHD is whole-body irradiation of the recipients. Several methods are available for this purpose: the most common is a ^{60}cobalt source (γ-irradiation); less common are a ^{137}cesium source (γ-irradiation) and a linear (particle) accelerator (photons). Differences between these radiation techniques can occur and can unexpectedly interfere with the results of the experiments. In this chapter, the materials and methods for bone-marrow transplantation in mice, with particular emphasis on the different radiation techniques, are explained; furthermore, the advantages and disadvantages in regard to the underlying physical principles will be discussed.

Key Words: Radiation; whole body irradiation; bone-marrow transplantation; cobalt; cesium; linear accelerator; particle accelerator; incidence; GVHD; GVHR; mice.

1. Introduction

Bone-marrow transplantation is an approved curative treatment for many hemato-oncologic diseases, such as immunodeficiency (SCID, Wiskott-Aldrich syndrome), acute leukemia, aplastic anemia, chronic leukemia, hemoglobinopathies (thalassemia major), myelodysplasia, enzymatic defects (Gaucher's disease), lymphoma, myeloma, and after whole-body irradiation of carcinomas with myelosuppressive side effects. Allogeneic bone-marrow transplantation is the treatment of choice for patients with lymphomas or leukemias. Despite significant improvements since the beginning

of the modern era of allogeneic bone-marrow transplantation, the side effects of this therapy can be tremendous and life-threatening. In particular, the disease caused by the immunological reaction of immunocompetent donor cells against the immuno-compromised host (graft-vs-host disease [GVHD]) is still a major problem. An acute and a chronic form of GVHD can be differentiated. The acute form of GVHD can be very dangerous and life-threatening and manifests mainly at the skin, the liver, and the gastrointestinal tract. The chronic form resembles an autoimmune disease, and severe complications are mainly caused by the immunosuppressive therapy.

The treatment of a patient with a severe acute clinical course of GVHD is frequently not successful. Acute GVHD must, therefore, be prevented by potent immunosuppressive drugs, with their inherent range of risks and side effects. Therefore, a main goal in bone-marrow transplantation is to specifically suppress the GVH reaction without impairing the physiological immune response to pathogens and residual leukemic cells. For this reason, it is of major importance to develop more specific therapeutic strategies in bone-marrow transplantation.

Mice are frequently used as experimental models to test new therapeutic approaches in the treatment of GVHD after allogeneic bone-marrow transplantation. They have the advantage that several genetically defined inbred, transgenic, and knock-out mouse strains are available. These can be used to examine GVHD pathophysiology and GVHD prevention in several informative combinations. In the following, a mouse model is presented that allows the study of GVHD under defined conditions.

The first step to induce acute GVHD is whole-body irradiation of the host. In the clinical setting, this serves three purposes: first, lethal irradiation destroys malignant cells underlying the leukemic disease. Second, irradiation destroys host lymphocytes and in turn prevents or ameliorates the rejection of the allogeneic bone-marrow inoculum. Third, irradiation is thought to create space in the bone marrow by destroying host bone-marrow cells, thereby improving the engraftment of the injected bone-marrow cells. Several methods are available to irradiate animals in an experimental setting: the most commonly used radiation source is [60]cobalt (γ-irradiation); less frequently used are [137]cesium (γ-irradiation) and the linear (particle) accelerator (photon irradiation).

After irradiation, bone-marrow cells are purified from the donor. In the clinical setting, multiple bone-marrow aspirates are harvested from the donor, whereas in animal models bone-marrow cells are obtained from the donor tibia and femur.

Finally, bone-marrow cells are injected intravenously. The outcome is followed by regularly checking the weight and inspection for signs of GVHD.

2. Materials

1. Phosphate buffered saline (PBS): 28.0 mM NaH$_2$PO$_4$, 7.2 mM Na$_2$HPO$_4$, and 0.14 M NaCl; 9.55 g/L bidistilled water; without calcium and magnesium; may be stored indefinitely without contamination at 4°C.
2. Anesthesia with ketamine (ketamine hydrochloride) and Rompun (xylazine hydrochloride): mixture of 0.5 mL ketamine hydrochloride and 0.5 mL xylazine hydrochloride, dissolved in 9 mL sterile PBS; light-sensitive; stable at room temperature for up to 1 mo. Ketamine (10%): 0.08 mL/100 g i.p. (80 mg/kg); Rompun (2%): 0.01 mL/100 g i.p. (2 mg/kg). Two-hundred fifty microliters per mouse.

3. Irradiation equipment: a ^{60}cobalt source, a linear accelerator, or a ^{137}cesium source.
4. Mouse cages made of plexiglas for irradiation.
5. Medium 199 (TC 199): Hank's salt solution with L-glutamine without NaHCO$_3$: 10.61 g/L bidist. water; stable at 4°C for 2 mo if kept sterile.
6. One liter hemolysis buffer: pH 7.3, 8.34 g NH$_4$Cl, 0.037 g EDTA, and 1.00 g NaHCO$_3$; stable at 4°C for up to 2 mo if kept sterile.
7. One hundred milliliters trypan blue: 8 mL of a 2% stock solution, dissolved in a 92-mL NaCl solution; store at 4°C indefinitely.
8. Surgical instruments (forceps, scissors).
9. Fifteen-milliliter plastic tubes.
10. Polystyrene cell-culture dishes (Petri dishes).
11. Sieve with 0.6-mm mesh size.
12. Sieve with 0.2-µm mesh size.
13. Fifty-milliliter polypropylene tube.
14. Counting chamber (Neubauer's hematocytometer).
15. BL/LB, 0.40 × 12 mm, 27 gage × 0.5 in. disposable injection needles.
16. BL/LB, 0.90 × 40 mm, 20 gage × 1.5 in. disposable injection needles.
17. Five-milliliter, 10-mL, and 20-mL disposable syringes.

3. Methods

Mice should be kept under clean, preferably "specific pathogen free" conditions. Following lethal irradiation and bone-marrow reconstitution, the mice are temporarily immunodeficient until the bone marrow has produced sufficient immunocompetent cells to protect the mice from infections.

The anesthetized recipients are lethally irradiated 24 h before the injection of donor cells. Donor animals are sacrificed about 6 h before the planned injection to allow for the collection of bone marrow and lymph-node cells (*see* **Note 1**), and to have sufficient time for cell processing.

Donors and recipients should be age and sex matched in order to avoid undesired immune responses to minor (H-Y) antigens that might affect the GVH reaction under study.

3.1. Irradiation of the Recipients

To prevent rejection of the allogeneic bone-marrow cells, the recipients are lethally irradiated by a single dose of whole-body irradiation. The recipient animals are contained in special cages during the irradiation.

3.1.1. Anesthesia

To achieve a homogenous radiation effect, the animals are kept still by general anesthesia. Therefore, the animals are anesthetized with 250 µL of the ketamine-Rompun mixture, applied intraperitoneally with a 27-gage needle. Anesthesia lasts for about 20 min and is sufficient for the duration of the irradiation procedure.

3.1.2. Cage Design

The size of the radiation cage must be large enough to accommodate the mice in one plane, side by side, to achieve a homogenous irradiation effect. The cage should contain air holes to provide sufficient ventilation. Usually, a cage contains a maxi-

mum of eight mice. A suitable radiation cage can measure 16 cm in length, 10 cm in width, and 2.5 cm in height. The lid of the cage should close directly above the animals with as little space between them and the lid as possible (*see* **Note 2**). A mouse cage for irradiation can be made of safety glass, plexiglas, or cardboard carton, and should be secured to prevent escape of the animals.

3.1.3. Irradiation Equipment

See **Note 3**. Irradiation with a ^{60}cobalt source is carried out at a distance of 75 cm between the device and the animals for a radiation dose of 9 Gy. A 0.5-cm thick plexiglas plate should be placed on top of the cage to achieve optimal tissue distribution.

3.2. Collection of Donor Cells

For the collection of bone-marrow and lymph-node cells the animals are sacrificed by cervical dislocation, following anesthesia with carbon dioxide. The level of anesthesia is checked by controlling for spontaneous movements, posture of the head, reflexes, spontaneous breathing, and heartbeat of the mouse.

3.2.1. Preparation of Lymph-Node Cells

1. Donor animals are fixed on their back and disinfected with 70% EtOH.
2. Then a transverse skin incision is made, starting 1 cm below the xiphoid process.
3. The skin is manually pulled upwards and downwards, exposing the abdomen and thorax up to the neck and front legs.
4. The submandibular, axillar, and brachial lymph nodes are removed with a curved anatomic forceps, taking care not to include surrounding fat.
5. The lower part of the skin is drawn caudally towards the hind legs, and the inguinal lymph nodes are removed.
6. Then a midline incision is made through the abdominal wall to expose the intestines. Lymph nodes are collected from the intestinal mesentery, taking particular care to exclude fat.
7. Lymph nodes are collected in sterile, ice-cold TC 199 medium in 15-mL tubes that are usually kept on ice in a styrofoam container.
8. Under sterile conditions, the lymph nodes are transferred to a sterile sieve (mesh size: 0.6 mm) and ground with a spade. Subsequently, the sieve is rinsed with 10 mL TC 199. The cell suspension is collected in a cell-culture dish (Petri dish) and is flushed through another sieve (mesh size: 0.2 µm) to exclude cell debris.
9. The resulting single-cell suspension is collected in a 50-mL plastic tube and is centrifuged (10 min, 300g, 4°C). Cells are taken up in 10 mL sterile PBS, and viable cells are counted after trypan blue staining in a microhemocytometer.
10. The optimal number of cells for induction of GVHD depends on the chosen model (*see* **Note 4**).

3.2.2. Preparation of Bone-Marrow Cells

After collecting the lymph-node cells, the bone marrow is harvested.

1. Bone-marrow cells are harvested from the tibia and femur of donor mice: after stripping the skin from both hind legs, the femoral bones are disarticulated at the hip joint. Care is taken not to damage or splinter the bones, as this makes later flushing inefficient. Subsequently, muscle tissue is carefully dissected away from the bones. The bones are collected in 20 mL sterile TC 199 at 4°C in 50-mL plastic tubes.
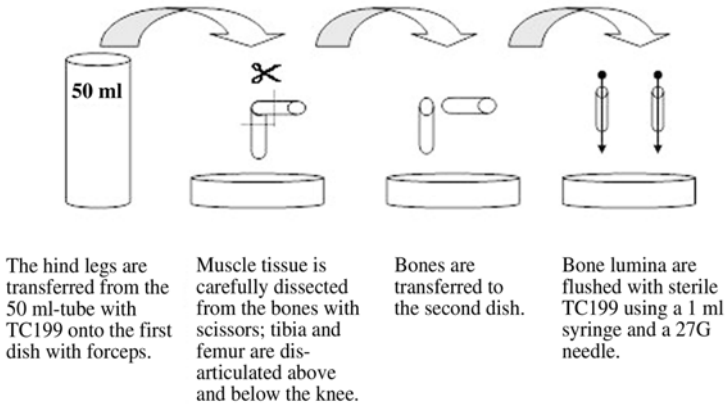
Fig. 1. Harvesting of bone-marrow cells.

2. Under sterile conditions, three cell-culture dishes are prepared, each containing 10 mL sterile TC 199. Scissors and forceps should be disinfected with 70% EtOH regularly during this process. First, the bones are collected in the first dish. Femur and tibia are disarticulated at the knee joint (*see* **Fig. 1**) and the separated bones are collected in the second dish. There, the distal ends of both bones are cut off with scissors to access the bone-marrow cavity. The bone marrow is harvested by flushing the bone cavities with a 27-gage needle on a 1-mL syringe containing TC199 into the third dish.

3. Bone-marrow cells are then repeatedly resuspended with a 20-gage needle on a 20-mL syringe (TC 199) until the cell suspension is homogenized. Then cells are transferred to a 50-mL plastic tube and centrifuged (10 min, 4°C, 300g).

4. After centrifugation, the bone-marrow cell suspension is incubated with sterile hemolysis buffer at room temperature for 5 min. Then it is filtered through a sieve (mesh size: 0.2 μm) to remove bone fragments and other particulate material. The cell suspension is collected in a 50-mL plastic tube and is washed twice in sterile PBS. Thereafter, the cells are taken up with 10 mL sterile PBS to count them with trypan blue (vitality control).

5. Similar to the clinical situation, in which 2×10^8 bone-marrow cells per kg body weight are administered to the patient, mice should receive on average 5×10^6 cells (*see* **Note 5**).

3.3. Injection of Donor Cells

To inject the cells intravenously, the four tail veins of the mouse can be expanded and visualized by patting them with a swab and warm water. Water should not be too hot or boil. It is recommended to inject the tail vein with no more than 200 μL of volume. Only the lateral tail veins are suitable for injections.

For this procedure the mouse must be restrained in a holding device. At best, the mouse is placed in a body-adjusted plastic tube or cylinder to restrain the mouse inside the tube, and to allow the tail to hang out. Care should be taken not to exert unnecessary force against the animals.

The injection is carried out with a 27-gage injection needle on a 1-mL disposable syringe.

3.4. Diagnosing GVHD

After bone-marrow reconstitution, the recipients are checked every other d for at least 100 d (*see* **Note 6**) for weight changes, and are checked daily for survival. In addition, the skin is inspected and the defense reaction is tested. If skin lesions such as alopecia, desquamations, or ulcerous-erosive changes appear, the animals should be sacrificed. Similarly, animals should be sacrificed upon severe weight loss or apathetic behavior. The liver, the gastrointestinal tract, and the skin should be examined by histology. It is recommended to take photos for documentation of skin lesions and a hunched back. *See* **Note 7** for the clinical course of chronic GVHD.

4. Notes

1. In contrast to human beings, in whom acute GVHD is caused by allogeneic bone-marrow cells alone, mature T-cells must be added to the bone-marrow inoculum in most experimental mouse models in order to induce acute GVHD. It is reported that with total body irradiation of 8.5 Gy ([60]cobalt source) and 3×10^7 bone-marrow cells in a major histocompatibility complex (MHC)-I disparate mouse model, about 40% of recipients survived the first 3 mo after bone-marrow transplantation *(1)*. Many studies confirm that the murine bone marrow contains only a low frequency of mature T-cells (1–3% of all bone-marrow cells) *(2–5)*. In marked contrast, the proportion of immunocompetent T-cells in humans amounts to 8% ± 1.6% of the bone-marrow pool *(6)*, and is therefore considerably higher than in the mouse. Another factor necessitating the addition of mature T-lymphocytes from secondary lymphoid organs (spleen, lymph nodes) is the high proportion of immunoregulatory cells in murine bone marrow. Thirty to 50% of bone-marrow αβ-T-cell antigen receptor (TCR) T-cells are NK1.1^{+} cells *(7)*; about 30% of CD3^{+} cells are CD4^{-}CD8^{-} double negative T-cells *(8)*. So far, experiments in autoimmune disease and GVHD models have proven the immunoregulatory function of both of these cell types *(9–14)*. The mechanism of immunoregulation has been attributed to the secretion of interleukin (IL)-4 by these cells *(5)*. Therefore, NK1.1CD4^{-}CD8^{-} T-cells have been termed "natural suppressor cells" *(15)*. Both the low frequency of mature immunocompetent T-cells and the high percentage of immunoregulatory T-cells could explain the unsuccessful induction of GVHD in mice reconstituted with bone-marrow cells only. This is why, even with higher cell numbers, mature T-cells cannot induce a GVHD reaction as expected—they are still suppressed by the concomitant increase in the number of transferred suppressor cells. In summary, in contrast to the human system, bone-marrow cells alone are unable to reliably induce a GVH reaction in the mouse. It is necessary to add mature T-cells from secondary lymphoid organs, such as lymph nodes or spleen, to increase the ratio of immunocompetent vs immunoregulatory T-cells in the bone-marrow inoculum (*see* **Note 4** for further details).

2. Should an alternative design of an irradiation cage be used, it is important to remember that the effect of irradiation is more diminished, the greater the distance between the animals and the lid of the cage. The dose needed to achieve the same irradiation effect increases with the second power of the distance between the irradiation source and the target. Ideally, the lid should close directly on top of the back of the animals in order to achieve perfect irradiation distribution. To achieve optimal radiation results, it is necessary to optimize the radiation conditions. First, it is important to construct an optimal cage. If the lid does not close directly above the back of the recipients, a higher radiation dose might be necessary. In our own experience, the mortality of recipients of allogeneic
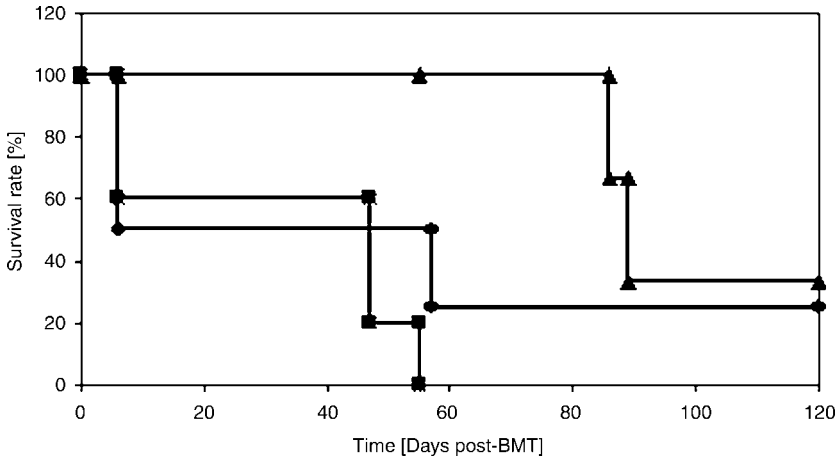
Fig. 2. Lethal graft-vs-host disease after irradiation by a particle accelerator (5 MeV) in cages of different height (2.5 cm, 5 cm). K^b mice were reconstituted with 5×10^6 Des-T-cell antigen receptor (TCR) (anti-K^b TCR) bone-marrow cells. Three experimental groups were analyzed: (1) 12 Gy irradiation, 5 cm height, 1×10^6 added lymph-node cells (LNC); (2) 11 Gy, 2.5 cm, 1×10^6 added LNC; (3) 11 Gy, 2.5 cm, 5×10^6 added LNC.

bone marrow was higher in a group that was irradiated with a smaller dose (11 Gy) of a particle accelerator in a smaller box (2.5 cm high; $n = 5$; survival rate: 0% at 55 d after bone-marrow transplantation) than with a higher dose (12 Gy) of the same particle accelerator in a higher box (5 cm high; $n = 3$; survival rate: 33% after 89 d post bone marrow transplantation) (unpublished, **Fig. 2**). This can be explained by the build-up effect of radiation beams. With too much space between lid and the irradiated objects, the build-up dose will be lost and has to be "rebuilt" in the object itself. In this scenario, the dose maximum is not optimally focused, which can lead to misleading results. In summary, it is recommended that the irradiation cage should have a maximum height of 2.5 cm.

As mentioned above, another modification to focus the build-up dose and the depth dose, and to optimize the radiation effect, is to place a plate on the cage. Usually, a plexiglas plate is put on top of the cage to distribute the radiation homogenously and to focus the maximum of the radiation optimally on the body of the recipient. The optimum thickness of such a plate can vary from 1 to 4 cm, depending on the radiation device and the employed energy of the radiation source. Alternatively, the use of moulages has been recommended in the literature *(16,17)* for oncologic radiation patients. Moulages are wax molds (lexan) with tissue-like characteristics adapted to the body forms of the patients. In the experimental situation, the moulages would have to be placed on top of the cage.

3. Different radiation devices are available for GVHD induction in experimental models. The three most commonly used are [60]cobalt, [137]cesium, and particle (linear) accelerators. The biological effects, for instance with respect to GVHD induction or side effects, differ considerably depending on the radiation source used. Characteristics of these radiation sources are summarized in **Table 1**.

Table 1
Characteristics of Different Radiation Sources

^{60}Cobalt	Linear accelerator	^{137}Cesium
• Naturally found radioactive source	• Electrons are accelerated by electromagnetic high frequency waves	• Naturally found radioactive source
• Radioactive decay	• Photon radiation	• Radioactive decay
• β- and γ- radiation[a]	• Used energies (monoenergetic): between 6 MV and 25 MV	• β- and γ- radiation[a]
• Energy: 1.25 MV[b]	• Maximum doses with:	• Energy: 662 keV[b] (monoenergetic)
• Maximum dose at 0.5 cm depth	23 MV at 3.0 cm depth; 6 MV at 1.5 cm depth	• Maximum dose at <0.5 cm depth
• Formation of penumbra[c]	• No formation of penumbra[c]; extensive continuous spectrum	• Formation of penumbra[c]
• Half-life: about 5.25 yr	• No half-life	• Half-life: about 30 ys

[a] β-radiation is absorbed by the technical device; only the γ-radiation will have an effect.

[b] The ^{60}cobalt source emits two equally powerful γ-lines of 1.17 and 1.33 MeV. For practical reasons they are calculated as one monochromatic line of 1.25 MeV. In contrast, the ^{137}cesium source emits only one monoenergetic line.

[c] Within the radiation field, the dose is roughly constant, but decreases towards the margins of the radiation field. In the area within these margins, the dose reduction is geometrically very steep; outside of these margins and the radiation field it converts into a flat runner. The dose value in the main axis of the radiation field is defined as 100%. The distance between two distinct dose values in the area of the radiation field margins (dose reductions) is called "penumbra." The term "penumbra" therefore deals with the flat dose reduction at the margins of the radiation field. Often the distance between the 80% and the 20% value will be given (again, 100% is according to the main field axis). The formation of the penumbra is influenced by the size of the radiation source and its focus, and by the construction of the collimator system. Particle accelerators have a penumbra region of only a few millimeters, which are therefore smaller than those of γ-irradiation devices *(17)*.

Table 2
Results of Different Irradiation Modalities With the Same Radiation Dose (9 Gy) and Injected Lymph-Node Cell Number [a]

Radiation device	Number of treated mice	Dose (Gy)	Height of cage (cm)	Cell number of injected lymph-node cells	Death rate (Days after BMTx)	Survival rate (%)
Cobalt	6	9	5	5×10^5	7, 11 (2x), 14 (2x), 23, 27	0
Particle accelerator	12	9	5	5×10^5	7, 8, 12, 14, 42, 46, 73	42
Cesium	5	9	—[b]	5×10^5	20, 82, 113	40

[a] For legend, *see* **Table 1**.

[b] For technical reasons, the mice were placed inside a special metal cylinder (18 cm high, base area 58 cm^2). The metal cylinder with the mice inside rotated around its vertical axis close to the cesium source for equivalent dose distribution.

Experiments were performed to compare the different radiation sources after allogeneic bone-marrow transplantation (Schwarte and Hoffmann, unpublished). Using 9 Gy irradiation with [60]cobalt and 5×10^5 lymph-node cells plus 5×10^6 bone-marrow cells, all recipients died from acute GVHD within 30 d. With the same treatment but with the other radiation devices, recipient mice could live longer than 120 d (**Table 2**).

It can be observed that with these other two radiation techniques, the mice developed skin lesions, such as alopecia or ulcerative-erosive skin desquamations, especially after radiation with the [137]cesium source. Acute GVHD could not be induced by these two radiation modalities. In contrast, it was confirmed that the dose of 9 Gy with the latter two radiation sources was lethal in the absence of bone-marrow reconstitution. All irradiated mice died within 14 d, irrespective of the presence or absence of an acute GVHD reaction.

The high lethality in the radiation control groups (without treatment) showed that the radiation was sufficient to induce a lethal tissue injury, particularly of the bone marrow, but was not able to set the recipient into a GVHD-inducable state.

The different reactions to the radiation techniques and their effects on GVHD results can be explained by the underlying physical principles and some immunological concepts.

The main reason for these findings and different GVHD incidence, dependent on the different radiation devices, is the principle of the build-up dose and the depth dose maximum.

One particularly important quality of these radiation devices is the dose build-up effect with increasing tissue depth. After hitting the body surface, the radiation dose changes with increasing depth along the central axis of the beam, which is caused by various physical effects *(18)*. The graphic description of these dose distributions in the radiated object is termed *isodose curves*.

The explanation for the phenomenon of the build-up dose is as follows: at first, as the radiation decreases, the dose is reduced. The relative depth dose of the [60]cobalt source at the surface amounts to about 90%, of the particle accelerator with 5 MeV to 70%, and with 16 MeV to 40% *(17)*.

At the surface of the object, only electrons from the radiation source, the surrounding area (mainly air), and backscattered electrons from the object have an effect; in the irradiated object itself, significantly more electrons are removed and transmitted, proportional to the total amount of available photons (so-called photonfluence).

As a consequence of the limited range of liberated electrons, the total sum of electrons increases with increasing depth until they have lost their motion energy. At the end of their course and, therefore, at the end of their defined depth range, a maximum of liberated electrons can be observed. At the same time, the effect of each liberated, secondary electron adds up to the primary photon beam, which is absorbed by the object and is therefore further diminished. On the whole, an increase of dose is achieved up to a defined depth in the tissue, though the primary beam is decreased.

A depth dose maximum of 100% is achieved with the [60]cobalt source at 0.5 cm, with the particle accelerator at 1.5 cm (6 MeV) to 3.0 cm (23 MeV), and with the [137]cesium source at less than 0.5 cm. Beyond this depth, the dose decreases, mainly due to the effect of photoabsorption *(17,19)*.

With the [60]cobalt equipment, an acute GVHD can be induced in murine recipients. The depth dose maximum is at 0.5 cm. Beyond this point, the dose decreases steeply. Nonetheless, this is sufficient to induce an acute GVHD. The only technical disadvantage is that due to its short half-life (approx 5 yr) a [60]cobalt source needs to be checked and replaced at regular intervals.

The [137]cesium source has a lower energy (662 KeV) than [60]cobalt (1.25 MeV) and the linear accelerators. Therefore, the dose depth maximum is <0.5 cm, which is quite close the surface, even if the dose is built up appropriately under optimized conditions. Below this point, the dose decreases even more steeply than with a [60]cobalt source. This is why the irradiation is most effective at the surface, but significantly decreases in effectiveness with increasing tissue depth. Due to these considerations, [137]cesium is no longer used as a telegamma radiation device in the clinical routine, but only for brachytherapy of tumors *(20)*. Furthermore, the surface effects can explain why in experimental models so many recipient mice develop skin lesions compared to other radiation devices ([60]cobalt, linear accelerator): the maximum radiation effect at the surface leads to a heavy injury of the skin, resulting in a high incidence of skin lesions, but without the effects in the depth. In turn, the recipient organism is not sufficiently immunosuppressed to allow for the induction of acute GVHD; only a mild, chronic GVHD can be induced. Other studies prove the interdependences between radiation source and the induction of GVHD *(21)*.

It has previously been observed that organisms vary in their biological response to the different radiation techniques. With [137]cesium, a higher secretion of IL-1 and IL-6 could be detected, whereas with a conventional X-ray device, a higher secretion of interferon (IFN)-γ and tumor necrosis factor (TNF)-α was identified *(21)*.

In contrast, linear accelerators use more energy than the [60]cobalt source. The maximum depth dose is at 1.5 cm (6 MeV) or 3.0 cm (23 MeV). Considering the small size of an animal such as a mouse for irradiation, problems with the use of higher energies (e.g., 23 MeV) may occur. The dose lethally damages the organism. However, irrespective of the death of the irradiated mouse, the suboptimal distribution and depth dose, the same effect as with the [137]cesium source will be obtained. If lower energies are used, irradiation will have to be optimized, i.e., the cage design and the plate for the build-up dosing must be adjusted (2.0 cm for a 6 MeV linear accelerator and 4.5 cm for a 25 MeV linear accelerator).

It was determined that the mouse strains respond differently to irradiation *(22)*. BALB/c, C3H/OuJ, C3H/HeJ, and C57BL/6 mice were exposed to [60]cobalt and [137]cesium sources. The lethality rate decreased in the following sequence: BALB/c > C3H/OuJ = C3H/HeJ > C57BL/6. The C57BL/6 mouse strain was, therefore, the most radiation resistant. The reason for this difference is still unclear. It is assumed that probably DNA-repair systems in some strains do not work as efficiently as in other strains, or that the pool of radiosensitive stem cells differs between the mouse strains.

4. Only the addition of mature T-cells from secondary lymphatic organs, such as lymph nodes or spleen, to the bone-marrow inoculum can induce acute GVHD in the mouse (*see* **Note 2** for further details).With that in mind, the number of added cells determines the form and clinical course of the GVH-reaction *(23)*. In a murine GVHD-model with CBA-mice as donors and BALB/c mice as recipients, which had been irradiated 5 to 6 h before bone-marrow transplantation with 750 cGy (γ-irradiation), the recipients were given 5×10^6 CBA bone-marrow cells with varying numbers of spleen cells. Less than 1×10^5 spleen cells did not lead to any GVH reaction at all, or at least only to a mild course of GVHD; 2.5 to 4×10^5 spleen cells led to a moderate to severe GVHD; 1×10^6 or more spleen cells were associated with a hyperacute form of GVHD in which most of the BALB/c recipients died within 8 d after bone-marrow transplantation *(4)*. The various mouse strains differ in their extent of immune responses. That is why a defined number of cells to induce an acute GVHD cannot be given in general. Nevertheless, in all mouse strains, mature T-cells must be added to induce lethal acute GVHD.

5. In the literature, varying numbers of transferred cells can be found. Therefore, many alternatives to this mentioned cell count are possible. The amount of 5×10^6 bone-marrow cells is related to the clinical setting, in which the patient is given 2×10^8 bone-marrow cells per kg body weight, calculated with an average mouse weight of 25 g.

6. Alternatives for monitoring for a GVHD course: every d for mortality and once a wk for weight changes. It is dependent on the question of interest and of data survey for statistical analysis. The definition of the acute form of GVHD is that it appears during the first 100 d after bone-marrow transplantation; the chronic form of GVHD by definition starts after 100 d. That is why bone-marrow transplant recipients should be controlled for at least 100 d if the acute form is the objective for experiments.

7. Mice developing a chronic GVHD typically show the following disease course: In the first wk after cell transfer, the mice get visibly and evidently ill: they lose weight and show bristled fur. Then the status of a few mice can worsen, resulting in their death within the next 2 wk. In most cases, however, the recipients recover for a certain period of time. These mice exhibit only marginal body weight loss, the skin lesions improve at the end of the second wk after bone-marrow transplantation, and the mice show regular, almost normal physical activity. After 4 wk, the mice develop a severe and progressive body weight loss with diarrhea and a hunched back. Most of them die within the next 1 to 2 wk; the body weight loss can then be severe, sometimes up to more than 40% *(24)*. The described course of chronic GVHD in mice, also in the study cited above *(24)*, is frequently observed. In that study, the chronic GVHD was caused by injection of purified CD8+ T-cells, without CD4+ T-cells. That study is seen as evidence that CD8+ T-cells more likely induce a chronic GVHD, rather than an acute form. Even in standard textbooks this study is cited for this interrelation *(25)*. It is striking, though, that in publications with observations of a chronic GVHD by CD8+ T-cells, the recipient mice were lethally irradiated by a ^{137}cesium source *(23–29)*. Therefore, the general statement that CD8+ T-cells lead to chronic GVHD cannot be maintained. The reaction of the recipient is also influenced by the radiation source during the conditioning for the bone-marrow transplantation. Since the immunological reactions following irradiation and bone-marrow transplantation do not necessarily lead to an acute GVH reaction, but rather to a mild and chronic GVHD, the donor cells somehow react in another way than expected. In another study, three possible concepts were proposed as explanations for this observation *(30)*: the activation-induced cell death, tolerance by internalization of the T-cell receptor, and anergy of the donor T-cells. The immune response of the recipient and the induction of the GVHD is dependent on various factors, e.g., the combination of the mouse strains and the different radiation modalities. In summary, based on the physical-technical characteristics, it is easiest and most reliable to work with a ^{60}cobalt source for the induction of an acute GVHD, at least in the experimental setting with mice. In contrast, linear accelerators and ^{137}cesium sources are rather unreliable for this purpose.

Acknowledgment

References

1 Waer, M., Ang, K. K., Schueren, E. van der, and Vandeputte, M. (1984) Increased incidence of murine graft-versus-host disease after allogeneic bone marrow transplantation by previous infusion of syngeneic bone marrow cells. *Transplantation* **38,** 396–400.

2   Eberl, G., Lees. R, Smiley, S. T., Taniguchi, M., Grusby, M. J., and MacDonald, H. R. (1999) Tissue-specific segregation of CD1d-dependent and CD1d-independent NK T cells. *J. Immunol.* **162,** 6410–6419.

3   Zeng, D.,Gazit, G., Dejbakhsh-Jones, S., et al. (1999) Heterogeneity of NK1.1⁻ T cells in the bone marrow: divergence from the thymus. *J. Immunol.* **163,** 5338–5345.

4   Rosario, M. L. U. del, Zucali, J. R., and Kao, K. J. (1999) Prevention of graft-versus-host disease by induction of immune tolerance with ultraviolet b-irradiated leukocytes in H-2 disparate bone marrow donor. *Blood* **93,** 3558–3564.

5   Zeng, D., Lewis, D., Dejbakhsh-Jones, S., et al. (1999) Bone marrow NK1.1⁻ and NK1.1⁺ T cells reciprocally regulate acute graft versus host disease. *J. Exp. Med.* **189,** 1073–1081.

6   Fauci, A. S. (1975) Human bone marrow lymphocytes: I. Distribution of lymphocyte sub-populations in the bone marrow of normal individuals. *J. Clin. Invest.* **56,** 98–110.

7   Zeng, D., Hoffmann, P., Lan, F., Huie, P., Higgins, J., and Strober, S. (2002) Unique patterns of surface receptors, cytokine secretion, and immune functions distinguish T cells in the bone marrow from those in the periphery: impact on allogeneic bone marrow transplantation. *Blood* **99,** 1449–1457.

8   Sykes, M. (1990) Unusual T cell populations in adult murine bone marrow. Prevalence of CD3⁺CD4⁻CD8⁻ and αβTCR⁺NK1.1⁺ cells. *J. Immunol.* **145,** 3209–3215.

9   Gombert, J. M., Herbelin, A., Tancrede-Bohin, E., Dy, M., Carnaud, C., and Bach, J. F. (1996) Early quantitative and functional deficiency of NK1⁺-like thymocytes in the NOD mouse. *Eur. J. Immunol.* **26,** 2989–2998.

10 Baxter, A. G., Kinder, S. J., Hammond, K. J., Scollay, R., and Godfrey, D. I. (1997) Association between αβTCR⁺CD4⁻CD8⁻ T-cell deficiency and IDDM in NOD/Lt mice. *Diabetes* **46,** 572–582.

11 Hammond, K. J. L., Poulton, L. D., Palmisano, L. J., Silveira, P. A., Godfrey, D. I., and Baxter, A. G. (1998) α/β-T cell receptor (TCR)⁺CD4⁻CD8⁻ (NKT) thymocytes prevent insulin-dependent diabetes mellitus in nonobese diabetic (NOD)/Lt mice by the influence of interleukin (IL) 4 and/or IL-10. *J. Exp. Med.* **187,** 1047–1056.

12 Palathumpat, V., Dejbakhsh-Jones, S., Holm, B., Wang, H., Liang, O., and Strober, S. (1992) Studies of CD4⁻CD8⁻ αβ bone marrow T cells with suppressor activity. *J. Immunol.* **148,** 373–380.

13 Sykes, M., Hoyles, K. A., Romick, M. L., and Sachs, D. H. (1990) In vitro and in vivo analysis of bone marrow-derived CD3⁺, CD4⁻, CD8⁻, NK1.1⁺ cell lines. *Cell. Immunol.* **129,** 478–493.

14 Strober, S., Cheng, L., Zeng, D., et al. (1996) Double negative (CD4⁻CD8⁻αβ⁺) T cells which promote tolerance induction and regulate autoimmunity. *Immunol. Rev.* **149,** 217–230.

15 Strober, S. (2000) Natural killer 1.1⁺ T cells and "natural suppressor" T cells in the bone marrow. *J. Allergy. Clin. Immunol.* **106,** S113–114.

16. Quast, U. and Hoederath, A. (1996) Ganzkörperbestrahlung. In: *Strahlentherapie: Radiologische Onkologie.* Scherer, E. and Sack, H. eds., Springer, New York, NY, pp. 207–218.

17. Richter, J. and Schwab, F. (1998) Charakterisierung und Eigenschaften von Dosisverteilungen, in *Strahlenphysik für die Radioonkologie.* Richter, J. and Flentje, M., eds., Thieme Stuttgart, New York, NY, pp. 43–59.

18. Verhey, L. J. (1998) Principles of radiation physics. In: *Textbook of Radiation Oncology.* Leibel, S. A. and Phillips, T. L. eds. WB Saunders, Philadelphia, PA, pp. 91–114.

19. Laubenberger, T. and Laubenberger, J. (eds.) (1994) *Technik der medizinischen Radiologie: Diagnostik, Strahlentherapie, Strahlenschutz für Ärzte, Medizinstudenten und MTRA; mit Anleitung zur Strahlenschutzbelehrung in der Röntgendiagnostik.* Deutscher Ärzte-Verlag, Köln, Germany.

20. Schmidt, R. (1998) Geräte zur Erzeugung ionisierender Strahlung. In: *Strahlenphysik für die Radioonkologie.* Richter, J. and Flentje, M. eds. Thieme Stuttgart, New York, NY, pp. 27–38.

21 Sykes, M., Pearson, D. A., Taylor, P. A., Szot, G. L., Goldman, S. J., and Blazar, B. R. (1999) Dose and timing of interleukin (IL)-12 and timing and type of total-body irradiation: effects on graft-vs.-host disease inhibition and toxicity of exogenous IL-12 in murine bone marrow transplant recipients. *Biol. Blood Marrow Transplant.* **5,** 277–284.

22 Henning, U. G. G., Wang, Q., Gee, N. H., and von Borstel, R. C. (1996) Protection and repair of γ-radiation-induced lesions in mice with DNA or deoxyribonucleoside treatments. *Mutat. Res.* **350,** 247–254.

23 Baker, M. B., Altman, N. H., Podack, E. R., and Levy, R. B. (1996) The role of cell-mediated cytotoxicity in acute GVHD after MHC-matched allogeneic bone marrow transplantation in mice. *J. Exp. Med.* **184,** 2645–2656.

24 Sprent, J., Schaefer, M., Gao, E. K., and Korngold, R. (1988) Role of T cell subsets in lethal graft-versus-host disease (GVHD) directed to class I versus class II H-2 differences. I. L3T4+ cells can either augment or retard GVHD elicited by Lyt-2+ cells in class I-different hosts. *J. Exp. Med.* **167,** 556–569.

25 Sprent, J., Schaefer, M., and Korngold, R. (1990) Role of T cell subsets in lethal graft-versus-host disease (GVHD) directed to class I versus class II H-2 differences. *J. Immunol.* **144,** 2946–2954.

26 Graubert, T. A., Russell, J. H., and Ley, T. (1996) The role of granzyme B in murine models of acute graft-versus-host disease and graft rejection. *Blood* **87,** 1232–1237.

27 Graubert, T. A., DiPersio, J. F., Russell, J. H., and Ley, T. J. (1997) Perforin/granzyme-dependent and independent mechanisms are both important for the development of graft-versus-host disease after murine bone marrow transplantation. *J. Clin. Invest.* **100,** 904–911.

28 Korngold, R. and Sprent, J. (1985) Surface markers of T cells causing lethal graft-vs-host disease to class I vs class H-2 differences. *J. Immunol.* **135,** 3004–3010.

29. Sprent, J., Schaefer, M., Lo, D., and Korngold, R. (1986) Properties of purified T cell subsets. II. In vivo responses to class I vs. class II H-2 differences. *J. Exp. Med.* **163,** 998–1011.

30. Dey, B., Yang, Y. G., Preffer, F., Shimizu, A., Swenson, K., Dombkowski, D., and Sykes, M. (1999) The fate of donor T-cell receptor transgenic T cells with known host antigen specificity in a graft-versus-host disease model. *Transplantation* **68,** 141–149.

30

Induction of Chimerism and Tolerance Using Freshly Purified or Cultured Hematopoietic Stem Cells in Nonmyeloablated Mice

Nikos Emmanouilidis and Christian P. Larsen

Summary

The development of protocols to induce a state of durable mixed allogeneic hematopoietic chimerism to confer robust donor-specific transplant tolerance has been a major focus of the transplant community for the past decade. High levels of mixed allogeneic hematopoietic chimerism across a full major histocompatibility complex (MHC) barrier can be achieved by total myeloablation and transfusion of host and donor bone-marrow cells *(1)* or, as shown more recently, can be achieved with nonmyeloablative preconditioning regimes in combination with donor bone-marrow transfusions *(2–4)* or transfusion of purified hematopoietic stem cells (HSC) *(5–7)*. Here we illustrate useful experimental techniques for the study of hematopoietic chimerism in rodents by describing a system in which chimerism can be induced using nonmyeloablative conditioning, short-term costimulation blockade, and transplantation of purified or cultured hematopoietic stem cells.

Key Words: Hematopoietic stem cell; Sca-1; chimerism; tolerance; magnetic bead selection; MACS; busulfan; anti-CD40-ligand; CTLA4-Ig.

1. Introduction

Three factors are crucial for the establishment and long-term maintenance of hematopoietic chimerism across allogeneic barriers in mice. First, deletion or anergy of donor-specific allo-reactive T-cells, which is necessary to avoid rejection of the bone-marrow graft. In this model, this is achieved by blocking the CD28 and CD40 co-stimulatory pathways using CTLA4-Ig and anti-CD40L along with the administration of donor antigen. Second, niches for donor stem cells need to be available within the recipient's bone-marrow microenvironment. This can be achieved by administration of a single nonmyeloablative dose of busulfan, which selectively kills HSC, thus freeing stem-cell niches and making them available for the engraftment of transplanted donor HSC. Third, the transfused cells must contain multipotent HSC capable of homing, engraftment, and self-renewal.

It is widely recognized that HSC in mice can be identified using flow cytometry by their expression of stem-cell antigen 1 (SCA-1) *(8)* and lack of expression of various lineage markers (e.g., CD3, CD19, and so on). HSC in mice are a minor fraction within the bone-marrow compartment and represent only about 0.05–0.1% of total bone-marrow cells, which necessitates the development of specialized techniques in order to study hematopoietic stem cell behavior in detail. In this chapter we will describe how to purify Sca-1^{pos}Lin^{neg} HSC using a magnetic cell-sorting procedure and how to use these HSC for the induction of durable and robust hematopoietic chimerism in a fully allogeneic transplant model in non-myeloablated mice. The preconditioning of recipient mice in this model takes 5 d and involves the induction of anergy in recipient donor-reactive T-cells, the administration of a myelotoxic drug, and transfusion of donor antigen. Anergy or deletion of donor specific allo-reactive T-cells in this model is achieved by blocking the CD28 and CD40 co-stimulatory pathways using CTLA4-Ig and anti-CD40L along with the administration of donor antigen (e.g., unseparated bone-marrow cells, splenocytes, and so on). These agents prevent the early destruction of donor HSC and allow sufficient time for newly evolving donor antigen-presenting cells (APC) to migrate to the thymus, where they participate in the process of shaping the T-cell repertoire through central deletion of new donor-specific T-cells. Nonmyeloablative preconditioning regimens, whether involving myelotoxic drugs or γ-irradiation, have been proven to be sufficient and reliable for the induction of robust long-term hematopoietic chimerism *(2–7,9)*. Thus we describe a regime that makes use of a single dose of busulfan, an agent with stem-cell selective toxicity, which, if administered 1 d before transfusion of the engrafting HSC dose, frees stem-cell niches within the recipient bone-marrow compartment and makes them available for donor HSC engraftment.

Recent results have shown the ability to expand HSC ex vivo *(10–14)* and the potency of these cells for self-renewal and long-term bone-marrow engraftment *(5,6)*. Thus, we also provide a brief example of how short-term in vitro cultured HSC can be studied within this protocol.

2. Materials

1. Adult male 6–8-wk-old C57BL/6 (H-2^b) *(1)* and adult male 6–8-wk-old BALB/c (H-2^d) mice (JAX, Bar Harbor, ME).
2. Murine anti-CD40L (MR1) (BioExpress, West Lebanon, NH).
3. Human CTLA4-Ig (Bristol-Myers Squibb, New York, NY).
4. Biotinylated Mouse Lineage Panel (PharMingen, San Diego CA).
5. Anti-Biotin Microbeads® (Miltenyi Biotec, Bergisch-Gladbach, Germany).
6. Anti-FITC Multisort® Kit (Miltenyi Biotec).
7. Auto-MACS® cell sorter (Miltenyi Biotec).
8. FITC-conjugated anti-Sca1 (Ly-6A/E), (PharMingen).
9. APC-conjugated anti-biotin mAB (PharMingen).
10. F$_c$-block (Fc_ III/II receptor) (PharMingen).
11. Whole blood cell lysis kit (R&D Systems, Minneapolis, MN).
12. R10-medium: RPMI-1640 (Mediatech, Herndon, VA) with 10% fetal calf serum (FCS) (Mediatech).
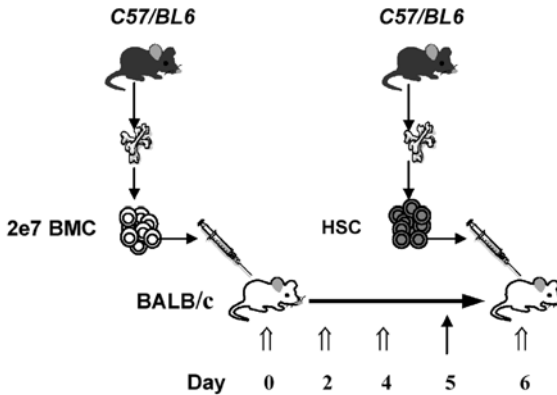
Fig. 1. Unseparated C57/BL6 bone-marrow cells, 2×10^7 are administered on d 0, followed by injection of costimulation-blocking molecules anti-CD40L and CTLA4-Ig (↑) on d 0, 2, 4, and 6. Busulfan (↑) is administered on d 5, one day before donor hematopoietic stem cells are injected on d 6.

13. MACS buffer: Dulbecco's 1X phosphate-buffered saline (1X PBS) (Mediatech) with 2 m*M* ethylene-diamine-tetraacetic acid (EDTA) (Sigma-Aldrich, St. Louis, MO) and 0.5% bovine serum albumin (BSA) (Sigma-Aldrich).
14. RINSE buffer: Dulbecco's 1X phosphate-buffered saline (1X PBS) (Mediatech) with 2 m*M* ethylene-diamine-tetraacetic acid (EDTA) (Sigma-Aldrich).
15. Histopaque® 1083g/mL (Sigma-Aldrich).
16. Trypan blue solution, liquid 0.4% (Sigma-Aldrich).
17. Twenty-four-well cell-culture flat-bottom plate (Fisher Scientific, Pittsburgh, PA).
18. Serum-free expansion medium (SFEM®) (Stem Cell Technology, Vancouver, Canada).
19. Mouse stem-cell factor (SCF), mouse Flt-3/Flk-2 ligand (FLT3L), recombinant mouse interleukin (IL)-3, recombinant mouse IL-6 (all from Sigma-Aldrich): resolve lyophilized growth factors to 100 ng/10 μL SCF, 100 ng/10 μL FLT3L, 20 ng/10 μL IL-3, and 20 ng/10 μL IL-6 in R10-medium, aliquot to volumes of 100 μL per tube, and store at –20°C.
20. Scissors and microsurgical forceps (Fine Science Tools, North Vancouver, BC, Canada).

3. Methods

3.1. Preconditioning of Recipient Mice

To avoid rejection of transferred hematopoietic stem cells in allogeneic donor/recipient settings, alloreactive recipient T-cells must be either depleted or suppressed. A 6-d recipient preconditioning protocol is outlined in **Fig. 1**, utilizing costimulatory pathway-blocking molecules anti-CD40 ligand and CTLA4-Ig as immunosupressive drugs and busulfan as a non-myeloablative agent to create space within the recipient bone-marrow microenvironment.

Day 1:

1. Euthanize C57BL/6 donor mice (*n* = 4) by cervical dislocation. Harvest tibiae, femura, and humeri with sterile instruments.

2. Flush out the bone marrow from bone shafts onto a Petri dish with cold sterile R10 medium using a syringe and a 26-gage needle. Aspirate bone-marrow cylinders repeatedly to disaggregate cells.

3. Pass cells through a 40-µm cell strainer into a 50-mL conical tube and add R10 medium to a total volume of 50 mL.

4. Spin down cells at 300g and 4°C, resuspend the pellet in 25 mL of RBC-lysis buffer, and incubate for 15 min on ice.

5. Rescue cells by adding 25 mL cold R10 medium and spin down at 300g and 4°C.

6. Resuspend the pellet by adding 20 mL of sterile saline. Take out 10 µL of the cell suspension into a 1.5-mL Eppendorf tube and add 986 µL of 1X PBS. Add 4 µL of the fluorescent dye and count the nucleated cells on a fluorescent microscope using a standard hematocytometer (alternatively, stain cells by adding 4 µL of trypan blue and count cells on a phase-contrast microscope).

7. Take out desired cell number (2.0×10^7 cells per recipient) and add sterile saline to bring the cell suspension to a concentration of 2.0×10^7 cells/300 µL.

8. For each recipient mouse, prepare one 1-mL syringe with a 30-gage needle and 300 µL of the cell suspension (2.0×10^7 cells) and store syringes on ice.

9. Anesthetize BALB/c recipient mice and administer 500 µg anti-CD40L and 500 µg CTLA4-Ig per recipient intraperitoneally. Each recipient is then injected with 2.0×10^7 C57BL/6 bone-marrow cells via penile-vein injection.

Days 2 and 4:

Each BALB/c recipient receives 500 µg anti-CD40L and 500 µg CTLA4-Ig intraperitoneally on d 2 and 4.

Day 5:

Busulfan is administered at 600 µg/mouse intraperitoneally.

Day 6:

See **Subheading 3.2.**

3.2. Purification of Sca1^{pos}Lin^{neg} Hematopoietic Stem Cells

The purification procedure takes about 8 h *(2)* from harvest of bones to final elution of *Sca1^{pos}Lin^{neg}* hematopoietic stem cells from the Auto-MACS®.

3.2.1. Harvest of Cells

1. Euthanize C57BL/6 donor mice ($n = 10$) *(3)* by cervical dislocation. Harvest tibiae, femura, and humeri with sterile instruments.

2. Flush out the bone marrow from bone shafts onto a Petri dish placed on ice with cold sterile R10 medium using a syringe and a 26-gage needle.

3. Aspirate bone-marrow cylinders repeatedly to disaggregate cells.

4. Pass the cells through a 40-µm cell strainer into a 50-mL conical tube, add R10 medium to a total volume of 50 mL, and spin down cells at 300g and 4°C.

5. Resuspend the pellet in 25 mL of RBC-lysis buffer and incubate for 15 min on ice.

6. Recover cells by adding 25 mL cold R10 medium and spin down at 300g and 4°C.

7. Resuspend the pellet by adding 14 mL of rinse buffer.

8. Take two 15-mL conical tubes and fill each with Histopaque® 1083 at room temperature. Divide the cell suspension into two equal volumes and carefully load cells as a second layer in each tube on top the Histopaque® 1083 layer.

9. Spin down both tubes at 20°C and 400g for 20 min with slow acceleration and centrifuge brakes off.
10. Take out the middle layer with a Pasteur pipet and resuspend cells in 14 mL cold R10 medium.
11. Count nucleated cells: mix well, take out 10 μL of the cell suspension into a 1.5-mL Eppendorf tube, and add 986 μL of MACS buffer. Add 4 μL of a fluorescent dye and count the nucleated cells on a fluorescent microscope using a standard hematocytometer (alternatively, stain cells by adding 4 μL of trypan blue and count cells on a phase-contrast microscope).
12. Spin down remaining cells at 300g for 15 min at 4°C and resuspend the pellet in MACS buffer at 150 μL/10^8 cells.

3.2.2. Labeling With Magnetic Beads

1. To reduce nonspecific binding of antibodies and beads, pre-incubate cells with F_c-block (Fcγ III/II receptor) by adding 5 μL per 10^8 cells (per 150 μL cell suspension) and incubate at 6–12°C for 10 min.
2. Add 4 μL of anti-Sca1-FITC monoclonal antibody, mix well, and incubate in the dark at 6–12°C for 20 min.
3. Add MACS buffer to a total volume of 15 mL and spin down at 300g for 15 min.
4. Discard supernatant and repeat the washing step a second time at 15 mL total volume, spin down at 300g at 4°C, and resuspend the pellet by adding 900 μL MACS buffer per 10^8 cells.
5. Pass the cells through a 40-μm nylon-mesh filter into a 15-mL conical tube.
6. Add anti-FITC microbeads at 100 μL per 10^8 cells (per 900 μL cell suspension), mix well, and incubate in the dark at 6–12°C for 20 min.
7. Divide cell suspension into equal volumes in two 15-mL conical tubes, add ice-cold MACS buffer to each tube to a total volume of 15 mL, and spin down at 300g at 4°C.
8. Repeat the washing step a second time, unite the pellets, and resuspend the cells in MACS buffer at a total volume of 2500 mL.
9. Filter cells through a 40 μm nylon-mesh filter before moving to the next step.

3.2.3. Magnetic Cell Sorting by Auto-MACS

3.2.3.1. First Step: Sca-1^{pos} Selection

1. Place the tube with the labeled cells under the uptake port and place 15-mL conical tubes under each eluent cock to save labeled (Sca1^{pos}) and nonlabeled (Sca1^{neg}) cells.
2. Select *PosselDS* as the sorting mode and hit start *(4)*.
3. Right before the cell uptake is completed, add 500 μL of MACS buffer to make sure that all cells are loaded onto the columns.
4. After elution of cells, save cells on ice and rinse the Auto-MACS following the manufacturer's protocol.
5. Place the negative fraction from the first magnetic separation under the uptake port and hit *PosselDS* a second time to sort out any remaining Sca1^{pos} cells. Collect labeled cells into the same 15-mL tube as the first time.
6. Count nucleated cells from the labeled (Sca1^{pos}) fraction: mix well, take out 10 μL of the cell suspension, and add 89 μL of MACS buffer. Add 1 μL of the fluorescent dye and count the nucleated cells on a fluorescent microscope using a standard hematocytometer (alternatively, stain cells by adding 1 μL of trypan blue and count cells on a phase-contrast microscope).

Lineage [CD3e, CD11b, Ly-6G,
CD45RB220, Ter119] – neg. APC
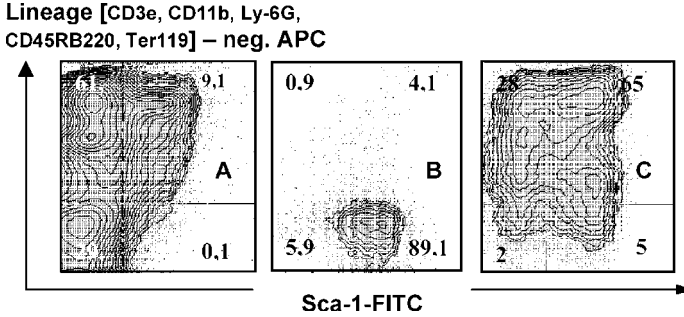
Fig. 2. Percentage of Sca1^{pos}Lin^{neg} cells in C57/BL6 mice from unseparated bone marrow (**A**), after magnetic bead selection (**B**), and after 6-d Sca1^{pos}Lin^{neg} in-vitro culture (**C**).

3.2.3.2. SECOND STEP: LINEAGE DEPLETION

1. Take Sca1^{pos} cells, add 100 µL of release agent per 4 mL of cell suspension, and incubate for 30 min at 4°C.
2. Spin down cells at 300g for 10 min and resuspend the pellet in 50 µL MACS buffer per 10^7 cells.
3. Add 30 µL of stop agent per 10^7 cells and incubate for 5 min.
4. Add the biotinylated lineage panel at 20 µL of each antibody per 10^7 cells and incubate for 20 min on ice.
5. Wash cells twice by adding MACS buffer to total volumes of 10 mL and spin down cells at 300g for 10 min.
6. Resuspend the pellet in 80 µL of MACS buffer per 10^7 cells, add 20 µL of anti-biotin microbeads per 10^7 cells, and incubate at 4°C for 20 min.
7. Wash cells once by adding MACS buffer to a total volume of 14 mL, spin down at 300g for 10 min, and finally resuspend the pellet in 1500 µL MACS buffer.
8. Load the sample under the uptake port of the AutoMACS and run the sample on Deplete mode.
9. Right before the cell uptake is completed, add 500 µL of MACS buffer so that all cells will be loaded on the columns.
10. Save the cells in 15-mL conical tubes on ice.
11. Count the nonlabeled fraction (Sca1^{pos}Lin^{neg} cells): mix well, take out 1.0 µL of the cell suspension, and add 9 µL of MACS buffer. Add 0.5 µL of a fluorescent dye and count the nucleated cells on a fluorescent microscope using a standard hematocytometer (alternatively, stain cells by adding 0.5 µL of trypan blue and count live cells on a phase-contrast microscope).
12. Use Sca1^{pos}Lin^{neg} cells for injection (*see* **Subheading 3.3.**) or cell culture (*see* **Subheading 3.4.**). Save a fraction of sorted cells to quantify purity and yield of HSC magnetic bead selection by flow cytometry (*see* **Fig. 2** and **Subheading 3.5.1.**).

3.3 Injection of Hematopoietic Stem Cells

1. Take desired cell number of Sca1^{pos}Lin^{neg} cells and prepare for injection: either add sterile saline in order to dilute to desired cell concentration or transfer cells into 2-mL

Eppendorf tubes and spin down tubes on a microfuge for 7 min at 300g to increase cell concentration *(5)*.

2. Discard supernatant and add sterile saline to desired cell concentration for injection volumes of 250–300 µL per mouse.
3. Save remaining cells on ice to determine purity of the purification procedure by flow cytometry.
4. Anesthetize recipient mice and use 1-mL syringes with 30-gage needles for penile-vein injections. Beginners should make use of a microscope or magnifying goggles with ×3–5 magnification.
5. Simultaneously each BALB/c is injected with 500 µg anti-CD40L and 500 µg CTLA4-Ig intraperitoneally.

3.4. HSC Short-Term Culture in Serum-Free Expansion Medium

In order to use short-term cultured HSC as engrafting cells within the described chimerism-induction protocol, Sca1^{pos}Lin^{neg} HSC must be purified and plated in culture on the first d of the recipient preconditioning.

1. Purify HSC as described in **Subheading 3.2.**
2. Prepare a 24-flat-bottom-well plate by adding 460 µL of fresh and sterile SFEM® medium and place in an incubator at 37°C with 5% CO_2 and 97% humidity.
3. Take desired number of purified Sca1^{pos}Lin^{neg} cells (20,000 cells per well), bring to a minimum spinning volume of 2000 µL by adding fresh SFEM medium, and spin down at 300g for 5 min.
4. Resuspend the pellet in SFEM medium at 20,000 cells/500 µL.
5. Add 20,000 cells (500 µL volume) to each well.
6. Add 100 ng SCF, 100 ng FLT3L, 20 ng IL3, and 20 ng IL6 to each well.
7. Place plate in an incubator at 37°C with 5% CO_2 and 97% humidity.
8. Exchange half of the medium volume after 2, 4, and 5 d by carefully aspirating 540 µL of the medium from the sides of each well and add 500 µL of warmed fresh SFEM medium. Further, renew growth factors on each medium change by adding 100 ng/10 µL SCF, 100 ng/10 µL FLT3L, 20 ng/10 µL IL-3, and 20 ng/10 µL IL-6. Examine the cell-culture once a day on an inverted phase contrast microscope to verify the viability of the plated cell (**Fig. 3**).
9. Harvest cells after 6 d of culture by washing the cloudy layer off the bottom of each well.
10. Transfer cells into a 15-mL conical tube, spin down at 300g for 10 min, and resuspend the pellet in sterile saline to the desired cell concentration.
11. Prepare 1-mL syringes with 30-gage needles with injection volumes of 250–300 µL cell suspension.
12. Use remaining cells to characterize the cells and to quantify percentage of Sca1^{pos} Lin^{neg} cells by flow cytometry (proceed to **Subheading 3.5.2.**).

3.5. Flow Cytometry

3.5.1. Freshly Isolated HSC

1. Spin down cells at 300g for 5 min on a microfuge.
2. Discard supernatant using a Pasteur pipet.
3. Add 100 µL of MACS buffer.
4. Add 1.0 µL of APC-labeled anti-biotin mAB and incubate in the dark for 7–10 min at 4°C.
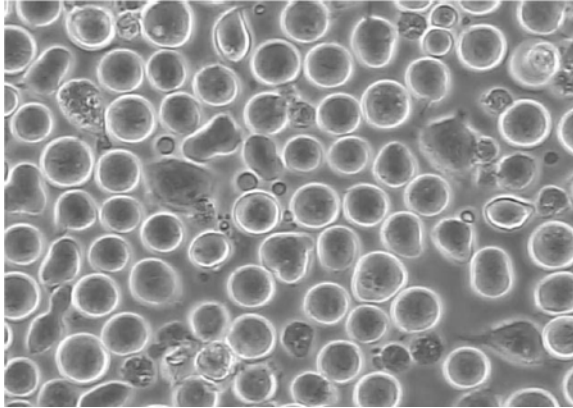
Fig. 3. Sca1^{pos}Lin^{neg} hematopoietic stem cells after 4 d in serum-free expansion medium supplemented with SCF, FLT3L, interleukin-3, and interleukin-6.

5. Wash once by adding 900 μL MACS buffer and spin down for 5 min at 300g on a microfuge.
6. Discard supernatant, resuspend the pellet in about 150 μL of rinse buffer, and proceed to flow cytometry.

3.5.2. Cultured HSC

1. Take 1.0–5.0 × 10^6 cells per tube and staining.
2. Spin down cells at 300g for 5 min on a microfuge.
3. Discard supernatant using a Pasteur pipet.
4. Resuspend pellet in 80 μL of MACS buffer per 10^7 cells.
5. Add the biotinylated lineage panel at 20 μL of each antibody per 10^7 cells and add 0.5 μL of anti-Sca1-FITC.
6. Incubate for 20 min on ice.
7. Add 500 μL of wash buffer (e.g., MACS buffer) and spin down at 300g for 5 min on a microfuge.
8. Resuspend the pellet in 100 μL MACS buffer, add 1.0 μL of APC-labeled anti-biotin mAB, and incubate in the dark for 7–10 min at 4°C.
9. Wash once by adding 900 μL MACS buffer and spin down for 5 min at 300g on a microfuge.
10. Discard supernatant, resuspend the pellet in about 150 μL of rinse buffer, and proceed to flow cytometry.

3.5.3. Screening BALB/c Recipient Mice
for Hematopoietic Chimerism After HSC Transfusion

1. Harvest 50 μL of peripheral blood from each recipient.
2. Transfer blood onto a 96-V-bottom-well plate.
3. Add 150 μL of RBC-lysis buffer per well and incubate on ice for 15 min.
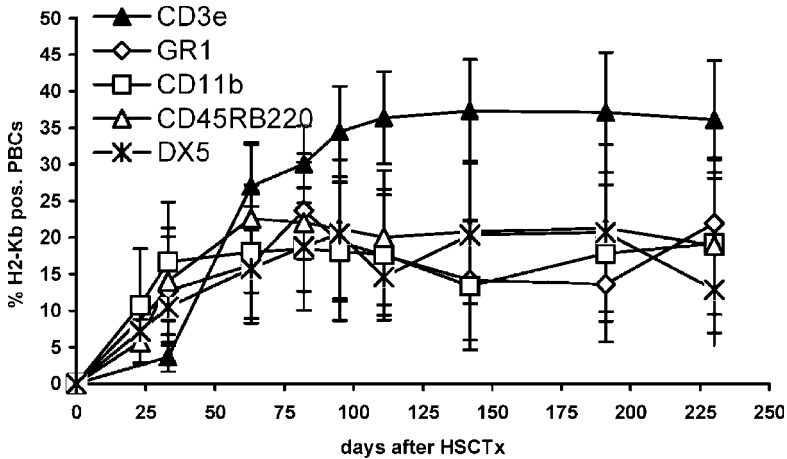
Fig. 4: Expression levels of C57/BL6 H2-K^b (MHC-I) on different lineages of peripheral blood cells in fully allogeneic preconditioned BALB/c H2-K^d-positive mice after transfusion of 20,000 C57/BL6 Sca1^{pos}Lin^{neg} hematopoietic stem cells.

4. Spin down the plate at 300g and 4°C for 5 min.
5. Discard supernatant and add 50 µL of MACS buffer per well.
6. Add 0.5 µL of anti-H2-K^b FITC and 0.5 µL of either anti-CD3e-PE, anti-Ly6G-PE, anti-CD11b-PE, or anti-CD45RB220-PE and incubate in the dark at 4°C for 10 min.
7. Wash by adding 150 µL MACS buffer and spin down at 300g for 5 min.
8. Discard supernatants, resuspend pellets in 100 µL rinse buffer, and proceed to flow cytometry. (Chimerism is measured as percentage of H2-K^b [MHC-I]-antigen-positive cells in peripheral blood, **Fig. 4**.)

4. Notes

1. Expression levels of Sca-1 (Ly-6A/E) on HSC vary between different mouse strains from high to very low and even nonexpression. Mice with a Ly-6.1 haplotype (such as BALB/c, C3H/He, or CBA) have few Ly-6A/E-positive hematopoietic stem cells and are not suitable for HSC purification by Sca-1 bead selection *see* **Subheading 2.1.**).
2. The viability of sorted cells greatly depends on avoiding unnecessary delays. Therefore, work fast and have ice-cold buffers ready to use before starting the experiment.
3. The total cell number of unseparated bone-marrow cells at baseline should be at least 5.0 × 10^8 cells. Using tibiae, femura, and humeri will give a total of 0.7–1.0 × 10^8 bone-marrow cells and about 0.7–1.0 × 10^5 HSC per mouse.
4. Magnetic columns should not be older than 1 wk. Using two new columns per experiment will greatly increase yield and purity of the final cell sort.
5. Mark the orientation of Eppendorf tubes as inserted in microfuges to avoid accidental loss of the pellet when discarding supernatants. Pellets of cell numbers as low as 50,000 cells are barely visible. Use a Pasteur pipet with a rubber suction ball to carefully discard supernatants from Eppendorf tubes.

References

1 Ildstad, S. T. and Sachs, D. H. (1984) Reconstitution with syngeneic plus allogeneic or xenogeneic bone marrow leads to specific acceptance of allografts or xenografts. *Nature* **307(5947),** 168–170.

2 Wekerle, T., Sayegh, M. H., Ito, H., et al. (1999) Anti-cd154 or ctla4ig obviates the need for thymic irradiation in a non-myeloablative conditioning regimen for the induction of mixed hematopoietic chimerism and tolerance. *Transplantation* **68(9),** 1348–1355.

3 Wekerle, T., Kurtz, J., Ito, H., et al. (2000) Allogeneic bone marrow transplantation with co-stimulatory blockade induces macrochimerism and tolerance without cytoreductive host treatment. *Nat. Med.* **6(4),** 464–469.

4 Durham, M. M., Bingaman, A. W., Adams, A. B., et al. (2000) Cutting edge: Administration of anti-cd40 ligand and donor bone marrow leads to hemopoietic chimerism and donor-specific tolerance without cytoreductive conditioning. *J. Immunol.* **165(1),** 1–4.

5 Bachar-Lustig, E., Li, H. W., Marcus, H., and Reisner, Y. (1998) Tolerance induction by megadose stem cell transplants: Synergism between sca-1+ lin– cells and nonalloreactive t cells. *Transplant. Proc.* **30(8),** 4007–4008.

6 Uchida, N., Tsukamoto, A., He, D., et al. (1998) High doses of purified stem cells cause early hematopoietic recovery in syngeneic and allogeneic hosts. ***J. Clin. Invest.* 101(5),** 961–966.

7 Emmanouilidis, N., Hussain, A., Adams, A. B., et al. (2002) Costimulation Blockade, administration of Busulfan and Infusion of purified Sca1^{pos}Lin^{neg} bone marrow cells leads to hematopoietic chimerism in a full MHC disparate mouse model. *Am. J. Trans.* **Suppl. 3(2),** 211.

8 Spangrude, G. J., Heimfeld, S., and Weissman, I. L. (1988) Purification and characterization of mouse hematopoietic stem cells. *Science* **241(4861),** 58–62.

9 Adams, A. B., Durham, M. M., Kean, L., et al. (2001) Costimulation blockade, busulfan, and bone marrow promote titratable macrochimerism, induce transplantation tolerance, and correct genetic hemoglobinopathies with minimal myelosuppression. *J. Immunol.* **167(2),** 1103–1111.

10 Fraser, C. C., Szilvassy, S. J., Eaves, C. J., and Humphries, R. K. (1992) Proliferation of totipotent hematopoietic stem cells in vitro with retention of long-term competitive in vivo reconstituting ability. *Proc. Natl. Acad. Sci. USA* **89(5),** 1968–1972.

11 Petzer, A. L., Hogge, D. E., Landsdorp, P. M., Reid, D. S., and Eaves, C. J. (1996) Self-renewal of primitive human hematopoietic cells (long-term-culture-initiating cells) in vitro and their expansion in defined medium. *Proc. Natl. Acad. Sci. USA* **93(4),** 1470–1474.

12 Neben, S., Donaldson, D., Sieff, C., et al. (1994) Synergistic effects of interleukin-11 with other growth factors on the expansion of murine hematopoietic progenitors and maintenance of stem cells in liquid culture. *Exp. Hematol.* **22(4),** 353–359.

13. Koller, M. R., Oxender, M., Brott, D. A., and Palsson, B. O. (1996) Flt-3 ligand is more potent than c-kit ligand for the synergistic stimulation of ex vivo hematopoietic cell expansion. *J. Hematother.* **5(5),** 449–459.

14. Bryder, D. and Jacobsen, S. E. (2000) Interleukin-3 supports expansion of long-term multilineage repopulating activity after multiple stem cell divisions in vitro. *Blood* **96(5),** 1748–1755.

31

Induction of Mixed vs Full Chimerism to Potentiate GVL Effects After Bone-Marrow Transplantation

Markus Y. Mapara and Megan Sykes

Summary

Graft-vs-host (GVH) alloresponses mediated by delayed donor lymphocyte infusions (DLI) can occur in the absence of GVHD (graft-vs-host disease). These GVH responses are confined to the lymphohematopoietic system and mediate graft-vs-leukemia (GVL) reactions without causing GVHD. Although interaction of donor T-cells with host-derived antigen-presenting cells (APC) is central to the development of GVHD, we were able to show that this T-cell/APC interaction is also critical for the induction of GVL, which can occur in the absence of GVHD if donor T-cell administration is delayed to a time point after bone-marrow transplant (BMT) when conditioning-induced inflammation has subsided. Induction of mixed hematopoietic chimerism using the method described below allows analysis of these interactions between host APC and donor T-cells.

Key Words: Mixed chimerism; donor lymphocyte infusions; GVL; GVH; transplantation.

1. Introduction

Rodent studies have shown that administration of donor lymphocyte infusions (DLI) to mixed hematopoietic chimeras can mediate a graft-vs-host (GVH) reaction that is restricted to the lymphohematopoietic system, as indicated by the conversion from mixed chimerism to full chimerism without the concomitant development of GVH disease (GVHD) *(1,2)*. This suggested an approach to using the GVH alloresponse to achieve graft-vs-leukemia (GVL) without GVHD. In humans, GVL effects have been achieved by the administration of DLI to patients with relapsed chronic myeloid leukemia (CML) after allogeneic bone marrow transplant (BMT) *(3,4)*. In a clinical trial at our institution, mixed chimeras induced with nonmyeloablative conditioning have enjoyed striking remissions of advanced, refractory lymphoid malignancies, both with and without the administration of DLI *(5,6)*. Based on these surprisingly powerful GVL effects, we hypothesized that nontolerant donor lymphocytes might result in stronger GVL effects when administered to mixed hematopoietic chimeras than to full donor chimeras (*see* **Fig. 1**). DLI administration to mixed chimeras produced dramati-
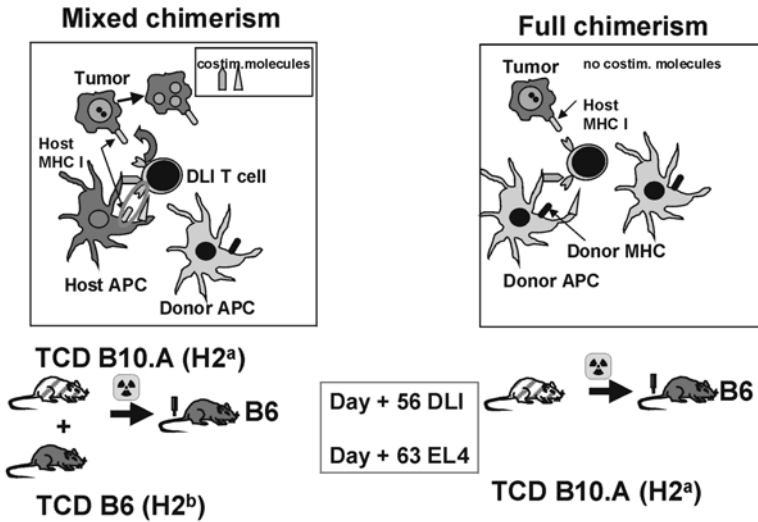
Fig. 1. Generation of mixed and full donor hematopoietic chimeras.

cally improved leukemia-free survival compared to administration of the same DLI to full allogeneic chimeras. DLI also converted mixed chimeras to full chimeras without causing GVHD. The magnitude of the GVL effect was dependent on the level of major histocompatibility complex (MHC) class I expression on recipient hematopoietic cells in mixed chimeras. Thus, induction of mixed chimerism followed by delayed DLI provides an approach to inhibiting GVHD that optimizes GVL effects *(7)*.

2. Materials

2.1. Animals

1. C57BL/6 mice.
2. B10.A mice.
3. B6.β2m$^{-/-}$ mice.

2.2. Operating Tools

1. Microdissecting scissors.
2. Small forceps.
3. Small operating scissors.

2.3. Apparatus and Chemicals

1. Fifty-milliliter conical tubes.
2. Sterile spleen mesh.
3. Syringes (3 cc, 20 to 35 cc).
4. Nineteen-gage, 23-gage, 25-gage needles.

5. Petri dishes, 100×20 mm.
6. CO_2 chamber for euthanasia.
7. CML medium: 500 mL RPMI 1640, 50 mL fetal calf serum (FCS; complement-inactivated 30 min at 55°C), 5 mL 100X nonessential amino acids, 0.146 g L-glutamine (final concentration 2 m*M*), 0.05 g sodium pyruvate (final concentration 1m*M*), 5 mL 1 m*M* HEPES buffer (final concentration 0.01 m*M*), 1 mL 12.5 m*M* 2-mercaptoethanol (final concentration 0.025 m*M*), 50,000 U penicillin, 50 mg streptomycin.
8. Bone marrow medium (BMM): 500 mL Media 199, 5 mL HEPES buffer, 5 mL DNAse (1 mg/mL in H_2O), 40 μL gentamycin (at 50 mg/mL).
9. FACS buffer: 100 mL 10X Hanks balanced salt solution, 900 mL D.I. H_2O, 210 μL of 1 *N* sodium hydroxide (NaOH), 1 g sodium azide (NaN_3), 1 g bovine serum albumin (BSA) fraction V.
10. Antibodies for target cell depletion:
    a. In vitro T-cell depletion: a-CD4 (GK1.5), α-CD-8 (2.43).
    b. In vivo natural killer (NK) cell depletion: NK1.1.

3. Methods

3.1. Animals

B10.A (H-2^a: K^k, A^k, E^k, D^d, L^d) female donor mice purchased from Frederick Cancer Research Facility, NCI, were used at 8 to 12 wk of age. Female C57BL/6 (B6: H-2^b, I-E$^-$) recipient mice were purchased from Frederick Cancer Research Facility, NCI, and used at 10 wk of age. In some experiments, B6.β2m$^{-/-}$ animals and wild-type control B6 mice were purchased from Jackson Laboratories (Bar Harbor, ME). All mice were housed in autoclaved micro-isolator environments, and all manipulations were performed in a laminar flow hood (*see* **Note 1**).

3.2. Bone-Marrow Harvest, Transplantation, and Generation of Mixed and Full Donor Chimeras

1. Animals were sacrificed by CO_2 inhalation and dissected under sterile conditions.
2. The femora and tibiae were collected and flushed with BMM.
3. After cell counting, cells were subjected to in vitro T-cell depletion by antibody-complement lysis (*see* **Subheading 3.3.**).
4. B6 (H2^b) mice received 10.25 Gy total body irradiation from a ^{37}Cs irradiator in a single dose (dose rate 1cGy/min, *see* **Note 2**) and were reconstituted with either a mixture of T-cell-depleted (TCD) B6 (5×10^6 bone-marrow cells) plus B10.A (H2^a) (15×10^6) bone-marrow cells or with TCD B10.A bone marrow cells (15×10^6) alone by lateral tail-vein injection 4 h after irradiation. The complete experimental setup is depicted in **Fig. 1**.

3.3. In Vitro T-Cell Depletion

In vitro depletion of CD4 and CD8 T-cells from the bone-marrow inoculum was performed using mAbs and rabbit low toxic complement lysis (*see* **Note 3**) as previously described *(7)*:

1. BMC were adjusted to a working cell concentration of 5×10^7 cells/mL with BMM.
2. After washing, cells were labeled with a predetermined (by separate titrations of depletion activity) amount of anti-CD4 (Gk1.5) and anti-CD8 (2.43) antibodies from ascites for 30 min at room temperature.

3. Thereafter, cells were washed twice and incubated with a predetermined amount of low-toxic rabbit complement for 45 min at 37°C.

4. Thereafter cells were washed and T-cell depletion efficiency was determined by flow cytometry.

5. Complete T-cell depeletion is critical for establishing mixed chimeras, as residual host or donor T-cells from the bone-marrow graft will lead to spontaneous development of either full host or full donor chimerism, respectively *(8)*.

3.4. In Vivo NK Cell Depletion

To demonstrate the role of direct allorecognition, it was necessary to establish mixed chimeras in which host hematopoietic cells were devoid of MHC class expression. This was performed by reconstituting wild-type B6 mice with a mixture of T-cell-depleted B10.A marrow and T-cell-depleted B6.β2m$^{-/-}$ marrow. It is known that recipient NK cells reject MHC class I deficient bone-marrow cells, a phenomenon also known as "hybrid resistance," which describes the observation that F1 mice reject the parental bone-marrow grafts due to the missing self MHC I molecules. In order to achieve engraftment of MHC I deficient B6.β2m$^{-/-}$ marrow in animals receiving B10.A plus B6.β2m$^{-/-}$ bone-marrow cells, recipient mice received 150 µg of mAb PK136 (NK1.1) on d –6 and –1 prior to BMT.

3.5. Phenotyping of Chimeras

Chimerism in white blood cells (WBC) and bone marrow was assessed by two-color or three-color flow cytometry (FCM) using a FACScan cytometer (Becton Dickinson, Mountain View, CA).

1. Peripheral blood was collected into heparinized Eppendorf tubes and subjected to deionized water lysis.

2. For double or triple color staining, 10^6 cells were incubated in the presence of directly fluorescein-isothiocyanate (FITC)-, phycoerythrin (PE)-, or biotin (Bio)-conjugated monoclonal antibodies (mAbs) for 30 min at 4°C.

3. Development of bio-labeled mAbs was performed by subsequent incubation with phycoerythrin-conjugated avidin (PEA) for 10 min.

4. To reduce nonspecific binding of mAbs, 10 µL of 2.4G2 (anti-Fcγ-RII-receptor, CDw32) hybridoma supernatant *(9)* were added to all tubes. The following antibodies were used for chimerism analyses in various cell lineages: anti-CD4-FITC, anti-CD8β-FITC, anti-B220-FITC (all purchased from PharMingen, San Diego CA), anti-Mac-1-FITC (CalTag, San Francisco, CA), and 34-2-12-Bio (anti-H2-D^d prepared in our laboratory). Nonreactive control mAb HOPC-FITC or HOPC-Bio (mouse IgG2a prepared in our laboratory) and rat IgG2b-PE (Pharmingen) were used as negative controls.

5. The percentage of donor cells within each leukocyte population was determined using the following formula: Net percent donor cells of a particular lineage × 100%/(net percent donor cells of a particular lineage + net percent host cells of a particular lineage), where net refers to the percentage obtained after subtraction of staining with control antibody. For the H-2 class I allele-specific mAb, the mouse strain (donor or host) not bearing the allele recognized by the mAb was used as the negative control and the strain expressing the allele was used as the positive control to determine the cutoffs for reactivity with the H2-specific mAb. Exclusion of dead cells was performed by propidium iodide (PI) staining and live gating on PI negative cells. Ten thousand events were collected and ana-

lyzed. The different peripheral blood leukocyte populations were distinguished by their forward scatter (FSC) and side scatter (SSC) properties: FSC low and SSC low (lymphocytes), SSC high (granulocytes), and FSC high and SSC low (monocytes).

3.6. Preparation of DLI

For preparation of DLI, B10.A spleens were harvested and gently teased in ACK lysing buffer (Biowhittaker, Walkersville, MD). Single-cell suspensions were filtered through nylon mesh. Donor lymphocytes were administered in the form of 3×10^7 B10.A spleen cells on d 56 post-BMT. Animals were randomized between cages to avoid cage-related bias.

3.7. EL4 Cell Culture

The T-cell leukemia cell line EL4 (500 cells) was administered intravenously on d 63. EL4 cells were originally obtained from ATCC and were cultured in CML medium. A new vial of a working bank of EL4 cells was thawed for each experiment and maintained in culture for a maximum of 2 wk.

4. Notes

1. As in all BMT experiments, it is extremely important to have an animal facility that complies with specific pathogen-free (SPF) or SPF-like standards to prevent the development of opportunistic infections after allogeneic bone-marrow transplantation.
2. In order to prevent conditioning-induced mortality, it is important to use a low dose rate (100 rad/min) for total body irradiation.
3. Achieving complete T-cell depletion of the bone-marrow graft is crucial for obtaining stable mixed chimerism and avoiding GVH reactions that might induce a proinflammatory state that could persist at the time of DLI and lead to GVHD. The method described in **Subheading 3.3.** is based on antibody-complement-mediated lysis of T-cells. Appropriate antibody titers of Gk1.5 and 2.43 antibodies have to be predetermined by titration, to allow optimal coating of target cells and to avoid anticomplementarity due to excess antibody. It is also important to select rabbit complement batches that have a very low background toxicity (i.e., low lysis without antibody preincubation). Alternatively, thorough T-cell depletion also can be achieved using magnetic cell separation with MACS beads from Miltenyi.

Acknowledgments

References

1 Sykes, M., Sheard, M. A., and Sachs, D. H. (1988) Graft-versus-host-related immunosuppression is induced in mixed chimeras by alloresponses against either host or donor lymphohematopoietic cells. *J. Exp. Med.* **168,** 2391–2396.
2 Pelot, M. R., Pearson, D. A., Swenson, K., et al. (1999) Lymphohematopoietic graft-vs-host reactions can be induced without graft-vs.-host disease in murine mixed chimeras established with a cyclophosphamide-based nonmyeloablative conditioning regimen. *Biol. Blood Marrow Transplant.* **5,** 133–143.

3 Kolb, H. J., Mittrmuller, J., Clemm, C., et al. (1990) Donor leukocyte transfusions for treatment of recurrent chronic myelogenous leukemia in marrow transplant patients. *Blood* **76,** 2462–2465.

4 Kolb, H.-J., Schattenberg, A., Goldman, J. M., et al. (1995) Graft-versus-leukemia effect of donor lymphocyte transfusions in marrow grafted patients. European Group for Blood and Marrow Transplantation Working Party Chronic Leukemia. *Blood* **86,** 2041–2050.

5 Spitzer, T. R., McAfee, S., Sackstein, R., et al. (2000) Intentional induction of mixed chimerism and achievement of antitumor responses after nonmyeloablative conditioning therapy and HLA-matched donor bone marrow transplantation for refractory hematologic malignancies. *Biol. Blood Marrow Transplant.* **6,** 309–320.

6 Sykes, M., Preffer, F., McAffee, S., et al. (1999) Mixed lymphohaemopoietic chimerism and graft-versus-lymphoma effects after non-myeloablative therapy and HLA-mismatched bone-marrow transplantation. *Lancet* **353,** 1755–1759.

7 Mapara, M. Y., Kim, Y.-M., Wang, S. P., Bronson, R., Sachs, D. H., and Sykes, M. (2002) Donor lymphocyte infusions mediate superior graft-versus-leukemia effects in mixed compared to fully allogeneic chimeras: a critical role for host antigen-presenting cells. *Blood* **100,** 1903–1909.

8. Ildstad, S. T., Wren, S. M., Bluestone, J. A., Barbieri, S. A., Stephany, D., and Sachs, D. H. (1986) Effect of selective T cell depletion of host and/or donor bone marrow on lymphopoietic repopulation, tolerance, and graft-vs-host disease in mixed allogeneic chimeras (B10 + B10.D2——B10). *J. Immunol.* **136,** 28–33.

9. Unkeless, J. C. (1979) Characterization of a monoclonal antibody directed against mouse macrophage and lymphocyte Fc receptors. *J. Exp. Med.* **150,** 580–596.

32

Application of Donor Lymphocytes Expressing a Suicide Gene for Early GVL Induction and Later Control of GVH Reactions After Bone-Marrow Transplantation

Attilio Bondanza, Fabio Ciceri, and Chiara Bonini

Summary

Allogeneic hematopoietic stem cell transplantation (allo-SCT) is the treatment of choice for many malignant diseases. It is recognized that the curative potential of allo-SCT relates closely to the immune advantage conferred by allogeneic T-lymphocytes. In allo-SCT donor T-lymphocytes favor engraftment, provide early immune reconstitution, and fight the underlying malignancy—the so-called graft-vs-leukemia (GVL) effect. These benefits are counterbalanced by the occurrence of a life-threatening disease: graft-vs-host disease (GVHD). A suicide gene encodes a protein able to convert a nontoxic prodrug into a toxic product. Therefore, cells expressing the suicide gene become selectively sensitive to the prodrug. The transfer of a suicide gene into donor lymphocytes could allow, upon administration of the prodrug, the in vivo selective elimination of transduced lymphocytes, resulting in the switch-off of GVHD, thus allowing full exploitation of the curative potential of donor T-lymphocytes in the context of allo-SCT. In this chapter the rationale, the materials, and the methods of the suicide-gene strategy with human T-lymphocytes are described.

Key Words: Bone marrow transplantation; graft-vs-leukemia, graft-vs-host disease, stem cells.

1. Introduction

1.1. Adoptive Transfer of Donor T-Lymphocytes in Allo-SCT

Both preclinical and clinical data suggest that the curative potential of allo-SCT closely relates to the immune advantage of allogeneic lymphocytes. Although neither the nature of effector cells nor the antigenic targets have been fully elucidated, the allogeneic advantage in abating relapse probability is well documented *(1)*. Furthermore, the administration of donor lymphocytes has become a new tool for treating relapse of hematologic malignancies occurring after allo-SCT *(2,3)* and holds promise also for the cure of solid tumors *(4)*.

Before donor lymphocyte infusion (DLI) became a standard treatment, patients relapsing after allo-SCT had a very poor prognosis. Since 1989, many patients affected by hematologic malignancies relapsing after allo-SCT achieved complete remissions after DLI without requiring any further cytoreductive therapy *(2,5–10)*, thus demonstrating the efficacy of the allogeneic immune advantage in allo-SCT. Unfortunately, clinical success was often associated with the occurrence of GVHD, especially when high numbers of T-cells were infused *(3,11)*. New DLI regimens—i.e., infusion of escalating dose of lymphocytes—lowered the incidence of GVHD, but this complication remains the major obstacle for success of DLI *(13)*.

A possible alternative strategy relies on the generation and infusion of leukemia-specific T-lymphocytes. Up to now, adoptive immunotherapy with antigen-specific T-cells has been used in viral disease such as cytomegalovirus (CMV) reactivation syndromes *(14)* and Epstein–Barr virus lymphoproliferative disease (EBV-LPD) *(15)*, and has been investigated for the cure of metastatic solid tumors such as melanoma *(16)*.

The overall results of adoptive immunotherapy with virus-specific T-cells are encouraging, with good efficacy and virtually no occurrence of GVHD *(17)*. Thus, results of such an approach targeted on leukemia produced high expectations, till now still to be met *(18–20)*. Indeed, despite the fact that GVHD and GVL are potentially mediated by donor T-lymphocytes with different specificities, we cannot yet differentiate GVL and GVHD effector cells.

1.2. The Suicide-Gene Strategy

In allo-SCT, the transfer of a heterogeneous population of donor T-cells with a wide range of antigen specificities offers some clear advantages over strategies involving infusion of antigen-specific cells. First, such a population can provide more complete immune reconstitution in immune-compromised allo-SCT patients. Furthermore, since most targets of GVL are still unknown, the use of the entire T-cell repertoire seems to be the best option to fully exploit GVL. To reduce the risks of uncontrolled GVHD associated with DLI, genetic modification of donor lymphocytes to confer an inducible suicide phenotype has been proposed and tested at clinical level. A suicide gene encodes for a protein able to convert a nontoxic prodrug into a toxic product. Therefore, cells expressing the suicide gene become selectively sensitive to the prodrug and can be selectively eliminated if unwanted effects such as GVHD occur (**Fig. 1**).

Different suicide genes have been investigated and described in recent years. Up to now, the thymidine kinase of herpes simplex virus (HSV*tk*) seems to be the most effective and was the first tested in clinical trials *(21,22)*.

1.3. Suicide-Gene Therapy in Allo-SCT: The Technology

1.3.1. The Vectors

Genetic modification of primary human T-lymphocytes is currently tested for the treatment of inherited and acquired disease. This is commonly accomplished through replication-defective retroviral vectors (RV). RV based on the Moloney murine leukemia virus were the first utilized in clinical trials and remain the most effective approach for introduction of genes into human T-lymphocytes. RV are produced by packaging
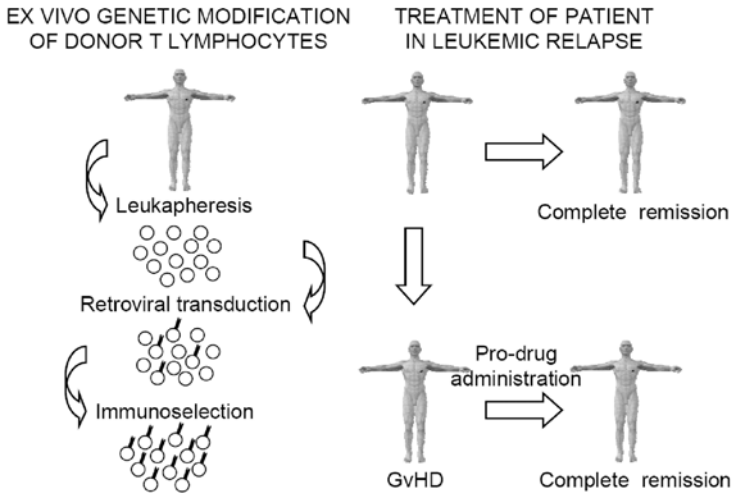
Fig. 1. Schematic representation of the suicide gene strategy. Donor T-lymphocytes are harvested by leukapheresis, transduced with a retroviral vector carrying a suicide gene (i.e., thymidine kinase of herpes simplex virus [HSV*tk*]) and a cell-surface marker (i.e., ΔLNGFR, *see* text), and immunoselected to homogenous expression. If disease relapse occurs after a T-cell-depleted bone-marrow transplant, transduced donor lymphocytes are infused into the patient in order to obtain a graft-vs-leukemia effect. If graft-vs-host disease occurs, a specific prodrug (i.e., ganciclovir) selectively toxic to the transduced cells is administered to the patient, aiming at switch-off of the disease.

cell lines that are laboratory "factories" specialized in producing high titers of replication-defective RV *(23)*. Practically, gene transfer by RV is usually accomplished by high-speed centrifugation of the target cells within the packaging cell line supernatant (spinoculation). It is also possible to preconcentrate the virus particles onto plates coated with the CH-296 fragment of fibronectin (Retronectin) for higher transduction efficiency *(24)*.

Because RV transduce only proliferating cells, target T-cells are induced to active cell proliferation through polyclonal stimulation *(25,26)* before transduction with a suicide vector. This allows the transduction of a polyclonal T-cell population, potentially representative of all T-cell precursors circulating in healthy donors *(27)*, including precursors able to mediate antitumor and antiviral responses *(21)*. However, the variability in response to activation stimuli, activation-induced cell death (AICD), exposure to rhIL-2, and proliferation-induced T-cell exhaustion could alter the half-life, the immune repertoire, and the immune competence of transduced cells *(28)*. RV transduction often results in an inversion of the physiologic CD4/CD8 ratio, enrichment in memory cells associated with loss of naive T-cells *(29)*, a skew in the T-cell antigen receptor (TCR) repertoire to oligoclonality as assessed by the analysis of the Vβ families *(30)*, and a reduced in vivo alloreactivity *(31,32)*. Indeed, the latter modi-
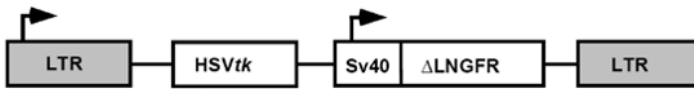
Fig. 2. Schematic map of integrated SFCMM3 proviral genome. Gray boxes indicate long terminal repeat sequences. White boxes indicate the transgenes. HSV*tk* codes for the herpes simplex virus thymidine kinase and ΔLNGFR codes for a truncated form of the low-affinity receptor for nerve-growth factor. The latter transgene is preceded by the control of the simian virus 40 (Sv40). Arrows indicate transcription promoters.

fications are attributed more appropriately to ex vivo culture than to the gene transfer procedure. As a matter of fact, transduction protocols that include optimal T-cell activation and shorter culture times better preserve the immune competence of transduced T-cells *(29)*. To overcome alterations of immune competence secondary to in vitro culture, new cell manipulation protocols are being investigated. Co-stimulation through CD28 along with TCR triggering appear to reduce the skewing in the Vβ families of the TCR *(30,33)* and to partially preserve the anti-EBV immune response *(34)*. Alternative vectors with reduced cell manipulation requirements, such as lentiviral vectors, may improve immunocompetence of transduced cells *(35)*.

1.3.2. The Selection Marker

Because even the most efficient RV cannot transduce the totality of proliferating T-lymphocytes, it is necessary, along with the gene of interest, to insert into the cell a gene that enables for the selection of genetically modified cells (GMC) to virtually 100% purity (selection marker). The RV vector we are currently using is depicted in **Fig. 2**.

There are two types of selection marker genes currently utilized in clinical trials. The first are intracellular factors, such as the gene coding for neomycin phosphotransferase resistance (NeoR) and its analog G418 *(36)*. Selection of GMC requires prolonged culture with a drug that can be toxic, albeit to a lower extent, also to GMC *(31,34)*. Moreover, resistance marker genes cannot be detected by easy means such as flow cytometry *(37)*. Newly designed resistance marker genes are expected to solve many of the limitations of NeoR *(38)*.

An alternative approach relies on the use of a surface marker not expressed by target cells *(26)*. A gene encoding for the truncated form of the low-affinity cell-surface receptor of human nerve growth factor (ΔLNGFR) was the first surface marker successfully utilized in clinical suicide-gene therapy trials *(39)*. New chimeric surface markers such as the fusion gene between HSV*tk* and the surface molecule CD34 *(40,41)*, or the CD20 molecule, have now been developed. Advantages of these new markers rely on the double role of marker and suicide genes.

1.3.3. The Suicide Gene

A suicide gene encodes for a protein able to convert a nontoxic prodrug into a toxic product. Different suicide genes have been investigated and described in recent years.

HSV*tk*   Cellular kinases

GCV ⟶ pGCV ⟶ pppGCV

Incorporation into DNA:
- chain termination
- strand breaks

Cell Death ◀
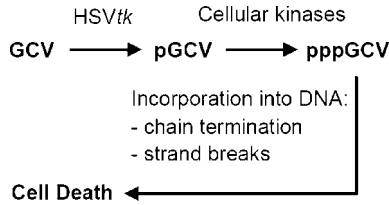
Fig. 3. Mechanism of toxic activity of the prodrug gancyclovir (GCV) on herpes simplex thymidine kinase (HSV*tk*)-expressing cells. Upon entry into the cells, HSV*tk* metabolizes GCV to a monophosphate intermediate derivative (pGCV). Cellular kinases further phosphorylate it to a triphosphate compound (pppGCV), which is the toxic form. pppGCV is then incorporated into DNA, resulting in efficient inhibition of DNA elongation and causing strand breaks. This ends up with selective death of HSV*tk*-expressing cells *(27)*.

Table 1
Overview of the Characteristics of Different Suicide Genes in Allo-SCT

Suicide gene	Prodrug	Prodrug approved for clinical use	Cell cycle dependence	Immunogenicity
HSV*tk*	GCV	Yes	Yes	Yes
ΔFas	AP1903	No	No	No
CD20	Rituximab	Yes	No	No

HSV*tk*, Thymidine kinase of herpes simplex virus; GCV, ganciclovir.

Up to now, HSV*tk* seems to be the most effective (**Fig. 3**). The HSV*tk* has been successfully transferred into different cell lines to confer ganciclovir (GCV) sensitivity, and its efficacy has been shown both in vitro and in vivo *(36,42)*. Only recently, a molecular mechanism for GCV resistance in human HSV*tk*-expressing T-lymphocytes was described *(43,44)*.

HSV*tk* was the first suicide gene to be used in clinical trials of allo-SCT *(37,45)*. Despite its efficacy and safety, the HSV*tk*/GCV approach has some limitations *(28)*. Firstly, HSV*tk* is a gene of viral origin, which can induce a cytotoxic CD8^{+} T-cell response leading to the elimination of GMC *(21)*. Moreover, HSV*tk*-mediated killing of transduced lymphocytes is cell-cycle dependent. GMC elimination can be a problem with slowly proliferating cells. Initially considered as a disadvantage, the latter phenomenon has been recently proposed as a platform for the separation of GVHD from the GVL effect by tuning on the kinetics of GCV administration *(46,47)*. Finally, the use of GCV for the treatment of CMV results in undesired clearance of HSV*tk* donor lymphocytes.

To circumvent these limitations (see overview on suicide genes depicted in **Table 1**), novel suicide switches were designed. The first proposed was based on the human Fas receptor to trigger cell death in primary human T-lymphocytes *(50,51)*. Another prom-

ising suicide gene is represented by the CD20 molecule, physiologically expressed on the surface of B- and not T-lymphocytes *(50)*. Since the humanized chimeric mono-clonal antibody directed against human CD20 (Rituximab) is able to kill CD20-express-ing cells *(51)*, CD20 expression on T-lymphocytes can serve both as a suicide gene and as a selection marker *(52)*.

1.4. Suicide-Gene Therapy in Allo-SCT: Clinical Results

Suicide-gene therapy with GMC after allo-SCT proved to be safe and effective in phase I clinical trials *(22,23,53–55.)*

The first study performed at HSR in Milan showed that the infusion of HSV*tk*-transduced donor lymphocytes to eight patients, who underwent allogeneic transplan-tation and had subsequent disease relapse or EBV-induced lymphoproliferative disorders, was effective in five out of eight, with three patients obtaining complete remission. Two patients developed acute GVHD and were treated with GCV with clearance of circulating GMC and complete regression of GVHD. In one patient, who developed chronic GVHD, GCV administration allowed for a reduction of GMC and a partial clinical response.

Tiberghien et al. at the University Hospital (CHU), Besancon, treated 12 patients with escalating doses of cells transduced with HSV*tk* and NeoR, as prophylaxis against disease relapse after HLA-identical T-cell-depleted marrow transplantation *(23)*. The presence of circulating GMC was shown in 10 out of 11 patients. The treatment with GCV resulted in a significant reduction of GMC in all patients and in complete remis-sion of the GVHD signs in two out of three patients, with acute GVHD of a grade = II and in one of one patient with chronic GVHD.

In a pilot study conducted by Link et al., in which GMC with HSV*tk* and NeoR were administered as DLI after allo-SCT, the percentage of circulating transduced lymphocytes ranged from 0 to 3.8 %. Three patients responded to the infusion in terms of antitumoral activity. One patient developed chronic GVHD that did not respond to conventional therapy but did respond to GCV *(53,54)*.

Champlin et al. conducted a phase I/II study with GMC with HSV-tk for relapse after allo-SCT. Twenty-three patients were treated with one to four doses per patient (from 0.7 to 190×10^6 cells/kg). In almost all the patients, it was possible to document the presence of circulating GMC, and there was no adverse reaction to the treatment. Two patients, affected by chronic myelogenous leukemia, had complete remission with a dose of 50 or 85×10^6 cells/kg, and four had a stabilization of the disease. Only one patient developed grade I GVHD, for which no therapy was needed *(55)*.

Different levels of clinical response obtained in different pilot studies are in part explained by the complexity of the ex vivo manipulation procedures. Published stud-ies utilized different culture conditions and different degrees of in vitro expansion of GMC. This has been shown to affect in vivo survival, expansion, and effector poten-tial of GMC. Despite these difficulties, in all clinical studies, it was possible to kill GMC in vivo upon administration of GCV and to control GVHD.

The full exploitation of the strategy requires validation of the technology in extended multicentric trials. This challenging process is now ongoing.

2. Materials

2.1. Preparation of Human Lymphocytes
Retrovirally Transduced to Express a Suicide Gene

2.1.1. Activation and Transduction of Human Lymphocytes
With a Retroviral Vector Carrying the Suicide Gene and the Marker Gene

1. Lymphoprep (Nycomed, Oslo, Norway). Store at 4°C.
2. Medium for T-cell culture: RPMI 1640 (BioWhittaker Europe, Verviers, Belgium). For 500 mL final: Add 5 mL of 200 m*M* glutamine (GibcoGrand Island, NY), 0.5 mL of 100.000 UI/mL penicillin (Pharmacia, Milan, Italy), 0.5 mL of 100.000 UI/mL streptomicin (Bristol-Myers Sqiubb, Sermoneta, LT), 25 mL autologous serum, 1 mL of hu-r-IL-2 (Chiron Milan, Italy), 50.000 U/mL. Store at 4°C.
3. Phytoemoagglutinine (PHA) (Boehringer Mannheim-Roche GmbH, Mannheim, Germany). Stock solution 1 mg/mL. Store at –20°C. Use at the final concentration of 2 μg/mL.
4. Anti-CD3 mAb (OKT3) (Orthoclone, Milan, Italy). Stock solution 1 mg/mL. Prepare working solution at 100 μg/mL. Store at 4°C. Use at the final concentration of 30 ng/mL.
5. Anti-CD28 mAb (PharMingen, San Diego, CA). Stock solution 1 mg/mL. Store at 4°C. Use at the final concentration of 1 μg/mL.
6. Polybrene (Sigma-Aldrich Chemie GmbH, Steinhgeim, Germany). Stock solution at 0.8 mg/mL. Store at 4°C.

2.1.2. Cytofluorimetric Analysis and Immune Selection of Transduced Cells

1. mAb 20.4 specific for LNGFR (HB8737) (American Type Culture Collection [ATCC], Rockville, MD). Store at 4°C in the dark.
2. FITC-conjugated goat-antimouse Ab (DAKO, Glostrup, Denmark). Store at 4°C in the dark.
3. Goat antimouse-IgG1 coated magnetic beads (Dynabeads M-450, Dynal AS, Oslo, Norway). Store at 4°C in the dark.

2.1.3. Analysis of Transduced and Selected Cells

1. Ganciclovir (Syntex, Palo Alto, CA). Prepare aliquots at 100 μ*M* and store at –20°C.
2. Radiolabeled thymidine (³H-Thy; Dupont, Boston, MA). Stored at 4°C.

3. Methods

3.1. Preparation of Human Lymphocytes
Retrovirally Transduced to Express a Suicide Gene

The preparation of genetically modified cells is based on different steps:

1. Activation and transduction of human lymphocytes with a retroviral vector carrying the suicide gene and the marker gene.
2. Immune selection of transduced cells. This step exploits the expression of the cell surface marker gene by genetically modified cells.
3. Analysis of transduced cells in terms of purity and suicide phenotype.

3.1.1. T-Cell Transduction With SFCMM-3 Retroviral Vector

Primary human lymphocytes are transduced with a replication competent retrovirus (RCR)-free supernatant coding for the suicide gene and a marker. As an example, we can utilize the SFCMM-3 vector *(21)*, encoding for the suicide gene HSV-tk and for a

truncated form of the low-affinity receptor for nerve growth factor (ΔLNGFR) as a cell-surface marker *(27)*.

The protocol of T-cell manipulation is the following:

1. Day 0: Primary human lymphocytes harvested from healthy donors are isolated by leukapheresis and Ficoll-Hypaque gradient separation (Lymphoprep Nycomed, Pharma AS, Oslo, Norway) and activated in vitro. Different activation signals can be utilized.
2. Phytoemoagglutinine (PHA), 2 µg/mL.
3. Anti-CD3 mAb (OKT3), 30 ng/mL
4. Anti-CD3 mAb 30 ng/mL plus anti-CD28 mAb, 1 µg/mL.
5. Activated T-cells are cultured at 1×10^6 cells/mL, in medium for T-cell culture.
6. Day 2. First round of transduction is performed by one cycle of 2 h centrifugation of T-cells in viral supernatant in the presence of polybrene (8 µg/mL) at a multiplicity of infection (MOI) = 3/1. Cells are plated in medium for T-cell culture at 37°C for 18 h.
7. Day 3. Second round of transduction is performed by one cycle of 2 h centrifugation of T-cells in viral supernatant in the presence of polybrene (8 µg/mL) at an MOI = 3/1. Cells are plated in medium for T-cell culture at 37°C.
8. Day 5. Transduction efficiency is determined by FACS analysis. To this purpose, 0.2×10^6 transduced cells are stained with 100 µL of the mouse antihuman LNGFR mAb 20.4 for 30 min at 4°C and washed twice in PBS. Cells are then stained with FITC-conjugated goat-antimouse Ab for 30 min at 4°C. Transduced cells stained only with FITC-conjugated goat-antimouse Ab are used as negative controls. After two additional washes with PBS, samples are analyzed on FACSCalibur® (Becton Dickinson) using CellQuest software (BD Biosciences).

3.1.2. Immuneselection of Transduced Cells

This step exploits the expression of the cell-surface marker gene by genetically modified cells. During this step, cells are immunoselected to homogeneous transgene expression.

1. Day 6. Transduced cells are stained with the anti-LNGFR MAb for 30 min at 4°C, washed twice with PBS, and stained with goat-antimouse-IgG1 coated magnetic beads for an additional 30 min at 4°C. After two additional washes with PBS, transduced cells are selected on magnetic beads according to manufacturer's instructions. Cells are plated in medium for T-cell culture.
2. Day 7. Beads are eliminated from selected cells by exposure to the magnet.

3.1.3. Analysis of Transduced Cells
in Terms of Purity and Suicide Phenotype

During this step, the efficiency of the overall procedure is analyzed: this requires the analysis of purity after T-cell selection and the analysis of ganciclovir sensitivity of transduced/selected cells.

1. Day 8. Selection efficiency is analyzed by FACS as described in **Subheading 3.1.1., step 8** (method utilized at d 5). A purity of at least 90% is usually obtained and allows us to perform further experiments in the absence of an additional step of cell immune selection.
2. Within the following wk, GCV sensitivity of transduced and selected cells is analyzed. Since GCV-mediated killing requires cell proliferation, cells are restimulated in vitro following the same conditions described on d 0 in the presence of increasing GCV con-

centrations (0.01 to 10 μ*M*), in 96-well plates at 0.1×10^6 cells/well in triplicates. After 4 d, radiolabeled thymidine (1 μCi/well; specific activity 87 Ci/mmol) is added and DNA is harvested after an additional 16 h. Cpm are counted in a beta scintillation counter (Wallac 1205 BetaPlate). The effect of GCV on transduced lymphocytes is expressed as percentage of growth inhibition or as relative proliferation, referring to proliferation in the absence of ganciclovir. A GCV concentration of 0.1 μ*M* induces more than 90% growth inhibition in T-cells transduced with SFCMM-3.

References

1 Horowitz, M. M., Gale, R. P., Sondel, P. M., et al. (1990) Graft-versus-leukemia reactions after bone marrow transplantation. *Blood* 7**5,** 555–562.

2 Kolb, H. J., Mittermuller, J., Clemm, C., et al. (1990) Donor leukocyte transfusions for treatment of recurrent chronic myelogenous leukemia in marrow transplant patients. *Blood* **76,** 2462–2465.

3 Kolb, H. J., Schattenberg, A., Goldman, J. M., et al. (1995) Graft-versus-leukemia effect of donor lymphocyte transfusions in marrow grafted patients. European Group for Blood and Marrow Transplantation Working Party Chronic Leukemia. *Blood* **86,** 2041–2050.

4 Childs, R., Chernoff, A., Contentin, N., et al. (2000) Regression of metastatic renal-cell carcinoma after nonmyeloablative allogeneic peripheral-blood stem-cell transplantation. *N. Engl. J. Med.* **343,** 750–758.

5 Drobyski, W. R., Keever, C. A., Roth, M. S., et al. (1993) Salvage immunotherapy using donor leukocyte infusions as treatment for relapsed chronic myelogenous leukemia after allogeneic bone marrow transplantation: efficacy and toxicity of a defined T-cell dose. *Blood* **82,** 2310–2318.

6 Szer, J., Grigg, A. P., Phillips, G. L., and Sheridan, W. P. (1993) Donor leucocyte infusions after chemotherapy for patients relapsing with acute leukaemia following allogeneic BMT. *Bone Marrow Transplant.* **11,** 109–111.

7 Porter, D. L., Roth, M. S., McGarigle, C., Ferrara, J. L., and Antin, J. H. (1994) Induction of graft-versus-host disease as immunotherapy for relapsed chronic myeloid leukemia. *N. Engl. J. Med.* **330,** 100–106.

8 van Rhee, F., Lin, F., Cullis, J. O., et al. (1994) Relapse of chronic myeloid leukemia after allogeneic bone marrow transplant: the case for giving donor leukocyte transfusions before the onset of hematologic relapse. *Blood* **83,** 3377–3383.

9 Slavin, S., Naparstek, E., Nagler, A., et al. (1996) Allogeneic cell therapy with donor peripheral blood cells and recombinant human interleukin-2 to treat leukemia relapse after allogeneic bone marrow transplantation. *Blood* **87,** 2195–2204.

10 Tricot, G., Vesole, D. H., Jagannath, S., Hilton, J., Munshi, N., and Barlogie, B. (1996) Graft-versus-myeloma effect: proof of principle. *Blood* **87,** 1196–1198.

11 Collins, R. H., Jr., Shpilberg, O., Drobyski, W. R., et al. (1997) Donor leukocyte infusions in 140 patients with relapsed malignancy after allogeneic bone marrow transplantation. *J. Clin. Oncol.* **15,** 433–444.

12 Mackinnon, S., Papadopoulos, E. B., Carabasi, M. H., et al. (1995) Adoptive immunotherapy evaluating escalating doses of donor leukocytes for relapse of chronic myeloid leukemia after bone marrow transplantation: separation of graft-versus-leukemia responses from graft-versus-host disease. *Blood* **86,** 1261–1268.

13 Guglielmi, C., Arcese, W., Dazzi, F., et al. (2002) Donor lymphocyte infusion for relapsed chronic myelogenous leukemia: prognostic relevance of the initial cell dose. *Blood* **100,** 397–405.

14 Riddell, S. R., Watanabe, K. S., Goodrich, J. M., Li, C. R., Agha, M. E., and Greenberg, P. D. (1992) Restoration of viral immunity in immunodeficient humans by the adoptive transfer of T cell clones. *Science* **257,** 238–241.

15 Rooney, C. M., Smith, C. A., Ng, C. Y., et al. (1995) Use of gene-modified virus-specific T lymphocytes to control Epstein-Barr-virus-related lymphoproliferation. *Lancet* **345,** 9–13.

16 Yee, C., Thompson, J. A., Byrd, D., et al. (2002) Adoptive T cell therapy using antigen-specific CD8+ T cell clones for the treatment of patients with metastatic melanoma: in vivo persistence, migration, and antitumor effect of transferred T cells. *Proc. Natl. Acad. Sci. USA* **99,** 16,168–16,173.

17 Papadopoulos, E. B., Ladanyi, M., Emanuel, D., et al. (1994) Infusions of donor leukocytes to treat Epstein-Barr virus-associated lymphoproliferative disorders after allogeneic bone marrow transplantation. *N. Engl. J. Med.* **330,** 1185–1191.

18 Molldrem, J. J., Lee, P. P., Wang, C., et al. (2000) Evidence that specific T lymphocytes may participate in the elimination of chronic myelogenous leukemia. *Nat. Med.* **6,** 1018–1023.

19 Bellantuono, I., Gao, L., Parry, S., et al. (2002) Two distinct HLA-A0201-presented epitopes of the Wilms tumor antigen 1 can function as targets for leukemia-reactive CTL. *Blood* **100,** 3835–3837.

20 Marijt, W. A., Heemskerk, M. H., Kloosterboer, F. M., et al. (2003) Hematopoiesis-restricted minor histocompatibility antigens HA-1- or HA-2-specific T cells can induce complete remissions of relapsed leukemia. *Proc. Natl. Acad. Sci, USA* **100,** 2742–2747.

21 Bonini, C., Ferrari, G., Verzeletti, S., et al. (1997) HSV-TK gene transfer into donor lymphocytes for control of allogeneic graft-versus-leukemia. *Science* **276,** 1719–1724.

22 Tiberghien, P., Ferrand, C., Lioure, B., et al. (2001) Administration of herpes simplex-thymidine kinase-expressing donor T cells with a T-cell-depleted allogeneic marrow graft. *Blood* **97,** 63–72.

23 Miller, A. D. and Buttimore, C. (1986) Redesign of retrovirus packaging cell lines to avoid recombination leading to helper virus production. *Mol. Cell Biol.* **6,** 2895–2902.

24 Lamers, C. H., Willemsen, R. A., Luider, B. A., Debets, R., and Bolhuis, R. L. (2002) Protocol for gene transduction and expansion of human T lymphocytes for clinical immunogene therapy of cancer. *Cancer Gene Ther.* **9,** 613–623.

25 Culver, K. W., Anderson, W. F., and Blaese, R. M. (1991) Lymphocyte gene therapy. *Hum. Gene Ther.* **2,** 107–109.

26 Mavilio, F., Ferrari, G., Rossini, S., et al. (1994) Peripheral blood lymphocytes as target cells of retroviral vector-mediated gene transfer. *Blood* **83,** 1988–1997.

27 Verzeletti, S., Bonini, C., Marktel, S., et al. (1998) Herpes simplex virus thymidine kinase gene transfer for controlled graft-versus-host disease and graft-versus-leukemia: clinical follow-up and improved new vectors. *Hum. Gene Ther.* **9,** 2243–2251.

28 Bonini, C. and Bordignon, C. (1997) Potential and limitations of HSV-TK-transduced donor peripheral blood lymphocytes after allo-BMT. *Hematol. Cell Ther.* **39,** 273–274.

29 Marktel, S., Magnani, Z., Ciceri, F., et al. (2003) Immunologic potential of donor lymphocytes expressing a suicide gene for early immune reconstitution after hematopoietic T-cell-depleted stem cell transplantation. *Blood* **101,** 1290–1298.

30 Ferrand, C., Robinet, E., Contassot, E., et al. (2000) Retrovirus-mediated gene transfer in primary T lymphocytes: influence of the transduction/selection process and of ex vivo expansion on the T cell receptor beta chain hypervariable region repertoire. *Hum. Gene Ther.* **11,** 1151–1164.

31 Contassot, E., Murphy, W., Angonin, R., et al. (1998) In vivo alloreactive potential of ex vivo-expanded primary T lymphocytes. *Transplantation* **65,** 1365–1370.

32 Drobyski, W. R., Majewski, D., Ozker, K., and Hanson, G. (1998) Ex vivo anti-CD3 antibody-activated donor T cells have a reduced ability to cause lethal murine graft-versus-host disease but retain their ability to facilitate alloengraftment. *J. Immunol.* **161,** 2610–2619.

33 Berger, C., Blau, C. A., Clackson, T., Riddell, S. R., and Heimfeld, S. (2003) CD28 costimulation and immunoaffinity-based selection efficiently generate primary gene-modified T cells for adoptive immunotherapy. *Blood* **101,** 476–484.

34 Sauce, D., Tonnelier, N., Duperrier, A., et al. (2002) Influence of ex vivo expansion and retrovirus-mediated gene transfer on primary T lymphocyte phenotype and functions. *J. Hematother. Stem Cell Res.* **11,** 929–940.

35 Cavalieri, S., Cazzaniga, S., Geuna, M., et al. (2003) Human T lymphocytes transduced by lentiviral vectors in the absence of TCR activation maintain an intact immune competence. *Blood* **102,** 497–505.

36 Tiberghien, P., Reynolds, C. W., Keller, J., et al. (1994) Ganciclovir treatment of herpes simplex thymidine kinase-transduced primary T lymphocytes: an approach for specific in vivo donor T-cell depletion after bone marrow transplantation? *Blood* **84,** 1333–1341.

37 Tiberghien, P., Cahn, J. Y., Brion, A., et al. (1997) Use of donor T-lymphocytes expressing herpes-simplex thymidine kinase in allogeneic bone marrow transplantation: a phase I-II study. *Hum. Gene Ther.* **8,** 615–624.

38 Aints, A., Belusa, R., Andersson, R. M., Guven, H., and Dilber, M. S. (2002) Enhanced ouabain resistance gene as a eukaryotic selection marker. *Hum. Gene Ther.* **13,** 969–977.

39 Bonini, C., Grez, M., Traversari, C., et al. (2003) Safety of retroviral gene marking with a truncated NGF receptor. *Nat. Med.* **9,** 367–369.

40 Fehse, B., Kustikova, O. S., Li, Z., et al. (2002) A novel 'sort-suicide' fusion gene vector for T cell manipulation. *Gene Ther.* **9,** 1633–1638.

41 Rettig, M. P., Ritchey, J. K., Meyerrose, T. E., Haug, J. S., and DiPersio, J. F. (2003) Transduction and selection of human T cells with novel CD34/thymidine kinase chimeric suicide genes for the treatment of graft-versus-host disease. *Mol. Ther.* **8,** 29–41.

42 Moolten, F. L., Wells, J. M., Heyman, R. A., and Evans, R. M. (1990) Lymphoma regression induced by ganciclovir in mice bearing a herpes thymidine kinase transgene. *Hum. Gene Ther.* **1,** 125–134.

43 Garin, M. I., Garrett, E., Tiberghien, P., et al. (2001) Molecular mechanism for ganciclovir resistance in human T lymphocytes transduced with retroviral vectors carrying the herpes simplex virus thymidine kinase gene. *Blood* **97,** 122–129.

44 Chalmers, D., Ferrand, C., Apperley, J. F., et al. (2001) Elimination of the truncated message from the herpes simplex virus thymidine kinase suicide gene. *Mol. Ther.* **4,** 146–148.

45 Bordignon, C., Bonini, C., Verzeletti, S., et al. (1995) Transfer of the HSV-tk gene into donor peripheral blood lymphocytes for in vivo modulation of donor anti-tumor immunity after allogeneic bone marrow transplantation. *Hum. Gene Ther.* **6,** 813–819.

46 Cohen, J. L., Saron, M. F., Boyer, O., et al. (2000) Preservation of graft-versus-infection effects after suicide gene therapy for prevention of graft-versus-host disease. *Hum. Gene Ther.* **11,** 2473–2481.

47 Litvinova, E., Maury, S., Boyer, O., et al. (2002) Graft-versus-leukemia effect after suicide-gene-mediated control of graft-versus-host disease. *Blood* **100,** 2020–2025.

48 Ashkenazi, A., and Dixit, V. M. (1998) Death receptors: signaling and modulation. *Science* **281,** 1305–1308.

49 Thomis, D. C., Marktel, S., Bonini, C., et al. (2001) A Fas-based suicide switch in human T cells for the treatment of graft-versus-host disease. *Blood* **97,** 1249–1257.

50 Introna, M., Barbui, A. M., Bambacioni, F., et al. (2000) Genetic modification of human T cells with CD20: a strategy to purify and lyse transduced cells with anti-CD20 antibodies. *Hum. Gene Ther.* **11,** 611–620.

51. Cerny, T., Borisch, B., Introna, M., Johnson, P., and Rose, A. L. (2002) Mechanism of action of rituximab. *Anticancer Drugs* **13 Suppl 2,** S3–10.

52 Di Gaetano, N., Cittera, E., Nota, R., et al. (2003) Complement activation determines the therapeutic activity of rituximab in vivo. *J. Immunol.* **171,** 1581–1587.

53 Link, C. J., Burt, R. K., Traynor, A. E., et al. (1998) Adoptive immunotherapy for leukemia: donor lymphocytes transduced with the herpes simplex thymidine kinase gene for remission induction. ***Hum. Gene Ther. 9,*** 115.

54. Link, C. J., Drobyski, W. R., Traynor, A. E., et al. (1999) Adoptive immunotherapy for leukemia: donor lymphocytes transduced with the Herpes Simplex thymidine kinase (HStk) gene. *Blood* **94,** 1631a.

55. Champlin, R., Besinger, W., Henslee-Downey, J., K. et al. (1999) Phase I/II study of thymidine kinase (TK)-transduced donor lymphocyte infusions (DLI) in patients with hematologic malignanicies. *Blood* **94,** 1448a.

Index